High-order renormalization of scalar quantum fields

Dissertation

zur Erlangung des akademischen Grades

doctor rerum naturalium (Dr. rer. nat.)
im Fach Physik, Spezialisierung: Theoretische Physik

eingereicht an der

Mathematisch-Naturwissenschaftlichen Fakultät der Humboldt-Universität zu Berlin

von

M. Sc. Paul-Hermann Balduf

Präsidentin der Humboldt-Universität zu Berlin
Prof. Dr. Julia von Blumenthal

Dekanin der Mathematisch-Naturwissenschaftlichen Fakultät
Prof. Dr. Caren Tischendorf

Gutachter: 1. Prof. Dr. Dirk Kreimer
2. Prof. David Broadhurst
3. Prof. Gerald Dunne, PhD

Tag der mündlichen Prüfung: 6. Januar 2023

Preface

Quantum field theory is a monster: Unmanageable in terms of the sheer number of different, sometimes contradictory, principles, formalisms, definitions, and results that have been amassed in the past 100 years, often without clear relation to each other. It suffers from mathematical conundrums, incomprehensible heuristic constructions, and being declared hopeless or obsolete once every few years; while at the same time its computational techniques are being used successfully in ever more remote areas of research.

For the present thesis, this has two consequences: Firstly, I spend extraordinarily much effort on explaining the background of relevant constructions, discussing their relations and demonstrating the logical order of their development, as well as the practical applicability in 150 examples. And secondly, I generally prefer to reference original work, instead of merely the latest reviews, in order to acknowledge the historical background. At five points, complete sections are marked as *Digression*, they are not relevant for the understanding of the thesis, but contain additional remarks, motivations, or related topics I found interesting.

More than 70 years after its inception, text books about quantum field theory are now readily available for the general audience, e.g. [1–5], as well as for almost any profession, from mathematicians [6] over economists [7] to gifted amateurs [8]. Nevertheless, chapter 1 is a self-contained introduction to make the thesis accessible to readers without a background in quantum field theory. Conversely, in chapter 2, I review the mathematical formalism, before introducing the concept of renormalization. The following chapter 3 concerns the renormalization group, which lies at the heart of the present thesis. Most of my own results are contained in chapter 4, where I examine different renormalization schemes. Finally, chapter 5 contains the results of a second research project, concerning transformations of the field variable.

To make the thesis more accessible to the general audience, I have included a non-technical abstract in German in the beginning. The appendix is – apart from the bibliography – mostly for entertainment.

Occasionally, I quote from works in their original language German or French. A friend mocked this as “a very continental attitude”, a verdict I can live with. The reader can rest assured that those quotes only serve to illustrate some qualitative remarks of mine, and that they are completely irrelevant for the main text.

Kreuzberg, October 2022

Zusammenfassung

Thema dieser Dissertation ist die Renormierung von perturbativer skalarer Quantenfeldtheorie bei großer Schleifenzahl. Der Hauptteil der Arbeit ist dem Einfluss von Renormierungsbedingungen auf renormierte Greenfunktionen gewidmet.

Zunächst studieren wir ausführlich Dyson-Schwinger-Gleichungen und die Renormierungsgruppe, inklusive der Gegenterme in dimensionaler Regularisierung. Anhand zahlreicher Beispiele illustrieren wir, wie die verschiedenen Größen in konktreten Fällen berechnet werden und welche Relationen es zwischen ihnen gibt.

Alsdann diskutieren wir, welche Freiheitsgrade ein Renormierungsschema hat und wie diese mit den Gegentermen und den renormierten Greenfunktionen zusammenhängen. Für ungekoppelte Dyson-Schwinger-Gleichungen stellen wir fest, dass alle Renormierungsschemata bis auf eine Verschiebung $\delta(\alpha, \epsilon)$ des Renormierungspunktes äquivalent sind. Die Verschiebung zwischen verschiedenen kinematischen Renormierungsschemata ist eine Konstante $\delta \in \mathbb{R}$. Die Verschiebung zwischen kinematischer Renormierung und Minimaler Subtraktion ist eine Funktion der Kopplung α und des Regularisierungsparameters ϵ. Wir leiten eine neuartige Formel für den Fall einer linearen Dyson-Schwinger Gleichung vom Propagatortyp her. Sie erlaubt es, die Verschiebung direkt aus der Mellintransformation des Integrationskerns zu berechnen, ohne die Dyson-Schwinger-Gleichung explizit in Minimaler Subtraktion lösen zu müssen.

Schließlich berechnen wir obige Verschiebung störungstheoretisch für drei beispielhafte nichtlineare Dyson-Schwinger-Gleichungen. Wir stellen dabei fest, dass die Koeffizienten der Reihendarstellung ein ähnliches asymptotisches Wachstum zeigen wie die Koeffizienten der anormalen Dimension.

Ein zweites, nachgeordnetes Thema der vorliegenden Arbeit sind Diffeomorphismen der Feldvariable in einer Quantenfeldtheorie. Wir präsentieren eine Störungstheorie des Diffeomorphismusfeldes im Impulsraum und verifizieren, dass der Diffeomorphismus keinen Einfluss auf messbare Größen hat. Weiterhin untersuchen wir die Divergenzen des Diffeomorphismusfeldes und stellen fest, dass die Divergenzen Wardidentitäten erfüllen, die die Abwesenheit dieser Terme von der S-Matrix ausdrücken. Trotz der Wardidentitäten bleiben unendlich viele Divergenzen unbestimmt, damit ist die Diffeomorphismustheorie perturbativ unrenormierbar.

Den Abschluss der vorliegenden Arbeit bildet ein Kommentar über die numerische Quadratur von Periodenintegralen.

Abstract

This thesis concerns the renormalization of perturbative quantum field theory. More precisely, we examine scalar quantum fields at high loop order. The bulk of the thesis is devoted to the influence of renormalization conditions on the renormalized Green functions.

Firstly, we perform a detailed review of Dyson-Schwinger equations and the renormalization group, including the counterterms in dimensional regularization. Using numerous examples, we illustrate how the various quantities are computable in a concrete case and which relations they satisfy.

Secondly, we discuss which degrees of freedom are present in a renormalization scheme, and how they are related to counterterms and renormalized Green functions. We establish that, in the case of an un-coupled Dyson-Schwinger equation, all renormalization schemes are equivalent up to a shift $\delta(\alpha, \epsilon)$ in the renormalization point. The shift between different kinematic renormalization points is a constant $\delta \in \mathbb{R}$. The shift between kinematic renormalization and Minimal Subtraction is a function of the coupling α and the regularization parameter ϵ. We derive a novel formula for the case of a linear propagator-type Dyson-Schwinger equation. It allows us to compute the shift directly from the Mellin transform of the kernel, without explicitly solving the Dyson-Schwinger equation in Minimal Subtraction.

Thirdly, we compute the shift perturbatively for three examples of non-linear Dyson-Schwinger equations. We find that the series coefficients show a similar asymptotic growth as the coefficients of the anomalous dimension.

A second, smaller topic of the present thesis are diffeomorphisms of the field variable in a quantum field theory. We present the perturbation theory of the diffeomorphism field in momentum space and find that the diffeomorphism has no influence on measurable quantities. Moreover, we study the divergences in the diffeomorphism field and establish that they satisfy Ward identities, which ensure their absence from the S-matrix. Nevertheless, the Ward identities leave infinitely many divergences unspecified and the diffeomorphism theory is perturbatively unrenormalizable.

Finally, we remark on a third topic, the numerical quadrature of Feynman periods.

Populärwissenschaftliche Zusammenfassung

Der Haupttext dieser Arbeit mag abschnittsweise technisch erscheinen. Aus diesem Grunde fassen wir die Kernaussagen hier qualitativ zusammen, ohne auf die mathematischen Details einzugehen.

Grundsätzlich handelt die Dissertation von Quantenfeldtheorie, das ist die Beschreibung von Feldern, die den Prinzipien der Quantenmechanik unterliegen. Man kann sich ein Quantenfeld grob als ein Feld vorstellen, das die Wahrscheinlichkeit für das Antreffen eines Teilchens, des Quants, angibt. Quantenfelder können mit anderen Quantenfeldern interagieren. In dieser Dissertation betrachten wir ausschließlich den Fall, dass ein einziges Feld mit sich selbst interagiert. Anschaulich bedeutet das, dass ein Quant des besagten Feldes, während es sich bewegt, weitere Quanten desselben Feldes aussenden oder einfangen kann.

Um eine Quantenfeldtheorie zu konstruieren, beschreibt man die Ausbreitung und Wechselwirkung der Teilchen mit Hilfe einer sogenannten *Lagrangedichte* (def. 6). Darin sind alle möglichen Prozesse aufgeführt, an denen ein Teilchen teilnehmen kann, und jeder von ihnen ist mit einer sogenannten *Kopplungskonstante* gewichtet.

Viele Interaktionen von Quanten können als *Streuprozesse* (section 1.2.5) verstanden werden: Eine gewisse Gruppe von Quanten stößt zusammen, dabei kommt es zu eine Wechselwirkung und möglicherweise werden einige Quanten dabei absorbiert oder entstehen neu. Das Verhalten solcher Streuprozesse ist in den Greenfunktionen $G^{(n)}$ (def. 46) kodiert: $G^{(n)}$ ist im Prinzip die Wahrscheinlichkeit dafür, dass ein Prozess stattfindet, an dem n Quanten beteiligt sind. Folglich ist eines der primären Ziele der Quantenfeldtheorie, die Greenfunktionen $G^{(n)}$ zu berechnen.

Bei der Berechnung der Greenfunktionen gibt es einen Stolperstein: Die Lagrangedichte enthält gewisse Parameter – die Kopplungskonstanten – deren Zahlenwert man zunächst nicht kennt. Wenn man nun eine Greenfunktion berechnet, dann enthält auch diese Funktion die unbekannten Kopplungskonstanten, und folglich kann man mit dieser Greenfunktion keine Wahrscheinlichkeit für einen konkreten Streuprozessen vorhersagen. Abhilfe schafft eine Prozedur namens *Renormierung* (section 2.2): Man berechnet einige der Greenfunktionen und misst dann die betreffenden Wahrscheinlichkeiten in einem Experiment. Dadurch erhält man eine Gleichung – die *Renormierungsbedingung* – für die unbekannten Kopplungskonstanten. Wenn man diese Gleichung löst, erfährt man den Wert der Kopplungskonstanten und kann fortan die Wahrscheinlichkeit für alle anderen Streuprozesse vorhersagen. Dieses konkrete Verfahren nennt sich *kinematische Renormierung* (def. 91), es gibt aber auch andere *Renormierungsschemata*. Die Greenfunktionen, bei denen die Kopplungskonstanten durch ihren physikalischen Wert ersetzt wurden, bezeichnet man als *renormierte Greenfunktionen* $G^{(n)}_{\mathcal{R}}$ (def. 90).

Im Zuge der Renormierung tritt ein technisches Problem auf: Viele der rechnerischen Größen sind unendlich. Diese *Divergenzen* (section 2.3.1) kann man intuitiv verstehen: Ein Quant ist ein punktförmiges Teilchen ohne räumliche Ausdehnung. Naiv betrachtet dürfte es daher nie zu Wechselwirkungen kommen: Die Quanten sind zu klein, um sich jemals zu treffen. Andererseits wissen wir aus Experimenten, dass sehr wohl Wechselwirkung zwischen Quanten stattfindet.

Formell gesehen kann man den Widerspruch auflösen, wenn man annimmt, dass die Teilchen nicht nur unendlich klein sind, sondern gleichzeitig eine unendlich hohe Wechselwirkungsrate haben, falls sie sich doch einmal treffen. Der Formalismus der Renormierung erlaubt es, mit derartigen unendlichen Größen zu arbeiten. Bei manchen Quantenfeldtheorien ist garantiert, dass ein messbares Endergebnis – also eine renormierte Greenfunktion $G^{(n)}_{\mathcal{R}}$ – niemals eine der unendlichen Größen enthält, sondern stets einen sinnvollen endlichen Wert hat. Solche Theorien heißen *renormierbar* (section 2.3). Vermutlich ist das Auftreten von Divergenzen lediglich ein Artefakt unseres etwas unbeholfenen Formalismus, bei dem wir die Theorie aus Streuprozessen zwischen punktförmigen Teilchen aufbauen (section 3.2.3). In Wirklichkeit ist jedes Quant von einer ausgedehnten Wolke aus anderen Quanten umgeben, die auch an Wechselwirkungen teilnehmen, und bekommt dadurch eine effektive Größe, die verschieden von Null ist.

Im Detail handelt diese Dissertation davon, dass verschiedene mögliche Renormierungsbedingungen letztendlich zu denselben physikalischen Vorhersagen für renormierte Greenfunktionen $G^{(n)}_{\mathcal{R}}$ führen. Für die oben beschriebene kinematische Renormierung ist das naheliegend – es sollte keinen Unterschied machen, ob man beispielsweise einen Streuprozess bei einer anderen Energie oder einem anderen Winkel der beteiligten Teilchen als Referenz nimmt. Allerdings ist es auch möglich, eine abstraktere Renormierungsbedingung zu wählen, die darauf abziehlt, lediglich die Divergenzen aus der Theorie zu entfernen, ohne dabei eine konkrete physikalische Interpretation vorzugeben. Dieses Renormierungsschema heißt *Minimale Subtraktion* (def. 108), und sie hat zwei Effekte: Erstens erhält man, verglichen mit kinematischer Renormierung, einen anderen Zahlenwert der Kopplungskonstanten, und zweitens hat die renormierte Greenfunktion $G^{(n)}_{\mathcal{R}}$ eine andere Form. In der vorliegenden Dissertation wird demonstriert, dass, abgesehen von gewissen Sonderfällen, die Ergebnisse für kinematische Renormierung und für Minimale Subtraktion äquivalent sind (section 4.4). Die Minimale Subtraktion entspricht dann einer kinematischen Renormierung bei einer gewissen Energie δ, deren Wert wir für einige Beispielsysteme bestimmen (section 4.5).

Das Ergebnis hat keinerlei Anwendung in der Industrie oder im Alltag. Allerdings ist es nützlich für theoretische Berechnungen in der Quantenfeldtheorie, denn wir erhalten dadurch eine größere Freiheit bei der Wahl der Renormierungsbedingungen. Ohne systematisch danach zu suchen, sind wir auf zwei Fälle gestoßen, in denen die Berechnung der Greenfunktion in jeweils einem bestimmten Schema sehr viel einfacher ist als in anderen (section 4.2.4). Die betreffende Quantenfeldtheorie ist – wie alle Theorien, die in dieser Dissertation behandelt werden – ein extrem vereinfachtes Beispielsystem. Die realen Fälle in der Natur sind sehr viel komplizierter und man sollte nicht erwarten, dass bestimmte Renormierungsschemata zu derartig einfachen Lösungen führen. Nichtsdestotrotz ist die Äquivalenz von Renormierungsschemata auch dort von Bedeutung, beispielsweise für die Frage, welche Terme bei Quantenkorrekturen den größten Einfluss haben und welche eher vernachlässigt werden können (section 6.2.1).

Contents

wir sind ameisen und bauen an schwerem gerät

Elisa Weinkötz [9]

1. Introduction to perturbative quantum field theory

1.1. Conventions

The following notation and conventions should be familiar to the physicist reader.

Definitions will be indicated by ":=", where $A := B$ means that A is defined to be equal to B. The real numbers are $\mathbb{R}$, the natural numbers $\mathbb{N}$ do not include zero, and $\mathbb{N}_0 = \mathbb{N} \cup \{0\}$. The sign $\propto$ means "exactly proportional to", while $\sim$ denotes "of the order" or "approximately proportional to". With $\overset{!}{=}$ we denote "is demanded to be equal". The center dot $\cdot$ is used to visually highlight a multiplication. It does not indicate a special type of multiplication, such as a scalar product between vectors.

Integrals act as operators on products to the right of them, but not on sums:

$$\int \mathrm{d}x \left(f(x)g(x) + h(x)\right) \neq \int \mathrm{d}x\, f(x)g(x) + h(x) = \left(\int \mathrm{d}x\, f(x)g(x)\right) + h(x).$$

An integral without explicit integration domain is meant to cover the complete space.

In this thesis, we assume a flat D-dimensional spacetime. A point in this spacetime is a D-vector, that is an ordered tuple

$$\underline{x} := \left(x^0, \mathbf{x}\right) := \left(x^0, x^1, \ldots, x^{D-1}\right),$$

consisting of one time coordinate x^0 and a $(D-1)$-dimensional vector $\mathbf{x}$ which denotes the position in space.

Definition 1. The D-dimensional real vector space together with the pseudo scalar product eq. (1.1) is called *Minkowski space* $\mathbb{M}^D$. The *Minkowski metric* is the $D \times D$-matrix

$$\eta := \mathrm{diag}\,(1, -1, \ldots, -1) = \begin{pmatrix} 1 & 0 & \ldots & 0 \\ 0 & -1 & \ldots & 0 \\ \vdots & & \ddots & \vdots \\ 0 & \ldots & 0 & -1 \end{pmatrix}.$$

The magnitude of a vector is given by the scalar product

$$\underline{x}\underline{y} := \sum_{i=0}^{D-1} \sum_{j=0}^{D-1} x^i \eta_{ij} y^j = \sum_{i=0}^{D-1} x^i y_i =: x_i y^i. \tag{1.1}$$

Here, we have introduced Einstein's sum convention: If an index (the i in the last formula) appears twice, it is being summed over. Equation (1.1) is a pseudo scalar product, it can take positive and negative values.

Occasionally, we use *Euclidean spacetime*, where the metric is $\mathbb{1}_{D\times D} = \mathrm{diag}\,(1,\ldots,1)$. The transition between Euclidean and Minkowski metric is formally achieved by exchanging $x^0 = t \leftrightarrow i\tau$. This can be interpreted as continuation to imaginary times, and is called *Wick rotation*.

Definition 2 ([10, 11])**.** Let η be the Minkowski metric (def. 1). A *Lorentz transformation* is a transformation of coordinates $x'^\mu = \Lambda^\mu{}_\nu x^\nu$, where the transformation matrix satisfies

$$\Lambda^\mu{}_\rho \Lambda^\nu{}_\sigma \eta_{\mu\nu} = \eta_{\rho\sigma}, \qquad \text{or short} \qquad \Lambda^T \eta \Lambda = \eta.$$

Transformations between different inertial frames are given by the group of Lorentz transformations. In $D = 4$ spacetime dimensions, a Lorentz transformation has 6 parameters, representing rotations around 3 axes and changes in the relative velocity along 3 axes. The Lorentz group is closely related to causality [12].

Definition 3 ([13])**.** A *Poincaré transformation* is a transformation of coordinates $x'^\mu = \Lambda^\mu{}_\nu x^\nu + a^\mu$, where Λ is a Lorentz transformation (def. 2) and $\underline{a}$ is a D-dimensional constant vector.

We use *natural units*, that is, we choose the units such that the speed of light is $c = 1$ and the reduced Planck constant [14] is $\hbar = 1$. Thereby, all quantities we encounter have the same unit, which one can choose to be mass.

Definition 4. If, in natural units, a quantity has the unit $(\text{mass})^n$ for some n, we say it has *mass dimension* n. Equivalently, the unit $(\text{length})^n$ amounts to a mass dimension $-n$.

A Fourier transform involves a factor 2π, which we include into the momentum-integral,

$$\tilde{f}(k) = \int \mathrm{d}x\; f(x) e^{ikx} \quad \Leftrightarrow \quad f(x) = \int \frac{\mathrm{d}k}{2\pi}\; f(k) e^{-ikx}.$$

Definition 5 ([15])**.** Let $\nu \in \mathbb{R}$ and $-\nu \notin \mathbb{N}_0$. The *Euler Gamma function* is defined as

$$\Gamma(\nu) := \int_0^\infty \mathrm{d}t\; t^{\nu-1} e^{-t}.$$

For later use, we note here two formulae regarding the D-dimensional Fourier transforms of a monomial. Let $\nu \in \mathbb{C}$ with real part $-\nu \notin \mathbb{N}_0$ and $\nu - D/2 \notin \mathbb{N}_0$, and $n \in \mathbb{N}$, then [16, pp. 155, 163]

$$\begin{aligned} \int \frac{\mathrm{d}^D k}{(2\pi)^D} \frac{1}{(\underline{k}^2)^\nu} e^{-i\underline{k}\underline{x}} &= \frac{1}{4^\nu \pi^{\frac{D}{2}}} \frac{\Gamma\left(\frac{D}{2} - \nu\right)}{\Gamma(\nu)} (\underline{x}^2)^{\nu - \frac{D}{2}} \\ \int \frac{\mathrm{d}^D k}{(2\pi)^D} (\underline{k}^2)^n e^{-i\underline{k}\underline{x}} &= (-1)^n (\partial_\mu \partial^\mu)^n \delta(\underline{x}), \qquad n \in \mathbb{N}. \end{aligned} \tag{1.2}$$

The D-dimensional Euclidean Gaussian [17] integral is

$$\int \frac{\mathrm{d}^D \underline{k}}{(2\pi)^D} \, e^{i\alpha \underline{k}^2 - i\underline{k}\underline{x}} = \left(\frac{i}{4\pi\alpha}\right)^{\frac{D}{2}} e^{-\frac{i\underline{x}^2}{4\alpha}}. \tag{1.3}$$

1.2. From classical field theory to perturbative QFT

This thesis concerns perturbative quantum field theory (QFT). Before we discuss the technical points, the present section is a brief introduction to the subject. The content is readily available in any QFT course or textbook, such as [1, 3–5]. The reader familiar with the basics is invited to skip directly to section 1.3.

1.2.1. Classical field theory

Colloquially, a field is an object which takes a value depending on a point in spacetime. In the present thesis, we almost exclusively consider scalar fields, this means that the value of the field is a single, real number (as opposed to a vector or a matrix) at each point. More formally, a field is a function $\phi : \mathbb{M}^D \to \mathbb{R}$. A *field theory* is a set of fields, together with so-called *equations of motion* which describe the behaviour of these fields.

One way to specify a field theory is through the corresponding Lagrangian density, short *Lagrangian*. It contains the field variables and information about how the fields interact with themselves or with each other.

Definition 6. A Lagrangian is a function $\mathcal{L}$ with the following properties:

1. $\mathcal{L}(\underline{x})$ can depend on $\underline{x}$, on $\phi(\underline{x})$, and on finitely many derivatives of $\phi(\underline{x})$, all evaluated at the same spacetime point $\underline{x}$ ("locality").
2. $\mathcal{L}(\underline{x})$ is a scalar under Poincaré transformations (def. 3), $\mathcal{L}(\underline{x}) \mapsto \mathcal{L}(\Lambda\underline{x})$.
3. $\mathcal{L}(\underline{x})$ depends on the field $\phi(\underline{x})$ only via the value $\phi(\underline{x})$ itself and its first derivatives $\partial_\mu\phi(\underline{x})$, not via higher derivatives of $\phi(\underline{x})$.
4. $\mathcal{L}(\underline{x})$ has mass dimension (def. 4) D in a D-dimensional spacetime. Equivalently, the action (def. 7) carries no units.

We write $\mathcal{L}(\underline{x})$ or equivalently $\mathcal{L}(\phi, \partial_\mu\phi)$ for $\mathcal{L}(\underline{x}, \phi(\underline{x}), \partial_\mu\phi(\underline{x}))$.

We restrict ourselves to Lagrangians that do not depend on $\underline{x}$ explicitly. Property 2 implies that the field variables are representations of the Poincaré group (def. 3). A closer inspection of the structure of this group [11] reveals that fields, and in a quantum theory their corresponding particles, can be classified according to a half-integer parameter *spin* and a real, non-negative parameter *mass*. Property 3 is subtle. At this point, we take it as an axiom without obvious physical reason, but we will explore the motivation and implications in section 2.4.

Definition 7. The *action* is the D-dimensional spacetime integral of the Lagrangian,

$$S[\phi] := \int \mathrm{d}^D\underline{x}\, \mathcal{L}(\underline{x}).$$

Example 1: Free scalar field, Lagrangian.

The Lagrangian density of the free scalar field reads

$$\mathcal{L} = \frac{1}{2}\partial_\mu\phi(\underline{x})\partial^\mu\phi(\underline{x}) - \frac{1}{2}m^2\phi^2(\underline{x}).$$

In this,

- The prefactors $\frac{1}{2}$ are convention.
- The first summand, $\frac{1}{2}\partial_\mu\phi(\underline{x})\partial^\mu\phi(\underline{x})$, is called *kinetic term*. For each field, a Lagrangian density needs to have one kinetic term, which is the product of two field variables and involves at least one derivative.
- The second summand, $\frac{1}{2}m^2\phi^2(\underline{x})$, is called *mass term*. It is quadratic in the field without derivative. The constant $m \in \mathbb{R}$ has mass dimension (def. 4) $[m] = 1$. The mass term is optional, fields can be massless.

Both summands in the free Lagrangian density are quadratic in the field variable. Since the Lagrangian has mass dimension $[\mathcal{L}] = D$, the field variable must have mass dimension

$$[\phi] = \frac{D-2}{2}.$$

The Lagrangian of a free field theory is quadratic in the field variables, it can be expressed with a differential operator $\hat{s}$ in the form

$$\mathcal{L} = \frac{1}{2}\phi\hat{s}\phi. \tag{1.4}$$

Definition 8. The *offshell variable* s_p is the Fourier transform of the free field differential operator from eq. (1.4),

$$s_p \cdot e^{i\underline{p}\underline{x}} := \hat{s}e^{i\underline{p}\underline{x}},$$

A momentum $\underline{p}$ is said to be *onshell* if $s_p = 0$, otherwise $\underline{p}$ is called *offshell*. For numbered momenta, we use the shorthand notation $s_{i+j} := s_{p_i+p_j}$.

Example 2: Scalar field, field differential operator.

The Lagrangian from example 1 amounts to the field differential operator $\hat{s} = -\partial_\mu\partial^\mu - m^2$ and the offshell variable $s_p = \underline{p}^2 - m^2$. A particle is onshell if $\underline{p}^2 = m^2$.

The corresponding massless theory is obtained by setting $m = 0$, i.e.

$$\mathcal{L} = -\frac{1}{2}\phi\partial_\mu\partial^\mu\phi, \qquad \hat{s} = -\partial_\mu\partial^\mu, \qquad s_p = \underline{p}^2.$$

Any summand of higher than second power represents an interaction between fields. We only consider interactions that are monomials in the field, which amounts to a Lagrangian

$$\mathcal{L} = \frac{1}{2}\partial_\mu\phi(\underline{x})\partial^\mu\phi(\underline{x}) - \frac{1}{2}m^2\phi^2(\underline{x}) - \sum_{n=3}^{\infty}\frac{\lambda_n}{n!}\phi^n(\underline{x}). \tag{1.5}$$

Here, the parameters λ_n are called *coupling constants*. In classical field theory they take a pre-defined finite numerical value. From now on, we will mostly skip the argument $(\underline{x})$, understanding that all terms in a Lagrangian are to be evaluated at the same point.

Example 3: ϕ^n theory, Lagrangian.

The so-called ϕ^n theory is a model with only a single interaction monomial $\propto \phi^n$. The most popular examples are ϕ^3- and ϕ^4 theory. The Lagrangian of ϕ^n theory is

$$\mathcal{L} = \frac{1}{2}\partial_\mu\phi\partial^\mu\phi - \frac{1}{2}m^2\phi^2 - \frac{\lambda_n}{n!}\phi^n.$$

Following def. 6 and example 1, we conclude the mass dimension of the coupling constant

$$[\lambda_n] = D - n\frac{D-2}{2}, \quad \Rightarrow \quad [\lambda_3] = 3 - \frac{1}{2}D, \quad [\lambda_4] = 4 - D.$$

Example 4: Liouville theory, Lagrangian.

A typical example of non-polynomial interaction are theories of Liouville-type [18]

$$\mathcal{L} = \frac{1}{2}\partial_\mu\phi\partial^\mu\phi - c\exp(\lambda\cdot\phi).$$

In this case $[\phi] = \frac{D-2}{2}$ and $[\lambda] = \frac{2}{D-2}$ and $[c] = D$.

The classical equations of motion can be obtained by requesting that the action (def. 7) be invariant under infinitesimal changes of the field ϕ,

$$\delta S[\phi] \overset{!}{=} 0. \tag{1.6}$$

A series expansion of the Lagrangian in the field variable, assuming the properties of def. 6 are fulfilled, leads to the Lagrangian equation of motion,

$$\frac{\partial\mathcal{L}}{\partial\phi} - \frac{\mathrm{d}}{\mathrm{d}\,x^\mu}\left(\frac{\partial\mathcal{L}}{\partial(\partial_\mu\phi)}\right) = 0. \tag{1.7}$$

Here, all functions and derivatives are to be taken at the same spacetime point. This is a second order partial differential equation, it requires two initial conditions: The field $\phi(0,\mathbf{x})$ at the starting time and its time derivative $\partial_0\phi(0,\mathbf{x}) =: \dot{\phi}(0,\mathbf{x})$, both for the complete space.

Example 5: Free scalar field, classical solution.

The free Lagrangian from example 1 results in

$$\frac{\partial \mathcal{L}}{\partial \phi} = -m^2\phi, \qquad \frac{\partial \mathcal{L}}{\partial(\partial_\mu \phi)} = \partial_\mu \phi$$

and the Lagrangian equation of motion is the Klein-Gordon equation [19–21]

$$\left(\partial_\mu \partial^\mu + m^2\right) \phi(\underline{x}) = 0. \tag{1.8}$$

Its solutions in infinitely large spacetime are superpositions of plane waves of the form

$$\phi(\underline{x}) = A \cdot \sin\left(\underline{k} \cdot \underline{x}\right) + B \cdot \cos(\underline{k} \cdot \underline{x}), \tag{1.9}$$

where A and B are arbitrary constants and $\underline{k}^2 - m^2 = 0$. The last equation means that $\underline{k}$ is onshell (def. 8). Since eq. (1.8) is a *linear* partial differential equation, any sum of such solutions is a solution as well. Physically, this means that any number of such waves can exist simultaneously without disturbing each other, there is no interaction between them, the theory is a *free* field as claimed.

We remark that a mode expansion, that is, an expansion into fundamental solutions of the differential operator, is fruitful in field theory much more generally. For example, the *quasinormal modes* [22] framework allows to treat the behaviour of the electromagnetic field (example 7) in finite size cavities. Also dissipation can be included by allowing for complex energies k^0, which effectively give rise to exponentially decaying solutions. In QFT, this amounts to unstable particles, see [23].

Example 6: Interacting scalar fields, classical equations of motion.

ϕ^n theory from example 3 leads to the equation of motion

$$\left(\partial^\mu \partial_\mu + m^2\right) \phi(\underline{x}) + \frac{\lambda}{(n-1)!}\phi^{n-1}(\underline{x}) = 0.$$

Liouville theory from example 4 produces $\partial^\mu \partial_\mu \phi(\underline{x}) + \lambda \exp\left(\lambda \cdot \phi(\underline{x})\right) = 0$.

Both differential equations are non-linear in the field variable $\phi(\underline{x})$, a superposition of two solutions is not a solution. Hence, they describe a field with self-interaction, not a free field. One can obtain a perturbative solution in terms of iterated integrals by recursively inserting the *Green functions* (eq. (1.23)) of the free field, see e.g. [24].

Example 7: Classical electrodynamics.

The electromagnetic field describes many familiar phenomena in physics, such as light, heat radiation, radio waves, or the binding between atoms. Due to its high popularity, we will occasionally use it as an example. Classical electrodynamics can be formulated in terms of a scalar potential $\Phi(\underline{x})$ and a vector potential $\mathbf{A}(\underline{x})$. In the relativistic formulation, the two are merged into the 4-component vector potential $A^\mu(\underline{x}) := (\Phi(\underline{x}), \mathbf{A}(\underline{x}))$.

The field strength tensor $F_{\mu\nu} := \partial_\mu A_\nu - \partial_\nu A_\mu$ is a 4×4-matrix, its entries are the classical electric field $\mathbf{E}$ and magnetic field $\mathbf{B}$:

$$F_{\mu\nu} = \begin{pmatrix} 0 & E_x & E_y & E_z \\ -E_x & 0 & -B_z & B_y \\ -E_y & B_z & 0 & -B_x \\ -E_z & -B_y & B_x & 0 \end{pmatrix}.$$

Recall that we defined the speed of light to be $c = 1$, otherwise, the E-fields appear as $\frac{E_j}{c}$ in $F_{\mu\nu}$. The Lagrangian of electrodynamics is

$$\mathcal{L} = -\frac{1}{4} F_{\mu\nu} F^{\mu\nu}.$$

Let $\epsilon^{\mu\nu\rho\sigma}$ be a completely antisymmetric tensor with $\epsilon^{1234} = 1$. The Euler Lagrange equations of motion (eq. (1.7)) arising from $\mathcal{L}$ are the vacuum Maxwell equations [25]

$$\partial_\mu F^{\mu\nu} = 0, \qquad \partial_\mu \epsilon^{\mu\nu\rho\sigma} F_{\rho\sigma} = 0.$$

In terms of $\mathbf{E}$ and $\mathbf{B}$, the first equation reads $\nabla \cdot \mathbf{E} = 0, \nabla \times \mathbf{B} - \partial_t \mathbf{E} = 0$, and the second equation is $\nabla \cdot \mathbf{B} = 0, \nabla \times \mathbf{E} + \partial_t \mathbf{B} = 0$.

The electromagnetic field interacts with fermions, most notable electrons. In classical electrodynamics, they appear as point charges or continuous charge densities. For later, it will be useful to introduce a fermionic field $\psi(\underline{x})$ which carries a charge $e \in \mathbb{R}$ and a mass $m \in \mathbb{R}_+$. This field is Dirac spinor [26], it is a vector in spinor space, operated on by the Dirac matrices γ^μ, and $\bar{\psi} := \psi^\dagger \gamma^5$ is the adjoint spinor. The Lagrangian of the fermion field is

$$\mathcal{L} = \bar{\psi} \left(i \gamma^\mu \partial_\mu - m \right) \psi.$$

The coupling between the electromagnetic and the fermionic field has a particular structure, called *gauge-covariant derivative*, which will be motivated in example 127,

$$D_\mu := \partial_\mu - ieA_\mu.$$

The Lagrangian of the electromagnetic field, coupled to the fermion field, is then

$$\mathcal{L} = \bar{\psi} \left(i \gamma^\mu D_\mu - m \right) \psi - \frac{1}{4} F_{\mu\nu} F^{\mu\nu}.$$

The equations of motion (eq. (1.7)) arising from this Lagrangian are the Dirac equation for the fermion field, and the Maxwell equations for the electromagnetic field, where the fermion density $\bar{\psi}\psi$ appears as a source term:

$$\begin{aligned} \left(i \gamma^\mu \partial_\mu - m \right) \psi(\underline{x}) &= 0 \\ \partial_\mu \epsilon^{\mu\nu\rho\sigma} F_{\rho\sigma} = 0, \qquad \partial_\mu F^{\mu\nu} &= e \bar{\psi} \psi. \end{aligned}$$

For the construction of a quantum field theory, we need the Hamiltonian description of classical field theory. To this end, we introduce the canonical conjugate momentum field,

$$\pi := \frac{\partial \mathcal{L}}{\partial(\partial_0 \phi)}, \tag{1.10}$$

where $\partial_0 \phi =: \dot{\phi}$ is the time-derivative of ϕ. We assume that eq. (1.10) is invertible so that we can express $\dot{\phi}$ as a function of π.

Definition 9. The *Hamiltonian density* is defined as the Legendre transform (to be defined in def. 53) of the Lagrangian density,

$$\mathcal{H}(\underline{x}) := \pi(\underline{x})\dot{\phi}(\pi) - \mathcal{L}\left(\phi, \dot{\phi}(\pi)\right).$$

The Hamiltonian density is a function of ϕ and π, there is no dependence on $\dot{\phi}$ any longer.

Example 8: Free scalar field, Hamiltonian density.

The Hamiltonian density of a free field (example 1) reads

$$\mathcal{H}(\underline{x}) = \frac{1}{2}\pi^2(\underline{x}) + \frac{1}{2}\left(\nabla\phi(\underline{x})\right)^2 + \frac{1}{2}m^2\phi^2(\underline{x}).$$

Definition 10. The *Hamilton function*, or *Hamiltonian*, is the spatial integral of the Hamiltonian density def. 9,

$$H := \int \mathrm{d}^{D-1}\mathbf{x}\, \mathcal{H}(\mathbf{x}, t).$$

From eq. (1.7) and def. 10 one derives the *Hamiltonian equations of motion*,

$$\dot{\phi}(t, \mathbf{x}) = \frac{\delta H}{\delta \pi(t, x)}, \qquad \dot{\pi}(t, \mathbf{x}) = -\frac{\delta H}{\delta \phi(t, \mathbf{x})}. \tag{1.11}$$

Definition 11. The *Poisson bracket* of two functionals $A[\phi, \pi]$ and $B[\phi, \pi]$ is defined as

$$\{A, B\}(t) := \int \mathrm{d}^{D-1}\mathbf{x} \left(\frac{\delta\, A}{\delta\phi(t, \mathbf{x})}\frac{\delta B}{\delta\pi(t, \mathbf{x})} - \frac{\delta B}{\delta\phi(t, \mathbf{x})}\frac{\delta A}{\delta\pi(t, \mathbf{x})}\right).$$

By direct calculation, we find

$$\begin{aligned} \{\phi(t, \mathbf{x}), \pi(t, \mathbf{y})\} &= \delta(\mathbf{x} - \mathbf{y}) \\ \{\phi(t, \mathbf{x}), \phi(t, \mathbf{y})\} &= 0 = \{\pi(t, \mathbf{x}), \pi(t, \mathbf{y})\}. \end{aligned} \tag{1.12}$$

The equations of motion eq. (1.11) can be expressed with Poisson brackets (def. 11) as

$$\dot{\phi}(t, \mathbf{x}) = \{\phi(t, \mathbf{x}), H\}, \qquad \dot{\pi}(t, \mathbf{x}) = \{\pi(t, \mathbf{x}), H\}. \tag{1.13}$$

1.2.2. Canonical quantization

Canonical quantization produces a quantum field theory out of a given classical field theory in Hamilton formalism. Concretely, it amounts to two formal steps:

1. Promote the field variable $\phi(t, \mathbf{x})$ and the canonical momentum $\pi(t, \mathbf{x})$ to operators on a suitable Hilbert space of states.

2. Replace the Poisson brackets eq. (1.12) $\{\ ,\ \}$ by commutators $-i\hbar[\ ,]$ between the operators.

There are numerous justifications, constraints and technical details to this procedure both from the physics and the mathematics side. While the first formulation in the 1920s [27–30] was based on physical intuition, a contemporary approach called *deformation quantization* [31–34] is more mathematically rigorous. The interested reader finds more modern perspectives about quantization in [35–38], an amusing collection of "mathematical surprises" in [39], and some examples of contradictions and open problems in [40–43].

A more sophisticated approach to canonical quantization is based on operators acting on smooth test functions and avoids the notion of a "field at spacetime point $\underline{x}$". For Minkowski spacetime, this gives rise to the *Wightman axioms* [44, 45], in Euclidean spacetime one has the *Osterwalder-Schrader axioms* [46, 47]. For completeness, we state the Wightman axioms, following [42], without introducing all technical terms.

Definition 12. A quantum field theory can be defined by the *Wightman axioms*:

1. All states of the system are vectors in a separable Hilbert space which is equipped with a strongly continuous unitary representation of the Poincaré group $P_+^\uparrow$. There is a unique vacuum state $|0\rangle$ which is invariant under Poincaré transformations (def. 3).

2. The spectrum of the energy-momentum operator p_μ lies in the closed forward light cone, that is, $p_\mu p^\mu \geq 0$.

3. For each Schwartz function f there are operators $\phi_1(f), \ldots, \phi_n(f)$ ("quantum fields") and their adjoints $\phi_1^\dagger(f), \ldots, \phi_n^\dagger(f)$, defined on a dense subset D of the Hilbert space containing the vacuum and stable under actions of the Poincaré group.

4. The quantum fields transform covariantly under the Poincaré group.

5. If the support of f, g is spacelike separated then $[\phi(f), \phi(g)] = 0$.

The free scalar quantum field in infinitely large spacetime can be expanded in modes like the classical free field (example 5),

$$\phi(\underline{x}) = \int \frac{\mathrm{d}^{D-1}\,\mathbf{k}}{(2\pi)^{D-1}} \frac{1}{2\omega(\mathbf{k})} \left(a(\mathbf{k}) e^{-i\underline{kx}} + a^\dagger(\mathbf{k}) e^{i\underline{kx}} \right). \tag{1.14}$$

We have introduced $\omega(\mathbf{k}) := \sqrt{\mathbf{k}^2 + m^2}$. The operator-valued coefficients $a(\mathbf{k})$ and $a^\dagger(\mathbf{k})$ are called *annihilation- and creation operators*. Replacing the Poisson brackets eq. (1.12) by commutators leads to the fundamental commutation relations

$$\begin{aligned} \left[a(\mathbf{k}), a^\dagger(\mathbf{k}')\right] &= (2\pi)^{D-1} 2\omega(\mathbf{k})\hbar\delta(\mathbf{k}-\mathbf{k}'), \\ \left[a(\mathbf{k}), a(\mathbf{k}')\right] &= 0 = \left[a^\dagger(\mathbf{k}), a^\dagger(\mathbf{k}')\right]. \end{aligned} \tag{1.15}$$

The Hamilton function (def. 10) becomes the Hamiltonian operator of the free field theory, which computes the energy of a state. Further, it governs time-evolution via the quantized version of the Hamiltonian equation of motion (eq. (1.13)),

$$\dot{\phi}(t, \mathbf{x}) = [\phi(t, \mathbf{x}), H(\underline{t})]\,. \tag{1.16}$$

We are operating in the *Heisenberg picture* of quantum mechanics: The operators are time-dependent, while the states are not. An explicit calculation of various commutators reveals that the operator $a^\dagger(\mathbf{k})$ increases the momentum of a state by $\mathbf{k}$ and the energy by $\omega(\mathbf{k})$, this justifies the interpretation that $a^\dagger(\mathbf{k})$ creates one non-interacting particle of momentum $\mathbf{k}$ and mass m. The vacuum $|0\rangle$ does not contain a particle which could be annihilated,

$$a(\mathbf{k})|0\rangle = 0, \qquad \langle 0|a^\dagger(\mathbf{k}) = 0, \qquad \forall \mathbf{k}. \tag{1.17}$$

In general, it is possible to add a position-independent constant to the Lagrangian eq. (1.5) and to the field eq. (1.14). Such constant amounts to a shift of the vacuum expectation value of the field, which is, for example, relevant when the field is coupled to gravity. However, for the QFTs considered in the present thesis, the absolute value of the field is not observable, therefore we choose this constant to vanish. Equation (1.17) then implies

$$\langle 0|\phi(\underline{x})|0\rangle = 0. \tag{1.18}$$

1.2.3. 2-point correlation functions

Following the general principle of the Copenhagen interpretation of quantum mechanics [48], it is impossible to directly observe quantum fields. The only quantities accessible to measurements are *observables*, given by hermitian operators.

The requirement in the Wightman axioms def. 12 that the subset spanned by quantum fields be dense in the Hilbert space means that all states in it can be reasonably expressed by products of quantum field operators $\phi(\underline{x}), \phi^\dagger(\underline{x})$. This entails that all observables are expressible in terms of vacuum expectation values of products of fields. In practice, one can circumvent the somewhat arcane notion of operator-valued distributions, and their precise physical interpretation, by taking the correlation functions as primary objects. Alternatively, instead of the Wightman axioms for the field operators, a quantum field theory can also be defined by an equivalent set of axioms for its corresponding *Wightman distributions* in the first place [42, 44].

Definition 13. The *Wightman distributions* are the vacuum expectation values of a product of n quantum fields, given by n Schwartz functions:

$$\tilde{W}^{(n)}(f_1, \dots, f_n) := \langle 0|\phi(f_1)\cdots\phi(f_n)|0\rangle.$$

Using the Fourier expansion eq. (1.14) and eq. (1.17), the 2-point distribution is

$$\tilde{W}^{(2)}(f_1, f_2) = \int \frac{\mathrm{d}^D \underline{k}}{(2\pi)^D}\, 2\pi\theta(p^0)\delta(\underline{k}^2 - m^2)\tilde{f}_1^*(\underline{k})\tilde{f}_2(\underline{k}). \tag{1.19}$$

Here, $\tilde{f}_j$ are the Fourier transforms of the Schwartz functions f_j.

If one demands the Schwartz functions $f_j(\underline{x})$ to be localized arbitrarily closely around some spacetime points $\underline{x}_j$, then the Wightman distributions (def. 13) become the local *Wightman functions* $\tilde{W}^{(n)}(\underline{x}_1, \dots, \underline{x}_n)$. Colloquially, this limit is denoted by $f_j \to \delta(\underline{x} - \underline{x}_j)$ in position space, or $\tilde{f}_j(\underline{p}) \to e^{i\underline{k}\underline{x}_j}$ in momentum space. In doing so, one leaves the territory of well-defined axiomatic QFT. The functions $\tilde{W}^{(n)}$ will generally have singularities, see section 1.2.8. The "local" limit of the distribution in eq. (1.19) is obtained by replacing $\tilde{f}_j(\underline{p}) \to e^{i\underline{p}\underline{x}_j}$,

$$\tilde{W}^{(2)}(\underline{x}_1, \underline{x}_2) = \int \frac{\mathrm{d}^D \underline{k}}{(2\pi)^D}\, 2\pi\theta(k^0)\delta(\underline{k}^2 - m^2)e^{-i\underline{k}(\underline{x}_1 - \underline{x}_2)} = \int \frac{\mathrm{d}^{D-1}\mathbf{k}}{(2\pi)^{D-1}}\, \frac{e^{i\underline{k}(\underline{x}_1 - \underline{x}_2)}}{2\sqrt{\mathbf{k}^2 + m^2}}.$$

This function depends only on the difference $\underline{x}_1 - \underline{x}_2$. Further, it is manifestly singular in the case $\underline{x}_1 = \underline{x}_2$. The integrand $\theta(p^0)\delta(\underline{p}^2 - m^2) =: \delta_+(\underline{p}^2 - m^2)$ has a physical interpretation, it ensures that only the positive-energy solution $p^0 = +\sqrt{\mathbf{p}^2 + m^2} \equiv +\omega(\mathbf{p})$ contributes. One uses the residue theorem (see fig. 1.1) to rewrite

$$\tilde{W}^{(2)}(\underline{z}) = 2\pi i \int \frac{\mathrm{d}^{D-1}\underline{k}}{(2\pi)^D} \frac{-i}{2\omega(\mathbf{k})} e^{i\underline{k}\underline{z}} = \int \frac{\mathrm{d}^{D-1}\underline{k}}{(2\pi)^D} \int \mathrm{d}p^0 \frac{i}{(k^0 - \omega(\mathbf{p}))(k^0 + \omega(\mathbf{p}))} e^{-ik^0 z^0} e^{i\mathbf{k}\mathbf{z}}. \tag{1.20}$$

In this, we have to integrate k^0 around the right pole of $((k^0 - \omega(\mathbf{p}))(k^0 + \omega(\mathbf{p}))^{-1} = (\underline{k}^2 - m^2)^{-1}$. The function is holomorphic everywhere else, the integration path can be extended to include the full real axis, passing the poles on the right side, see fig. 1.1.

In eq. (1.20), it is still cumbersome to remember the different integration contours of fig. 1.1. They can be enforced by introducing an infinitesimal $\epsilon > 0$ and using

$$\tilde{W}^{(2)}(\underline{z}) = \lim_{\epsilon \to 0} \mathrm{sgn}(z^0) \int \frac{\mathrm{d}^4 \underline{k}}{(2\pi)^4} \frac{i}{\underline{k}^2 - m^2 + \mathrm{sgn}(z^0) i\epsilon} e^{-i\underline{k}\underline{z}}. \tag{1.21}$$

In this case, no information about the integration contour of k^0 needs to be provided, see fig. 1.2: It extends along the real axis and it is closed either above or below, depending on the sign of z^0, such that $e^{-i\underline{k}\underline{z}}$ decays on the semi-circle for $|\Im p^0| \to \infty$. This setup is called *$i\epsilon$-prescription.*

The Wightman functions have a straightforward relation to the field operators ϕ, but for the computation of physical observables, the *time-ordered correlation functions* are more relevant [49–52].

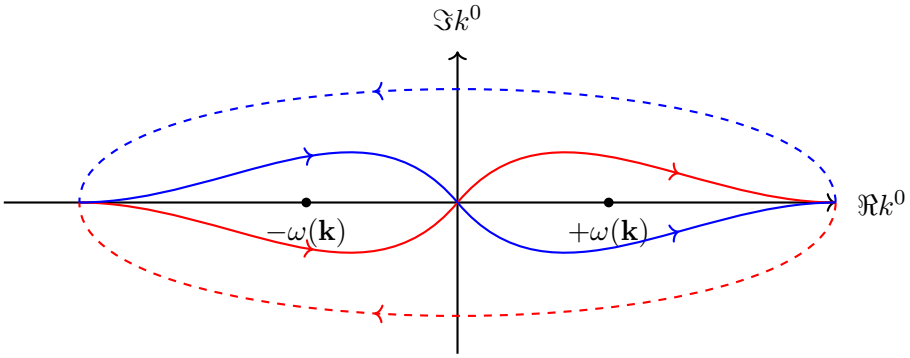

Figure 1.1.: Integration contour for the Wightman propagator for $z^0 > 0$ (red) and $z^0 < 0$ (blue). In both cases, the integral runs along the real line in positive direction $\rightarrow$ and it encloses only the right pole.

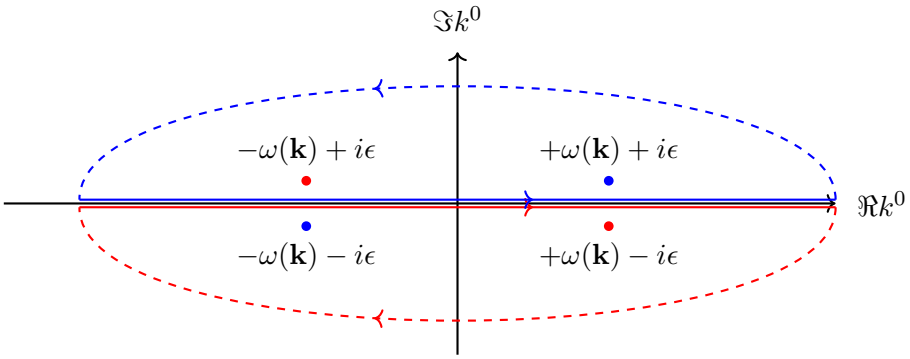

Figure 1.2.: Poles of eq. (1.21). For $z^0 > 0$ (red), the integral needs to be closed on the negative imaginary k^0-plane to make $e^{-ik^0 z^0}$ decay. In that case, only the right pole (red) is enclosed. Analogously for $z^0 < 0$ (blue), again only the right pole is enclosed.

Definition 14. The (not necessarily connected,) time-ordered *n-point functions*, or *Green functions*, are the correlation functions of n field operators,

$$\tilde{G}^{(n)}(\underline{x}_1, \ldots, \underline{x}_n) := \langle 0 | T\left(\phi(\underline{x}_1) \cdots \phi(\underline{x}_n)\right) | 0 \rangle.$$

Here, the operator T switches the order of its arguments such that the factors are sorted with respect to the time coordinate x^0, where the largest time stands to the left. We write $G_F^{(n)}$ if ϕ is a free field, and $G^{(n)}$ for interacting fields.

Definition 15. The *Feynman propagator* is the time-ordered 2-point Green function (def. 14) of a free field. By Lorentz covariance, it depends only on the difference of its two arguments,

$$G_F(\underline{x}_1 - \underline{x}_2) = G_F(\underline{x}_1, \underline{x}_2) := \tilde{G}^{(2)}(\underline{x}_1, \underline{x}_2) - \tilde{G}^{(1)}(\underline{x}_1)\tilde{G}^{(1)}(\underline{x}_2).$$

We have included the subtraction of 1-point-functions for completeness, this qualifies G_F as the *connected* 2-point function (def. 20). Within our setup, this makes no difference because the second summand vanishes thanks to eq. (1.18). The Feynman propagator (def. 15) is related to the Wightman propagator (def. 13) by

$$G_F(\underline{x}_1, \underline{x}_2) = G_F(\underline{z}) = \begin{cases} W^{(2)}(\underline{z}), & z^0 > 0 \\ W^{(2)}(-\underline{z}), & z^0 < 0. \end{cases} \tag{1.22}$$

An inspection of eq. (1.21) shows that eq. (1.22) amounts to taking the right pole for $z^0 > 0$ and the left one for $z^0 < 0$ in fig. 1.2. That can be achieved by leaving out the factors $\operatorname{sgn}(z^0)$ in the $i\epsilon$-prescription eq. (1.21). The Feynman propagator is given by

$$G_F(\underline{z}) = \int \frac{\mathrm{d}^D \underline{k}}{(2\pi)^D} \frac{i}{\underline{k}^2 - m^2 + i\epsilon} e^{-i\underline{k}\underline{z}}. \tag{1.23}$$

Again, it is automatic on which side to close the contour, as shown in fig. 1.3. This integral is a Fourier transform, we read off the Feynman propagator in momentum space:

$$G_F(\underline{p}) = \frac{i}{\underline{p}^2 - m^2 + i\epsilon} = \frac{i}{s_p + i\epsilon} =: \frac{i}{s_p} \tag{1.24}$$

In the last equation, we used the offshell variable s_p (def. 8). From now on, the summand $+i\epsilon$ is always implied, even if we do not write it explicitly.

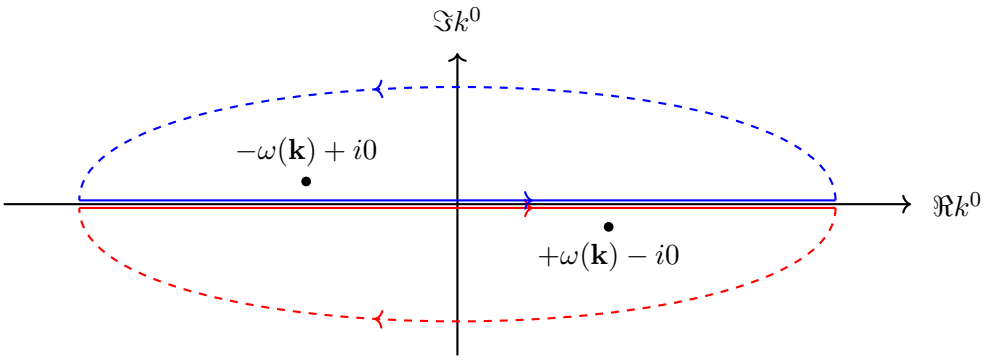

Figure 1.3.: Integration path of the Feynman propagator (def. 15) in the complex k^0-plane for $z^0 > 0$ (red) and $z^0 < 0$ (blue).

From the momentum-space representation eq. (1.24), it follows that the Feynman propagator is a Green function of the Klein-Gordon equation, that is, it fulfils

$$\left(\partial_\mu \partial^\mu + m^2\right) G_F(\underline{z}) = -i\delta(\underline{z}). \tag{1.25}$$

This explains the name *propagator*: it describes how the field at $\underline{z}$ reacts to a point-like "source" at $\underline{0}$. The poles in the propagator are the eigenvalues of the time-evolution (eq. (1.16)), even if we were to set up a free quantum field on more exotic timelike hypersurfaces [53]. All other possible combinations of signs for $i\epsilon$ in eqs. (1.21) and (1.24) amount to solutions of eq. (1.25), which differ only in the boundary conditions.

Using the Fourier transforms given in eq. (1.2), we can solve the integral eq. (1.23) for the massless Feynman propagator in position space, and obtain

$$G_F(\underline{x}) = \frac{\Gamma\left(\frac{D}{2}\right)}{4\pi^{\frac{D}{2}}} \frac{i}{(\underline{x}^2)^{\frac{D}{2}-1}}. \tag{1.26}$$

For the massive field, the Feynman propagator in position space is given by Bessel functions, for example in four spacetime dimensions [54, p. 30]

$$G_F(\underline{x}) = \frac{m}{4\pi^2} \begin{cases} \frac{1}{\sqrt{\underline{x}^2}} \frac{i\pi}{2} H_1^{(1)}\left(m\sqrt{\underline{x}^2}\right), & \underline{x}^2 > 0 \\ \frac{1}{\sqrt{-\underline{x}^2}} K_1\left(m\sqrt{-\underline{x}^2}\right), & \underline{x}^2 < 0. \end{cases} \tag{1.27}$$

Both the massive and the massless propagator scale like $(\underline{x}^2)^{-1}$ in the limit $\underline{x}^2 \to 0^+$. This seemingly mundane statement has profound consequences for the theory of renormalization, see section 2.3.1: For the high-energy behaviour of a quantum field theory, it is largely irrelevant if the involved quanta are massive or not.

Finally, we want to mention a remarkable result from axiomatic QFT, underlining the conceptual importance of particularly the 2-point functions:

Theorem 1 (Jost-Schroer-Federbush-Johnson-Pohlmeyer [55–57])**.** If the 2-point Wightman distribution $W^{(2)}$ of a quantum field theory equals that of a free quantum field theory with mass $m \geq 0$, then the theory in question is a free theory of that mass.

1.2.4. n-point correlation functions of the free field

To compute the time-ordered correlation functions (def. 14) of ($n > 2$) factors of the free quantum field, we split the field eq. (1.14) into positive and negative frequency solutions, $\phi(\underline{x}) = \phi^-(\underline{x}) + \phi^+(\underline{x})$, where

$$\phi^-(\underline{x}) := \int \frac{\mathrm{d}^3\mathbf{p}}{(2\pi)^3} \frac{1}{2\omega(\mathbf{p})} a^\dagger(\mathbf{p}) e^{i\underline{p}\underline{x}}, \qquad \phi^+(\underline{x}) := \int \frac{\mathrm{d}^3\mathbf{p}}{(2\pi)^3} \frac{1}{2\omega(\mathbf{p})} a(\mathbf{p}) e^{-i\underline{p}\underline{x}}.$$

Definition 16. A product of quantum field operators is *normal ordered* if all annihilation operators appear to the right of all creation operators. It is denoted $:\phi(\underline{x}_1)\cdots\phi(\underline{x}_n):$.

By eq. (1.17), the vacuum expecation value of any normal ordered product vanishes. An explicit calculation shows that

$$T\left(\phi(\underline{x})\phi(\underline{y})\right) =: \phi(\underline{x})\phi(\underline{y}) : + \begin{cases} [\phi^+(\underline{x}), \phi^-(\underline{y})], & x^0 > y^0 \\ [\phi^+(\underline{y}), \phi^-(\underline{x})], & x^0 < y^0. \end{cases} =: \phi(\underline{x})\phi(\underline{y}) : + \overbrace{\phi(\underline{x})\phi(\underline{y})} \tag{1.28}$$

We have defined the contraction $\overbrace{\phi\phi}$ as a shorthand for the conditional commutator expression. Taking the vacuum expectation value, the left hand side by def. 14 equals the Feynman propagator, while the normal ordered product vanishes. Consequently $\langle 0|\overbrace{\phi(\underline{x})\phi(\underline{y})}|0\rangle = G_F(\underline{x}, \underline{y})$. By induction, any time-ordered product can be expanded into a sum where each term is a product of normal-ordered and pairwise contracted factors like in eq. (1.28).

Theorem 2 (Wick [58])**.** For a free scalar quantum field ϕ, the time-ordered (def. 14) and normal ordered (def. 16) products of fields fulfil

(1) $T\left(\phi(\underline{x}_1)\cdots\phi(\underline{x}_n)\right) = :\phi(\underline{x}_1)\cdot\phi(\underline{x}_n): +$ sum of all contractions

(2) $\tilde{G}_F^{(n)} = \langle 0|T\left(\phi(\underline{x}_1)\cdots\phi(\underline{x}_n)\right)|0\rangle = \begin{cases} \text{sum of all complete contractions} & n \text{ even} \\ 0 & n \text{ odd.} \end{cases}$

Here, a *contraction* is a product of Feynman propagators (def. 15) between pairs of the spacetime points, where all remaining non-contracted field operators are normal ordered. A *complete contraction* is a product where all factors are contracted and no normal ordered factor prevails.

There is an obvious graphical notation for Wick's theorem: Any single contraction $\overbrace{\phi(\underline{x}_1)\phi(\underline{x}_2)}$ involves precisely two distinct points in spacetime, hence, it can be drawn as a line joining the points $\underline{x}_1$ and $\underline{x}_2$. Wick's theorem then states that the n-point function will be the sum of all ways of joining the n distinct points pairwise with edges.

Example 9: Free scalar field, Four-point function.

Let $\phi(\underline{x}_j) =: \phi_j$, then

$$\begin{aligned} T\left(\phi_1\phi_2\phi_3\phi_4\right) =: \phi_1\phi_2\phi_3\phi_4 : \quad &+ :\phi_1\phi_2:\overbrace{\phi_3\phi_4} + 5 \text{ similar terms} \\ &+ \overbrace{\phi_1\phi_2}\overbrace{\phi_3\phi_4} + \overbrace{\phi_1\overbrace{\phi_2\phi_3}\phi_4} + \overbrace{\phi_1\overbrace{\phi_2\phi_3}\overbrace{\phi_4}}, \\ \tilde{G}_F^{(n)} &= \langle 0|T\left(\phi_1\phi_2\phi_3\phi_4\right)|0\rangle \\ &= G_F(\underline{x}_1,\underline{x}_2)G_F(\underline{x}_3,\underline{x}_4) + G_F(\underline{x}_1,\underline{x}_3)G_F(\underline{x}_2,\underline{x}_4) + G_F(\underline{x}_1,\underline{x}_4)G_F(\underline{x}_2,\underline{x}_3). \end{aligned}$$

Denoting the spacetime points as points in a plane, the 4-point function of the free field has the following graphical representation:

$\tilde{G}_F^{(4)} = \langle 0|T\left(\phi_1\phi_2\phi_3\phi_4\right)|0\rangle =$

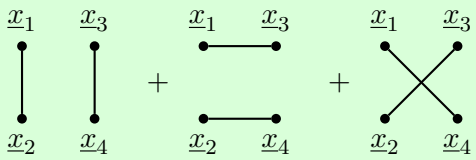

Clearly, the n-point functions vanish for odd n: There is no way to connect an odd number of points into pairs.

We often encounter symmetric sums over all permutations of certain terms, therefore we introduce a shorthand notation:

Definition 17. Let $f(x_1,\ldots,x_n)$ be a function of $n \in \mathbb{N}$ arguments. The expression $\langle k\rangle f(x_1,x_2,\ldots,x_n)$ denotes the sum over all $k \in N$ different permutations of arguments in the function $f(x_1,\ldots,x_n)$.

Example 10: Permutations of four-point amplitude.

The four-point amplitude from example 9 is the sum over three permutations (def. 17),

$$\tilde{G}_F^{(4)}(\underline{x}_1, \underline{x}_2, \underline{x}_3, \underline{x}_4) = \langle 3 \rangle \, G_F(\underline{x}_1, \underline{x}_2) G_F(\underline{x}_3, \underline{x}_4).$$

In this notation, we assumed the known symmetry $G_F(\underline{x}_1, \underline{x}_2) = G_F(\underline{x}_2, \underline{x}_1)$ of the Feynman propagator eq. (1.23).

The derivation of Wick's theorem made use of operator identities in QFT, but there is an entirely different perspective, concerning multivariate normal distributions [17]:

Theorem 3 (Isserlis [59])**.** Let $x_1, \ldots, x_n$ be independent normal distributed with zero mean, $\mathbb{E}(x_j) = 0 \; \forall j$. Let $\mathcal{P}$ be the set of all partitions of $\{1, \ldots, n\}$ into pairs, then

$$\mathbb{E}\left(x_1 \cdots x_n\right) = \sum_{p \in \mathcal{P}} \prod_{\{j,k\} \in p} \mathbb{E}\left(x_j x_k\right).$$

A normal distribution is the ground state wave function of a quantum-mechanical harmonic oscillator. In this sense, a free quantum field can be thought of as an infinite collection of uncoupled harmonic oscillators.

We remark that, instead of using $\tilde{G}^{(n)}$ (def. 14), one can formulate perturbative QFT in terms of $W^{(n)}$ (def. 13) [60]. This was originally proposed by Schwinger [61–63], but it involves rather intransparent nested commutators. Feynman's and Dyson's formulation entirely in terms of $\tilde{G}^{(n)}$, see e.g. [64], avoids this problem. Still, an analysis of the relationship between $\tilde{G}^{(n)}$ and $W^{(n)}$ is fruitful even if one is eventually only interested in $\tilde{G}^{(n)}$, because it reveals certain analytic properties of $\tilde{G}^{(n)}$, compare section 1.2.8.

1.2.5. The S-matrix

For an interacting theory, it is useful to introduce the notion of *scattering processes*. A scattering process amounts to a transition of the system from some *asymptotic state* Ψ_1 at the infinite past to some new asymptotic state Ψ_2 at the infinite future, where we assume that interactions take place only in the intermediate process but not in the asymptotic states. Effectively, the asymptotic states are assumed to be states of a free field, which is sometimes called *adiabatic hypothesis*, see e.g. [65]. We do especially require that the asymptotic states are physically valid states of the system. That includes that the momenta of all particles are onshell (def. 8) and all symmetries of the system are satisfied.

The existence of asymptotic free states faces considerable mathematical obstacles known as *Haag's theorem* [42, 66]. For example, theorem 1 prevents any state of an interacting theory to truly propagate like a free field, because a theory with the propagator of a free field is a free theory altogether. These problems however have been circumvented by a more careful construction, known as *Haag-Ruelle theory* [67–69], which sharply distinguishes between states themselves being equal, and expectation values of certain operators being equal.

Moreover, the naive relationship between states of an interacting and a free quantum field theory also rises concerns from a philosophical perspective [70]: In an interacting theory, the

state generated by the field operators $\phi(\underline{x}_1)\phi(\underline{x}_2)|0\rangle$ will in general not have twice the energy of a single particle $\phi(\underline{x})|0\rangle$, therefore it is strictly no longer obvious in what sense this state is to be interpreted as "two quanta". We will however resort to the assumption that the asymptotic states resemble free quanta "close enough", especially, to be indistinguishable by real-world experiments, which can never measure the *complete* 2-point function or the *exact* energy of a state.

Definition 18. The *S-matrix* is the operator that takes the asymptotic initial state to the asymptotic final state,

$$\Psi_2 =: S\Psi_1.$$

The S-matrix becomes an actual (infinitely large) matrix [71] as soon as we define a basis for the space of asymptotic states. Each state contains a countable number of particles. For a fixed number n of particles, one can take any basis of the corresponding n-particle Hilbert space H_n, for example the states with well-defined onshell (def. 8) momenta. They can be written in terms of field operators in momentum space,

$$|0\rangle, \quad |\phi(\underline{k}_1)\rangle, \quad |\phi(\underline{k}_1)\phi(\underline{k}_2)\rangle, \quad \dots \qquad \text{where} \;\; s_{k_j} = 0 \;\forall j.$$

The space of asymptotic states is the direct sum $\bigoplus_{n=0}^{\infty} H_n$ of the n-particle Hilbert spaces, or equivalently the symmetric tensor algebra of H_1, this is a *Fock space* [72]. The S-matrix elements in momentum space are then given by expectation values of the form

$$\langle \phi(\underline{k}_1)\cdots\phi(\underline{k}_n)|S|\phi(\underline{k}_{n+1})\cdots\phi(\underline{k}_m)\rangle \qquad \text{where} \;\; s_{k_j} = 0 \;\forall j. \tag{1.29}$$

Similarly, matrix elements can be defined in position space. The *LSZ-formula* makes the link between the S-matrix (which is observed in scattering experiments) and the time-ordered Green functions.

Theorem 4 (Lehmann-Symanzik-Zimmermann formula [52])**.** The S-matrix element for a $2 \to 2$-scattering between particles with 4-momenta $\underline{p}_i$ and masses m_i is given by

$$\langle \phi(\underline{p}_1)\phi(\underline{p}_2)|S|\phi(\underline{p}_3)\phi(\underline{p}_4)\rangle \propto \int\cdots\int \mathrm{d}^D\underline{x}_1\cdots\mathrm{d}^D\underline{x}_4 \left[e^{i(\underline{p}_1\underline{x}_1+\underline{p}_2\underline{x}_2-\underline{p}_3\underline{x}_3-\underline{p}_4\underline{x}_4)} \left(\prod_{i=1}^{4}\left(\partial_{\mu,i}\partial^{\mu}_{,i}+m_i^2\right)\right)\tilde{G}^{(4)}(\underline{x}_1,\underline{x}_2,\underline{x}_3,\underline{x}_4)\right].$$

Here, $\partial_{\mu,i}$ is short for $\frac{\partial}{\partial x_i^{\mu}}$ and $\tilde{G}^{(4)}$ is the time-ordered Green function (def. 14) of the interacting field.

The prefactor is essentially a normalization factor for the wave functions. We will see in section 2.3.4 that this factor needs to be fixed by experiment. The LSZ-formula (theorem 4) can be generalized for more than four external particles by including additional terms for the new arguments $\underline{x}_j$.

Note that the only difference between incoming and outgoing particles is their sign in the exponential. If we flip all 4-momenta of outgoing particles $(\underline{p}_1, \underline{p}_2) \to (-\underline{p}_1, -\underline{p}_2)$, then

the formula becomes completely symmetric with respect to incoming and outgoing particles. From now on, we will count all external momenta of scattering processes as pointing towards the interaction.

The S-matrix elements eq. (1.29) are *onshell* by definition, whereas the time-ordered correlation functions $G^{(4)}(\underline{x}_1, \underline{x}_2, \underline{x}_3, \underline{x}_4)$ are not restricted. Their relationship in the LSZ-formula (theorem 4) becomes more clear if one considers the Green functions in momentum space:

$$G^{(4)}(\underline{p}_1, \underline{p}_2, \underline{p}_3, \underline{p}_4) := \int \cdots \int \mathrm{d}^D \underline{x}_1 \cdots \mathrm{d}^D \underline{x}_4 \; e^{-i(\underline{p}_1\underline{x}_1 + \underline{p}_2\underline{x}_2 + \underline{p}_3\underline{x}_3 + \underline{p}_4\underline{x}_4)} G^{(4)}(\underline{x}_1, \underline{x}_2, \underline{x}_3, \underline{x}_4).$$

Theorem 5 (LSZ formula in momentum space)**.** The S-matrix elements in momentum space are given, up to prefactors, by the *amputated* time-ordered Green functions def. 14 in momentum space, where *amputated* means that the 2-point function of external particles, including its quantum corrections, is to be left out.

$$\langle \phi(\underline{p}_1)\phi(\underline{p}_2)|S|\phi(\underline{p}_3)\phi(\underline{p}_4)\rangle \propto \left(\prod_{i=1}^{4} \left(\underline{p}_i^2 - m_i^2\right)\right) G^{(4)}\left(\underline{p}_1, \underline{p}_2, \underline{p}_3, \underline{p}_4\right).$$

The S-matrix elements computed by the LSZ theorem are not yet the total scattering cross sections observed in real-world experiments, but only *scattering amplitudes*. To obtain cross-sections, one first needs to square the amplitudes, and secondly, integrate over *phase space*, which is the space of all possible, but unobservable, configurations of the system. These can be angles or energies outside the range of the detector, unobserved types of particles, or integrals over energy-bins of a detector with limited resolution. The phase space integration is outside the scope of this work, even if it is closely related to the Feynman integrals in theorem 6 via *loop-tree duality* [73–78].

1.2.6. Perturbative computation of the S-matrix

The Lagrangian of an interacting field, eq. (1.5), gives rise to a Hamiltonian density (def. 9)

$$\mathcal{H} = \underbrace{\frac{1}{2}\pi^2(\underline{x}) + \frac{1}{2}\left(\nabla\phi(\underline{x})\right)^2 + \frac{1}{2}m^2\phi^2(\underline{x})}_{=:\mathcal{H}_0} + \underbrace{\sum_{n=3}^{\infty} \frac{\lambda_n}{n!}\phi^n(t, \mathbf{x})}_{=:\mathcal{H}_I}. \tag{1.30}$$

Here, we have separated the Hamiltonian $\mathcal{H}_0$ of the free field (example 8). Spatial integration leads to the Hamiltonian (def. 10)

$$H(t) = H_0(t) + \sum_{n=3}^{\infty} \int \mathrm{d}^{D-1}\mathbf{x} \; \frac{\lambda_n}{n!}\phi^n(t, \mathbf{x}) =: H_0(t) + H_I(t). \tag{1.31}$$

The sum of interaction terms constitutes the *interacting Hamiltonian* H_I. With this definition, we can formally separate the evolution of free fields, governed by H_0, from the interaction H_I which we will treat perturbatively. As remarked below eq. (1.16), the free fields $\phi(\underline{x})$ constructed via canonical quantization are in the Heisenberg picture of quantum mechanics, they are time-dependent operators acting on time-independent state vectors.

For interacting fields, we use the free field operators as basis vectors, governed again by the Heisenberg equation 1.16, where H_0 replaces H. Due to the presence of H_I in eq. (1.31), the state vectors, i.e. the coefficients of the expansion in free fields, are now time-dependent as well. Their time evolution is given by an unitary *time evolution operator*

$$|\Psi(t)\rangle = U(t, t_0)|\Psi(t_0)\rangle. \tag{1.32}$$

Concretely, the time evolution operator is given by the formal time-ordered exponential of the interaction Hamiltonian, called *Dyson Series* [64],

$$U(t, t_0) = T\left(\exp\left(-i\int_{t_0}^{t} \mathrm{d}\tau\ H_I(\tau)\right)\right). \tag{1.33}$$

Here, "formal" means that the exponential generates a series expansion and we make no claim about convergence, see section 2.1.1. To concretely compute $U(t, t_0)$, one expands the exponential and obtains a series of integrals over time-ordered products of the interacting Hamiltonian,

$$U(t, t_0) = \mathbb{1} + \sum_{k=1}^{\infty} \frac{(-i)^k}{k!} \int \cdots \int_{t_0}^{t} \mathrm{d}\tau_1 \cdots \mathrm{d}\tau_k\ T\left(H_I(\tau_1) \cdots H_I(\tau_k)\right).$$

The Hamiltonian eq. (1.31) is itself a spatial integral over the Hamiltonian density eq. (1.30), which in turn consists of powers of the field operators, hence

$$\begin{aligned} U(t, t_0) = \mathbb{1} + \sum_{k=1}^{\infty} \frac{(-i)^k}{k!} \int \cdots \int_{t_0}^{t} \mathrm{d}\tau_1 \cdots \mathrm{d}\tau_k \int \cdots \int_{-\infty}^{\infty} \mathrm{d}\mathbf{x}_1 \cdots \mathrm{d}\mathbf{x}_k \cdot \\ \cdot T\left(\left(\sum_{n_1=3}^{\infty} \frac{\lambda_{n_1}}{n_1!}\phi^{n_1}(\tau_1, \mathbf{x}_1)\right) \cdots \left(\sum_{n_k=3}^{\infty} \frac{\lambda_{n_k}}{n_k!}\phi^{n_k}(\tau_k, \mathbf{x}_k)\right)\right). \end{aligned}$$

The adiabatic hypothesis asserts that in the limit $t \to \infty, t_0 \to -\infty$, the states approach the states of a free field, and are hence time-independent. In this limit, the time evolution operator becomes the S-matrix,

$$S = \lim_{t\to\infty} \lim_{t_0\to-\infty} U(t, t_0). \tag{1.34}$$

Simultaneously, the combined integrals now run over all Mikowsky space for each of the spacetime points. Exchanging summation and time-ordering, we identify time-ordered n-point Green functions (def. 14) $\tilde{G}_F^{(n)}$ of a *free* field,

$$S = \mathbb{1} + \sum_{k=1}^{\infty} \frac{(-i)^k}{k!} \sum_{n_1=3}^{\infty} \frac{\lambda_{n_1}}{n_1!} \cdots \sum_{n_k=3}^{\infty} \frac{\lambda_{n_k}}{n_k!} \int \cdots \int \mathrm{d}\underline{x}_1 \cdots \mathrm{d}\underline{x}_k \cdot \tag{1.35}$$

$$\cdot\, \tilde{G}_F^{(n_1+\ldots+n_k)}(\underbrace{\underline{x}_1, \ldots \underline{x}_1}_{n_1 \text{ times}}, \ldots, \underbrace{\underline{x}_k, \ldots, \underline{x}_k}_{n_1 \text{ times}}). \tag{1.36}$$

One is interested in the time evolution from one concrete state to another one. Owing to the adiabatic hypothesis, these "external" states are free field states, hence generated by products of $\phi(\underline{x})$ operators. They can be included in the above derivation to obtain a series for arbitrary S-matrix elements (def. 18) in position space. One needs to divide by the vacuum S-matrix eq. (1.35) in order to normalise the result.

Theorem 6. For S-matrix (def. 18) elements in position space, the Dyson series takes the following form, where $G_F^{(n)}$ are the n-point time ordered Green functions of a free field (def. 14), given by theorem 2.

$$\langle \phi(\underline{z}_1)\cdots\phi(\underline{z}_j)|S|\phi(\underline{y}_1)\cdots\phi(\underline{y}_i)\rangle = \frac{1}{S}\sum_{k=1}^{\infty}\frac{(-i)^k}{k!}\sum_{n_1=3}^{\infty}\frac{\lambda_{n_1}}{n_1!}\cdots\sum_{n_k=3}^{\infty}\frac{\lambda_{n_k}}{n_k!}$$
$$\int\cdots\int \mathrm{d}\underline{x}_1\cdots\mathrm{d}\underline{x}_k \cdot G_F^{(j+n_1+\ldots+n_k+i)}\big(\underline{z}_1,\ldots,\underline{z}_j,\underbrace{\underline{x}_1,\ldots\underline{x}_1}_{n_k\text{ times}},\ldots,\underbrace{\underline{x}_k,\ldots,\underline{x}_k}_{n_1\text{ times}},\underline{y}_1,\ldots,\underline{y}_i\big).$$

Here, we have assumed that the initial and final states are not identical, so that the summand $\mathbb{1}$ in the numerator vanishes. The integrals appearing in theorem 6 are called *Feynman integrals*.

It appears at first that by the Dyson series (theorem 6), even the amplitudes of interacting QFT are reduced to free 2-point functions just as for the free field in Wick's theorem 2. But note two striking differences:

1. Wick's theorem involves only finitely many summands, whereas the Dyson series requires us to add up infinitely many terms.
2. In Wick's theorem, all we have to do is multiply known functions. For the Dyson series, we have to *integrate* such products. Compare also section 5.2.3.

1.2.7. The Path integral

Instead of canonical quantization as outlined in section 1.2.2, one can also use the *path integral* formalism [49, 51, 79, 80]. Here, the fundamental object is the path integral, which is a formal integral over all possible field configurations $\mathcal{D}\phi$, weighted with an imaginary Boltzmann factor of their respective classical action (def. 7):

$$Z[J] := \int \mathcal{D}\phi\; e^{iS[\phi]+i\int \mathrm{d}^D\underline{x}\; J(\underline{x})\phi(\underline{x})}. \tag{1.37}$$

We have introduced a *source field* $J(\underline{x})$ such that the functional derivative of $Z[J]$ with respect to $J(\underline{x})$ produces factors $\phi(\underline{x})$ in the path integral. Equivalently, eq. (1.37) can be interpreted as an infinite dimensional Fourier transform of the functional $e^{iS[\phi]}$ [81, Sec. 3.4].

The path integral is very much analogous to statistical mechanics. A Wick rotation to Euclidean spacetime eliminates the imaginary units and one recovers a partition function of a 4-dimensional statistical system [82, 83]. Just like in statistical physics, the vacuum expectation value of products of fields, that is, the correlation functions (def. 13), can be computed by including the corresponding terms into the integral and normalizing the result:

$$\begin{aligned}\langle 0|T\left(\phi(\underline{x}_1)\cdots\phi(\underline{x}_n)\right)|0\rangle &= \frac{\int\mathcal{D}\phi\;\phi(\underline{x}_1)\cdots\phi(\underline{x}_n)e^{iS[\phi]+i\int\mathrm{d}^D\underline{x}J(\underline{x})\phi(\underline{x})}\Big|_{J(\underline{x})\equiv 0}}{\int\mathcal{D}\phi\; e^{iS[\phi]+i\int\mathrm{d}^D\underline{x}J(\underline{x})\phi(\underline{x})}\Big|_{J(\underline{x})\equiv 0}} \\ &= \frac{(-i)^n}{Z[0]}\frac{\delta}{\delta J(\underline{x}_1)}\cdots\frac{\delta}{\delta J(\underline{x}_n)}Z[J]\Big|_{J(\underline{x})\equiv 0}.\end{aligned} \tag{1.38}$$

In the sense of eq. (1.38), $Z[J]$ is a *generating functional* of the time-ordered Green functions. The path integral framework does not have any notion of operator-valued distributions and therefore circumvents many of their conceptual problems (section 1.2.2). Also, it comes with a physical interpretation along the lines of "quantum field theory means summing over all possible fields, weighting them with their classical action". However, this view is deceptive: The path integral is a mathematically highly non-trivial object which can, in relevant cases, not be computed in any conventional sense. Also, the path integral is dominated entirely by non-continuous "trajectories" [84, 85], which have little in common with the classical "path of a particle".

The free part, analogous to eq. (1.30), of the path integral eq. (1.38) is a Gaussian integral which can be solved analytically. A series expansion in the coupling constants λ_n of the remaining interaction Lagrangian then leads to the same Feynman integrals and Feynman graphs as does canonical quantization in theorem 6. One even recovers the $i\epsilon$-prescription (eq. (1.21)) for the propagator from the path integral [86].

Conversely, knowing Feynman integrals as series coefficients, one can *define* the path integral as their formal generating functional, irrespective of convergence issues:

$$\sum_{n=0}^{\infty} \frac{1}{n!} i^n \langle T\left(\phi(\underline{x}_1) \cdots \phi(\underline{x}_n)\right)\rangle J(\underline{x}_1) \cdots J(\underline{x}_n) =: Z[J]. \tag{1.39}$$

In this sense, the path integral or the canonical quantization procedure are equivalent, and either one produces Feynman integrals (theorem 6) as a perturbation series. In section 1.3.11, we will motivate *Dyson-Schwinger equations* from perturbation theory, they can also be derived from the path integral (e.g. [24]), or one takes Dyson-Schwinger equations as primary objects and derives from them the perturbation series.

The pragmatic view in the present thesis will therefore be that Feynman integrals are the correct series coefficients of the S-matrix, irrespective of the mathematical truth of their derivation. This is in the spirit of 't Hooft and Veltman 1973 [86]:

> Whatever approach is used, the result is always that the S-matrix is expressed in terms of a certain set of Feynman diagrams. [...] The situation must be reversed: Diagrams form the basis from which everything must be derived. [...] Using diagrams as a starting point seems [...] to be a capitulation in the struggle to go beyond perturbation theory. It is unthinkable to accept as a final goal a perturbation theory, and it is not our purpose to forward such a notion. On the contrary, it becomes more and more clear that perturbation theory is a very useful device to discover equations and properties that may hold true even if the perturbation expansion fails.

As for the last sentence, much progress has been reached in the last 50 years in the framework of *resurgence*, which we comment on in section 2.1.2.

1.2.8. Digression: History and alternative ways to compute the S-matrix

We have seen in theorem 6 that we can compute the S-matrix as an infinite series of Feynman integrals. Following this approach naively, however, has shortcomings. Amongst them

1. The whole derivation was based on quantum field operators, whose physical significance is not completely clear, see section 1.2.2.
2. Feynman graphs are often divergent. This is for most of the physically relevant cases solved by *renormalization* (section 2.2).
3. The individual integrals are hard to solve and the number of Feynman integrals grows rapidly with rising order in the Dyson series (see section 6.2), or with rising number of external particles. The resulting functions are highly non-trivial.
4. The perturbation series diverges even if individual integrals are finite. It appears unclear what information it carries about the true, non-perturbative solution. This is to some extent solved by *resurgence* (section 2.1.2).

As an illustration for the third problem, take the anomalous magnetic momentum in QED, which, after decades of effort, is now computed perturbatively to 4^{th} (!) order [87] as

$$\frac{g}{\mu_{\text{B}}} = 1 + 0.5\left(\frac{\alpha}{\pi}\right) - 0.3285\left(\frac{\alpha}{\pi}\right)^2 + 1.181\left(\frac{\alpha}{\pi}\right)^3 - 1.912\left(\frac{\alpha}{\pi}\right)^4 + \dots.$$

The numerical coefficients are known to thousands of digits. At order 4, individual Feynman integrals take values in the 100s or 1000s. All these large numbers almost completely cancel, leaving the result -1.912. See also [88].

One possibility to, at least partially, overcome the computational problem 3. is the massive use of numerical calculations. Firstly, one can resort to numerical quadrature of Feynman integrals, compare for example section 6.2. Secondly, the framework of lattice QFT [89, 90] aims at an ab-initio simulation of quantum fields in a small, discretized region of Euclidean spacetime, where QFT essentially becomes statistical physics [83, 91].

An alternative approach to computing S-matrix element goes broadly by the name of (constructive/axiomatic) *S-matrix theory*. It consists of several different, closely related methods with the aim of establishing as many general properties as possible which a sensible S-matrix must fulfil. Trivial examples are Lorentz covariance and macroscopic conservation laws for charges and momentum. Another line of thought is the intuition that a scattering process of many particles with local interactions should decompose into "elementary" clusters in a consistent manner [92]. A more sophisticated examination concerns the analytic structure of scattering amplitudes. Being not based on QFT, analogous statements for the S-matrix exist, for example, in classical optics, where they relate scattering amplitudes to the optical resonances of a system [22, 93, 94].

The goal of constructive S-matrix theory is to establish sufficiently many conditions such that the whole S-matrix is fixed by them. In the early days of quantum field theory, the main motivation was to circumvent the technical and conceptual difficulties of canonical quantization outlined above. In the best case, constructive S-matrix theory would be able to replace quantum field theory altogether and produce all observables without any reference to an unobservable "microscopic" theory. This is in the spirit of Heisenberg's dictum [29] from 1920s quantum mechanics:

> Die anschauliche Deutung der Quantenmechanik ist bisher noch voll innerer Widersprüche, die sich im Kampf der Meinungen um Diskontinuumus- und Kontinuumstheorie, Korpuskeln und Wellen auswirken. Schon daraus möchte man schließen, daß eine Deutung der Quantenmechanik mit den gewohnten kinematischen und mechanischen Begriffen jedenfalls nicht möglich ist. Die Quantenmechanik war ja gerade aus dem Versuchen entstanden, mit jenen gewohnten kinematischen Begriffen zu brechen und an ihre Stelle Beziehnungen zwischen konreten experimentell gegebenen Zahlen zu setzen.

Heisenberg himself doubled down on this perspective in his introduction of the S-matrix [71], and it eventually lead to an understanding of *renormalization* (section 2.2). Interestingly, the same principle was also the crucial ingredient for the second revolution in 20^{th}-century physics, Einstein's general relativity [95]

> Eine Antwort auf diese Frage [das Mach'sche Paradox] kann nur dann als erkenntnistheoretisch befriedigend anerkannt werden, wenn die als Grund angegebene Sache eine *beobachtbare Erfahrungstatsache* ist; denn das Kausalitätsgesetz hat nur dann den Sinn einer Aussage über die Erfahrungswelt, wenn als Ursachen und Wirkungen letzten Endes nur *beobachtbare Tatsachen* auftreten.

In the 1960s, the technical problems 1. and 2. were largely sorted out for quantum electrodynamics, leading to Feynman integral calculations becoming a widely used tool in quantum field theory. In hindsight, Weinberg remarks about this period [96]

> One problem with the S-matrix program was in formulating what is meant by the analyticity of the S-matrix. What precisely are the analytic properties of a multi-particle S-matrix element? I don't think anyone ever knew. I certainly didn't know [...]. By the mid-1960's it was clear that S-matrix theory had failed in dealing with the one problem it had tried hardest to solve, that of pion–pion scattering.

By theorem 6, Feynman integrals are supposed to be summands of the S-matrix element and therefore they naturally inherit many of its analytic properties. Consequently, the approaches of axiomatic-constructive S-matrix theory and perturbative quantum field theory heavily informed each other. Notable outcomes of this interplay are, amongst others, the *Källen-Lehmann representation* of the 2-point function [97, 98], the Landau equations [99], *Cutkosky's theorem* [100–103], and a classification of particles and their propagators in terms of the Lorentz group [104–108]. The correspondence between Wightman functions (def. 13) and time-ordered Green functions (def. 14) noted in sections 1.2.3 and 1.2.4 gives rise to the *Steinman relations* [109, 110] for the latter. Expressing the Feynman propagator in terms of Wightman propagators is the starting point for the *cutting formula* [23, Sec 2]

The success of such analytic considerations in perturbation theory has been unbroken. Still today, extended and refined versions are routinely used in the computation of Feynman integrals, see for example [111–114]. The reader interested in historic anecdotes will also like [115]. Another aspect is to use analytic properties in order to restrict the class of functions appearing as solutions of certain Feynman integrals, and specify their properties and relations, e.g. [116–121]. These methods nowadays primarily attack the third problem above, the difficulty to solve individual Feynman integrals. They add to the vast amount of identities and methods to simplify Feynman integrals, for example [122–126].

Another modern branch of analytic methods goes by the label *on-shell methods*. It has proven especially valuable for amplitudes with complicated Lorentz structure. These are notably QCD amplitudes with many external particles, see for example [127–134], and theories with higher spin [135–138].

But even after decades of successful perturbative QFT, the second original motivation for S-matrix theory is still relevant, namely the computation of scattering amplitudes when the microscopic theory is not understood. This applies to quantum gravity, which so far resisted every attempt to be described by a convincing quantum field theory, see section 5.2.1. Still, it is possible to deduce many features of the graviton-scattering S-matrix from general considerations without knowing the microscopic theory, e.g. [117, 139–146]. Conversely, there are dozens of hypothetical microscopic explanations for quantum gravity, ranging from string theory [147–149] over causal dynamic triangulation [150, 151] to causal fermionic systems [152]. For these approaches, S-matrix theory can be a guideline and criterion to check their predictions for plausibility.

Summary of section 1.2.

1. One can construct quantum field theory "by analogy" (section 1.2.2) to classical field theory (section 1.2.1).
2. We have discussed in detail the 2-point functions of a free quantum field (section 1.2.3) and how they determine all n-point functions via Wick's theorem (2).
3. All information about an interacting quantum field theory is encoded in its S-matrix (section 1.2.5), which can be computed perturbatively with the Dyson series (theorem 6) in terms of Feynman integrals.
4. The path integral provides another way to define a QFT, leading to the same Feynman integrals as a perturbative solution (section 1.2.7).
5. A brute-force computation of Feynman integrals is inefficient, and there are numerous advanced tricks for improvement. Moreover, there are approaches to QFT which do not involve Feynman integrals at all (section 1.2.8).

1.3. Feynman graphs

In this section, we discuss several properties of the Feynman graphs which appear as a graphical notation of the perturbative solution to a QFT.

1.3.1. Graphical representation of Feynman integrals

The correlation functions of the interacting theory are, by the Dyson series theorem 6, expressed in terms of *Feynman integrals* over products of propagators (def. 15). These integrals inherit the graphical notation of Wick's theorem, introduced in section 1.2.4, we obtain *Feynman graphs* [50].

From theorem 6 we learn that these graphs can involve vertices of valence k if and only if the Lagrangian (eq. (1.5)) contains an interaction term $\frac{-\lambda_k}{k!}\phi^k$. To compute the interacting $G^{(n)}$, we need to sum over all possible graphs which have exactly n external 1-valent vertices, but arbitrarily many internal ones. The vacuum S-matrix (eq. (1.35)) amounts to the sum over all graphs without external vertices. Dividing through S in theorem 6 entails that we can leave out all graphs which are disconnected from all of the external points of $G^{(n)}$. Eventually, the Dyson series (theorem 6) takes the form

$$\tilde{G}^{(n)}(\underline{x}_1, \dots, \underline{x}_n) = \sum_{\Gamma \in \tilde{\Gamma}^{(n)}} \mathrm{sym}(\Gamma) \cdot \mathcal{F}[\Gamma](\underline{x}_1, \dots, \underline{x}_n). \tag{1.40}$$

Here, $\tilde{\Gamma}^{(n)}$ is the set of all graphs with n external vertices corresponding to the points $\underline{x}_1, \dots, \underline{z}_n$. We have absorbed all combinatorial prefactors into the *symmetry factor* $\mathrm{sym}(\Gamma)$ which is discussed in section 1.3.8. All integrals and coupling constants are absorbed into the *Feynman rules* $\mathcal{F}(\Gamma)$, to be discussed in section 1.3.5. The graphs in $\bar{\Gamma}^{(n)}$ have at most n components.

In the Feynman integral, two spacetime points $\underline{x}, \underline{y}$ are joined by a propagator $G_F(\underline{x}, \underline{y})$ if and only if there is an edge between the two vertices representing $\underline{x}$ and $\underline{y}$ in the corresponding Feynman graph. Conversely, if a graph Γ has two connected (def. 22) components $\Gamma = \gamma_1 \cup \gamma_2$, that is two subgraphs which are not connected to each other, then the corresponding variables in the Feynman integral are independent.

$$\Gamma = \gamma_1 \cup \gamma_2, \gamma_1 \cap \gamma_2 = \emptyset \quad \Rightarrow \quad \mathcal{F}[\Gamma] = \mathcal{F}[\gamma_1] \cdot \mathcal{F}[\gamma_2]. \tag{1.41}$$

Definition 19. The *connected combinatorial Green function* $\bar{\Gamma}^{(n)}$ is the set of all connected (def. 22) Feynman graphs with n external edges, including their symmetry factor (theorem 13) and powers of coupling constants.

Definition 20. The *connected analytic Green function* $\bar{G}^{(n)}$ is the restriction of the analytic Green function eq. (1.40) to only connected graphs (def. 19), namely $\bar{G}^{(n)} = \sum_{\Gamma \in \bar{\Gamma}^{(n)}} \mathcal{F}(\Gamma)$.

Equivalently, the connected Green function $\bar{G}^{(n)}$ arises from the non-connected Green functions $\tilde{G}^{(n)}$ (def. 14) by subtraction of all products of smaller valence,

$$\bar{G}^{(1)}(\underline{x}) = \tilde{G}^{(1)}(\underline{x}), \qquad \bar{G}^{(2)}(\underline{x}_1, \underline{x}_2) = \tilde{G}^{(2)}(\underline{x}_1, \underline{x}_2) - \tilde{G}^{(1)}(\underline{x}_1)\tilde{G}^{(1)}(\underline{x}_2)$$
$$\bar{G}^{(3)}(\underline{x}_1, \underline{x}_2, \underline{x}_3) = \tilde{G}^{(3)}(\underline{x}_1, \underline{x}_2, \underline{x}_3) - \langle 3 \rangle \cdot \tilde{G}^{(2)}\tilde{G}^{(1)} - \tilde{G}^{(1)}(\underline{x}_1)\tilde{G}^{(1)}(\underline{x}_2)\tilde{G}^{(1)}(\underline{x}_3), \qquad \dots.$$

Here, $\langle 3 \rangle$ denotes permutations (def. 17). In terms of generating functionals, the relationship between $\bar{G}$ and $\tilde{G}$ is that of exponentiation or logarithm. If $Z[J]$ is the generating series of all Green functions (eq. (1.39)), then the connected Green functions are generated by $\ln Z[J] =: W[J]$ [83, 153]. Finally, we generally exclude all graphs which contain self-loops, or tadpoles (def. 29). A more detailed account of this decision will be given in section 5.1.4.

Example 11: ϕ^3 theory, connected Feynman graphs.

Consider the connected 2-point graphs (def. 19) of ϕ^3 theory (example 3). There is a single graph without loops, namely an edge. Next there is one 1-loop graph, the 1-loop multiedge. At two loops, there are already four graphs. In this example, we write the coupling constants as explicit prefactors, they can alternatively be included into the definition of the graphs.

$\bar{\Gamma}^{(2)} =$ 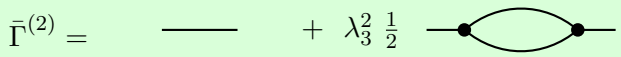 $+ \lambda_3^2 \frac{1}{2}$

$+\lambda_3^4 \Big(\frac{1}{4}$ 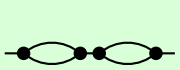 $+ \frac{1}{2}$ 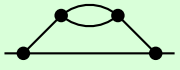 $+ \frac{1}{2}$ 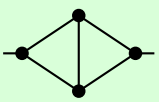 $\Big) + \dots$

There are infinitely many more graphs contributing to $\bar{\Gamma}^{(2)}$. Similarly, $\bar{\Gamma}^{(3)}$ starts with

$\bar{\Gamma}^{(3)} =$ λ_3  $+ \lambda_3^3 \Big($ 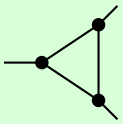 $+ \langle 3 \rangle \frac{1}{2}$ 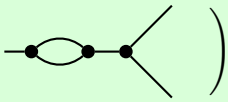 $\Big)$

$+\lambda_3^5 \langle 3 \rangle \Big(\frac{1}{2}$ 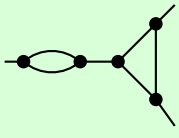 $+ \frac{1}{2}$ 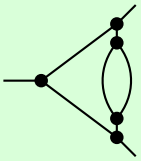 $+$ 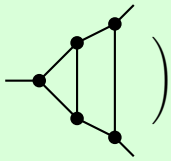 $\Big) + \lambda_3^5 \frac{1}{2}$ 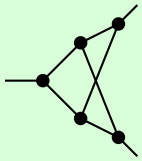 $+ \dots$

The factor $\langle 3 \rangle$ means that these graphs can be oriented in 3 different ways (def. 17). The very last graph is symmetric under exchange of the three external edges and does not obtain a factor $\langle 3 \rangle$. Altogether, there are 15 different connected graphs contributing up to loop number 2.

1.3.2. Basic definitions

Definition 21. An *un-amputated Feynman graph* Γ is a graph given by disjoint vertex sets $(V_\Gamma, V_{\Gamma,\text{ext}})$ and edge sets $(E_\Gamma, E_{\Gamma,\text{ext}})$ where

1. V_Γ are called *internal vertices* of Γ. The valence (def. 23) of them is at least 3.
2. $V_{\Gamma,\text{ext}}$ are called *external vertices* of Γ. They have valence 1.
3. E_Γ are the *internal edges* of Γ. An edge $e \in E_\Gamma$ is an ordered pair $e = \{v_1, v_2\}$ where both $v_j \in V_\Gamma$.
4. $E_{\Gamma,\text{ext}}$ are the *external edges* of Γ. An edge $e \in E_{\Gamma,\text{ext}}$ is an ordered pair $e = \{v_1, v_2\}$ where $v_1 \in V_\Gamma$ and $v_2 \in V_{\Gamma,\text{ext}}$.
5. Every edge comes with a *mass* $0 \leq m_e \in \mathbb{R}$ and a power $\nu_e \in \mathbb{R}$ and a 4-momentum $\underline{k}_e$. Unless otherwise specified, we will assume that $\nu_e = 1$.

This definition allows for *multigraphs*, that is, graphs with multiple parallel edges between the same two vertices. Also, the two end-vertices of an internal edge can be the same vertex, which is called *tadpole* in physics and *loop* in mathematics (not to be confused with *loop* in the physical nomenclature, def. 28). Further, def. 21 is a *directed* graph which is not strictly necessary for a scalar theory since the scalar Feynman propagator eq. (1.23) is symmetric with respect to exchanged arguments. However, we will use the direction of edges to fix the direction of the edge-momentum $\underline{k}_e$.

Moreover, a Feynman graph according to def. 21 need not be connected.

Definition 22. A graph is *connected* if for any two vertices, there is a path of edges to go from the first vertex to the second one. A *connected component* $\gamma \subset \Gamma$ is a connected graph γ that is not connected to the remainder $\Gamma \setminus \gamma$.

Definition 23. The *valence* (=degree) of a vertex is the number of edges incident to it. A graph is j-regular if and only if all its vertices have valence j.

Thanks to the LSZ formula (theorem 5), we will mostly be working with amputated graphs.

Definition 24. An (amputated) *Feynman graph* Γ, derived from a non-amputated Feynman graph Γ' (def. 21), is a graph given by disjoint vertex sets, $V_\Gamma = V_{\Gamma,\text{int}} \cup V_{\Gamma,\text{ext}}$ and an edge set E_Γ where

1. $V_{\Gamma,\text{ext}}$ are called *external vertices* of Γ. They have valence at least 2. These are the vertices $v \in V_{\Gamma'}$ that used to be connected to external edges of Γ'. Especially, $V_{\Gamma,\text{ext}} \subseteq V_{\Gamma'}$ and $V_{\Gamma,\text{ext}} \nsubseteq V_{\Gamma',\text{ext}}$.
2. $V_{\Gamma,\text{int}}$ are called *internal vertices* of Γ. Their valence is at least 3. In Γ', they were not adjacent to any external edge.

3. The edges $E_\Gamma = E_{\Gamma'}$ are the *internal edges* of Γ'.

4. To every edge $e \in E_\Gamma$ we assign a *mass* $0 \leq m_e \in \mathbb{R}$ and a power $\nu_e \in \mathbb{R}$ and a 4-momentum $\underline{k}_e$. Unless otherwise specified, we will assume that $\nu_e = 1$.

The information about which vertices are external and internal is not trivial, it can in general not be reconstructed from (a drawing of) the graph Γ alone without knowing the underlying Γ'. If we know that Γ' is j-regular (def. 23) then those vertices $v \in \Gamma$ with valence lower than j are exactly the ones where, in Γ', external edges used to be attached.

Definition 25. A *subgraph* $\gamma \subseteq \Gamma$ of a Feynman graph Γ (def. 24) is a Feynman graph such that $E_\gamma \subseteq E_\Gamma$ and γ contains all the vertices adjacent to any edges $e \in E_\gamma$. That is, γ may contain disconnected (def. 22) vertices, but no edges without their end vertices.

Definition 26. The *residue* $\mathrm{res}(\Gamma)$ of an unamputated Feynman graph Γ (def. 21) is the product of its external edges, $\mathrm{res}(\Gamma) = \prod_{e \in E_{\Gamma,\mathrm{ext}}} e$. Especially, the residue of a single vertex is the product of edges adjacent to it.

The physical interpretation of Feynman graphs is that each edge represents a field variable. In that case, the residue is a monomial in the field variables.

Definition 27. Let $\gamma \subset \Gamma$ be a proper subgraph (def. 25) of a Feynman graph Γ. The *contracted graph* $\frac{\Gamma}{\gamma}$ is the graph Γ, but every connected component of γ is replaced by its residue, that is, by a single vertex.

Example 12: Dunce's cap.

Traditionally, one chooses as an example the following Feynman graph, known as the *dunce's cap*:

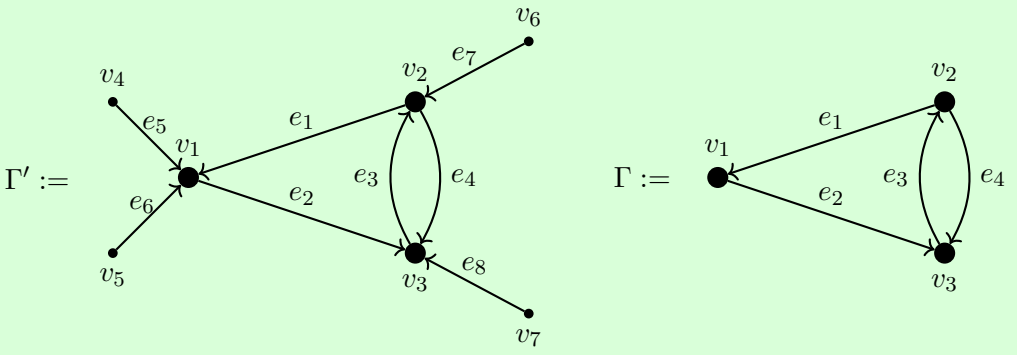

Here Γ' is the graph including external vertices and external edges (def. 21), while in Γ, the external edges have been amputated (def. 24), following theorem 5.

For Γ', the internal vertices are $V_{\Gamma'} = \{v_1, v_2, v_3\}$ while the external vertices are $V_{\Gamma',\mathrm{ext}} = \{v_4, v_5, v_6, v_7\}$. Likewise, the internal edges are $E_{\Gamma'} = \{e_1, e_2, e_3, e_4\}$ and the external edges are $E_{\Gamma',\mathrm{ext}} = \{e_5, e_6, e_7, e_8\}$. This graph is 4-regular (def. 23), and it is connected (def. 22). The external edges are directed inwards by convention, the orientation of inner edges is fixed arbitrarily. Each edge represents the propagation of the same type of field ϕ, hence the residue (def. 26) of the unamputated graph is $\mathrm{res}(\Gamma') = |V_{\Gamma',\mathrm{ext}}| = \phi^4$.

In the amputated graph Γ, all three vertices are *external* vertices, $V_{\Gamma,\mathrm{ext}} = \{v_1, v_2, v_3\}$ since all of them used to be connected to an external edge prior to amputation. The residue of Γ is not well-defined, unless one specifies the valence of the external vertices. If we provide the information that the un-amputated graph is 4-regular (def. 26), then one can infer the amputated external edges and that $\mathrm{res}(\Gamma) = \phi^4$.

Definition 28. The *loops* L_Γ of a Feynman graph Γ (def. 24) are a basis of the graph's cycle space, that is, a choice of linearly independent closed paths. For a given graph Γ, this choice need not be unique. The *loop number* $|L_\Gamma|$ is the dimension of the cycle space, it is unique for a fixed Γ. In mathematical terminology, $|L_\Gamma| = b_1(\Gamma)$ is the first Betti number.

Definition 29. A *tadpole* is a Feynman graph γ that has one external edge. More generally, a tadpole $\gamma \subset \Gamma$ is a graph γ that is connected to the remainder $\Gamma \setminus \gamma$ by only a single vertex.

Theorem 7 (Euler's formula [154])**.** For a connected (def. 22) graph Γ, the number of edges $|E_\Gamma|$, vertices $|V_\Gamma|$ and loops $|L_\Gamma|$ are related by

$$|E_\Gamma| - |V_\Gamma| + 1 = |L_\Gamma| \,.$$

It is sometimes useful to rephrase Euler's formula in terms of the number of external edges $|E_{\Gamma,\mathrm{ext}}|$ and the number of j-valent vertices, n_j.

$$\sum_{j=3}^{\infty} (j-2)\, n_j = |E_{\Gamma,\mathrm{ext}}| - 2 + 2\,|L_\Gamma| \,. \tag{1.42}$$

Especially, if Γ is n-regular (def. 23) then $n_n = |V_\Gamma|$ and $n_{j\neq n} = 0$ and

$$(n-2)\,|V_\Gamma| = |E_{\Gamma,\mathrm{ext}}| - 2 + 2\,|L_\Gamma| \,, \qquad |E_{\Gamma,\mathrm{int}}| = \frac{|E_{\Gamma,\mathrm{ext}} - n|}{n-2} + \frac{n}{n-2}\,|L_\Gamma| \,. \tag{1.43}$$

Example 13: Dunce's cap, loops.

A possible choice of loops (def. 28) for the dunce's cap (example 12) is

$$L_{\Gamma'} = \{\{e_1, e_2, -e_4\}, \{e_3, e_4\}\}.$$

We have used different signs to account for the direction of edges along the loop. The dunce's cap has loop number (def. 28) $|L'_\Gamma| = 2$. Euler's formula (theorem 7) is fulfilled: $8 - 7 + 1 = 2$. Since Γ' is 4-regular, eq. (1.43) holds: $(4-2)\cdot 3 = 6 = 4 - 2 + 2\cdot 2$.

The amputated graph Γ has the same set of loops and therefore still has loop number $|L_\Gamma| = 2$. Despite the missing edges, it still satisfies theorem 7: $4 - 3 + 1 = 2$.

1.3.3. Graph matrices

In order to handle larger graphs algorithmically, it is useful to express them not as a set of edges and vertices as in def. 24, but rather in terms of matrices, which encode these elements.

Definition 30. The *incidence matrix* I_Γ of a Feynman graph Γ (def. 24) is a $|E_\Gamma| \times |V_\Gamma|$ matrix whose entries correspond to edges $\{v_1, v_2\} = e \in E_\Gamma$ and vertices $v \in V_\Gamma$,

$$(I_\Gamma)_{e,v} := \begin{cases} 1 & v = v_1 \\ -1 & v = v_2 \\ 0 & \text{else.} \end{cases}$$

Definition 31. The undirected *adjacency matrix* A_Γ of a Feynman graph Γ (def. 24) is a $|V_\Gamma| \times |V_\Gamma|$ matrix where the entry $(A_\Gamma)_{i,j}$ is the number of edges – regardless of direction – between vertices v_i and v_j.

The transposed incidence matrix I_Γ^T defines a map $E_\Gamma \to V_\Gamma$ whose kernel is the cycle space (def. 28). Hence, by solving $I_\Gamma^T \vec{e} = \vec{0}$ for linearly independent vectors $\vec{e}$, we obtain a possible choice of loops, see example 14.

Definition 32. The undirected *degree matrix* D_Γ of a Feynman graph Γ (def. 24) is a $|V_\Gamma| \times |V_\Gamma|$ matrix where the entry $(D_\Gamma)_{i,i}$ is the valence (def. 23) of v_i, and $(D_\Gamma)_{i,j\neq i} = 0$.

Lemma 8 (e.g. [155])**.** Let I_Γ be the incidence matrix (def. 30), A_Γ the adjacency matrix (def. 31) and D_Γ the degree matrix (def. 32) of a graph Γ (def. 24). The following two expressions coincide, and they define the $|V_\Gamma| \times |V_\Gamma|$ *Laplace matrix* M_Γ:

$$M_\Gamma := I_\Gamma^T I_\Gamma = D_\Gamma - A_\Gamma.$$

There are straightforward generalizations of defs. 31 and 32 for directed multigraphs: For the adjacency matrix, let $(A_\Gamma)_{i,j}$ be the number of edges directed from i to j. A tadpole (def. 29) at v_i corresponds 1 to $(A_\Gamma)_{i,i}$. For the degree matrix, let $(D_\Gamma)_{i,i}$ be the number of directed edges entering v_i. For our applications, due to the use of scalar fields, it will be sufficient to consider undirected matrices.

Example 14: Dunce's cap, graph matrices.

Consider the dunce's cap from example 12. The incidence matrix of Γ' is

$$I_{\Gamma'} = \begin{pmatrix} -1 & 1 & 0 & 0 & 0 & 0 & 0 \\ 1 & 0 & -1 & 0 & 0 & 0 & 0 \\ 0 & -1 & 1 & 0 & 0 & 0 & 0 \\ 0 & 1 & -1 & 0 & 0 & 0 & 0 \\ 1 & 0 & 0 & -1 & 0 & 0 & 0 \\ 1 & 0 & 0 & 0 & -1 & 0 & 0 \\ 0 & 1 & 0 & 0 & 0 & -1 & 0 \\ 0 & 0 & 1 & 0 & 0 & 0 & -1 \end{pmatrix}$$

We note that the 4 external edges result in a 4×4 block identity matrix $-\mathbb{1}_{4\times 4} \subset I_\Gamma$. The incidence matrix of the amputated graph is the remainder after removing said block,

$$I_\Gamma = \begin{pmatrix} -1 & 1 & 0 \\ 1 & 0 & -1 \\ 0 & -1 & 1 \\ 0 & 1 & -1 \end{pmatrix}.$$

From this matrix, one obtains the loops (def. 28) with the simple calculation

$$I_\Gamma^T \vec{e} = \vec{0} \quad \Rightarrow \quad \vec{e} = (a, a, b, b-a), \quad a, b \in \mathbb{R}.$$

Choosing, for example, $a = 1$ and $b = 0$, we have $\vec{e} = (1, 1, 0, -1)$, which amounts to the loop $\{e_1, e_2, -e_4\}$. The choice $a = 0$ and $b = 1$ yields the loop $\{e_3, e_4\}$. This reproduces the loops from example 13. Note how the result respects the direction of edges in the loop.

The undirected adjacency matrix and degree matrix of Γ are

$$A_\Gamma = \begin{pmatrix} 0 & 1 & 1 \\ 1 & 0 & 2 \\ 1 & 2 & 0 \end{pmatrix}, \qquad D_\Gamma = \begin{pmatrix} 2 & 0 & 0 \\ 0 & 3 & 0 \\ 0 & 0 & 3 \end{pmatrix}.$$

The two matrices in lemma 8 coincide and give rise to the Laplace matrix

$$M_\Gamma = \begin{pmatrix} 2 & -1 & -1 \\ -1 & 3 & -2 \\ -1 & -2 & 3 \end{pmatrix}.$$

For comparison, the directed Laplace matrix (with directions as indicated in example 12) is

$$M_\Gamma = \begin{pmatrix} 1 & 0 & -1 \\ -1 & 1 & -1 \\ 0 & -1 & 2 \end{pmatrix}.$$

Definition 33.

1. A *tree* is a connected Feynman graph (def. 24) with zero loops (def. 28). Those trees which contribute to a given amplitude are called *treelevel graphs*.
2. A *j-forest* is a disjoint set of exactly j trees, that is, a Feynman graph with exactly j connected components and zero loops.

For a tree T, Euler's formula (theorem 7) specializes to

$$|V_T| = |E_T| + 1. \tag{1.44}$$

Lemma 9 (Cayley's formula, [156–158])**.**
There are $|V_T|^{|V_T|-2}$ labelled trees with distinguishable (=labelled) vertices.

Definition 34. Let Γ be a connected Feynman graph (def. 24).

1. A *spanning tree* of Γ is a connected subgraph $T \subseteq \Gamma$ (def. 25) such that T is a tree and $V_T = V_\Gamma, V_{T,\text{ext}} = V_{\Gamma,\text{ext}}$. By $T_\Gamma^{(1)}$ we denote the set of all spanning trees of Γ.
2. A *spanning j-forest* of a Feynman graph Γ is a subgraph $F \subseteq \Gamma$ (def. 25) such that F is a forest with exactly j components, and $V_F = V_\Gamma, V_{F,\text{ext}} = V_{\Gamma,\text{ext}}$. By $T_\Gamma^{(j)}$ we denote the set of all spanning j-forests of Γ.

Since our definition of Feynman graph (def. 24) is a directed graph, its spanning trees will be directed as well. Under the name *directed acyclic graphs*, directed trees are prominently used in blockchain technology [159].

Theorem 10 (Matrix tree theorem, Kirchhoff's theorem [156, 157, 160])**.** Let M_Γ be the Laplace matrix (def. 35) and let $M_\Gamma(i,j)$ be M_Γ where the row i and the column j are deleted. Then, $(-1)^{i+j} \det M_\Gamma(i,j)$ is the number of spanning trees in Γ, irrespective of the choice of (i,j).

If, instead, M_Γ is the directed Laplace matrix, then $\det M_\Gamma(i,i)$ is the number of directed spanning trees in Γ, originating from v_i.

There are numerous generalizations and alternative proofs of matrix tree theorems [161].

Example 15: Dunce's cap, trees.

For the dunce's cap example 12, we have

$$M_\Gamma(3,3) = \begin{pmatrix} 2 & -1 \\ -1 & 3 \end{pmatrix}, \qquad \det M_\Gamma(3,3) = 5,$$

indicating by theorem 10 that Γ has 5 different spanning trees. Explicitly, they are

$$T_\Gamma = \{\{e_1,e_2\},\{e_1,e_3\},\{e_1,e_4\},\{e_2,e_3\},\{e_2,e_4\}\}.$$

The cofactors of the directed Laplacian matrix (example 14) are

$$M_{\Gamma'}(1,1) = \begin{pmatrix} 1 & -1 \\ -1 & 2 \end{pmatrix}, \qquad M_{\Gamma'}(2,2) = \begin{pmatrix} 1 & -1 \\ 0 & 2 \end{pmatrix}, \qquad M_{\Gamma'}(3,3) = \begin{pmatrix} 1 & 0 \\ -1 & 1 \end{pmatrix}.$$

Consequently, there are $(1,2,1)$ oriented spanning trees starting at vertices (v_1,v_2,v_3),

$$(\{e_2,e_3\}, \quad \{\{e_1,e_2\},\{e_1,e_4\}, \quad \{e_1,e_3\}\}).$$

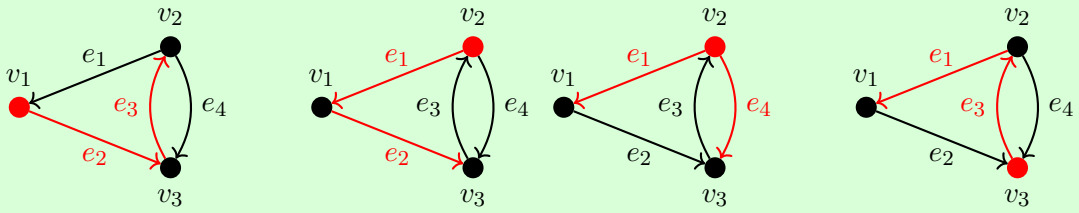

The spanning j-forests (def. 34) of the dunce's cap are

$$T_\Gamma^{(2)} = \{\{\{e_1\},\{v_3\}\},\{\{e_2\},\{v_2\}\},\{\{e_3\},\{v_1\}\},\{\{e_4\},\{v_1\}\}\}$$
$$T_\Gamma^{(3)} = \{\{\{v_1\},\{v_2\},\{v_3\}\}\}, \qquad T_\Gamma^{(j\geq 4)} = \emptyset.$$

1.3.4. Graph polynomials

It is possible to obtain even more information than the mere number of spanning trees from theorem 10. To this end, assign a formal variable a_e to each edge $e \in E_\Gamma$. Instead of re-defining all the above matrices (defs. 30 to 32), we directly give the Laplace matrix.

Definition 35. Let Γ be a Feynman graph (def. 24). The *(labelled) Laplace matrix* M_Γ is a $|V_\Gamma| \times |V_\Gamma|$-matrix with entries

$$(M_\Gamma)_{i,j} := \sum_e a_e, \text{ where } e \text{ joins } v_i \text{ with } v_j \text{ and } i \neq j,$$
$$(M_\Gamma)_{i,i} := -\sum_e a_e, \text{ where } e \text{ is incident to } v_i.$$

Theorem 11 (Labelled Kirchhoff's theorem)**.** Let Γ be a connected graph. Let M_Γ be the labelled Laplace matrix (def. 35) and $M_\Gamma(i,j)$ the same matrix with row i and column j deleted. Then, for every choice (i,j),

$$(-1)^{i+j} \det M_\Gamma(i,j) =: \tilde{\psi}_\Gamma(\{a_e\})$$

is the same polynomial in the edge variables $\{a_e\}$ called *Kirchhoff polynomial*. Every monomial in $\tilde{\psi}_\Gamma$ corresponds to a spanning tree (def. 34) of Γ,

$$\tilde{\psi}_\Gamma(\{a_e\}) = \sum_{T \in T_\Gamma^{(1)}} \prod_{e \in T} a_e.$$

Definition 36. Let Γ be a connected Feynman graph with amputated external edges. The *first Symanzik polynomial* ψ_Γ is defined to be the dual Kirchhoff polynomial (theorem 11),

$$\psi_\Gamma(\{a_e\}) := \tilde{\psi}_\Gamma\left(\left\{\frac{1}{a_e}\right\}\right) \cdot \prod_{e \in E_\Gamma} a_e = \sum_{T \in T_\Gamma^{(1)}} \prod_{e \notin T} a_e.$$

Intuitively, the polynomial is identical no matter which row and column (i,j) are deleted because each edge ends in two vertices. Therefore, knowing all but one vertices allows to reconstruct the missing information. If, however, a larger subset of the rows and columns is deleted, one obtains a different polynomial. These are the *Dodgson polynomials*, they are useful for a study of subgraphs of Feynman graphs, for example in [162, 163].

Example 16: Dunce's cap, first Symanzik polynomial.

For the dunce's cap (example 12) one finds the labelled Laplace matrix (def. 35)

$$M_\Gamma = \begin{pmatrix} -a_1 - a_2 & a_1 & a_2 \\ a_1 & -a_1 - a_3 - a_4 & a_3 + a_4 \\ a_2 & a_3 + a_4 & -a_2 - a_3 - a_4 \end{pmatrix}.$$

The Kirchhoff polynomial is

$$\begin{aligned} \tilde{\psi}_\Gamma = \det M_\Gamma(1,1) &= (a_1 + a_3 + a_4)(a_2 + a_3 + a_4) - (a_3 + a_4)(a_3 + a_4) \\ &= a_1a_2 + a_1a_3 + a_1a_4 + a_2a_3 + a_2a_4. \end{aligned}$$

The monomials exactly correspond to the spanning trees stated in example 15. Conversely, the first Symanzik polynomial (def. 36) is

$$\psi_\Gamma = a_3a_4 + a_2a_4 + a_2a_3 + a_1a_4 + a_1a_3.$$

In quantum field theory, there is a 4-momentum $\underline{k}_e$ associated to each edge. Take a spanning 2-forest $F = \{T_1, T_2\} \in T_\Gamma^{(2)}$ (def. 34). It divides the graph Γ into exactly two connected components. We consider the edges of Γ which lead from one component to the other,

$$C_F := \{e \in E_\Gamma | e = \{v_1, v_2\}, v_1 \in T_i, v_2 \in T_{j\neq i}\}.$$

Note that in general $C_F \neq \Gamma \setminus \{T_1 \cup T_2\}$. Now let

$$Q(F) := \sum_{e \in C_F} \bar{k}_e, \tag{1.45}$$

where $\bar{k}_e = \underline{k}_e$ if the edge e is directed from T_1 to T_2, and $\bar{\underline{k}_e} = -\underline{k}_e$ if e is directed from T_2 to T_1. Hence, $Q(F)$ is the total momentum flowing from the first component T_1 of the spanning forest F into the second component T_2. Due to momentum conservation in Feynman graphs, $Q(F)$ is at the same time the total external momentum entering T_1, or leaving T_2.

Definition 37. Let Γ be a connected amputated Feynman graph (def. 24). Let $Q(F)$ be defined as in eq. (1.45). The *second Symanzik polynomial* is given by

$$\phi_\Gamma := -\sum_{F \in T_\Gamma^{(2)}} Q(F)^2 \prod_{e \notin F} a_e + \psi_\Gamma \sum_{e \in E_\Gamma} m_e^2 a_e.$$

For more details and alternative definitions of the Symanzik polynomials, refer to [164].

Lemma 12.

1. The first Symanzik polynomial (def. 36) is homogeneous of degree $|L_\Gamma|$ (def. 28) in the variables $\{a_e\}$ and no a_e appears with higher than first power.
2. The second Symanzik polynomial (def. 37) is homogeneous of degree $|L_\Gamma| + 1$ in $\{a_e\}$.
3. The second Symanzik polynomial is homogeneous of degree two in masses and momenta.

Proof. By eq. (1.44), a spanning tree contains exactly $|V_\Gamma| - 1$ edges. Using theorem 7, the number of edges not in the spanning tree is $|E_\Gamma| - |V_\Gamma| + 1 = |L_\Gamma|$, the number of edges not in a spanning 2-forest is $|L_\Gamma| + 1$. The remaining points follow from the definitions. □

Example 17: Dunce's cap, second Symanzik polynomial.

We define the external momenta of the dunce's cap as follows:

$\Gamma =$ 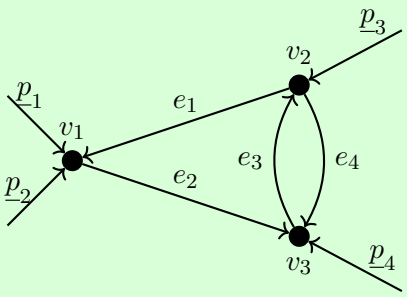

The total external momentum is zero, $\underline{p}_1 + \underline{p}_2 + \underline{p}_3 + \underline{p}_4 = \underline{0}$, this allows to express any sum of three momenta by the fourth one. The spanning 2-forests of the dunce's cap are listed in example 15, the first Symanzik polynomial has been computed in example 16. The second Symanzik polynomial (def. 37) is

$$\begin{aligned}\phi_\Gamma = &-\underline{p}_4^2 a_2a_3a_4 - \underline{p}_3^2 a_1a_3a_4 - (\underline{p}_1+\underline{p}_2)^2 a_1a_2a_4 - (\underline{p}_1+\underline{p}_2)^2 a_1a_2a_3 \\ &+ (a_3a_4 + a_2a_4 + a_2a_3 + a_1a_4 + a_1a_3)\left(m_1^2a_1 + m_2^2a_2 + m_3^2a_3 + m_4^2a_4\right).\end{aligned}$$

Example 18: Multiedges, Symanzik polynomials.

The l-loop multiedge graph consists of $l+1$ parallel edges.

$M^{(l)} :=$ 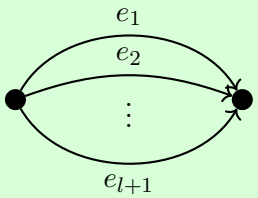

Each edge is a spanning tree and there is exactly one spanning 2-forest, hence $M^{(l)}$ has the following Symanzik polynomials (defs. 36 and 37):

$$\psi_{M^{(l)}} = \sum_{e=1}^{l+1} \frac{1}{a_e} \prod_{n=1}^{l+1} a_n, \qquad \phi_{M^{(l)}} = -\underline{p}^2 \prod_{e=1}^{l+1} a_e + \psi_{M^{(l)}} \sum_{e=1}^{l+1} m_e^2 a_e.$$

Especially

$$\psi_{M^{(1)}} = a_1 + a_2, \qquad \phi_{M^{(1)}} = -\underline{p}^2 a_1a_2 + (a_1+a_2)(m_1^2a_1 + m_2^2a_2).$$

1.3.5. Feynman rules in position space

Definition 38. We will use the term *Feynman rules* with two closely related, but not quite identical, meanings:

1. The *Feynman rules of a theory* are a set of vertices, edges, and rules how to connect them to build Feynman graphs of that theory.
2. The *Feynman rules* $\mathcal{F}$ in a closer sense are a map that takes a Feynman graph and returns the corresponding Feynman amplitude, given by the Feynman integral.

We have already established point 1 in section 1.3.1. The second point, how exactly to compute the amplitude $\mathcal{F}(\Gamma)$ from a given graph Γ, follows from theorems 2 and 6. In the spirit of sections 1.2.2 and 1.2.8, we take the resulting algorithm as a definition, rather than a theorem, in order to skip a technical discussion about the precise relation between quantum fields and Feynman amplitudes.

Example 19: ϕ^3 theory, Feynman rules in position space.

Consider ϕ^3 theory with the Lagrangian from example 3 and $m = 0$. By section 1.3.1, it gives rise to Feynman graphs which contain (a single type of) edges, and 3-valent vertices. The Feynman rules of these graphical building blocks are

$$\mathcal{F}\Big[\text{—}\Big] = \frac{\Gamma\left(\frac{D}{2}\right)}{4\pi^{\frac{D}{2}}} \frac{1}{(\underline{x}^2)^{\frac{D}{2}-1}}, \qquad \mathcal{F}\Big[\text{—<}\Big] = -i\lambda_3.$$

The Feynman rules of a graph without internal vertices are the product of the Feynman rules of its component. If the graph Γ contains internal vertices, then $\mathcal{F}[\Gamma]$ is an integral.

Definition 39. Let $\Gamma = (V_{\Gamma,\text{int}}, V_{\Gamma,\text{ext}}, E_\Gamma)$ be a Feynman graph (def. 24). The corresponding *Feynman amplitude in position space* $\mathcal{F}[\Gamma]$ is obtained by the following steps:

1. Identify each internal vertex v_i with a spacetime point $\underline{x}_i$.
2. Identify each external vertex with a spacetime point $\underline{y}_i$ of an external particle.
3. For each internal edge $e = \{\underline{x}_1, \underline{x}_2\}$, write one Feynman propagator (eqs. (1.26) and (1.27)) $\left(G^{(2)}(\underline{x}_2 - \underline{x}_1, m)\right)^{\nu_e}$, where m_e is the mass of the particle and ν_e the propagator power, $\nu_e = 1$ unless otherwise mentioned.
4. Write one integral $\int \mathrm{d}^D \underline{x}_i$ for each of the internal spacetime points $\underline{x}_i$.
5. For each internal k-valent vertex, multiply the amplitude by a factor $-i\lambda_k$.

The Feynman amplitude $\mathcal{F}(\Gamma)$ resulting from def. 39 is a nD-fold integral, where D is the dimension of spacetime and n the number of internal vertices. The amplitude is a function

of the positions $\underline{y}_i$ of external particles, and of the mass(es) of particles. Conceptually, it has the following form:

$$\mathcal{F}[\Gamma]\left(\{\underline{y}_i\},\{m_i\}\right) = \prod_{v\in V_\Gamma}(-i\lambda_{|v|})\cdot\int\cdots\int \mathrm{d}^D\underline{x}_1\cdots\mathrm{d}^D\underline{x}_n \prod_{e\in E_\Gamma}\left(G_F(\underline{x}_{e_1},\underline{x}_{e_2},m_e)\right)^{\nu_e}. \tag{1.46}$$

Here, the points $\{\underline{x}_{e_1},\underline{x}_{e_2}\}$ of the edges can be either internal points $\underline{x}_i$ or external points $\underline{y}_i$ of the underlying Feynman graph.

Example 20: Multiedges, Feynman amplitude in position space.

The amputated (def. 24) *l-loop multiedge* is the following Feynman graph, consisting of $l+1$ parallel edges between two external points $\underline{y}_1,\underline{y}_2$:

$M^{(l)} :=$ 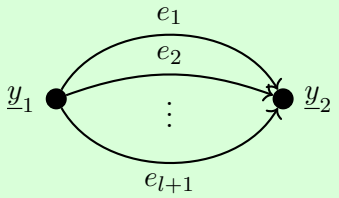

By Lorentz invariance, the function $\mathcal{F}[M^{(l)}]$ can not depend on the two individual positions, but only on the magnitude of the difference $\underline{y} := \underline{y}_2 - \underline{y}_1$. We assume that all masses are equal and all propagator powers are $\nu_e = 1$ and that there is one external edge at each vertex. The two vertices then each have valence $l+2$. The graph has no internal vertices, therefore the Feynman rules in position space (def. 39) do not involve any integration.

$$\mathcal{F}\left[M^{(l)}\right](\underline{y}^2) = (-i\lambda_{l+2})^2\prod_{e=1}^{l+1}G_F(\underline{y},m) = -\lambda_{l+2}^2\left(G_F(\underline{y},m)\right)^{l+1}.$$

1.3.6. Feynman rules in momentum space

The series expansion of Green functions in terms of Feynman graphs in momentum space is exactly the same as in position space, eq. (1.40). But one needs the Feynman amplitudes as functions of momenta of external particles, $\mathcal{F}[\Gamma](\underline{p}_1,\ldots)$.

The Feynman propagator has a simple representation in momentum space (eq. (1.24)), therefore it is often convenient to formulate the Feynman rules directly in momentum space. Consider a Feynman graph with P external points and $|V_\Gamma|$ internal vertices and $|E_\Gamma|$ internal edges. By Lorentz invariance, it depends on $P-1$ of the external positions. Moreover, it involves $|V_\Gamma|$ integrals over the internal vertices. Perform a Fourier transform of the P external positions, this introduces P integrals $\int \mathrm{d}^D\underline{y}_j \ \ldots e^{i\underline{y}_j\underline{p}_j}$. Now replace each Feynman propagator $G_F(\underline{z})$ with the Fourier transform eq. (1.23). This introduces another $|E_\Gamma|$ integrations $\int \mathrm{d}^D\underline{q}_j \ \ldots e^{-i\underline{y}_j\underline{z}_j}$.

In the resulting expression, the only dependence on internal points $\underline{x}_i$ is via exponentials of the form $e^{i\underline{x}_i(\underline{q}_i+\underline{q}_j+\ldots)}$. Hence, all integrals over internal points can be done explicitly, resulting in $|V_\Gamma|$ delta functions $\delta(\underline{q}_i+\underline{q}_j+\ldots)$, which enforce conservation of momentum at every internal vertex. One of these delta functions can be rewritten to express overall momentum conservation between all external momenta. The remaining delta functions allow to eliminate $|V_\Gamma|-1$ of the integrations $\int \mathrm{d}^D\underline{q}_j$ over edge momenta. What remains are $|E_\Gamma|-|V_\Gamma|+1$ integrations over undetermined edge momenta. By Euler's formula theorem 7, this is exactly the loop number $|L_\Gamma|$ (def. 28) of Γ. The freedom to choose an arbitrary linearly independent set of cycles as the loops in def. 28 corresponds to the freedom of choosing a set of internal momenta as integration variables. By convention, the overall delta function of a Feynman amplitude in momentum space is not written explicitly.

Example 21: ϕ^3 theory, Feynman rules in momentum space.

In momentum space, the Feynman rules of ϕ^3 theory (example 3) are

$$\mathcal{F}\left[\text{—}\right] = \frac{i}{\underline{p}^2-m^2}, \qquad \mathcal{F}\left[\text{—<}\right] = -i\lambda_3.$$

The Feynman rules of a treelevel graph (def. 33) are the product of the Feynman rules of its components, but as soon as the graph Γ contains loops (def. 28), $\mathcal{F}[\Gamma]$ is an integral.

Example 22: Quantum electrodynamics.

Quantum electrodynamics (QED)is the quantized version of classical electrodynamics (example 7). It is defined by the Lagrangian

$$\mathcal{L} = \bar{\psi}\left(i\gamma^\mu\left(\partial_\mu - ieA_\mu\right) - m\right)\psi - \frac{1}{4}F_{\mu\nu}F^{\mu\nu}.$$

The two involved fields correspond to two different types of particles. The particles represented by the field A^μ are massless *photons*, they carry spin 1 (that is, A^μ behaves like an ordinary vector under Lorentz transformations). In Feynman diagrams, they are represented by a wavy line ~~. Since A^μ carries one Lorentz index, the Feynman propagator is a tensor with two indices, representing the two fields in $\langle A^\mu(\underline{0})A^\nu(\underline{x})\rangle$. The precise Feynman rule for the propagator depends on the chosen gauge (see example 127), parametrized by a constant $\xi\in\mathbb{R}$,

$$\mathcal{F}\left[\text{~~}\right] = \frac{i}{\underline{p}^2}\left(\eta^{\mu\nu}+\xi\frac{\underline{p}_\nu\underline{p}_\mu}{\underline{p}^2}\right).$$

The fermion ψ has spin $\frac{1}{2}$ and is represented by an arrow $\rightarrow$ in Feynman graphs. Its propagator is a tensor in spinor space, but a scalar with respect to Lorentz indices,

$$\mathcal{F}\left[\text{—>}\right] = \frac{i}{\gamma^\mu\underline{p}_\mu - m} = \frac{i}{\underline{p}^2-m^2}\left(\gamma^\mu\underline{p}_\mu + m\right).$$

Observe that this propagator scales as $|\underline{p}|^{-1}$, and not $|\underline{p}|^{-2}$.

QED contains only a single type of interaction, given by the term $ieA_\mu\bar{\psi}\psi$ in the Lagrangian. In Feynman graphs, it is represented as a 3-valent vertex with Feynman rule

$$\mathcal{F}\left[\text{}\right] = ie\gamma^\mu.$$

The index of γ^μ amounts to the Lorentz index of the incoming photon line.

Definition 40. Let Γ be a Feynman graph and $\left\{\underline{p}_i\right\}$ a set of external momenta, pointing towards the graph. The Feynman amplitude in momentum space is obtained by the following procedure:

1. Assign to each internal edge e a 4-momentum $\underline{k}_e$.
2. For all momenta $\{\underline{q}_i\}$ flowing into a vertex, enforce momentum conservation $\underline{0} = \sum_i \underline{q}_i$. This will reduce the total number of independent internal momenta k_i to $|L_\Gamma|$.
3. For each internal edge e, write a momentum-space Feynman propagator eq. (1.24) with mass m_e, propagator power ν_e and momentum k_e corresponding to that edge.
4. Integrate over the $|L_\Gamma|$ independent internal momenta, $\int\cdots\int \frac{\mathrm{d}^D\underline{k}_1}{(2\pi)^D}\cdots\frac{\mathrm{d}^D\underline{k}_{|L_\Gamma|}}{(2\pi)^D}$.
5. For each internal n-valent vertex, multiply the integral by one factor λ_n.

In general, $|V_\Gamma| \neq |E_\Gamma|$. This means that the number of D-dimensional integrations in position space (def. 39) is different from the number in momentum space (def. 40). Compare section 5.2.3 for a particularly striking example. The *treelevel* (def. 33) Feynman graphs are the solution of the corresponding classical field theory. Loops represent quantum corrections. Observe that, therefore, in momentum space the quantum corrections are given by loop integrals, whereas the classical solution involves no integral. This is different from position space, there, even the treelevel graphs are integrals over internal spacetime points.

Including propagator powers ν_e, the Feynman integral in momentum space has the form

$$\mathcal{F}[\Gamma] = \prod_{v\in V_\Gamma}(-i\lambda_{|v|})\cdot\left(\prod_{l\in L_\Gamma}\int\frac{\mathrm{d}^D\underline{k}_l}{(2\pi)^D}\right)\prod_{e\in E_\Gamma}\left(G_F(\underline{k}_e)\right)^{\nu_e}, \tag{1.47}$$

where the momenta $\{\underline{k}_e\}$ and $\{\underline{k}_l\}$ are related via momentum conservation at each vertex.

Example 23: Multiedges, Feynman amplitude in momentum space.

Consider the l-loop multiedge graph from example 20. In momentum space, assign an external momentum $\underline{p}$ to the external vertices:

$M^{(l)} :=$ 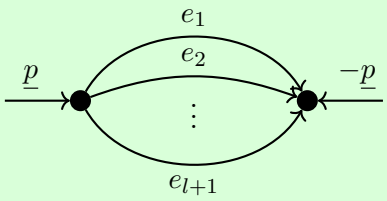

By Lorentz invariance $\mathcal{F}\left[M^{(l)}\right]$ is a function of the scale $s := \underline{p}^2$ of the external momentum. The Feynman integral in momentum space reads

$$-\lambda_{l+2}^2 \left(\prod_{e=1}^{l} \int \frac{\mathrm{d}^D \underline{k}_e}{(2\pi)^D}\right) \frac{i^{l+1}}{\left(\underline{k}_1^2 - m_1^2\right)^{\nu_1} \cdots \left(\underline{k}_l^2 - m_l^2\right)^{\nu_l} \left(\left(\underline{p} - \ldots - \underline{k}_l\right)^2 - m_{l+1}^2\right)^{\nu_{l+1}}}.$$

This is an $(l \cdot D)$-fold integral, while $\mathcal{F}(M^{(l)})(\underline{y})$ in position space (example 20) is merely a product. Instead of solving the momentum-space integral, the result can conveniently be found by Fourier-transform of the position-space expression [165].

1.3.7. Feynman rules in parametric space

Integration in parametric space is described in [166]. We will only review the principles relevant for the present thesis, loosely following the exposition in [167].

The goal of parametric space is to eliminate all integrals over D-vectors and instead rewrite the Feynman rules as integrals over one scalar *Schwinger parameter* for each edge. The first step is the integral representation of the Gamma function, def. 5. With a change of integration variable, one obtains

$$\frac{1}{(\underline{p}^2 - m^2)^\nu} = \frac{1}{\Gamma(\nu)} \int_0^\infty \mathrm{d}a \; a^{\nu-1} e^{-a(\underline{p}^2 - m^2)}. \tag{1.48}$$

This identity is sometimes called *Schwinger trick*, the variable a is the Schwinger parameter. We construct the scalar momentum-space version of parametric Feynman integrals. An analogous construction can be done based on position space Feynman rules (def. 39). For them, one uses the Gaussian integral eq. (1.3) to obtain $G_F(\underline{z})$ as a parametric integral [168, eq (1.10)] analogous to eq. (1.48). Moreover, a generalization to gauge theories is possible using the *corolla polynomial* [169–171].

Starting from the Feynman rules in momentum space (def. 40), we introduce one Schwinger Parameter a_e for each edge. The Feynman integral eq. (1.47) then becomes

$$\mathcal{F}[\Gamma] = i^{|E_\Gamma|} \prod_{v \in V_\Gamma} (-i\lambda_{|v|}) \prod_{l \in L_\Gamma} \int \frac{\mathrm{d}^D \underline{k}_l}{(2\pi)^D} \prod_{e \in E_\Gamma} \int_0^\infty \frac{\mathrm{d}a_e \; a_e^{\nu_e - 1}}{\Gamma(\nu_e)} \exp\left(-\sum_{e \in E_\Gamma} a_e \left(\underline{k}_e^2 - m_e^2\right)\right).$$

We recall that the momenta $\underline{k}_e$ are related to each other via the delta functions at the vertices. Solving these relations amounts to a linear transformation of integration variables. It turns out that the general solution can be expressed in terms of the Symanzik polynomials. After this transformation, the momentum-integrals are independently Gaussian and can therefore be performed analytically:

$$\mathcal{F}[\Gamma] = \frac{i^{|E_\Gamma|}}{(4\pi)^{|L_\Gamma|\frac{D}{2}}} \prod_{v\in V_\Gamma} (-i\lambda_{|v|}) \prod_{e\in E_\Gamma} \int_0^\infty \frac{\mathrm{d}a_e\, a_e^{\nu_e-1}}{\Gamma(\nu_e)} \frac{\exp\left(-\frac{\phi_\Gamma}{\psi_\Gamma}\right)}{\psi_\Gamma^{\frac{D}{2}}}. \tag{1.49}$$

Here, $\psi_\Gamma(\{a_e\})$ is the first (def. 36) and $\phi_\Gamma(\{a_e\})$ the second Symanzik polynomial (def. 37). Rescaling all Schwinger parameters $a_e \to t \cdot a_e$ and using lemma 12, the integration over the magnitude t results in yet another another Gamma function. It is useful to combine propagator powers, spacetime dimension and loop number into a single expression ω_Γ.

Definition 41. For an amputated Feynman graph Γ (def. 24), the *superficial degree of convergence* is defined as

$$\omega_\Gamma := \sum_{e\in E_\Gamma} \nu_e - |L_\Gamma| \frac{D}{2}.$$

The Feynman amplitude in parametric space now has the following form:

$$\mathcal{F}[\Gamma] = \frac{i^{|E_\Gamma|}}{(4\pi)^{|L_\Gamma|\frac{D}{2}}} \prod_{v\in V_\Gamma} (-i\lambda_{|v|})\Gamma(\omega_\Gamma) \prod_{e\in E_\Gamma} \int_0^\infty \frac{\mathrm{d}a_e\, a_e^{\nu_e-1}}{\Gamma(\nu_e)}\, \delta\left(1 - \sum_{e=1}^{|E_\Gamma|} a_e\right) \frac{\psi^{\omega_\Gamma-\frac{D}{2}}}{\phi_\Gamma^{\omega_\Gamma}}. \tag{1.50}$$

Example 24: Massless 1-loop multiedge.

We know the graph polynomials of multiedge graphs from example 18. For the massless 1-loop case, the resulting Feynman integral eq. (1.49) is the integral representation of Euler's beta function (e.g. [172]). Let $s := \underline{p}^2$ be the external momentum squared. Then

$$\begin{aligned}\mathcal{F}\big[M^{(1)}\big](s) &= \frac{(-i\lambda_3)^2 i^2}{(4\pi)^{\frac{D}{2}}\Gamma(\nu_1)\Gamma(\nu_2)} \int_0^\infty \mathrm{d}a_1 \int_0^\infty \mathrm{d}a_2\, a_1^{\nu_1-1} a_2^{\nu_2-1} \frac{\exp\left(-\frac{a_1 a_2 s}{a_1+a_2}\right)}{(a_1+a_2)^{\frac{D}{2}}} \\ &= \frac{\lambda_3^2}{(4\pi)^{\frac{D}{2}}} \frac{\Gamma\left(\nu_1+\nu_2-\frac{D}{2}\right)}{\Gamma(\nu_1)\Gamma(\nu_2)} \frac{1}{s^{\nu_1+\nu_2-\frac{D}{2}}} \frac{\Gamma\left(\frac{D}{2}-\nu_1\right)\Gamma\left(\frac{D}{2}-\nu_2\right)}{\Gamma\left(D-\nu_1-\nu_2\right)}.\end{aligned}$$

This result is widely known. One of the earlier articles showing a derivation is [173]. The superficial degree of convergence (def. 41) is $\omega = \nu_1 - \nu_2 - \frac{D}{2}$, the prefactor is $\Gamma(\omega)$ as expected from eq. (1.50). As a remark, amplitudes of multiedges for non-scalar fields, or with propagator powers in the numerator, can be found in [122, 124, 174–177].

Example 25: Massless l-loop multiedges.

We found in example 24 that the Feynman amplitude of the massless 1-loop multiedge itself has the form of a massless propagator $\frac{1}{(\underline{k}^2)^{\nu_e}}$, but with the propagator power $\nu_e := \nu_1 + \nu_2 - \frac{D}{2}$. This means that we can insert the amputated 1-loop multiedge into another 1-loop multiedge and obtain an expression for the 2-loop multiedge without any explicit integration. Keeping track of the various prefactors, the result is

$$\mathcal{F}\big[M^{(2)}\big](s) = \frac{-\lambda_4^2 i^3}{(4\pi)^{2\frac{D}{2}}} \frac{\Gamma\left(\nu_1+\nu_2+\nu_3-2\frac{D}{2}\right)}{\Gamma(\nu_1)\Gamma(\nu_2)\Gamma(\nu_3)} \frac{1}{s^{\nu_1+\nu_2+\nu_3-2\frac{D}{2}}} \cdot \frac{\Gamma\left(\frac{D}{2}-\nu_1\right)\Gamma\left(\frac{D}{2}-\nu_2\right)\Gamma\left(\frac{D}{2}-\nu_3\right)}{\Gamma\left(3\frac{D}{2}-\nu_1-\nu_2-\nu_3\right)}.$$

By induction, one confirms a formula for arbitrary loop number l. To this end, define $\nu := \sum_e \nu_e$. The superficial degree of convergence (def. 41) is $\omega = \nu - l\frac{D}{2}$.

$$\mathcal{F}\big[M^{(l)}\big](s) = \frac{-\lambda_{l+2}^2 i^{l+1}}{(4\pi)^{l\frac{D}{2}}} \frac{\Gamma(\omega)}{\prod_e \Gamma(\nu_e)} \frac{1}{s^\omega} \frac{\prod_e \Gamma\left(\frac{D}{2}-\nu_e\right)}{\Gamma\left((l+1)\frac{D}{2}-\nu\right)}.$$

Again, the result includes the expected factor $\Gamma(\omega)$.

Unfortunately, the massless multiedges from example 25, and the massless triangles where one external momentum vanishes, are essentially the only infinite class of 4-dimensional Feynman integrals that can be solved explicitly. As soon as a massive propagator is involved, the recursion becomes much more complicated, see [178, 179].

Example 26: Second chain graph.

We call the following graph in a massless ϕ^3 theory "second chain graph" S:

$S :=$

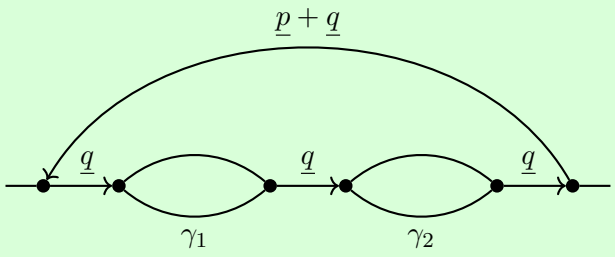

Assume that all propagator powers are $\nu_e = 1$. There are two subgraphs γ_1 and γ_2. They are 1-loop multiedges and they carry the same momentum $t := \underline{q}^2$, hence, by example 24,

$$\mathcal{F}[\gamma_1] = \mathcal{F}[\gamma_2] = \frac{\lambda_3^2}{(4\pi)^{\frac{D}{2}}} \frac{\Gamma\left(2 - \frac{D}{2}\right)}{1} \frac{\Gamma\left(\frac{D}{2} - 1\right)\Gamma\left(\frac{D}{2} - 1\right)}{\Gamma\left(D - 2\right)} \frac{1}{t^{2-\frac{D}{2}}}.$$

These two graphs are connected with three propagators $\frac{i}{t}$ (eq. (1.24)), each of which carries momentum t. The complete chain therefore has the amplitude

$$\left(\frac{\lambda_3^2}{(4\pi)^{\frac{D}{2}}} \Gamma\left(2 - \frac{D}{2}\right) \frac{\Gamma\left(\frac{D}{2} - 1\right)\Gamma\left(\frac{D}{2} - 1\right)}{\Gamma\left(D - 2\right)}\right)^2 \frac{1}{t^{4-D}} \frac{i^3}{t^3}.$$

The amplitude of this chain is again similar to a propagator, but with exponent $7 - D$ and a prefactor. Hence, we can evaluate it once again with example 24 and obtain (for $s := \underline{p}^2$)

$$\mathcal{F}[S] = \frac{-\lambda_3^6}{(4\pi)^{\frac{3}{2}D}} \frac{\Gamma^2\left(2 - \frac{D}{2}\right)\Gamma\left(8 - \frac{3}{2}D\right)\Gamma^5\left(\frac{D}{2} - 1\right)\Gamma\left(\frac{3}{2}D - 7\right)}{\Gamma^2\left(D - 2\right)\Gamma(7 - D)\Gamma\left(2D - 8\right)} \frac{1}{s^{8-3\frac{D}{2}}}.$$

Later, we will also need the graphs S_i where the subgraph γ_i is contracted (def. 27),

$\frac{S}{\gamma_1} =: S_1 =$ 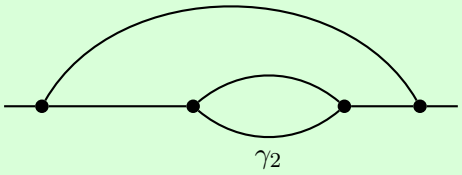

Both S_1 and S_2 have the same amplitude

$$\mathcal{F}\big[S_1\big] = \mathcal{F}\big[S_2\big] = \frac{i\lambda_3^4}{(4\pi)^D} \frac{\Gamma\left(2 - \frac{D}{2}\right)\Gamma\left(5 - D\right)\Gamma^3\left(\frac{D}{2} - 1\right)\Gamma\left(D - 4\right)}{\Gamma\left(D - 2\right)\Gamma(4 - \frac{D}{2})\Gamma\left(\frac{3}{2}D - 5\right)} \frac{1}{s^{5-D}}.$$

Besides the three forms (sections 1.3.5 to 1.3.7) we discussed, there are several other ways to express Feynman integrals. We will not go into details because computational techniques for individual graphs are out of the scope of this thesis. The interested reader is referred to the literature. Examples include representations by the Lee-Pomeransky polynomial $G_\Gamma := \psi_\Gamma + \phi_\Gamma$ [180], which can be understood as a special case of a GKZ hypergeometric function [126, 181–183], or the Baikov representation [184–186], or as solutions of differential or difference equations [123, 187–191]. For the various polynomials, it is also fruitful to consider their geometric realizations such as Newton polytopes, see e.g. [183, 192, 193].

1.3.8. Symmetry factors

By Wick's theorem (theorem 2), the correlation functions $G_F^{(n)}$ of the free field are given by "all contractions". But, as soon as some of the arguments of $G_F^{(n)}$ coincide, some of the contractions start to become identical.

Example 27: Contraction of the four-point function.

Consider the 4-point function from example 9, but, for the time being, assume that $\underline{x}_1 = \underline{x}_2$ and $\underline{x}_3 = \underline{x}_4$. Out of the three complete contractions, two now become identical.

$$G_F^{(4)}(\underline{x}_1, \underline{x}_2, \underline{x}_3, \underline{x}_4) =$$

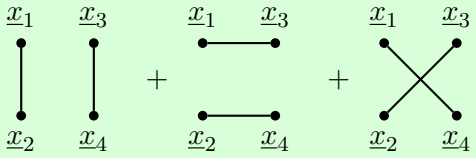

$$\Rightarrow \quad G_F^{(4)}(\underline{x}_1, \underline{x}_1, \underline{x}_3, \underline{x}_3) =$$

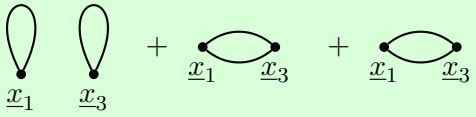

The fact that graphs can potentially become identical when vertices are merged gives rise to non-trivial combinatoric prefactors in the Dyson series (eq. (1.40)). We will discuss the fundamental mechanism that leads to these *symmetry factors* by examining the two most basic examples.

Before going to the examples, we quickly recall why in many cases there is *no* non-trivial symmetry factor. Each k-valent vertex in a Feynman graph corresponds to an interaction term ϕ^k, which comes with a prefactor $\frac{1}{k!}$ in the Lagrangian (eq. (1.5)). Assume that in the Dyson series, k arguments of $G_F^{(n)}$ are identified. That means, before identification, there were k distinct 1-valent vertices, which are now merged to a single k-valent vertex. The k adjacent edges had, in general, $k!$ different permutations of which edge joins which of the original 1-valent vertices. Hence, there were $k!$ different original graphs, which all become identical as soon as the vertices are merged. The resulting graph would have a prefactor $k!$, were it not for the factor $\frac{1}{k!}$ in the Lagrangian which precisely cancels it. The resulting graph therefore has a prefactor of unity.

Similarly, the order n in the Dyson series is given by graphs with n internal vertices. In the Feynman integral, each internal vertex is integrated over the whole space. Therefore, all n vertices are interchangeable. All graphs which differ only by a labelling of the vertices are actually the same graph. For n vertices, this would give rise to a prefactor $n!$. But the Dyson series (theorem 6) contains a prefactor $\frac{1}{n!}$ for the order-n term, arising from the exponential function. Once more, both prefactors cancel and the resulting graph appears with a prefactor of unity.

The mechanism outlined in the last two paragraphs works only as long as the initial edges or vertices were distinguishable. We will now see the two most basic cases where this is not the case, and why they give rise to non-trivial symmetry factors.

Firstly, examine a tadpole (def. 29), such as in the first summand in example 27: Each 2-valent vertex comes with a prefactor $\frac{1}{2!}$, but for each vertex there is only a single way

to build the tadpole. The "other" way would be exchanging the two ends of the tadpole edge, which gives the same graph. Consequently, the first summand in $G_F^{(4)}(\underline{x}_1, \underline{x}_1, \underline{x}_3, \underline{x}_3)$ has a prefactor $\frac{1}{2} \cdot \frac{1}{2} = \frac{1}{4}$. It is straightforward to see that, irrespective of the valence of the vertices, every tadpole produces a prefactor $\frac{1}{2}$.

Secondly, look at multiedges. Thehe second and third summand in example 27 are examples of 2-edge multiedges. Starting from $\underline{x}_1$, there are two ways of attaching an edge to $\underline{x}_3$. They are symbolized by the two (identical) graphs in $G_F^{(4)}(\underline{x}_1, \underline{x}_1, \underline{x}_3, \underline{x}_3)$. But again, each of the two vertices has a factor $\frac{1}{2}$, and adding the two identical graphs, we obtain an overall factor $\frac{1}{2} \cdot \frac{1}{2} + \frac{1}{2} \cdot \frac{1}{2} = \frac{1}{2}$. In this case, not a tadpole, but a multiedge (example 25) leads to the mismatch of prefactors: If there are n parallel edges, then there are $n!$ ways of attaching them, but each of the two vertices comes with a prefactor $\frac{1}{n!}$. Therefore, a n-edge multiedge produces an overall symmetry factor $n! \cdot \frac{1}{n!} \cdot \frac{1}{n!} = \frac{1}{n!}$.

In general, one finds that such "overcompensation" of prefactors always occurs whenever a graph Γ has multiple subgraphs which can be interchanged without altering Γ. In the case of multiedges, these subgraphs were just the individual edges. Tadpoles are a limiting case, namely exchanging the order $\{v_1, v_2\} \leftrightarrow \{v_2, v_1\}$ in an edge, which only ever leaves the graph unaltered if $v_1 = v_2$. For the exchange of more complicated subgraphs, it is helpful to introduce the notion of a *graph automorphism*.

Definition 42. An *isomorphism* between two undirected graphs Γ_1, Γ_2, where both edges and vertices are labelled, is a a map $f : E_{\Gamma_1} \to E_{\Gamma_2}, V_{\Gamma_1} \to V_{\Gamma_2}$ such that $\{v_i, v_j\} = e \in E_{\Gamma_1}$ if and only if $\{f(v_i), f(v_j)\} = f(e) \in E_{\Gamma_1}$.

Definition 43. An *automorphism* of an amputated Feynman graph Γ (def. 24) is an isomorphism $f : \Gamma \to \Gamma$ (def. 42). Additionally, we demand that an automorphism acts trivially on the external vertices $V_{\Gamma,\text{ext}}$, and that reversing the "direction" of a tadpole edge is considered an automorphism. The set of all automorphisms of a graph forms the *automorphism group* $\text{Aut}(\Gamma)$.

Example 28: Automorphism group of a 2-loop graph.

Consider the following graph Γ, where v_1 and v_4 are external vertices:

$\Gamma :=$ 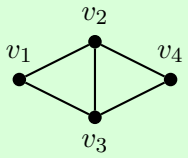

$\Gamma' :=$ 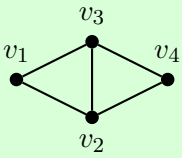

The graph Γ' is an automorphism (def. 43) of Γ: It is exactly the same drawing, but labels are exchanged, and every edge that was present in Γ is still present in Γ'. Since the external vertices v_1 and v_4 are fixed, Γ' is the only non-trivial automorphism of Γ and $|\,\text{Aut}(\Gamma)| = 2$. If we write the graphs as an abstract list of edges (instead of drawing them), then

$$\Gamma = \{\{v_1, v_2\}, \{v_2, v_4\}, \{v_2, v_3\}, \{v_1, v_3\}, \{v_3, v_4\}\} = \Gamma'.$$

The automorphism here is the exchange $v_2 \leftrightarrow v_3$, which leaves the list unchanged apart from the direction of the central edge, $\{v_2, v_3\} \leftrightarrow \{v_3, v_2\}$. But we are considering undirected graphs, so both edges are identical.

One can also consider Γ' as "a different way of drawing Γ". But this is not the point: There are infinitely many different ways of drawing the same graph on a plane. The automorphism is about exchanging labelled parts of the graph without changing the drawing.

Theorem 13. In the Dyson series (eq. (1.40)), each graph appears with a *symmetry factor* which is the inverse of the size of its automorphism group (def. 43),

$$\mathrm{sym}(\Gamma) = \frac{1}{|\mathrm{Aut}(\Gamma)|}.$$

Proof. A mathematically rigorous proof can be found for example in [194, Sec. 2.3]. It is based on the *orbit-stabilizer-theorem*, namely that the size of a group equals the number of orbits times the size of each orbit, which is a specialization of the Cauchy–Frobenius-Burnside lemma [195, 196] or the Redfield–Pólya theorem [197, 198]. The case of multiedges and tadpoles has been discussed in detail above. What remains is the relabelling of vertices. The permutations of all $|V_\Gamma|$ (labelled) vertices are the symmetric group $S_{|V_\Gamma|}$ with size $|V_\Gamma|!$. The automorphism group $\mathrm{Aut}(\Gamma)$ is the stabilizer group of $S_{|V_\Gamma|}$ acting on V_Γ. The orbit $\mathrm{Orb}(\Gamma)$ of $S_{|V_\Gamma|}$ acting on the labelled graph Γ amounts to all the copies of Γ which are created by Wick's theorem (theorem 2). The Dyson series (theorem 6) introduces a prefactor $\frac{1}{|V_\Gamma|!}$, the result is

$$\frac{1}{|V_\Gamma|!}\,|\mathrm{Orb}(\Gamma)|\cdot\Gamma = \frac{1}{|\mathrm{Orb}(\Gamma)|\,|\mathrm{Aut}(\Gamma)|}\,|\mathrm{Orb}(\Gamma)|\cdot\Gamma = \frac{1}{|\mathrm{Aut}(\Gamma)|}\cdot\Gamma$$

□

Symmetry factors are compatible with cutting, in the sense that summing all possible ways to cut a set of graphs into smaller components is the same as summing all subgraphs with all ways to join them. See [194, 199] or example 29 for more details. This fact has important consequences for Dyson-Schwinger equations (section 1.3.11) in gauge theories.

Example 29: Cutting a 2-loop graph.

Choose Γ_1, Γ_2 as indicated, then each of them has symmetry factor $\frac{1}{2}$ (for the exchange of $1 \leftrightarrow 2$ or $4 \leftrightarrow 5$). The numbered edges are supposed to be internal in the final graph, so they are not excluded from graph automorphisms (def. 43). There are $3! = 6$ possibilities to join Γ_1 to Γ_2, resulting in the graphs $\Gamma_A, \Gamma_B, \Gamma_C$.

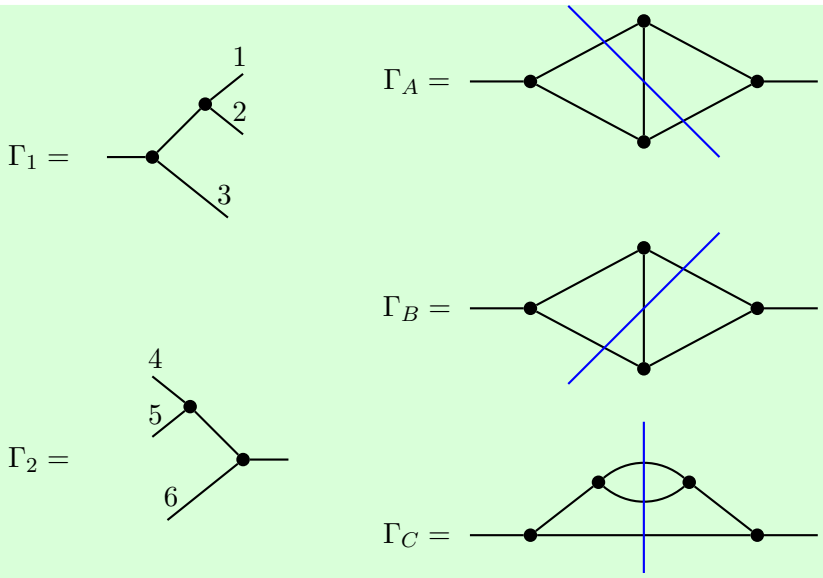

Two of the 6 possible connections result in Γ_C, producing an overall factor of $2 \cdot \frac{1}{2} \cdot \frac{1}{2}$, which is the correct symmetry factor $\mathrm{sym}(\Gamma_C) = \frac{1}{2}$. The 4 other possibilities produce the topology $\Gamma_A = \Gamma_B$ with an overall factor $4 \cdot \frac{1}{2} \cdot \frac{1}{2} = 1$. There are two distinct ways of cutting this topology into Γ_1 and Γ_2. The correct symmetry factor is respected in the sum over both cuts, $2 \cdot \mathrm{sym}(\Gamma_A) = 2 \cdot \frac{1}{2} = 1$. This summation over all possible cuts, although it appears slightly odd at first, is exactly what one needs in QFT, for example for gauge theory [169, 200, 201], see example 131, or field diffeomorphisms [199, 202], see chapter 5.

1.3.9. Digression: Electrical networks

The theoretical analysis of electrical networks was first started by Ohm's discovery of the fundamental law $U = R \cdot I$ for the voltage U, resistance R and current I in directed current circuits [203]. In 1847, Kirchhoff gave a more systematic treatment, accounting for charge conservation by his famous two rules (from today's perspective, these rules are a graph-discretized version of Maxwell's equations [25] for the electric field). In passing, we will now see what the original meaning of the Kirchhoff polynomial theorem 11 for electrical networks was.

To turn a graph into an electrical network, the edges become resistors inheriting the direction of the edge, and we add additional lines and dots to make the drawing rectangular. Each resistor has a conductance $c_i := \frac{1}{R_i}$. We assume that current flows from one vertex s to another vertex t through the network. All other vertices are not connected to any external potential, marked nc, hence no current can enter or leave here.

Example 30: Dunce's cap as an electrical network.

Choosing arbitrarily one of the vertices as s and one as t, the dunce's cap (example 12) becomes the following electrical network:

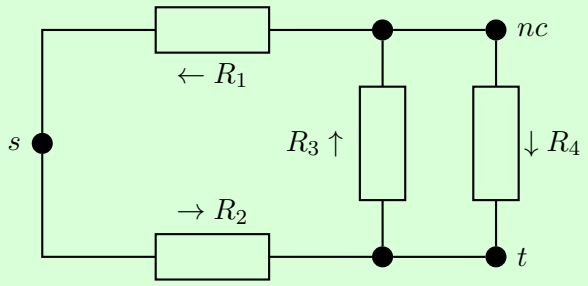

For any spanning tree $T \in T_\Gamma^{(1)}$ (def. 34), let its *weight* be the product of the conductances in the tree, $c_T := \prod_{e \in T} c_e$. Each spanning tree defines a unique directed path from s to t. Assume that a current of magnitude 1 flows from s to t. Then, Kirchhoff's theorem [155, 160] states that the current through R_i is

$$I_i = \frac{N(s, R_i^+, t) - N(s, R_i^-, t)}{\tilde{\psi}\left(\langle c_e \rangle\right)}. \tag{1.51}$$

In eq. (1.51), $N(s, R_i^+, t)$ is the sum of the weights c_T of all spanning trees T which, on their way from s to t, pass through R_i in positive direction. $N(s, R_i^-, t)$ is defined accordingly for negative direction, and $\tilde{\psi}$ is the Kirchhoff polynomial (theorem 11). For readability, we skipped the physical units in eq. (1.51).

Example 31: Dunce's cap, currents in the edges.

For the network shown in example 30, we know the Symanzik polynomial from example 16. Using eq. (1.51), we find

$$\begin{aligned}
I_1 &= \frac{0 - (c_1c_3 + c_1c_4)}{c_1c_2 + c_1c_3 + c_1c_4 + c_2c_3 + c_2c_4} \\
I_2 &= \frac{(c_2c_3 + c_2c_4 + c_1c_2) - 0}{c_1c_2 + c_1c_3 + c_1c_4 + c_2c_3 + c_2c_4} \\
I_3 &= \frac{(c_2c_3) - (c_1c_3)}{c_1c_2 + c_1c_3 + c_1c_4 + c_2c_3 + c_2c_4} \\
I_4 &= \frac{(c_2c_4) - (c_1c_4)}{c_1c_2 + c_1c_3 + c_1c_4 + c_2c_3 + c_2c_4}.
\end{aligned}$$

Knowing all currents, we can reconstruct all other properties of the network. For example, by Ohm's law [203], the voltage between s and t is the voltage over R_2,

$$U_{s\to t} = U_2 = R_2 I_2 = \frac{1}{c_2} \frac{c_2c_3 + c_2c_4 + c_1c_2}{c_1c_2 + c_1c_3 + c_1c_4 + c_2c_3 + c_2c_4} = \frac{c_3 + c_4 + c_1}{c_1c_2 + c_1c_3 + c_1c_4 + c_2c_3 + c_2c_4}.$$

The voltage in turn delivers the total resistance of the network because the total current is 1 (where the unit Ampere is left out): $R = U_{s\to t}/1 = U_{s\to t}$. A manual calculation with the rules for parallel/serial resistors, known from high school physics, confirms this result.

Current conservation in electrical networks is analogous to momentum conservation in Feynman graphs. It is therefore not surprising that solving for the individual currents in an electrical network involves the same graph polynomial as does the resolution of all internal momenta in a Feynman graph with respect to a chosen set of loop momenta. The Schwinger trick eq. (1.48) can be interpreted as minimizing the power dissipation of an electrical network, see [204].

The analogy between Feynman graphs and electrical networks has sometimes been mentioned in the literature, but concrete applications remain rare. In electrical networks, a triangle of resistors can always be replaced by a "star", joining the three corners to a new central vertex. A similar relation for Feynman integrals is known as *uniqueness identity* [205–208],

$$\int \mathrm{d}^D t \, \frac{1}{((\underline{x}-\underline{t})^2)^a} \frac{1}{\left((\underline{y}-\underline{t})^2\right)^b} \frac{1}{((\underline{z}-\underline{t})^2)^c} \propto \frac{1}{\left((\underline{x}-\underline{y})^2\right)^{\frac{D}{2}-a}} \frac{1}{\left((\underline{y}-\underline{z})^2\right)^{\frac{D}{2}-b}} \frac{1}{((\underline{z}-\underline{x})^2)^{\frac{D}{2}-c}}.$$

The uniqueness identity holds only for $a+b+c = D$, while the replacement of stars in electrical networks is always possible. In [209], the star-triangle relation for electrical circuits is used to restrict the analytic form of 1-loop massless 3-point functions.

1.3.10. 1PI graphs

In momentum space, the Feynman rules (def. 40) require integration for every linearly independent loop. Conversely, if two Feynman graphs Γ_1, Γ_2 are connected by only a single edge, then they can not be part of the same loop and hence the total amplitude factors,

$$\mathcal{F}\big[\Gamma_1 \cdot e \cdot \Gamma_2\big] = \mathcal{F}\left[\Gamma_1\right] \cdot \mathcal{F}[e] \cdot \mathcal{F}\left[\Gamma_2\right]. \tag{1.52}$$

Definition 44. An amputated Feynman graph Γ (def. 24) is *1-particle irreducible* or 1PI if it is 2-edge connected. That is, Γ is connected and it stays connected (def. 22) when any one of the internal edges is removed.

Example 32: ϕ^3 theory, 1PI graphs.

In example 11, we gave the first graphs contributing to the connected Green functions. The 1PI graphs are a subset of those. For the 2-point function, there was only one non-1PI graph and what remains is

$\Gamma^{(2)} =$ 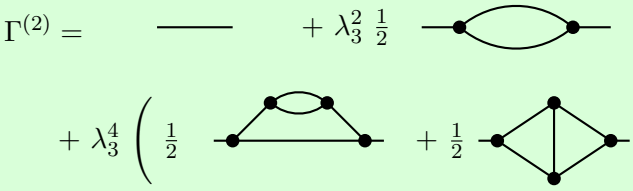 $+ \ldots$

For the 3-point function, two of the given topologies are connected but not 1PI. The 1PI ones are

$\Gamma^{(3)} =$ 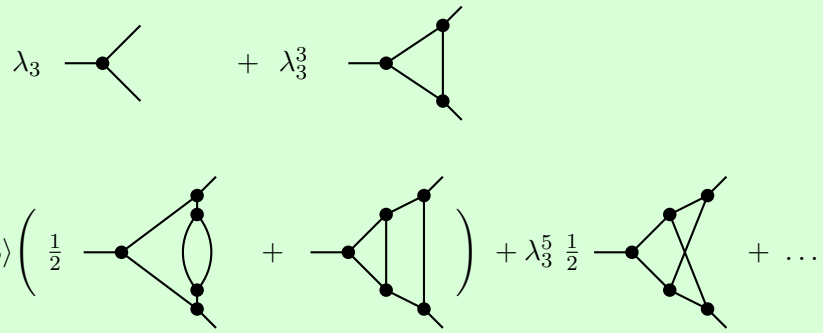 $+ \ldots$

There are in total nine 1PI graphs contributing up to loop number 2, down from 15 connected graphs in example 11.

Definition 45. The *combinatorial 1PI Green function* Γ^r is the sum of all 1PI graphs (def. 44) with residue r (def. 26), weighted with their symmetry factors (theorem 13) and coupling constants, the latter rescaled to match the loop number (def. 28).

$$\Gamma^r(\alpha) := \sum_{\Gamma \text{ 1PI}, \text{res}(\Gamma)=r} \alpha^{|L_\Gamma|} \, \text{sym}(\Gamma) \cdot \Gamma.$$

For a ϕ^n theory, the residue are monomials of ϕ, we write $r = (j)$ to indicate the residue ϕ^j. By $\Gamma \in \Gamma^r$ we mean that Γ is 1PI and $\text{res}(\Gamma) = r$.

Observe that 1PI Green functions are not the same as amputated (theorem 5) Green functions. They coincide for 2-point and 3-point graphs, but from 4 external edges on, the amputated Green function can contain an internal edge making it 1-particle reducible.

Definition 46. The 1PI Green function G^r is the combinatorial 1PI green function Γ^r (def. 45), evaluated with the Feynman rules (def. 38):

$$G^r := \mathcal{F}\big[\Gamma^r\big]$$

For 2-point graphs, the relation between connected and 1PI graphs is given by a geometric series. If we consider the functions as operators, this is a Neumann series [210]. The connected 2-point function $\bar{G}^{(2)}$ equals the sum of any number of products of the 1PI 2-point

function $\Sigma^{(2)}$, all of them with the same momentum $\underline{p}$ and connected by propagators $\frac{i}{s_p}$ (eq. (1.24)):

$$\begin{aligned}\bar{G}^{(2)}(\underline{p}) &= \frac{i}{s_p} + \frac{i}{s_p}\Sigma^{(2)}(\underline{p})\frac{i}{s_p} + \frac{i}{s_p}\Sigma^{(2)}(\underline{p})\frac{i}{s_p}\Sigma^{(2)}(\underline{p})\frac{i}{s_p} + \dots \\ &= \frac{i}{s_p}\sum_{k=0}^{\infty}\left(\frac{i}{s_p}\Sigma^{(2)}(\underline{p})\right)^k = \frac{i}{s_p}\frac{1}{1-\frac{i}{s_p}\Sigma^{(2)}(\underline{p})} =: \frac{i}{s_p G^{(2)}(\underline{p})}. \end{aligned} \tag{1.53}$$

Definition 47. The *1PI 2-point function* is defined as

$$G^{(2)}(\underline{p}) := 1 - \frac{i}{s_p}\Sigma^{(2)}(\underline{p})$$

where $\Sigma^{(2)}(\underline{p})$ represents the *self energy*, the sum of all 1PI 2-point quantum corrections. Consequently, the connected 2-point function, replacing the treelevel propagator eq. (1.24), is $\bar{G}^{(2)}(\underline{p}) = \frac{i}{s_p G^{(2)}(\underline{p})}$. For def. 45, it is $\bar{\Gamma}^{(2)} = \frac{1}{\Gamma^{(2)}}$.

The relationship between connected and 1PI 2-point functions is consistent with the Feynman propagator (eq. (1.24)). For example, instead of using the massive propagator, one can use the massless propagator and take the mass term of the Lagrangian (example 1) as a 2-valent vertex. Then, every internal line in a graph can be dressed with infinitely many of these vertices, which eventually add up to the massive Feynman propagator.

1PI graphs are "building blocks" of connected Feynman graphs, in the same sense that trees are built of vertices, which in turn are generated by the classical action (def. 7).

Definition 48. The *effective action* $\Gamma[J]$ is the formal (def. 51) generating functional of all 1PI Green functions.

If $W[J]$ is the generating functional of connected amplitudes (eq. (1.39)), then $\Gamma[J]$ is the Legendre transform (def. 53) of $W[J]$ [82, 153, 211, 212]. We will discuss the correspondence between graphs and power series in section 2.1.4. Amongst other things, it can be used to count graphs, see example 56, or [194] for a detailed account.

1.3.11. Dyson-Schwinger equations

So far, we have viewed the graphs appearing in the Dyson series (eq. (1.40)) as isolated objects. But for a given graph Γ, the subgraphs $\gamma \subset \Gamma$ are graphs themselves. This observation will now be used to organize the graphs in the Dyson series according to their residue (def. 26). The resulting identity is called *Dyson-Schwinger equation*, and it can be stated in various equivalent forms. In the present section, we stay rather general and "qualitative". More precise equations will be given in sections 2.2.5 and 3.3.

Definition 49. The *residues of the Lagrangian* are a set $\mathfrak{L}$ of pairs (g, T) associated to the monomials of the Lagrangian (def. 6). g is the residue (def. 26), that is, a monomial of field variables, while T is the tensor structure, that is, a monomial in masses or momenta.

We write $\Gamma \in \mathfrak{L}$ if there is a $(g, T) \in \mathfrak{L}$ such that $\text{res}(\Gamma) = g$ and Γ projected onto T does not vanish at $\underline{p} = \underline{0}, m = 0$. As shown in example 33, the second condition is not trivial.

Example 33: ϕ^n theory, residues of the Lagrangian.

In massive ϕ^n theory (example 3), the kinetic term amounts to $(\phi^2, \underline{p}^2) \in \mathfrak{L}$, the mass term contributes $(\phi^2, m^2) \in \mathfrak{L}$ and the interaction term is $(\phi^n, 1) \in \mathfrak{L}$.

Assume now that Γ is a graph contributing to a 2-point function with momentum $\underline{p}$, but $\mathcal{F}[\Gamma] \propto \underline{p}^4$, then $\Gamma \notin \mathfrak{L}$ for the ϕ^n theory.

Let $\Gamma \in \Gamma^{(n)}$ be a graph contributing to the combinatorial 1PI n-point Green function (def. 44). Into every edge $e \in \Gamma$ one can insert any 2-valent graph $\gamma \in \Gamma^{(2)}$, and the result is a valid Feynman graph of $\Gamma^{(n)}$. Similarly, one can replace every j-valent vertex with any $\gamma \in \Gamma^{(j)}$. A closer inspection shows that such insertion, when done consistently, produces the correct symmetry factors (theorem 13) for the newly created graphs.

Definition 50. Let $\Gamma^{(n)}$ be the combinatorial 1PI n-point Green function (def. 45). A *kernel graph* $K \in \Gamma^{(n)}$ is a 1PI (def. 44) Feynman graph with n external edges such that there is no proper subgraph $\gamma \subset K$ with $\gamma \in \mathfrak{L}$ (def. 49). The set of all kernel graphs for $\Gamma^{(n)}$ is denoted $\mathfrak{K}^{(n)}$.

Theorem 14 (Dyson-Schwinger equations (DSEs) for Feynman graphs)**.** The 1PI combinatorial Green function $\Gamma^{(n)}$ (def. 45) is given by a (possibly infinite) sum of kernel graphs (def. 50) $\mathfrak{K}^{(n)}$, and for each $K \in \mathfrak{K}^{(n)}$, all j-valent vertices $v_j \in K$ are replaced by the series $\Gamma^{(j)}$, and all edges by $\bar{\Gamma}^{(2)} = \frac{1}{\Gamma^{(2)}}$ (def. 47).

A special role is played by the 2-point function $\Gamma^{(2)}$: We insert the connected 2-point function, but the DSE is usually written for the 1PI 2-point function. The relationship def. 47 entails that the DSE for the 2-point function contains a minus sign in front of all kernel graphs.

Example 34: ϕ^3 propagator, combinatorial Dyson-Schwinger equation .

Consider the 2-point function of ϕ^3 theory. The first graphs are shown in example 32. The propagator DSE only involves a single kernel graph, which has symmetry factor $\frac{1}{2}$ (theorem 13). To avoid double-counting, one needs to disentangle the series into three parts, see also [200, 213, 214]. Again, we write the DSE for the 1PI 2-point function $\Gamma^{(2)}$, not for the connected one, see def. 47.

$\Gamma^{(3)} =:$  $\bar{\Gamma}^{(2)} =:$  $\bar{\Gamma}^{(2)} - - =:$ 

$\Gamma^{(2)} = \quad 1 \quad - \lambda_3^2 \ \frac{1}{2}$ 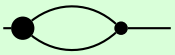 $- \lambda_3^2$ 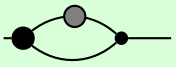 $- \lambda_3^2 \ \frac{1}{2}$ 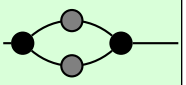

Compare this to theorem 1: We see that the presence of interaction, that is $\Gamma^{(3)} \neq 0$, necessarily alters the 2-point function.

Example 35: ϕ^3 propagator, simplified combinatorial DSE.

A drastic simplification of the propagator DSE can be obtained by ignoring all quantum corrections to the vertex, that is setting $\Gamma^{(3)} =$. This produces a DSE where $\Gamma^{(2)}$ is the only unknown function. Such DSEs will be discussed further in section 3.3.2.

$\Gamma^{(3)} =$  $\bar{\Gamma}^{(2)} =:$  $\Rightarrow \quad \Gamma^{(2)} = \quad 1 \quad - \lambda_3^2 \ \frac{1}{2}$ 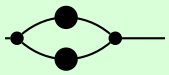

Example 36: ϕ^3 vertex, combinatorial Dyson-Schwinger equation.

Consider massless ϕ^3 theory (example 3) where $\mathfrak{L} = \left\{\left(\phi^2, \underline{p}^2\right), \left(\phi^3, 1\right)\right\}$ (example 33). In example 32, we depicted the first graphs contributing to the 1PI (def. 44) 3-point function $\Gamma^{(3)}$. Indeed, some of them have subgraphs with 2 or 3 external edges which can be identified as coefficients of the series $\Gamma^{(2)}$ and $\Gamma^{(3)}$. Without such subgraphs, there is one graph at order α^3 and one at order α^5 (in 3 different orientations). Into each edge we insert the *connected* 2-point function $\bar{\Gamma}^{(2)}$ (see eq. (1.53)).

$\Gamma^{(3)} =:$  $\bar{\Gamma}^{(2)} =:$ 

$\Gamma^{(3)} = \quad \lambda_3$  $+ \ \lambda_3^3$ 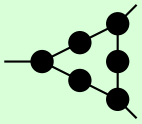 $+ \lambda_3^5 \ \frac{1}{2}$ 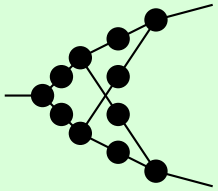 $+ \ \ldots$

Unlike the propagator DSE (example 34), the vertex DSE involves infinitely many kernel graphs. Counting the different orientations, we now have three kernel graphs up to loop number 2, down from nine 1PI graphs in example 32.

As it stands, theorem 14 is a mildly interesting combinatoric statement about the sum of infinitely many graphs and their subgraphs. But these graphs ultimately represent Feynman integrals, and consequently, theorem 14 actually amounts to a set of integral equations for the 1PI Green functions (def. 46).

Theorem 15 (Dyson-Schwinger integral equations [215–218])**.** A Green function $G^{(n)}$ is given by a series of integrals, encoded by kernel graphs (def. 50), where the j-valent vertices are replaced by the function $G^{(j)}$ and the edges are replaced by the function $\bar{G}^{(2)}$ (def. 47).

Example 37: ϕ^3 propagator, simplified integral DSE.

Consider the simplified propagator DSE of example 35, that is, setting the vertex Green function to $\mathcal{F}\big[\Gamma^{(3)}\big] = G^{(3)} \stackrel{!}{=} -i\lambda_3$. Define the 2-point functions as in def. 47. One then has, using $(-i)^2 i^2 = 1$ and the propagator eq. (1.24),

$$G^{(2)}(\underline{p}) = 1 - \frac{i}{s_p}\lambda_3^2 \frac{1}{2} \int \frac{\mathrm{d}^D \underline{k}}{(2\pi)^D} \frac{1}{s_k} \frac{1}{s_{k+p}} \left(G^{(2)}(\underline{k})\right)^{-1} \left(G^{(2)}(\underline{k}+p)\right)^{-1}.$$

In both forms (theorems 14 and 15), the Dyson-Schwinger equations are *fixed-point equations*, this means that the objects on the left hand side of these equations also appear in the right hand side. To solve a DSE, one needs to find a self-consistent solution. One possible approach is to consider all quantities as series in a coupling parameter and to solve the DSE recursively order by order. We will discuss this procedure in detail in section 4.2.

Our formulation of Dyson-Schwinger equations are based on kernel graphs (def. 50) which have one out of finitely many residues (def. 26). This entails that only finitely many Dyson-Schwinger equations are coupled. On the other hand, one generally has to include an infinite set of kernel graphs. An alternative version involves only a small number of graphs for each residue, but all (infinitely many) equations are coupled. See e.g. [219] for an entertaining presentation. These DSEs are again fixed-point equations, the most compact way to write them is if one identifies Green functions with derivatives of the path integral as in eq. (1.38).

Theorem 16 (Dyson-Schwinger equations for generating functionals)**.** Let $Z[J]$ be the path integral (eq. (1.37)) and $S[\phi]$ the classical action (def. 7), then

$$\left.\frac{\delta S[\phi]}{\delta \phi(\underline{x})}\right|_{\phi \to \frac{\delta}{\delta J}} Z[J] = 0.$$

Observe the similarity to the classical equations of motion $\delta S = 0$ (eq. (1.6)).

As announced in section 1.2.7, Dyson-Schwinger equations provide another possible way to define a quantum field theory. Their series expansion leads to the same set of Feynman rules. Indeed, that was their original motivation [216]:

> The construction of these [Green functions] for coupled fields is usually considered from the viewpoint of perturbation theory. [...] It is desirable to avoid founding the formal theory of the Green's functions on the restricted basis provided by the assumption of expandability in powers and coupling constants.

Summary of section 1.3.

1. Feynman integrals appearing in the Dyson series can be represented graphically as Feynman graphs, and it is sufficient to consider connected graphs (sections 1.3.1 and 1.3.2).
2. We reviewed graph theory and learned about various matrices and polynomials associated to graphs, and how they can be used to systematically compute quantities of interest (sections 1.3.3 and 1.3.4).
3. We established a concrete algorithm to turn a given Feynman graph into the corresponding integral in position space, called *Feynman rules* (section 1.3.5).
4. Feynman rules can equivalently be formulated in momentum space (section 1.3.6) or in parametric space (section 1.3.7).
5. We derived the symmetry factor of Feynman graphs in the Dyson series, which is given by the size of the automorphism group (section 1.3.8).
6. Connected graphs can be decomposed into 1PI graphs and it is usually sufficient to compute the 1PI ones (section 1.3.10).
7. The structure of nested subgraphs of Feynman graphs can be expressed by Dyson-Schwinger equations. They are fixed-point equations and can be formulated in various ways, either as a statement for sums of graphs, or for the generating functionals, or for Green functions (section 1.3.11).

2. Hopf algebra theory of renormalization

2.1. Combinatorics and Hopf algebras

In this section, we introduce the mathematical background needed for the later work. The concepts are well-known, but usually not taught in physics courses. The mathematically experienced reader might want to skip directly to section 2.2

2.1.1. Formal power series

Definition 51. Let R be a commutative ring and t a formal parameter. Then, $R[[t]]$ denotes the ring of all formal power series in the parameter t over with coefficients in R. A *formal power series* $f \in R[[t]]$ is a sequence of coefficients $f_j \in R$, each of which is indexed by a power of the parameter t, and extracted by $[t^j]f(t) = f_j$:

$$f(t) = \sum_{j=0}^{\infty} f_j t^j.$$

As opposed to ordinary power series and analytic functions, a formal power series has no notion of convergence. t is merely a symbol to indicate coefficients, it is not supposed to have any numerical value. Operations such as differentiation, integration or series reversion are identities between series coefficients, which agree with the formulas for analytic functions if the power series converges. For example, a formal power series can be differentiated using $f_j \mapsto (j+1)f_{j+1}$ even if the series $f(t)$ does not converge to a differentiable function in the ordinary sense. A standard reference on formal series is [220], for further details see [153, 212, 221].

Definition 52 ([222], [223, p 134])**.** Let $k \in \mathbb{N}_0, n \in \mathbb{N}_0$ and $k \leq n$ be fixed. The partial *Bell polynomial* is given by

$$B_{n,k}(x_1, x_2, x_3, \ldots) = \sum_S \frac{n!}{j_1! j_2! \cdots j_n!} \left(\frac{x_1}{1!}\right)^{j_1} \left(\frac{x_2}{2!}\right)^{j_2} \left(\frac{x_3}{3!}\right)^{j_3} \cdots \left(\frac{x_n}{n!}\right)^{j_n},$$

where the sum extends over all sets $\{j_i\}_{i\in\{1,\ldots,k\}}$ such that

$$S = \{j_i \geq 0 \ \forall i, \quad j_1 + j_2 + j_3 + \ldots + j_k = k \quad j_1 + 2j_2 + 3j_3 + \ldots + (n-k)j_{n-k} = n\}.$$

The generating function of the Bell polynomials is

$$\sum_{n=0}^{\infty} \sum_{k=0}^{n} B_{n,k}(x_1, x_2, \ldots) u^k \frac{t^n}{n!} = \exp\left(u \sum_{j=1}^{\infty} x_j \frac{t^j}{j!}\right). \tag{2.1}$$

Example 38: Some values of Bell polynomials.

The Bell polynomials contain several sets of combinatorially interesting numbers and have various relations amongst themselves and to other polynomials, see for example [223–226]. Some straightforward evaluations are:

$$B_{0,0} = 1, \qquad B_{n,0} = 0, \quad n > 0, \qquad B_{n,k} = 0, \quad k > n$$

$$B_{n,1} = x_n, \quad n > 0, \qquad B_{n,n} = x_1^n, \quad n > 0 \qquad B_{n,2} = \sum_{k=1}^{n-1} \frac{1}{2}\binom{n}{k} x_k x_{n-k}$$

$$B_{n,k}(1,2,3,\ldots) = \binom{n}{k} k^{n-k} \qquad B_{n,k}(1^0, 2^1, 3^2, 4^3, \ldots) = \binom{n-1}{k-1} n^{n-k}.$$

The Bell polynomials encode all combinatoric information to solve two of the standard tasks of formal power series, finding the inverse of a series, and concatenating two series.

Theorem 17 (Lagrange inversion [227–229])**.** Let $f(t) = f_1 t + f_2 t^2 + f_3 t^3 + \ldots$ be a formal power series and $f^{-1}(t) =: g_1 t + g_2 t^2 + g_3 t^3 + \ldots$ its combinatorial inverse, that is, $f^{(-1)}\big(f(t)\big) = t$. Let $B_{n,k}$ be the partial Bell polynomials (def. 52). Then for all $n \geq 1$,

$$\left(f^{-1}\right)_n = g_n = \frac{1}{n!} \sum_{k=1}^{n-1} \frac{1}{f_1^{n+k}} B_{n-1+k,k}\left(0, -2!f_2, -3!f_3, \ldots\right), \quad g_1 = \frac{1}{f_1}. \tag{2.2}$$

Alternatively, for power series of exponential type,

$$f(t) = \sum_{n=0}^{\infty} f_n \frac{t^n}{n!}, \qquad \text{and} \qquad f^{-1}(t) =: g(t) = \sum_{n=1}^{\infty} g_n \frac{t^n}{n!},$$
$$g_n = \sum_{k=1}^{n-1} \frac{1}{f_1^{n+k}} B_{n-1+k,k}\left(0, -f_2, -f_3, \ldots\right), \qquad g_1 = \frac{1}{f_1}.$$

Example 39: First coefficients of the inverse series.

For a series $f(t) = t + f_2 t^2 + f_3 t^3 + \ldots$, the inverse series begins with

$$f^{-1}(t) = t - f_2 t^2 + \left(-f_3 + 2f_2^2\right) t^3 + \left(-f_4 - 5f_2^3 + 5f_2 f_3\right) t^4 + \ldots.$$

Similarly, for an exponential series $f(t) = t + f_2\frac{t^2}{2!} + f_3\frac{t^3}{3!} + \dots$, the coefficients are

$$f^{-1}(t) = t - f_2\frac{t^2}{2} + \left(3f_2^2 - f_3\right)\frac{t^3}{3!} + \left(-15f_2^3 + 10f_2f_3 - f_4\right)\frac{t^4}{4!} + \left(105f_2^4 - 105f_2^2f_3 + 10f_3^2 + 15f_2f_4 - f_5\right)\frac{t^5}{5!} + \dots$$

It might appear unaesthetic that the summands in the individual parentheses are monomials of different order. Indeed, they are very much aesthetic, see example 53.

Theorem 18 (Faà di Brunos formula [230])**.** Let $f(t) = f_0 + f_1t + f_2t^2 + \dots$ and $g(t) = g_1t + g_2t^2 + g_3^3 + \dots$ be formal power series. Then, the coefficients h_n of the concatenation $f(g(t)) =: h_0 + h_1t + h_2t^2 + \dots$ are given by $h_0 = f_0$ and the partial Bell polynomials (def. 52)

$$h_n = \sum_{k=1}^{n} \frac{k!}{n!} f_k \cdot B_{n,k}\left(1!g_1, 2!g_2, \dots, (n+1-k)!g_{n+1-k}\right), \qquad n \geq 1.$$

If, instead,

$$f(t) = \sum_{n=0}^{\infty} f_n\frac{t^n}{n!}, \qquad g(t) = \sum_{n=1}^{\infty} g_n\frac{t^n}{n!}, \qquad f(g(t)) =: h(t) = \sum_{n=0}^{\infty} h_n\frac{t^n}{n!},$$

then $h_0 = f_0$ and

$$h_n = \sum_{k=1}^{n} f_k \cdot B_{n,k}\left(g_1, \dots, g_{n+1-k}\right), \qquad n \geq 1.$$

Example 40: First coefficients of the concatenation of series.

Let $f(t) = f_0 + f_1t + f_2t^2 + \dots$ and $g(t) = g_1t + g_2t^2 + g_3^3 + \dots$, then by theorem 18

$$h(t) = f_0 + f_1g_1t + \left(f_2g_1^2 + f_1g_2\right)t^2 + \left(f_3g_1^2 + 2f_2g_1g_2 + f_1g_3\right)t^3 + \left(f_4g_1^4 + 3f_3g_1^2g_2 + f_2g_2^2 + 2f_2g_1g_3 + f_1g_4\right)t^4 + \dots$$

In defs. 9 and 48 we have used the Legendre transform without formally defining it. For formal power series, it is once again a statement about combinatorics of their coefficients, irrespective of analytic properties of functions [153, 212].

Definition 53. Let $f(t)$ be a formal power series (def. 51) and let $u(t) = \partial_t f(t)$ be its formal derivative. Further, let $t(u)$ be the combinatorial inverse of $u(t)$, given by Lagrange inversion (theorem 17). The *Legendre transform* of f is defined as the series

$$g(u) := -t(u) \cdot u + f(t(u)).$$

2.1.2. Divergent power series

Physics courses tend to focus heavily on Taylor expansions, supporting the impression that every physically sensible function should be identified with a convergent power series. A similarly radical view was also prominent in mathematics 200 years ago, as Borel [231] reproduces a famous quote by Abel (1826):

> Les séries divergentes sont en général quelque chose de bien fatal et c'est une honte qu'on ose y fonder aucune démonstration.

However, by now it is established that divergent series can contain a large amount of information on the "true" function they are supposed to represent. First steps in that direction were already taken in the 1800s [232]. The modern treatment is based on *Borel resummation* and, more generally, *resurgence*. This is a very active field of research with an immense literature, a starting point can be one of the reviews [233–238]. More sophisticated examples related to physics can be found in [213, 239–253].

Example 41: Divergence of the QED perturbation series.

Without any mathematical analysis of the growth behaviour of coefficients, one can conclude from physical arguments that the Dyson series (eq. (1.40)) in QED (example 22) can not be convergent [254]. The perturbative expansion parameter is the fine structure constant α [255], which has a positive value $\alpha \approx \frac{1}{137} > 0$ in nature. If the Green functions of QED were convergent functions of α around the expansion point $\alpha = 0$, then it would be possible to continue them to small negative α, where they are still convergent. Physically, a negative value of α corresponds to an "electrodynamics" where equal charges attract each other and opposite charges are repelled. By charge conservation, quantum fluctuations can only produce pairs of particles with opposite charges. In a world where $\alpha < 0$, these particles would repel each other instead of merging back to the vacuum. Consequently, the vacuum would "decay" into a large number of particles if $\alpha < 0$. The ground state of this theory would not be a vacuum state, but filled with matter. Consequently, the Green functions of QED must abruptly have different properties as soon as α becomes infinitesimally negative, they can not be analytic around $\alpha = 0$.

Definition 54. An *asymptotic power series* is a formal power series (def. 51) where the remainder term $R_N(t)$, defined by

$$f(t) =: \sum_{n=0}^{N} f_n t^n + R_N(t),$$

fulfils

$$\lim_{t\to 0} t^{-N} |R_N(t)| = 0, \qquad N \text{ fixed.}$$

Every convergent power series is asymptotic, but the converse is not true. Observe that for a convergent power series one has, instead of a limit $t \to 0$ as in def. 54,

$$\lim_{N\to\infty} |R_N(t)| = 0, \qquad t \text{ fixed.}$$

Definition 55 ([256])**.** For $k \in \mathbb{N}$, a formal power series $\sum_{n=0}^{\infty} f_n t^n$ is called *Gevrey-k* if

$$\sum_{n=0}^{\infty} \frac{f_n}{(n!)^k} t^n$$

has a positive radius of convergence.

Definition 56. Let $f(t)$ be a formal power series. The *Borel transform* of f is the power series obtained by the mapping $B : f_n \mapsto \frac{f_n}{n!}$, that is

$$f(t) = \sum_{n=0}^{\infty} f_n t^n \qquad \Leftrightarrow \qquad B[f](u) = \sum_{n=0}^{\infty} \frac{f_n}{n!} u^n.$$

The complex u-plane is called *Borel plane*. The inverse mapping $L : f_n \mapsto n! f_n$ is called *Laplace transform*.

The Borel transform is convergent near the origin if the original function is Gevrey-1 (def. 55), and this is the case we will be dealing with for the rest of the thesis.

For convergent power series, def. 56 is consistent with the ordinary analytic Laplace transform (in the variable $\frac{1}{t}$), given by the integral

$$L[f](t) = \frac{1}{t} \int_0^{\infty} \mathrm{d}u \; f(u) e^{-u\frac{1}{t}} = \int_0^{\infty} \mathrm{d}u \; e^{-u} f\left(ut\right),$$

upon recalling the definition of the Gamma function (def. 5) $\int_0^{\infty} \mathrm{d}u \; e^{-u} u^n = \Gamma(n+1) = n!$.

Example 42: Borel transform of factorially divergent series.

Consider the factorially divergent power series

$$f(t) := \sum_{n=0}^{\infty} (-1)^n n! t^n.$$

Its Borel transform (def. 56) is analytic at the origin $u = 0$,

$$B[f](u) = \sum_{n=0}^{\infty} (-1)^n \frac{n!}{n!} u^n = \frac{1}{1+u}.$$

It turns out that, starting from a divergent Gevrey-1 power series $f(t)$, performing the Borel transform and then the Laplace transform, one can arrive at a well-defined function. This is called *Borel resummation* of the series,

$$S[f](t) = L[B[f]](t) = \frac{1}{t}\int \mathrm{d}u\; B[f](u) e^{-u\frac{1}{t}}. \tag{2.3}$$

Example 43: Exponential integral.

The Borel resummation of example 42 is

$$S[f](t) = \frac{1}{t}\int_0^\infty \mathrm{d}u\; \frac{1}{1+u} e^{-u\frac{1}{t}} = \frac{1}{t} e^{\frac{1}{t}} \int_1^\infty \mathrm{d}u \frac{e^{-u\frac{1}{t}}}{u} = \frac{1}{t} e^{\frac{1}{t}} E_1\left(\frac{1}{t}\right).$$

Here we have introduced the exponential integral (incomplete Gamma function)

$$E_1(z) := \int_1^\infty \mathrm{d}t\; \frac{e^{-zt}}{t} = \int_z^\infty \mathrm{d}t\; \frac{e^{-t}}{t}.$$

The exponential integral has, for $z > 0$, the convergent series representation

$$E_1(z) = -\gamma_E - \ln|z| - \sum_{k=1}^\infty \frac{(-z)^k}{k!k}.$$

We have replaced $f(t)$ by a convergent series in $z = \frac{1}{t}$. Despite its intimidating looks, the Borel resummed function $S[f](t)$ is perfectly finite at the origin $t = 0$, and its derivatives are exactly the coefficients of the original series $f(t)$ from example 42. Unlike its Taylor series $f(t)$, the function $S[f](t)$ has a finite numeric value for $t > 0$.

Curiously, this example was given by Euler [257], 66 years before Abel's comment at the beginning of the present section.

Example 43 illustrates that the class of formal power series in one variable t is too small to capture Borel transforms, we at least need to allow for powers of exponentials such as $e^{\frac{1}{t}}$. Including also logarithms, the resulting class of series is a generalization of formal power series by the name of *transseries*, see [258] for an introduction.

Definition 57 ([259–261])**.** A *transseries* is a formal power series (def. 51) in the three monomials $t, e^{-\frac{S}{t}}$ and $\ln t$. It has the form

$$f(t) = \sum_{p=0}^\infty \sum_{q=0}^\infty \sum_{l=1}^{q-1} c_{p,q,l} \cdot t^p \cdot e^{-q\cdot\frac{S}{t}} \cdot (\ln t)^l. \tag{2.4}$$

The term $q \cdot S$ is called the *q-instanton action*, in more general cases it can also be a non-trivial function $S_q(t)$. Transseries are sufficient to express all functions definable from

addition, multiplication and exponentiation [262], and the field of transseries is closed under differentiation, integration, composition, inversion, Borel transforms and various other operations [263, 264].

As seen in example 42, the Borel transform (def. 56) of a Gevrey-1 (def. 55) power series can have poles in the Borel plane. Assume that there is a simple pole at $u = u_0$ closest to the origin,

$$B[f](u) = \phi(u) \left(1 - \frac{u}{u_0}\right)^{-\beta}, \tag{2.5}$$

where $\phi(u)$ is smooth at u_0 and $\beta \in \mathbb{R}$. This functional form has an implication for the series expansion $B[f](u) =: \sum_{n=0}^{\infty} b_n u^n$ of $B[f](u)$ near the origin $u = 0$. Namely for $n \to \infty$ the coefficients asymptotically behave like

$$b_n \sim \frac{\Gamma(n+\beta)}{\Gamma(n+1)\Gamma(\beta)} \frac{1}{u_0^n} \left(\phi(u_0) - \frac{(\beta-1)u_0\phi'(u_0)}{(n+\beta-1)} + \dots\right). \tag{2.6}$$

Since b_n are the coefficients of the Borel transform (def. 56), the coefficients of the original function $f(t)$ grow like

$$f_n \sim \frac{\Gamma(n+\beta)}{\Gamma(\beta)} \frac{1}{u_0^n} \left(\phi(u_0) - \frac{(\beta-1)u_0\phi'(u_0)}{(n+\beta-1)} + \dots\right). \tag{2.7}$$

A detailled discussion as well as many more examples and theorems regarding asymptotic power series can be found in the book [265].

Definition 58. If the coefficients of a formal power series f grow asymptotically like

$$f_n \sim S \cdot A^n \cdot \Gamma(n+\beta) \left(1 + \mathcal{O}\left(\frac{1}{(n+\beta-1)}\right)\right), \qquad n \to \infty,$$

then f is called a *factorially divergent power series* with *Stokes constant* S.

Owing to $\Gamma(n+\beta)/\Gamma(n) \sim n^\beta$, all factorially divergent power series are Gevrey-1 (def. 55).

The relationship eq. (2.7) is the first step towards a general theory of *resurgence*: We observe that the asymptotic factorial growth of the coefficients of a divergent power series contains information about poles in the Borel plane. The next step would be to examine the general form of the Laplace transform of eq. (2.5), which is the Borel resummation of $f(t)$. One finds that the coefficients of the subleading corrections in eq. (2.7) reappear as coefficients of the perturbative fluctuations around the 1-instanton term $e^{-\frac{S}{t}}$ (def. 57) of the resummed transseries.

On the other hand, the subleading corrections in eq. (2.7) are given by derivatives $\phi^{(n)}(u_0)$ of the function $\phi(u)$ from eq. (2.5). If $B[f](u)$ has a second pole, other than $u = u_0$, at $u = u_1$. Then the asymptotic growth of the expansion coefficients of $\phi(u)$ around u_0 will be dominated by the pole at u_1, in the same way that the pole at u_0 determines the coefficients b_n in eq. (2.6). This construction can be continued indefinitely, until eventually all correction coefficients in def. 58 are expressed via the locations and exponents of poles of the Borel transform. They in turn determine the fluctuations around all q-instanton terms in the resummed function $B[f](t)$ (eq. (2.3)).

In this heuristic account, we have skipped all sorts of difficulties which can potentially appear. The detailed mathematical theory of resurgence was developed by Ecalle [266], by now there are comprehensive reviews such as [236, 237]. Some particularly instructive cases are used in [249] to compute asymptotic expansions.

In practical calculations, we often only know a finite set of coefficients $\{f_n\}$ and we want to determine the subleading corrections of factorially divergent powerseries (def. 58), after stripping off a known factorial growth. That is, we want to compute the constants $\{a_j\}$ for in the asymptotic expansion

$$f_n \sim a_0 + a_1 \frac{1}{n} + a_2 \frac{1}{n^2} + \mathcal{O}\left(\frac{1}{n^3}\right), \qquad n \to \infty. \tag{2.8}$$

Formally, the coefficients can be extracted from their definition, like $a_0 = \lim_{n\to\infty} f_n$, but this procedure is imprecise unless we know f_n for very high n. It is more practical to algebraically eliminate subleading corrections. Define a discrete series derivation operator

$$\Delta f_n := f_{n+1} - f_n. \tag{2.9}$$

With this operator, we find

$$\Delta\left(nf\right) = (n+1)f_{n+1} - nf_n = a_0 + \mathcal{O}\left(\frac{1}{n^2}\right).$$

Th quantity $\Delta(nf)$ can be expected to converge to a_0 more quickly than f_n itself.

Definition 59 ([267])**.** Assume a sequence $\{f_n\}$ behaves asymptotically like eq. (2.8). Let $\Delta(f) := \{f_{n+1} - f_n\}$, then the order-$k$ *Richardson extrapolation* is the sequence

$$R_k[f] := \frac{1}{k!}\Delta^k\left(n^k f\right) = a_0 + \mathcal{O}\left(\frac{1}{n^{k+1}}\right).$$

The order-k Richardson extrapolation operator is only applicable if we know at least $k+1$ elements of the sequence $\{f_n\}$. Moreover, the cancellations of small differences in computing $\Delta^k(n^k f)$ usually require that we know the numbers f_n to arbitrary precision, and not just as numerical estimates.

The higher asymptotic coefficients $a_{j>0}$ can be extracted by applying Richardson extrapolation (def. 59) to a sequence where lower coefficients are subtracted, for example

$$\Delta\left(n^2(f-a_0)\right) = (n+1)^2(f_{n+1}-a_0) - n^2(f_n - a_0) = a_1 + \mathcal{O}\left(\frac{1}{n^2}\right).$$

2.1.3. Basics of Hopf algebras

In the present section, we review those aspects of Hopf algebra theory which become important later in the thesis. A comprehensive introduction to Hopf algebras is contained in the book [268]. Here and in the following, $\otimes$ denotes a tensor product while $\circ$ denotes concatenation of maps.

Definition 60. Let K be a field. An associative, unital *algebra* A over K is a vector space endowed with two vector space homomorphisms

$$\begin{aligned} m : A \otimes A \to A \qquad & \text{(product)} \\ \mathbb{1} : K \to A \qquad & \text{(unit),} \end{aligned}$$

subject to the conditions

$$\begin{aligned} m \circ (m \otimes \mathrm{id}) = m \circ (\mathrm{id} \otimes m) \qquad & \text{(associativity of } m\text{)} \\ m \circ (\mathbb{1} \otimes \mathrm{id}) = m \circ (\mathrm{id} \otimes \mathbb{1}) = \mathrm{id} \qquad & (\mathbb{1} \text{ is a left and right unit}). \end{aligned}$$

Strictly speaking, there is a unit element 1 in the field K, and the homomorphism $\mathbb{1}$, and a unit element in the algebra. We will slightly abuse notation by calling the latter also $\mathbb{1}$, namely we identify $\mathbb{1}(1) =: \mathbb{1} \in A$. Further, we will generally assume our algebras to be commutative, that is $m(a, b) = m(b, a)\ \forall a, b \in A$.

Example 44: Algebra of quadratic matrices.

For $n \in \mathbb{N}$, the $n \times n$-matrices are the elements of an algebra, where m is matrix multiplication and $\mathbb{1}$ is the identity matrix.

Definition 61. Let K be a field. A coassociative couintal *coalgebra* C over K is a vector space equipped with two vector space homomorphisms

$$\begin{aligned} \Delta : C \to C \otimes C \qquad & \text{(coproduct)} \\ \tilde{\mathbb{1}} : C \to K \qquad & \text{(couint)} \end{aligned}$$

subject to the conditions

$$\begin{aligned} (\mathrm{id} \otimes \Delta) \circ \Delta = (\Delta \otimes \mathrm{id}) \circ \Delta \qquad & \text{(coassociativity of } \Delta\text{)} \\ \left(\tilde{\mathbb{1}} \otimes \mathrm{id}\right) \circ \Delta = \left(\mathrm{id} \otimes \tilde{\mathbb{1}}\right) \circ \Delta = \mathrm{id} \qquad & (\tilde{\mathbb{1}} \text{ is a left and right unit}). \end{aligned}$$

Definition 62. A coalgebra C is *cocommutative* if the two factors of the coproduct are interchangeable, that is, if for all elements $h \in C$,

$$\Delta(h) = \sum_i h'_i \otimes h''_i = \sum_i h''_i \otimes h_i.$$

Definition 63. The *augmentation ideal* Aug is the kernel of $\tilde{\mathbb{1}}$. By P_{Aug} we denote the projection to the augmentation ideal such that the identity map is $\mathrm{id} = P_{\mathrm{Aug}} + \tilde{\mathbb{1}}$.

Definition 64. The *reduced coproduct* of a coalgebra $C \ni h$ is

$$\Delta_1(h) := (P_{\mathrm{Aug}} \otimes P_{\mathrm{Aug}})\Delta(h).$$

Definition 65. Let C be a coalgebra. An element $h \in C$ is called *primitive* if $\Delta(h) = h \otimes 1 + 1 \otimes h$, or equivalently $\Delta_1(h) = 0$. An element $h \in C$ is called *grouplike* if $\Delta(h) = h \otimes h$.

Example 45: Polynomials as algebra and coalgebra.

Let K be a field. The polynomials $K[t]$ in one variable t are an algebra, where m is the ordinary product and $\mathbb{1}$ is the polynomial $1t$. For example, let $K[t] \ni f = 1 + 3t^2$ and $K[t] \ni g = 2 + t$, then

$$m(f, g) = f \cdot g = (1 + 3t^2)(2 + t) = 2 + t + 6t^2 + 3t^3.$$

Polynomials can also be given the structure of a coalgebra by the following construction: First, define the counit $\tilde{\mathbb{1}}(t^n) := \delta_{n,0} \in K$. Consequently, the augmentation ideal (def. 63) are all those polynomials which are not constants.

Next, we let $\Delta(t) := 1 \otimes t + t \otimes 1$. This implies that the polynomial t is a primitive element (def. 65). Then, by the homomorphism property $\Delta(ab) = \Delta(a)\Delta(b)$, one finds the coproduct of any monomial,

$$\Delta(t^n) = \sum_{j=0}^{n} \binom{n}{j} t^j \otimes t^{n-j}, \qquad \tilde{\mathbb{1}} t^n = \delta_{n,0} \in K,$$

The two factors in the tensor product can be exchanged, the coproduct is cocommutative (def. 62). By linearity, one obtains the coproduct of any polynomial, for example

$$\Delta(1 + 3t^2) = 1 \cdot \Delta(t^0) + 3 \cdot \Delta(t^2) = 1 \otimes 1 + 3\left(1 \otimes t^2 + 2t \otimes t + t^2 \otimes 1\right)$$
$$\Delta(2 + t) = 2(1 \otimes 1) + 1 \otimes t + t \otimes 1.$$

Definition 66. Let K be a field. A *bialgebra* B over K is a vector space over K endowed with the vector space homomorphisms

$m : B \otimes B \to B$	(product)
$\mathbb{1} : K \to B$	(unit)
$\Delta : B \to B \otimes B$	(coproduct)
$\tilde{\mathbb{1}} : B \to K$	(counit)

such that $(B, m, \mathbb{1})$ is an algebra (def. 60), and $(B, \Delta, \tilde{\mathbb{1}})$ is a coalgebra (def. 61), and Δ and $\tilde{\mathbb{1}}$ are morphisms of the algebra $(B, m, \mathbb{1})$. Explicitly, the latter reads

$$\begin{aligned}\Delta \circ m &= (m \otimes m) \circ (\mathrm{id} \otimes \mathrm{flip} \otimes \mathrm{id}) \circ (\Delta \otimes \Delta)\\ \mathbb{1} \otimes \mathbb{1} &= \Delta \circ \mathbb{1}\\ \tilde{\mathbb{1}} \otimes \tilde{\mathbb{1}} &= \tilde{\mathbb{1}} \circ \Delta\\ \tilde{\mathbb{1}} \circ \mathbb{1} &= \mathrm{id},\end{aligned}$$

where $\mathrm{flip}(a \otimes b) = b \otimes a$ denotes exchange of two arguments

Example 46: Polynomials as bialgebra.

In example 45, we saw that the polynomials $K[t]$ form an algebra and a coalgebra. In fact, they form a bialgebra. For the example polynomials above, compatibility of the product and the coproduct reads

$$\begin{aligned}&\Delta \circ m(f, g) = \Delta\left(2 + t + 6t^2 + 3t^3\right)\\ &= 2(1 \otimes 1) + 1 \otimes t + t \otimes 1 + 6(1 \otimes t^2 + 2t \otimes t + t^2 \otimes 1)\\ &\quad + 3\left(1 \otimes t^3 + 3t \otimes t^2 + 3t^2 \otimes t + t^3 \otimes 1\right)\\ &= m\left(1 \otimes 1 + 3\left(1 \otimes t^2 + 2t \otimes t + t^2 \otimes 1\right), 2(1 \otimes 1) + t \otimes 1 + 1 \otimes t\right) = m\left(\Delta f, \Delta g\right).\end{aligned}$$

Definition 67. A *Hopf algebra* H over K is a bialgebra (def. 66) equipped with a linear map

$$S : H \to H \qquad \text{(antipode)}$$

such that

$$m\left(S \otimes \mathrm{id}\right)\Delta = m\left(\mathrm{id} \otimes S\right)\Delta = \mathbb{1} \circ \tilde{\mathbb{1}}.$$

Automatically, $S(\mathbb{1}) = \mathbb{1}$. Def. 67 together with def. 63 implies for the antipode:

$$S(h) = -m\left(S \otimes P_{\mathrm{Aug}}\right)\Delta(h), \qquad h \in \mathrm{Aug}\,. \tag{2.10}$$

For a primitive (def. 65) element $h \in H$ we immediately find

$$S(h) = -h. \tag{2.11}$$

Similarly, a grouplike element $h \in H$ has $S(h) = h^{-1}$, such that $m(h \otimes h^{-1}) = \mathbb{1}$.

Definition 68. A Hopf algebra H is *graded* if

$$H = \bigoplus_{k=0}^{\infty} H^{(k)},$$
$$\Delta H^{(n)} \subseteq \sum_{i+j=n} H^{(i)} \otimes H^{(j)}$$
$$H^{(i)} \cdot H^{(j)} \subseteq H^{(i+j)}.$$

For $h \in H$, the degree is denoted $|h| \in \mathbb{N}_0$, that is $|h| = n \Leftrightarrow h \in H^{(n)}$. We let $Y : H \to H$ be the linear operator counting the degree,

$$Y(h) = |h| \cdot h \qquad \forall h \in H.$$

The degree counting operator is a *derivation*, that means, for $h_1, h_2 \in H$ it fulfils

$$Y(h_1 \cdot h_2) = Y(h_1) \cdot h_2 + h_1 \cdot Y(h_2). \tag{2.12}$$

If, in a graded Hopf algebra, $H^{(0)} = K\mathbb{1}$, then it is called *connected*. In that case eq. (2.10) is sufficient to uniquely define an antipode, therefore, every graded connected bialgebra is automatically a Hopf algebra.

Example 47: Polynomials as Hopf algebra.

The bialgebra of polynomials (example 46) is actually a graded, connected, cocommutative Hopf algebra H_P. The grade of a polynomial is the exponent of its highest monomial. The operator Y is a derivation (eq. (2.12)), for example

$$\begin{aligned} Y\big((3t^2+1)(t^4-t^2)\big) &= Y(3t^6 - 2t^4 - t^2) = 6(3t^6 - 2t^4 - t^2) = 6(3t^2+1)(t^4-t^2) \\ &= 2(3t^2+1)(t^4-t^2) + (3t^2+1)4(t^4-t^2) \\ &= Y(3t^2+1)\cdot(t^4-t^2) + (3t^2+1)\cdot Y(t^4-t^2). \end{aligned}$$

H_P is connected because there is a unique degree zero polynomial $\mathbb{1} = 1 \in H_P$, not to be confused with e.g. the polynomial 5, which is $5 \in K$ multiplied with $1 \in H_P$. So the grade zero component (def. 68) is indeed $H_P^{(0)} = K \cdot \mathbb{1}$.

Finally, H_P has an antipode. Trivially, $S(\mathbb{1}) = \mathbb{1} \in H_P$. The monomial t is primitive, its antipode is $S(t) = -t$. Using eq. (2.10), we find the antipode

$$S(t^2) = -2S(t)t - S(1)t^2 = 2t^2 - t^2 = t^2.$$

Generally, $S(t^n) = (-1)^n t^n = (-t)^n$ as can be seen from the induction step

$$S(t^n) = -\sum_{k=0}^{n} \binom{n}{k} S(t^k) P_{\mathrm{Aug}}(t^{n-k}) = -\sum_{k=0}^{n-1} \binom{n}{k} (-1)^k 1^{n-k} t^n = -(1-1)^n t^n + (-1)^n t^n.$$

Definition 69. A *Hopf ideal* I of a Hopf algebra H (def. 67) is a subset $I \subset H$ such that

$$\begin{aligned} H \cdot I &\subset I \\ \Delta(I) &\subset H \otimes I + I \otimes H \\ S(I) &\subset I \end{aligned}$$

If $I \subset H$ is a Hopf ideal then the quotient Hopf algebra mimics the usual construction of dividing a ring by an ideal, the elements are unique up to addition of elements of the ideal:

$$\frac{H}{I} := \{h \in H \text{ where } h_1 = h_2 \Leftrightarrow h_1 - h_2 \in I\}\,. \tag{2.13}$$

Expressed differently, dividing by an ideal means that all elements of the ideal are set to zero. Consequently, their coproduct and antipode are also set to zero.

Lemma 19. Let H be a Hopf algebra (def. 67) and $I \subset H$ a Hopf ideal (def. 69). Then, the quotient $U := \frac{H}{I}$ (eq. (2.13)) is a sub Hopf algebra, that is,

$$\Delta(U) \subseteq U \otimes U, \qquad S(U) \subseteq U.$$

We have seen in def. 65 that primitive elements in the Hopf algebra are characterized by a particularly simple coproduct. This notion can be generalized, namely, we count how often a coproduct has to be applied recursively before the remainder becomes primitive.

Definition 70. The *iterated coproduct* of a Hopf algebra H is

$$\Delta^1 := \Delta, \qquad \Delta^k := (\Delta \otimes \mathrm{id} \otimes \cdots \otimes \mathrm{id})\,(\Delta \otimes \mathrm{id} \cdots \otimes \mathrm{id}) \cdots (\Delta \otimes \mathrm{id})\,\Delta.$$

It is well-defined thanks to coassociativity (def. 61) of Δ. Further, using the projector P_{Aug} (def. 63), we define the iterated reduced coproduct,

$$\Delta_0 := P_{\mathrm{Aug}}, \qquad \Delta_1 := (P_{\mathrm{Aug}} \otimes P_{\mathrm{Aug}})\,\Delta, \qquad \Delta_k := P_{\mathrm{Aug}}^{\otimes(k+1)} \Delta^k.$$

The iterated reduced coproduct is a generalization of the reduced coproduct Δ_1 from def. 64. It induces the *coradical filtration*

$$H^0 \subset H^1 \subset \ldots \qquad \text{where} \qquad H^n := \left\{x \in H \middle| \Delta_n(x) = 0\right\}. \tag{2.14}$$

Definition 71. Let $H \ni h$ be a Hopf algebra. Using the iterated coproduct (def. 70), the *coradical degree* of h is defined as

$$\operatorname{cor}(h) = n \quad \Leftrightarrow \quad \Delta_n = 0 \text{ and } \Delta_k \neq 0 \quad \forall k < n.$$

An element $h \in H$ is primitive (def. 65) if and only if it has coradical degree one. The coradical filtration is not to be confused with the grading (def. 68). But there is the bound

$$\operatorname{cor}(h) \leq |h| \qquad \forall h \in H. \tag{2.15}$$

Example 48: Polynomials, coradical degree.

Using the coproduct (example 45) of polynomials, one finds that

$$\begin{aligned} \Delta^1(t^2) &= \Delta(t^2) = \mathbb{1} \otimes t^2 + 2t \otimes t + t^2 \otimes \mathbb{1}, \qquad \Delta_1(t^2) = 2t \otimes t \\ \Delta^2(t^2) &= \mathbb{1} \otimes \mathbb{1} \otimes t^2 + 2(\mathbb{1} \otimes t + t \otimes \mathbb{1}) \otimes t + \Delta(t^2) \otimes \mathbb{1}, \qquad \Delta_2(t^2) = 0 \end{aligned}$$

and hence $\operatorname{cor}(t^2) = 2$. A simple inductive proof shows that $\operatorname{cor}(t^n) = n$.

The homomorphisms of a Hopf algebra H can be given the structure of a cochain complex as follows [269–271]. For $n \in \mathbb{N}_0$, the n-cochains are the elements of $\operatorname{Hom}(H, H^{\otimes n})$, that is, linear maps $L_n : H \to H^{\otimes n}$. Here, $H^{\otimes 0} = \mathbb{K}$ is the underlying field. The coboundary operator is

$$\begin{aligned} b_n &: \operatorname{Hom}(H, H^{\otimes n}) \to \operatorname{Hom}(H, H^{\otimes (n+1)}) \\ b_n L_n &:= (\operatorname{id} \otimes L_n)\, \Delta + \sum_{j=1}^{n} \Big((-1)^j \operatorname{id}^{\otimes (j-1)} \otimes \Delta \otimes \operatorname{id}^{\otimes (n-j)} \Big) L_n + (-1)^{n+1} L_n \otimes \mathbb{1}. \end{aligned}$$

We will only need the first two instances,

$$\begin{aligned} b_0 L_0 &= m\, (\operatorname{id} \otimes L_0)\, \Delta - \mathbb{1} L_0 \\ b_1 L_1 &= (\operatorname{id} \otimes L_1)\, \Delta - \Delta L_1 + L_1 \otimes \mathbb{1}. \end{aligned}$$

Definition 72. Let H be a Hopf algebra (def. 67) and L_n be a homomorphism $H \to H^{\otimes (n+1)}$. If $b_n L_n = 0$ then L_n is called *n-cocycle*. If $L_n = b_{n-1} M_{n-1}$ for a homomorphism M_{n-1}, then L_n is called *n-coboundary*.

Automatically, every n-coboundary is also a n-cocycle because the coassociativity of Δ (def. 61) implies $b_{n+1} \circ b_n = 0$. The quotient space, that is, those n-cocycles which are not n-coboundaries, is called the n^{th} cohomology group.

Definition 73. Let H be a Hopf algebra. A *Hochschild 1-cocycle* is a homomorphism $B_+ : H \to H$ such that, for all $h \in H$,

$$\Delta\left(B_+(h)\right) = B_+(h) \otimes \mathbb{1} + (\mathrm{id} \otimes B_+)\,\Delta(h).$$

Lemma 20. Hochschild-1 cocycles B_+ (def. 73) have the following properties:

1. The reduced coproduct (def. 64) is $\Delta_1\left(B_+(h)\right) = h \otimes B_+(\mathbb{1}) + (\mathrm{id} \otimes B_+)\Delta_1(h)$.
2. If B_+ is a 1-cocycle, then from any homomorphism $L_0 : H \mapsto \mathbb{K}$ we obtain another 1-cocycle by adding the 0-coboundary $b_0 L_0$ to B_+.
3. $B_+(\mathbb{1})$ is primitive (def. 65) and it has no freedom to add 0-coboundaries.
4. B_+ increases the coradical degree (def. 71) by exactly one.

Proof. (1) $(P_{\mathrm{Aug}} \otimes P_{\mathrm{Aug}})\Delta(B_+(h)) = (P_{\mathrm{Aug}} \otimes P_{\mathrm{Aug}})\,(\mathrm{id} \otimes B_+)\,(\mathbb{1} \otimes h + h \otimes \mathbb{1} + \Delta_1(h))$
(2) If we add a 0-coboundary $L_1 = b_0 L_0$ then $b_1(B_+ + L_1) = b_1 B_+ + b_1 b_0 L_0 = b_1 B_+$ since $b_1 b_0 = 0$. Hence, $(B_+ + L_1)$ is a 1-cocycle, fulfilling $\Delta(B_+(h) + L_1(h)) = (B_+(h) + L_1(h)) \otimes \mathbb{1} + (\mathrm{id} \otimes (B_+ + L_1))\Delta(h)$.
(3) Every homomorphism $L_0 : H \to \mathbb{K}$ maps $\mathbb{1} \mapsto 1 \in \mathbb{K}$. Therefore, $b_0 L_0(\mathbb{1}) = (\mathrm{id} \otimes L_0)(\mathbb{1} \otimes \mathbb{1}) - L_0(\mathbb{1}) \otimes \mathbb{1} = 0$. Consequently, a 0-boundary necessarily vanishes when applied to $\mathbb{1}$ and $B_+(\mathbb{1}) + b_0 L_0(\mathbb{1}) = B_+(\mathbb{1})$. Its coproduct is

$$B_+(\mathbb{1}) \otimes \mathbb{1} + (\mathrm{id} \otimes B_+)\,(\mathbb{1} \otimes \mathbb{1}) = B_+(\mathbb{1}) \otimes \mathbb{1} + \mathbb{1} \otimes B_+(\mathbb{1}),$$

which certifies that $B_+(\mathbb{1})$ is primitive (def. 65).
(4) Induction on the coradical degree. Let h have coradical degree n, so $\Delta_{n-1}(h) \neq 0$.

$$\Delta(B_+(h)) = B_+(h) \otimes \mathbb{1} + (\mathrm{id} \otimes B_+)(h \otimes \mathbb{1} + \mathbb{1} \otimes h + \Delta_1(h)) = \ldots + h \otimes B_+(\mathbb{1}) + \ldots$$

It is $\Delta_n = (\Delta_{n-1} \otimes P_{\mathrm{Aug}})\Delta$. This coproduct does not vanish since $P_{\mathrm{Aug}} B_+(\mathbb{1}) \neq 0$ and $\Delta_{n-1}(h) \neq 0$. But all higher ones vanish since $\Delta_1(B_+(\mathbb{1})) = 0$ by (2). □

Definition 74. Let H be a Hopf algebra (def. 67) and A an algebra (def. 60). An A-valued *character* is a map

$$\phi : H \to A,$$

linear under multiplication, that is, $\phi(m_H(h_1, h_2)) = m_A(\phi(h_1) \otimes \phi(h_2))$ where m_H is the multiplication in H and m_A is the multiplication in A.

Definition 75. Let $\phi, \psi : H \to A$ be two characters (def. 74) from a Hopf algebra H to an algebra A. The *convolution product* $\phi \star \psi$ is again a character, defined as

$$\phi \star \psi = m_A(\phi \otimes \psi)\Delta.$$

Together with the convolution product $\star$, the characters $H \to A$ form a group G_A^H. Using def. 67, one confirms that the inverse of a character $\phi \in G_A^H$ is given by

$$\phi^{-1} = \phi \circ S. \tag{2.16}$$

Coassociativity of the coproduct (def. 61) implies associativity of the convolution product,

$$(\phi_1 \star \phi_2) \star \phi_3 = \phi_1 \star (\phi_2 \star \phi_3)\,.$$

Example 49: Polynomials, Hopf algebra characters.

Let $H_P = K[t]$ from example 47. A group $G_K^{H_P}$ of K-valued characters ϕ_t on H_P is given by the evaluation at $a \in K$. Namely, let $p \in H_P$, then

$$\phi_a \in G_K^{H_P}, \qquad \phi_a(p) = p(a) \in K.$$

This group $G_K^{H_P}$ with operation $\star$ is isomorphic to the group K under addition. Using the coproduct from example 45, we see that the basis elements behave as expected:

$$(\phi_a \star \phi_b)\,(t^n) = m\,(\phi_a \otimes \phi_b)\,\Delta(t^n) = (a+b)^n = \phi_{a+b}(t^n).$$

The antipode from example 47 gives the inverse character according to eq. (2.16),

$$\left(\phi_a \star \phi_a^{-1}\right)(t^n) = m\,(\phi_a \otimes \phi_a \circ S) \sum_{j=0}^{n} \binom{n}{j} t^j \otimes t^{n-j} = m\,(\phi_a \otimes \phi_a) \sum_{j=0}^{n} \binom{n}{j} t^j \otimes (-t)^{n-j}$$
$$= \sum_{j=0}^{n} \binom{n}{j} a^j \otimes (-a)^{n-j} = 0^n = \phi_0(t^n) = \phi_{a-a}(t^n).$$

Recall that the neutral element of addition is indeed 0, not 1.

We remark that the behaviour of many familiar functions under addition of their arguments can be expressed through a coalgebra [272]. Another such case, apart from polynomials, are trigonometric functions such as $\sin(a+b) = \sin(a)\cos(b) + \cos(b)\sin(a) =: (\Delta \sin)\,(a, b)$. Especially, the exponential function $e^{a+b} = e^a \cdot e^b$ amounts to a grouplike (def. 65) element, $\Delta e^{\cdot} = e^{\cdot} \otimes e^{\cdot}$. This case will become important later in section 3.2.3.

Theorem 21 (Milnor-Moore-Cartier-Quillen [273, 274])**.** The dual of a Hopf algebra is the universal enveloping algebra of a Lie algebra.

The character group G_K^H (def. 74) is a Lie group, see [275, 276] for details.

Definition 76. An *infinitesimal character* is a character (def. 74) $\sigma : H \to A$ which fulfils, for $h_1, h_2 \in H$,

$$\sigma(h_1 h_2) = \tilde{\mathbb{1}}(h_1)\sigma(h_2) + \tilde{\mathbb{1}}(h_2)\sigma(h_1).$$

The set of all infinitesimal characters form a Lie algebra $\mathfrak{g}_A^H$ with Lie bracket given by the convolution product (def. 75): $[\sigma_1, \sigma_2] := \sigma_1 \star \sigma_2 - \sigma_2 \star \sigma_1$.

The elements of $\mathfrak{g}_A^H$ act as generators of the Lie group G_A^H by the exponential map

$$G_A^H \ni \phi = \exp^\star(\sigma) := \sum_{n=0}^{\infty} \frac{1}{n!}\sigma^{\star n} = \tilde{\mathbb{1}} + \sigma + \frac{1}{2}\sigma \star \sigma + \dots . \tag{2.17}$$

The action of the exponential map on the Hopf algebra H itself justifies the notions of primitive and grouplike elements (def. 65): If $p \in H$ is primitive, then

$$H \ni g := \mathbb{1} + p + \frac{1}{2}p^2 + \ldots = \exp(p) \tag{2.18}$$

is grouplike, as can be verified by explicitly using $\Delta(p) = p \otimes \mathbb{1} + \mathbb{1} \otimes p$. In a Hopf algebra, the set of all grouplike elements forms a group under multiplication m.

Example 50: Polynomials, infinitesimal characters.

Polynomials can trivially be identified with their Taylor series at the origin. Any character ϕ_a (example 49) is given by the series

$$\phi_a = \exp\left(a \left.\frac{\partial}{\partial t}\right|_{t=0}\right).$$

The infinitesimal characters are thus the first derivatives, $\sigma_a = a\partial_t|_{t=0}$. They extract the linear coefficient of a polynomial. They fulfil the condition def. 76 because the product of two polynomials can only have a linear term if one of the two factors contains a constant term. But $\tilde{\mathbb{1}}$ is exactly the projection onto constants, namely for two monomials

$$\begin{aligned} \sigma_a(t^m) &= a\partial_t(t^m)_{t=0} = am \cdot t^{m-1}|_{t=0} = am \cdot \delta_{m=1} \\ \sigma_a(t^m \cdot t^n) &= a\partial_t(t^{m+n})_{t=0} = a(m+n)\delta_{m+n=1} = \tilde{\mathbb{1}}(t^n)\sigma_a(t^m) + \tilde{\mathbb{1}}(t^m) \cdot \sigma_a(t^n). \end{aligned}$$

2.1.4. Faà di Bruno Hopf algebra

In section 2.1.3, we have used polynomials as a central example for a Hopf algebra, where the coproduct merely corresponds to the usual product between two polynomials. The Faà di Bruno Hopf algebra H_{FdB} [277–280] expresses formal power series, but, contrary to the polynomials, the coproduct operation is not multiplication of series, but concatenation. Also, the algebraic perspective is different: The algebra elements are no longer the power series themselves, but rather their coefficient extraction operators. Let $f(t)$ be a formal power series (def. 51), then the elements of H_{FdB} are the operators $\mathfrak{C}_n$ for $n \in \mathbb{N}$, extracting the n^{th} coefficient,

$$\mathfrak{C}_n(f) = f_n = [t^n]f(t) = \frac{1}{n!}\partial_t^n f(t)\Big|_{t=0}.$$

A formal power series $f(t)$ over a field K can then be viewed as a linear map that associates a value – the coefficient $f_n \in K$ – to each of the algebra elements $\mathfrak{C}_n$:

$$\begin{aligned} f : H_{\mathrm{FdB}} &\to K[t] \\ \{f_1, f_2, \ldots\} &\mapsto f_1 t + f_2 t^2 + \ldots. \end{aligned}$$

We demand that this map is a character (def. 74) of the Hopf algebra, where the product of power series is concatenation, not ordinary multiplication:

$$f \star g := f \circ g.$$

On the other hand, the $\star$ product of characters amounts to the coproduct in the Hopf algebra,

$$(f \star g)\,\mathfrak{C}_n = \mathfrak{C}_n\,(f(g(t))) = m \circ (f(t) \otimes g(t))\,\Delta\mathfrak{C}_n. \tag{2.19}$$

In this way, one obtains the coproduct of the Faà di Bruno Hopf algebra. Observe the notation: The operator $\mathfrak{C}_n$ extracts coefficients of the power series, and hence, it effectively acts to the left, and the notation is consistent with section 2.1.3. From Faà di Bruno's theorem 18, we know the coefficients of series concatenation, namely

$$(f \star g)\,\mathfrak{C}_n = \sum_{k=1}^{n} \frac{k!}{n!} f_k \cdot B_{n,k}\left(1!g_1, \ldots, (n+1-k)!g_{n+1-k}\right).$$

In this formula, f_j and g_j are once again coefficients, extracted from the power series f, g by suitable operators $\mathfrak{C}_j$. Therefore, the coproduct of the Faà di Bruno Hopf algebra reads

$$\Delta\mathfrak{C}_n = \sum_{k=1}^{n} \frac{k!}{n!} \mathfrak{C}_k \otimes B_{n,k}\left(1!\mathfrak{C}_1, 2!\mathfrak{C}_2, \ldots, (n+1-k)!\mathfrak{C}_{n+1-k}\right). \tag{2.20}$$

Generally, $f(g(t))$ and $g(f(t))$ are not the same series, while $f(t)g(t)$ and $g(t)f(t)$ are. Consequently, the coproduct eq. (2.20) is not cocommutative (def. 62) while the one of the polynomials (example 45) is.

From eq. (2.20), one obtains $\Delta(\mathfrak{C}_1) = \mathfrak{C}_1 \otimes \mathfrak{C}_1$, this element is grouplike (def. 65). By rescaling all involved power series, we set $\mathfrak{C}_1 = \mathbb{1} \in H_{\mathrm{FdB}}$ to ensure that $\mathfrak{C}_1$ has an inverse. The Faà di Bruno Hopf algebra is connected. The inverse character is given by the antipode eq. (2.16). The antipode is obtained either by demanding that the character f^{-1} be the

inverse series under concatenation, or by using eq. (2.10). Unsurprisingly, the result in both cases is the Lagrange inversion formula (theorem 17), where $f_1 = 1$:

$$S\mathfrak{C}_n = \frac{1}{n!}\sum_{k=1}^{n-1}(-1)^k B_{n-1+k,k}\left(0, 2!\mathfrak{C}_2, 3!\mathfrak{C}_3, \ldots\right) = \frac{1}{n!}\sum_{k=1}^{n-1} B_{n-1+k,k}\left(0, -2!\mathfrak{C}_2, -3!\mathfrak{C}_3, \ldots\right). \tag{2.21}$$

Example 51: Faà di Bruno Hopf algebra, coproducts and antipodes.

The first coproducts eq. (2.20) are

$$\begin{aligned}
\Delta(\mathfrak{C}_2) &= \mathfrak{C}_2 \otimes \mathbb{1} + \mathbb{1} \otimes \mathfrak{C}_2 \\
\Delta(\mathfrak{C}_3) &= \mathfrak{C}_3 \otimes \mathbb{1} + \mathbb{1} \otimes \mathfrak{C}_3 + 2\mathfrak{C}_2 \otimes \mathfrak{C}_2 \\
\Delta(\mathfrak{C}_4) &= \mathfrak{C}_4 \otimes \mathbb{1} + \mathbb{1} \otimes \mathfrak{C}_4 + \mathfrak{C}_2 \otimes \left(\mathfrak{C}_2^2 + 2\mathfrak{C}_3\right) + 3\mathfrak{C}_3 \otimes \mathfrak{C}_2.
\end{aligned}$$

Compare this with the coefficients in example 40. The antipodes agree with example 39,

$$\begin{aligned}
S\mathfrak{C}_2 &= -\mathfrak{C}_2 \\
S\mathfrak{C}_3 &= -\mathfrak{C}_3 + 2\mathfrak{C}_2^2 \\
S\mathfrak{C}_4 &= -\mathfrak{C}_4 + 5\mathfrak{C}_2\mathfrak{C}_3 - 5\mathfrak{C}_2^3.
\end{aligned}$$

There is a beautiful graphical representation of the Faà di Bruno Hopf algebra as rooted trees. We identify $\mathfrak{C}_n$ with a vertex with n lower edges, called *hairs*. This can be motivated intuitively: $\mathfrak{C}_n$ corresponds to a term t^n in a power series, so it "takes" a value t and "returns" n copies of it, which it multiplies.

$\mathfrak{C}_1 =$  $\mathfrak{C}_2 =$  $\mathfrak{C}_3 =$  $\mathfrak{C}_4 =$ 

Figure 2.1.: Identification of the Faà di Bruno Hopf Hopf algebra elements with trees.

A concatenation $f \circ g$ of two functions corresponds to replacing the argument t of $f(t)$ with the series g, so attaching the vertices of g at the lower ends of the vertices of f. We obtain plane trees (without crossing edges) of depth two with arbitrary many vertices. A tree with n hairs contributes to $(f \circ g)\mathfrak{C}_n$, so to the coefficient t^n of $f(g(t))$. With the notation of eq. (2.20), the left factor in the tensor product corresponds to the upper vertex, the right factor is the lower vertex. Note that each tree with n hairs corresponds to a partition of $\{1, \ldots, n\}$ into k non-empty sets, where k is the number of hairs of the upper vertex. In total, $\Delta\mathfrak{C}_n$ is given by all these plane trees, so it is a sum over all such partitions. This is precisely the sum over Bell polynomials (def. 52), counting trees reproduces the formula eq. (2.20) for the coproduct.

Example 52: Series concatenation as trees.

Let us see explicitly how trees reproduce the coefficients of $f(g(t))$ from example 40. We show the trees and below them the corresponding terms in the coproduct (example 51), where the left factor is the upper vertex and the right factor are the lower vertices.

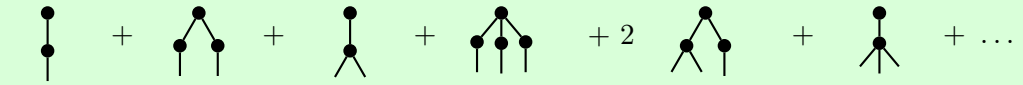

$$\mathfrak{C}_1 \otimes \mathfrak{C}_1 \;+\; \mathfrak{C}_2 \otimes \mathfrak{C}_1^2 \;+\; \mathfrak{C}_1 \otimes \mathfrak{C}_2 \;+\; \mathfrak{C}_3 \otimes \mathfrak{C}_1^3 \;+\; 2\,\mathfrak{C}_2 \otimes \mathfrak{C}_2\mathfrak{C}_1 \;+\; \mathfrak{C}_1 \otimes \mathfrak{C}_3 \;+\; \dots$$

$$f_1 g_1\, t \;+\; \left(f_2 g_1^2 \;+\; f_1 g_2\right) t^2 \;+\; \left(f_3 g_1^3 \;+\; 2\; f_2 g_2 g_1 \;+\; f_1 g_3\right) t^3 + \dots$$

Note how the combinatorial factor 2 exactly accounts for the two ways of attaching the lower vertices to the upper one, namely left or right.

Knowing the coproduct, the antipode can be constructed recursively using eq. (2.10). We skip the details, the end result is that the antipode is given by the sum of *all* trees, not just the ones of depth 2. Additionally, each vertex of the trees carries a factor -1. For any n, $S\mathfrak{C}_n$ corresponds to the sum of all those trees with exactly n leaves. There are infinitely many trees which differ from each other just by adding chains of 2-valent vertices. These infinite sums, viewed as a geometric series, eventually correspond to the factors $\frac{1}{f_1}$ in theorem 17, compare eq. (1.53). The condition $f_1 = 1$, or equivalently $\mathfrak{C}_1 = \mathbb{1}$, amounts to leaving out all such chains and keeping only non-trivial trees. Of course, working out the tree-counting with the help of set partitions reproduces the Lagrange inversion theorem 17 and eq. (2.21).

Example 53: Series inversion as trees.

Assume $\mathfrak{C}_1 = \mathbb{1}$, then there are no 2-valent vertices and the edges contribute a factor $\mathbb{1}$ to the value of a tree. To improve readability, we also leave out all + signs between the various summands.

$$\mathbb{1} \quad (-\mathfrak{C}_2) \quad (-\mathfrak{C}_3) \quad 2(-\mathfrak{C}_2)^2 \quad (-\mathfrak{C}_4) \quad 3(-\mathfrak{C}_2)(-\mathfrak{C}_3) \quad 4(-\mathfrak{C}_2)^3 \quad (-\mathfrak{C}_2)^3 \quad 2(-\mathfrak{C}_2)(-\mathfrak{C}_3)$$

$$1t \quad -\,f_2 t^2 \quad +\left(-\,f_3 + f_2^2\right)t^3 \quad +\left(-\,f_4 \quad +5 f_2 f_3 \quad -5 f_2^3\right)t^4$$

Observe that different tree topologies contribute to the same monomial at order t^4. As claimed, the end result equals the inverse series given in example 39.

$S\mathfrak{C}_n$ amounts to the sum of all trees with alternating signs. To facilitate notation, define

$$\mathfrak{B}_n := i^n S\mathfrak{C}_n. \tag{2.22}$$

This operator extracts the n-th coefficient of the inverse of a given power series,

$$f(t)\mathfrak{B}_n = i^n[t^n]f^{-1}(t) = i^n n!\left.\frac{\partial^n f^{-1}(t)}{\partial t^n}\right|_{t=0}. \tag{2.23}$$

The antipode of $\mathfrak{B}_n$ essentially extracts coefficients of f,

$$f(t)\left(S\mathfrak{B}_n\right) = f^{-1}(t)\mathfrak{B}_n = i^n[t^n]f(t) = f(t)\left(i^n\mathfrak{C}_n\right).$$

Example 54: Faà di Bruno Hopf algebra, inverse operators.

Using eq. (2.21), one finds

$$\begin{aligned}\mathfrak{B}_4 &= \left(-\mathfrak{C}_4 + 5\mathfrak{C}_2\mathfrak{C}_3 - 5\mathfrak{C}_2^3\right) i^4\\ \mathfrak{B}_5 &= \left(-\mathfrak{C}_5 + 6\mathfrak{C}_2\mathfrak{C}_4 + 3\mathfrak{C}_3^2 - 21\mathfrak{C}_2^2\mathfrak{C}_3 + 14\mathfrak{C}_2^4\right) i^5\end{aligned}$$

Up to the factors i^n, we have merely exchanged the meaning of $\mathfrak{C}_n$ and $S\mathfrak{C}_n$ with $S\mathfrak{B}_n$ and $\mathfrak{B}_n$. This appears to be a technical subtlety, but becomes convenient for the coproduct $\Delta(\mathfrak{B}_n)$. The latter now computes the coefficients of two concatenated *inverse* series. Note that by Coxeter's rule, $f^{-1}\circ g^{-1} = (g\circ f)^{-1}$, so

$$\begin{aligned}m\left(f\otimes g\right)\Delta(\mathfrak{B}_n) &= \left(f\circ g\right)\mathfrak{B}_n = \left(g^{-1}\circ f^{-1}\right)^{-1}\mathfrak{B}_n = i^n\left(g^{-1}\circ f^{-1}\right)\mathfrak{C}_n\\ &= i^n m\left(g\otimes f\right)\left(S\otimes S\right)\Delta\mathfrak{C}_n = m\left(f\otimes g\right) i^n\mathrm{flip}\left(S\otimes S\right)\Delta(\mathfrak{C}_n).\end{aligned}$$

Translating this to our graphical representation, $\mathfrak{B}_j$ equals the sum of all plane trees with exactly j leaves. Observe the difference between $\Delta(\mathfrak{B}_n)$ and $\Delta(\mathfrak{C}_n)$ (eq. (2.20)): For $\Delta(\mathfrak{C}_n)$, we sum over all trees of depth exactly two, where the upper vertex is the left factor in the tensor product, whereas for $\Delta(\mathfrak{B}_n)$, there is no restriction to the depth and the factors are exchanged. The upper part of the cut tree, which is a tree itself, represents the right factor in the tensor product. The lower part of the cut tree is a product of trees and appears to the left. One can include an additional flip operation into the definition to reverse this change.

Theorem 22. Let $\mathfrak{B}_n$ be the operator from eq. (2.22). In the graphical representation as rooted trees, where $\mathfrak{B}_n$ corresponds to the sum of all trees with n leaves, the coproduct is given by

$$\Delta(\mathfrak{B}_n) = \sum_{C=R\cup P}\mathfrak{B}_P\otimes\mathfrak{B}_R.$$

Here, C is the set of all possible cuts of the trees which separate the root from the leaves, including the trivial cuts above the root or below the leaves. Each path in the trees from above the roots to below the trees is cut exactly once. R denotes the component including the root, P is a disjoint union of trees containing all the leaves, and $\mathfrak{B}_P$ denotes the product of all the $\mathfrak{B}_j$ corresponding to the disjoint trees. The summands $\mathfrak{B}_R, \mathfrak{B}_P$ correspond to individual trees, they become well-defined tree-sums $\mathfrak{B}_n$ only in the sum over C.

Proof. The non-trivial assertion of this theorem is that, when summing over all cuts of all trees representing some $\mathfrak{B}_n$, the cut components once again add up to $\mathfrak{B}_j$, without any trees missing or doubled. On the one hand, this is a standard fact of enumerating *all* plane trees: One obtains exactly *all* trees by joining all smaller trees in all possible ways, and our cut formula reverses this operation. On the other hand, it can be shown by retreating to $\Delta(\mathfrak{C}_n)$: Cutting the trees of depth two produces all trees of depth one, that is, vertices. Using eq. (2.22), we replace each vertex with j leaves with a sum of all trees with j leaves. □

Example 55: Faà di Bruno Hopf algebra, coproduct of inverse operators.

To understand the coproduct of theorem 22, let us examine $\Delta(\mathfrak{B}_3)$ in detail. That means, we are looking for the coefficient of t^3 in the concatenation

$$g^{-1}(f^{-1}(t)) = \ldots + \left(-f_3 + 2f_2^2 - g_3 + 2g_2^2 + 2f_2g_2\right) \cdot t^3 + \ldots .$$

$\mathfrak{B}_3$ is represented by two different trees, both of which have 3 leaves. They are shown in the top row. Below them are all the possibilities of cutting them according to theorem 22. Next, we reorder the cut components to obtain $\mathfrak{B}_j$.

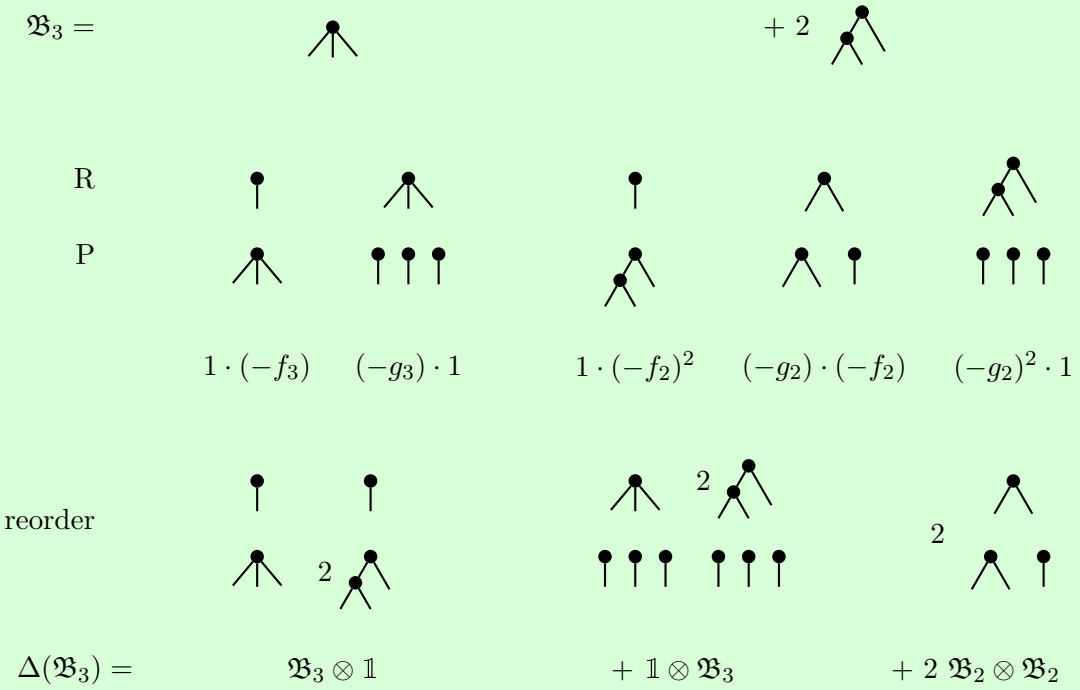

The individual trees we obtained in R and P are not necessarily Hopf algebra elements $\mathfrak{B}_j$, but, as expected, they appear in just the right multiplicities that the total sum consists of $\mathfrak{B}_j$. A similar construction produces the coproduct

$$\Delta(\mathfrak{B}_4) = \mathfrak{B}_4 \otimes \mathbb{1} + \mathbb{1} \otimes \mathfrak{B}_4 + \mathfrak{B}_2^2 \otimes \mathfrak{B}_2 + 2\mathfrak{B}_3 \otimes \mathfrak{B}_2 + 3\mathfrak{B}_2 \otimes \mathfrak{B}_3.$$

For more details about the Faà di Bruno Hopf algebra, see for example [280–282]. We remark that, instead of ordinary power series $f(t) = f_1 t + f_2 t^2 + \ldots$, it is more customary to base the whole construction on exponential power series $f(t) = f_1 \frac{t}{1!} + f_2 \frac{t^2}{2!} + \ldots$. This only changes numerical prefactors, namely, one then has to consider *all* permutations of

lower edges, not only the planar ones. For example, the factor 2 in $\Delta(\mathfrak{C}_3)$ becomes a 3, in accordance with the three ways to permute the leaves of the tree in example 52.

At least two close cousins of the Faà di Bruno Hopf algebra are worth mentioning: Firstly, the Connes-Moscovici Hopf algebra H_{CM} which appears in the study of elliptic operators on foliations [283]. Very loosely speaking, for the most simple case, if $f(t)$ is a formal power series (def. 51), then the basis elements $\delta_k \in H_{\mathrm{CM}}$ extract the coefficients of $\ln\left(\partial_t f^{-1}(t)\right)$. Thereby, δ_n are similar to $\mathfrak{B}_n$ from eq. (2.23), only that they operate on the logarithm of power series. The elements $\delta_k \in H_{\mathrm{CM}}$ can again be represented by certain rooted trees [284], see example 59.

Secondly, the Butcher group [285–288] expresses the concatenation of Runge-Kutta numerical integration methods [289, 290]. Not too surprisingly, the combinatorics of this process is once more expressible by joining certain rooted trees.

We mentioned the correspondence between trees and their generating formal power series in section 1.3.10. Now we are in the position to understand the Legendre transform (def. 53) graphically: Given some vertices, by inverting the series, compare to eq. (2.23), it produces all possible trees made from these vertices. For details on counting graphs, see [153, 212, 249, 252, 291].

Example 56: ϕ^3 theory, counting treelevel graphs.

To illustrate how the Legendre transform can in principle be used to count graphs, consider ϕ^3 theory in $D = 0$ spacetime dimensions. This means that there is no kinematic dependence, every Feynman graph evaluates to a constant number. Without integrals, the classical action (def. 7) equals the Lagrangian (example 3); it is the generating function of the vertices. The 3-valent vertex has amplitude λ_3 and an edge has amplitude $\frac{1}{p}$. The Legendre transform (def. 53) can be computed in closed form:

$$\mathcal{L}(t) = \frac{1}{2}pt^2 - \frac{\lambda_3}{3!}t^3, \qquad \frac{\partial\,\mathcal{L}}{\partial t} = pt - \frac{1}{2}\lambda_3 t^2 \qquad \left(\frac{\partial\,\mathcal{L}}{\partial t}\right)^{-1} = \frac{p - \sqrt{p^2 - 2\lambda_3 t} - p}{\lambda_3}$$

$$\begin{aligned} -\left(\frac{\partial\,\mathcal{L}}{\partial t}\right)^{-1}\cdot t + \mathcal{L}\left(\left(\frac{\partial\,\mathcal{L}}{\partial t}\right)^{-1}\right) &= \frac{p^3}{3\lambda_3^2} - \frac{pt}{\lambda_3} - \frac{\left(p^2 - 2\lambda_3 t\right)^{\frac{3}{2}}}{3\lambda_3^2} \\ &= -\frac{1}{p}\frac{t^2}{2!} - \frac{\lambda_3}{p^3}\frac{t^3}{3!} - 3\frac{\lambda_3^2}{p^5}\frac{t^4}{4!} - 15\frac{\lambda_3^3}{p^7}\frac{t^5}{5!} - 105\frac{\lambda_3^4}{p^9}\frac{t^6}{6!} - \dots \\ &= -\sum_{n=2}^{\infty}(2n-5)!!\frac{\lambda_3^{n-2}}{p^{2n-3}}\frac{t^n}{n!}. \end{aligned}$$

In the resulting series, the coefficient of $\frac{t^n}{n!}$ corresponds to all trees with n external edges. Powers of λ_3 count vertices, powers of p^{-1} count edges. Hence, there are exactly $(2n-5)!!$ trees with n external edges, and each of them contains $(n-2)$ 3-valent vertices and $2n-3$ edges (of which n are external edges). This satisfies the Euler characteristic eq. (1.44).

2.1.5. Connes-Kreimer Hopf algebra

The Faà di Bruno Hopf algebra (section 2.1.4) has a natural interpretation as rooted trees, and its coproduct is given by cutting these trees into an upper and a lower part (theorem 22). The elements $\mathfrak{B}_n$ of the (inverse) Faà di Bruno Hopf algebra are the sums of all rooted trees with n leaves. The coproduct and the antipode in the Faà di Bruno Hopf algebra do not actually require that the Hopf algebra elements are sums of *all* rooted trees, it is possible to understand these operations for each individual tree. To this end, we need a Hopf algebra where the elements are not sums of trees, but individual trees. This is the Connes-Kreimer Hopf algebra of rooted trees H_{CK} [269, 283, 292, 293]. In fact, there are several closely related Hopf algebras of rooted trees, see also [280, 294–297], the latter with the cheerful introduction "We study here a type of algebra which deserves more attention than it has been given".

In the following, we attach 1-valent vertices at the top and bottom of any tree, so the leaves are now vertices, not edges. Every edge now is incident to precisely two vertices.

Definition 77. The *Connes-Kreimer Hopf algebra* H_{CK} is a graded (def. 68) Hopf algebra (def. 67) where the basis elements are non-plane rooted trees, that means, different ways of drawing trees count as the same element. Multiplication of trees is disjoint union, the unit is the empty tree, the counit annihilates all trees but the empty tree. The coproduct is given in analogy to theorem 22: Let an admissible cut $\emptyset \neq c \subseteq E_T$ be a subset of the edges of a tree $T \in H_{\mathrm{CK}}$ such that every path from the root of T to any of its leaves contains at most one edge $e \in c$. Removing c disconnects the tree, let $R^c(T)$ be the component containing the root and $P^c(T)$ all other components. Then $T - c = P^c(T) \oplus R^c(T)$. Let $C(T)$ be the set of all cuts c, then the coproduct and antipode of H_{CK} are

$$\Delta(T) = T \otimes \mathbb{1} + \mathbb{1} \otimes T + \sum_{\emptyset \neq c \in C} P^c(T) \otimes R^c(T)$$
$$S(T) = -T - \sum_{\emptyset \neq c \in C} S\big(P^c(T)\big) R^c(T).$$

The degree of a tree is the number of vertices, counted by the operator $Y : H_{\mathrm{CK}} \to H_{\mathrm{CK}}$ according to $Y(T) = |T| \cdot T$ (def. 68).

Example 57: Rooted trees, coproducts and antipodes.

Recall the reduced coproduct from def. 70.

$$\Delta(\bullet) = \bullet \otimes \mathbb{1} + \mathbb{1} \otimes \bullet, \qquad \Delta_1(\bullet) = 0, \qquad S(\bullet) = -\bullet,$$
$$\Delta_1\Big(\begin{array}{c}\bullet\\[-2pt]\bullet\quad\bullet\end{array}\Big) = 2\,\bullet \otimes \begin{array}{c}\bullet\\[-2pt]\bullet\end{array} + \bullet\bullet \otimes \bullet, \qquad \Delta_2\Big(\begin{array}{c}\bullet\\[-2pt]\bullet\quad\bullet\end{array}\Big) = 2\,\bullet \otimes \bullet \otimes \bullet,$$
$$S\Big(\begin{array}{c}\bullet\\[-2pt]\bullet\quad\bullet\end{array}\Big) = -\begin{array}{c}\bullet\\[-2pt]\bullet\quad\bullet\end{array} + 2\,\bullet\begin{array}{c}\bullet\\[-2pt]\bullet\end{array} - \bullet\bullet\bullet.$$

Multiplicativity $\Delta(h_1 h_2) = \Delta(h_1)\Delta(h_2)$ results in (compare $\Delta(t^n)$ in example 45)

$$\Delta(\underbrace{\bullet\bullet\cdots\bullet}_{n \text{ factors}}) = \sum_{j=0}^{n} \binom{n}{j} \underbrace{\bullet\bullet\cdots\bullet}_{n-j \text{ factors}} \otimes \underbrace{\bullet\bullet\cdots\bullet}_{j \text{ factors}}.$$

The degree (def. 68) is counted by Y, this operator is a derivation (eq. (2.12)):

$$Y\Big(\ \Big) = 2\ , \qquad Y\Big(\ \Big) = 7\ = Y\Big(\ \Big)\ + \ Y\Big(\ \Big).$$

Theorem 23 (Universal property [269, Sec. 3 thm. 2])**.** Let A be an algebra and $L : A \to A$ an endomorphism. Then there is a unique morphism $U : H_{\mathrm{CK}} \to A$ such that $U \circ B_+ = B_+ \circ L$ and $U \circ m_{H_{\mathrm{CK}}} = m_A \circ U$ and $U \circ \mathbb{1}_{H_{\mathrm{CK}}} = \mathbb{1}_A \circ U$.

Especially, if A in theorem 23 is a Hopf algebra itself, then U is a Hopf algebra morphism.

Example 58: Rooted trees of Faà di Bruno Hopf algebra.

One obtains Connes-Kreimer trees for the inverse Faà di Bruno Hopf algebra by omitting the hairs,

$$\mathfrak{B}_1 = \mathbb{1}, \qquad \mathfrak{B}_2 = \bullet, \qquad \mathfrak{B}_3 = 2\ + \bullet, \qquad \mathfrak{B}_4 = 4\ + \ + 5\ + \bullet.$$

Computing the coproduct of these forests, one confirms the result of example 55.

Example 59: Rooted trees of Connes-Moscovici Hopf algebra.

The generators of the Connes-Moscovici Hopf algebra are obtained recursively by *natural growth* $N : H_{\mathrm{CK}} \to H_{\mathrm{CK}}$. This amounts to adding one new leaf at every possible vertex of the preceding forest. The first generators are

$$N(\mathbb{1}) = \bullet =: \delta_1, \qquad N(\delta_1) = \ =: \delta_2, \qquad N(\delta_2) = \ + \ =: \delta_3$$

$$N(\delta_3) = \ + \ + 3\ + \ =: \delta_4.$$

These weights can be computed from the tree factorial [284], and they show interesting behaviour in QFT [298].

Definition 78. The *1-cocycle* (def. 73) B_+ of the Connes-Kreimer Hopf algebra H_{CK} (def. 77) takes a disjoint union of trees $T_1 \cdots T_n$ as argument and joins all of them to a newly created root, producing a tree $B_+(T_1 \cdots T_n)$.

Example 60: Rooted trees, cocycle.

$B_+(\mathbb{1}) = \bullet$, $B_+(\bullet\bullet\bullet) =$  , $B_+\Big($  $\Big) =$  .

Example 61: Bamboos.

The *bamboos* are the rooted trees without branches, namely

$b_0 = \mathbb{1}$, $b_1 = \bullet$, $b_2 =$, $b_n =$  n , $Y(b_n) = nb_n$.

All bamboos can be generated from the cocycle (def. 78) by setting $b_1 = B_+(\mathbb{1})$ and $b_n = B_+(b_{n-1})$. b_n has exactly $n-1$ edges. Explicit construction gives the coproduct

$$\Delta(b_n) = \sum_{k=0}^{n} b_{n-k} \otimes b_k.$$

The coproduct of bamboos is symmetric under exchange of the two factors, and both factors consist of bamboos exclusively. Hence, the bamboos form a cocommutative (def. 62) sub Hopf algebra of H_{CK}. Especially, the sum of all bamboos is a grouplike (def. 65) element

$$G_B := \sum_{n=0}^{\infty} b_n, \quad \Rightarrow \quad \Delta(G_B) = G_B \otimes G_B.$$

The antipode of bamboos can be written as

$$S(b_n) = \sum_{k=1}^{n} (-1)^k \sum_{s_1+\ldots+s_k=n} b_{s_1} \cdots b_{s_k}.$$

We have seen in eq. (2.18) that grouplike elements are the exponential function of primitive elements. Conversely, we expect to find primitive elements by taking the "logarithm" of grouplike elements. This operation can be made precise using a Dynkin operator.

Definition 79. The *Dynkin operator* is defined to be the convolution product (def. 75) of the antipode with the degree operator (def. 68):

$$S \star Y : H_{\mathrm{CK}} \to H_{\mathrm{CK}}, \qquad (S \star Y)(h) = m\,(S \otimes Y)\,\Delta(h).$$

The Dynkin operator is an infinitesimal character def. 76. Using the cocycle property (def. 73) of B_+ (def. 78), $\Delta(B_+(h)) = B_+(h) \otimes 1 + (\mathrm{id} \otimes B_+)\,\Delta(h)$, together with $Y(\mathbb{1}) = 0$, one finds that for all $h \in H_{\mathrm{CK}}$, the coradical degree (def. 71) falls,

$$\mathrm{cor}\left((S \star Y)(h)\right) < \mathrm{cor}(h). \tag{2.24}$$

Effectively, the Dynkin operator realizes a logarithm. Applied to the grouplike element G_B of example 61, we obtain an infinite set of primitive forests, one for each degree. Let b_n be a bamboo (example 61), then a primitive forest of degree k is given by

$$p_n = \frac{1}{n}\left(S \star Y\right)(b_n) = \frac{1}{n}\sum_{k=1}^{n} kS(b_{n-k})b_k. \tag{2.25}$$

Example 62: Rooted trees, primitive elements.

$p_1 =$, $p_2 =$ $-\frac{1}{2}$, $p_3 =$ $-$ $+\frac{1}{3}$.

These elements are non-trivial examples of the bound eq. (2.15): $1 = \mathrm{cor}(p_k) \leq |p_k| = k$. When applied to arbitrary trees, the Dynkin operator does not necessarily produce a primitive element. For example $F := (S \star Y)\left(\right.$ $\left.\right) = 3$  $- 4 \bullet$  $+ \bullet\bullet\bullet$ is not primitive, but $\Delta_1(F) = 2 \bullet \otimes p_2 - 4p_2 \otimes \bullet$ and therefore $\mathrm{cor}(F) = 2 < 3 = \mathrm{cor}($ $)$, see eq. (2.24).

2.1.6. Fixed-point equations for rooted trees

The Cocycle def. 78 can be used to construct a fixed-point equation for some forest $X(\alpha) \in H_{\mathrm{CK}}$, depending on a parameter α. We restrict ourselves to the form

$$X(\alpha) = \mathbb{1} + \alpha B_+\Big(X(\alpha) \cdot Q(\alpha)\Big). \tag{2.26}$$

Here, $Q(\alpha) \in H_{\mathrm{CK}}$ is a forest, the most relevant case for us is

$$Q(\alpha) := X(\alpha)^w, \qquad w \in \mathbb{R}. \tag{2.27}$$

If we allow for labelled rooted trees then every labelled vertex $\bullet$ comes with its own cocycle B_+^n and we can consider a generalization of eq. (2.26),

$$X(\alpha) = \mathbb{1} + \sum_k \alpha^k B_+^k\Big(X(\alpha) \cdot Q^k(\alpha)\Big). \tag{2.28}$$

Example 63: Linear fixed-point equation.

The choice $w = 0$ amounts to $Q = \mathbb{1}$ and therefore the eqation

$$X(\alpha) = \mathbb{1} + \alpha B_+\left(X(\alpha)\right).$$

We call this a *linear* fixed-point equation, because the argument of B_+ is a linear function of $X(\alpha)$. Clearly, the order zero solution is $X(\alpha) = \mathbb{1} + \mathcal{O}(\alpha)$. If we insert this into the DSE, we obtain $X(\alpha) = \mathbb{1} + \alpha B_+(\mathbb{1}) + \mathcal{O}(\alpha^2) = \mathbb{1} + \bullet + \mathcal{O}(\alpha^2)$. By induction, the unique power-series solution of the linear fixed-point equation is given by the bamboos

(example 61),

$$X(\alpha) = \mathbb{1} + \alpha \bullet + \alpha^2 \; \begin{smallmatrix}\bullet\\ \bullet\end{smallmatrix} \; + \alpha^3 \; \begin{smallmatrix}\bullet\\ \bullet\\ \bullet\end{smallmatrix} \; + \ldots = \sum_{n=0}^{\infty} \alpha^n b_n.$$

Using the cocycle property (def. 73), we see

$$\begin{aligned}\Delta(X(\alpha)) &= \Delta(\mathbb{1}) + \alpha B_+ \left(X(\alpha)\right) \otimes \mathbb{1} + \left(\mathrm{id} \otimes B_+\right) \Delta \left(X(\alpha)\right) \\ &= X(\alpha) \otimes \mathbb{1} + \left(\mathrm{id} \otimes B_+\right) \Delta \left(X(\alpha)\right)\end{aligned}$$

which has the solution $\Delta \left(X(\alpha)\right) = X(\alpha) \otimes X(\alpha)$. The solution of a linear fixed point equation is grouplike (def. 65). Taking coefficients in α, we learn that the bamboos are cocommutative, without explicitly constructing their coproduct (compare example 61).

The cocycle B_+ (def. 78) joins all its arguments to a new root. If B_+ is given $(w+1)$ factors as an argument, it will produce a root vertex with $(w+1)$ children. Consequently, a parameter $w \in \mathbb{N}_0$ defines the maximum fertility of the trees in the series $X(\alpha)$: There will be trees with up to $(w+1)$ children per vertex. If y is negative or non-integer, then a formal series expansion is understood:

$$X(\alpha) = \mathbb{1} + Y(\alpha) \qquad \Rightarrow \qquad X(\alpha)^{w+1} := \sum_{n=0}^{\infty} \binom{w+1}{n} Y(\alpha)^n.$$

This series terminates for $w+1 \in \mathbb{N}$, otherwise it is infinite. In particular, the choice $w = -2$ produces the geometric series

$$X(\alpha)^{-2+1} = \frac{1}{\mathbb{1} + Y(\alpha)} = \sum_{n=0}^{\infty} (-1)^n Y(\alpha)^n.$$

The general solution of the fixed point equation 2.28 is a series

$$X(\alpha) = \mathbb{1} + \sum_{k=1}^{\infty} \alpha^k x_k, \tag{2.29}$$

where the coefficients $x_k \in H_{\mathrm{CK}}$ are sums of rooted trees.

Theorem 24 (Kreimer, Bergbauer, Van Suijlekom, Foissy [270, 271, 299, 300])**.** Consider the Connes-Kreimer Hopf algebra H_{CK} (def. 77). Let eq. (2.29) be the unique power series solution of eq. (2.28) where $Q = X^w$. Then

1. $\Delta \left(X(\alpha)\right) = \sum_{j=0}^{\infty} X(\alpha) \alpha^j Q^j(\alpha) \otimes x_j$.
2. The coefficients x_k of the solution $X(\alpha)$ generate a sub Hopf algebra of H_{CK}.
3. If $w \in \mathbb{N}_0$, then x_k is a sum of rooted trees with at most $w+1$ children at each vertex.

Summary of section 2.1.

1. Power series are useful even if they do not converge as functions. Many "analytic" operations can rigorously be defined term-wise (section 2.1.1).
2. Divergent power series contain information about their non-perturbative completion in the way the coefficients grow (section 2.1.2).
3. Hopf algebras are a systematic mathematical framework for operations that require a "deconcatenation", given by the coproduct (section 2.1.3).
4. In the Faà di Bruno Hopf algebra, the coproduct describes insertion of power series into each other, and the antipode gives the inverse series. Elements can be denoted as rooted trees with hair (section 2.1.4).
5. The Connes-Kreimer Hopf algebra of rooted trees is the general framework in which almost all Hopf algebras can be understood graphically (section 2.1.5).
6. Fixed point equations, expressed by the Hochschild cocycle B_+, generate sub Hopf algebras. Linear fixed point equations have grouplike solutions (section 2.1.6).

2.2. Renormalization

In constructing the perturbative expansion for QFT observables, namely the Dyson series eq. (1.33), we have so far ignored one conceptual problem: Every observable is given by an infinite series in the coupling parameter α, therefore, no measurement can tell us the value of α directly. To infer α, we need to invert the series corresponding to that observable. The process of adjusting the *bare* parameters to match experimental values for the observables is called *renormalization*.

2.2.1. Renormalization of a formal power series

To understand the combinatorics of renormalization, we first examine an illustrative example without any reference to QFT. This section partially follows [279, 280, 301]. Assume that we are given a formal power series in a parameter λ_0, where coefficients depend on another variable s,

$$f(\lambda_0, s) = \lambda_0 + f_{0,2}(s)\lambda_0^2 + f_{0,3}(s)\lambda_0^3 + \mathcal{O}\left(\lambda_0^4\right). \tag{2.30}$$

Our task is to evaluate this series as a function of s. We have no information about λ_0. Instead, we are given the value of the function at some point $s = s_0$, called *renormalization point*:

$$f(\lambda_0, s_0) =: \lambda. \tag{2.31}$$

This equation is called a *renormalization condition*. Since s_0 is a constant, we can view the renormalization condition as a formal power series $\lambda(\lambda_0)$. The value λ is called *renormalized coupling*. Given this data, we can in principle invert the series eq. (2.30) in order to find the value of λ_0. But in practice, we would like to express all predictions in terms of the observable λ instead of always doing the inversion whenever we get a new value λ. Therefore, we define the *renormalized function*

$$f_{\mathcal{R}}(\lambda, s) := f\big(\lambda_0(\lambda), s\big) \tag{2.32}$$

where

$$\lambda_0(\lambda) =: c_1\lambda + c_2\lambda^2 + c_3\lambda^3 + \ldots \;=: Z_\lambda(\lambda)\cdot\lambda. \tag{2.33}$$

is the inverse series of eq. (2.31). We have defined the *Z-factor* , $Z_\lambda(\lambda)$. Our task now reduces to a purely combinatorial problem for the series coefficients. First, determine the coefficients c_j of the Z-factor by inverting eq. (2.31), and second, insert the series $\lambda_0(\lambda)$ into eq. (2.30) to produce the renormalized series eq. (2.32). Both are standard operations for formal power series (section 2.1.1). Using theorem 17, we find the Z-factor as in example 39,

$$Z_\lambda(\lambda) = 1 - f_{0,2}(s_0)\lambda + \left(2f_{0,2}^2(s_0) - f_{0,3}(s_0)\right)\lambda^3 + \ldots.$$

With the help of theorem 18, we arrive at our renormalized function eq. (2.32),

$$f_{\mathcal{R}}(\lambda, s) = \lambda + \underbrace{\left(f_{0,2}(s) - f_{0,2}(s_0)\right)}_{=:f_2(s)}\lambda^2 + \Big(f_{0,3}(s) - f_{0,3}(s_0) - 2f_{0,2}(s_0)\underbrace{\left(f_{0,2}(s) - f_{0,2}(s_0)\right)}_{=f_2(s)}\Big)\lambda^3 + \ldots$$

Explicit formulas for f_j and c_j can be constructed in terms of Bell polynomials (def. 52).

Although we did not make any reference to physics, our result exhibits some typical properties one also observes for renormalization in QFT:

1. The renormalized function features so called "subtractions" $\big(f_{0,j}(s) - f_{0,j}(s_0)\big)$ as "building blocks". In Feynman graphs, they will correspond to *superficial divergences*.
2. At order λ^n there are terms involving $\big(f_{0,j}(s) - f_{0,j}(s_0)\big)$ for $j < n$. For Feynman graphs, they correspond to subgraphs.
3. There are seemingly non-trivial signs and combinatoric factors. In fact, they arise from the inversion and concatenation of series (section 2.1.1).

To transfer our findings to a more general setting, we rewrite them in the abstract language of the Faà di Bruno Hopf algebra H_{FdB} (section 2.1.4). We take s, s_0 as fixed parameters and let λ, λ_0 be the power series argument. The bare function f, and the renormalized function $f_{\mathcal{R}}$, are supposed to be characters (def. 74) in H_{FdB}:

$$\begin{aligned} n! c_n &= \mathfrak{C}_n\left(\lambda_0(\lambda)\right) \\ n! f_{0,n} &= \mathfrak{C}_n\left(f(\lambda_0)\right) \\ n! f_n &= \mathfrak{C}_n\left(f_{\mathcal{R}}(\lambda)\right) = \mathfrak{C}_n\left(f_{\mathcal{R}}(\lambda_0(\lambda))\right). \end{aligned}$$

Definition 80. The kinematic renormalization operator $\mathcal{R}$ is the evaluation of a power series $f(s, \lambda, \ldots)$ at a fixed value s_0 of the kinematic scale variable s,

$$\mathcal{R}\big(f(\lambda, s)\big) := f_{\mathcal{R}}(\lambda, s_0).$$

In eq. (2.32), the renormalized function is given as a concatenation of the unrenormalized function with the series $\lambda_0(\lambda)$ from eq. (2.33). In the Faà di Bruno Hopf algebra, the coefficient of such concatenated series is expressed by the coproduct (eq. (2.19)):

$$f_{\mathcal{R}}\mathfrak{C}_n = m(\lambda_0 \circ f)\Delta\mathfrak{C}_n = (\lambda_0 \star f)\mathfrak{C}_n.$$

By the renormalization condition eq. (2.31), $\lambda_0(\lambda)$ is the inverse series of f, evaluated at $s = s_0$. Using the kinematic renormalization operator def. 80, this reads

$$\lambda_0\mathfrak{C}_n = \left(f(\lambda, s_0)\right)^{-1}\mathfrak{C}_n = \left(\mathcal{R}\left(f\right)\right)^{-1}\mathfrak{C}_n = \mathcal{R}\left(f\right)S\mathfrak{C}_n = \mathcal{R}\circ f \circ S\mathfrak{C}_n. \tag{2.34}$$

Despite the abstract algebraic language, there is an intuitive understanding of the situation: The operator $(S\mathfrak{C}_n)$ extracts the n-th coefficient of the inverse of the function standing on the left of it, and that very function is $f(\lambda_0, s)$, evaluated at $s = s_0$. Consequently, the n-th coefficient of the renormalized series is

$$f_{\mathcal{R}}\mathfrak{C}_n = \left(\mathcal{R}fS \star f\right)\mathfrak{C}_n. \tag{2.35}$$

The combinatoric properties of the convolution product (def. 75) ensure that we are multiplying and adding the correct coefficients on the right hand side. We can rewrite eq. (2.35) in a "recursive" fashion by splitting off the augmentation ideal (def. 63), namely $P_{\mathrm{Aug}} + \tilde{\mathbb{1}} = \mathrm{id}$, and noting that $\Delta\mathfrak{C}_n$ contains a summand $\mathfrak{C}_n \otimes \mathbb{1}$. Further, we use $\mathcal{R}(\mathcal{R}(f)) = \mathcal{R}(f)$ and eq. (2.10), $S = -m(S \otimes P_{\mathrm{Aug}})\Delta$, to arrive at

$$\begin{aligned} f_{\mathcal{R}}\mathfrak{C}_n &= m\left(\mathcal{R}fS \otimes f\right)\Delta\mathfrak{C}_n = m\left(\mathcal{R}fS \otimes fP_{\mathrm{Aug}}\right)\Delta\mathfrak{C}_n + m\left(\mathcal{R}fS \otimes f\right)\left(\mathfrak{C}_n \otimes \mathbb{1}\right) \\ &= \left(\mathrm{id} - \mathcal{R}\right)\left(m\left(\mathcal{R}fS \otimes fP_{\mathrm{Aug}}\right)\Delta\mathfrak{C}_n\right) = \left(\mathrm{id} - \mathcal{R}\right)\left(\mathcal{R}fS \star fP_{\mathrm{Aug}}\right)\mathfrak{C}_n. \end{aligned}$$

These formulas hold for every single coefficients. Therefore, they also hold for the overall renormalized power series $f_{\mathcal{R}}(\lambda)$ (eq. (2.32)) fulfilling the renormalization condition eq. (2.31),

$$f_{\mathcal{R}}(t) = \mathcal{R}fS \star f = (\mathrm{id} - \mathcal{R})\left(\mathcal{R}fS \star fP_{\mathrm{Aug}}\right). \tag{2.36}$$

2.2.2. Classification of Feynman amplitudes

The renormalization procedure as developed in section 2.2.1 involves only a single power series. In most situations in QFT, renormalization will be applied to multiple power series simultaneously, namely to different Green functions. In the present section, we establish a classification for the various Green functions which can appear in a given QFT.

Definition 81 ([302, 303])**.** Assume that $\{\underline{p}_j\}$ are the external momenta to some Green function in momentum space. We define the *scale* s as the square of any non-vanishing linear combination of them such that $s = 0$ only when all external momenta vanish. All other momenta are then expressed as dimensionless ratios, such as $\theta_1 = \frac{\underline{p}_1 \underline{p}_2}{s}$, which we collectively call *angles* θ. Sometimes, we also express the internal masses as angles by scaling to s.

A n-point Green function has $(n-1)$ independent momenta due to momentum conservation. By Lorentz covariance, it depends only on the $(n-1)$ magnitudes $\underline{p}_i^2$ and the $\frac{(n-1)(n-2)}{2}$ scalar products $\underline{p}_i \underline{p}_j$, so $\frac{n(n-1)}{2}$ scalar variables in total. One of them is the scale, and there are $\frac{n(n-1)}{2} - 1$ angles. This number is reduced by n if the external edges are required to be onshell (def. 8).

Example 64: Mandelstam variables of 4-point functions.

A 4-point scattering process, where masses are not counted as angles, has five angle variables. If the external edges are onshell, then one angle remains. It is typically expressed in terms of the Lorentz-invariant Mandelstam variables [100],

$$s := \left(\underline{p}_1 + \underline{p}_2\right)^2, \qquad t := \left(\underline{p}_1 + \underline{p}_3\right)^2, \qquad u := \left(\underline{p}_1 + \underline{p}_4\right)^2.$$

As always, all four momenta are counted as incoming. One can choose, for example, s as a scale, then $\theta_1 = \frac{t}{s}$ and $\theta_2 = \frac{u}{s}$ are angles. They are related by $s + t + u = m_1^2 + m_2^2 + m_3^2 + m_4^2$.

Example 65: Scale invariance.

Spacial or temporal translations are generated by the operator ∂_k, rotations by $x_i\partial_j - x_j\partial_i$ and scale transformations by $x_j\partial_j + \Delta$, where Δ is a constant, the dimension of the field in question (we will compute it in def. 103). All theories considered in this thesis are invariant under translations and rotations, namely Poincaré transformations (def. 3).

If they are additionally scale invariant, then the 2-point function (of a scalar field) is $G^{(2)}(\underline{x}_1, \underline{x}_2) \propto (\underline{x}_{12}^2)^{-\Delta}$, where $\underline{x}_{12} = \underline{x}_2 - \underline{x}_1$. This function, thereby, only depends on the scale (def. 81). If the theory would contain a mass, then the mass-dependence would enter in the form of an angle, breaking scale invariance. Likewise, the 3-point function of a scale-invariant theory has the form

$$G^{(3)} \propto |\underline{x}_{12}|^{-3\Delta} f(\theta_1, \theta_2),$$

where $\theta_1 = \frac{|\underline{x}_{13}|}{|\underline{x}_{12}|}$ and $\theta_2 = \frac{|\underline{x}_{23}|}{|\underline{x}_{12}|}$.

The same relations hold for scale-invariant functions in momentum space. The 2-point function depends only on $s := \underline{p}^2$, while the 3-point function depends on s and two angles.

A similar, but not identical, situation arises for a non-scale-invariant theory, where we take the masses fixed, not expressing them as angles. In that case, one can consider *onshell* Green functions by setting $\underline{p}_j^2 = m^2$ for every external $\underline{p}$. Both the 2-point function and the 3-point function are mere numbers in that case, there is no degree of freedom left.

Example 66: Conformal invariance.

Conformal symmetry has the generators $\underline{x}^2\partial_j - 2x_j x_i \partial_i - 2\Delta \cdot x_j$. If a theory is not only scale invariant (example 65), but also conformally invariant, then the 3-point function is entirely fixed to be

$$G^{(3)}(\underline{x}_1, \underline{x}_2, \underline{x}_3) \propto |\underline{x}_{12}|^{-\Delta} |\underline{x}_{13}|^{-\Delta} |\underline{x}_{23}|^{-\Delta}.$$

The first non-trivial correlation function of a conformally invariant theory is the 4-point function, depending (non-trivially) on two angles. Generally, a conformally invariant n-point function has $\frac{n(n-3)}{2}$ degrees of freedom [304, 305].

Definition 82. The *tensor structure* T of a Feynman amplitude G is, in a scalar theory, a monomial in the external momenta of the Green function. Especially, the mass dimension (def. 4) is $[T] = [G]$.

Let g be the residue (def. 26) of a Green function, and T be its tensor structure (def. 82). In general, g can contain multiple different field types and the tensor structure T may also involve Dirac matrices or tensors corresponding to internal symmetries. By (g, T), we denote the Green function with residue g, projected onto the tensor T. Here and in the following, we assume that T is *compatible* with g, that is, the number and type of kinematic variables in the tensor T matches the external fields in the residue g. This pair (g, T) can be used to classify all the Green functions of a QFT. For a fixed residue, the sum over all tensors T is defined as $G^g := \sum_T T \cdot (g, T)$. For a theory with a single scalar field, the external structure is simply the number of fields, we write $G^{(n)} := G^{\phi^n}$ for a Green function with n external fields.

Example 67: Decomposition of Green functions for scalar fields.

Consider massive ϕ^4 theory in $D = 4$ dimensions (example 3). The 2-point function contains summands proportional to $\underline{p}^2$ and summands proportional to m^2, so there are two components, $(\phi^2, \underline{p}^2)$ and (ϕ^2, m^2). Consequently, $G^{(2)} = \underline{p}^2 f_1 + m^2 f_2$, where f_1 and f_2 are functions of scale-free ratios of momenta.

The 4-point function is not proportional to momenta, we write $(\phi^4, 1)$. This does not imply that the 4-point function is constant, it can still depend on angles, and on the scale in a non-polynomial way. The 6-point function behaves like $(\phi^6, \underline{p}^{-2})$. The massive theory also has (ϕ^6, m^{-2}). The massless theory has exactly one Green function for each $n \in \mathbb{N}$, namely (ϕ^{2n}, s^{2-n}) with the scale $s := \underline{p}^2$.

Example 68: Decomposition of Green functions for QED.

The 2-point function of the fermion ψ in QED (to be introduced in example 22) is $G^{\bar{\psi}\psi} = (\psi\bar{\psi}, p^\mu \gamma_\mu)$, where γ_μ are the Dirac matrices. The massless photon A_μ has two different 2-point functions, a longitudinal one $(A^\mu A^\nu, p^\mu p^\nu)$, and a transversal one $(A^\mu A^\nu, \eta^{\mu\nu}\underline{p}^2 - p^\mu p^\nu)$. The tensors of amplitudes with a higher number of non-scalar particles are conveniently classified in terms of spin-helicity variables [127, 128, 306].

2.2.3. Hopf algebra of Feynman graphs

Definition 83. The *set of amplitudes needing renormalization* $\mathfrak{R}$ is a set of pairs $(g, T) = r$, where g is the residue (def. 26) of a Green function, and T is a kinematic tensor structure compatible with g. The notion $\mathfrak{R} = \infty$ means that $\mathfrak{R}$ contains *all* amplitudes (g, T).

For a connected Feynman graph Γ, we denote $\Gamma \in \mathfrak{R}$ if $\mathrm{res}(\Gamma) = g$ for some $(g, T) \in \mathfrak{R}$ and $\mathcal{F}(\Gamma)$ projected onto T does not vanish. $\Gamma \in \mathfrak{R}_+$ means that $\Gamma \in \mathfrak{R}$ and $|L_\Gamma| > 0$ (def. 28). Similarly, a non-connected graph Γ is $\in \mathfrak{R}$ if all connected components are.

For the present section, the precise choice of $\mathfrak{R}$ is irrelevant. In section 2.3.4, we see why certain $\mathfrak{R}$ are physically sensible.

Example 69: ϕ^n theory, amplitudes needing renormalization.

For massive ϕ^4 theory in $D = 4$ dimensions with propagator powers $\nu_e = 1$, we choose

$$\mathfrak{R} = \left\{ \left(\phi^2, m^2\right), \left(\phi^2, \underline{p}^2\right), \left(\phi^4, 1\right) \right\}.$$

For the massless theory, leave out the m^2 residue. ϕ^3 theory in $D = 6$ dimensions has

$$\mathfrak{R} = \left\{ \left(\phi^2, m^2\right), \left(\phi^2, p^2\right), \left(\phi^3, 1\right) \right\}.$$

Definition 84. The Hopf algebra (def. 67) of Feynman graphs H_F contains all Feynman graphs (def. 24) as algebra elements. The product m is given by disjoint union, it is commutative. $\mathbb{1}$ is the empty graph. Let $\mathfrak{R}$ be a set of amplitudes needing renormalization (def. 83), then the coproduct of a Feynman graph $\Gamma \in H_F$ is

$$\Delta_{\mathfrak{R}}(\Gamma) = \sum_{\Gamma \supset \gamma \in \mathfrak{R}_+} \gamma \otimes \frac{\Gamma}{\gamma}.$$

Here, γ does not need to be connected, but every component must have at least one loop (def. 28). $\frac{\Gamma}{\gamma}$ denotes contraction (def. 27). H_F is graded by the loop number and connected, the antipode follows from eq. (2.10).

Example 70: Dunce's cap, renormalization coproduct.

Consider the dunce's cap from example 12. It has exactly one proper subgraph γ with $\mathrm{res}(\gamma) \in \mathfrak{R}_+$ (example 69), the multiedge $\gamma = \{e_3, e_4\}$. The cograph $\frac{\Gamma}{\gamma}$ is a multiedge $\{e_1, e_2\}$. Note that $\{e_1, e_2, e_3\} \notin \mathfrak{R}$ because this graph has 6 external edges.

$\Gamma :=$ 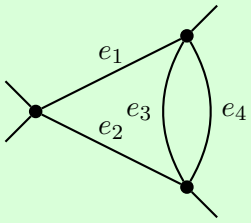

$\gamma :=$ 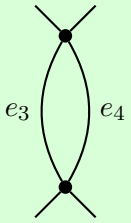

$\frac{\Gamma}{\gamma} =$ 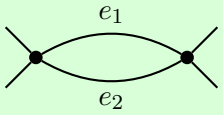

Hence, the coproduct of the dunce's cap is

$$\Delta_{\mathfrak{R}}(\Gamma) = \mathbb{1} \otimes \Gamma + \Gamma \otimes \mathbb{1} + \{e_3, e_4\} \otimes \{e_1, e_2\}\,.$$

Definition 85. The *core Hopf algebra* of Feynman graphs is a Hopf algebra of Feynman graphs (def. 84), where the coproduct Δ_∞ is given by $\mathfrak{R} = \infty$ (def. 83). That is, there is a factor $\gamma \otimes \frac{\Gamma}{\gamma}$ for every subgraph γ which has at least one loop.

Example 71: Dunce's cap, core coproduct.

The dunce's cap from example 70 has two subgraphs with 6 external edges. Contracting them, one obtains a tadpole (self-loop) on a single vertex. We denote the tadpole made of edge e_j by t_j. The core-coproduct (def. 85) reads

$$\Delta_\infty(\Gamma) = \Delta_{\mathfrak{R}}(\Gamma) + \{e_1, e_2, e_3\} \otimes t_4 + \{e_1, e_2, e_4\} \otimes t_3.$$

Definition 86. In the Hopf algebra H_F (def. 84), a graph Γ is said to be *primitive* (def. 65) if $\Gamma \in \mathfrak{R}_+$ (def. 83) and there is no proper subgraph $\gamma \subset \Gamma$ with $\gamma \in \mathfrak{R}_+$.

Example 72: ϕ^4 theory, primitive graphs.

All 1-loop Feynman graphs Γ with $\Gamma \in \mathfrak{R}$ are primitive because they can not have proper subgraphs with at least one loop. The dunce's cap (example 12) is not primitive due to the subgraph $\gamma = \{e_3, e_4\} \in \mathfrak{R}_+$. But there are primitive graphs with more than one loop in ϕ^4 theory, for example:

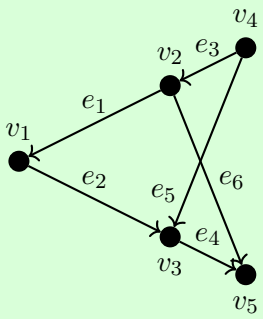

The fact that there is more than one primitive element in H_F has an interesting consequence for the Hochschild cocycle B_+ (def. 73). Namely, by lemma 20, $B_+(\mathbb{1})$ is primitive, therefore, there must be multiple B_+ in H_F, one for each primitive Feynman graph.

Definition 87. Let $\Gamma \in H_F$ be a primitive (def. 86) graph. Then there is a Hochschild 1-cocycle $B_+^\Gamma : H_F \to \mathrm{Aug}$ (def. 73) such that $B_+^\Gamma(\mathbb{1}) = \Gamma$ and

$$B_+^\Gamma(h) = \frac{1}{|I|} \sum_I \text{insert } h \text{ into } \Gamma,$$

where I is the set of all possible insertion places of h into Γ. Here, h can be a product (=disjoint union) of multiple graphs, and the operation returns the empty graph in case h has too many, or incompatible, components.

Example 73: Cocycle of Feynman graphs.

Let

$\Gamma =$ 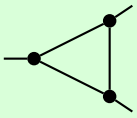 $\gamma =$ 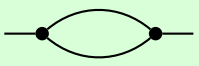

then

$B_+^\Gamma(\gamma) = \frac{1}{3}$ 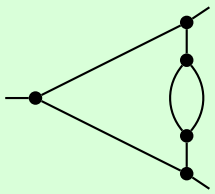 $+ \frac{1}{3}$ 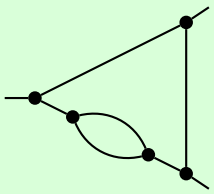 $+ \frac{1}{3}$ 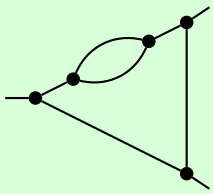

We have mentioned in section 2.1.5 that the Hopf algebra of rooted trees H_{CK} (def. 77) is a universal description for all graded connected Hopf algebras (theorem 23). Consequently, there is a mapping of Feynman graphs H_{F} (def. 84) into H_{CK}.

Theorem 25 (Kreimer [292, 307])**.** The following algorithm is a Hopf algebra homomorphism from H_{F} to a vertex-labelled H_{CK}. Let $\Gamma \in H_{\mathrm{F}}$ be a Feynman graph.

1. Let $\gamma \subset \Gamma$ with $\gamma \in \mathfrak{R}_+$ (def. 83). Assume there are zero or more graphs $\gamma' \subset \gamma$ with $\gamma' \in \mathfrak{R}_+$. If $\frac{\gamma}{\bigcup \gamma'} \in \mathfrak{R}_+$, but $\gamma - \bigcup \gamma'$ is not in $\mathfrak{R}_+$, then γ corresponds to a vertex v_γ, labelled by γ, of a rooted tree.

2. If $\gamma_1 \subset \gamma_2$ both correspond to vertices by point 1, then the vertex v_{γ_1} is attached below v_{γ_2}.

3. If $\gamma \subset \gamma_1$ and $\gamma \subset \gamma_2$ but $\gamma_1 \not\subseteq \gamma_2$ and $\gamma_2 \not\subseteq \gamma_1$, then draw two trees, one where v_γ is attached below v_{γ_1} and one where v_γ is attached below v_{γ_2}.

Without the labels of the rooted trees, one can, in general, not reproduce the corresponding Feynman graph, compare examples 76 and 78.

Example 74: Chain graphs, rooted trees.

The conditions in point 1 of theorem 25 may appear intransparent. To clarify them, consider a chain of n multiedges in ϕ^3 theory (example 69):

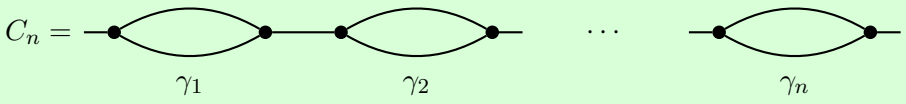

Every single γ_j is $\in \mathfrak{R}$ and has one loop and does not have any non-trivial subgraphs, so each γ_j amounts to one vertex in the rooted tree. Now consider the connected subgraph $\gamma' := \gamma_1 \cup e \cup \gamma_2$. It is also $\in \mathfrak{R}_+$ and, for example,

$$\frac{\gamma'}{\gamma_1} = \gamma_2 \cup e \in \mathfrak{R}_+.$$

Still, γ' does not map to a vertex in the rooted trees because $\gamma' - \gamma_1 = \gamma_2 \cup e \in \mathfrak{R}_+$. Restricting ourselves again to unlabelled trees, theorem 25 yields (compare example 57)

$$C_n \mapsto \underbrace{\bullet\bullet\cdots\bullet}_{n \text{ factors}}.$$

Example 75: Second chain graph, rooted trees.

The graph S in example 26 is called "second chain graph" because its subgraph is the second chain C_2 from example 74. Under theorem 25, ignoring vertex labels,

$$S \mapsto$$  .

Observe how $C_2 = \gamma_1\gamma_2 \mapsto \bullet\bullet$ is attached below the root vertex. The graphs with only one subgraph from example 26 map to $\Gamma/\gamma_i = \Gamma_i \mapsto$  . This is the same rooted tree as the dunce's cap (example 77), despite the Feynman graphs being different. The coproduct is

$$\Delta(S) = \quad S \otimes \mathbb{1} + \mathbb{1} \otimes \quad S \quad + (\gamma_1 \otimes S_1 + \gamma_2 \otimes S_2) + \gamma_1\gamma_2 \otimes \gamma$$

$$\mapsto$$  $\otimes \mathbb{1} + \mathbb{1} \otimes$  $+ \quad 2 \bullet \otimes$  $+ \bullet\bullet \otimes \bullet$.

Example 76: Bamboos from rainbows.

In example 61 we saw that the bamboos are an interesting class of rooted trees. The *rainbow* Feynman graphs are a possible counterpart in H_{F}:

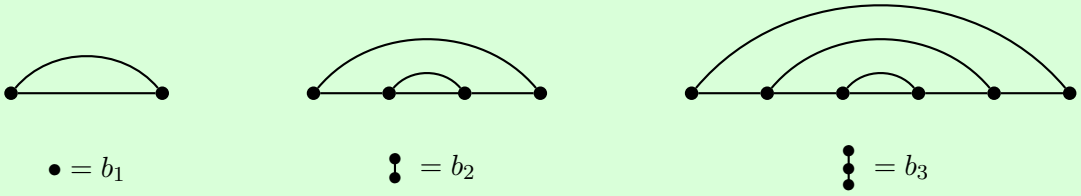

The coproduct (def. 84) of the Feynman graphs clearly matches the coproduct of example 61, as every subgraph and cograph of a rainbow graph is again a (smaller) rainbow graph.

Example 77: Dunce's cap, rooted trees.

In the renormalization Hopf algebra, the dunce's cap has only a single subgraph (example 70). Using unlabelled rooted trees, by theorem 25

$$\Gamma \mapsto$$.

The coproduct of this rooted tree (def. 77) exactly matches the one of Γ,

$$\Delta_{\mathfrak{R}}(\Gamma) = \mathbb{1} \otimes \Gamma + \Gamma \otimes \mathbb{1} + \{e_3, e_4\} \otimes \{e_1, e_2\}$$

$$\Delta\left(\text{  }\right) = \mathbb{1} \otimes$$ $+$ $\otimes \mathbb{1} + \bullet \otimes \bullet$.

As anticipated, the unlabelled trees are missing information: • denotes both $\{e_3, e_4\}$ and $\{e_1, e_2\}$, and we do not know if $\{e_3, e_4\}$ is inserted into the left or right vertex of $\{e_1, e_2\}$.

Example 78: Bamboos from ladders.

As announced below theorem 25, the mapping $H_{\mathrm{F}} \to H_{\mathrm{CK}}$ is not invertible for unlabelled trees. As an illustration, the *ladder graphs* represent another class of Feynman graphs which are mapped to the (unlabelled) bamboos just like the rainbows (example 76).

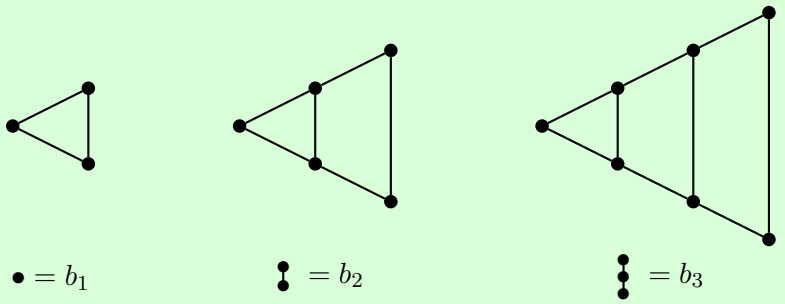

In ϕ^3 theory, the ladders contribute to the vertex $\Gamma^{(3)}$, the rainbows to the propagator $\Gamma^{(2)}$.

2.2.4. Renormalized Feynman rules

The Feynman rules are a character (def. 74) in the Hopf algebra H_F (def. 84). The cocycle B_+^Γ (def. 87) of H_F corresponds to a linear operator for the Feynman rules, namely integration:

$$\mathcal{F}\left[B_+^\Gamma(h)\right] = \int \mathrm{d}_\Gamma \, \mathcal{F}[h]. \tag{2.37}$$

Here $\int \mathrm{d}_\Gamma$ denotes the integral over the respective integration variables of the Feynman integral $\mathcal{F}[\Gamma]$, and it is understood that $\mathcal{F}[h]$ is to be evaluated at the corresponding arguments.

Using theorem 25, one can reformulate the Feynman rules to act not on graphs, but on labelled rooted trees. Besides being a useful tool to organize the combinatorial aspects of ordinary amplitudes, these *tree Feynman rules* allow to construct simplified toy models for renormalization. This can be useful to study the combinatorics while skipping the technical difficulties of solving ordinary Feynman integrals [288, 308, 309].

Example 79: Toy model Feynman rules.

Let $t \in H_{\mathrm{CK}}$ be a forest of unlabelled rooted trees, and $\epsilon \in \mathbb{R}$ a regularization parameter. One possible toy model [307, 308] is given by

$$\mathcal{F}\left[B_+(t)\right](s) := \int_0^\infty \mathrm{d}x \frac{x^{-\epsilon}}{x+s} \mathcal{F}[t](x).$$

Morally, this resembles a theory with a single primitive.

Having established the Hopf algebra of Feynman graphs, renormalization now is conceptually very simple. All we have to do is apply eq. (2.36) to Feynman graphs. For a more precise discussion of the various Hopf algebras involved in renormalization, see [278, 287, 310–312].

Definition 88. The *renormalized Feynman rules* are given by

$$\mathcal{F}_{\mathcal{R}} = S^{\mathcal{F}}_{\mathcal{R}} \star \mathcal{F} = (\mathrm{id} - \mathcal{R}) \left(S^{\mathcal{F}}_{\mathcal{R}} \star \mathcal{F} P_{\mathrm{Aug}}\right).$$

Here, $\mathcal{F}$ are the Feynman rules (def. 38), $\star$ is the convolution product (def. 75), $S^{\mathcal{F}}_{\mathcal{R}}$ is the *counterterm* (def. 89), and P_{Aug} projects onto Aug (def. 63). We write $\mathcal{F}_{\mathcal{R}}[\Gamma](L)$ to indicate the Feynman rules acting on Γ, evaluated at L.

Definition 89. The *counterterm* is the twisted antipode, given recursively by eq. (2.10),

$$S^{\mathcal{F}}_{\mathcal{R}}[\Gamma] = -\mathcal{R}\Big(m\left(S^{\mathcal{F}}_{\mathcal{R}} \otimes \mathcal{F} P_{\mathrm{Aug}}\right)\Delta(\Gamma)\Big) = -\mathcal{R}\Big((S^{\mathcal{F}}_{\mathcal{R}} \star \mathcal{F} P_{\mathrm{Aug}})\Gamma\Big).$$

Here, $\mathcal{R}$ denotes the renormalization operator to be made precise in def. 97.

Note that the counterterm involves nested applications of the renormalization operator, in general $S^{\mathcal{F}}_{\mathcal{R}}[\Gamma] \neq \mathcal{R}\left(S(\Gamma)\right)$. We see this effect explicitly later in example 107.

Definition 90. The *renormalized 1PI Green functions* arise from the combinatorial 1PI Green functions (def. 45) via the renormalized Feynman rules (def. 88),

$$G^r_{\mathcal{R}} := \mathcal{F}_{\mathcal{R}}\left[\Gamma^r\right] = \sum_{\Gamma \text{ 1PI, } \mathrm{res}(\Gamma)=r} \alpha^{|L_\Gamma|} \,\mathrm{sym}(\Gamma) \mathcal{F}_{\mathcal{R}}[\Gamma].$$

Example 80: Dunce's cap, renormalized amplitude.

The coproduct of the dunce's cap Γ has been computed in example 70. If $M^{(1)} = \{e_3, e_4\}$ is a 1-loop multiedge (example 24) then $S(M^{(1)}) = -M^{(1)}$, and as always $S(\mathbb{1}) = \mathbb{1}$. Further, $\mathcal{F}[\mathbb{1}] = 1$ and $P_{\mathrm{Aug}}(\mathbb{1}) = 0$ (def. 63). Hence, the renormalized Feynman rules

(def. 88) of the dunce's cap are

$$\begin{aligned}\mathcal{F}_{\mathcal{R}}[\Gamma] &= (\mathrm{id} - \mathcal{R})\, m\, (\mathcal{R}\mathcal{F}S \otimes \mathcal{F}P_{\mathrm{Aug}})\, \Delta_{\mathfrak{R}}(\Gamma) \\ &= (\mathrm{id} - \mathcal{R}) \Big(\mathcal{R}\mathcal{F}S(\mathbb{1}) \cdot \mathcal{F}[\Gamma] + 0 + \mathcal{R}\mathcal{F}S(\{e_3, e_4\}) \cdot \mathcal{F}[\{e_1, e_2\}] \Big) \\ &= (\mathrm{id} - \mathcal{R}) \Big(\mathcal{F}[\Gamma] - \mathcal{R}\mathcal{F}[\{e_3, e_4\}] \cdot \mathcal{F}[\{e_1, e_2\}] \Big). \\ S^{\mathcal{F}}_{\mathcal{R}}[\Gamma] &= -\mathcal{R}\mathcal{F}[\Gamma] + \mathcal{R}\Big(\mathcal{R}\mathcal{F}[\{e_3, e_4\}] \cdot \mathcal{F}[\{e_1, e_2\}] \Big).\end{aligned}$$

As expected, the combinatorics of this procedure is non-trivial, but everything is encoded in the Hopf algebra coproduct (def. 84).

We do not print the full result here because it is a complicated function. See example 87.

Asymptotically for large scale s, the finite term scales like $(\ln s/s_0)^2$ [173]. We will understand this in theorem 35.

Unrenormalized Feynman rules are multiplicative for disjoint graphs (eq. (1.41)), which has the interpretation of *locality*, namely that two processes are independent if they happen far apart from each other. Renormalization might spoil this property, but we demand that also the renormalized Feynman rules be multiplicative,

$$\mathcal{F}_{\mathcal{R}}\big[h_1 \cdot h_2\big] = \mathcal{F}_{\mathcal{R}}\big[h_1\big] \cdot \mathcal{F}_{\mathcal{R}}\big[h_2\big]. \tag{2.38}$$

More precisely, we want $\mathcal{F}_{\mathcal{R}}$ to be a character (def. 74) on H_{F} (def. 84). Effectively, this is a condition for the counterterm $S^{\mathcal{F}}_{\mathcal{R}}$ (def. 89), which needs to be a character as well. This requires [284, 310, 313, 314] that the renormalization operator $\mathcal{R}$ is a *Rota-Baxter operator* [315, 316],

$$\mathcal{R}\Big(f(x)g(x)\Big) + \mathcal{R}\left(f(x)\right)\mathcal{R}\left(g(x)\right) \overset{!}{=} \mathcal{R}\Big(\mathcal{R}\left(f(x)\right)g(x)\Big) + \mathcal{R}\Big(f(x)\mathcal{R}\left(g(x)\right)\Big). \tag{2.39}$$

The most straightforward renormalization operator $\mathcal{R}$ is the analogue of def. 80, with the only difference that it acts on functions G which, in general, depend on more than one variable.

Definition 91. Let $G \in \mathfrak{R}$ (def. 83) be an amplitude needing renormalization. In the *kinematic renormalization scheme*, or *MOM-scheme*, or *BPHZ-scheme*, the renormalization operator $\mathcal{R}$ evaluates G at a fixed value s_0, θ_0 of the angle and scale variables (def. 81),

$$\mathcal{R} : G(s, \theta, m, \ldots) \mapsto G(s_0, \theta_0, m, \ldots).$$

The kinematic renormalization operator has the special property that

$$\mathcal{R}\Big((\mathcal{R}f(s)) \cdot g(s)\Big) = \mathcal{R}\Big(f(s_0) \cdot g(s)\Big) = f(s_0) \cdot g(s_0) = \mathcal{R}\Big(f(s) \cdot g(s)\Big) = \Big(\mathcal{R}f(s)\Big) \cdot \Big(\mathcal{R}g(s)\Big).$$

Thereby, it trivially fulfils the Rota-Baxter equation 2.39, and the couterterm (def. 89) in kinematic renormalization indeed turns out to be $S^{\mathcal{F}}_{\mathcal{R}}[\Gamma] = \mathcal{R}\left(S(\Gamma)\right)$.

Owing to the cocycle property (def. 73), the renormalized Feynman rules (def. 88) acting on B_+ (eq. (2.37)) decompose into subtraction of a superficial divergence, $(\mathrm{id} - \mathcal{R})$, and renormalization of subdivergences, $\mathcal{F}_{\mathcal{R}}[h]$ [270]:

$$\mathcal{F}_{\mathcal{R}}\left[B_+^\Gamma(h)\right] = (\mathrm{id} - \mathcal{R}) \int \mathrm{d}_\Gamma \, \mathcal{F}_{\mathcal{R}}[h] = (\mathrm{id} - \mathcal{R}) \mathcal{F}\left[B_+^\Gamma(\mathcal{F}_{\mathcal{R}}[h])\right]. \tag{2.40}$$

2.2.5. Dyson-Schwinger equations revisited

In section 1.3.11, we have introduced Dyson-Schwinger equations in a rather colloquial way. The Hopf algebra of Feynman graphs allows us to give them a much more concrete form.

By the DSE theorem 14, every internal edge in a kernel graph Γ (def. 50) is to be replaced by the connected 2-point function (def. 47), given by the series $\left(\Gamma^{(2)}\right)^{-1}$. Equivalently, one can "distribute" the factor $\Gamma^{(2)}$ to the two vertices adjacent to the edge by using $\Gamma^{(2)} = \left(\Gamma^{(2)}\right)^{\frac{1}{2}} \cdot \left(\Gamma^{(2)}\right)^{\frac{1}{2}}$. The square root of a set of graphs is explained by its formal (def. 51) series expansion,

$$\sqrt{1+t} = \sum_{n=0}^{\infty} \binom{\frac{1}{2}}{n} t^n = \sum_{n=0}^{\infty} \frac{(2n)!(-1)^{n+1}}{(n!)^2(2n-1)4^n} t^n = 1 + \frac{1}{2}t - \frac{1}{8}t^2 + \frac{1}{16}t^3 \mp \dots.$$

Products of graphs are disjoint unions (def. 84). Every n-valent internal vertex $v \in V_\Gamma$ is adjacent to exactly n edges, and every edge is adjacent to two vertices. In the following, it turns out to include the Green functions of adjacent edges together with the vertex into a single object, the invariant charge.

Definition 92. Let v be a n-valent vertex and Γ^v its combinatorial 1PI Green function (def. 45). Let $e \sim v$ be edges adjacent to v and Γ^e the 1PI propagator corresponding to e. The combinatorial *invariant charge* is

$$Q_v = \left(\frac{\Gamma^v}{\prod_{e \sim v} \sqrt{\Gamma^e}} \right)^{\frac{2}{n-2}}.$$

The exponent $\frac{2}{n-2}$ in def. 92 is a matter of convention, here it is chosen such that the loop number (def. 28) matches the power of Q_v.

Example 81: Invariant charges.

In scalar ϕ^n theory, the invariant charges for the n-valent vertices are

$$Q_n = \frac{\left(\Gamma^{(n)}\right)^{\frac{2}{n-2}}}{\left(\Gamma^{(2)}\right)^{\frac{n}{n-2}}}, \qquad Q_3 = \frac{\left(\Gamma^{(3)}\right)^2}{\left(\Gamma^{(2)}\right)^3}, \qquad Q_4 = \frac{\Gamma^{(4)}}{\left(\Gamma^{(2)}\right)^2}.$$

QED has a photon , and an electron , and a vertex with invariant charge

$$Q_{\mathrm{QED}} = \frac{\left(\Gamma^{\text{}}\right)^2}{\left(\Gamma^{\text{}}\right)^2 \Gamma^{\text{}}}.$$

QCD has gluons, quarks, and ghosts, and four different vertices:

$$Q_{\text{gluon}} = \frac{\left(\Gamma^{\text{gluon}}\right)^2}{\left(\Gamma^{\text{gluon}}\right)^3}, \qquad Q_{\text{quark}} = \frac{\Gamma^{\text{quark}}}{\left(\Gamma^{\text{gluon}}\right)^2}, \qquad Q_{\text{ghost}} = \frac{\left(\Gamma^{\text{ghost}}\right)^2}{\left(\Gamma^{\text{ghost}}\right)^2 \Gamma^{\text{gluon}}}, \qquad Q_{\text{3g}} = \frac{\left(\Gamma^{\text{3g}}\right)^2}{\left(\Gamma^{\text{quark}}\right)^2 \Gamma^{\text{gluon}}}.$$

Theorem 26 (Combinatorial Dyson-Schwinger equations)**.** Consider a scalar QFT with a single n-valent interaction term. Rescale $\lambda_n^{\frac{2}{n-2}} =: \alpha$. Let $\Gamma^{(n)}$ be the n-point 1PI graphs (def. 45), where $\Gamma^{(n)}$ is divided by $(i\lambda_n)$ such that the treelevel vertex is normalized to $\mathbb{1}$. Let $\Gamma^{(2)}$ be the 1PI 2-point function (def. 47). Let $K^{(n)}$ be the set of kernel graphs (def. 50) with residue ϕ^n. Then the Dyson-Schwinger equations (theorem 14) can be expressed using the Hochschild 1-cocycle B_+ (def. 87) as

$$\Gamma^{(2)} = \mathbb{1} - \sum_{\Gamma \in K^{(2)}} \alpha^{|L_\Gamma|} \operatorname{sym}(\Gamma) B_+^\Gamma \left(\Gamma^{(2)} \cdot Q_n^{|L_\Gamma|}\right)$$
$$\Gamma^{(n)} = \mathbb{1} + \sum_{\Gamma \in K^{(n)}} \alpha^{|L_\Gamma|} \operatorname{sym}(\Gamma) B_+^\Gamma \left(\Gamma^{(n)} \cdot Q_n^{|L_\Gamma|}\right).$$

Proof. The Cocycle $B_+^\Gamma(h)$ (def. 87) of Feynman graphs inserts the subgraph h into Γ, by the identification eq. (2.37). This is exactly what is being done in a graphical Dyson-Schwinger equation (theorem 14). To be shown is that the argument of B_+^Γ is sufficient to replace exactly all internal edges and vertices of Γ. Consider the propagator DSE. By eq. (1.43), a graph $\Gamma \in K^{(2)}$ has $\frac{n}{n-2}|L_\Gamma| - 1$ internal edges and $\frac{2}{n-2}|L_\Gamma|$ vertices. Therefore B_+^Γ requires the argument

$$\left(\Gamma^{(2)}\right)^{-\left(\frac{n}{n-2}|L_\Gamma|-1\right)} \left(\Gamma^{(n)}\right)^{\frac{2}{n-2}|L_\Gamma|} = \Gamma^{(2)} \left(\frac{\Gamma^{(n)}}{\left(\Gamma^{(2)}\right)^{\frac{n}{2}}}\right)^{\frac{2}{n-2}|L_\Gamma|} = \Gamma^{(2)} \cdot Q_n^{|L_\Gamma|}.$$

The vertices of this graph contribute $\lambda_3^{\frac{2}{n-2}|L_\Gamma|} = \alpha^{|L_\Gamma|}$. Analogous for the vertex DSE. □

Example 82: Multiedge DSE, algebraic form.

In example 34 we have introduced a simplified DSE for the propagator by setting the 3-valent vertex to its treelevel value. Thanks to our rescaling, this now amounts to

$$\Gamma^{(3)} = \mathbb{1}, \qquad \Rightarrow \qquad Q_3 = \left(\Gamma^{(2)}\right)^{-3}.$$

The DSE has only one single kernel graph,  , with symmetry factor (theorem 13) $\operatorname{sym}(\text{}) = \frac{1}{2}$. In the form of theorem 26, the DSE reads

$$\Gamma^{(2)} = \mathbb{1} - \alpha \cdot \frac{1}{2} B_+^{\text{}} \left(\left(\Gamma^{(2)}\right)^{-2}\right).$$

The exponent -2 means that one can insert two $\left(\Gamma^{(2)}\right)^{-1}$ into the two edges of .

There are also Dyson-Schwinger equations for those Green functions which do not require (superficial) renormalization. For a renormalizable scalar ϕ^n theory, these are all $\Gamma^{(m)}$ with $m > n$. Let t be any of the trees with m external edges, then, by eq. (1.42), t contains $|V_t| = \frac{m-2}{n-2}$ vertices and $|E_t| = \frac{m-n}{n-2}$ internal edges. Define

$$T^{(m)} := \frac{\left(\Gamma^{(n)}\right)^{\frac{m-2}{n-2}}}{\left(\Gamma^{(2)}\right)^{\frac{m-n}{n-2}}}$$

and let $\bar{K}^{(m)}$ be the set of all 1PI kernel graphs (def. 50) Γ with $\mathrm{res}(\Gamma) = \phi^m$ without sub-divergences. Unlike theorem 26, these $K^{(m)}$ are not divergent themselves. Then

$$\Gamma^{(m)} = \sum_{\Gamma \in \bar{P}^{(m)}} \alpha^{|L_\Gamma|} \operatorname{sym}(\Gamma) B_+^\Gamma \left(T^{(m)} \cdot Q_n^{|L_\Gamma|} \right). \tag{2.41}$$

Observe that this DSE is missing the summand $\mathbb{1}$ because $\Gamma^{(m)}$ has no treelevel vertex, and it is a 1PI Green function (def. 45), so the tree $T^{(m)}$ itself does not contribute to $\Gamma^{(m)}$.

Using eq. (2.40), one can directly map theorem 26 to a set of integral equations for renormalized Green functions.

Definition 93. The renormalized invariant charge is the renormalized Feynman rule (def. 88) acting on the combinatorial invariant charge (def. 92),

$$\mathcal{Q}(\alpha, L) := \mathcal{F}[Q(\alpha)](L), \qquad \mathcal{Q}_\mathcal{R}(\alpha, L) := \mathcal{F}_\mathcal{R}[Q(\alpha)](L).$$

In kinematic renormalization (def. 91), we must fix all angles at the renormalization point symmetrically, such that all Green functions involved in $\mathcal{Q}_n$ are evaluated at the same scale.

Theorem 27. Let $G^r_\mathcal{R}$ be the renormalized 1PI Green function (defs. 47 and 90) with residue r, where the treelevel term is normalized to unity. Let P^r be the set of subdivergence-free (but not necessarily superficially divergent) graphs with residue r. Then the Dyson-Schwinger equations from theorem 26 and eq. (2.41) can be expressed using the Hochschild 1-cocycle B_+ (eq. (2.37)) as

$$G^r_\mathcal{R} = 1 \pm (\mathrm{id} - \mathcal{R}) \sum_{\Gamma \in P^{(j)}} \alpha^{|L_\Gamma|} \operatorname{sym}(\Gamma) \mathcal{F}\left[B_+^\Gamma \left(G^r_\mathcal{R} \cdot \mathcal{Q}_\mathcal{R}^{|L_\Gamma|} \right) \right], \quad r \in \mathfrak{R}$$

$$G^r_\mathcal{R} = \sum_{\Gamma \in P^r} \alpha^{|L_\Gamma|} \operatorname{sym}(\Gamma) \mathcal{F}\left[B_+^\Gamma \left(T^{(m)} \cdot \mathcal{Q}_\mathcal{R}^{|L_\Gamma|} \right) \right], \qquad r \notin \mathfrak{R}.$$

Summary of section 2.2.

1. Renormalization means to express bare parameters by observables, which are themselves power series in the bare parameters. Technically, this amounts to insertion and reversion of power series, leading to the formula $f_{\mathcal{R}} = Sf\mathcal{R} \star f$ (section 2.2.1).

2. In QFT, there are multiple power series, corresponding to the Green functions. They can be classified with respect to their residue and their tensor structure (section 2.2.2).

3. Feynman graphs form a Hopf algebra H_{F}. The coproduct is given by extraction and contraction of all subgraphs which are classified in a set $\mathfrak{R}$. There is a homomorphism between Feynman graphs and rooted trees. The abstract Hochschild-1-cocycle B_+ amounts, for Feynman graphs, to the insertion of subgraphs (section 2.2.3).

4. Feynman rules are a character in H_{F}. The renormalized Feynman rules $\mathcal{F}_{\mathcal{R}} = S^{\mathcal{F}}_{\mathcal{R}} \star \mathcal{F}$ are a character as well, they implement one renormalization condition for each Green function in $\mathfrak{R}$ (section 2.2.4).

5. For Feynman amplitudes, B_+ is the integral operator which appears in the Dyson-Schwinger equations. The arguments can be regrouped so that, instead of vertex Green functions Γ^v, they involve one invariant charge Q_v for each vertex v of the theory.

2.3. Divergences and renormalizability

The alert physicist reader might wonder by now how we have introduced renormalization without any reference to "removing infinities". This is not an accident: Renormalization is a rigorous method of expressing power series in terms of observable parameters, which themselves are given by power series. It is completely unrelated to the question if certain integrals are divergent, and it is necessary in just the same way if they are not. Nonetheless, in the present section we see that renormalization also eliminates certain types of divergences from the theory.

2.3.1. Divergences of Feynman graphs

Before we discuss the general case, we consider a simple illustration for the qualitative behaviour of Feynman integrals. Let L and n be integers, $n + L \neq 0$ and consider the L-dimensional integral (ignoring integration constants)

$$\int_{\Lambda_0}^{\Lambda_1} \mathrm{d}^L t \; t^n = \int_{\Lambda_0}^{\Lambda_1} \mathrm{d}t \cdots \int_{\Lambda_0}^{\Lambda_1} \mathrm{d}t \; t^n = \frac{n!}{(n+L)!} \left(\Lambda_1^{n+L} - \Lambda_0^{n+L} \right). \tag{2.42}$$

The limit $\Lambda_1 \to \infty$ is called *ultraviolet (UV) limit* while $\Lambda_0 \to 0$ is the *infrared (IR) limit*. This naming is motivated physically: Ultraviolet light carries higher energy ("$t \to \infty$") per photon than visible light, while infrared light carries less ("$t \to 0$").

Clearly, the expression eq. (2.42) is divergent in the UV limit if $n + L > 0$. We call this phenomenon an *UV-divergence*. Similarly, the integral has an *IR-divergence* if $n + L < 0$. If $n + L = 0$, the result will be a logarithm which is both UV-divergent and IR-divergent.

Now consider a Feynman integral in momentum space, eq. (1.47),

$$\mathcal{F}[\Gamma] = \prod_{v \in V_\Gamma} (-i\lambda_{|v|}) \cdot \prod_{l \in L_\Gamma} \int \frac{\mathrm{d}^D \underline{k}_l}{(2\pi)^D} \prod_{e \in E_\Gamma} \left(G_F(\underline{k}_e) \right)^{\nu_e}. \tag{2.43}$$

By choosing spherical coordinates, we can split each D-dimensional integration $\mathrm{d}^D \underline{k}_l$ into a *scale* t_l and $D - 1$ *angles* $\{\underline{\theta}_l\}$, compare def. 81. The scale is to be integrated from 0 to ∞ with a measure $\mathrm{d}t_l \; t_l^{D-1}$, while the integration domain of the angles is compact. Next, for each integration scale t_l, we extract a common factor t such that $t_l = t \cdot c_l$ and the quantities c_l represent the ratio between two scales, fixing e.g. $c_1 = 1$. There are $|L_\Gamma|$ (def. 28) integrations over different t_l, hence the integration over t has a measure $\mathrm{d}t \; t^{|L_\Gamma| D - 1}$.

Definition 94. Let t_l be as above. A *superficial UV divergence* is a divergence of the Feynman integral in the limit where all $t_l \to \infty$ jointly, that is, the limit $t \to \infty$ with finite c_l. Conversely, if the integral diverges in the case where only a subset of the t_l goes $\to \infty$, then it is said to have an *UV subdivergence*.

In the limit $t \to \infty$, the Feynman propagator eq. (1.24) behaves like t^{-2}, regardless of the value of the mass m_e. Consequently, the integrand in eq. (2.43) scales like

$$\prod_{e \in E_\Gamma} \left(G_F(\underline{k}_e) \right)^{\nu_e} \sim \prod_{e \in E_\Gamma} \left(t^{-2} \right)^{\nu_e} = t^{-2 \sum_{e \in E_\Gamma} \nu_e}, \qquad t \to \infty.$$

Including the integration measure $\mathrm{d}t\ t^{|L_\Gamma|D-1}$, we find that in the superficial UV limit, $t \to \infty$, the Feynman integral eq. (1.47) behaves like

$$\int^{\Lambda_1} \mathrm{d}t\, t^{|L_\Gamma|D-1-2\sum_{e\in E_\Gamma}\nu_e} \cdot (\text{angle integrations}) \propto \left(\Lambda_1^2\right)^{|L_\Gamma|\frac{D}{2}-\sum_{e\in E_\Gamma}\nu_e}, \qquad \Lambda_1 \to \infty. \quad (2.44)$$

The exponent $|L_\Gamma|\,\frac{D}{2} - \sum_{e\in E_\Gamma}\nu_e = -\omega_\Gamma$ is nothing but the negative superficial degree of convergence (def. 41). This justifies the name: The Feynman integral is superficially UV-divergent if $\omega_\Gamma \leq 0$. A UV subdivergence (def. 94) of $\mathcal{F}[\Gamma]$ amounts to a superficial UV divergence of the integral of some subgraph $\gamma \subset \Gamma$. One finds that again, the sub-integral is divergent if $\omega_\gamma \leq 0$.

Theorem 28 (Weinberg power counting theorem [317])**.** The Feynman integral $\mathcal{F}[\Gamma]$ of a Feynman graph Γ is UV-convergent if the superficial degree of convergence def. 41 fulfils

1. $\omega_\Gamma > 0$ and
2. $\omega_\gamma > 0$ for all subgraphs $\emptyset \neq \gamma \subset \Gamma$.

At the same time, each factor t_l is the magnitude of a 4-momentum. Consequently, its mass dimension (def. 4) is $[t_l] = 1$ and the superficial degree of convergence equals the mass dimension of the overall Feynman integral:

$$\text{assuming } [\lambda_j] = 0, \qquad \left[\mathcal{F}[\Gamma]\right] = -2\omega_\Gamma = |L_\Gamma|\,D - 2\sum_{e\in E_\Gamma}\nu_e. \quad (2.45)$$

If the coupling constants λ_j themselves have a non-vanishing mass dimension, then

$$\left[\mathcal{F}[\Gamma]\right] = -2\omega_\Gamma + \sum_{v\in V_\Gamma}[\lambda_{|v|}]. \quad (2.46)$$

We further remark that the UV-limit in momentum space corresponds to a short-distance limit in position space. Instead of using the Feynman integral in momentum space (eq. (2.43)), the same conclusions can be reached in position space or in the parametric representation, see e.g. [303]. Inspecting eq. (1.50), we can confirm that the prefactor $\Gamma(\omega_\Gamma)$ causes the expression to diverge as soon as ω_Γ is a non-positive integer, in accordance with theorem 28.

Example 83: Multiedges, mass dimension.

For the massless multiedge graphs, the only quantity with a nonvanishing mass dimension are the external momentum $s := \underline{p}^2$, with $[s] = 2$, and potentially the coupling constants. The monomial s^n has mass dimension $2n$. Indeed, the amplitude of the 1-loop-multiedge (example 24) is $\mathcal{F}\left[M^{(1)}\right] \propto \lambda_3^2 s^{-\omega}$ as expected from eq. (2.46), $\left[\mathcal{F}[M^{(l)}]\right] = 2[\lambda_{l+2}] - 2\omega$.

Definition 95. A Feynman integral $\mathcal{F}[\Gamma]$ is said to be *logarithmically UV divergent* if the superficial degree of convergence (def. 41), or equivalently the mass dimension (eq. (2.45)), is $\omega_\Gamma = 0$. It is said to be *quadratically UV divergent* if $\omega_\Gamma = -1$, and so on.

Returning to our initial example eq. (2.42), we can repeat the whole procedure for the infrared limit, analyzing "superficial" infrared divergences. The result is a statement analogous to theorem 28, the *Lowenstein Zimmerman power counting theorem* [318].

Infrared singularities arise if the denominators in Feynman propagators (eq. (1.24)) vanish at the lower integration limit, which is only possible for massless particles $m_e = 0$. However, the fact that $\underline{k}_e^2$ can be both positive or negative means that the denominator can also vanish in other regions of the integration domain, which can depend on the external kinematics. Consequently, there are two different classes of infrared divergences:

1. Infrared divergences in a closer sense are *soft* and *collinear* IR divergences, they occur in the limit of vanishing momentum in massless propagators. Although they make the individual integrals diverge, these divergences always cancel if one sums up all processes contributing to a physically observable process by the *Kinoshita Lee Nauenberg theorem* [319–322]. One can avoid them for example by giving a small artificial mass to internal edges or by choosing suitable momenta of external edges [323].

2. In a wider sense, massive propagators can also become singular if they are onshell (def. 8), $\underline{k}_e^2 = m_e^2 > 0$. Unlike UV and IR divergences, these situations reflect an expected physical behaviour of scattering amplitudes, for example, a branch cut as soon as the total energy of external particles is sufficient to create a real intermediate state. The amplitude will not be holomorphic at such points, but, choosing appropriate integration contours and Riemann sheets, it will not diverge overall. See section 1.2.8 for some comments on the analytic structure of Feynman amplitudes.

We conclude that, although infrared singularities can be a formidable challenge in concrete calculations, they are not conceptionally relevant for the topic of the present thesis, which is UV renormalization. In the following, we will largely ignore infrared singularities and instead focus on the ultraviolet ones.

2.3.2. Analytic regularization

Feynman integrals are UV-divergent if their superficial degree of convergence (def. 41) is a non-positive integer, as can be seen from eq. (1.50). To work with these expressions in a mathematically sensible way, we need to *regularize* them so that they become infinite only in some well-defined limit. The most basic regularization is a *cutoff* in the integral like Λ_0, Λ_1 in eq. (2.42). However, a cutoff breaks Lorentz invariance.

Breaking a symmetry in the regularization is not necessarily catastrophic, because a regularized amplitude is only an intermediate object without direct physical significance. But the missing symmetry makes computations cumbersome, the various cutoffs become increasingly intransparent if we consider subdivergences, and special care is required to make sure that symmetries are properly restored if the regulator is removed. We therefore concentrate on those regularization schemes that preserve Lorentz symmetry.

Analytic regularization amounts to choosing $\nu_e \notin \mathbb{N}$. Physically, this means that we slightly change the short-distance, or high-energy, behaviour of propagators. The resulting amplitude will be divergent in the *physical limit* $\{\nu_e \to 1\}$. We can introduce parameters $\nu_e := 1 + \varepsilon_e$, where the physical limit is $\varepsilon_e \to 0$. It is generally unnecessary to alter every single propagator, as long as ω_γ becomes non-integer for every divergent subgraph γ.

Example 84: Massless l-loop multiedges, analytic regularization.

We can specialize the amplitude from example 25 to $D = 4$ dimensions:

$$\mathcal{F}\big[M^{(l)}\big](s) = \frac{-\lambda_{l+2}^2 i^{l+1}}{(4\pi)^{2l}} \frac{\Gamma(\omega)}{\prod_e \Gamma(\nu_e)} \frac{1}{s^\omega} \frac{\prod_e \Gamma\left(2-\nu_e\right)}{\Gamma\left(2(l+1)-\nu\right)}.$$

Here, $\nu := \nu_1 + \ldots + \nu_{l+1}$. Choose, $\nu_e =: 1 + \varepsilon$ with the same parameter ε for all edges. In that case $\nu = l + 1 + (l+1)\varepsilon$ and $\omega = (l+1)(1+\varepsilon) - 2l = 1 - l + (l+1)\varepsilon$.

$$\mathcal{F}\big[M^{(l)}\big](s) = \frac{-\lambda_{l+2}^2 i^{l+1}}{(4\pi)^{2l}} \frac{\Gamma(1-l+(l+1)\varepsilon)}{\left(\Gamma(1+\varepsilon)\right)^{l+1}} \frac{1}{s^\omega} \frac{\left(\Gamma\left(1-\varepsilon\right)\right)^{l+1}}{\Gamma\left((l+1)-(l+1)\varepsilon\right)}.$$

We are interested in a series expansion of the regularized amplitude in the regularization parameter(s). For the Euler Gamma function (def. 5), this is easily done:

$$\begin{aligned} z\Gamma(z) = \Gamma(1+z), \qquad \Gamma(z)\Gamma(1-z)\sin(\pi z) = \pi, \\ \Gamma(1+z) = \exp\left(-\epsilon\gamma_E + \sum\nolimits_{m=2}^{\infty} \frac{(-z)^m}{m}\zeta(m)\right). \end{aligned} \tag{2.47}$$

Here, $\gamma_E = 0{,}577\ldots$ is Euler's constant [324]. The Riemann Zeta function [325] is

$$\zeta(m) := \sum_{t=1}^{\infty} \frac{1}{t^m}. \tag{2.48}$$

Example 85: Massless 1-loop multiedge, series expansion.

The 1-loop multiedge from example 84, with the choice $\nu_e = 1 + \varepsilon$, requires ratios like

$$\left(\frac{\Gamma\left(1-\epsilon\right)}{\Gamma(1+\epsilon)}\right)^n = \exp\left(2n\epsilon\gamma_E + 2n\sum_{m=1}^{\infty} \frac{\epsilon^{2m+1}}{2m+1}\zeta(2m+1)\right).$$

As expected, the regularized Feynman amplitude is divergent in the limit $\varepsilon \to 0$:

$$\begin{aligned} \mathcal{F}\big[M^{(1)}\big](s) &= \frac{\lambda_3^2}{(4\pi)^2} \frac{1}{s^{2\epsilon}} \frac{1}{2\epsilon(1-2\varepsilon)} \exp\left(2\sum_{m=1}^{\infty} \frac{\left((-2)^{2m+1}+2\right)\varepsilon^{2m+1}}{2m+1}\zeta(2m+1)\right) \\ &= \frac{\lambda_3^2}{(4\pi)^2}\left(\frac{1}{2\varepsilon} + 1 - \ln s + \left(2 - 2\ln s + (\ln s)^2\right)\varepsilon + \ldots\right). \end{aligned}$$

2.3.3. Dimensional regularization

In section 2.3.2, we saw that the Feynman amplitude can be regularized by letting the superficial degree of convergence ω (def. 41) be non-integer. Instead of choosing $\nu_e \notin \mathbb{Z}$ as in section 2.3.2, one can also introduce a non-integer dimension according to

$$D := D_0 - 2\epsilon,$$

where $D_0 \in \mathbb{N}$. This is *dimensional regularization* [326, 327],[328, Chap. 3.3]. To ensure that all mass dimensions (def. 4) are consistent, one generally needs to introduce an arbitrary reference mass scale s_0 as soon as D is altered, compare def. 104.

The notion of a D-dimensional integral needs explanation in the case of $D \notin \mathbb{N}$. Precise constructions can be found in [326, 327], but the general idea is very much in the spirit of the above discussion of divergence in eq. (2.44): One first splits off $D_0 - 1$ spatial "angular" integrals which work as usual. The remaining $(1 - 2\epsilon)$-dimensional "radial" integral is then done by analytic continuation similar to eq. (2.42). This analytic continuation is already implicit in the parametric integrand (eq. (1.50)) which does contain D only as function arguments, but not as dimension of an integral. Similarly, the analytic continuation is unproblematic for Fourier transforms of monomials (eq. (1.2)). In $D = 4 - 2\epsilon$ dimensions, the massless Feynman propagator in position space (eq. (1.23)) involves corrections $\in \mathcal{O}(\epsilon)$,

$$G_F(x) = \int \frac{\mathrm{d}^D k}{(2\pi)^D} \frac{i}{\underline{k}^2} e^{-ikx} = \frac{i}{(2\pi)^2 \underline{x}^2} \left(1 + \epsilon \left(\gamma_E + \ln(\pi \underline{x}^2 / \underline{x}_0^2)\right) + \mathcal{O}(\epsilon^2)\right). \tag{2.49}$$

A Feynman amplitude in dimensional regularization will be a Laurent series in ϵ. If no IR divergences are present then there are no higher order poles than $\epsilon^{-|L_\Gamma|}$ [329] (see examples 86 and 88 and theorem 55), otherwise, with IR divergences, poles can be $\epsilon^{-2|\Gamma|}$ [112]. For one loop graphs, this IR pole gives rise to terms $\propto \ln(s/s_0)^2$, known as *Sudakov double logarithms* [330]. Moreover, the pole terms in the Laurent series will generally depend on kinematic variables (in momentum-space). This is called *nonlocal divergence* because, after Fourier transform to position space, such terms are not proportional to $\delta(\underline{x})$.

Lemma 29. Let $H_n = \sum_{j=1}^n j^{-1}$ be the n^{th} harmonic number and define $s := \underline{p}^2$ to be the scale (def. 81), where $s_0 \in \mathbb{R}$ is an arbitrary, but fixed, reference scale. Then in $D = 4 - 2\epsilon$ dimensions, the massless l-loop multiedge (example 18) with propagators $i(k^2)^{-1}$, not including the symmetry factor (theorem 13), has the Feynman amplitude

$$\mathcal{F}\left[M^{(l)}\right] = \frac{\lambda_{l+2}^2 (-is)^{l-1}}{(4\pi)^{2l} (l!)^2} \left(\frac{1}{\epsilon} + (2l+1)H_l - 1 + l\left(\ln(4\pi) - \gamma_E\right) - l \ln\left(\frac{s}{s_0}\right)\right) + \mathcal{O}(\epsilon).$$

Proof. We skip the trivial prefactor $(-i\lambda_{l+2})^2$. Set $D = 4 - 2\epsilon$ and $\nu_e = 1$ in example 24 to obtain

$$M^{(l)}(s) = \frac{s^{l-1-l\epsilon}}{(4\pi)^{l(2-\epsilon)}} \left(\Gamma(1-\epsilon)\right)^{l+1} \frac{\Gamma(-l+1+l\epsilon)}{\Gamma(l+1-(l+1)\epsilon)}. \tag{2.50}$$

The only singular factor for $\epsilon \to 0$ is the second gamma function in the numerator. Its series representation is eq. (2.47),

$$\Gamma(-l+1+l\epsilon) = \frac{(-1)^{l-1}}{l!} \left(\frac{1}{\epsilon} + l\psi(l) + \mathcal{O}(\epsilon)\right).$$

Here, $\psi(l)$ is the digamma function, with integer argument $l > 0$ it has the value [331, §5.4]

$$\psi(l) = \sum_{k=1}^{l-1} \frac{1}{k} - \gamma_E = H_{l-1} - \gamma_E$$

where γ_E is Euler's constant. All other factors in eq. (2.50) are regular for $\epsilon \to 0$, consequently their $\mathcal{O}(\epsilon^1)$ coefficients need to be included to produce an overall $\mathcal{O}(\epsilon^0)$ result. These are

$$\frac{1}{\Gamma\left(l+1-(l+1)\epsilon\right)} = \frac{1}{\Gamma(l+1)} + \epsilon(l+1)\frac{\psi(l+1)}{\Gamma(l+1)} + \mathcal{O}\left(\epsilon^2\right) = \frac{1}{l!}\left(1 + \epsilon(l+1)\left(H_l - \gamma_E\right) + \mathcal{O}\left(\epsilon^2\right)\right),$$

$$\left(\Gamma(1-\epsilon)\right)^{l+1} = 1 + \epsilon(l+1)\gamma_E + \mathcal{O}\left(\epsilon^2\right), \qquad s^{l-1-l\epsilon} = s^{l-1}\left(1 - \epsilon l \ln s + \mathcal{O}\left(\epsilon^2\right)\right),$$
$$(4\pi)^{-2l+l\epsilon} = (4\pi)^{-2l}\left(1 + \epsilon l \ln(4\pi) + \mathcal{O}\left(\epsilon^2\right)\right).$$

Finally, use $H_l = H_{l-1} + l^{-1}$ and include a factor i^{l+1} for $l+1$ internal propagators. □

Example 86: Massless 1-loop multiedge, dimensional regularization.

The 1-loop multiedge, by lemma 29, has the amplitude

$$\mathcal{F}\left[M^{(1)}\right] = \frac{\lambda_3^2}{(4\pi)^2}\left(\frac{1}{\epsilon} + 2 - \gamma_E + \ln(4\pi) - \ln\left(\frac{s}{s_0}\right) + \mathcal{O}\left(\epsilon\right)\right).$$

Compare to example 85. Both series have a simple pole in the regulator and the finite term is $-\ln(s)$ up to constants, which differ between the two regularizations. Similarly,

$$\mathcal{F}\left[M^{(2)}\right](s) = \frac{-is\lambda_4^2}{4(4\pi)^4}\left(\frac{1}{\epsilon} + \frac{11}{2} - 2\gamma_E + 2\ln(4\pi) - 2\ln\left(\frac{s}{s_0}\right)\right).$$

Example 87: Dunce's cap in dimensional regularization.

In a massless theory, the multiedge graph $M^{(l)} \propto s^{-\omega}$ (example 25) amounts to a propagator with the non-integer power ω. This means that a triangle graph, where the edges are replaced with multiedes, equals, up to prefactors, a massless triangle graph where the edges carry said non-integer propagator power. If two of the external edges are on-shell then triangle graphs can be computed recursively like the multiedges (example 25), and evaluate to Gamma functions. For arbitrary momenta, the triangle graph evaluates to Appel's hypergeometric F_4 functions [332, 333]. Without any multiedge insertions, the graph is convergent in 4 dimensions and computed in [334, Eq. (2.11)].

The dunce's cap corresponds to the insertion of a 1-loop multiedge in one of the edges of the triangle. Its unrenormalized amplitude, without the symmetry factor $\frac{1}{2}$, reads [335] (compare also [336, 337])

$$\mathcal{F}[\Gamma](s_1, s_2, s_3) = \frac{1}{2(4\pi)^4}\left(\frac{1}{\epsilon^2} + \left(5 - 2\gamma_E - 2\ln\left(\frac{s_3}{s_0}\right) + 2\ln(4\pi)\right)\frac{1}{\epsilon} + \text{finite terms}\right).$$

Again, the amplitude contains a nonlocal divergence.

Example 88: Second chain graph in dimensional regularization.

Consider the second chain graph. We have computed its amplitude in example 26. Using $D = 6 - 2\epsilon$, and leaving out the prefactors $\propto \frac{\lambda^2}{(4\pi)^{\frac{D}{2}}}$, we find

$$\mathcal{F}[S_i] = is^{1-2\epsilon}\frac{\Gamma(-1+\epsilon)\Gamma(-1+2\epsilon)\Gamma(2-2\epsilon)\Gamma^3(2-\epsilon)}{\Gamma(4-3\epsilon)\Gamma(4-2\epsilon)\Gamma(1+\epsilon)}$$
$$\mathcal{F}[S] = -s^{1-3\epsilon}\frac{\Gamma^2(-1+\epsilon)\Gamma(-1+3\epsilon)\Gamma(2-3\epsilon)\Gamma^5(2-\epsilon)}{\Gamma(4-4\epsilon)\Gamma^2(4-2\epsilon)\Gamma(1+2\epsilon)}.$$

Observe how the various integers count the loops, subgraphs, edges etc.. The factors $\Gamma(-1+\ldots)$ are divergent for $\epsilon \to 0$, a series expansion results in

$$\mathcal{F}[S] = -s\Big(-\frac{1}{648\epsilon^3} + \frac{-35+9\gamma_E}{1944\epsilon^2} + \frac{1}{216\epsilon^2}\ln\left(\frac{s}{s_0}\right) + \frac{-2984+18\gamma_E(70-9\gamma_E)+9\pi^2}{23328\epsilon} + \frac{35-9\gamma_E}{648\epsilon}\ln\left(\frac{s}{s_0}\right) - \frac{1}{144\epsilon}\ln\left(\frac{s}{s_0}\right)^2 + \mathcal{O}(\epsilon^0)\Big).$$

Some of the pole terms depend on $\ln(s/s_0)$. They are a nonlocal divergence.

Definition 96. Let Γ be a Feynman graph in $D_0 \in \mathbb{N}$ dimensions, free of IR-divergences, logarithmically UV-divergent (def. 95), and without UV-subdivergences (def. 94), and let $0 < \nu_e \in \mathbb{N}$. The *Feynman period* of Γ is given by the convergent integral

$$\mathcal{P}[\Gamma] = \prod_{e\in E_\Gamma}\int_0^\infty \frac{\mathrm{d}a_e\, a_e^{\nu_e-1}}{\Gamma(\nu_e)}\,\delta\left(1-\sum_{e=1}^{|E_\Gamma|}a_e\right)\frac{1}{\psi^{\frac{D_0}{2}}}.$$

Especially, the Feynman period is independent of kinematics.

The proof for finiteness, and many more properties, can be found in [338–342]. The name *period* is borrowed from mathematics: A period is an absolutely convergent integral of a rational function with rational coefficients and an integration domain given by polynomial inequalities with rational coefficients [343].

Theorem 30. Let Γ be a Feynman graph without any subdivergences (def. 94) in $D_0 \in \mathbb{N}$ dimensions, free of IR-divergences, and logarithmically UV-divergent (def. 95). Let $s \propto \underline{p}^2$ be the momentum scale, s_0 a fixed reference scale, and $\{\theta\}$ angles (def. 81). Then the Feynman amplitude of Γ in dimensional regularization has the form

$$\mathcal{F}[\Gamma] = \Lambda\left(\frac{\mathcal{P}[\Gamma]}{|L_\Gamma|}\frac{1}{\epsilon} - \mathcal{P}[\Gamma]\ln\left(\frac{s}{s_0}\right) + C_\Gamma(\{\theta\}) + \mathcal{O}(\epsilon)\right).$$

Here, $\Lambda = i^{|E_\Gamma|}(4\pi)^{|L_\Gamma|(-\frac{D_0}{2})}\prod_{v\in V_\Gamma}(-i\lambda_{|v|})$, and $\mathcal{P}[\Gamma]$ is the period (def. 96), and C_Γ is a finite quantity which might depend on the angles $\{\theta\}$, but not on the scale s.

Proof. Consider the Feynman rules in parametric space (eq. (1.50)). Without subdivergences, the only divergence comes from $\Gamma(\omega_\Gamma)$. In dimensional regularization

$$\omega_\Gamma = \sum_{e\in E_\Gamma} \nu_e - |L_\Gamma| \frac{D_0}{2} + |L_\Gamma|\,\epsilon =: -n + |L_\Gamma|\,\epsilon,$$

where $n \in \mathbb{N}_0$ and $-n$ amounts to the unregularized superficial degree of divergence (def. 95), $n = 0$ by assumption. Let $H_n = \sum_{k=1}^{n} \frac{1}{k}$ be the harmonic numbers. Using eq. (2.47), we find

$$\Gamma\left(-n + |L_\Gamma|\,\epsilon\right) = \frac{\Gamma\left(1 + |L_\Gamma|\,\epsilon\right)}{\prod_{k=1}^{n}\left(-k + |L_\Gamma|\,\epsilon\right)} = \frac{(-1)^n}{n!\,|L_\Gamma|\,\epsilon} + \frac{(-1)^n}{n!}\left(H_n - \gamma_E\right) + \mathcal{O}\left(\epsilon\right). \tag{2.51}$$

By lemma 12, we can extract the scale factor $\phi_\Gamma = s \cdot \tilde{\phi}_\Gamma$ from the second Symanzik polynomial. With this, the Feynman rules in parametric space (eq. (1.50)) read

$$\Lambda \cdot \Gamma(|L_\Gamma|\,\epsilon) s^{-|L_\Gamma|\epsilon} \prod_{e\in E_\Gamma} \int_0^\infty \frac{\mathrm{d}a_e\; a_e^{\nu_e - 1}}{\Gamma(\nu_e)}\; \delta\left(1 - \sum_{e=1}^{|E_\Gamma|} a_e\right) \frac{\psi^{-\frac{D_0}{2} + (|L_\Gamma|+1)\epsilon}}{\tilde{\phi}_\Gamma^{|L_\Gamma|\epsilon}}.$$

Expand in ϵ. $\Gamma(|L_\Gamma|\,\epsilon)$ has a simple pole $\frac{1}{|L_\Gamma|\epsilon}$ by eq. (2.51). Setting $\epsilon = 0$ in the integral, we obtain the Feynman period (def. 96), which is independent from angles. Next, expand $(s/s_0)^{-|L_\Gamma|\epsilon} = e^{-|L_\Gamma|\epsilon \ln(s/s_0)}$ to first order. Finally, the constant term C_Γ is given by the order ϵ^1 of the integral, which will involve $\tilde{\phi}_\Gamma$ and therefore depend on the angles. The exponent ϵ in the prefactor $\Lambda = i^{|E_\Gamma|}(4\pi)^{|L_\Gamma|(\epsilon - \frac{D_0}{2})} \prod(-i\lambda_{|v|})$ can be left out, because it results in momentum-independent, non-singular contributions, which can always be absorbed into C_Γ.

Note the result is well-defined for any choice of the scale (def. 81), since a rescaling $s \to c \cdot s$ as c can be absorbed into $C_\Gamma \to C_\Gamma - \ln c$. A more rigorous proof, concerning especially the convergence of the integral and the precise dependence on angle variables, is given in [303, 344]. □

Theorem 30 (together with analogous statements for other regularization schemes) is the core of renormalization theory, therefore it deserves some explanation. The statement of theorem 30 is not that "every primitive graph depends on the overall momentum like $\ln s$". This is certainly false, to see this, consider any massive graph which has non-trivial analytic properties as soon as the energy is sufficient to create real massive intermediate particles. The masses are expressed in terms of angles such as $\theta = m^2/s$. If masses are fixed then θ changes with s, and theorem 30 has nothing to say about the behaviour of the amplitude in this case, because $C_\Gamma(\theta)$ can be any function. Instead, what we are asking is "If all energies and all masses are scaled with the same factor s, what does the amplitude do?". The surprising answer of theorem 30 is that this *does* change something, namely, it alters the amplitude by $\mathcal{P}[\Gamma] \ln s$. Phrased differently, primitive graphs are *not* scale invariant.

Example 89: Massless multiedge, period.

If we leave out tadpole graphs (def. 29, compare the discussion in section 5.1.4), then a multiedge (example 18) has no subdivergence (def. 94). Consequently, the prefactor of $\frac{1}{\epsilon}$ in lemma 29 represents the period by theorem 30. The only caveat is that we have to exclude a prefactor s^{l-1} from the multiedge. Concretely, in $D = 4 - 2\epsilon$, we find the following period for the l-loop multiedge $M^{(l)}$:

$$i^{l+1}(4\pi)^{l(-2)}(-i\lambda_{l+2})^2 \cdot \frac{\mathcal{P}\left[M^{(l)}\right]}{l} \overset{!}{=} \frac{\lambda_{l+2}^2 (-i)^{l-1}}{(4\pi)^{2l}(l!)^2}$$
$$\mathcal{P}\left[M^{(l)}\right] = \frac{-(-1)^l}{l!(l-1)!}.$$

Example 90: Second chain graph, nontrivial primitive.

In example 62, we saw that the Connes-Kreimer Hopf algebra contains primitive elements other than $\bullet$. The first of these is $p_2 :=$  $- \frac{1}{2} \bullet\bullet$. Using theorem 25, one possible realization of these trees as Feynman graphs is  $\simeq S_i$ and $\bullet \simeq \gamma_i$ from examples 26 and 75. Let $P_2 := S_i - \frac{1}{2}\gamma_i \frac{i}{s}\gamma_i$, where all momenta are to be taken equal to s (the momentum dependence would require more care if we had chosen a graph  where the subgraph has a different external edge structure). Using example 88, we find

$$\mathcal{F}[P_2] = is\left(\frac{11}{432}\frac{1}{\epsilon} - \frac{11}{216}\ln\left(\frac{s}{\mu}\right) + \frac{535 - 132\gamma_E}{2592} + \mathcal{O}(\epsilon)\right).$$

This is indeed the form predicted by theorem 30, with a period $\mathcal{P}[P_1] = \frac{11}{216}$.

We will be using dimensional regularization with the sole purpose of making intermediate expressions finite. One can, however, take it at face value to obtain results in a truly different dimension of spacetime. Examples in that regard are [345–347]. A more drastic step is to extend D all the way to negative integers $D = -n$, interpreting an integral $\int \mathrm{d}^D \underline{x}$ as a derivative $\partial^n_{\underline{x}}$. This gives rise to the *negative dimensional integration method* to solve Feynman integrals [333, 348–350]. Recent more algebraic perspectives are [351, 352].

2.3.4. Renormalizability

Amplitudes needing renormalization and residues of the Lagrangian

We have based the renormalized Feynman rules (def. 88) on the arbitrary set $\mathfrak{R}$ of *amplitudes needing renormalization* (def. 83), without restricting to "physical" choices. By construction, each amplitude $G \in \mathfrak{R}$ is a power series which is assigned exactly one renormalization condition.

On the other hand, going back to the simplified example section 2.2.1, we see that, in order to carry out the series inversion eq. (2.33), the unrenormalized series needs to have a non-vanishing first order term. Translated to Feynman graphs, this means that each amplitude $G \in \mathfrak{R}$ must have a non-vanishing treelevel term. But those vertices are precisely the set $\mathfrak{L}$ of *residues of the Lagrangian* (def. 49). We record this finding as a theorem:

Theorem 31. Renormalization of Feynman graphs based on the amplitudes $\mathfrak{R}$ (def. 83) is only possible if $\mathfrak{R} \subseteq \mathfrak{L}$ (def. 49). Also, one needs to provide exactly one renormalization condition for each $(g, T) \in \mathfrak{R}$.

On the other hand, if $\mathfrak{R} \subsetneq \mathfrak{L}$ then there are constants in $\mathfrak{L}$ to which we do not assign values by any renormalization condition. Mathematically, this is possible, but physically questionable, since the result then contains unknown bare parameters. From now on, we assume that $\mathfrak{R} = \mathfrak{L}$.

In concrete QFTs, the interplay between $\mathfrak{R}$ and $\mathfrak{L}$ works as follows: We start with an "initial guess" of a Lagrangian. Then, by calculation (see theorem 32), we obtain the set $\mathfrak{R}$, which might or might not be a subset of $\mathfrak{L}$. In the latter case, we need to include additional monomials in the Lagrangian $\mathfrak{L}$ and repeat the calculation, until eventually theorem 31 is satisfied. In general, this will force us to add all possible terms of given mass dimension (def. 4) because quantum corrections lead to *operator mixing*, that is, a quantum correction originating from one such term will generally include all possible terms of the same mass dimension which are not forbidden by symmetries [353].

Example 91: Renormalization of a massless scalar field.

Theorem 31 has an interesting, albeit slightly philosophical, consequence for massless theories: Starting with a massive interacting Lagrangian (eq. (1.5)), we obtain a renormalized theory where the mass needs to be determined by renormalization conditions. We can choose the renormalized theory to be massless by imposing the renormalization condition $m = 0$ for the renormalized mass term. In this way, effectively, we can leave out all mass terms and work with a massless Lagrangian from the start. The true reason is not that mass corrections can not arise, but that we demand them to vanish, compare [354]. Symmetries change the picture, as we will see in section 5.1.1.

Finiteness and subdivergences

The third aspect to the process of renormalization is the question whether a renormalized amplitude will be finite. Let Γ be a 1-loop graph. It is UV-divergent if and only if $\omega_\Gamma \leq 0$ (theorem 28). By def. 86, Γ is primitive iff $\Gamma \in \mathfrak{R}$. Now observe that by renormalization (def. 88), a primitive graph is mapped to the renormalized Feynman rules

$$\mathcal{F}_\mathcal{R}[\Gamma] = (\mathrm{id} - \mathcal{R})\,\mathcal{F}[\Gamma] = \mathcal{F}[\Gamma] - \mathcal{R}\mathcal{F}[\Gamma].$$

If $\mathcal{R}$ denotes kinematic renormalization (def. 91), then $\mathcal{F}_\mathcal{R}[\Gamma]$ is finite by theorem 30, because the period is independent of external momenta and therefore $\mathcal{P}[\Gamma]\frac{1}{\epsilon} - \mathcal{R}\mathcal{P}[\Gamma]\frac{1}{\epsilon} = 0$. We conclude that the renormalized Feynman rules of all 1-loop graphs are finite provided that $\Gamma \in \mathfrak{R}$ for all Γ where $\omega_\Gamma \leq 0$.

Definition 97. A *renormalization scheme* is a choice of a renormalization operator $\mathcal{R}$ such that

1. The Rota-Baxter equation eq. (2.39) is fulfilled, and
2. The renormalized Feynman rules (def. 88) $(\mathrm{id} - \mathcal{R})\mathcal{F}[\Gamma]$ are finite for every primitive (def. 86) Feynman graph Γ.

In all renormalization schemes, the treelevel term of a Green function has the value unity, that is, we project onto the treelevel tensor (see section 2.2.2).

Theorem 32. Assume that $\Gamma \in \mathfrak{R}$ (def. 83) whenever the superficial degree of convergence (def. 41) is $\omega_\Gamma \leq 0$. Let $\mathcal{R}$ be a renormalization scheme (def. 97). Then the renormalized Feynman rules (def. 88) $\mathcal{F}_\mathcal{R} = S^\mathcal{F}_\mathcal{R} \star \mathcal{F}$ are finite.

Proof. For a detailed proof, see [269, 293, 307, 355].

Use induction on the coradical degree. For primitive graphs, $\mathcal{F}_\mathcal{R}$ is finite by definition (def. 97). Assume that $\mathcal{F}_\mathcal{R}(\gamma)$ is finite for all Feynman graphs γ with $\mathrm{cor}(\gamma) < n \in \mathbb{N}$. By the Dyson-Schwinger equation theorem 26, the graphs of coradical degree n are of the form

$$\Gamma' = B^\Gamma_+ \left(P(\{\gamma\}) \right).$$

Here, Γ is a primitive (kernel) graph and $P(\{\gamma\})$ is a polynomial in the graphs γ of coradical degree smaller than n. Using eq. (2.38) (which needs the Rota-Baxter equation assumed in def. 97) and the induction assumption, the renormalized Feynman rules $\mathcal{F}_\mathcal{R}[P(\{\gamma\})] = P\left(\{\mathcal{F}_\mathcal{R}[\gamma]\}\right)$ are finite. The renormalized amplitude of Γ' is, by theorem 27,

$$\mathcal{F}_\mathcal{R}\left[\Gamma'\right] = (\mathrm{id} - \mathcal{R}) \int \mathrm{d}_\Gamma \, \mathcal{F}_\mathcal{R}\left[P(\{\gamma\})\right].$$

The integral on the right hand side does not contain subdivergences, so $(\mathrm{id} - \mathcal{R})$ applied to it is finite by assumption. Similarly, one can establish that the counterterms $S^\mathcal{F}_\mathcal{R}[\Gamma]$ (def. 89) are local.

The non-Hopf algebra version of this theorem is known as *Zimmermann forest formula*, named after the forests of rooted trees corresponding to nested sub-divergences (theorem 25). This combinatorial procedure (which we nowadays encode in the coproduct Δ), together with the kinematic renormalization operator $\mathcal{R}$ (def. 91), is called *BPHZ-renormalization* [168, 356, 357] (def. 91). See also [328, 358, 359]. □

We have used only simple subtractions $(\mathrm{id} - \mathcal{R})$, which, on first sight, are insufficient for quadratically divergent (def. 95) amplitudes. However, our procedure works in full generality because we project on the tensors. Consider an amplitude $(g, T) \in \mathfrak{R}$, where the tensor is $T \propto \left(\underline{p}^2\right)^n$ with $n \geq 1$, that is, the underlying graph Γ is divergent of degree $2n$. In that case, one also needs to include $(g, 1), (g, \underline{p}^2), \ldots, (g, (\underline{p}^2)^{n-1}) \in \mathfrak{R}$ and in total, $n + 1$ renormalization conditions must be provided. Each of these amplitudes can be treated with a simple subtraction, but all of the together are equivalent to a subtraction of the first $n + 1$ powers of momenta in $\mathcal{F}[\Gamma]$.

Predictive power of a renormalized theory

Theorem 32 tells us that we can make any Feynman graph finite by including the residue of every possible subgraph into $\mathfrak{R}$. We then obtain the core Hopf algebra (def. 85). If $\mathfrak{R}$ contains infinitely many amplitudes, then, by theorem 31, one needs to provide infinitely many renormalization conditions to give a physical meaning to the renormalized amplitude. This makes the theory *unpredictive*: No finite set of (measured) input values allows to predict all remaining observables.

Definition 98. A quantum field theory is called *renormalizable* if there is a finite set $\mathfrak{R}$ (def. 83) such that, if Γ is a superficially divergent graph (def. 94) without subdivergences, then $\Gamma \in \mathfrak{R}$.

In detail, def. 98 implies two conditions: (1) There are only finitely many residues $g = \text{res}(\Gamma)$ of graphs such that $\omega_\Gamma \leq 0$. And (2) For any such residue, there are only finitely many tensors T such that $(g, T) \in \mathfrak{R}$.

The superficial degree of convergence (def. 41) is nothing but the negative mass dimension (def. 4) of a graph, see eq. (2.46). Euler's formula (eq. (1.42)) implies two other useful characterizations of renormalizability. They have long been known (e.g. [360]) and can be derived using Euler's formula eq. (1.42).

Lemma 33. A quantum field theory is renormalizable (def. 98) if the superficial degree of convergence ω_Γ (def. 41) is independent of the loop number $|L_\Gamma|$, and $\omega_\Gamma \leq 0$ for only finitely many residues of graphs.

Lemma 34. A quantum field theory is renormalizable (def. 98) if all coupling constants λ_n in its Lagrangian (def. 6) have mass dimension (def. 4) zero.

A slightly different perspective on renormalizability originates from Dyson-Schwinger equations. There, renormalizability (def. 98) is equivalent to having only *finitely many* DSEs of the upper type in theorem 27. The renormalization condition, encoded in the operator $\mathcal{R}$, is a boundary condition for the solutions $G^r_\mathcal{R}$ of these DSEs. Once these functions are fixed, all remaining $G^m_\mathcal{R}$, where $m \notin \mathfrak{R}$, can be computed without further renormalization, that is, without providing additional input data.

Example 92: Second chain graph, renormalized amplitude.

Consider the second chain graph from example 26. It is not primitive and, correspondingly, has non-local divergences (example 88). The appropriate set $\mathfrak{R}$ for ϕ^3 theory is the one we chose in example 69, fulfilling lemma 33. We will use the notation $S_i = S/\gamma_i$ and $\gamma = S/(\gamma_1\gamma_2)$, the corresponding rooted trees are shown in example 75.

First, we renormalize S_1, which has one subgraph γ_2 needing renormalization.

$$\Delta(S_1) = S_1 \otimes \mathbb{1} + \mathbb{1} \otimes S_1 + \gamma_2 \otimes \gamma, \qquad \text{antipode: } S(S_1) = -S_1 + \gamma_2\gamma.$$

Eventually, all graphs are proportional to s, we leave out this overall factor. The counterterm and renormalized amplitude are

$$S^{\mathcal{F}}_{\mathcal{R}}[S_1] = \mathcal{R}\left(-\mathcal{F}[S_1] + \mathcal{R}\left(\mathcal{F}[\gamma_2]\right)\frac{i}{s}\mathcal{F}[\gamma]\right) = \left(\frac{1}{72\epsilon^2} + \frac{7}{144\epsilon} - \frac{\gamma_E + \ln s_0}{36\epsilon} + \mathcal{O}(\epsilon^0)\right) i.$$

If we take $\mathcal{R}$ to be kinematic renormalization at $s = s_0$ (def. 91), then

$$\begin{aligned}\mathcal{F}_{\mathcal{R}}[S_1] &= \mathcal{F}[S_1] + S^{\mathcal{F}}_{\mathcal{R}}[S_1] + S^{\mathcal{F}}_{\mathcal{R}}[\gamma_2]\frac{i}{s}\mathcal{F}[\gamma] \\ &= \frac{1}{72} i \ln^2\left(\frac{s}{s_0}\right) - \frac{11}{216} i \ln\left(\frac{s}{s_0}\right) + \mathcal{O}(\epsilon).\end{aligned}$$

As it should be, the result is finite for $\epsilon \to 0$ and it vanishes at $s = s_0$.

Now consider the full graph S (not to be confused with the antipode) from example 26.

$$\begin{aligned}\Delta(S) &= S \otimes \mathbb{1} + \mathbb{1} \otimes S + \gamma_1 \otimes S_1 + \gamma_2 \otimes S_2 + \gamma_1\gamma_2 \otimes \gamma \\ S(S) &= -S + \gamma_1 S_1 + \gamma_2 S_2 - \gamma_1\gamma_2\gamma, \qquad S(\gamma_1\gamma_2) = \gamma_1\gamma_2 \\ S^{\mathcal{F}}_{\mathcal{R}}[S] &= \mathcal{R}\Big(-\mathcal{F}[S] + \mathcal{R}\left(\mathcal{F}[\gamma_1]\right)\mathcal{F}[S_1] + \mathcal{R}\left(\mathcal{F}[\gamma_2]\right)\mathcal{F}[S_2] - \mathcal{R}\left(\mathcal{F}[\gamma_1]\right)\mathcal{R}\left(\mathcal{F}[\gamma_2]\right)\mathcal{F}[\gamma]\Big) \\ &= -\frac{1}{648\epsilon^3} + \left(-\frac{37}{3888} + \frac{\gamma_E + \ln s_0}{216}\right)\frac{1}{\epsilon^2} + \mathcal{O}\left(\frac{1}{\epsilon}\right).\end{aligned}$$

The renormalized amplitude is (again, assuming kinematic renormalization)

$$\begin{aligned}\mathcal{F}_{\mathcal{R}}[S] &= \mathcal{F}[S] + S^{\mathcal{F}}_{\mathcal{R}}[S] + 2S^{\mathcal{F}}_{\mathcal{R}}[\gamma_i]\mathcal{F}[S_i] + S^{\mathcal{F}}_{\mathcal{R}}[\gamma_1\gamma_2]\mathcal{F}[\gamma] \\ &= -\frac{1}{648}\ln^3\left(\frac{s}{s_0}\right) + \frac{11}{1296}\ln^2\left(\frac{s}{s_0}\right) - \frac{85}{3888}\ln\left(\frac{s}{s_0}\right) + \mathcal{O}(\epsilon).\end{aligned}$$

Example 93: Renormalizability of Liouville theory.

We introduced Liouville theory in example 4, its Lagrangian is

$$\mathcal{L} = \frac{1}{2}\partial_\mu\phi\partial^\mu\phi - \exp(g\phi).$$

In two dimensions, classical Liouville theory is solved by mapping its solutions to modes of a free field via Bäcklund transformation [361]. As a quantum theory, Liouville theory is renormalizable in $D = 2$ dimensions by lemma 34. It enjoyed significant attention in the 1980s [362, 363] for its connection to string theory [148].

In four dimensions, the coupling has mass dimension (def. 4) $[g] = 1$ and Liouville theory is not renormalizable by lemma 34. This requires to introduce additional constraints, apart from the usual renormalization conditions, in order to fully fix the Green functions [364–366]. Compare example 143.

The topic of renormalizability is vast, but the space in this thesis is not. We are therefore content with a few stenographical comments without further explanation:

1. The Hopf algebraic description of renormalization can be extended to also subtract infrared singularities, using a $\mathcal{R}^*$-operation in place of $\mathcal{R}$ [329, 367–370].

2. The LSZ formula (theorem 5) requires *amputated* graphs. This means amputation of the renormalized full 2-point function, not just of the bare propagator.

3. An integral can be renormalized according to def. 88 on the level of the integrand, see for example [303]. All integrals are then convergent and regularization is not needed.

4. Renormalization can be carried out graphically if one introduces a n-valent *counterterm vertex* with amplitude $Z^{(n)} - 1$ for the Z-factor (eq. (2.33)) of each amplitude $(n) \in \mathfrak{R}$.

5. It is possible to mix different regularization schemes, the counterterms will then in general depend on all the regulators. The results in kinematic renormalization are unaltered. This freedom is essential to the removal of tadpoles, see later in section 5.1.4. If one uses a renormalization scheme that depends on the regulator (such as the MS-scheme to be introduced in def. 108), the results differ for different choices of regulators.

6. All physically sensible renormalization schemes are equivalent up to a changed, potentially α-dependent renormalization point. This will be the topic of chapter 4.

7. A theory is called *superrenormalizable* if the coupling constants have positive mass dimension, or, equivalently, if there are finitely many graphs (not residues) with $\omega_\Gamma \leq 0$.

8. The problem with non-renormalizable theories is that they need infinitely many renormalization conditions. If $|\mathfrak{R}| = \infty$ but still the renormalization conditions are dictated by some other mechanism, the theory can potentially still be predictive.

9. The correspondence between a sensible series expansion and the mass dimensions of coupling constants has been remarked as early as 1927 [29], before QFT was even formulated.

10. The physical intuition that divergences would be cured by re-defining results in terms of observable quantities also dates earlier than theorem 32. Bethe, observing the divergence in his computation of the Lamb shift, notes [371]:

    > This shift [of energy levels] comes out infinite in all existing theories, and has therefore always been ignored. However, it is possible to identify the most strongly divergent term in the level shift with an electromagnetic mass effect [...]. This effect should properly be regarded as already included in the observed mass of the electron, and we must therefore subtract from the theoretical expression, the corresponding expression for a free electron [...].

Summary of section 2.3.

1. Feynman integrals can be divergent. The superficial degree of convergence ω_Γ determines whether an integral is UV-divergent. IR-divergences are conceptually less problematic (section 2.3.1).

2. Divergent Feynman amplitudes can be regularized if one introduces non-integer powers ν_e of the propagators. This is analytic regularization (section 2.3.2).

3. Dimensional regularization amounts to choosing a non-integer spacetime dimension. A divergent graph without subdivergences then takes the form $\mathcal{F}[\Gamma] \propto \mathcal{P}[\Gamma]/\left|L_\Gamma\right| \frac{1}{\epsilon} - \mathcal{P}[\Gamma] \ln(s/\mu) + C_\Gamma$, where $\mathcal{P}[\Gamma]$ is the period, independent of kinematics (section 2.3.3).

4. If one includes the amplitude of every superficially divergent graph into $\mathfrak{R}$ then the renormalized Feynman rules are finite. If this is possible with a finitely large set $\mathfrak{R}$ then the theory is called renormalizable. It needs only a finite amount of input data in order to predict all correlation functions (section 2.3.4).

2.4. Digression: Order of derivatives and dimension of spacetime

Having finished our survey of Hopf algebra renormalization theory, we return to the axioms on the Lagrangian at the very beginning of the thesis. In def. 6, we demanded that a Lagrangian must not depend on higher than first derivatives of the field. The present section explores some motivation and consequences of this assumption, partially following [372].

In classical mechanics, Ostrogradsky's theorem [373] asserts that if a Lagrangian function contains time derivatives of higher than first order, the Hamilton function, or the total energy, is unbounded from below. To see this, consider a Lagrangian function $L(x, \dot{x}, \ddot{x})$ depending on the second derivative with respect to time in the form of a monomial $(\ddot{x})^n$, where $n \neq 1$. The requirement that the first variation of the classical action vanishes, $\delta S = 0$ (eq. (1.6)), leads to the Euler-Lagrange equation (1.7),

$$\frac{\partial L}{\partial x} - \frac{\mathrm{d}}{\mathrm{d}t}\frac{\partial L}{\partial \dot{x}} + \frac{1}{2}\frac{\mathrm{d}^2}{\mathrm{d}t^2}\frac{\partial L}{\partial \ddot{x}} = 0.$$

Since $\frac{\partial L}{\partial \ddot{x}} \sim \ddot{x}^{n-1}$, this is a differential equation of fourth order in time, as opposed to second order for a conventional Lagrangian function depending only on $x, \dot{x}$.

The Hamiltonian formalism for this generalized Lagrangian is sometimes called *Ostrogradsky formalism*. Hamilton equations of motion are supposed to be first order differential equations, hence we need four canonical variables. Choose

$$q_1 := x, \qquad q_2 := \dot{x}, \qquad p_1 := \frac{\partial L}{\partial \dot{x}} - \frac{\mathrm{d}}{\mathrm{d}t}\frac{\partial L}{\partial \ddot{x}}, \qquad p_2 := \frac{\partial L}{\partial \ddot{x}}.$$

With this definition, only p_1 involves the third derivative $\dddot{x}$, the other three canonical variables only depend on $\{x, \dot{x}, \ddot{x}\}$. Inverting these relations, one can hence express the Langrangian in terms of q_1, q_2, p_2, without using p_1. The Hamilton function (def. 9) is

$$H(q_1, q_2, p_1, p_2) := p_1\dot{x} + p_2\ddot{x}(q_1, q_2, p_2) - L(q_1, q_2, p_2). \tag{2.52}$$

This choice satisfies the Hamilton equations of motion (1.11) as expected,

$$\dot{q}_1 = \frac{\partial H}{\partial p_1}, \qquad \dot{q}_2 = \frac{\partial H}{\partial p_2}, \qquad \dot{p}_1 = -\frac{\partial H}{\partial q_1}, \qquad \dot{p}_2 = -\frac{\partial H}{\partial q_2}.$$

A closer look at the Hamilton function eq. (2.52) reveals that it is unbounded: The variable $\dot{x} = q_2$ is an independent degree of freedom, not expressed through p_1 (as it would be in the ordinary Hamilton formalism). The Lagrangian is independent of the variable p_1, hence the Hamilton function H eq. (2.52) is linear in p_1, and hence unbounded.

In quantum mechanics, at least if interactions are present, generally all possible states of a system will participate in the dynamics. A theory with unbounded energy has no stable ground state [374] and a different structure of Hilbert space compared to our construction [375]. On physical grounds, it must be rejected, compare also the discussion in [376].

Canonical quantization (section 1.2.2) involves certain additional subtleties, regarding the correspondence between classical objects and quantum field operators, as soon as higher derivatives are present [377]. A theory with second derivatives in the Lagrangian gives, qualitatively, a propagator

$$G_F(\underline{p}) = \frac{i}{\underline{p}^4 - m^4} = \frac{i}{(\underline{p}^2 + m^2)(\underline{p}^2 - m^2)},$$

which inevitably has poles at $\underline{p}^2 = +m^2$ and $\underline{p}^2 = -m^2$. Depending on conventions and interpretation, one of them corresponds to a physically absurd particle called *Ostrogradsky ghost*, showing either a negative rest mass or negative probabilities.

On the other hand, for example, ϕ^3 theory is a QFT with unbounded potential energy and yet at least a perturbative treatment is possible. It has been argued that, similarly, a higher-derivative QFT can be given meaning at least in the massless case by considering a delicate limit of vanishing masses [378, 379].

A different perspective on higher derivatives comes from dimensional analysis. A theory with n-th derivatives in the Lagrangian has a propagator which scales, for large momenta, as $(\underline{p}^2)^{-n}$. Using eq. (1.2), we find the short-distance behaviour in position space: A field with n-th derivatives propagates $\sim (r^2)^{n-\frac{D}{2}}$, see also eq. (1.26). Assuming a flat D-dimensional spacetime with one time dimension, there are $D-1$ spatial dimensions. The surface area of a sphere with radius r is

$$A_{D-1}(r) = \frac{2\pi^{\frac{D-1}{2}}}{\Gamma\left(\frac{D-1}{2}\right)} r^{D-2}. \tag{2.53}$$

Together, these two scaling laws mean that the total spatial flow of the field, that is the propagator integrated over the spherical surface, scales as $r^{2n-D} \cdot r^{D-2} = (r^2)^{n-1}$. Irrespective of the dimension of spacetime, the flow is conserved only in the case $n = 1$, that is, for a Lagrangian with first derivatives only. This heuristic argument implies that with $n \neq 1$, the theory will not be unitary, as indicated by the above Ostrogradsky ghosts.

At this point, we could settle for the conclusion that theories with higher than first derivatives are not sensible, were it not for quantum gravity. The latter is perturbatively non-renormalizable and introducing higher derivatives is one speculative way to solve the problem. We will discuss details in section 5.2.1, after having developed all the necessary concepts. Nevertheless, we are confident that prohibiting higher derivatives in def. 6 is at least a sensible choice for most of the typical cases in QFT.

3. Renormalized Green functions in kinematic renormalization

3.1. Renormalization and momentum-dependence

We have established in section 2.3.4 that renormalization amounts to the iterative subtraction of subdivergences. These subtractions do not only remove divergences, but they also impose a certain structure on the finite renormalized amplitudes. In the present section, we discuss some of the properties that are consequences of the renormalization process.

3.1.1. Angles and scales

In def. 81, we have split the arguments of a Feynman amplitude into one scale variable s and arbitrary many scale-free angles θ. From now on, we ignore the possible dependence on angles unless otherwise mentioned. This is not as much of a restriction as it seems. Observe that for a primitive graph (theorem 30), the dependence on angles resides in the finite part $C_\Gamma(\{\theta\})$, unrelated to the scale dependence given by $\mathcal{P}[\Gamma] \cdot L$. In this, the angle dependence is analogous to the divergent part, which, for a primitive graph, is independent of the scale as well. Essentially the same recursive construction that leads to renormalizability (section 2.3.4), $\mathcal{F}_\mathcal{R}(s/s_0) = (\mathcal{F}(s_0))^{-1} \star \mathcal{F}(s)$, also allows a factorization of angles and scales [271, 302, 303],

$$\mathcal{F}_\mathcal{R}(s, \theta) = \mathcal{F}_\mathcal{R}(s)\Big|_{\theta \text{ fixed}} \star \mathcal{F}_\mathcal{R}(\theta)\Big|_{s \text{ fixed}}. \tag{3.1}$$

In the remainder of section 3.1, we will see that the scale-dependence of a renormalized amplitude is to a large extent fixed by the structure of renormalization. On the other hand, little can be said about the angle dependence, even though by eq. (3.1), the Feynman rules factor "symmetrically" into a scale-dependent and an angle-dependent part. The pivotal reason is that the dependence of a primitive graph on scale is simply a linear function $\mathcal{P}[\Gamma] \cdot L$ (theorem 30), while the dependence on angles is almost arbitrary, subject to the analytic conditions mentioned in section 1.2.8.

3.1.2. Expansion in Logarithmic momenta

Unless otherwise stated, we assume that a Feynman amplitude $\mathcal{F}_\mathcal{R}[\Gamma]$ is projected to its treelevel tensor (def. 82) and coupling constant. That is, $\mathcal{F}_\mathcal{R}[\Gamma]$ is a scalar under Lorentz transformations (def. 2) and its power series starts with a constant independent of the coupling α. More precisely, in kinematic renormalization, $\mathcal{F}_\mathcal{R}[\Gamma] = 1 + \mathcal{O}(\alpha)$.

Definition 99. We express the external momenta as angles and scales (def. 81), and we introduce some arbitrary *reference scale* s_0. Define the *logarithmic scale* as

$$L := \ln \frac{s}{s_0}.$$

The point $L = 0$ amounts to $s = s_0$. In the present chapter, we restrict ourselves to kinematic renormalization (def. 91) and choose s_0 as the renormalization point. The renormalized Feynman rules (def. 88) are a character (eq. (2.38)) and hence, they are generated (with respect to the scale L) by some infinitesimal character according to eq. (2.17).

Definition 100. The infinitesimal character (def. 76) σ which generates the Feynman rules (def. 88) in kinematic renormalization is called *infinitesimal Feynman rule* and it is related to $\mathcal{F}_\mathcal{R}$ via eq. (2.17),

$$\mathcal{F}_\mathcal{R}[\Gamma](L) = \exp^\star (L\sigma)\,[\Gamma], \qquad \sigma[\Gamma] := \frac{\partial}{\partial L}\mathcal{F}_\mathcal{R}[\Gamma]\Big|_{L=0}.$$

The zeroth power $\sigma_0[\Gamma] := \sigma^{\star 0}[\Gamma] = \mathcal{F}_\mathcal{R}[\Gamma]|_{L=0}$ extracts the value at the renormalization point. In kinematic renormalization, $\sigma_0 = \tilde{\mathbb{1}}$ (def. 61) because every renormalized amplitude vanishes at $L = 0$ (def. 91), except for the treelevel amplitude, which is rescaled to $1 = \tilde{\mathbb{1}} \circ \mathbb{1}$. The behaviour in non-kinematic renormalization will be discussed in section 4.1.1. The empty graph does not depend on momenta, so $\sigma(\mathbb{1}) = 0$ in every renormalization scheme.

Example 94: Infinitesimal character for a primitive graph.

For a primitive graph Γ, we know from theorems 30 and 32 that $\mathcal{F}_\mathcal{R}[\Gamma] = \Lambda\mathcal{P}[\Gamma]\cdot L + \Lambda C_\Gamma$, where in kinematic renormalization $C_\Gamma = 0$. Indeed, def. 100 produces

$$\begin{aligned}\mathcal{F}_\mathcal{R}[\Gamma] &= \tilde{\mathbb{1}}(\Gamma) + L\cdot\sigma[\Gamma] + \frac{1}{2}L^2\cdot m\circ(\sigma\otimes\sigma)\Delta(\Gamma) + \mathcal{O}\left(L^3\right)\\ &= 0 + L\cdot\Lambda\mathcal{P}[\Gamma] + 0 + \mathcal{O}\left(L^3\right).\end{aligned}$$

We used $\Delta(\Gamma) = \Gamma\otimes\mathbb{1} + \mathbb{1}\otimes\Gamma$ and $\sigma(\mathbb{1}) = 0$. All higher orders in L vanish.

Theorem 35 ([303])**.** Let Γ be a Feynman graph free of IR-divergences, then the renormalized Feynman rules (def. 88), projected on the treelevel tensor (def. 82), depend on the scale s (def. 81) in the form

$$\mathcal{F}_\mathcal{R}[\Gamma](L) = \sum_{j=0}^{\mathrm{cor}(\Gamma)} g_j(\theta)\cdot L^j.$$

Here, L is the logarithm of the scale (def. 99) and $\mathrm{cor}(\Gamma)$ is the coradical degree (def. 71). The coefficients g_j can be different for different renormalization schemes.

Proof. The coefficients g_j will in general depend on θ because the overall amplitude does. By theorem 32, they are finite. Now, by def. 100, the term proportional to L^n is given by

$$\frac{1}{n!}\sigma^{\star n}[\Gamma] = \frac{1}{n!} m \circ \sigma^{\otimes n} \circ \Delta^n(\Gamma).$$

The iterated coproduct Δ^n (def. 70) involves factors of $\mathbb{1}$ for all Γ with $\mathrm{cor}(\Gamma) > n$ (def. 71). But $\sigma(\mathbb{1}) = 0$ and therefore $\sigma^{\star n}(\Gamma) = 0$ in those cases.

Alternatively, the statement can also be shown from Dyson-Schwinger integral equations (theorem 15), without using infinitesimal characters (def. 100), upon noticing that

$$\int \frac{\mathrm{d}s}{s} (\ln s)^n = \frac{(\ln s)^{n+1}}{n+1}.$$

The coradical degree is then the number of nested integrals. This gives a "pedestrian" derivation which does not require the Hopf algebra knowledge that an infinitesimal character *must* exist. □

Lemma 36. Let $n > 1$. In kinematic renormalization, the character $\sigma^{\star n}[\Gamma]$, and hence g_n in theorem 35, are completely determined by amplitudes of proper subgraphs $\gamma \subsetneq \Gamma$.

Proof. For a graph Γ, $c_n = \sigma^{\star n}[\Gamma] = m(\sigma \otimes \sigma^{\star(n-1)})\Delta(\Gamma)$. But $\sigma(\mathbb{1}) = 0$ in kinematic renormalization, therefore only $\Delta_1(\Gamma)$ (def. 64) contributes, consisting entirely of subgraphs. □

Example 95: Second chain graph, scale dependence.

Consider the graph $S \simeq$ from examples 26 and 92, where

$$\mathcal{F}_{\mathcal{R}}[S] = -\frac{1}{648}\ln^3\left(\frac{s}{s_0}\right) + \frac{11}{1296}\ln^2\left(\frac{s}{s_0}\right) - \frac{85}{3888}\ln\left(\frac{s}{s_0}\right)$$
$$\mathcal{F}_{\mathcal{R}}[S_i] = \frac{1}{72} i \ln^2\left(\frac{s}{s_0}\right) - \frac{11}{216} i \ln\left(\frac{s}{s_0}\right), \qquad \mathcal{F}_{\mathcal{R}}[\gamma] = \frac{1}{6}\ln\left(\frac{s}{s_0}\right).$$

The infinitesimal Feynman rules (def. 100), applied to these graphs, are

$$\sigma[S] = -\frac{85}{3888}, \qquad \sigma[S_i] = -\frac{11}{216} i, \qquad \sigma[\gamma] = \frac{1}{6}.$$

Note that $\sigma[S_i]$ equals the period $\mathcal{P}[P_2]$ of the 2-loop primitive P_2 constructed from S_i in example 90. Now, use $\Delta(S_i) = \gamma_i \otimes \gamma$ to find that indeed

$$\exp^{\star}(L\sigma)[S_i] = L\sigma[S_i] + \frac{1}{2}L^2\sigma[\gamma_i]\sigma[\gamma] = -\frac{11}{216} i L + \frac{1}{2}\left(\frac{1}{6}\right) i \left(\frac{1}{6}\right) = \mathcal{F}_{\mathcal{R}}[S_i].$$

As expected, $\sigma^{\star 2}[S_i] = \frac{1}{2}\sigma[\gamma_i]\sigma[\gamma]$ is completely determined by the subgraph $\gamma_i \simeq \gamma$. The factor i is to correct the intermediate propagator $\frac{i}{s}$, we divide out the tensor s as usual.

By example 75, $\Delta(S) = S \otimes \mathbb{1} + \mathbb{1} \otimes S + 2\gamma_i \otimes S_i + \gamma_1\gamma_2 \otimes \gamma$. Further, $\sigma[\gamma_1\gamma_2] = 0$ and therefore

$$\sigma^{\star 2}[S] = 2\sigma[\gamma_i]\sigma[S_i] = 2\left(\frac{1}{6}\right) i \left(-\frac{11}{216} i\right) = \frac{11}{648}$$

$$\sigma^{\star 3}[S] = 2\sigma[\gamma_i]\sigma^{\star 2}[S_i] + \sigma^{\star 2}[\gamma_1\gamma_2]\sigma[\gamma] = 2\sigma[\gamma]^3 = 2i^2\left(\frac{1}{6}\right)^3 = -\frac{1}{108}.$$

With these numbers, we correctly reproduce example 92,

$$\exp^{\star}(L\sigma)[S] = L\sigma[S] + \frac{1}{2}L^2\sigma^{\star 2}[S] + \frac{1}{6}\sigma^{\star 3}[S] = -\frac{85}{3888}L + \frac{11}{1296}L^2 - \frac{1}{648}L^3.$$

$\sigma[S]$ is the only non-trivial input, all higher orders in L are determined by subgraphs.

Summing over all graphs, and suppressing the dependence on angles, theorem 35 delivers an expansion of the renormalized Green function, again projected to a treelevel tensor (def. 82), in terms of logarithms,

$$G^r_{\mathcal{R}}(\alpha, L) = \sum_{j=0}^{\infty} \gamma^r_j(\alpha) \cdot L^j. \tag{3.2}$$

Observe that L^j denotes a power while ^{r} in γ^r is the residue $r := \operatorname{res}(G^r)$ (def. 26). By theorem 35, the functions γ^r_j obtain contributions only from graphs Γ with $\operatorname{cor}(\Gamma) \geq j$. They are given by the infinitesimal Feynman rules (def. 100) acting on the combinatorial Green functions (def. 45),

$$\gamma^r_j(\alpha) = \frac{1}{j!} \sum_{\Gamma \text{ 1PI}, \operatorname{res}(\Gamma)=r} \alpha^{|L_\Gamma|} \operatorname{sym}(\Gamma) \cdot \sigma^{\star j}[\Gamma] = \frac{1}{j!}\sigma^{\star j}\big[\Gamma^r(\alpha)\big]. \tag{3.3}$$

3.1.3. Mellin transforms

We can rewrite L (def. 99) in theorem 35 as derivatives,

$$L^j = \partial^j_\rho e^{L\rho}\big|_{\rho=0} = \partial^j_\rho \left(\frac{s}{s_0}\right)^\rho \Bigg|_{\rho=0} \qquad \Rightarrow \mathcal{F}_{\mathcal{R}}[\gamma](L) = \sum_{j=0}^{\operatorname{cor}(\gamma)} g_j(\theta)\partial^j_\rho \left(\frac{s}{s_0}\right)^\rho \Bigg|_{\rho=0}. \tag{3.4}$$

At this point, we assume that γ is a 1PI propagator-type graph for concreteness. Then $s = p^2$ is the external momentum of γ and $g_j(\theta) = g_j$ is independent of angles. By eq. (2.37), $\mathcal{F}\big[B^\Gamma_+\left(\mathcal{F}_{\mathcal{R}}[\gamma]\right)\big] = \int \mathrm{d}_\Gamma\, \mathcal{F}_{\mathcal{R}}[\gamma]$. In the momentum representation (eq. (1.47)), γ replaces one of the edges in Γ according to

$$\frac{i}{s_p} \to \frac{i}{s_p} s_p \mathcal{F}_{\mathcal{R}}[\gamma](s) \frac{i}{s_p} = \frac{-1}{s_p}\mathcal{F}_{\mathcal{R}}[\gamma](s).$$

If we further assume the field to be massless, then $s_p = s = \underline{p}^2$ and

$$\begin{aligned}\int \mathrm{d}_\Gamma \, \mathcal{F}_{\mathcal{R}}[\gamma] &= \prod_{v\in V_\Gamma} (-i\lambda_{|v|}) \cdot \prod_{l\in L_\Gamma} \int \frac{\mathrm{d}^D \underline{k}_l}{(2\pi)^D} \frac{-1}{s} \sum_{j=0}^{\mathrm{cor}(\gamma)} g_j(\theta) \partial_\rho^j \left(\frac{s}{s_0}\right)^\rho \Big|_{\rho=0} \prod_{e\neq 1} \frac{i}{s_e} \\ &= -\sum_{j=0}^{\mathrm{cor}(\gamma)} g_j(\theta) \partial_\rho^j \frac{1}{(s_0)^\rho} \prod_{v\in V_\Gamma} (-i\lambda_{|v|}) \cdot \prod_{l\in L_\Gamma} \int \frac{\mathrm{d}^D \underline{k}_l}{(2\pi)^D} \frac{1}{s^{1-\rho}} \prod_{e\neq 1} \frac{i}{s_e} \Big|_{\rho=0} \\ &=: -\mathcal{F}_{\mathcal{R}}[\gamma] \, (\partial_\rho) \, \frac{1}{(s_0)^\rho} \prod_{v\in V_\Gamma} (-i\lambda_{|v|}) \tilde{F}_\gamma \left(\rho, 0, \ldots, 0\right) \Big|_{\rho=0}.\end{aligned}$$

Definition 101. The *Mellin transform* of a Feynman graph Γ with $E = |E_\Gamma|$ internal edges and $L = |L_\Gamma|$ loops is defined by raising each of its propagators to a variable power ρ_e,

$$\tilde{F}_\Gamma \left(\rho_1, \ldots, \rho_E\right) := \int \frac{\mathrm{d}^{LD} \underline{k}}{(2\pi)^{LD}} \frac{1}{\left(\underline{k}_1^2\right)^{1-\rho_1}} \cdots \frac{1}{\left(\underline{k}_E^2\right)^{1-\rho_E}}$$

Up to global factors, the Mellin transform equals the Integral $\mathcal{F}[\Gamma]$ in analytic regularization (section 2.3.2) with exponents $\nu_j = 1-\rho_j$. By eq. (2.45), the Mellin transform is proportional to the scale (def. 81) $s^{kD/2-E+\sum \rho_j}$. For renormalization, we evaluate at $s = s_0$, therefore, we factor out this dependence and define

$$s^{k\frac{D}{2}-\frac{E}{+}\sum_j \rho_j} F_\Gamma \left(\rho_1, \ldots, \rho_E\right) := \tilde{F}_\Gamma \left(\rho_1, \ldots, \rho_E\right).$$

If Γ is primitive divergent (def. 86) and we restrict ourselves to only one $\rho \neq 0$, then

$$F_\Gamma \left(\rho\right) = \sum_{j=0}^{\infty} c_j \rho^{j-1}. \tag{3.5}$$

Example 96: 1-loop multiedge, Mellin transform.

The Mellin transform can directly be read off from example 24 (compare also example 85)

$$F_{M^{(1)}}(\rho_1, \rho_2) = \frac{1}{(4\pi)^{\frac{D}{2}}} \frac{\Gamma\left(-\rho_1-\rho_2+2-\frac{D}{2}\right)\Gamma\left(\frac{D}{2}-1+\rho_1\right)\Gamma\left(\frac{D}{2}-1+\rho_2\right)}{\Gamma\left(D-2+\rho_1+\rho_2\right)\Gamma(1-\rho_1)\Gamma(1-\rho_2)}.$$

For the sake of brevity, we skip all prefactors 4π. Set $\rho_2 = 0$ and $D = 4-2\epsilon$:

$$F_{M^{(1)}}(\rho, 0)\Big|_{D=4-2\epsilon} = \frac{\Gamma\left(\epsilon-\rho\right)\Gamma\left(1-\epsilon+\rho\right)\Gamma\left(1-\epsilon\right)}{\Gamma\left(2-2\epsilon+\rho\right)\Gamma(1-\rho)}.$$

Conversely, set $D = 4$ and use eq. (2.47):

$$F_{M^{(1)}}(\rho_1, \rho_2)\Big|_{D=4} = \frac{-1}{(\rho_1+\rho_2)(1+\rho_1+\rho_2)} \frac{\Gamma\left(1-\rho_1-\rho_2\right)\Gamma\left(1+\rho_1\right)\Gamma\left(1+\rho_2\right)}{\Gamma\left(1+\rho_1+\rho_2\right)\Gamma(1-\rho_1)\Gamma(1-\rho_2)}$$

Combining both the previous lines, we obtain simple rational functions:

$$F_{M^{(1)}}(\rho,0)\Big|_{D=4} = \frac{-1}{\rho(1+\rho)}, \qquad F_{M^{(1)}}(\rho,0)\Big|_{D=6} = \frac{1}{\rho(1+\rho)(2+\rho)(3+\rho)}.$$

The Mellin transform allows to write an explicit formula for the action of the cocycle B_+^Γ (def. 87) on the level of Feynman amplitudes. This is the mapping between different B_+ announced in the universal property (theorem 23), from the Hopf algebra of Feynman graphs to the Hopf algebra of formal power series in L. We assume that γ is inserted into edge $e = 1$ in Γ, then

$$\mathcal{F}\Big[B_+^\Gamma\left(\mathcal{F}_{\mathcal{R}}[\gamma]\right)\Big](L) = -\prod_{v\in V_\Gamma}(-i\lambda_{|v|})\mathcal{F}_{\mathcal{R}}[\gamma]\left(\partial_\rho\right)e^{L\rho}F_\Gamma\left(\rho\right)\Big|_{\rho=0}. \tag{3.6}$$

Kinematic renormalization (def. 91) amounts to subtraction at $L = 0$, therefore

$$\mathcal{F}_{\mathcal{R}}\Big[B_+^\Gamma\left(\mathcal{F}_{\mathcal{R}}(\gamma)\right)\Big](L) = -\prod_{v\in V_\Gamma}(-i\lambda_{|v|})\mathcal{F}_{\mathcal{R}}[\gamma]\left(\partial_\rho\right)\left(e^{L\rho}-1\right)F_\Gamma(\rho)\Big|_{\rho=0}. \tag{3.7}$$

The product of series $\mathcal{F}_{\mathcal{R}}[\gamma]$ and F_Γ in eq. (3.7) can be reordered to obtain

$$\mathcal{F}_{\mathcal{R}}\Big[B_+^\Gamma\left(\mathcal{F}_{\mathcal{R}}[\gamma]\right)\Big](L) = -\int_0^L \mathrm{d}t\ \sum_{k=0}^{\mathrm{cor}(\gamma)} c_k\frac{\partial^k}{\partial t^k}\mathcal{F}_{\mathcal{R}}[\gamma](t). \tag{3.8}$$

The precise algebraic nature of these maps regarding the universal property is explained in [308]. Following lemma 20, the integral $-c_0\int \mathrm{d}t$ is the crucial ingredient to make this map a cocycle, all higher summands can be viewed as a coboundary b_0L_0 (def. 72). In the more conventional language of physics, c_0 defines the *leading-log-order* of an amplitude, while $c_{j>0}$ give next-to-leading-log corrections, see section 3.3.3.

Example 97: Tree Feynman rules.

Using eq. (3.8), we can assign an amplitude to every rooted tree. Firstly, $\mathcal{F}_{\mathcal{R}}[\mathbb{1}] = 1$. Since trees are unlabelled, this represents a single primitive, and insertion of the same primitive as subgraphs.

$$\mathcal{F}_{\mathcal{R}}[\bullet] = \mathcal{F}_{\mathcal{R}}\left[B_+(\mathbb{1})\right] = -\int_0^L \mathrm{d}t\ c_0\mathcal{F}_{\mathcal{R}}[\mathbb{1}] = -c_0L$$

$$\mathcal{F}_{\mathcal{R}}\Big[\ \Big] = -\int_0^L \mathrm{d}t\ \left(c_0(-c_0t) + c_1\partial_t(-c_0t)\right) = \frac{1}{2}c_0^2L^2 + c_0c_1L$$

$$\mathcal{F}_{\mathcal{R}}\Big[\ \Big] = \mathcal{F}_{\mathcal{R}}\left(B_+\left(\mathcal{F}_{\mathcal{R}}[\bullet]^2\right)\right) = -\frac{1}{3}c_0^3L^3 - c_0^2c_1L^2 - 2c_0^2c_2L$$

$$\mathcal{F}_{\mathcal{R}}\Big[\ \Big] = \frac{1}{12}c_0^4L^4 + \frac{2}{3}c_0^3c_1L^3 + c_0^2\left(2c_0c_2+c_1^2\right)L^2 + c_0^2\left(c_0c_3+4c_1c_2\right)L.$$

Observe that the highest order in L is determined by c_0, the next-to-highest order involves c_0, c_1 and so on. This will be made precise in section 3.3.3.

Example 98: Toy model, Mellin transform.

For the toy model (example 79) at $\epsilon = 0$, the Mellin transform is

$$F(\rho) = \int_0^\infty \mathrm{d}x \, \frac{x^\rho}{x+1} = \frac{-\pi}{\sin(\pi\rho)} = -\frac{1}{\rho} \exp\left(\sum_{n=1}^\infty \zeta(2n) \frac{\rho^{2n}}{n}\right) = -\frac{1}{\rho} - \frac{\pi^2}{6}\rho - \frac{7\pi^4}{360}\rho^3 + \dots .$$

We used eq. (2.47) and $\zeta(2n) = (-1)^{n+1} 2^{2n+1} B_{2n}/(2n)! \pi^{2n}$ with the Bernoulli numbers B_j. Consequently, the tree amplitudes (example 97) for the toy model are

$$\mathcal{F}_\mathcal{R}[\mathbb{1}] = 1, \qquad \mathcal{F}_\mathcal{R}\left(\bullet\right) = -L, \qquad \mathcal{F}_\mathcal{R}\Big[\; \Big] = \frac{1}{2}L^2$$

$$\mathcal{F}_\mathcal{R}\Big[\; \Big] = -\frac{1}{3}L^3 - \frac{\pi^2}{6}L, \qquad \mathcal{F}_\mathcal{R}\Big[\; \Big] = \frac{1}{12}L^4 + \frac{\pi^2}{6}L^2.$$

Summary of section 3.1.

1. Feynman amplitudes factorize, under the convolution product $\star$, into a scale-dependent and an angle-dependent part (section 3.1.1). We are mostly concerned with the scale dependent part.

2. We expanded the scale-dependence of the Feynman rules in powers of the logarithmic scale L. The infinitesimal Feynman rules σ extract the linear coefficient in L, and the exponential of the operator σ reproduces the full Feynman amplitude by acting with σ on subgraphs (section 3.1.2).

3. The action of the cocycle B_+, that is insertion of subgraphs, on Feynman amplitudes can be expressed as a series convolution with the Mellin transform of the underlying graph (section 3.1.3).

3.2. Renormalization group in kinematic renormalization

Up to this point, we have examined the scale-dependence of individual graphs. In the present section, we consider full Green functions and additionally use the information that they are solutions of Dyson-Schwinger equations.

3.2.1. Callan-Symanzik equation

Our exposition of the renormalization group loosely follows [270, 271, 380]. The convolution product $\star$ (def. 75) is a homomorphism, this implies that it is linear under multiplication, $L \cdot \sigma[\Gamma] = \sigma[L \cdot \Gamma]$. A product can thus be expanded according to

$$\Big((L_1 + L_2)\sigma\Big) \star \Big((L_1 + L_2)\sigma\Big) = L_1^2\sigma \star \sigma + L_1 L_2 \sigma \star \sigma + L_2 L_1 \sigma \star \sigma + L_2^2 \sigma \star \sigma.$$

Collecting all the prefactors, we obtain

$$\Big((L_1 + L_2)\sigma\Big) \star \Big((L_1 + L_2)\sigma\Big) = (L_1 + L_2)^2 \, \sigma \star \sigma.$$

The same argument applies to all higher monomials, consequently, the Feynman rules (def. 100) factorize with respect to scales.

Lemma 37. Let $\mathcal{F}_\mathcal{R}$ be the renormalized Feynman rules in kinematic renormalization, given by def. 100. Let $L_1, L_2 \in \mathbb{R}$ be two arbitrary, but fixed scales, then

$$\mathcal{F}_\mathcal{R}[\Gamma](L_1 + L_2) = e^{\star(L_1+L_2)\sigma}\Gamma = \Big(e^{\star L_1 \sigma} \star e^{\star L_2 \sigma}\Big)\Gamma = \Big(\mathcal{F}_\mathcal{R}\big|_{L_1} \star \mathcal{F}_\mathcal{R}\big|_{L_2}\Big)\Gamma. \tag{3.9}$$

Algebraically, lemma 37 means that the Feynman rules at fixed angles (def. 81) form a group with respect to $\star$, this is the *renormalization group*. It is a Lie group, its generator are the infinitesimal Feynman rules σ (def. 100) as seen from eq. (2.17).

The star product $\star$ does not directly correspond to an ordinary product, so despite lemma 37, we generally have $\mathcal{F}_\mathcal{R}[\Gamma](L_1 + L_2) \neq \mathcal{F}_\mathcal{R}[\Gamma](L_1) \cdot \mathcal{F}_\mathcal{R}[\Gamma](L_2)$. But still, the renormalization group has deep consequences for the momentum-dependence of renormalized Green functions. To see this, recall that every physically sensible Green function satisfies a combinatoric DSE (theorem 26),

$$\Gamma^r = \mathbb{1} \pm \sum_{\Gamma \in K^r} \alpha^{|L_\Gamma|} \operatorname{sym}(\Gamma) B_+^\Gamma \left(\Gamma^r \cdot Q^{|L_\Gamma|}\right).$$

Denote the insertion into all k-loop kernels by

$$B_+^{r,k} = \sum_{|L_\Gamma|=k,\ \operatorname{res}(\Gamma)=r} \operatorname{sym}(\Gamma) B_+^\Gamma. \tag{3.10}$$

We skip the superscript ^{r} for now. Then, the DSE becomes

$$\Gamma = \mathbb{1} \pm \sum_{k=1}^{\infty} \alpha^k B_+^k \left(\Gamma \cdot Q^k\right). \tag{3.11}$$

The combinatorial Green function Γ (def. 45) is a series in α. We obtain the 1PI Green function (def. 90) by applying the renormalized Feynman rules,

$$G_{\mathcal{R}}(L, \alpha) = \mathcal{F}_{\mathcal{R}}[\Gamma(\alpha)](L). \tag{3.12}$$

We now want to translate lemma 37 into a statement about the behaviour of eq. (3.12) under a shift in the scale L (def. 99). We remark that such a shift can equivalently be viewed as a change of the renormalization point $s_1 \leftrightarrow s_0$,

$$L' := \ln \frac{s}{s_2} = \ln \frac{s}{s_1} + \ln \frac{s_1}{s_2} = L + \delta, \quad \Leftrightarrow \quad s_2 = e^{\delta} \cdot s_1.$$

Definition 102. Let $\mathcal{Q}_{\mathcal{R}}(\alpha, L)$ be the renormalized invariant charge (def. 93). The *running coupling* $\tilde{\alpha}$ at the energy scale L is

$$\tilde{\alpha}(\alpha, L) = \alpha \mathcal{Q}_{\mathcal{R}}(\alpha, L).$$

In kinematic renormalization with renormalization point $L = 0$, we have $\tilde{\alpha}(\alpha, 0) = \alpha$.

Lemma 38. Let $L, \delta \in \mathbb{R}$ be two arbitrary, but fixed, logarithmic scales (def. 99). Let $G_{\mathcal{R}}(\alpha, L)$ be a solution of a DSE in kinematic renormalization (def. 91) and let $\tilde{\alpha}$ be the running coupling (def. 102). Then

$$G_{\mathcal{R}}(\alpha, L + \delta) = G_{\mathcal{R}}(\alpha, \delta) \cdot G_{\mathcal{R}}\left(\tilde{\alpha}(\alpha, \delta), L\right).$$

Proof. Under a shift of scale, the Feynman rules transform according to lemma 37:

$$\mathcal{F}_{\mathcal{R}}[\Gamma](\delta + L) = \left(\mathcal{F}_{\mathcal{R}}\Big|_{\delta} \star \mathcal{F}_{\mathcal{R}}\Big|_{L}\right)\Gamma.$$

Γ fulfils the DSE eq. (3.11), hence we know $\Delta(\Gamma)$ from theorem 24:

$$\begin{aligned} \mathcal{F}_{\mathcal{R}}[\Gamma](L') &= \sum_{j=0}^{\infty} \mathcal{F}_{\mathcal{R}}\left[\Gamma \cdot Q^j\right](\delta) \cdot \alpha^j \mathcal{F}_{\mathcal{R}}\left[\Gamma_j\right](L) \\ &= \mathcal{F}_{\mathcal{R}}[\Gamma](\delta) \cdot \sum_{j=0}^{\infty} \left(\alpha \mathcal{F}_{\mathcal{R}}[Q](\delta)\right)^j \cdot \mathcal{F}_{\mathcal{R}}[\Gamma_j](L). \end{aligned} \tag{3.13}$$

Here we have used multiplicativity (eq. (2.38)) to write $\mathcal{F}_{\mathcal{R}}[Q^j] = \mathcal{F}_{\mathcal{R}}[Q]^j$. The invariant charge $\mathcal{F}_{\mathcal{R}}[Q](\delta) = \mathcal{Q}_{\mathcal{R}}(\alpha, \delta)$ (def. 93) evaluated at a fixed δ is simply a fixed number, it rescales the coupling α according to def. 102. In eq. (3.13), $\Gamma_j := [\alpha^j]\Gamma$ is the series coefficient of the Green function. The sum over j is nothing but the Green function, but at the running coupling. □

We emphasize how nicely the correspondence between lemma 37 and lemma 38 fits with our understanding of the renormalization Hopf algebra as an "advanced variant of the the Faà di Bruno Hopf algebra" (section 2.1.4), compare section 2.2.1: The $\star$-product in the Hopf algebra of Feynman graphs *really* amounts to inserting Green functions into each other.

Definition 103. Let $G^r_{\mathcal{R}}$ be the renormalized 1PI Green function (def. 90) in kinematic renormalization (def. 91) with renormalization point $L = 0$, and let $\tilde{\alpha}(\alpha, L)$ be the running coupling (def. 102). The *anomalous dimension* in kinematic renormalization is defined as

$$\gamma^r(\alpha) := \frac{\partial}{\partial L} G^r_{\mathcal{R}}(\alpha, L)\Big|_{L=0} = \sigma\left[\Gamma^r\right].$$

The *Symanzik beta function* in kinematic renormalization is

$$\beta(\alpha) := \frac{\partial}{\partial L} \tilde{\alpha}(\alpha, L)\Big|_{L=0} = \alpha\sigma\left[Q\right].$$

Here, σ (def. 100) is the infinitesimal Feynman rule.

The anomalous dimension expresses the fact that interaction in a quantum field theory can effectively change the mass dimension of the field, compare for example [381] or our discussion in section 2.4.

Theorem 39 ([382, 383])**.** In kinematic renormalization, with β, γ^r from def. 103, the renormalized Green function, projected onto its treelevel tensor (def. 82), satisfies the *Callan-Symanzik equation*,

$$\frac{\partial}{\partial L} G^r_{\mathcal{R}}(\alpha, L) = \left(\gamma^r(\alpha) + \beta(\alpha) \cdot \frac{\partial}{\partial \alpha}\right) G^r_{\mathcal{R}}(\alpha, L). \tag{3.14}$$

Proof. Deriving lemma 38 with respect to δ, we obtain

$$\frac{\partial}{\partial \delta} \ln G_{\mathcal{R}}(\alpha, L + \delta) = \frac{\partial}{\partial \delta} \ln G_{\mathcal{R}}(\alpha, \delta) + \frac{\partial}{\partial \delta}\tilde{\alpha}(\alpha, \delta) \cdot \frac{\partial}{\partial \tilde{\alpha}(\delta)} \ln G_{\mathcal{R}}(\tilde{\alpha}(\delta), L).$$

Consider the point $\delta = 0$. According to kinematic renormalization conditions, $\tilde{\alpha}(0) = \alpha$ and $G_{\mathcal{R}}(\alpha, 0) = 1$, therefore $\partial_L \ln G|_{L=0} = \partial_L G|_{L=0}$ and

$$\frac{\partial}{\partial L} \ln G_{\mathcal{R}}(\alpha, L) = \frac{\partial}{\partial L} G_{\mathcal{R}}(\alpha, L)\Big|_{L=0} + \frac{\partial}{\partial L}\tilde{\alpha}(\alpha, L)\Big|_{L=0} \cdot \frac{\partial}{\partial \alpha} \ln G_{\mathcal{R}}(\alpha, L).$$

Identify def. 103 to obtain the Callan-Symanzik equation. □

A variant of the Callan-Symanzik equation can be obtained if we exchange $L \leftrightarrow \delta$ in lemma 38 and then derive that equation with respect to δ at $\delta = 0$:

$$\frac{\partial}{\partial L} G^r_{\mathcal{R}}(\alpha, L) = G^r_{\mathcal{R}}(\alpha, L) \cdot \gamma^r\left(\tilde{\alpha}(\alpha, L)\right) \quad \Leftrightarrow \quad \frac{\partial}{\partial L} \ln G^r_{\mathcal{R}}(\alpha, L) = \gamma^r(\tilde{\alpha}(\alpha, L)). \tag{3.15}$$

Further variants and generalizations of the Callan-Symanzik equation exist [384–388]. Recall that we project the Green function to its tensor structure (section 2.2.2). In realistic theories, there are multiple tensors, and hence multiple Green functions (example 67). Each of them has their own γ^r and the Callan-Symanzik equation can involve additional terms, such as $\gamma^m(\alpha)\frac{\partial}{\partial m}$ for a massive theory. For the present thesis, theorem 39 is sufficiently general.

For our later calculations it is useful to rewrite the Callan-Symanzik equation in terms of the expansion functions $\gamma_j^r(\alpha)$ of the log-expansion eq. (3.2),

$$G_{\mathcal{R}}^r(\alpha, L) = \sum_{j=0}^{\infty} \gamma_j^r(\alpha) \cdot L^j. \tag{3.16}$$

Theorem 40 ([200, 270, 389])**.** Let γ_j^r be the coefficients of the log expansion eq. (3.16), where ^{r} is an index, not a power. Let β, γ be the beta function and anomalous dimension (def. 103) of the corresponding DSE. Then

$$\gamma_{j>1}^r(\alpha) = \frac{1}{j} \left(\gamma^r(\alpha) + \beta(\alpha) \cdot \partial_\alpha\right) \gamma_{j-1}^r(\alpha).$$

Proof. Act on eq. (3.13) with the infinitesimal Feynman rules (def. 100), or equivalently insert the expansion eq. (3.2) into theorem 39. □

Lemma 41. Assume $G^r(\alpha, L)$ is a formal power series (def. 51) in α. Assume that $\gamma^{(r)}$ and β have a non-vanishing term $\propto \alpha$. Then, the coefficients in eq. (3.16) are of order

$$\gamma_k(\alpha) \in \mathcal{O}\left(\alpha^k\right) \qquad \forall k \geq 0. \tag{3.17}$$

Proof. Clearly $\gamma_0(\alpha) = G(\alpha, L = 0) \in \mathcal{O}\left(\alpha^0\right)$. We have rescaled the DSE eq. (3.11) such that the first correction is of order one, $\Gamma = \mathbb{1} \pm \alpha B_+^1(\mathbb{1})$. But $B_+(\mathbb{1})$ is primitive by lemma 20, therefore its amplitude is linear in L by theorem 30 and consequently $\gamma = \partial_L \Gamma \in \mathcal{O}(\alpha)$. The higher $k \geq 1$ follow from theorem 40 by induction. It is even possible that some coefficients of the power series vanish and that $\gamma_k(\alpha)$ actually starts with a higher order than k. □

Lemma 42. Consider ϕ^n theory with vertex $G_{\mathcal{R}}^v$ and propagators $G_{\mathcal{R}}^e$ in kinematic renormalization (def. 91). Let $e \sim v$ denote that e is incident to v. Then, the beta function (def. 103) can be computed from the various anomalous dimensions according to

$$\beta(\alpha) = \frac{2\alpha}{n-2} \left(\gamma^v(\alpha) - \frac{1}{2} \sum_{e \sim v} \gamma^e(\alpha)\right). \tag{3.18}$$

Proof. The invariant charge (def. 92) is a monomial in the various Green functions, consequently, the beta function is related to the various anomalous dimensions. Consider the logarithm $\ln \mathcal{Q}_{\mathcal{R}} = \frac{2}{n-2} \ln G_{\mathcal{R}}^v - \sum_{e \sim v} \frac{1}{n-2} \ln G_{\mathcal{R}}^e$. By def. 103,

$$\beta(\alpha) = \alpha \partial_L \mathcal{Q}_{\mathcal{R}}|_{L=0} = \mathcal{Q}_{\mathcal{R}}(0) \cdot \partial_L \ln \mathcal{Q}_{\mathcal{R}}|_{L=0}.$$

In kinematic renormalization (def. 91), $\mathcal{Q}_{\mathcal{R}}(0) = 1$ and we obtain

$$\beta(\alpha) = \frac{\partial}{\partial L} \ln \mathcal{Q}_{\mathcal{R}}|_{L=0} = \frac{2\alpha}{n-2} \left(\partial_L G_{\mathcal{R}}^v\big|_{L=0} - \sum_{e \sim v} \frac{1}{2} \partial_L G_{\mathcal{R}}^e\big|_{L=0}\right).$$

□

Example 99: ϕ^n theory, relation between anomalous dimensions.

In ϕ^n theory, there are exactly n identical propagators attached to each vertex, hence

$$\beta(\alpha) = \alpha\sigma[Q] = \frac{2\alpha}{n-2}\left(\gamma^{(n)}(\alpha) - \frac{n}{2}\gamma^{(2)}(\alpha)\right).$$

Concretely, in ϕ^3 theory, $\beta = 2\alpha\gamma^{(3)} - 3\alpha\gamma^{(2)}$. In ϕ^4 theory, $\beta = \alpha\gamma^{(4)} - 2\alpha\gamma^{(2)}$.

Finally, all the renormalization group equations can be rewritten for the running coupling (def. 102). Use def. 92 to find

$$\frac{\partial}{\partial L}\ln \mathcal{Q}_{\mathcal{R}} = \frac{2}{n-2}\frac{\partial}{\partial L}\ln G^v_{\mathcal{R}} - \sum_{e\sim v}\frac{1}{n-2}\frac{\partial}{\partial L}\ln G^e_{\mathcal{R}}.$$

Apply theorem 39 and eq. (3.15) to each summand and use lemma 42 to collect the terms:

$$\frac{\partial}{\partial L}\tilde{\alpha}(\alpha, L) = \tilde{\alpha}\frac{\partial}{\partial L}\ln \mathcal{Q}_{\mathcal{R}}(\alpha, L) = \beta(\tilde{\alpha}(\alpha, L)) = \left(\beta(\alpha) + \beta(\alpha)\frac{\partial}{\partial \alpha}\right)\mathcal{Q}_{\mathcal{R}}(\alpha, L). \tag{3.19}$$

Note that, by def. 103, β is the derivative $\partial_L\tilde{\alpha}$ at $L = 0$, while eq. (3.19) holds for all L. Using separation of variables, one obtains a formal solution:

$$\mathrm{d}\tilde{\alpha}(\alpha, L)\frac{1}{\beta(\tilde{\alpha}(\alpha, L))} = \mathrm{d}L, \quad \tilde{\alpha}(\alpha, 0) = \alpha \qquad \Rightarrow \qquad L = \int_{\alpha}^{\tilde{\alpha}(L)} \mathrm{d}u \frac{1}{\beta(u)}. \tag{3.20}$$

Example 100: Multiedge DSE, beta function and anomalous dimension.

In example 34, we introduced a simplified DSE for the ϕ^3 propagator by setting $G^{(3)}_{\mathcal{R}} = \prec = \mathbb{1}$. In that case, the 3-point function is not momentum-dependent and we have $\gamma^{(3)} = 0$. By lemma 42, the beta function of this model is

$$\beta(\alpha) = -3\alpha\gamma^{(2)}(\alpha).$$

We want to stress that even if the vertex function is trivial, there still is a non-trivial running coupling (eq. (3.19)). Hence, the L-dependence of the coupling is ultimately given by the anomalous dimension γ of the propagator. This relationship is called *propagator-coupling duality* in [390].

We can slightly generalize this model by letting the invariant charge (def. 92) be $Q = \left(G^{(2)}\right)^w$. In that case, $w = -3$ is the ordinary physical choice and $w = 0$ amounts to a linear DSE and the beta function is

$$\beta(\alpha) = w \cdot \alpha\gamma^{(2)}(\alpha).$$

3.2.2. Counterterms and ϵ-dependence

So far, we have concentrated on renormalized quantities, most prominently the renormalized Green functions $G_{\mathcal{R}}$ (def. 90). In our initial example (section 2.2.1), we interpreted renormalization as a rescaling of the bare coupling constant by the *Z-factor* $\lambda_0 =: Z_\lambda(\lambda) \cdot \lambda$ (eq. (2.33)). Similar Z-factors can be introduced in the full QFT picture. Their form depends on the chosen regularization scheme. For concreteness, we work in dimensional regularization (section 2.3.3) here and for the rest of the thesis, unless stated otherwise.

Consider the Lagrangian of massless ϕ^n theory (example 3). In this Lagrangian, two quantities can be rescaled: The coupling constant λ_n, and the field variable ϕ. This matches the two residues $\mathfrak{L}$ of the Lagrangian (example 33). Like in the DSE (theorem 27), we redefine the coupling $\lambda_n^{\frac{2}{n-2}} =: \alpha$ to ensure that α corresponds to the loop order of the graphs.

Definition 104. Let s_0 be an arbitrary, but fixed, mass scale. For massless ϕ^n theory, the *Z-factors* in dimensional regularization (section 2.3.3) are

$$\alpha_0 := Z_\alpha(\alpha, \epsilon) s_0^\epsilon \cdot \alpha, \qquad \phi_0 := (Z_\phi(\alpha, \epsilon))^{\frac{1}{2}} \cdot \phi.$$

The factor s_0^ϵ in the definition of Z_α is to make α dimensionless regardless of ϵ. It will cause significant effects later, therefore we want to stress that there is not the option to leave out s_0 in order to simplify later calculations. If we were to leave it out, then the renormalized coupling would, for $\epsilon \neq 0$, obtain a non-vanishing mass dimension (def. 4). In that case, we would be forced to introduce a new, arbitrary, mass scale into the theory at a later point in order to construct a sensible expansion in a massless parameter. In most cases, we will not write s_0^ϵ explicitly, but rather implicitly redefine $s_0^\epsilon \alpha \to \alpha$.

In perturbation theory, a Z-factors is a power series in the renormalized coupling α, and a Laurent series in the regulator ϵ, they can always be chosen to not depend on masses [391]. For convenience, we introduce

$$Z^{(2)}(\alpha, \epsilon) := Z_\phi(\alpha, \epsilon), \qquad Z^{(n)}(\alpha, \epsilon) := Z_\alpha^{\frac{n-2}{2}}(\alpha, \epsilon) s_0^{\left(\frac{n-2}{2}\right)\epsilon} (Z_\phi(\alpha, \epsilon))^{\frac{n}{2}}. \tag{3.21}$$

The overall factor $Z_\alpha^{\frac{n-2}{2}}$ in $Z^{(n)}$ arises from our convention that $G^{(n)}$ is rescaled to the treelevel, $G^{(n)} = \lambda + \ldots$. With these factors, and absorbing s_0^ϵ into α, the n-point 1PI (not the connected one) Green function (def. 90) is renormalized according to

$$G_{\mathcal{R}}^{(n)}(\alpha, L) := Z^{(n)}(\alpha, \epsilon) \cdot G^{(n)}(Z_\alpha(\alpha, \epsilon) \cdot \alpha, L). \tag{3.22}$$

Equation (3.22) is the analytic manifestation of the abstract relation $\mathcal{F}_{\mathcal{R}} = S_{\mathcal{R}}^{\mathcal{F}} \star \mathcal{F}$ (def. 88), where

$$S_{\mathcal{R}}^{\mathcal{F}} \left[\Gamma^{(j)}\right] \equiv Z^{(j)} \tag{3.23}$$

is the counterterm (def. 89).

eq. (3.22) is structurally similar to the behaviour of $G_{\mathcal{R}}$ under finite changes of the energy scale (lemma 38). Indeed, the Z-factors (def. 104) are defined analogous to the running coupling (def. 102). Consequently, to express a renormalized amplitude at a given energy scale, the coupling constant is rescaled multiplicatively two times [392–395]. Firstly, Z_α in def. 104 ensures that the renormalized coupling α takes its pre-described value at the

renormalization point s_0 (eq. (2.31)). Secondly, the invariant charge $\mathcal{Q}_{\mathcal{R}}(L)$ (def. 93) adjusts α to its effective value at $L \neq 0$. Schematically,

$$\alpha_0 \overset{Z_\alpha s_0^\epsilon}{\longrightarrow} \alpha \overset{\mathcal{Q}_{\mathcal{R}}(L)}{\longrightarrow} \tilde{\alpha}(L). \tag{3.24}$$

The renormalized invariant charge (def. 93) is related to its unrenormalized counterpart via the counterterm Z_α (def. 104),

$$\mathcal{Q}_{\mathcal{R}}(\alpha, L) = Z_\alpha s_0^\epsilon \cdot \mathcal{Q}\left(Z_\alpha \alpha, L\right). \tag{3.25}$$

At this point, we can motivate that multiplicative renormalization (def. 104) and the L-dependence in the renormalization group are *one and the same thing*. Indeed, the exact same construction that lead to the renormalization group in section 3.2.1 is also used for renormalization itself. Schematically, we start with an un-renormalized DSE (theorem 26) and insert the rescalings eqs. (3.21) and (3.22) to obtain

$$\begin{aligned} G^{(2)}(\alpha_0) &= 1 - \sum_{k=1}^{\infty} \alpha_0^k B_+^{(2),k}\left(G^{(2)}(\alpha_0) \cdot \mathcal{Q}(\alpha_0)^k\right) \\ \Rightarrow \quad Z^{(2)} G^{(2)}\left(Z_\alpha \cdot \alpha\right) &= Z^{(2)}\left(1 - \sum_{k=1}^{\infty} (Z_\alpha \cdot \alpha)^k B_+^{(2),k}\left(G^{(2)}(\alpha) \cdot \mathcal{Q}(Z_\alpha \cdot \alpha)^k\right)\right). \end{aligned}$$

An analogous replacement is possible for the vertex-type DSE. Using eq. (3.25), the general form is

$$G_{\mathcal{R}}^{(n)}(\alpha) = Z^{(n)} \pm \sum_{k=1}^{\infty} \alpha^k B_+^{(n),k}\left(G_{\mathcal{R}}^{(n)}(\alpha) \cdot \mathcal{Q}_{\mathcal{R}}(\alpha)^k\right). \tag{3.26}$$

The cocycle B_+ is an integral operator (eq. (2.40)). If we were to write eq. (3.24) non-recursively, using the DSE eq. (3.26), then we would obtain to every fixed order in α an expression involving finitely many nested integrals, where the boundaries are either the renormalization point s_0 or the physical scale L. This construction is known as *Chen's lemma* [284], the Hopf algebra (def. 88) implements the combinatorics of the permuted integral boundaries. The *renormalization group* describes the fact that the intermediate scale s_0 is arbitrary, that is, the process eq. (3.24) can involve arbitrarily many intermediate steps, each of which comes with its own Z-factors. The convolution product $\star$ (def. 75) is the group operation of the renormalization group, $Z = Z_1 \star Z_2$ just like, in def. 88, $\mathcal{F}_{\mathcal{R}} = Z \star \mathcal{F}$ where $Z = S_{\mathcal{R}}^{\mathcal{F}}$ (def. 89). Comparing def. 100, we see that the renormalization group is generated by the infinitesimal Feynman rule σ. For a linear DSE, there is no non-trivial nesting and the resulting integrals can be written down explicitly, see eq. (3.32).

The Z-factors depend on ϵ, in order to work with them, we need to extend the renormalization group theory of section 3.2.1 to include ϵ-dependence of γ, β and $G_{\mathcal{R}}$.

Definition 105. For $\epsilon \neq 0$, we extend def. 102: the *running coupling* is defined as

$$\tilde{\alpha}(\alpha, \epsilon, L) := \alpha e^{-\epsilon L} \mathcal{Q}_{\mathcal{R}}(\alpha, \epsilon, L).$$

The running coupling $\tilde{\alpha}(\alpha, \epsilon, s)$ at a certain physical scale s (def. 81), and at the physical dimension $\epsilon = 0$, is an observable, it is the numerical value of a scattering amplitude at that energy. Renormalization involves the arbitrary intermediate renormalization scale s_0 in eq. (3.24). Consequently, $\tilde{\alpha}(s)$ must not change if we change s_0. Consequently,

$$0 = s_0 \cdot \frac{\mathrm{d}\tilde{\alpha}}{\mathrm{d}s_0} = \frac{\mathrm{d}\tilde{\alpha}}{\mathrm{d}\ln s_0} = \frac{\partial\tilde{\alpha}}{\partial \ln\alpha}\frac{\mathrm{d}\ln\alpha}{\mathrm{d}\ln s_0} + \frac{\partial\tilde{\alpha}}{\partial L}\frac{\mathrm{d}L}{\mathrm{d}\ln s_0}. \tag{3.27}$$

Owing to def. 99, $\frac{\mathrm{d}L}{\mathrm{d}\ln s_0} = -1$. This equation is valid for all values of L. Specify to $L = 0$, then the second summand, in the limit $\epsilon = 0$, becomes the beta function $\beta(\alpha) := \frac{\partial\tilde{\alpha}}{\partial L}|_{L=0}$ from def. 103,

$$0 = \frac{\partial\tilde{\alpha}}{\partial\alpha}\Big|_{L=0,\epsilon=0} \alpha s_0 \frac{\mathrm{d}}{\mathrm{d}s_0}\ln\alpha\Big|_{\epsilon=0} - \beta(\alpha).$$

On the other hand, owing to def. 102, there will always be a trivial summand $\epsilon\tilde{\alpha}$ in the derivative of $\tilde{\alpha}$ for $\epsilon \neq 0$,

$$0 = \frac{\partial\tilde{\alpha}}{\partial\alpha}\Big|_{L=0} \alpha s_0 \frac{\mathrm{d}}{\mathrm{d}s_0}\ln\alpha + \epsilon\tilde{\alpha}\Big|_{L=0} - \alpha\frac{\partial\mathcal{Q}_\mathcal{R}}{\partial L}\Big|_{L=0}.$$

For later convenience, we *define* the ϵ-dependent beta function to not contain the term $\epsilon\tilde{\alpha}$. Furthermore, in kinematic renormalization, $\tilde{\alpha}(\alpha, \epsilon = 0, L = 0) = \alpha$ and $\partial_\alpha\tilde{\alpha} = 1$. In other renormalization schemes, this derivative is non-trival, and it turns out (see theorem 51), that one should include it into the definition of the beta function.

Definition 106. Let $\mathcal{Q}_\mathcal{R}$ be the invariant charge (def. 93). In dimensional regularization, the ϵ-dependent *beta-function* is defined as

$$\beta(\alpha,\epsilon) := \frac{1}{\frac{\partial\tilde{\alpha}}{\partial\alpha}\big|_{L=0}}\alpha\frac{\partial\mathcal{Q}_\mathcal{R}}{\partial L}\Big|_{L=0} = \alpha s_0\frac{\mathrm{d}}{\mathrm{d}s_0}\ln\alpha(s_0,\alpha_0)\Big|_{\alpha_0 \text{ fixed}} + \frac{\tilde{\alpha}\epsilon}{\frac{\partial\tilde{\alpha}}{\partial\alpha}}\Big|_{L=0}.$$

In kinematic renormalization with renormalization point $L = 0$, and in the limit $\epsilon \to 0$, this reproduces def. 103:

$$\beta(\alpha) := \alpha\frac{\partial}{\partial L}\mathcal{Q}_\mathcal{R}(\alpha, L)\Big|_{L=0} = \alpha s_0\frac{\mathrm{d}}{\mathrm{d}s_0}\ln\alpha(s_0,\alpha_0)\Big|_{\alpha_0 \text{ fixed}}.$$

For the remainder of this section, we will again assume kinematic renormalization conditions We remark that the first equation in def. 106 holds in all renormalization schemes (def. 97), while the second one is only valid in kinematic renormalization (def. 91).

Def. 106 implies an equation for the Z-factors. From def. 104, one obtains

$$s_0\frac{\mathrm{d}}{\mathrm{d}s_0}\ln\alpha = s_0\frac{\mathrm{d}}{\mathrm{d}s_0}(\ln\alpha_0 - \ln Z_\alpha - \epsilon\ln s_0) = -s_0\frac{\mathrm{d}}{\mathrm{d}s_0}\ln\alpha\cdot\frac{\partial}{\partial\ln\alpha}\ln Z_\alpha - \epsilon.$$

The first summand on the right hand can be expressed by the beta function (def. 106), and therefore

$$\beta(\alpha,\epsilon) + \big(\beta(\alpha,\epsilon) - \alpha\epsilon\big)\alpha\frac{\partial}{\partial\alpha}\ln Z_\alpha(\alpha,\epsilon) = 0. \tag{3.28}$$

Comparing eq. (3.28) with eq. (3.19), $\beta(\alpha) + \beta(\alpha)\partial_\alpha \ln \mathcal{Q}_\mathcal{R} = \alpha \partial_L \ln \mathcal{Q}_\mathcal{R}$, we see that Z_α is the L-independent part of $\tilde{\alpha}$, as stated in eq. (3.24), while on the other hand $\mathcal{Q}_\mathcal{R}$ is the finite part for $\epsilon \to 0$. Knowing either Z_α or $\beta(\alpha, \epsilon)$, one can compute the other,

$$\begin{aligned} \beta(\alpha,\epsilon) &= \frac{-\epsilon}{\frac{\partial}{\partial\alpha} \ln\left(\alpha \cdot Z_\alpha\left(\alpha,\epsilon\right)\right)} + \alpha\epsilon, \\ Z_\alpha(\alpha,\epsilon) &= \exp\left(-\int_0^\alpha \frac{\mathrm{d}u}{u} \frac{\beta(u,\epsilon)}{\beta(u,\epsilon) - u\epsilon}\right) = \prod_{j=1}^{\infty} \exp\left(\frac{1}{\epsilon^j} \int_0^\alpha \frac{\mathrm{d}u}{u} \left(\frac{\beta(u,\epsilon)}{u}\right)^j\right). \end{aligned} \tag{3.29}$$

For $\epsilon \neq 0$, not only the beta function, but also the anomalous dimension can obtain a non-trivial ϵ-dependent part. It arises from the ϵ-dependence of $G^{(2)}_\mathcal{R}$ in eq. (3.16),

$$\gamma^{(2)}(\alpha,\epsilon) := -s_0 \partial_{s_0} G^{(2)}_\mathcal{R}(\alpha,\epsilon).$$

Expressed in terms of Z-factors (def. 104), using eq. (3.22) and def. 106, this means

$$\gamma^{(2)}\left(\alpha,\epsilon\right) = -\left(\beta(\alpha,\epsilon) - \alpha\epsilon\right) \partial_\alpha \ln Z_\phi(\alpha,\epsilon), \qquad Z_\phi(\alpha,\epsilon) = \exp\left(-\int_0^\alpha \mathrm{d}u \, \frac{\gamma^{(2)}(u,\epsilon)}{\beta(u,\epsilon) - u\epsilon}\right). \tag{3.30}$$

The relations between the renormalization group functions and the counterterms are called *Gross-'t Hooft relations* [392, 396, 397]. Observe how they resemble the finite rescaling eq. (3.20): As expected from eq. (3.24), the Z-factor and the finite rescaling $\alpha \to \tilde{\alpha}$ are structurally similar.

The so-defined ϵ-dependent functions satisfy, in kinematic renormalization, all the properties from section 3.2.1. We collect them in a theorem for later reference.

Theorem 43. In kinematic renormalization, with renormalization point $L = 0$, the renormalization group equations theorems 39 and 40 and eqs. (3.15) and (3.19) hold for $\epsilon \neq 0$ in the form

$$\begin{aligned} \partial_L \ln G_\mathcal{R}(\alpha,\epsilon,L) &= \gamma(\tilde{\alpha}(\alpha,\epsilon,L),\epsilon) \\ \partial_L G^r_\mathcal{R}(\alpha,\epsilon,L) &= \big(\gamma^r(\alpha,\epsilon) + \left(\beta(\alpha,\epsilon) - \alpha\epsilon\right)\partial_\alpha\big) G^r_\mathcal{R}\left(\alpha,\epsilon,L\right), \\ \gamma^r_{j>1}(\alpha,\epsilon) &= \frac{1}{j}\left(\gamma^r(\alpha,\epsilon) + \left(\beta(\alpha,\epsilon) - \alpha\epsilon\right)\cdot\partial_\alpha\right)\gamma^r_{j-1}(\alpha,\epsilon), \\ \tilde{\alpha}(\alpha,\epsilon,L)\partial_L \ln \mathcal{Q}_\mathcal{R}(\alpha,\epsilon) &= \beta(\tilde{\alpha}(\alpha,\epsilon,L),\epsilon) \qquad \text{(there is no } -\alpha\epsilon \text{ here)}, \\ \partial_L \ln \mathcal{Q}_\mathcal{R}(\alpha,\epsilon) - \epsilon &= \big(\beta(\alpha,\epsilon) - \alpha\epsilon\big)\partial_\alpha \ln(\alpha \mathcal{Q}_\mathcal{R}(\alpha,\epsilon)). \end{aligned}$$

Moreover, for ϕ^n theory, the relation from lemma 42 is fulfilled even for $\epsilon \neq 0$,

$$\beta(\alpha,\epsilon) = \frac{2\alpha}{n-2}\left(\gamma^{(n)}(\alpha,\epsilon) - \frac{n}{2}\gamma^{(2)}(\alpha,\epsilon)\right).$$

3.2.3. Grouplike Green functions

Let $\Gamma \in H_{\mathrm{F}}$ be a grouplike (def. 65) combinatorial Green function (def. 45). We do not require at this point that Γ is a solution to a combinatorial DSE (eq. (2.28)). Owing to $\Delta(\Gamma) = \Gamma \otimes \Gamma$, we have $(\sigma \star \sigma)\Gamma = \sigma[\Gamma] \cdot \sigma[\Gamma]$. This holds as well for higher monomials, and the Feynman rules (def. 76) evaluate to

$$\exp^{\star}(L\sigma)[\Gamma] = \mathbb{1} + L\sigma[\Gamma] + \frac{1}{2}L^2\sigma[\Gamma]\sigma[\Gamma] + \frac{1}{6}L^3\sigma[\Gamma]\sigma[\Gamma]\sigma[\Gamma] + \ldots = e^{L\sigma[\Gamma]}.$$

In other words: The Feynman amplitude (def. 100) of a grouplike Hopf algebra element is a *scaling solution* (example 65), where the value $\sigma[\Gamma(\alpha)] = \gamma_1(\alpha)$ is the exponent,

$$\mathcal{F}_{\mathcal{R}}[\Gamma](L) = e^{L\gamma_1(\alpha)} = \left(\frac{s}{s_0}\right)^{\gamma_1(\alpha)}. \tag{3.31}$$

We have used def. 99 and the kinematic renormalization condition $\sigma^{\star 0}(\Gamma) = \tilde{\mathbb{1}}$. The same solution is also obtained from lemma 37 and $\Delta(\Gamma) = \Gamma \otimes \Gamma$, via the functional equation

$$\mathcal{F}_{\mathcal{R}}[\Gamma](L_1 + L_2) = m\left(\mathcal{F}_{\mathcal{R}}|_{L_1} \otimes \mathcal{F}_{\mathcal{R}}|_{L_2}\right)\Delta(\Gamma) = \mathcal{F}_{\mathcal{R}}[\Gamma](L_1) \cdot \mathcal{F}_{\mathcal{R}}[\Gamma](L_2).$$

Theorem 44. Let $\Gamma \in H_{\mathrm{CK}}$ or $\Gamma \in H_F$ be the solution of a linear DSE $\Gamma = \mathbb{1} + \sum_k \alpha^k B_+^k(\Gamma)$ (eq. (2.28)). Then the following holds:

1. Γ is grouplike (def. 65), $\Delta(\Gamma) = \Gamma \otimes \Gamma$.
2. The beta function (def. 106) vanishes, $\beta(\alpha, \epsilon) = 0$.
3. The renormalized Feynman amplitude in kinematic renormalization (def. 91) for $\epsilon = 0$ is $\mathcal{F}_{\mathcal{R}}[\Gamma](L) = \exp(L\gamma_1(\alpha))$, where $\gamma_1(\alpha) = \gamma(\alpha)$ is the anomalous dimension (def. 103).

Proof. Point 1 was remarked in example 63, and is a special case of theorem 24. Point 2 follows from def. 106 because in a linear DSE, $Q = \mathbb{1}$ is momentum-independent. The general form in point 3 follows from the Callan-Symanzik equation (theorem 39) using $\beta(\alpha) = 0$. In kinematic renormalization, we demand $\mathcal{F}_{\mathcal{R}}[\Gamma]|_{L=0} = 1$, hence there is no prefactor to $e^{L\gamma}$. Alternatively, use theorem 40 to find $\gamma_j = \frac{1}{j!}(\gamma_1)^j$. With these coefficients, eq. (3.2) takes the desired form. Clearly, $\partial_L \mathcal{F}_{\mathcal{R}}[\Gamma]|_{L=0} = \gamma_1 = \gamma$ is the anomalous dimension (def. 103). □

Compare theorem 44 with example 65: The scaling solution of a linear DSE is the 2-point function of a scale invariant theory. Moreover, for a scalar field theory, scale invariance implies conformal invariance [398], therefore, if a scalar theory is described by a linear DSE, then its correlation functions are severely restricted, see example 66.

Example 101: Infinite sums of rainbows or ladders.

Two realizations of grouplike Green functions in terms of Feynman graphs are the rainbows (example 76) and ladders (example 78). From theorem 44, we know, without performing any explicit computation, that these infinite sums of Feynman graphs add up to a Green function of the form eq. (3.31). The only remaining task is to determine $\gamma_1(\alpha)$, we will come back to this in theorem 45.

Another class of grouplike graphs are the wheels with spokes, recently featured in Super Yang-Mills theory [399, 400].

The simple scaling form of grouplike Green functions holds only for $\epsilon = 0$. For $\epsilon \neq 0$, we have the Callan-Symanzik equation (43),

$$\partial_L G_{\mathcal{R}}(\alpha, \epsilon, L) = (\gamma(\alpha, \epsilon) - \epsilon\alpha\partial_\alpha)\, G_{\mathcal{R}}(\alpha, \epsilon, L).$$

Using separation of variables and the boundary condition $G_{\mathcal{R}}(\alpha, \epsilon, 0) = 1$, we find

$$G_{\mathcal{R}}(\alpha, \epsilon, L) = \exp\left(- \int\limits_{\alpha e^{-\epsilon L}}^{\alpha} \mathrm{d}u \frac{\gamma(u, \epsilon)}{-u\epsilon} \right). \tag{3.32}$$

Compare this to the counterterm in eq. (3.30),

$$Z_G(\alpha, \epsilon) = \exp\left(- \int\limits_{0}^{\alpha} \mathrm{d}u\, \frac{\gamma(u, \epsilon)}{-u\epsilon} \right).$$

This is a particularly striking illustration of eq. (3.24): Owing to the ϵ in the denominator, the integral would be divergent, were it not for integration limits $(\alpha - \alpha e^{-\epsilon L}) \sim -\epsilon L \alpha$. The counterterm represents the divergent part of this integral, the renormalized Green function is merely a transition to the running coupling $\alpha e^{-\epsilon L} = \tilde{\alpha}$ (def. 105).

As an alternative to the integral in eq. (3.32), one can derive a series solution of the linear DSE by iterating the renormalization group equation for $\gamma_j(\alpha, \epsilon)$,

$$\gamma_j(\alpha, \epsilon) = \frac{1}{j} \left(\gamma_1(\alpha, \epsilon) - \alpha\epsilon\partial_\alpha\right) \gamma_{j-1}(\alpha, \epsilon).$$

The first order in ϵ is

$$\begin{aligned} G_{\mathcal{R}}(\alpha, \epsilon, L) &= e^{L\gamma_1(\alpha,\epsilon)} - \frac{1}{2}\epsilon L^2 e^{L\gamma_1(\alpha,\epsilon)} \alpha\partial_\alpha\gamma_1(\alpha, \epsilon) + \mathcal{O}\left(\epsilon^2\right) \\ &= e^{L\gamma_1(\alpha)} \left(1 + \epsilon \left([\epsilon^1]\gamma_1(\alpha, \epsilon) - \frac{1}{2} L^2 \alpha\partial_\alpha\gamma_1(\alpha) \right) + \mathcal{O}\left(\epsilon^2\right) \right). \end{aligned} \tag{3.33}$$

Here, we have introduced $\gamma_1(\alpha, \epsilon) =: \gamma_1(\alpha) + \epsilon[\epsilon^1]\gamma_1(\alpha, \epsilon) + \mathcal{O}(\epsilon^2)$.

Grouplike Green functions allow us to make an argument about counterterms in the physical dimension $\epsilon = 0$: To finite order in α, the counterterms (def. 104) are a sum of poles in ϵ and clearly infinite for $\epsilon \to 0$. But the 2-point Green functions carry an anomalous dimension, which will generally be non-integer. For grouplike functions (theorem 44), this anomalous dimension resembles analytic regularization (section 2.3.2). In that case, the Feynman integrals are not actually divergent when the regulator is removed, and "the theory regularizes itself" [401]. The Z-factors are then finite. See example 119 for the counterterm of a linear DSE. In the non-linear case, eq. (3.2) represents an expansion "around analytic regularization"[401]. The true non-perturbative status of Z-factors is unclear, but it is well possible that they turn out finite in the general case as well. This would be fortunate, because, in the traditional view of canonical quantization, they are introduced as probabilities and hence $Z \in [0, 1]$. A detailed discussion of the latter aspect can be found in [42].

3.2.4. Digression: History and variants of the renormalization group

The early developments, motivations and variants of the renormalization group are laid out in the foundational work [393]. For QFT, the renormalization group is intimately related to the quantum nature of the interaction, that is, the sum of all possible interactions as expressed by Dyson-Schwinger equations. Nonetheless, the renormalization group also appears in classical statistical physics [83, 402]. There, a change of scale amounts to averaging over microscopic degrees of freedom, in lattice models for example expressed by *Migdal-Kadanoff transformations* [403–406].

A first step towards the renormalization group equation in QFT was the *Gell-Mann-Low equation* [407, 408], which concerns the behaviour of interactions in QED at very high energies. From today's perspective, this analysis falls under *leading-log expansion*, to be introduced in section 3.3.3. See [402] for a detailed discussion of this point and a comprehensive historical review. Interestingly, without developing a formal theory, [408] already contains many of the features of the later renormalization group theory. The crucial point seems to be that later work, culminating in the Callan-Symanzik equation (theorem 39), realized that the renormalization group functions determine *all* scale dependence, while Gell-Mann and Low did not make a sharp distinction between the scale and the energy (compare example 65), and consequently understood their results only as an asymptotic approximation for very small distances, i.e. high energies, where scale and energy actually become equivalent.

The running of the coupling (def. 102) is governed (eq. (3.19)) by the behaviour of the beta function [213, 409, 410]. Especially, a value α^* such that $\beta(\alpha^*) = 0$ is a *fixed point* of the theory [411]. Once the energy scale L is such that $\tilde{\alpha}(L) = \alpha^*$, any further change of L will not change $\tilde{\alpha}$ any more, and therefore, the theory becomes *scale invariant*. This observation, together with *Bjorken scaling* [412, 413], guided the discovery of *asymptotic freedom* in QCD in the 1970s [414–417].

In our above language (def. 102), scale invariance means that the Dyson-Schwinger equations become linear, or that $\mathcal{Q}_{\mathcal{R}}(\alpha^*, L) = \mathbb{1}$. Clearly, $\alpha^* = 0$ is a fixed point, called *Gaussian fixed point* (because the free fields follow a Gaussian distribution, compare theorem 3). It is conceivable that a theory has additional *non-trivial fixed points* $\alpha^* \neq 0$. This implies that the linear DSEs studied in section 3.2.3 are not merely a technical example, but they are of high relevance for real-world QFT. Conversely, a non-vanishing beta function in the renormalization group (theorem 40) can be interpreted as a "perturbation around conformal field theory" [200, Sec. 4.2].

One can view the renormalization group equations (RGE, theorem 39) as yet another perspective – apart from implementing boundary conditions, rescaling Lagrangian parameters, and removing divergences as discussed in section 2.3.4 – on renormalizability. This is the perspective of *Wilson's renormalization group* [393, 418–422]. The RGE determine how beta functions change with the scale. Renormalizability then amounts to whether or not an effective action (def. 48) at high energies can have finite coupling constants, given the values we observe at lower energies. The conclusions are identical, but philosophically it is the opposite view compared to the "UV-finiteness" we usually demand: For us, the argument was that there must be no divergent high-energy unobservable quantum corrections to the processes we observe. In Wilson's perspective, the theory at a very high, but finite, scale is the fundamental object and the question is if it gives rise to a low-energy theory with non-zero effective couplings. For a non-renormalizable theory, the couplings *decrease* polynomially as the scale is *lowered*, rendering them effectively zero at observables. This phenomenon is called *triviality* and it can also occur for renormalizable theories, for example,

scalar ϕ^4 theory is assumed to be trivial in this sense [423], even though it is renormalizable perturbatively.

Computing the change of the effective action (as opposed to individual Green functions) with changing energy scales is the endeavour of *exact renormalization group theory* and the *Wetterich equation* [424–429]. A priori, this comes at the cost of manipulating, instead of functions, a potentially complicated functional, but in concrete calculations one truncates the functional to finitely many functions. This setup appears particularly suitable for finding non-trivial fixed points [430]. Especially, it might be that quantum gravity, despite not being renormalizable when formulated as a perturbation of a free theory (see section 5.2.1), has a sensible, finite, high-energy effective action, representing a non-trivial fixed point [431–434].

Finally, we have discussed the renormalization group only in terms of UV-behaviour. Especially for gauge theories, the IR-behaviour is interesting as well [402, 435–444].

Summary of section 3.2.

1. Upon changing the energy scale, a renormalized Green function varies according to the Callan-Symanzik equation (theorem 39). The change of the coupling parameter with changing energy scale is given by the beta function, such transformations generate the renormalization group. We concentrated on kinematic renormalization conditions in section 3.2.1.

2. In section 3.2.2, we extended the renormalization group to $\epsilon \neq 0$ in dimensional regularization, still using kinematic renormalization. We saw that removing divergences, and rescaling to different energy scales, is essentially the same process. In this transformation, the invariant charge represents the finite part, the counterterms a divergent, L-independent part. The latter are integrals of the renormalization group functions.

3. A linear DSE has grouplike combinatorial Green functions as solutions, and the corresponding analytic Green function is a simple monomial, called scaling solution. The functional form becomes more complicated when $\epsilon \neq 0$ (section 3.2.3).

4. Section 3.2.4 is a short survey of other aspects of renormalization group theory, which are not directly relevant for the present thesis. We observed that scaling functions appear at fixed-points of the renormalization group.

3.3. Dyson-Schwinger equations, third act

Equipped with knowledge about the renormalization group, we can finally carry out our last attack on Dyson-Schwinger equations. The previous sections about DSEs, sections 1.3.11 and 2.2.5, have been rather superficial and served to introduce the general, conceptional features of Dyson-Schwinger equations. Conversely, the purpose of the present section is to find concrete solutions of a certain class of DSEs.

3.3.1. Propagator-DSE as differential equation

We want to learn how to compute the anomalous dimensions (def. 103) systematically in kinematic renormalization. The method in question was derived gradually over 15 years in [213, 271, 389, 390, 401, 445, 446].

For this section, we restrict ourselves to a massless theory, and a single (non-coupled) Dyson-Schwinger equation of propagator type. Conceptually, the method can account for vertex corrections either by explicitly including kernel graphs (def. 50) with vertex-type subgraphs into the propagator DSE, or by introducing an additional functional dependence of kernels on angle parameters (def. 81) to allow for vertex-type DSEs. Both approaches greatly increase the computational difficulty and we will not pursue them further. It has been argued [447] that this approximation to DSEs is in the spirit of the Hartree-Fock method [448–450] in molecular physics: Instead of solving the full coupled system, one solves for one Green function at a time, keeping all others fixed.

The solution we are trying to find is a 1PI propagator Green function $G_{\mathcal{R}}^{(2)} =: G_{\mathcal{R}}$ and the invariant charge (def. 93) is a power of this Green function,

$$\mathcal{Q}_{\mathcal{R}} = G_{\mathcal{R}}^{w}. \tag{3.34}$$

Here, the exponent $w \in \mathbb{Z}$ is chosen corresponding to the vertex valence of the theory, see def. 92. We have encountered this setup already in example 82. In kinematic renormalization, eq. (3.34) implies $\beta(\alpha, \epsilon) = w \cdot \alpha\gamma(\alpha, \epsilon)$ (theorem 43). We shall see in theorem 49 that the same holds for all renormalization schemes.

Despite the simplifications, the DSE can still involve infinitely many kernel graphs (def. 50). We redefine the coupling constant such that it corresponds to the loop order $|\Gamma|$ of the kernels, that is, the first non-vanishing kernel is of order α^1, the next one α^2 etc.. In this way, the DSE has a form similar to theorem 27,

$$G_{\mathcal{R}} = 1 - (1-\mathcal{R}) \sum_{k=1}^{\infty} \alpha^k B_+^{(2),k} \left(G_{\mathcal{R}} \cdot \mathcal{Q}_{\mathcal{R}}^k \right) = 1 - (1-\mathcal{R}) \sum_{k=1}^{\infty} \alpha^k B_+^{(2),k} \left(G_{\mathcal{R}}^{1+wk} \right). \tag{3.35}$$

Here, B_+ is the sum of all cocycles of grade k, it is the analogue of eq. (3.10), but on the level of amplitudes, not on graphs. It is given by the Mellin transform (def. 101) according to eq. (3.7),

$$(1-\mathcal{R})\, B_+^{(2),k} \left(G_{\mathcal{R}}^{1+wk} \right) = \sum_{\Gamma} \underbrace{G_{\mathcal{R}}(\alpha, \partial_{\rho_1}) \cdots G_{\mathcal{R}}(\alpha, \partial_{\rho_E})}_{E=1+wk \text{ factors}} \left(e^{L \sum_j \rho_j} - 1 \right) F_\Gamma \left(\rho_1, \ldots, \rho_E \right) \Big|_{\rho=0}.$$

All graphs of order k have the same number $E = |E_\Gamma|$ of internal edges, therefore we can sum their Mellin transforms to obtain

$$F_k(\rho_1, \ldots, \rho_E) := \sum_{\Gamma, |\Gamma|=k} F_\Gamma \left(\rho_1, \ldots, \rho_E \right).$$

The DSE from eq. (3.35) now reads

$$G_{\mathcal{R}}(\alpha, L) = 1 - \sum_{k=1}^{\infty} \alpha^k G_{\mathcal{R}}(\alpha, \partial_{\rho_1}) \cdots G_{\mathcal{R}}(\alpha, \partial_{\rho_E}) \left(e^{L \sum_j \rho_j} - 1 \right) F_k(\rho_1, \ldots, \rho_E) \Big|_{\rho=0}. \quad (3.36)$$

This is a *pseudodifferential equation* version of the DSE, that is, a differential equation of potentially infinite order. Expanding in L results in an equation for the anomalous dimension in kinematic renormalization, $\gamma(\alpha) = \gamma_1(\alpha)$,

$$\gamma(\alpha) = -\sum_{k=1}^{\infty} \alpha^k G_{\mathcal{R}}(\alpha, \partial_{\rho_1}) \cdots G_{\mathcal{R}}(\alpha, \partial_{\rho_E}) \left(\sum_j \rho_j \right) F_k(\rho_1, \ldots, \rho_E) \Big|_{\rho=0}. \quad (3.37)$$

The Green functions $G_{\mathcal{R}}$ on the right hand side are determined from the anomalous dimension by the renormalization group equation (theorem 40), where $\beta = w\alpha\gamma$.

If the Mellin transform is known as a power series in ρ, computing $\gamma(\alpha)$ from eq. (3.37) is a merely combinatorial task, which can typically be done to hundreds of orders, e.g. [451] or even to all orders [389, 390]. Equation (3.36) implies especially that all information about the behaviour of $G_{\mathcal{R}}$ for high orders in α is encoded in the coefficients of the Mellin transforms, see [213, 409, 410]. A graphical interpretation of the coefficients of $\gamma(\alpha)$ is in terms of chord diagrams [162, 452–455]. By truncating the Mellin transform to a polynomial of low degree, the computation can be simplified even more [456, 457].

3.3.2. Insertions into a single edge

It is possible to turn eq. (3.37) into a non-recursive differential equation, if the following severe additional restrictions are imposed:

1. There are only kernel graphs of a single order, which we take $k = 1$.
2. The correction is only inserted into one of the edges at a time. Technically, this means that we restrict ourselves to one-parameter Mellin transforms $F(\rho) := F(\rho, 0, \ldots, 0)$. It is possible to include all edges, $F(\rho) := F(\rho, 0, \ldots) + F(0, \rho, \ldots)$, but this will still miss the insertions into multiple edges *simultaneously*.

Under these conditions, the DSE (theorem 15) takes the form

$$G(\alpha, s) = 1 + \alpha(1 - \mathcal{R}) \int \mathrm{d}y \; K(s, y) G(\alpha, y)^{1+w}, \quad (3.38)$$

where K is the sum of all kernel graphs and $w = -2$ in physical models. The DSE can be rewritten as a differential equation analogous to eq. (3.36),

$$G_{\mathcal{R}}(\alpha, L) = 1 - \alpha \left(G_{\mathcal{R}}^{1+w}(\alpha, \partial_\rho) e^{L\rho} F(\rho) - G_{\mathcal{R}}^{1+w}(\alpha, \partial_\rho) F(\rho) \right) \Big|_{\rho=0}. \quad (3.39)$$

Theorem 45. Consider a DSE at the physical dimension $\epsilon = 0$ of the form eq. (3.38), where $\mathbb{R} \ni w \neq 0$ and $F(\rho)$ is the Mellin transform (def. 101) of the sum of kernel graphs. Then, in kinematic renormalization (def. 91), the anomalous dimension is a solution of the pseudodifferential equation

$$\frac{1}{\rho \cdot F(\rho)}\Big|_{\rho \to \gamma(1+w\alpha\partial_\alpha)} \gamma(\alpha) = -\alpha.$$

If, in the same setup, $w = 0$, then $\gamma(\alpha)$ satisifies the algebraic equation

$$\frac{1}{F(\gamma(\alpha))} = -\alpha \quad \Leftrightarrow \quad \gamma(\alpha) = F^{-1}\left(-\frac{1}{\alpha}\right).$$

On the right hand side, F^{-1} denotes the inverse function, not $\frac{1}{F}$.

Proof. Conceptually, we use eq. (3.4) in reverse direction, namely $\partial_L^k e^{L\rho} = \rho^k e^{L\rho}$ and therefore

$$e^{L\rho} = \frac{1}{F(\rho)} \cdot F(\rho) e^{L\rho} = \frac{1}{F(\rho)}\Big|_{\rho \to \partial_L} \cdot F(\rho) e^{L\rho}.$$

Apply this differential operator to both sides of eq. (3.39):

$$\frac{1}{F(\rho)}\Big|_{\rho \to \partial_L} G_{\mathcal{R}}(\alpha, L) = -\alpha G_{\mathcal{R}}^{1+w}(\alpha, \partial_\rho) e^{L\rho}\Big|_{\rho=0} + 0 = -\alpha G_{\mathcal{R}}^{1+w}(\alpha, L).$$

The operator on the left hand side is a power series in ∂_L, starting at linear order. The Callan-Symanzik equation (theorem 39) in our case reads $\partial_L G_{\mathcal{R}} = \gamma(\alpha)(1 + w\alpha\partial_\alpha) G_{\mathcal{R}}$. Therefore, we can replace ∂_L and obtain

$$\begin{aligned} \frac{1}{F(\rho)}\Big|_{\rho \to \gamma(1+w\alpha\partial_\alpha)} G_{\mathcal{R}}(\alpha, L) &= -\alpha G_{\mathcal{R}}^{1+w}(\alpha, L) \\ \frac{1}{F(\rho)}\Big|_{\rho \to \gamma(1+w\alpha\partial_\alpha)} \left(1 + \gamma(\alpha)L + \gamma_2(\alpha)L^2 + \ldots\right) &= -\alpha \left(1 + \gamma(\alpha)L + \gamma_2(\alpha)L^2 + \ldots\right)^{1+w}. \end{aligned}$$

We will be interested in the order L^0. On the left hand side,

$$\gamma\left(1 + w\alpha\partial_\alpha\right) 1 = \gamma(\alpha), \qquad \left(\gamma\left(1 + w\alpha\partial_\alpha\right)\right)^j 1 = j!\gamma_j(\alpha) = \left(\gamma\left(1 + w\alpha\partial_\alpha\right)\right)^{j-1} \gamma(\alpha).$$

Consequently, if we reduce all powers of ρ in the differential equation by one, then the operator acts on $\gamma(\alpha)$ instead of on 1. We obtain the claimed form of the pseudodifferential equation.

In this equation, unlike eq. (3.38), the parameter w has an analytic, but no longer a combinatorial function, therefore we can allow $w \in \mathbb{R}$. The algebraic equation is the limit $w \to 0$ of the differential equation. □

In the literature, differential equations like theorem 45 have appeared for various concrete examples of Mellin transforms [213, 271, 390, 456]. Knowing a differential equation for the anomalous dimension allows to derive sophisticated statements about its behaviour beyond perturbation theory [244, 253, 458], see section 3.4.

We remark that for the original graphical DSE (eq. (3.38)) in physical models, every choice $w \notin \{-2, 0\}$ means that we insert subgraphs with non-standard prefactors, or only certain sets of subgraphs. The choice $w = -2$ is the only one where all subgraphs are used with their conventional QFT multiplicities. The choice $w = 0$ amounts to $Q = \mathbb{1}$ (eq. (3.34)) and therefore to a linear DSE. With $w = -1$, we obtain a non-recursive "DSE", which has the 1-loop graph $\gamma(\alpha) = -c_0\alpha$ as full solution, where c_0 is the first coefficient of $F(\rho)$ (eq. (3.5)).

It seems that the literature so far has mostly concentrated on the physically most relevant cases $w = 0$ (linear approximation, e.g. [401, 459, 460]) and $w = -2$ (one inverse Green function inserted into the kernel, e.g. [253, 390, 445, 451, 456–458]).

The setup discussed in [451, 456, 457] is based on an invariant charge $\mathcal{Q}_\mathcal{R} = G_\mathcal{R}^{-3}$, but still it is conceptually different from choosing $w = -3$ in our formalism: With $w = -3$, we insert the entire correction $G_\mathcal{R}^{-2}$ into only one of the two internal edges, while in [451, 456, 457], one copy $G_\mathcal{R}^{-1}$ is inserted into each of the two edges. See also [213, Sec. 5] for a discussion how insertion into only a subset of the available edges is equivalent to including additional primitive kernels.

Finally, we remark that theorem 45 represents a unique mapping between a DSE of the form eq. (3.38) at $\epsilon = 0$ and its perturbative solution. That is, knowing the anomalous dimension (as a power series) allows to reconstruct the Mellin transform of the kernel (as a power series for $\epsilon = 0$). No two different Dyson-Schwinger equations of this form have the same solution in kinematic renormalization.

Example 102: Toy model, linear DSE.

The toy model (example 79) gives rise to the renormalized DSE

$$G_\mathcal{R}(\alpha, s) = 1 - (1 - \mathcal{R})\,\alpha \int_0^\infty \frac{\mathrm{d}y\ (sy)^{-\epsilon}}{1+y} G_\mathcal{R}^{1+w}(\alpha, sy).$$

We have computed the Mellin transform $F(\rho) = \frac{\pi}{\sin(\pi\rho)}$ in example 98. By theorem 45, the linear DSE, for $\epsilon = 0$, has the all-order solution $G_\mathcal{R}(\alpha, L) = e^{L\gamma(\alpha)}$ with

$$\gamma(\alpha) = -\frac{1}{\pi}\arcsin(\pi\alpha) = -\alpha - \frac{\pi^2}{6}\alpha^3 - \frac{3\pi^4}{40}\alpha^5 - \frac{5\pi^6}{112}\alpha^7 - \dots.$$

Example 103: Multiedge DSE.

We consider insertions into one of the edges of the the 1-loop multiedge (example 23). Then the DSE reads

$$G_\mathcal{R}(\alpha, \epsilon, \underline{q}^2) = 1 - \lambda^2 \int \frac{\mathrm{d}^D \underline{k}}{(2\pi)^D} \frac{G_\mathcal{R}^{1+w}(\alpha, \epsilon, \underline{k}^2)}{(\underline{k}+\underline{q})^2\,\underline{k}^2} + \mathcal{R}\left(\lambda^2 \int \frac{\mathrm{d}^D \underline{k}}{(2\pi)^D} \frac{G_\mathcal{R}^{1+w}(\underline{k}^2)}{(\underline{k}+\underline{q})^2\,\underline{k}^2}\right).$$

If $D = D_0 - 2\epsilon$, then we obtain the form eq. (3.38) by rescaling the coupling $\alpha := \lambda(4\pi)^{-\frac{D_0}{2}}$.

Definition 107 ([461, 462])**.** For $n \in \mathbb{N}$, the *Catalan numbers* C_n are given by

$$C_n := \frac{1}{n+1}\binom{2n}{n}.$$

Example 104: Multiedge linear DSE.

The Mellin transform of the 1-loop multiedge in $D = 4$ was computed in example 96. The linear DSE in kinematic renormalization at $\epsilon = 0$ has a scaling solution (theorem 44), where the anomalous dimension satisfies (theorem 45)

$$\frac{1}{\frac{-1}{\gamma(\alpha)(1+\gamma(\alpha))}} = -\alpha \quad \Rightarrow \quad \gamma(\alpha) = \frac{\sqrt{1+4\alpha}-1}{2} = \sum_{n=1}^{\infty}(-1)^n C_{n-1}\alpha^n,$$

where C_n are the Catalan numbers (def. 107). This solution has long been known [459]. In a similar way, the Mellin transform of the same kernel in $D = 6$ is a rational function of degree four, leading to the anomalous dimension

$$\gamma(\alpha) = \frac{\sqrt{5+4\sqrt{1-\alpha}}-3}{2}.$$

Observe that theorem 45 does not make any reference to regularization, because essentially, the Mellin transform acts as an analytically regularized integral. But even without explicit regularization, it is based on kinematic renormalization conditions (def. 91). Earlier works on DSEs, such as [459, 460], do regulate the integrals using dimensional regularization (section 2.3.3), but they impose kinematic renormalization conditions nonetheless. In chapter 4, we consider DSEs with non-kinematic renormalization conditions.

3.3.3. Leading-log expansion

In eqs. (3.2) and (3.16), we expanded the renormalized 1PI Green function in powers of the logarithmic scale L (def. 99), where the coefficients $\gamma_j(\alpha)$ are functions of the renormalized coupling α. The *leading log expansion* is a reordering of the series, in powers of $\alpha \cdot L$:

$$G_{\mathcal{R}}(\alpha, x) = 1 + \sum_{k=1}^{\infty} H_k(\alpha L)\,\alpha^{k-1}. \tag{3.40}$$

The function $H_1(z)$ is the *leading-log contribution* to the Green function, and $H_k(z)$ represents the next-to^k leading log part. They can be obtained systematically from DSEs by mapping to chord diagrams [463, 464], or from the renormalization group equation in the Hopf algebra [271, 380, 465]. In the language of rooted trees (section 2.1.5), the leading log approximation amounts to a weighting of all trees with their *tree factorial* [167, 271].

Using eq. (3.8), we see that the leading-log order is the highest power in L for each graph, therefore it is given by the c_0-term of the Mellin transform (def. 101). Phrased differently, we obtain the leading-log solution of any theory by setting $c_{j\geq 1} = 0$ in the Mellin transform, and the next-to^k leading log by keeping only the first k coefficients c_j (compare example 97). Equivalently, H_k depends on the first k coefficients c_k of the anomalous dimension in kinematic renormalization (def. 91),

$$\gamma(\alpha) =: \sum_{j=1}^{\infty} c_j \alpha^j. \tag{3.41}$$

As remarked in section 3.2.4, this observation was the starting point for renormalization group theory in QED in [408, 466]: Knowing the first coefficient of the beta function, one can resum leading logarithms to all orders. Concretely, for a DSE with one insertion point (eq. (3.39)) which features the invariant charge $\mathcal{Q}_\mathcal{R} = G_\mathcal{R}^w$ (eq. (3.34)), where $w \neq 0$, one finds [380]:

$$H_1(z) = \frac{1}{(1 - wc_1 z)^{\frac{1}{w}}}, \qquad H_2(z) = \frac{-c_2 \ln(1 - wc_1 z)}{wc_1 (1 - wc_1 z)^{\frac{1}{w}+1}}, \tag{3.42}$$
$$H_3(z) = \frac{-w^2 c_1 (c_2^2 - c_1 c_3) z - wc_2^2 \ln(1 - wc_1 z) + \frac{c_2^2}{2}(1 + w) \ln^2(1 - wc_1 z)}{w^2 c_1^2 (1 - wc_1 z)^{\frac{1}{w}+2}}.$$

Example 105: Landau pole in QED.

The leading-log functions in eq. (3.42) are only valid for a theory with a single Green function. QED (example 22) contains two fields and three Green functions needing renormalization (the two propagators and the vertex). Thanks to the Ward identity to be discussed in example 128, in terms of renormalization, QED effectively behaves like a theory with only one Green function and $w = +1$. We are interested in the leading log expansion of the running coupling $\tilde{\alpha}$ (def. 102). By eq. (3.19), its momentum dependence is given by the beta function, so we have to replace γ with β in eq. (3.42). In QED, the first coefficient of the beta function (where one factor of α is removed by $\alpha\mathcal{Q}_\mathcal{R} = \tilde{\alpha} \leftrightarrow \mathcal{Q}_\mathcal{R}$) is $c_1 = \frac{\alpha}{3\pi} > 0$ [467, 468]. From eq. (3.42), we obtain

$$\tilde{\alpha}(\alpha, L) = \frac{\alpha}{1 - \frac{\alpha}{3\pi} L}.$$

This is the famous first order correction to the running coupling, obtained by Gell-Mann and Low [408, 466]. We see that $\tilde{\alpha}(\alpha, L^*) = \infty$ for a finite value L^*. This value is known as the Landau pole, or Moscow zero, of QED [407, 469, 470], indicating the breakdown of the leading-log expansion. The same pole will appear for all H_k, at the same L^*, unless the polynomials in the numerator cancel the pole. A slightly different perspective, based on Dyson-Schwinger equations rather than the leading-log expansion, is given in [409], with the outcome that the presence of a Landau pole depends on the asymptotic growth of primitive Feynman graphs.

Conversely, the leading log approximation in QED does not contain obvious poles for the infrared asymptotics $L \to -\infty$. Therefore, $H_k(z)$ do give the correct asymptotics for vanishing *scale*, but this limit implies simultaneously a vanishing of the electron mass (see example 65), so it is not the physical low-energy limit of QED.

The opposite situation occurs if the coefficient c_1 is smaller than zero [410]. Then, H_1 is not singular for $L \to \infty$ and the leading-log expansion produces the correct UV asymptotics [402]. Such theories are called *asymptotically free* [416, 417, 429] since for high energies, they become free field theories. But this time, the leading log expansion breaks down for low scales $L \to -\infty$. Quantum chromodynamics (QCD) is a theory of this kind.

At the same time, the (experimentally verified) existence of QCD is an argument for why the Landau pole in QED does not necessarily indicate a failure of quantum field theory: The coupling of QCD at low energies becomes strong and perturbation theory

breaks down, but the coupling stays finite nevertheless, as known e.g. from lattice calculations [471]. Finally, a non-Gaussian UV fixed point has been proposed for QED [472], rendering it finite despite the diverging low-order perturbation series. Compare the discussions in sections 3.2.4 and 5.2.1.

3.3.4. Non-physical spacetime dimension

So far, we have concentrated on the physical spacetime dimension $D = D_0$. But with small modifications, our theory is also applicable to the general case $D = D_0 - 2\epsilon$.

Theorem 46. Work in dimensional regularization (section 2.3.3) with $D = D_0 - 2\epsilon$. Consider a DSE of the form eq. (3.38), where $\mathbb{R} \ni w \neq 0$ and $F(\rho)$ is the ϵ-dependent Mellin transform of the sum of kernel graphs. Then, in kinematic renormalization (def. 91), the ϵ-dependent anomalous dimension is a solution of the pseudodifferential equation

$$\frac{1}{\rho \cdot F(\rho)}\Big|_{\rho \to \gamma + (w\gamma - \epsilon)\alpha\partial_\alpha} \gamma(\alpha, \epsilon) = -\alpha.$$

The ϵ-dependent solution of a linear DSE is given by the differential equation that arises by setting $w = 0$.

Proof. The proof of theorem 45 can be copied almost verbatim. The only difference is that we need the Mellin transform in D dimensions, including its ϵ-dependence, and the Callan-Symanzik equation with ϵ-dependence (theorem 43),

$$\big(\gamma(\alpha, \epsilon) + (w\gamma(\alpha, \epsilon) - \epsilon)\,\alpha\partial_\alpha\big) G_{\mathcal{R}}(\alpha, \epsilon, L) = \partial_L G_{\mathcal{R}}(\alpha, \epsilon, L).$$

The linear case still contains the derivative operator $-\epsilon\alpha\partial_\alpha$, it does not reduce to an algebraic equation in the ϵ-dependent case. □

The differential equation in theorem 46 implies a highly non-trivial mixing of the various orders in ϵ. This is because, in a series expansion of the anomalous dimension in ϵ, the various orders no longer commute. For example, the quantity $[\epsilon^0]\gamma\alpha\partial_\alpha\left([\epsilon^1]\gamma\right)$ is generally different from $[\epsilon^1]\gamma\alpha\partial_\alpha\left([\epsilon^0]\gamma\right)$. The situation becomes more manageable in the linear case ($w = 0$).

Theorem 47. Consider a linear DSE ($w = 0$) of the form eq. (3.38) with ϵ-dependent Mellin transform (def. 101) $F(\rho)$. Let $\frac{1}{F(\rho)} = T_0(\rho) + \epsilon T_1(\rho) + \mathcal{O}(\epsilon^2)$ and $\gamma(\alpha, \epsilon) =: \gamma(\alpha) + \epsilon g(\alpha) + \mathcal{O}(\epsilon^2)$, then

$$g(\alpha) = \frac{\alpha\partial_\alpha\gamma(\alpha) \cdot \left(\frac{1}{2}\partial_\rho^2 T_0(\rho)\Big|_{\rho\to\gamma(\alpha)}\right) - T_1(\gamma(\alpha))}{\left(\partial_\rho T_0(\rho)\Big|_{\rho\to\gamma(\alpha)}\right)}.$$

Proof. We have to extract the order ϵ^1 from theorem 46 in the linear case. First, observe that

$$\begin{aligned}[\epsilon^1]\left(\left(\gamma(\alpha,\epsilon)-\epsilon\alpha\partial_\alpha\right)^k\gamma(\alpha,\epsilon)\right) &= \left(\gamma(\alpha)\right)^k g(\alpha)+\sum_{j=1}^{k}\left(\gamma(\alpha)\right)^{k-j}\left(g(\alpha)-\alpha\partial_\alpha\right)\left(\gamma(\alpha)\right)^j \\ &= (k+1)\cdot\gamma(\alpha)^k g(\alpha)-\frac{k(k+1)}{2}\gamma(\alpha)^{k-1}\alpha\partial_\alpha\gamma(\alpha).\end{aligned}$$

Let $T_0(\rho) =: \sum_{k\geq 1} t_k\rho^k$, then the first order in ϵ of theorem 46 is $0 = T_1(\gamma(\alpha)) + [\epsilon^1]T_0(\gamma(\alpha,\epsilon))$,

$$\begin{aligned}0 &= T_1(\gamma(\alpha))+\sum_{k\geq 1}t_k\left(k\cdot\gamma(\alpha)^{k-1}g(\alpha)-\frac{k(k-1)}{2}\gamma(\alpha)^{k-2}\alpha\partial_\alpha\gamma(\alpha)\right) \\ &= T_1(\gamma(\alpha))+g(\alpha)\left(\partial_\rho T_0(\rho)\Big|_{\rho\to\gamma(\alpha)}\right)-\alpha\partial_\alpha\gamma(\alpha)\left(\frac{1}{2}\partial_\rho^2 T_0(\rho)\Big|_{\rho\to\gamma(\alpha)}\right).\end{aligned}$$

□

Example 106: Multiedge DSE, linear correction in ϵ.

The Mellin transform of the Multiedge is example 96, a series expansion results in

$$\begin{aligned}T_0(\rho) &= -\rho-\rho^2 \\ T_1(\rho) &= 2+4\rho+\gamma_E\rho(1+\rho)+\left(\pi\cot(\pi\rho)+2\psi(\rho)\right)\rho(1+\rho) \\ &= 1+(3-\gamma_E)\rho-\gamma_E\rho^2-2\sum_{j=1}^{\infty}\zeta(2j+1)(\rho^{2j+1}+\rho^{2j+2}).\end{aligned}$$

Here, $\psi(z) := \partial_z\Gamma(z)$ is the digamma function. Using the given series expansion and eq. (2.47), one finds the alternative representation

$$\left(\pi\cot(\pi\rho)+2\psi(\rho)\right)\rho = \rho\partial_\rho\ln\frac{\Gamma(1+\rho)}{\Gamma(1-\rho)}-1.$$

We have $\partial_\rho T_0 = -1-2\rho$ and $\frac{1}{2}\partial_\rho^2 T_0 = -1$. The anomalous dimension $\gamma(\alpha)$ for $\epsilon = 0$ was derived in example 104, consequently,

$$\begin{aligned}g(\alpha) &= \frac{\alpha\partial_\alpha\gamma(\alpha)+T_1(\gamma(\alpha))}{1+2\gamma(\alpha)} \\ &= 1+\frac{\alpha}{1+4\alpha}+\frac{\gamma(\alpha)+1}{2\gamma(\alpha)+1}\left(2\gamma(\alpha)\cdot\gamma_E+\rho\partial_\rho\ln\frac{\Gamma(1+\rho)}{\Gamma(1-\rho)}\Big|_{\rho\to\gamma(\alpha)}-1\right) \\ &= 1+2\alpha-7\alpha^2+(26-2\zeta(3))\alpha^3+(-99+8\zeta(3))\alpha^4+\ldots.\end{aligned}$$

Knowing the functions $\gamma(\alpha)$ and $g(\alpha)$, the first-order solution in ϵ of the linear DSE is given by eq. (3.33).

Summary of section 3.3.

1. A DSE for propagator-type Green functions can be written as an implicit pseudodifferential equation where the Mellin transforms of the kernel graphs are the input data (section 3.3.1).

2. If we further restrict ourselves to insertions into only a single internal edge of a single kernel graph, then the DSE turns into an explicit pseudodifferential equation for the anomalous dimension $\gamma(\alpha)$ (section 3.3.2).

3. The leading-log expansion is a reordering of the series expansion of $G_{\mathcal{R}}$ in powers of $(\alpha \cdot L)$. The next-to-k-leading-log approximation is determined by the first k coefficients of the anomalous dimension, or of the Mellin transform of the kernel. Depending on the sign of the first coefficient, the leading-log expansion describes the asymptotics of the theory either for $L \to \infty$ or for $L \to -\infty$ (section 3.3.3).

4. In section 3.3.4, we showed that for insertions into a single edge, essentially the same pseudodifferential equation holds for the full ϵ-dependent anomalous dimension $\gamma(\alpha, \epsilon)$ as for the earlier case of $\epsilon = 0$. However, it needs the ϵ-dependent Mellin transform as input. For a linear DSE, we derived an explicit formula for the coefficient $[\epsilon^1]\gamma(\alpha, \epsilon)$.

3.4. Asymptotics and nonperturbative contributions in MOM

In this section, we determine the behaviour of the series coefficients of the MOM-renormalized (def. 91) Green functions at high order in α for three examples of DSEs. We comment on its implications for non-perturbative completions by resurgence (section 2.1.2).

3.4.1. Multiedge DSE at $D = 4$

The multiedge DSE has been introduced in example 103. We stated the solution of the linear DSE in example 104. The Mellin transform of this model, as computed in example 96, is $F(\rho) = \frac{-1}{\rho(1+\rho)}$. By theorem 45, the anomalous dimension $\gamma(\alpha)$ for the nonlinear DSE, $w \neq 0$, is determined by the differential equation

$$(1 + \gamma(\alpha)\,(1 + w\alpha\partial_\alpha))\,\gamma(\alpha) = \alpha. \tag{3.43}$$

This ODE has a unique perturbative solution. Using a power series ansatz eq. (3.41),

$$\gamma(\alpha) =: \sum_{j=1}^{\infty} c_j \alpha^j, \tag{3.44}$$

we computed the coefficients c_j symbolically up to order α^{500}, for $w \in \{-5, \ldots, +5\}$.

w	$\gamma(\alpha)$
5	$\alpha - 6\alpha^2 + 102\alpha^3 - 2640\alpha^4 + 87804\alpha^5 - 3483072\alpha^6 + 158329512\alpha^7 - 8050087584\alpha^8$
4	$\alpha - 5\alpha^2 + 70\alpha^3 - 1485\alpha^4 + 40370\alpha^5 - 1306370\alpha^6 + 48365100\alpha^7 - 2000065725\alpha^8$
3	$\alpha - 4\alpha^2 + 44\alpha^3 - 728\alpha^4 + 15368\alpha^5 - 384960\alpha^6 + 11004672\alpha^7 - 350628096\alpha^8$
2	$\alpha - 3\alpha^2 + 24\alpha^3 - 285\alpha^4 + 4284\alpha^5 - 75978\alpha^6 + 1530720\alpha^7 - 34237485\alpha^8$
1	$\alpha - 2\alpha^2 + 10\alpha^3 - 72\alpha^4 + 644\alpha^5 - 6704\alpha^6 + 78408\alpha^7 - 1008480a^8$
0	$\alpha - \alpha^2 + 2\alpha^3 - 5\alpha^4 + 14\alpha^5 - 42\alpha^6 + 132\alpha^7 - 429\alpha^8$
-1	α
-2	$\alpha + \alpha^2 + 4\alpha^3 + 27\alpha^4 + 248\alpha^5 + 2830\alpha^6 + 38232\alpha^7 + 593859\alpha^8$
-3	$\alpha + 2\alpha^2 + 14\alpha^3 + 160\alpha^4 + 2444\alpha^5 + 45792\alpha^6 + 1005480\alpha^7 + 25169760\alpha^8$
-4	$\alpha + 3\alpha^2 + 30\alpha^3 + 483\alpha^4 + 10314\alpha^5 + 268686\alpha^6 + 8167068\alpha^7 + 281975715\alpha^8$
-5	$\alpha + 4\alpha^2 + 52\alpha^3 + 1080\alpha^4 + 29624\alpha^5 + 988288\alpha^6 + 38377152\alpha^7 + 1689250176\alpha^8$

Table 3.1.: First perturbative coefficients of the anomalous dimension in MOM for the $D = 4$ multiedge DSE as a function of the renormalized coupling α for various powers w of the invariant charge $Q = G^w$. Only insertions into a single internal edge were performed, regardless of the value of w.

Results up to order α^8 are reported in table 3.1. The sequence of coefficients for $w = 1$ is part of the OEIS [473, A177384]. As remarked below theorem 45, the case $w = -3$ in our setup is not equivalent to insertion into both edges of the kernel graph, even if the latter also corresponds to $w = -3$. For $w = -3$, we obtain

$$\gamma(\alpha) = \alpha + 2\alpha^2 + 14\alpha^3 + 160\alpha^4 + 2444\alpha^5 + 45792\alpha^6 + 1005480\alpha^7 + 25169760\alpha^8 \mp \ldots. \tag{3.45}$$

Compare eq. (3.45) to [451, Table 1], in which $G_{\mathcal{R}}(\alpha, x)$ is inserted into both the internal edges of the primitive. Our result eq. (3.45) reproduces the purely rational part of the latter,

but not the terms proportional to $\zeta(j)$. This can be understood heuristically: The rational contribution to $\gamma(\alpha)$ arises from a rational Mellin transform. For the multiedge (example 96), this is the Mellin transform $F(\rho_1, \rho_2)$ where one of the ρ_j is set to zero. But restricting this Mellin transform to only one non-vanishing ρ exactly amounts to inserting into only one edge, as we do for eq. (3.45).

The empirical values of table 3.1 suggest for the coefficients of eq. (3.44)

$$\begin{aligned} &c_0 = 0, \quad c_1 = 1, \quad c_2 = -(w+1), \quad c_3 = (1+w)(2+3w), \\ &c_4 = -(w+1)(2w+1)(7w+5), \quad c_5 = (1+w)(2+5w)(7+22w+17w^2). \end{aligned} \tag{3.46}$$

These formulae have been verified for $w \in \{-30, 30\}$. Observe how every $c_{j\neq 1}$ contains a factor $(w+1)$, indicating that the higher coefficients vanish for the non-recursive DSE $w = -1$ as expected. The limit $w \to 0$, that is, the coefficient w^0 of c_j, must reproduce the solution of the linear DSE (example 104), namely the Catalan numbers C_n (def. 107):

$$[w^0]c_n = -(-1)^n C_{n-1} = (-1)^{n-1}\frac{1}{n}\binom{2(n-1)}{n-1}.$$

It turns out that the first order can be expressed in a similar fashion,

$$[w^1]c_n = \frac{1}{2}(-1)^{n-1}\left(4^{n-1} - \binom{2(n-1)}{n-1}\right). \tag{3.47}$$

The anomalous dimension considered so far, $\gamma(\alpha) =: \gamma^{\text{pert}}(\alpha)$, is the perturbative solution to the differential equation eq. (3.43). This ODE has also non-perturbative solutions [253, 458] of the form

$$\gamma^{\text{non-pert}}(\alpha) = \alpha^{\beta(w)} \exp\left(\frac{\lambda(w)}{\alpha}\right)\left(1 + b^{(1)}(w)\alpha + b^{(2)}(w)\alpha^2 + \dots\right). \tag{3.48}$$

We use the method of [458, section V. A.] to determine the unknown coefficients[1]. The ansatz $\gamma(\alpha) = \gamma^{\text{pert}}(\alpha) + \gamma^{\text{non-pert}}(\alpha)$ is inserted into eq. (3.43) and the above coefficients c_j are used for γ^{pert}. The equation is then linearized in $\gamma^{\text{non-pert}}$. The resulting series in α has to vanish, this leads to the expressions

$$\begin{aligned} \lambda(w) &= \frac{1}{w}, \quad \beta(w) = -\frac{3+2w}{w}, \quad b^{(1)}(w) = \frac{(1+w)(1+3w)}{w}, \\ b^{(2)}(w) &= \frac{(1+w)(1+5w+3w^2-5w^3)}{2w^2} \\ b^{(3)}(w) &= \frac{(1+w)(1+5w-4w^2-20w^3+45w^4+81w^5)}{6w^3} \\ b^{(4)}(w) &= \frac{(1+w)(1+3w-23w^2-9w^3+259w^4-327w^5-2421w^6-2139w^7)}{24w^4}. \end{aligned} \tag{3.49}$$

Setting $w = -2$, these expressions reproduce [253, (14)].

The coefficients c_n of the perturbative solution of the non-linear DSE eq. (3.43), grow factorially (def. 58), which has been studied intensively [249, 253, 390, 456]. As indicated

[1]The author thanks Gerald Dunne for suggesting the method.

in eq. (2.6), the asymptotic behaviour of c_n is dictated by the non-perturbative solution eq. (3.48), [237]. The same result can be obtained with the methods of [456]. For $n \to \infty$,

$$c_n \sim S(w) \cdot \frac{1}{(-\lambda(w))^n} \cdot \Gamma\left(n - \beta(w)\right) \left(1 + \frac{-\lambda(w) \cdot b^{(1)}(w)}{(n - \beta(w) - 1)} + \frac{(-\lambda)^2 \cdot b^{(2)}}{(n-\beta-1)(n-\beta-2)} + \frac{(-\lambda)^3 \cdot b^{(3)}}{(n-\beta-1)(n-\beta-2)(n-\beta-3)} + \dots\right). \tag{3.50}$$

We computed 500 series coefficients of $\gamma^{\text{pert}}(\alpha)$ and extracted their asymptotic behaviour using order-70 Richardson extrapolation (def. 59). This produced at least 50 significant digits and confirmed the expressions $\lambda(s), \beta(s), b^{(1)}(s) \dots b^{(4)}(s)$ listed in eq. (3.49). Numerical values for the Stokes constant $S(s)$ is reported in table 3.2.

Knowing the parameters eq. (3.49) (and the infinitely many other $b^{(j)}$) does not yet fix the non-perturbative solution entirely. Our non-perturbative ansatz eq. (3.48), in resurgence terminology, corresponds to a 1-instanton correction. There are infinitely many more terms $\gamma^{\text{non-pert},k}$ of similar structure, each of which has coefficients determined from the asymptotic growth of the preceding one, see the discussion in section 2.1.2. The true non-perturbative solution is a transseries (def. 57)

$$\gamma(\alpha) = \gamma^{\text{pert}} + \sum_{k=1}^{\infty} t^k \gamma^{\text{non-pert},k}, \tag{3.51}$$

where $t \in \mathbb{C}$ is a free parameter expressing the boundary condition of the first order DSE. For the case $w = -2$, all $\gamma^{\text{non-pert},k}$ have been determined in [253].

w	$S(w)$
5	−0.025 296 711 447 842 155 554 062 589 810 922 604 262 477 942 805 771
4	−0.027 093 755 285 804 302 538 145 834 438 779 321 901 953 254 099 492
3	−0.027 514 268 695 235 967 509 951 466 619 196 206 136 028 416 088 749
2	−0.022 754 314 527 304 604 570 864 961 094 569 471 756 231 077 114 904
1	−0.005 428 317 993 266 202 636 748 034 138 132 075 286 101 589 263 688 3
-2	0.207 553 748 710 297 351 670 134 124 720 668 682 684 453 514 969 63
-3	0.129 235 675 811 091 778 715 229 366 859 663 994 914 292 887 084 30
-4	0.087 977 369 959 821 254 076 048 394 021 324 447 743 442 962 588 612
-5	0.065 314 016 354 658 749 144 010 387 750 377 100 215 558 556 707 446

Table 3.2.: First 50 digits of the Stokes constant $S(w)$ for the non-linear DSE in $D = 4$ in the asymptotic expansion eq. (3.50). The numerical values coincide with the special values given in eq. (3.52).

3.4.2. Stokes constant as a function of the exponent of the invariant charge

As remarked above, the ODE eq. (3.50) from theorem 45 contains the exponent w of the invariant charge $\mathcal{Q}_{\mathcal{R}} = G_{\mathcal{R}}^{w}$ (eq. (3.34)) as an arbitrary numerical parameter, void of combinatorial interpretation. Consequently, we can insert also non-integer $w \in \mathbb{Q}$. The asymptotic corrections in eq. (3.50) are analytic in w. We can numerically extract the Stokes constant $S(w)$ as a function of w using Richardson extrapolation (def. 59) as described below eq. (3.50).

Firstly, we searched for values of w where the Stokes constant is a recognizable number, by comparing the numerical values to monomials in $\sqrt{\pi}$, $\sqrt{e}$, $\ln(n)$ for $n \in \{2, \ldots, 10\}$, and zeta values. We found the following, including $S(-2)$ known from [253]:

$$S\left(w=-1\right) = S\left(w=0\right) = 0, \qquad S\left(w=-\frac{3}{2}\right) = \frac{2}{\pi e},$$
$$S\left(w=-2\right) = \frac{1}{\sqrt{\pi}e}, \qquad S\left(w=-3\right) = \frac{3}{\pi e^2}. \tag{3.52}$$

In the cases $w = 0$ and $w = -1$, the DSE has convergent perturbative solutions (example 104), that is, the coefficients c_n in eq. (3.44) do not grow factorially. Consequently, $S(0) = 0$ and $S(-1) = 0$. It turns out that $S(w)$ quickly oscillates in the interval $w \in (-1, 0)$, with growing amplitude as $w \to 0_-$, see fig. 3.1.

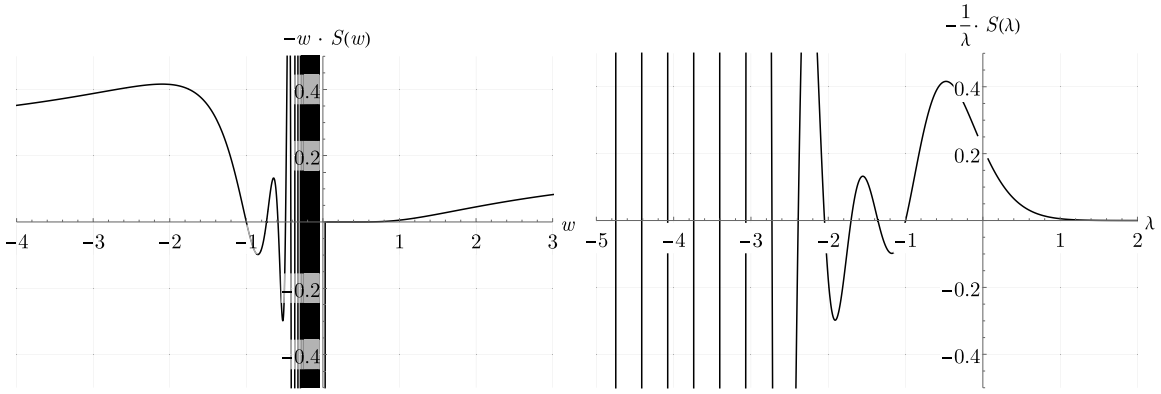

Figure 3.1.: Stokes constant of the anomalous dimension of the $D = 4$ multiedge DSE according to eq. (3.50). The plot is generated from $\sim 10^4$ individual evaluations of $S(w)$. The Stokes constant vanishes for $w = 0$ (linear DSE) and $w = -1$ (trivial DSE). Between these values, it is oscillating. In (b), the same data is shown as a function of $\lambda = \frac{1}{w}$, we see that the oscillations are regularly periodic in λ.

From the numerical data, we also conclude that $S(w)$ approaches zero faster than polynomially if $w \to 0_+$ from above. On the other hand, between $w = -1$ and $w = 0$ the function is oscillating with growing amplitude as w approaches zero from below. The first 50 nontrivial zeros were determined to six digits precision, starting with

$$z_j = \{-0.73658049, -0.586465, -0.488212, -0.418580, -0.366536, -0.326114, \ldots\}.$$

For large j, we find $j^2 \cdot (z_{j+1} - z_j) \to -3.000$ which indicates $z_j \sim \frac{-3}{j} + \mathcal{O}\left(\frac{1}{j^2}\right)$.

If we examine the Stokes constant as a function of $\lambda = \frac{1}{w}$, we see[2] that these oscillations are periodic in λ, with a period of $\frac{1}{3}$ as $\lambda \to -\infty$, shown in fig. 3.1 (b). To shed some light on the curious behaviour of $S(\lambda)$, we also express eq. (3.50) in terms of $\lambda = \frac{1}{w}$:

$$c_n \sim -\frac{1}{\lambda} S(\lambda) \frac{1}{\lambda^{n-1}} \Gamma\left(3\lambda + n + 2\right) \left(1 - \frac{\lambda^2 + 4\lambda + 3}{n} + \mathcal{O}\left(\frac{1}{n^2}\right)\right).$$

The heuristic physical interpretation of the parameter w is that it expresses the degree to which quantum corrections are taken into account: For $w = -1$, there are no quantum corrections, while $w = 0$ corresponds to a linear DSE, which includes all nested quantum corrections, but not yet the multiple insertions into the same edge. Consequently, we expect that the anomalous dimension $\gamma(\alpha)$ transitions smoothly between $w = -1$ and $w = 0$, or in the region $\lambda < -1$. On the other hand, the summand 3λ in $\Gamma(n + 2 + 3\lambda)$ will compete with the growth of n. Assuming that the c_n do not vary strongly as λ changes, the prefactor $S(\lambda)$ must absorb the shift, which leads to

$$S(\lambda) \sim \frac{1}{\Gamma(3\lambda + d(\lambda))}, \quad \lambda \to \infty. \tag{3.53}$$

Here, $d(\lambda) = d_0 + d_1 \frac{1}{\lambda} + \ldots$ is a subleading correction. Comparing with our numerical data, the formula eq. (3.53) qualitatively reproduces a correct factorial growth of $S(\lambda)$ for $\lambda \to 0_+$, and oscillations with period $\frac{1}{3}$ in λ, see fig. 3.2. We could even estimate the coefficients d_j, or find corrections to the formula eq. (3.53), but we will not pursue this further as we are currently lacking the theoretical background to rigorously understand the behaviour of $S(\lambda)$.

Prompted by the observations in fig. 3.1, David Broadhurst has independently reached similar conclusions as stated above, but greatly extended them by finding a variant of eq. (3.47) for all higher orders in w. With this, besides interesting number-theoretical and combinatorial findings, he was able to resum the first correction to the linear DSE [474]. It appears that, apart from this work, the behaviour of Dyson-Schwinger equations as functions of a continuous parameter w has never been examined in the literature. The author is convinced that a more detailed analysis can be fruitful, especially since it might provide a "continuous" way to introduce non-perturbative features into a theory, thereby clarifying their qualitative properties.

[2]The author thanks David Broadhurst for suggesting this variable, and for further discussions of this topic.

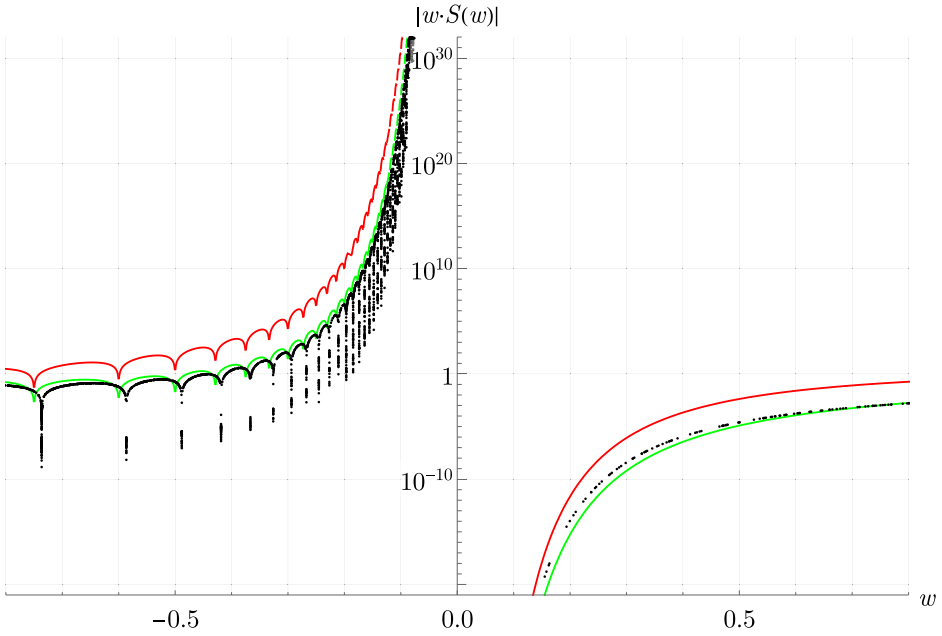

Figure 3.2.: Comparison of our numerical data (black) with the heuristic function eq. (3.53), plotted logarithmically as a function of $w = \frac{1}{\lambda}$. Red: $\frac{1}{\lambda}S(\lambda)$ from eq. (3.53) with $d(\lambda) = 0$. Green: The same function for $d(\lambda) = 3$. Visually, eq. (3.53) reproduces the observed behaviour of $S(\lambda)$.

3.4.3. Multiedge DSE at $D = 6$

We also examined the multiedge DSE (example 103) for the case $D = 6$, which differs from the $D = 4$ case only by a different Mellin transform, given in example 96. Consequently, the ODE of theorem 45 now takes the form

$$(3 + \gamma\,(1 + w\alpha\partial_\alpha))\,(2 + \gamma\,(1 + w\alpha\partial_\alpha))\,(1 + \gamma\,(1 + w\alpha\partial_\alpha))\,\gamma = -\alpha. \tag{3.54}$$

Again, we have computed the perturbative solution $\gamma^{\text{pert}}(\alpha) = \sum_{j=0}^{\infty} c_j \alpha^j$ to order α^{500} from this ODE, the first coefficients are

$$\begin{aligned}
c_1 &= -\frac{1}{6}, \quad c_2 = -\frac{11(w+1)}{6^3}, \quad c_3 = -\frac{(w+1)(206+291w)}{6^5}, \\
c_4 &= -\frac{(w+1)(4711+14887w+11326w^2)}{6^7}, \\
c_5 &= -\frac{(w+1)(119762+622327w+1036764w^2+556165w^3)}{6^9}.
\end{aligned}$$

Following the same procedure as in section 3.4.1, we insert the first few c_j and the non-perturbative ansatz eq. (3.48) into eq. (3.54), linarize, and solve for the parameters $\beta, \lambda, b^{(1)}, b^{(2)}, b^{(3)}$. Equation (3.54) is of third order, unlike in the case $D = 4$, we find three linearly independent

solutions:

$$\vec{\lambda}(w) = \left(-\frac{6}{w}, -\frac{12}{w}, -\frac{18}{w}\right), \quad \vec{\beta}(w) = \left(-\frac{35+29w}{6w}, -\frac{5+2w}{3w}, -\frac{15+13w}{2w}\right) \tag{3.55}$$

$$\vec{b}^{(1)}(w) = \left(\frac{275+267w-8w^2}{6\cdot 6^2 w}, \frac{-265-624w-359w^2}{3\cdot 6^2 w}, \frac{-85-241w-156w^2}{2\cdot 6^2 w}\right),$$

$$\vec{b}^{(2)}(w) = \left(\frac{75625+83790w-101849w^2-177828w^3-67814w^4}{93312w^2}, \right.$$
$$\left. \frac{70225+339690w+602764w^2+465258w^3+131959w^4}{23328w^2}, \frac{7225+37950w+69779w^2+51628w^3+12574w^4}{10368w^2}\right),$$

$$\vec{b}^{(3)}(w) = \left(\frac{20796875+8551125w-107422197w^2-206297091w^3-177713418w^4-90251478w^5-23658704w^6}{60466176w^3}, \right.$$
$$\frac{-18609625-138592350w-424432473w^2-687305592w^3-624311121w^4-303609366w^5-62154089w^6}{7558272w^3},$$
$$\left. \frac{-614125-4453575w-12499453w^2-16989843w^3-11830354w^4-4259034w^5-758520w^6}{2239488w^3}\right).$$

In order to match [458, eqs. (41)-(43)], the coefficient $b^{(1)}$ has to be multiplied by 3, $b^{(2)}$ by 9 and $b^{(3)}$ by 27.

w	$10^6 \cdot S(w)$
5	−48.879 979 612 936 267 148 575 174 247 043 686 402 701 421 680 529
4	−33.683 126 435 179 258 367 949 154 667 346 857 343 063 662 040 223
3	−16.197 057 487 106 552 084 835 982 615 789 341 267 879 644 562 145
2	−2.874 931 066 358 404 169 842 007 765 677 311 801 515 635 631 211 6
1	−0.005 037 643 852 252 104 613 165 864 641 040 152 093 341 435 216 537 2
-2	87 595.552 909 179 124 483 795 447 421 262 990 627 388 017 406 822
-3	17 853.256 793 175 269 493 347 991 077 950 813 245 133 374 820 922
-4	6637.593 110 037 931 650 951 894 178 458 603 722 595 701 766 465 0
-5	3384.186 761 682 513 227 965 148 628 942 508 807 465 013 504 317 6

Table 3.3.: First 50 digits of the Stokes constant $S(w)$ for the multiedge DSE in $D = 6$, from the asymptotics eq. (3.50).

In the ansatz eq. (3.48), the solution with smallest absolute λ is dominant, this is the first entry of the vectors eq. (3.55). Including order $1/n^3$, the large-order growth of c_n in eq. (3.50) is determined entirely by the first component of the vectors eq. (3.55). We have confirmed this behaviour numerically from the first 500 coefficients c_n for $w \in \{-5, \dots, +5\}$. The Stokes constant $S(w)$ is reported in table 3.3, we reproduce the value [458, (15)] which was obtained by a similar method as in our case, but only for $w = -2$.

As for $D = 4$ in eq. (3.51), the full non-perturbative solution requires to know $\gamma^{\text{non-pert},k}$, where this time k indicates contributions from all three fundamental solutions eq. (3.55), and there are three independent transseries parameters t_1, t_2, t_3. Moreover, the three non-perturbative solutions "overlap", giving rise to terms $\sim \ln(\alpha)$ in the full transseries solution. A detailed examination of the case $w = -2$ is [244].

3.4.4. Toy model

In the toy model (example 102), the Mellin transform (example 98) is not rational. Unlike the ODEs eqs. (3.43) and (3.54), the equation from theorem 45 is a pseudodifferential equation,

that is, it is of infinite order:

$$\frac{\sin(\pi u)}{\pi u}\Big|_{u\to\gamma(1+w\alpha\partial_\alpha)}\gamma(\alpha) = -\alpha. \tag{3.56}$$

Inserting a non-perturbative ansatz (eq. (3.48)) into eq. (3.56), we do not obtain a polynomial equation, therefore one can not simply read off the parameters of eq. (3.48). Instead, we computed a symbolic perturbative power series solution according eq. (3.44), $\gamma(\alpha) = \sum c_n \alpha^n$, of eq. (3.56). Since eq. (3.56) contains infinitely many derivative operators, a series solution is harder to compute than in the previous cases eqs. (3.43) and (3.54), our result includes order α^{450}. As above, we numerically extracted the asymptotic behaviour of c_j using Richardson extrapolation (def. 59). The result has the form eq. (3.50) for n odd. We find, empirically,

$$\beta(w) = -\frac{2+w}{w}. \tag{3.57}$$

Numerical values of the constants $S(w), b^{(1)}(w)$ and $b^{(2)}(w)$ are given in table 3.4. We did not recognize these numbers as rationals apart from the Stokes constant $S(-2) = 2/\pi$.

w	$S(w)$	$b^{(1)}(w)$	$b^{(2)}(w)$
5	−0.323 584 398 140 310 305 46	33.713 129 682 396 588 961	565.374 787 298 670
4	−0.391 335 083 719 234 905 86	28.505 508 252 042 547 410	405.630 022 359 080
3	−0.488 736 158 026 247 795 99	23.352 717 957 250 113 407	273.573 399 332 400
2	−0.620 736 529 443 448 896 58	18.337 005 501 361 698 274	169.862 094 180 663
1	−0.595 434 011 519 108 439 04	13.869 604 401 089 358 619	98.052 567 522 448 0
-2	0.636 619 772 367 581 343 08	−4.467 401 100 272 339 654 7	7.978 836 295 357 26
-3	0.526 186 295 467 803 784 50	−9.483 113 556 160 754 788 2	40.254 589 493 216 4
-4	0.419 256 495 256 609 057 56	−14.635 903 850 953 188 791	98.974 445 168 262 5
-5	0.343 587 215 470 932 442 58	−19.843 525 281 307 230 343	184.621 956 597 118

Table 3.4.: First digits of the Stokes constant $S(w)$ and subleading corrections of the asymptotic growth eq. (3.50) of the anomalous dimension in the toy model.

Summary of section 3.4.

1. We computed the perturbative anomalous dimension for the multiedge DSE in $D = 4$ to order α^{500} for various w. We derived formulas for their asymptotic growth and first corrections for variable w, and verified them numerically (section 3.4.1).
2. The Stokes constant $S(w)$ can be computed numerically for non-integer w. We recognized that it is a smooth function, oscillating between $w = 0$ and $w = -1$. We gave a tentative heuristic explanation for this observation (section 3.4.2).
3. For the $D = 6$ multiedge DSE, we derived the first coefficients for the asymptotic growth as a function of w and verified them numerically (section 3.4.3).
4. For the toy model DSE, we extracted the first growth coefficients numerically (section 3.4.4).

4. Renormalization group and DSEs in non-kinematic renormalization

4.1. Non-kinematic renormalization schemes

Up to this point, we have used the kinematic renormalization scheme (MOM, def. 91) exclusively. MOM has two advantages: Firstly, it allows for a clear physical interpretation of the renormalization process, namely, the redefinition of parameters in terms of their measured values, see section 2.2.1. Secondly, it contains a boundary condition for renormalized Green functions, $G_{\mathcal{R}}(\alpha, L = 0) = 1$, which is particularly helpful in deriving the renormalization group (section 3.2) and in solving Dyson-Schwinger equations, see sections 2.2.5 and 3.3. However, according to def. 97, other renormalization schemes are conceivable. In the present section, we examine how Feynman amplitudes change in a different scheme.

4.1.1. General infinitesimal Feynman rules

A drawback of the MOM scheme is that the counterterms (def. 104) are relatively complicated expressions. Conversely, the idea of the *Minimal Subtraction* is to choose the simplest possible counterterms which are sufficient to make renormalized amplitudes finite.

Definition 108. Assume that the regularized Feynman amplitude is a Laurent series in a regularization parameter ϵ, as it is in dimensional (section 2.3.3) or analytic (section 2.3.2) regularization. In the *Minimal Subtraction scheme* (MS), the renormalization operator $\mathcal{R}$ extracts the pole part from its argument Laurent series,

$$\hat{\mathcal{R}}\left(\sum_{k=-n}^{\infty} \epsilon^k c_k\right) := \sum_{k=-n}^{-1} \epsilon^k c_k.$$

In *modified Minimal Subtraction* (MS-bar, $\overline{\text{MS}}$), those parts of the $n = 0$ summand, which are powers of $\ln(4\pi)$ or γ_E, are extracted, too. The presence and precise form of such factors depends on the theory in question. To distinguish from MOM, we will denote the quantities in MS with a hat – $\hat{G}, \hat{Z}$, and quantities in MS-bar with a bar – $\bar{G}, \bar{Z}$.

Unlike with MOM, a MS-renormalized amplitude does not satisfy any particular pre-defined boundary condition at $\epsilon = 0$, apart from being finite. We stress that Minimal Subtraction is not the same as dimensional regularization (section 2.3.3), even if the two are often used in conjunction. For example (see section 4.2.2), one can perfectly use dimensional regularization, but with kinematic renormalization conditions instead of Minimal Subtraction.

We write $\mathcal{R}'$ for an arbitrary renormalization scheme (def. 97), while $\hat{\mathcal{R}}$ and $\bar{\mathcal{R}}$ indicate MS and MS-bar (def. 108), and $\mathcal{R}$ is reserved for kinematic renormalization at $L = 0$ (def. 91).

Acting on a Laurent series, the kinematic renormalization operator $\mathcal{R}$ amounts to a subtraction of *all* orders at $L = 0$, not only the pole terms as in def. 108:

$$\mathcal{R}\left(\sum_{k=-n}^{\infty} \epsilon^k c_k\right) = \sum_{k=-n}^{\infty} \epsilon^k c_k.$$

In this notation, the fact that we subtract at $L = 0$ is not visible explicitly, compare section 4.2.2.

Example 107: Second chain graph in MS.

In example 92 we computed the amplitude of the second chain graph in MOM for $D = 6 - 2\epsilon$. Now we repeat the computation in MS, where we skip powers of the coupling constant $\lambda_3^2/(4\pi)^2$. The reference scale s_0 in $L = \ln \frac{s}{s_0}$ (def. 99) does not have any specific significance for the renormalized Green function. The renormalized 1-loop multiedge (example 86) in MS is

$$\mathcal{F}_{\hat{\mathcal{R}}}[\gamma] = \frac{1}{6}L + \left(-\frac{4}{9} + \frac{\gamma_E}{6}\right).$$

In MOM, the operator $\mathcal{R}$ (def. 91) can be concatenated and multiplied without restrictions, this is not true for $\hat{\mathcal{R}}$ in MS. Namely, in MS, the twisted antipode (def. 89) is

$$S^{\mathcal{F}}_{\hat{\mathcal{R}}}[S_1] = -\hat{\mathcal{R}}\left[\mathcal{F}[S_1]\right] - \hat{\mathcal{R}}\big(\hat{\mathcal{R}}\big(\mathcal{F}[\gamma_2]\big) \cdot i \cdot \mathcal{F}[\gamma]\big) \neq \hat{\mathcal{R}}\Big(- \mathcal{F}[S_1] + \mathcal{F}[\gamma_2] \cdot i \cdot \mathcal{F}[\gamma]\Big).$$

For S_1, we obtain the following counterterm and renormalized amplitude:

$$\begin{aligned} S^{\mathcal{F}}_{\hat{\mathcal{R}}}[S_1] &= \left(\frac{1}{72\epsilon^2} - \frac{11}{432\epsilon}\right) i \\ \mathcal{F}_{\hat{\mathcal{R}}}[S_1] &= \frac{1}{72} i L^2 - \left(\frac{1}{8} - \frac{\gamma_E}{36}\right) iL + \left(\frac{791}{2592} - \frac{\gamma_E}{8} + \frac{\gamma_E^2}{72}\right) i. \end{aligned}$$

Now consider the full graph S. Again, $S^{\mathcal{F}}_{\hat{\mathcal{R}}}$ is computed recursively using def. 89.

$$\begin{aligned} S^{\mathcal{F}}_{\hat{\mathcal{R}}}[\gamma i \gamma] &= -\hat{\mathcal{R}}\big(\mathcal{F}[\gamma] \cdot i \cdot \mathcal{F}[\gamma]\big) + 2\hat{\mathcal{R}}\big(\hat{\mathcal{R}}\big(\mathcal{F}[\gamma]\big) \cdot i \cdot \mathcal{F}[\gamma]\big) \overset{2.39}{=} \hat{\mathcal{R}}\big(\mathcal{F}[\gamma]\big) \cdot i \cdot \hat{\mathcal{R}}\big(\mathcal{F}[\gamma]\big) \\ S^{\mathcal{F}}_{\hat{\mathcal{R}}}[S] &= -\hat{\mathcal{R}}\Big(\mathcal{F}[S] - \hat{\mathcal{R}}\left(\mathcal{F}[\gamma_i]\right) \cdot i \cdot \mathcal{F}[S_i] + \hat{\mathcal{R}}\big(\mathcal{F}[\gamma]\big) \cdot i \cdot \hat{\mathcal{R}}\big(\mathcal{F}[\gamma]\big) \cdot i \cdot \mathcal{F}[\gamma]\Big) \\ &= -\frac{1}{648\epsilon^3} + \frac{11}{3888\epsilon^2} + \frac{13}{23328\epsilon} \\ \mathcal{F}_{\hat{\mathcal{R}}}[S] &= \mathcal{F}[S] + S^{\mathcal{F}}_{\hat{\mathcal{R}}}[S] + 2S^{\mathcal{F}}_{\hat{\mathcal{R}}}[\gamma_i]\mathcal{F}[S_i] + S^{\mathcal{F}}_{\hat{\mathcal{R}}}[\gamma_1\gamma_2]\mathcal{F}[\gamma] \\ &= -\frac{1}{648}L^3 + \left(\frac{1}{48} - \frac{\gamma_E}{216}\right)L^2 + \left(-\frac{389}{3888} + \frac{\gamma_E}{24} - \frac{\gamma_E^2}{216}\right)L \\ &\quad + \frac{24155}{139968} - \frac{389\gamma_E}{3888} + \frac{\gamma_E^2}{48} - \frac{\gamma_E^3}{648} + \frac{\zeta(3)}{324}. \end{aligned}$$

Comparing with MOM (example 92), not only does the renormalized amplitude in MS contain a constant term independent of L, but also the coefficients of the non-constant terms are significantly more complicated. On the other hand, the counterterms in MS are very simple rational functions. Observe further that for each graph, the highest coefficient in L agrees between MS and MOM, as we will proof in theorem 56.

By def. 100, the Feynman rules $\mathcal{F}_{\mathcal{R}}$ in MOM are the exponential of the infinitesimal Feynman rule σ. The exponential formula relies on the condition $\mathcal{F}_{\mathcal{R}}|_{L=0} = \tilde{\mathbb{1}}\mathbb{1}$. To extend the procedure to non-kinematic schemes, we need to extract the amplitude at $L = 0$.

Definition 109. Let $\mathcal{R}'$ denote any renormalization scheme (def. 97). Let $s_0 \in \mathbb{R}$ be the reference scale (def. 99). The operator $\tau : H_F \to \mathbb{R}$ extracts the value at s_0,

$$\tau[\Gamma] := \mathcal{F}_{\mathcal{R}'}[\Gamma]\Big|_{s=s_0} = \mathcal{R} \circ \mathcal{F}_{\mathcal{R}'}[\Gamma], \qquad \tau[\mathbb{1}] = 1.$$

Here, $\mathcal{R}$ is the kinematic renormalization operator (def. 91).

In MOM with renormalization point s_0, we have $\tau = \tilde{\mathbb{1}} \circ \mathbb{1}$, as a MOM-renormalized amplitude vanishes at $L = 0$ for any graph except the empty graph. τ is an evaluation of $\mathcal{F}_{\mathcal{R}'}$ at the specific point, therefore, by eq. (2.38), it constitutes a character (def. 74):

$$\tau\big[\gamma_1 \cdot \gamma_2\big] = \mathcal{F}_{\mathcal{R}'}[\gamma_1 \cdot \gamma_2]\Big|_{s=s_0} = \left(\mathcal{F}_{\mathcal{R}'}[\gamma_1] \cdot \mathcal{F}_{\mathcal{R}'}[\gamma_2]\right)\Big|_{s=s_0} = \tau[\gamma_1] \cdot \tau[\gamma_2]. \tag{4.1}$$

Theorem 48 (Compare [271, 298])**.** Let $L = \ln \frac{s}{s_0}$ and $\sigma = \partial_L \mathcal{F}_{\mathcal{R}}|_{L=0}$ (def. 100), where $\mathcal{F}_{\mathcal{R}}$ is renormalized in MOM with renormalization point $L = 0$. Let $\mathcal{R}'$ be an arbitrary renormalization scheme (def. 97) with the corresponding operator τ (def. 109). The renormalized Feynman rules in $\mathcal{R}'$ are given by

$$\mathcal{F}_{\mathcal{R}'}[\Gamma](L) = \Big(\mathcal{F}_{\mathcal{R}'}(0) \star \mathcal{F}_{\mathcal{R}}(L)\Big)\Gamma = \Big(\tau \star \exp^{\star}(L\sigma)\Big)\Gamma.$$

Proof. Let $\mathcal{R}$ be the evaluation of the amplitude at s_0 (def. 91). By construction, a counterterm $S^{\mathcal{F}}_{\mathcal{R}'}$ (eq. (3.23)) does not depend on momenta (i.e. it is local), this implies $\mathcal{R}(S^{\mathcal{F}}_{\mathcal{R}'}) = S^{\mathcal{F}}_{\mathcal{R}'}$. Use def. 88 and def. 109:

$$\begin{aligned}\mathcal{F}_{\mathcal{R}'} &= S^{\mathcal{F}}_{\mathcal{R}'} \star \mathcal{F} = \left(\mathcal{R} \circ S^{\mathcal{F}}_{\mathcal{R}'}\right) \star \mathcal{F} = \left(\mathcal{R} \circ S^{\mathcal{F}}_{\mathcal{R}'}\right) \star (\mathcal{R} \circ \mathcal{F}) \star (\mathcal{R} \circ \mathcal{F})^{-1} \star \mathcal{F} \\ &= \left(\mathcal{R} \circ \left(S^{\mathcal{F}}_{\mathcal{R}'} \star \mathcal{F}\right)\right) \star S^{\mathcal{F}}_{\mathcal{R}} \star \mathcal{F} = \mathcal{R}\left(\mathcal{F}_{\mathcal{R}'}\right) \star \mathcal{F}_{\mathcal{R}} = \tau \star \mathcal{F}_{\mathcal{R}}.\end{aligned}$$

Here, $\mathcal{F}_{\mathcal{R}}$ are the Feynman rules in kinematic renormalization (def. 100), with renormalization point s_0 as used by $\mathcal{R}$. □

Owing to the Rota-Baxter equation (eq. (2.39)) in def. 97, renormalized Feynman rules, regardless of the scheme, are multiplicative with respect to disjoint unions (eq. (2.38)),

$$\mathcal{F}_{\mathcal{R}'}[\Gamma_1 \cdot \Gamma_2](L) = m\left(\tau \otimes e^{\star L\sigma}\right)\Delta(\Gamma_1)\Delta(\Gamma_2) = \mathcal{F}_{\mathcal{R}'}[\Gamma_1](L) \cdot \mathcal{F}_{\mathcal{R}'}[\Gamma_2](L). \tag{4.2}$$

Example 108: Second chain graph in MS, exponential formula.

In example 107, we computed

$$\tau[\gamma] = \mathcal{F}_{\hat{\mathcal{R}}}[\gamma]\Big|_{s=s_0} = -\frac{4}{9} + \frac{\gamma_E}{6}, \qquad \tau[S_i] = \left(\frac{791}{2592} - \frac{\gamma_E}{8} + \frac{\gamma_E^2}{72}\right) i$$
$$\tau[S] = \frac{24155}{139968} - \frac{389\gamma_E}{3888} + \frac{\gamma_E^2}{48} - \frac{\gamma_E^3}{648} + \frac{\zeta(3)}{324}.$$

The MOM-coefficients are known from example 92,

$$\sigma[\gamma] = \frac{1}{6}, \qquad \sigma[S_i] = -\frac{11}{216}i, \qquad \sigma[S] = -\frac{85}{3888}.$$

The summands of theorem 48 are:

$$\begin{aligned}
\left(\tau \star \tilde{\mathbb{1}}\right) S = \tau[S] &= \frac{24155}{139968} - \frac{389\gamma_E}{3888} + \frac{\gamma_E^2}{48} - \frac{\gamma_E^3}{648} + \frac{\zeta(3)}{324} \\
(\tau \star L\sigma)S &= \bar{L}\Big(\tau[S]\underbrace{\sigma[\mathbb{1}]}_{=0} + \underbrace{\tau[\mathbb{1}]}_{=1}\sigma[S] + 2\tau[\gamma]\sigma[S_i] + \underbrace{\tau[\gamma\gamma]}_{=\tau[\gamma]^2}\sigma[\gamma]\Big) \\
&= L\left(-\frac{85}{3888} + 2\left(-\frac{4}{9} + \frac{\gamma_E}{6}\right) i\left(-\frac{11}{216}i\right) + \left(-\frac{4}{9} + \frac{\gamma_E}{6}\right)^2 i^2 \frac{1}{6}\right) \\
&= \left(-\frac{389}{3888} + \frac{\gamma_E}{24} - \frac{\gamma_E^2}{216}\right) L
\end{aligned}$$

$$\left(\tau \star \frac{1}{2} L\sigma \star L\sigma\right) S = \frac{L^2}{2}\Big(2\tau[\gamma]\cdot\sigma[\gamma]\cdot\sigma[\gamma] + 2\sigma[\gamma]\cdot\sigma[S_i]\Big) = \left(\frac{1}{48} - \frac{\gamma_E}{216}\right) L^2$$
$$\left(\tau \star \frac{1}{6}\left(L\sigma\right)^{\star 3}\right) S = -\frac{1}{648} L^3.$$

These are the correct coefficients of $\mathcal{F}_{\hat{\mathcal{R}}}[S]$ as computed in example 107.

4.1.2. Renormalization group functions at the physical dimension

In section 3.2, we discussed the renormalization group in MOM. We found that the renormalization group functions β, γ (defs. 103 and 106) in kinematic renormalization simultaneously enjoy the following properties:

1. They are the L-derivative of $G_{\mathcal{R}}$ or $\mathcal{Q}_{\mathcal{R}}$ at $L = 0$ (def. 103).
2. They are the coefficients in the Callan-Symanzik equation (theorem 43).
3. If Q (def. 92) is a monomial in the functions $\Gamma^{(j)}$, then an equivalent relation (theorem 43) holds between β and the corresponding $\gamma^{(j)}$.
4. The beta function is the derivative of the renormalized coupling $\alpha(\alpha_0)$ with respect to the reference scale s_0 at fixed α_0 (def. 106).
5. The Z-factors are integrals of the renormalization group functions, or β and γ are derivatives of the Z-factors (eqs. (3.29) and (3.30)).

In deriving these properties in section 3.2, we repeatedly used the kinematic renormalization condition $G_{\mathcal{R}}(L=0)=1$. In non-kinematic renormalization schemes, all points except the first one are still satisfied by one set of functions β, γ (which are, however, different functions than in MOM). Only the first point is exclusive to MOM. In a concrete renormalization scheme, one will typically be able to compute the Z-factors unequivocally, therefore we take the last point as a definition:

Definition 110. In dimensional regularization, and for all renormalization schemes (def. 97), the ϵ-dependent renormalization group functions are defined as derivatives of the counterterms Z' (eq. (3.23)):

$$\begin{aligned}\beta'(\alpha,\epsilon) &:= \frac{-\epsilon}{\partial_\alpha \ln\left(\alpha \cdot Z'_\alpha(\alpha,\epsilon)\right)} + \alpha\epsilon \\ \gamma'^{(n)}(\alpha,\epsilon) &:= -\left(\beta'(\alpha,\epsilon) - \alpha\epsilon\right)\partial_\alpha \ln Z'^{(n)}(\alpha,\epsilon)\end{aligned}$$

For kinematic renormalization, this definition coincides with the earlier defs. 103 and 106.

Theorem 49. Let the functions β', γ' be defined as in def. 110. Then:

1. $Z'_\alpha(\alpha,\epsilon) = \exp\left(-\int_0^\alpha \frac{\mathrm{d}u}{u}\frac{\beta'(u,\epsilon)}{\beta'(u,\epsilon)-u\epsilon}\right)$,
2. $Z'_\phi(\alpha,\epsilon) = \exp\left(-\int_0^\alpha \mathrm{d}u\,\frac{\gamma'^{(2)}(u,\epsilon)}{\beta'(u,\epsilon)-u\epsilon}\right)$,
3. $Z'_\alpha(\alpha,\epsilon) = \left(Z'_\phi(\alpha,\epsilon)\right)^w$ if and only if $\beta'(\alpha,\epsilon) = w\alpha\gamma'^{(2)}(\alpha,\epsilon)$.

Proof. These are eqs. (3.29) and (3.30) and theorem 43. They follow from def. 110 upon solving for the Z-factors as shown in section 3.2.2. □

What remains to be shown is that the so-defined renormalization group functions satisfy the Callan-Symanzik equation (theorem 39).

In kinematic renormalization, $\mathcal{F}_{\mathcal{R}}$ is multiplicative under $\star$ with respect to scale, see lemma 37. In an arbitrary renormalization scheme, the latter equation is modified:

$$\begin{aligned}\mathcal{F}_{\mathcal{R}'}[\Gamma]\left(L_1+L_2\right) &= \left(\tau \star e^{\star L_1\sigma} \star e^{\star L_2\sigma}\right)\Gamma = \left(\mathcal{F}_{\mathcal{R}'}\Big|_{L_1} \star \mathcal{F}_{\mathcal{R}}\Big|_{L_2}\right)\Gamma \\ &\neq \left(\mathcal{F}_{\mathcal{R}'}\Big|_{L_1} \star \mathcal{F}_{\mathcal{R}'}\Big|_{L_2}\right)\Gamma.\end{aligned} \tag{4.3}$$

In terms of analytic Green functions, eq. (4.3) becomes the following lemma.

Lemma 50. Let Γ be the solution of a combinatorial DSE (eq. (2.28)) and $G_{\mathcal{R}'}(\alpha, L) = (\tau \star e^{\star L})\Gamma(\alpha)$ the renormalized analytic Green function according to theorem 48. Let $\tilde{\alpha}(\alpha) := \alpha\tau[Q(\alpha)] = \alpha\mathcal{Q}_{\mathcal{R}'}(\alpha, 0)$, then

$$G_{\mathcal{R}'}(\alpha, L) = G_{\mathcal{R}'}(\alpha, 0) \cdot G_{\mathcal{R}}(\tilde{\alpha}(\alpha), L).$$

Here, $G_{\mathcal{R}}$ is the renormalized Green function in MOM (def. 91).

Proof. The coproduct of Γ is given by theorem 24. Upon identification $e^{\star L\sigma} = \mathcal{F}_{\mathcal{R}}$ (def. 100), we find

$$\begin{aligned}\mathcal{F}_{\mathcal{R}'}[\Gamma](L) &= m(\tau \otimes \mathcal{F}_{\mathcal{R}}(L))\Delta(\Gamma) = \sum_{j=0}^{\infty} \tau\left[\Gamma\alpha^j Q^j\right] \cdot \mathcal{F}_{\mathcal{R}}[\Gamma_j](L) \\ &= \tau[\Gamma] \cdot \mathcal{F}_{\mathcal{R}}[\Gamma](L)\Big|_{\alpha\to\alpha\tau[Q]}.\end{aligned}$$

We have used eq. (4.1). By def. 109, the first factor is $G_{\hat{\mathcal{R}}}(\alpha, 0)$. □

By lemma 50, the non-kinematic Green function obtains an overall prefactor $G_{\mathcal{R}'}(\alpha, 0) =: \gamma_0'(\alpha)$. Qualitatively, the behaviour is indicated in fig. 4.1.

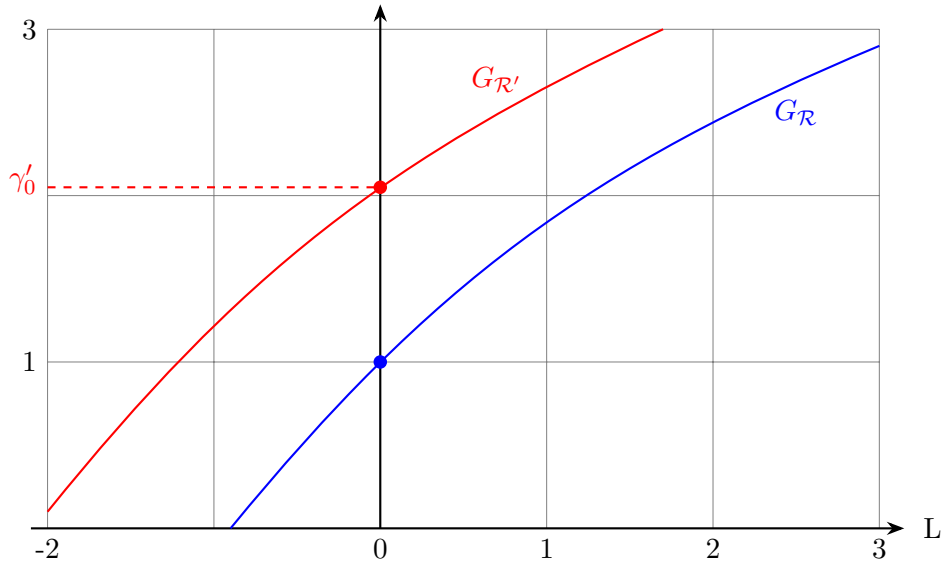

Figure 4.1.: A hypothetical Green function in MOM with renormalization point $L = 0$ (blue) and in a different scheme (red). Both curves are sketched for the same arbitrary, but fixed, value of the coupling. The value $\gamma_0' = \tau[G] = G_{\mathcal{R}'}(0)$ is indicated in red. By lemma 50, the Green functions are not merely multiples of each other, so $G_{\mathcal{R}'} \neq \gamma_0' \cdot G_{\mathcal{R}}$, because the coupling α is transformed, too.

Theorem 51. Let Γ be the solution of a combinatorial DSE (eq. (2.28)) and $G_{\mathcal{R}'}(\alpha, L) = (\tau \star e^{\star L})\Gamma(\alpha)$ the renormalized analytic Green function according to theorem 48. Then, for $\epsilon = 0$, the Callan-Symanzik equation (theorem 39) holds,

$$\frac{\partial}{\partial L} G_{\mathcal{R}'}(\alpha, L) = \left(\gamma'(\alpha) + \beta'(\alpha)\frac{\partial}{\partial \alpha}\right) G_{\mathcal{R}'}(\alpha, L),$$

where

$$\tilde{\alpha}(\alpha) := \alpha\tau[Q(\alpha)] = \alpha \mathcal{Q}_{\mathcal{R}'}(\alpha, 0), \qquad \gamma_0'(\alpha) := \tau[G(\alpha)] = G_{\mathcal{R}'}(\alpha, 0),$$
$$\beta'(\alpha) = \frac{\beta(\tilde{\alpha}(\alpha))}{\frac{\partial \tilde{\alpha}(\alpha)}{\partial \alpha}} \qquad \gamma'(\alpha) = \gamma(\tilde{\alpha}(\alpha)) - \frac{\beta'(\alpha)}{\gamma_0'(\alpha)}\frac{\partial \gamma_0'(\alpha)}{\partial \alpha}.$$

Proof. One can obtain the general Callan-Symanzik equation by repeating the steps of section 3.2, but using the renormalized Feynman rules theorem 48. Lemma 50 then takes the place of lemma 38.

Firstly, we derive lemma 50 with respect to α:

$$\frac{\partial}{\partial \alpha} G_{\mathcal{R}'}(\alpha, L) = \frac{\partial}{\partial \alpha}\gamma_0'(\alpha) \cdot G_{\mathcal{R}}(\tilde{\alpha}, L) + \gamma_0'(\alpha)\frac{\partial}{\partial \alpha}\tilde{\alpha}(\alpha) \cdot \frac{\partial}{\partial \tilde{\alpha}} G_{\mathcal{R}}(\tilde{\alpha}, L).$$

We want to make a connection with the MOM Green function $G_{\mathcal{R}}(\alpha, L)$, which satisfies the Callan-Symanzik equation (theorem 39). Write this equation with the variable $\tilde{\alpha}$ instead of α:

$$\frac{\partial}{\partial \tilde{\alpha}} G_{\mathcal{R}}(\tilde{\alpha}, L) = \frac{1}{\beta(\tilde{\alpha})}\frac{\partial}{\partial L} G_{\mathcal{R}}(\tilde{\alpha}, L) - \frac{\gamma(\tilde{\alpha})}{\beta(\tilde{\alpha})} G_{\mathcal{R}}(\tilde{\alpha}, L).$$

Insert this above:

$$\begin{aligned}\frac{\partial}{\partial \alpha} G_{\mathcal{R}'}(\alpha, L) &= \frac{\partial}{\partial \alpha}\gamma_0'(\alpha) \cdot G_{\mathcal{R}}(\tilde{\alpha}, L) + \frac{\gamma_0'(\alpha)}{\beta(\tilde{\alpha})} \cdot \frac{\partial \tilde{\alpha}(\alpha)}{\partial \alpha}\left(\frac{\partial}{\partial L} G_{\mathcal{R}}(\tilde{\alpha}, L) - \gamma(\tilde{\alpha}) G_{\mathcal{R}}(\tilde{\alpha}, L)\right) \\ &= \left(\frac{\partial \gamma_0'(\alpha)}{\partial \alpha} - \gamma(\tilde{\alpha})\frac{\gamma_0'(\alpha)}{\beta(\tilde{\alpha})}\frac{\partial \tilde{\alpha}(\alpha)}{\partial \alpha}\right) G_{\mathcal{R}}(\tilde{\alpha}, L) + \frac{\gamma_0'(\alpha)}{\beta(\tilde{\alpha})}\frac{\partial \tilde{\alpha}(\alpha)}{\partial \alpha}\frac{\partial}{\partial L} G_{\mathcal{R}}(\tilde{\alpha}, L).\end{aligned}$$

Owing to lemma 50, the L-derivative of $G_{\mathcal{R}'}$ is expressible in terms of $G_{\mathcal{R}}$:

$$G_{\mathcal{R}}(\tilde{\alpha}, L) = \frac{1}{\gamma_0'(\alpha)} G_{\mathcal{R}'}(\alpha, L), \qquad \frac{\partial}{\partial L} G_{\mathcal{R}}(\tilde{\alpha}, L) = \frac{1}{\gamma_0'(\alpha)} \partial_L G_{\mathcal{R}'}(\alpha, L).$$

Eventually, we find the Callan-Symanzik equation

$$\left(\gamma(\tilde{\alpha})\frac{\partial \tilde{\alpha}(\alpha)}{\partial \alpha} - \frac{\beta(\tilde{\alpha})}{\gamma_0'(\alpha)}\frac{\partial \gamma_0'(\alpha)}{\partial \alpha}\right) G_{\mathcal{R}'}(\alpha, L) + \beta(\tilde{\alpha})\frac{\partial}{\partial \alpha} G_{\mathcal{R}'}(\alpha, L) = \frac{\partial \tilde{\alpha}(\alpha)}{\partial \alpha}\frac{\partial}{\partial L} G_{\mathcal{R}'}(\alpha, L)$$

□

The concrete formulas for β', γ' in theorem 51 are only moderately useful because they require to know the MOM functions β, γ. But these relations allow us to prove the well-definedness of β', γ for $\epsilon = 0$, which would otherwise be unclear from def. 110. Remember that we always redefine the coupling such that the first quantum correction appears in order α^1, compare eq. (3.35).

Lemma 52. Assume that in MOM, the power series (def. 51) $\beta(\alpha)$ and $\gamma(\alpha)$ have non-vanishing terms $\propto \alpha^1$, and no constant terms. Then, to every finite order in perturbation theory, the renormalization group functions β', γ' from theorem 51 have finite series coefficients for $\epsilon \to 0$, and contain no pole terms in α.

Proof. β', γ' are computed from evaluations and derivatives of the renormalized quantities $\mathcal{Q}_{\mathcal{R}'}, G_{\mathcal{R}'}$. The individual factors are therefore finite by def. 97 and theorem 32.

We have to show that the fractions appearing in theorem 51 are not singular. It is

$$\frac{\partial\tilde{\alpha}(\alpha)}{\partial\alpha} = \mathcal{Q}_{\mathcal{R}'}(\alpha, 0) + \alpha \frac{\partial \mathcal{Q}_{\mathcal{R}'}(\alpha, L)}{\partial\alpha}\Big|_{L=0}.$$

The first summand can not vanish in general because it has the structure $\mathcal{Q}_{\mathcal{R}'}(\alpha, L) = 1 + C_0(\alpha) + C_1(\alpha) \cdot L$ where C_1 is, to leading order α^1, given by the periods of the involved graphs (theorem 30). The series $C_0(\alpha)$ starts at order α^1 and depends on the renormalization scheme. It is conceivable that $\mathcal{Q}_{\mathcal{R}'}(\alpha^*, 0) = 0$ for some value $\alpha^* \neq 0$, but in the limit $\alpha \to 0$, we have $\mathcal{Q}_{\mathcal{R}'} \to 1$ at least to finite order in perturbation theory. The denominator of $\beta'(\tilde{\alpha})$ is of order α^0 and β' is a power series without pole terms in α. The same holds for $\gamma'(\tilde{\alpha})$ because, if $\gamma'_0(\alpha) \in \mathcal{O}(\alpha^k)$ then $\partial_\alpha \gamma'_0(\alpha) \in \mathcal{O}(\alpha^{k-1})$ and $\beta \cdot \gamma'_0 \in \mathcal{O}(\alpha^k)$. □

Lemma 53. In the general renormalization scheme $\mathcal{R}'$, the renormalization group functions $\beta'(\alpha), \gamma'(\alpha)$ appearing in theorem 51 are the limit $\epsilon \to 0$ of the functions $\beta'(\alpha, \epsilon), \gamma'(\alpha, \epsilon)$ computed from the counterterms by def. 110.

Proof. Start from eq. (3.27),

$$0 = s_0 \cdot \frac{\mathrm{d}\tilde{\alpha}}{\mathrm{d}s_0} = \frac{\mathrm{d}\tilde{\alpha}}{\mathrm{d}\ln s_0} = \alpha s_0 \frac{\partial\tilde{\alpha}}{\partial\alpha}\frac{\mathrm{d}\ln\alpha}{\mathrm{d}s_0} - \frac{\partial\tilde{\alpha}}{\partial L},$$

and repeat the steps of section 3.2.2. Especially, note how def. 106 already contains the derivative $\frac{\partial\tilde{\alpha}}{\partial\alpha}$, which vanishes in MOM but is present in the beta function of general schemes in theorem 51. □

In its current form, the relationships between β, γ and β', γ' in theorem 51 only hold for $\epsilon = 0$. We will come back to the ϵ-dependence of β', γ' in section 4.3.

4.1.3. Properties of Minimal Subtraction

In this section, we derive two important properties of the Minimal Subtraction scheme.

Theorem 54. In Minimal Subtraction (def. 108), the renormalization group functions (def. 110) do not depend on the regularization parameter ϵ,

$$\hat{\beta}(\alpha,\epsilon) = \hat{\beta}(\alpha), \qquad \hat{\gamma}(\alpha,\epsilon) = \hat{\gamma}(\alpha).$$

Proof. By lemma 53, the renormalization group functions $\hat{\beta},\hat{\gamma}$ appearing in the counterterms of MS are the same ones which appear in the Callan-Symanzik equation. By lemma 52, they are finite for $\epsilon = 0$, therefore, they can not contain pole terms in ϵ. What remains to be shown is that they do not contain positive powers, either.

By def. 108, $\hat{Z}$ contains no positive powers of ϵ. Therefore, using theorem 49,

$$-\frac{\hat{\beta}(\alpha,\epsilon)}{\beta(\alpha,\epsilon)-\alpha\epsilon} = \frac{\hat{\beta}(\alpha,\epsilon)}{\alpha\epsilon}\sum_{k=0}^{\infty}\left(\frac{\hat{\beta}(\alpha,\epsilon)}{\alpha\epsilon}\right)^k \quad \text{must only contain negative powers of } \epsilon.$$

Assume that $\hat{\beta}(\alpha,\epsilon) = \ldots + c\cdot\epsilon$, then the fraction $\hat{\beta}/\epsilon$ contains a summand c which is not of negative order in ϵ. Therefore $\hat{\beta}(\alpha,\epsilon)$ can not contain positive order terms in ϵ. Hence it does not depend on ϵ at all. An analogous argument applies to $\hat{\gamma}(\alpha,\epsilon)$. □

Using the integral representation theorem 49, the counterterms are completely determined by the renormalization group functions $\hat{\beta},\hat{\gamma}$. In MOM, one needs to know the full ϵ-dependence of $\beta(\alpha,\epsilon)$ to compute the counterterm $Z_\alpha(\alpha,\epsilon)$, even to compute only the pole parts of Z_α. In MS, by theorem 54, we only have functions of a single variable α. Consequently, one can reconstruct the counterterm entirely from the renormalization group functions $\hat{\beta},\hat{\gamma}$ at the physical dimension.

We expand Z in orders of the pole term ϵ^{-1}, similarly to the expansion of the Green function in terms of L (eq. (3.2)):

$$\hat{Z}_\alpha(\alpha,\epsilon) =: \sum_{j=0}^{\infty}\hat{z}_j(\alpha)\epsilon^{-j}. \tag{4.4}$$

Theorem 55 (Scattering type formula [271, 311, 392], [81, Sec. 7])**.** Consider a single DSE with $Q = G^w$ (eq. (3.34). In MS, the coefficients of the counterterm eq. (4.4) satisfy $\hat{z}_{j<0} = 0$ and $\hat{z}_0(\alpha) = 1$ and

$$\alpha^2\partial_\alpha\hat{z}_1(\alpha) = \hat{\beta}(\alpha), \qquad \alpha^2\partial_\alpha\hat{z}_{j>1}(\alpha) = \hat{\gamma}(\alpha)\left(1+\hat{\beta}(\alpha)\alpha\partial_\alpha\right)\hat{z}_{j-1}(\alpha).$$

Here, $\hat{\gamma}(\alpha)$ is the anomalous dimension in MS.

Proof. Insert eq. (4.4) into the analogue of the Callan-Symanzik equation for the Z-factor, (eq. (3.28)),

$$\hat{\beta}(\alpha)\hat{Z}_\alpha(\alpha,\epsilon) + \big(\hat{\beta}(\alpha)-\alpha\epsilon\big)\alpha\frac{\partial}{\partial\alpha}\hat{Z}_\alpha(\alpha,\epsilon) = 0. \tag{4.5}$$

The resulting series is

$$\sum_{j=0}^{\infty} \hat{\beta}(\alpha)\hat{z}_j(\alpha)\epsilon^{-j} + \sum_{j=0}^{\infty} \hat{\beta}(\alpha)\alpha\frac{\partial}{\partial\alpha}\hat{z}_j(\alpha)\epsilon^{-j} = \sum_{j=0}^{\infty} \alpha^2\frac{\partial}{\partial\alpha}\hat{z}_{j+1}(\alpha)\epsilon^{-j}.$$

Compare orders in ϵ. By def. 108, $\hat{z}_0 = 1$ and therefore $\partial_\alpha z_0 = 0$. From this, $\alpha^2\partial_\alpha\hat{z}_1 = \hat{\beta}$. □

The second equation in theorem 55 can be integrated term by term with the boundary condition that $[\alpha^n]\hat{z}_j(\alpha) = 0$ whenever $n < j$.

It is instructive to note the duality of MOM and MS renormalization conditions. For concreteness, we assume a DSE of type eq. (3.35) with $Q = G^w$.

- In kinematic renormalization (def. 91), the order L^0 in $G_{\mathcal{R}}(\alpha, \epsilon, L)$ vanishes for all ϵ. This makes the log-expansion eq. (3.2) "simple", it only depends on $\gamma_1(\alpha, \epsilon)$, which is the anomalous dimension. The counterterms are given by theorem 49, which involves the non-trivial dependence of $\gamma(\alpha, \epsilon)$ on ϵ.
- In Minimal Subtraction (def. 108), the anomalous dimension $\hat{\gamma}(\alpha, \epsilon) = \hat{\gamma}(\alpha)$ is independent of ϵ, and the complete counterterm $\hat{Z}(\alpha, \epsilon)$ is determined entirely from $\hat{\gamma}(\alpha)$. This makes renormalization of concrete graphs "simple". Conversely, the renormalized Green function eq. (3.2) now involves a non-trivial function $\hat{\gamma}_0(\alpha, \epsilon) = G_{\hat{\mathcal{R}}}|_{L=0}$.

Further aspects of this dichotomy will be discussed in section 4.4.

4.1.4. Renormalization scheme independent quantities

Having established Minimal Subtraction, we now perform a quick survey of renormalization-scheme independent quantities. To this end, recall that grouplike elements of the Hopf algebra (def. 65) satisfy $\Delta(\Gamma) = \Gamma \otimes \Gamma$. In section 3.2.3, we examined them in kinematic renormalization. From theorem 48, we read off their Feynman amplitude for $\epsilon = 0$ in arbitrary schemes:

$$\mathcal{F}_{\mathcal{R}'}[\Gamma](L) = \mathcal{F}_{\mathcal{R}'}[\Gamma]\Big|_{s=s_0} \cdot \left(\frac{s}{s_0}\right)^{\gamma_1'(\alpha)} =: \gamma_0'(\alpha) \cdot \left(\frac{s}{s_0}\right)^{\gamma_1'(\alpha)}. \tag{4.6}$$

This is a scaling solution just like eq. (3.31), only with a non-trivial prefactor γ_0'. Both γ_0' and γ_1' are functions of the renormalized coupling α.

Theorem 56 (Compare [284, Sec. 4])**.** The following quantities are invariant under change of the renormalization scheme (def. 97):

1. The first coefficient of the anomalous dimension and of the beta function (def. 103) in the limit $\epsilon = 0$.
2. The highest pole in ϵ of the counterterms (def. 104) for every fixed order in α.
3. The coefficient $g_{\mathrm{cor}(\Gamma)}$ of the highest order term in the log expansion theorem 35.
4. The anomalous dimension of a linear DSE (theorem 44) for $\epsilon = 0$.

Proof. 1. The first coefficient is given by 1-loop graphs, which are, in particular, primitive. By theorem 30, the coefficient of their scale-dependence is the period, which is independent of renormalization schemes.

2. By theorem 49, the Z-factor is the exponential of a sum of type $\sum_j \left(\frac{\gamma(\alpha,\epsilon)}{\epsilon}\right)^j$. A term proportional to α^n can arise from $1 \leq j \leq n$ because the anomalous dimension has no constant term, $[\alpha^0]\gamma = 0$. However, j is the order of the pole. Therefore, the highest possible pole arises when $j = n$, and in that case, the numerator is $([\alpha^1]\gamma)^j$, so it is entirely determined by the first coefficient. These coefficients are independent of the renormalization scheme by point 1. A similar argument applies to Z_α and β.

3. The statement is obvious for primitive graphs since the period (def. 96) is independent of renormalization conditions.

The dependence of $\mathcal{F}_{\mathcal{R}'}$ on the renormalization scheme, by theorem 48, is entirely encoded in the operator τ (def. 109). We therefore have to demonstrate that the highest order coefficient is independent of τ. Apply theorem 48 to a cocycle (def. 87) $\Gamma = B_+(\gamma)$, using the reduced coproduct (def. 64)

$$\begin{aligned}\left(\tau \star e^{\star L\sigma}\right) B_+(\gamma) &= \tau\big[B_+(\gamma)\big] \cdot 1 + m\left(\tau \otimes e^{\star L\sigma} \circ B_+\right)\Delta(\gamma) \\ &= \tau\big[B_+(\gamma)\big] + \tau[\gamma] \cdot e^{\star L\sigma} B_+(\mathbb{1}) + e^{\star L\sigma} B_+(\gamma) + m\left(\tau \otimes e^{\star L\sigma} \circ B_+\right)\Delta_1(\gamma).\end{aligned}$$

Assume that $\mathrm{cor}(\gamma) = n$, then $\mathrm{cor}(B_+^\Gamma(\gamma)) = n+1$ by lemma 20, and $\Delta_1(\gamma)$ contains factors with coradical degree of at most $n-1$. The above sum contains only one summand of order L^{n+1},

$$[L^{n+1}]\left(\tau \star e^{\star L\sigma}\right) B_+(\gamma) = [L^{n+1}] e^{\star L\sigma} B_+(\gamma) = [L^{n+1}]\mathcal{F}_{\mathcal{R}}(\Gamma).$$

The right hand side is independent of τ, so is the left hand side.

4. On an algebraic level, this was remarked in [309, Ex. 5.12]. From theorem 44 we know that $\beta(\alpha) = 0$ in MOM. By theorem 51, $\beta'(\alpha) = 0$ in all schemes. Furthermore, $\mathcal{Q}_{\mathcal{R}'} = 1$ in every renormalization scheme since, regardless of the scheme, we still scale the treelevel graph to unity (def. 97). Hence $\tilde{\alpha} = \alpha$ for $\epsilon = 0$ and the statement follows from theorem 51.

□

Point 4 of theorem 56 fits with lemma 50: If there is no renormalization of the coupling constant, then the only difference between renormalization schemes is a finite overall factor $G_{\mathcal{R}'}(\alpha, 0) = \gamma_0'(\alpha)$. Point 1. in theorem 56 actually holds for the second order coefficients as well, see theorem 63.

Summary of section 4.1.

1. The renormalized Feynman rules in any renormalization scheme can be expressed by a variant of the exponential formula, $\mathcal{F}_{\mathcal{R}'} = \tau \star e^{\star L\sigma}$, where σ are the infinitesimal Feynman rules in kinematic renormalization and the operator τ evaluates at $L = 0$ (section 4.1.1).

2. The Callan-Symanzik equation holds for non-kinematic renormalization schemes, and the renormalization group functions are simultaneously derivatives of the counterterms. The only difference of the general case from the MOM case is that in MOM, the renormalization group functions are derivatives of renormalized Green functions with respect to L at the point $L = 0$ (section 4.1.2).

3. The renormalization group functions in MS are independent of ϵ, and the MS-counterterms $\hat{Z}$ can be reconstructed completely from knowing them at $\epsilon = 0$ (section 4.1.3).

4. In all renormalization schemes, the analytic Green function of a linear DSE for $\epsilon = 0$ is a scaling solution with an overall prefactor and an identical anomalous dimension. The first coefficients of various quantities are independent of the renormalization scheme (section 4.1.4).

4.2. Recursively solving a DSE

By now, we have introduced technical details of the renormalization group which might not be entirely obvious from standard textbooks. To convince ourselves of their soundness, it is useful to have a concrete example at hand. Therefore, before we continue with the theoretical development, we discuss, within a particularly accessible setting, how the various quantities can be computed concretely.

4.2.1. Expansion of the kernel of the DSE

We work in dimensional regularization (section 2.3.3), where ϵ is the regularization parameter. Or starting point is a propagator DSE of type eq. (3.38),

$$\begin{aligned} G_{\mathcal{R}}(\alpha, \epsilon, s) &= 1 - \alpha(1-\mathcal{R}) \int \mathrm{d}y \; K(s,y) G_{\mathcal{R}}(\alpha, \epsilon, y)^{1+w} \\ &= Z(\alpha, \epsilon) - \alpha \int \mathrm{d}y \; K(s,y) G_{\mathcal{R}}(\alpha, y)^{1+w}. \end{aligned} \tag{4.7}$$

The integration variable is generally a vector, and α is a rescaled coupling constant. The renormalization scheme $\mathcal{R}$ (def. 97) does not need to be a kinematic one. We have introduced the counterterm $Z(\alpha, \epsilon) := Z^{(2)}(\alpha, \epsilon)$ where α is the renormalized coupling. In our setup, we have $Z_\alpha = Z^w$, and the two different renormalization group functions (def. 106) are related by theorem 49,

$$\beta(\alpha, \epsilon) = w \cdot \alpha \gamma(\alpha, \epsilon). \tag{4.8}$$

It turns out that for an order-by-order solution of eq. (4.7), we need to know the Mellin transform (def. 101) of the kernel graph with arguments $-k\epsilon$, where $k \in \mathbb{N}_0$ is arbitrary. Observe that this quantity depends on ϵ in two different ways: Firstly, the Mellin transform itself is taken at a spacetime dimension $D_0 - 2\epsilon$, and secondly, its argument is $-k\epsilon$. Concretely, we expand each summand of eq. (3.5) in ϵ, and we factor out trivial powers of (4π). For the multiedge (example 103), this expansion reads

$$F(-k\epsilon) =: (4\pi)^{-\frac{D}{2}} e^{-\gamma_E \epsilon} \sum_{n=-1}^{\infty} f_n^{(k)} \epsilon^n. \tag{4.9}$$

Using the Mellin transform from example 96, we find

$$\sum_n f_n^{(k)} \epsilon^n = e^{\gamma_E \epsilon} \frac{\Gamma\left(-\frac{D}{2} + 2 + k\epsilon\right) \Gamma\left(\frac{D}{2} - 1\right) \Gamma\left(\frac{D}{2} - 1 - k\epsilon\right)}{\Gamma\left(1 + k\epsilon\right) \Gamma\left(D - 2 - k\epsilon\right)}.$$

It remains to expand the gamma functions using eq. (2.47). In $D = 4 - 2\epsilon$ dimensions,

$$\begin{aligned} &\Gamma := \frac{\Gamma((k+1)\epsilon)\Gamma(1-(k+1)\epsilon)\Gamma(1-\epsilon)}{\Gamma(1+k\epsilon)\Gamma(2-(k+2)\epsilon)} = \frac{e^{-\gamma_E}}{(k+1)\,(1-(k+2)\epsilon)\,\epsilon} \exp\left(\sum_{m=2}^{\infty} T_m^{(k)} \epsilon^m\right), \\ &\text{where} \qquad T_m^{(k)} := (m-1)!\left((-1)^m (k+1)^m + (k+1)^m + 1 - (-k)^m - (k+2)^m\right) \zeta(m). \end{aligned} \tag{4.10}$$

Expanding the prefactor in a geometric series, we obtain the coefficients of eq. (4.9),

$$f_n^{(k)} = \sum_{t=-1}^{n} \frac{(k+2)^{t+1}}{k+1} \frac{1}{(n-t)!} \sum_{m=0}^{n-t} B_{n-t,m}\left(0, T_2^{(k)}, T_3^{(k)}, \ldots, T_{n-t+1-m}^{(k)}\right). \tag{4.11}$$

Here $B_{n,k}$ are the Bell polynomials (def. 52).

Example 109: Coefficients for the 1-loop multiedge in $D = 4 - 2\epsilon$.

Unlike the Mellin transform at exactly $D = 4$ (example 96), the coefficients of eq. (4.11) do involve zeta values and powers of π^2:

$$f_{-1}^{(0)} = 1 \qquad f_0^{(0)} = 2 \qquad f_1^{(0)} = 4 - \frac{\pi^2}{12} \qquad f_2^{(0)} = 8 - \frac{\pi^2}{6} - \frac{7\zeta(3)}{3}$$
$$f_{-1}^{(1)} = \frac{1}{2} \qquad f_0^{(1)} = \frac{3}{2} \qquad f_1^{(1)} = \frac{9}{2} - \frac{\pi^2}{24} \qquad f_2^{(1)} = \frac{27}{2} - \frac{\pi^2}{8} - \frac{26\zeta(3)}{6}.$$

For $D = 6 - 2\epsilon$ dimensions, we have that

$$\frac{\Gamma\left(-1 + (k+1)\epsilon\right)\Gamma\left(2-\epsilon\right)\Gamma\left(2-(k+1)\epsilon\right)}{\Gamma\left(1+k\epsilon\right)\Gamma\left(4-(k+2)\epsilon\right)} = \frac{\epsilon - 1}{(3-(k+2)\epsilon)(2-(k+2)\epsilon)} \cdot \Gamma.$$

The gamma functions on the right hand side are the same as in $D = 4 - 2\epsilon$, consequently their series expansion is again given by the polynomials $T_m^{(k)}$ from eq. (4.10):

$$f_n^{(k)} = \sum_{t=-1}^{n} \left(-(k+1) + \frac{k}{2^{t+1}} - \frac{k-1}{3^{t+2}}\right) \frac{(k+2)^t}{2(k+1)} \frac{1}{(n-t)!} \sum_{m=0}^{n-t} B_{n-t,m}\left(0, T_2^{(k)}, \ldots, T_{n-t+1-m}^{(k)}\right). \tag{4.12}$$

As a last example, we consider the toy model (example 98):

$$\int_0^\infty \frac{\mathrm{d}y\; y^{-(k+1)\epsilon}}{1+y} = \frac{-\pi}{\sin(\pi(k+1)\epsilon)} = -\Gamma((k+1)\epsilon)\Gamma(1-(k+1)\epsilon) =: \sum_{n=-1}^{\infty} f_n^{(k)} \epsilon^n.$$

The Bernoulli numbers B_n [475] vanish when $n > 1$ is odd, therefore we can write

$$f_n^{(k)} := \frac{-1}{(k+1)} \sum_{m=0}^{n+1} \frac{1}{(n+1)!} B_{n+1,m}\left(0, T_2^{(k)}, \ldots, T_{n+2-m}^{(k)}\right), \qquad T_n^{(k)} := \Big(2\pi(k+1)\Big)^n \frac{|B_n|}{n}. \tag{4.13}$$

Observe that, in order to compute $f_n^{(k)}$, it is irrelevant whether the Mellin transform (example 96) is a simple rational function at $\epsilon = 0$ or not. The "analytic" approach (solving the ODE in theorem 45) is only feasible in practice in very limited cases, whereas our current "brute force" approach is applicable also for more complicated kernels, as long as $f_n^{(k)}$ can be determined with reasonable effort.

4.2.2. Series solution of the DSE

As always, the Green function $G_{\mathcal{R}}(\alpha, \epsilon, L)$ is scaled to its treelevel tensor, consequently, the order-zero solution of eq. (4.7) is

$$G_{\mathcal{R}}^{(0)}\left(\alpha, \epsilon, q^2\right) := 1. \tag{4.14}$$

Inserting this into the right hand side of the DSE (eq. (4.7)), the integral amounts to the Mellin transform (eq. (4.9)) at the argument zero, that is, $F(-k\epsilon)$ with $k = 0$. We will

assume for concreteness that our kernel is the 1-loop multiedge at $D = 4-2\epsilon$, all other cases are qualitatively similar. The correct choice to absorb trivial prefactors is then $\alpha = \lambda(4\pi)^{-2}$, and the order one solution of the DSE is given by the coefficients $f_n^{(0)}$:

$$\begin{aligned} G_{\mathcal{R}}^{(1)}(\alpha,\epsilon,q^2) &= 1-\alpha\,(1-\mathcal{R})\left[(4\pi)^{\epsilon}e^{-\gamma_E\epsilon}\left(\frac{q^2}{s_0}\right)^{-\epsilon}\sum_{r=-1}^{\infty} f_r^{(0)}\epsilon^r\right] \\ &= Z^{(1)}(\alpha,\epsilon) - \alpha(4\pi e^{-\gamma_E})^{\epsilon}\left(\frac{q^2}{s_0}\right)^{-\epsilon}\sum_{r=-1}^{\infty} f_r^{(0)}\epsilon^r. \end{aligned} \tag{4.15}$$

Here, s_0 is an arbitrary reference mass scale introduced for dimensional reasons. We have used that a renormalization operator $\mathcal{R}$ (def. 97) is local, that is, it results in a counterterm summand $Z^{(1)}$ that is independent of $\underline{q}^2$:

$$Z^{(1)}(\alpha,\epsilon) = 1+\alpha(4\pi e^{-\gamma_E})^{\epsilon}\mathcal{R}\left[\sum_{r=-1}^{\infty} f_r^{(0)}\epsilon^r\right].$$

We restrict ourselves to the following family of renormalization operators, which is parametrized by a number $\epsilon_{\max} \in \mathbb{Z}\cup\{\pm\infty\}$. Namely, we assume that the renormalization operator extracts the orders up to $\epsilon_{\max}$ of a given Laurent series $f(\epsilon)$:

$$\mathcal{R}[f(\epsilon)] = \mathcal{R}\left[\sum_{n=-\infty}^{\infty} f_n\epsilon^n\right] := \sum_{n=-\infty}^{\epsilon_{\max}} f_n\epsilon^n. \tag{4.16}$$

Three different options will be relevant to us:

1. If we chose $\epsilon_{\max} = -\infty$, then $\mathcal{R} = 0$ and we compute the unrenormalized Green function.

2. If we chose $\epsilon_{\max} = +\infty$, then $\mathcal{R}$ subtracts the complete function $f(\epsilon)$. Due to the prefactor $(\underline{q}^2/s_0)^{-\epsilon}$ in eq. (4.15), this amounts to kinematic renormalization (def. 91) at the renormalization point s_0.

3. The choice $\epsilon_{\max} = -1$ amounts to Minimal Subtraction (def. 108).

In concrete computations, to obtain the correct solution at $\epsilon = 0$ to order α^n, it is sufficient to chose $\epsilon_{\max} > n$. This is because every step in the iteration multiplies by ϵ^{-1}. For a linear DSE, it is even sufficient to let $\epsilon_{\max} = 1$ to obtain the correct MOM-solution at $\epsilon = 0$.

In order to streamline computations of higher orders, we define the coefficients $g_{t,r}^{(1)}$, which encode both the counterterm and the finite part of $G_{\mathcal{R}}^{(1)}$:

$$g_{1,r}^{(1)} := -f_r^{(0)}, \qquad g_{0,r}^{(1)} := \begin{cases} -g_{1,r}^{(1)} & r \le \epsilon_{\max} \\ 0 & \text{else.} \end{cases}$$

With this notation, the renormalized solution to order one, eq. (4.15), reads

$$G_{\mathcal{R}}^{(1)}(\alpha,\epsilon,q^2) = 1+\alpha\sum_{t=0}^{1}(4\pi e^{-\gamma_E})^{t\epsilon}\left(\frac{q^2}{s_0}\right)^{-t\epsilon}\sum_{r=-1}^{\infty} g_{t,r}^{(1)}\epsilon^r. \tag{4.17}$$

The 1-loop multiedge kernel graph gives rise to a factor $(4\pi e^{-\gamma_E})^{t\epsilon}$, which eventually produces finite contributions $\propto \gamma_E$ and $\propto \ln(4\pi)$. In MS renormalization, these terms are present in the finite part of $\hat{G}_{\mathcal{R}}$ while in MS-bar renormalization they are assigned to the MS-bar-counterterm $\bar{Z}$ and thus absent from $\bar{G}_{\mathcal{R}}$. To facilitate computations, we will absorb them into the momentum variable. In this way, choosing $\epsilon_{\max} = -1$, we obtain the MS-bar Green function of the new momentum variable, but our counterterm will be $\hat{Z}$ in MS, not in MS-bar:

$$\hat{x} := \frac{q^2}{s_0}, \qquad \bar{x} := \frac{e^{\gamma_E} q^2}{4\pi s_0} \equiv \frac{q^2}{\bar{s}_0}, \qquad \hat{G}_{\mathcal{R}}(\hat{x}) \equiv \bar{G}_{\mathcal{R}}(\bar{x}). \tag{4.18}$$

If we chose $\epsilon_{\max} = \infty$, that is, kinematic renormalization, then we can understand the transition $\hat{x} \leftrightarrow \bar{x}$ as a constant rescaling of the renormalization point $s_0 \leftrightarrow 4\pi e^{\gamma_E} s_0 =: \bar{s}_0$. Had we chosen a different kernel, such as the toy model (example 102), then the factor $(4\pi e^{-\gamma_E})$ would be different or not arise at all. In any case, we skip all decorations $\bar{x}, \hat{x}$, knowing that they can always be chosen to absorb superfluous constants. Observe that those constants have already been factored out of $f_n^{(k)}$ in eq. (4.9).

Example 110: Multiedge DSE, first order coefficients.

Consider the DSE of the 1-loop multiedge in $D = 4 - 2\epsilon$ dimensions. At 1-loop order, the solution is independent from the exponent w in the invariant charge eq. (3.34). In MOM renormalization, the coefficients of the solution are

$$\begin{aligned} g^{(1)}_{1,-1} &= -1, & g^{(1)}_{1,0} &= -2 & g^{(1)}_{1,1} &= -4 + \frac{\pi^2}{12} \\ g^{(1)}_{0,-1} &= 1, & g^{(1)}_{0,0} &= 2 & g^{(1)}_{0,1} &= 4 - \frac{\pi^2}{12}. \end{aligned}$$

In MS-bar renormalization, that is, $\epsilon_{\max} = -1$ in eq. (4.16) and $(4\pi e^{-\gamma_E})$ is absorbed as in eq. (4.18), we have

$$\begin{aligned} g^{(1)}_{1,-1} &= -1, & g^{(1)}_{1,0} &= -2 & g^{(1)}_{1,1} &= -4 + \frac{\pi^2}{12} \\ g^{(1)}_{0,-1} &= 1, & g^{(1)}_{0,0} &= 0 & g^{(1)}_{0,1} &= 0. \end{aligned}$$

Even if the only difference between MS-bar and MOM is in the counterterm $g^{(1)}_{0,r}$, this does not imply that the renormalized Green functions are equal.

Higher orders of the renormalized Green function are computed iteratively. Assume we know the order-m-solution in the form

$$G^{(m)}_{\mathcal{R}}(\alpha, \epsilon, x) = 1 + \sum_{n=1}^{m} \alpha^n \sum_{t=0}^{n} x^{-t\epsilon} \sum_{r=-n}^{\infty} g^{(n)}_{t,r} \epsilon^r =: 1 + \sum_{n=1}^{m} \alpha^n G_n(x, \epsilon),$$

where we defined functions $G_n(x, \epsilon)$. The latter do not depend on the order m. Next, we write a generic expansion of the invariant charge eq. (3.34) according to

$$G^{(m)}_{\mathcal{R}}(\alpha, \epsilon, x) \cdot \mathcal{Q}_{\mathcal{R}}(\alpha, \epsilon, x) \equiv \left(G^{(m)}_{\mathcal{R}}(\alpha, \epsilon, x)\right)^{w+1} =: 1 + \sum_{n=1}^{m} \alpha^n \sum_{t=0}^{n} x^{-t\epsilon} h^{(n)}_t(\epsilon). \tag{4.19}$$

The auxiliary functions $h_t^{(n)}(\epsilon)$ are Laurent series in ϵ with the highest pole order ϵ^{-n}. They are given by Faa di Bruno's formula (theorem 18) and the Binomial theorem, $B_{n,k}$ are Bell polynomials (def. 52):

$$\begin{aligned}\frac{1}{\left(G_{\mathcal{R}}^{(m)}(x)\right)^{-w-1}} &= \frac{1}{(-w-2)!}\sum_{n=0}^{\infty}\alpha^n\frac{1}{n!}\sum_{k=1}^{n}(-s-2+k)!B_{n,k}\left(1!G_1, 2!G_2, \ldots\right), \quad w<-1\\ \left(G_{\mathcal{R}}^{(m)}(x)\right)^{w+1} &= (w+1)!\sum_{n=0}^{\infty}\alpha^n\frac{1}{n!}\sum_{k=0}^{s+1}\frac{1}{(w+1-k)!}B_{n,k}\left(1!G_1, 2!G_2, \ldots\right), \quad w>-1.\end{aligned} \tag{4.20}$$

Knowing the functions $h_t^{(n)}(\epsilon)$, we integrate the sum eq. (4.19) term-wise. Each summand corresponds to a Mellin transform $F(-t\epsilon)$ in eq. (4.9), solving the integral amounts to multiplication with a suitable series $\sum_n f_n^{(t)}\epsilon^n$. Symbolically, the result is

$$g_{1,r}^{(1)} = -f_r^{(0)}, \qquad \bar{g}_{t,r}^{(n)} = -\sum_{u=-1}^{n+r-1}\left([\epsilon^{r-u}]\bar{h}_{t-1}^{(n-1)}\right)f_u^{(t-1)}, \qquad t\geq 1.$$

The overall minus sign is the $(-\alpha)$ in eq. (4.7). With these new coefficients, the next order solution of the DSE is

$$G_{\mathcal{R}}^{(m+1)}(\alpha,\epsilon,x) = G_{\mathcal{R}}^{(1)}(\alpha,\epsilon,x) + (1-\mathcal{R})\sum_{n=2}^{m+1}\alpha^n\sum_{t=1}^{n}x^{-t\epsilon}\sum_{r=-n}^{\infty}g_{t,r}^{(n+1)}\epsilon^r. \tag{4.21}$$

To renormalize, we compute the counterterm $Z^{(m+1)}(\alpha,\epsilon)$ according to eq. (4.16),

$$\begin{aligned}g_{0,r}^{(n)} &:= \begin{cases}-\sum_{t=1}^{n}g_{t,r}^{(n)}, & r\leq\epsilon_{\max}\\ 0, & \text{else,}\end{cases}\\ Z^{(m+1)}(\alpha,\epsilon) &= 1+\sum_{n=1}^{m+1}\alpha^n\sum_{r=-n}^{\infty}g_{0,r}^{(n)}\epsilon^r = 1+\sum_{n=1}^{m+1}\alpha^n\sum_{r=-n}^{\epsilon_{\max}}g_{0,r}^{(n)}\epsilon^r.\end{aligned}$$

As explained above eq. (4.18), if we use $\epsilon_{\max}=-1$, the quantity Z represents the MS (not MS-bar) counterterm, even though $G_{\mathcal{R}}$ in that case is the MS-bar renormalized Green function. In any case, the renormalized Green function to order $m+1$ reads

$$\begin{aligned}G_{\mathcal{R}}^{(m+1)}(\alpha,\epsilon,x) &= \sum_{n=1}^{m+1}\alpha^n\sum_{u=0}^{n}x^{-u\epsilon}\sum_{r=-n}^{\infty}g_{u,r}^{(n)}\epsilon^r\\ &= Z^{(m+1)}(\alpha,\epsilon)+\sum_{n=1}^{m+1}\alpha^n\sum_{t=1}^{n}x^{-t\epsilon}\sum_{r=-n}^{\infty}g_{t,r}^{(n)}\epsilon^r.\end{aligned} \tag{4.22}$$

Algebraically, our algorithm of solving the DSE can be understood as iterated matrix products, compare [476].

Example 111: Multiedge linear DSE in MOM, coefficients.

Consider the linear DSE, $w = 0$, of the 1-loop multiedge in $D = 4 - 2\epsilon$ dimensions and MOM renormalization. The 1-order solution is example 110. At two loops, the coefficients $g^{(1)}_{2,j}$ appear for the first time:

$$\begin{aligned}
g^{(2)}_{2,-2} &= \frac{1}{2} & g^{(2)}_{2,-1} &= \frac{5}{2}, & g^{(2)}_{2,0} &= \frac{19}{2} - \frac{\pi^2}{12} & g^{(2)}_{2,1} &= \frac{65}{2} - \frac{5\pi^2}{12} - \frac{16\zeta(3)}{3} \\
g^{(2)}_{1,-2} &= -1 & g^{(2)}_{1,-1} &= -4, & g^{(2)}_{1,0} &= -12 + \frac{\pi^2}{6} & g^{(2)}_{1,1} &= -32 + \frac{2\pi^2}{3} + \frac{14\zeta(3)}{3} \\
g^{(2)}_{0,-2} &= \frac{1}{2} & g^{(2)}_{0,-1} &= \frac{3}{2}, & g^{(2)}_{0,0} &= \frac{5}{2} - \frac{\pi^2}{12} & g^{(2)}_{0,1} &= -\frac{1}{2} - \frac{\pi^2}{4} + \frac{2\zeta(3)}{3}.
\end{aligned}$$

Example 112: Multiedge nonlinear DSE in MOM, coefficients.

Consider the same situation as in example 111, but this time a non-linear DSE with $w = 3$. The order one solution stays the same, but at two loops we find

$$\begin{aligned}
g^{(2)}_{2,-2} &= 2 & g^{(2)}_{1,-1} &= 10, & g^{(2)}_{2,0} &= 38 - \frac{\pi^2}{3} & g^{(2)}_{2,1} &= 130 - \frac{5\pi^2}{3} - \frac{64\zeta(3)}{3} \\
g^{(2)}_{1,-2} &= -4 & g^{(2)}_{1,-1} &= -16, & g^{(2)}_{1,0} &= -48 + \frac{2\pi^2}{3} & g^{(2)}_{1,1} &= -128 + \frac{8\pi^2}{3} + \frac{56\zeta(3)}{3} \\
g^{(2)}_{0,-2} &= 2 & g^{(2)}_{0,-1} &= 6, & g^{(2)}_{0,0} &= 10 - \frac{\pi^2}{3} & g^{(2)}_{0,1} &= -2 - \pi^2 + \frac{8\zeta(3)}{3}.
\end{aligned}$$

Example 113: Multiedge nonlinear DSE in MS, coefficients.

Consider the same DSE with $w = 3$, but this time in MS-bar renormalization, as introduced in example 110. The coefficients of the second order solution are

$$\begin{aligned}
g^{(2)}_{2,-2} &= 2 & g^{(2)}_{1,-1} &= 10, & g^{(2)}_{2,0} &= 38 - \frac{\pi^2}{3} & g^{(2)}_{2,1} &= 130 - \frac{5\pi^2}{3} - \frac{64\zeta(3)}{3} \\
g^{(2)}_{1,-2} &= -4 & g^{(2)}_{1,-1} &= -8, & g^{(2)}_{1,0} &= -16 + \frac{\pi^2}{3} & g^{(2)}_{1,1} &= -32 + \frac{2\pi^2}{3} + \frac{28\zeta(3)}{3} \\
g^{(2)}_{0,-2} &= 2 & g^{(2)}_{0,-1} &= -2, & g^{(2)}_{0,0} &= 0 & g^{(2)}_{0,1} &= 0.
\end{aligned}$$

We emphasize that the "highest order", the coefficients $g^{(n)}_{n,r}$, coincide between MS and MOM. This is a consequence of (or rather reason for) theorem 56.

4.2.3. Expansions of the renormalized Green function

The all-order perturbative solution $G_{\mathcal{R}}(\alpha, \epsilon, x)$ of eq. (4.7) is defined as the limit $m \to \infty$ in eq. (4.22), effectively it is an infinite sum over the orders α^m in the coupling. But the form eq. (4.22) is not yet practically useful because it contains pole terms, which only cancel if all summands of a given order are included. We can expose the log-expansion (eq. (3.2)), with the identification of the logarithmic scale $L = \ln x$ (eq. (4.18) and def. 99), by expanding

$$x^{-t\epsilon} = e^{-Lt\epsilon} = 1 - t\epsilon L + \frac{1}{2}t\epsilon^2 L^2 \mp \dots.$$

Reordering eq. (4.22), we obtain

$$G_{\mathcal{R}}(\alpha, \epsilon, x) = Z(\alpha, \epsilon) + \sum_{k=0}^{\infty} L^k \sum_{t=1}^{\infty} \frac{(-t)^k}{k!} \sum_{n=t}^{\infty} \alpha^n \sum_{r=-n}^{\infty} g_{t,r}^{(n)} \epsilon^{k+r}. \tag{4.23}$$

From this, we read off the expansion functions

$$\gamma_k(\alpha, \epsilon) = \sum_{t=1}^{\infty} \frac{(-t)^k}{k!} \sum_{n=t}^{\infty} \alpha^n \sum_{r=-n}^{\infty} g_{t,r}^{(n)} \epsilon^{k+r}, \tag{4.24}$$

especially, the limit $\gamma_k(\alpha, \epsilon = 0) =: \gamma_k(\alpha)$ is

$$\gamma_k(\alpha) = \sum_{t=1}^{\infty} \frac{(-t)^k}{k!} \sum_{n=t}^{\infty} \alpha^n g_{t,-k}^{(n)}, \qquad \gamma_1(\alpha) = -\sum_{t=1}^{\infty} t \sum_{n=t}^{\infty} \alpha^n g_{t,-1}^{(n)}. \tag{4.25}$$

Example 114: Multiedge linear DSE, anomalous dimension.

Consider the DSE from example 111. In MOM, $\gamma_0(\alpha, \epsilon) = 1$ and we find

$$\begin{aligned}\gamma_1(\alpha, \epsilon) = {} & \alpha - \alpha^2 + 2\alpha^3 - 5\alpha^4 + 14\alpha^5 - 42\alpha^6 + 132\alpha^7 \mp \dots \\ & + (2\alpha - 7\alpha^2 + (26 - 2\zeta(3))\alpha^3 + (-99 + 8\zeta(3))\alpha^4 + \dots)\epsilon + \mathcal{O}(\epsilon^2).\end{aligned}$$

The $[\epsilon^0]$- part of γ_1 is indeed the anomalous dimension known from example 104,

$$\gamma(\alpha) = \gamma_1(\alpha) = \frac{\sqrt{1 + 4\alpha} - 1}{2} = -\sum_{n=1}^{\infty} (-1)^n C_{n-1} \alpha^n.$$

The $[\epsilon^1]$-part coincides with our analytic calculation in example 106.

Example 115: Multiedge nonlinear DSE, expansion functions.

The DSE with $w = 3$ in MOM results in

$$\gamma_1(\alpha, \epsilon) = \alpha - 4\alpha^2 + 44\alpha^3 \mp \dots + (2\alpha - 28\alpha^2 + (572 - 56\zeta(3))\alpha^3 + \dots)\epsilon + \mathcal{O}(\epsilon^2).$$

In MS-bar, for $w = 3$, we find

$$\gamma_0(\alpha,\epsilon) = 1 - 2\alpha + 22\alpha^2 \pm \ldots + \left(\left(-4 + \frac{\pi^2}{12}\right)\alpha + (98 - \pi^2 - 12\zeta(3))\alpha^2 \mp \ldots\right)\epsilon + \mathcal{O}(\epsilon^2)$$
$$\gamma_1(\alpha,\epsilon) = \alpha - 12\alpha^2 + 212\alpha^3 \mp \ldots + \left(2\alpha + \left(-60 + \frac{\pi^2}{3}\right)\alpha^2 \mp \ldots\right)\epsilon + \mathcal{O}\left(\epsilon^2\right).$$

Example 116: Multiedge linear DSE, constant term in MS.

In MS-bar, the function $\gamma_0(\alpha,\epsilon)$ is not fixed by renormalization conditions. An explicit calculation for the linear DSE in $D = 4 - 2\epsilon$, using eq. (4.25), results in

$$\gamma_0(\alpha,\epsilon) = 1 - 2\alpha + \frac{11}{2}\alpha^2 + \left(-17 + \frac{2\zeta(3)}{3}\right)\alpha^3 + \left(\frac{447}{8} - \frac{10\zeta(3)}{3}\right)\alpha^4 + \ldots + \left(\left(-4 + \frac{\pi^2}{12}\right)\alpha + \left(\frac{49}{2} - \frac{\pi^2}{4} - 3\zeta(3)\right)\alpha^2 + \ldots\right)\epsilon + \mathcal{O}\left(\epsilon^2\right).$$

Using the coefficients up to order α^{25} and the series-lookup function of the OEIS [473], one discovers a closed formula for $[\epsilon^0]\gamma_0$. Firstly, laborious experimentation results in

$$\ln\gamma_0 - \ln\left(\frac{\sqrt{1+4\alpha}-1}{2\alpha(1+4\alpha)^{\frac{1}{4}}}\right) = \zeta(3)\left(2\frac{\alpha^3}{3} - 8\frac{\alpha^4}{4} + 30\frac{\alpha^5}{5} - 112\frac{\alpha^6}{6} + 420\frac{\alpha^7}{7} \mp \ldots\right) + \zeta(5)\left(2\frac{\alpha^5}{5} - 12\frac{\alpha^6}{6} + 56\frac{\alpha^7}{7} - 240\frac{\alpha^8}{8} \pm \ldots\right) + \zeta(7)\ldots.$$

At least up to $\zeta(11)$ and α^{25}, the coefficients of $\frac{\alpha^{j+m-1}}{j+m-1}$ in the term proportional to $\zeta(m)$ are given by the binomial coefficient $2\binom{2j+m-3}{j-1}$. Assuming that this holds universally, all series over α and then the remaining series in $\zeta(m)$ can be summed and yield known functions. The end result for $[\epsilon^0]\gamma_0$ is

$$\gamma_0(\alpha) = e^{\gamma_E(1-\sqrt{1+4\alpha})}\frac{\sqrt{1+4\alpha}-1}{2\alpha\,(1+4\alpha)^{\frac{1}{4}}}\frac{\Gamma\left(\frac{3}{2} - \frac{1}{2}\sqrt{1+4\alpha}\right)}{\Gamma\left(\frac{1}{2} + \frac{1}{2}\sqrt{1+4\alpha}\right)} = \frac{\gamma}{\alpha}\sqrt{\frac{\mathrm{d}\,\gamma}{\mathrm{d}\alpha}}e^{-2\gamma\gamma_E}\frac{\Gamma\left(1-\gamma\right)}{\Gamma\left(1+\gamma\right)}.$$

In this equation, $\gamma \equiv \gamma(\alpha)$ is the anomalous dimension from example 114. We remark that such a fraction of gamma functions is not uncommon in the computation of multiedge Feynman graphs, compare for example [178]. We will understand its relation to the multiedge amplitude (example 24) in theorem 68.

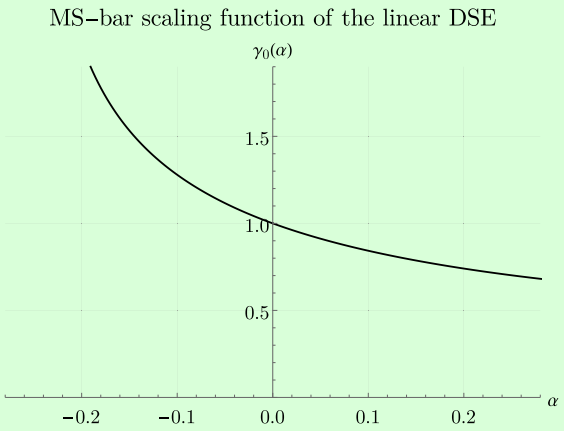

Example 117: Multiedge linear DSE, D=6, constant term.

In a very similar fashion to example 116, one finds empirically for the linear multiedge DSE in $D = 6$ dimensions the following functions:

$$\gamma(\alpha) = \frac{\sqrt{5 + 4\sqrt{1+\alpha}} - 3}{2}$$
$$\gamma_0(\alpha) = \frac{6\gamma}{\alpha}\sqrt{\frac{\mathrm{d}\,(6\gamma)}{\mathrm{d}\alpha}}e^{\gamma(1-2\gamma_E)}\frac{\Gamma\,(1-\gamma)}{\Gamma\,(1+\gamma)}$$

The anomalous dimension coincides with the expression quoted in example 104, derived from theorem 45.

Example 118: Toy model linear DSE, constant term.

For the linear DSE of the toy model (example 102), empirical calculation results in the tentative formula

$$\gamma_0(\alpha) = 1 + \left(\frac{\pi^2\alpha^2}{4}\right) + \frac{5}{2}\left(\frac{\pi^2\alpha^2}{4}\right)^2 + \ldots = \left(1 - \pi^2\alpha^2\right)^{-\frac{1}{4}} = \sqrt{\frac{\mathrm{d}\,\gamma}{\mathrm{d}\alpha}}.$$

Here, $\gamma = -\frac{1}{\pi}\arcsin(\pi\alpha)$ is the anomalous dimension from example 102.

For simple kernels such as the ones introduced in section 4.2.1, we can typically reach orders $\sim \alpha^{20}$ with a few hours computation time in Wolfram Mathematica. For computing the anomalous dimension in MOM, the analytic methods introduced in section 3.3 are tremendously more efficient: A power-series solution to the ODE in theorem 45 for the 1-loop multiedge in $D = 4$ dimensions can be obtained to hundreds of orders within minutes.

Nonetheless, the present brute-force algorithm for solving the DSE has two benefits. Firstly, it allows a seamless computation of the full ϵ-dependence of all quantities, especially also the counterterms, and secondly, it is not restricted to the MOM scheme. Therefore, it is indispensable to verify our theoretical study of "exotic" cases in the renormalization group.

Example 119: Multiedge linear DSE, MS counterterm.

Our calculation (up to order α^{25}) delivers for the counterterm in MS the series coefficients

$$\ln \hat{Z}(\alpha,\epsilon) = \frac{1}{\epsilon}\left(\alpha - \frac{\alpha^2}{2} + 2\frac{\alpha^3}{3} - 5\frac{\alpha^4}{4} + 14\frac{\alpha^5}{5} - 42\frac{\alpha^6}{6} \pm \dots\right).$$

Once more, we recognize the Catalan numbers and introduce $\gamma = \gamma(\alpha) = \frac{1}{2}\left(\sqrt{1+4\alpha} - 1\right)$ from example 114, which for $\epsilon = 0$ is the anomalous dimension both in MS and in MOM (theorem 56). The counterterm is indeed the integral of $\gamma(\alpha)$, as expected from theorem 49:

$$\hat{Z}(\alpha,\epsilon) = \exp\left(-\frac{1}{\epsilon}\sum_{n=1}^{\infty}(-1)^n C_{n-1}\frac{\alpha^n}{n}\right) = \left(\frac{e^{2\gamma}}{1+\gamma}\right)^{\frac{1}{\epsilon}} = e^{\frac{1}{\epsilon}\int_0^\alpha \frac{\mathrm{d}u}{u}\,\gamma(u)}. \tag{4.26}$$

Technically, $\hat{Z}(\alpha,\epsilon)$ is a transseries (def. 57) in ϵ.

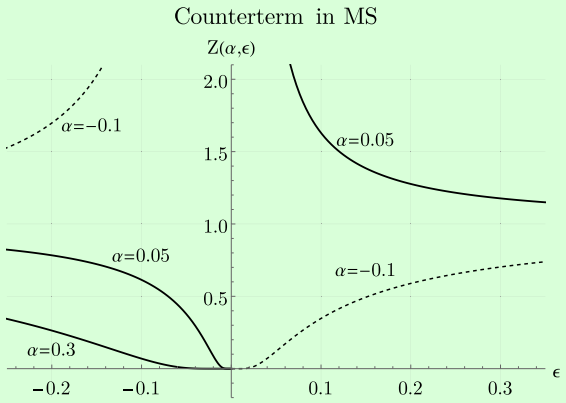

As long as α and ϵ have opposite signs, this function has the limit $\hat{Z}(\alpha, 0_+) = 0$ when $\epsilon \to 0$, see the figure. With eq. (4.26), the counterterm turns out to be a remarkably well-behaved function of ϵ, compared to its perturbative expansion, where every single term diverges as $\epsilon \to 0$. This is in line with [305] and a comment made in [401]: The all-order-solution example 114 "regulates itself" by its anomalous dimension, and the DSE (eq. (4.7)) does not contain a non-trivial counterterm at all. Compare the discussion at the end of section 3.2.3.

4.2.4. Exact solutions of the Toy model

Using the algorithm described above, one can solve the toy model DSE (example 102) for various values of w. In general, the results show the expected behaviour, but we made two curious observations which are worth mentioning.

Firstly, using kinematic renormalization and $w = -\frac{1}{2}$, the perturbative anomalous dimension turns out to be $\gamma(\alpha) = -\alpha + \mathcal{O}(\epsilon)$. This result was verified up to order α^{500} using theorem 45. We therefore assume that it holds to all orders in α, which means that for $w = -\frac{1}{2}$, the non-linear toy model DSE has a perturbative solution comparable to the non-recursive DSE ($w = -1$). Indeed, $w = -1$ corresponds to an anomalous dimension $\gamma(\alpha) = -\alpha$, where

we have rescaled $\frac{6\alpha}{\pi^2} \to \alpha$ to eliminate trivial factors. Let $L := \ln x$, then the non-recursive DSE (example 102) gives rise to the Callan-Symanzik equation (theorem 39)

$$\frac{\partial}{\partial L} G_{\mathcal{R}}(\alpha, L) = \gamma(\alpha) \left(1 + w\alpha \cdot \frac{\partial}{\partial \alpha}\right) G_{\mathcal{R}}(\alpha, L) = -\alpha G_{\mathcal{R}}(\alpha, L) + \alpha^2 \frac{\partial}{\partial \alpha} G_{\mathcal{R}}(\alpha, L).$$

The general solution of this partial differential equation is

$$G_{\mathcal{R}}(\alpha, L) = \alpha F_{-1}\left(L - \frac{1}{\alpha}\right),$$

where F_{-1} is an arbitrary function. The requirement $\partial_L G_{\mathcal{R}}|_{L=0} = \gamma(\alpha) = -\alpha$ and the boundary condition $G(\alpha, 0) = 1$ fix $F_{-1}(u) = -u$.

Although the anomalous dimension $\gamma(\alpha) = -\alpha$ of $w = -1$ coincides with the (supposed) one at $w = -\frac{1}{2}$, the latter gives rise to a slightly different Callan-Symanzik equation, namely

$$\frac{\partial}{\partial L} G_{\mathcal{R}}(\alpha, L) = -\alpha G_{\mathcal{R}}(\alpha, L) + \frac{1}{2}\alpha^2 \frac{\partial}{\partial \alpha} G_{\mathcal{R}}(\alpha, L).$$

This time, the general solution is

$$G_{\mathcal{R}}(\alpha, L) = \alpha^2 F_{-\frac{1}{2}}\left(L - \frac{2}{\alpha}\right).$$

The condition $G_{\mathcal{R}}(\alpha, 0) = 1$ translates to $F_{-\frac{1}{2}}(u) = \frac{1}{4}u^2$ and we find

$$G_{\mathcal{R}}(\alpha, L) = \frac{1}{4}\alpha^2 L^2 - \alpha L + 1. \tag{4.27}$$

At least within perturbation theory, eq. (4.27) represents an *exact* solution of a non-linear DSE. The same DSE with $w = -\frac{1}{2}$ in Minimal Subtraction (def. 108) gives rise to an anomalous dimension which seems to be a factorially divergent power series, and has no simple polynomial solution $\hat{G}_{\mathcal{R}}$.

The phenomenon occurs in reverse direction if we choose $w = -2$. In Minimal Subtraction, we find $\hat{\gamma}(\alpha) = -\alpha$ at least up to order α^{18}. By theorem 54, the latter is true even for $\epsilon \neq 0$. Assume again that $\hat{\gamma}(\alpha) = -\alpha$ holds to all orders of α, then the Callan-Symanzik equation (theorem 39) reads

$$\frac{\partial}{\partial L} G_{\hat{\mathcal{R}}}(\alpha, \epsilon, L) = -\alpha G_{\hat{\mathcal{R}}}(\alpha, \epsilon, L) + 2\alpha^2 \frac{\partial}{\partial \alpha} G_{\hat{\mathcal{R}}}(\alpha, \epsilon, L).$$

In MS, the Green function does not satisfy some simple boundary condition, therefore we can not derive an exact solution for $G_{\hat{\mathcal{R}}}$ from this differential equation. The MOM anomalous dimension for $w = -2$ is factorially divergent as its Stokes constant does not vanish (table 3.4).

It is unclear whether the toy model contains any concrete physical information, but nevertheless, the observations in this subsection serve as an example for how different renormalization conditions can give rise to qualitative different analytic features of the solution of the same DSE. As we shall see in theorem 57, these solutions are physically equivalent, but, thanks to renormalization of the coupling constant, they are expressed in terms of expansion parameters which are related non-linearly and therefore the corresponding series can look truly different. Concretely, the shift between MOM and MS can transform a factorially divergent power series (def. 58) into a trivial polynomial $\hat{\gamma}(\alpha) = -\alpha$.

Summary of section 4.2.

1. We consider propagator-type DSEs where the series expansion of the Mellin transform of the kernel is assumed to be known (section 4.2.1).

2. Starting from the treelevel $G_{\mathcal{R}}^{(1)} = 1$, the DSE can be solved order by order by algebraic operations on the Mellin coefficients. MOM and MS renormalization conditions can be implemented easily (section 4.2.2).

3. The resulting Green function is a triple series in α, ϵ and L. The n functions $\gamma_j(\alpha, \epsilon)$ or the counterterm $Z(\alpha, \epsilon)$ can be obtained by reordering the series (section 4.2.3).

4. The non-linear DSE of the toy model seems to have simple perturbative solutions in two particular cases. This is an example for the fact that different renormalization conditions can give rise to qualitatively different perturbative solutions (section 4.2.4).

4.3. Shifted kinematic renormalization point

We have examined non-kinematic renormalization schemes already in section 4.1. In the present section, we extend the previous analysis in two respects:

1. We consider the full ϵ-dependence of all quantities in dimensional regularization.
2. In theorem 48, non-kinematic renormalization schemes were expressed in terms of the quantity $\tau[\Gamma] = G_{\mathcal{R}'}(L=0) = \gamma_0'(\alpha)$. In the present section, we instead take the value $L = -\delta \neq 0$, where $G_{\mathcal{R}'}(L=-\delta) = 1$, as the primary object.

4.3.1. Shifted Green function

By theorem 48, a non-kinematic Green function $G_{\mathcal{R}'}$ has the value $G_{\mathcal{R}'}(L) = 1$ not at the point $L = 0$, but at some point δ. Instead of knowing the amplitude at $L = 0$, given by τ (def. 109), one can also ask at which point $L = -\delta$ the Green function is unity. In practice, the latter is often more physically sensible because, to limited order in perturbation theory, we expect our results to be accurate as long as the quantum corrections $(G_{\mathcal{R}'} - 1)$ are small. Consequently, a non-kinematic Green function will be reliable in the vicinity of $L = -\delta$, and not necessarily for small L [477, 478]. The set up is shown in fig. 4.2.

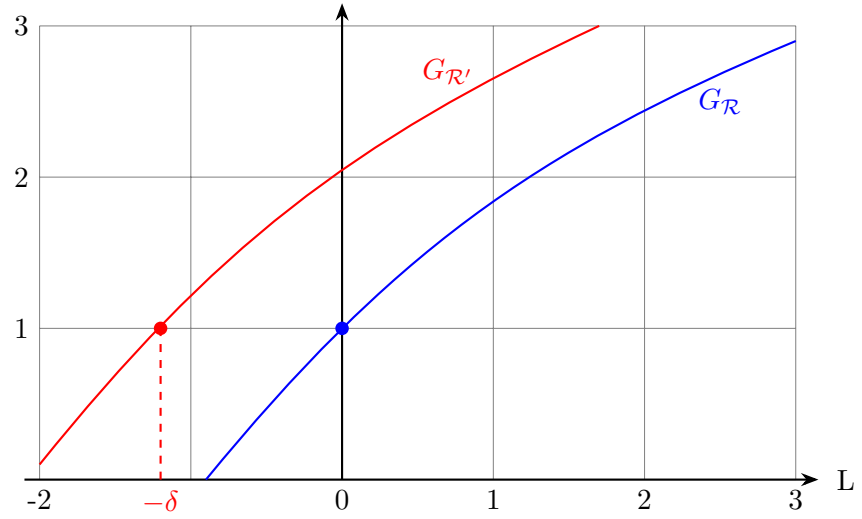

Figure 4.2.: A hypothetical Green function in MOM with renormalization point $L = 0$ (blue) and in shifted MOM according to def. 111 with $\delta = 1.2$ (red). Both are sketched for the same arbitrary, but fixed, value of the coupling.

Definition 111. Let $L = \ln \frac{s}{s_0}$ be the logarithmic scale (def. 99) and let $\delta(\alpha, \epsilon)$ be a power series (def. 51) in α and ϵ, regular at the origin. Let $\mathcal{F}_{\mathcal{R}}$ be the Feynman amplitude in kinematic renormalization (def. 91) with renormalization point $L = 0$. The *shifted kinematic renormalization scheme* $\mathcal{F}_{\mathcal{R}'}(L)$ is defined by the renormalization condition

$$\mathcal{F}_{\mathcal{R}'}(-\delta) \stackrel{!}{=} \tilde{\mathbb{1}} = \mathcal{F}_{\mathcal{R}}(0).$$

Theorem 57. Let $G_{\mathcal{R}'}$ be a renormalized Green function in any renormalization scheme (def. 97), which is a solution of a DSE. Let τ (def. 109) be the extraction of the value at $L = 0$ in $\mathcal{R}'$, and let $\sigma = \partial_L|_{L=0}$ be the infinitesimal Feynman rule in MOM (def. 100). Then, $G_{\mathcal{R}'}$ is the Green function (of the same DSE) in a shifted kinematic scheme (def. 111), provided the equation

$$\tau = \exp^\star(\delta \cdot \sigma)$$

can be satisfied with some power series $\delta(\alpha, \epsilon) \in \mathbb{R}[[\alpha, \epsilon]]$ (def. 51).

Proof. With def. 111, $\mathcal{F}_{\mathcal{R}'}(0) = \mathcal{F}_{\mathcal{R}}(\delta)$ is not unity. We can extract the value with the operator τ from def. 109. On the other hand, $\mathcal{F}_{\mathcal{R}}(\delta)$ is given by the ordinary exponential formula def. 100. Consequently, the relation between τ and δ must be the one claimed above, and if it is, then $\mathcal{F}_{\mathcal{R}'}(L + \delta) = \mathcal{F}_{\mathcal{R}}(L)$. □

In perturbation theory, the condition of theorem 57 can certainly be fulfilled: The operator τ, applied to a combinatorial Green function (def. 45), results in a formal power series in α with finite coefficients as $\epsilon \to 0$. Then, δ can be obtained by taking the combinatorial logarithm of this series. Algebraically, this is realized by the Dynkin operator def. 79, but one can understand its mechanism also by solving a DSE order by order as in section 4.2: At every new order, the Green function contains a higher power in L, and by shifting $L \to L+\delta$, one can always add a new free constant to adjust the absolute value. We will derive concrete algorithms to find δ in section 4.4.

Example 120: Multiedge DSE, manually computing the shift.

Consider the multiedge DSE in $D = 4 - 2\epsilon$ from example 110. The first-order solution is simply the kernel graph, in MOM it reads

$$G_{\mathcal{R}}(\alpha, \epsilon, L) = 1 + \alpha L + \mathcal{O}(\epsilon).$$

We use MS as an example of a non-kinematic renormalization scheme. In MS, the solution is

$$G_{\mathcal{R}'}(\alpha, \epsilon, L) = 1 + \alpha(L - 2) + \mathcal{O}(\epsilon).$$

Both Green functions are solutions to the same DSE, so by theorem 57, it should be possible to find a shift δ such that the MS-solution is a shifted kinematic scheme. That is, by def. 111, we want $G_{\mathcal{R}'}(-\delta) = 1$. Indeed, we can read off this value from the explicit solutions: $G_{\mathcal{R}'}(\alpha, \epsilon, 2) = 1 + \mathcal{O}(\epsilon)$, therefore,

$$\delta = -2 + \mathcal{O}(\epsilon) + \mathcal{O}(\alpha).$$

The extension of this "brute force algorithm" to higher orders in α and ϵ will be described in section 4.4.2

There are two rather philosophical obstacles to the relation between σ and τ in theorem 57:

1. If $\sigma[\Gamma] = 0$, then the right hand side is unity. If $G_{\mathcal{R}}$ is taken to be $\mathcal{Q}_{\mathcal{R}}$, then this case amounts to a fixed-point of the renormalization group. Moreover, this obstacle can arise in an empty DSE, that is, in a theory without any quantum corrections. The classification of such cases in full generality is rather complicated since a theory might have multiple beta functions, vanishing at different points. Geometrically, this case is simple to visualize: σ computes the derivative of $G_{\mathcal{R}}$, and if this value is zero somewhere then $G_{\mathcal{R}}$ can potentially have an absolute extreme value at that point and thus be not surjective. If in that case γ_0' is outside of the values of $G_{\mathcal{R}}$, then no shift can be found to relate $G_{\mathcal{R}}$ and $G_{\mathcal{R}'}$. Phrased differently: To find a shift, it is necessary that $G_{\mathcal{R}'}$ is unity *somewhere*, and the non-vanishing of the anomalous dimension and beta function guarantees that $G_{\mathcal{R}'}$ is monotonous and thus surjective.

2. Beyond perturbation theory, the operators σ, τ can, in principle, give rise to arbitrary functions with unknown analytic properties. In that case, we can not trivially resort to the combinatorial logarithm to solve for δ.

Both points will be irrelevant for the rest of the thesis because we only consider reasonably well-behaved DSEs in perturbation theory. There is, however, one very relevant caveat to the shift between renormalization schemes: Theorem 57 requires both Green functions to be solutions of the same combinatorial DSE. If the underlying graphs do not satisfy a DSE, then the exponential formula (def. 100) does not hold to start with and, in general, it is impossible to find a $\delta(\alpha, \epsilon)$ to relate the schemes. The chain approximation (section 4.5.4) is an example for the latter problem.

Before we turn to concrete algorithms for computing δ, we will first examine some general properties of the shifted scheme (def. 111).

4.3.2. Shifted counterterms

Definition 112. Let $\delta(\alpha, \epsilon)$ be the shifted renormalization point from def. 111 and $\mathcal{Q}_{\mathcal{R}'}$ be the invariant charge (def. 93) in the shifted theory. We define two *shifted couplings* α' and $\tilde{\alpha}$ in analogy to defs. 102, 104 and 105:

$$\alpha'(\alpha, \epsilon) := \alpha e^{-\epsilon\delta(\alpha,\epsilon)}, \qquad \mathcal{Q}_0(\alpha, \epsilon) := \mathcal{Q}_{\mathcal{R}'}(\alpha, \epsilon, 0)$$
$$\tilde{\alpha}(\alpha, \epsilon) := \alpha'(\alpha, \epsilon) \cdot \mathcal{Q}_0(\alpha, \epsilon) = \alpha e^{-\epsilon\delta(\alpha,\epsilon)} \mathcal{Q}_{\mathcal{R}'}(\alpha, \epsilon, 0).$$

In the special case of $\mathcal{Q}_{\mathcal{R}} = \mathbb{1}$ (linear DSE), the shifted couplings coincide, $\alpha' = \tilde{\alpha}$. Observe that all series in def. 112 start with a linear term in the coupling, therefore, using series reversion (theorem 17) and concatenation (theorem 18), one can compute the transformations between any pair of the three couplings $\{\alpha, \alpha', \tilde{\alpha}\}$. We will often indicate the dependence of functions by the corresponding decoration, for example $\tilde{\mathcal{Q}}_0(\tilde{\alpha}, \epsilon) := \mathcal{Q}_0(\alpha(\tilde{\alpha}), \epsilon)$ and $\mathcal{Q}_0'(\alpha', \epsilon) := \mathcal{Q}_0(\alpha(\alpha'), \epsilon)$.

Lemma 58. Let $G_{\mathcal{R}'}$ be a solution of a DSE in shifted kinematic renormalization (def. 111). Then

$$G_{\mathcal{R}'}(\alpha, \epsilon, L) = G_{\mathcal{R}'}(\alpha, \epsilon, 0) \cdot G_{\mathcal{R}}\left(\tilde{\alpha}(\alpha, \epsilon, \delta), \epsilon, L\right). \tag{4.28}$$

Proof. For the analytic Green function, the renormalization condition def. 111 is

$$G_{\mathcal{R}'}(\alpha, \epsilon, L) = G_{\mathcal{R}}(\alpha, \epsilon, L + \delta). \tag{4.29}$$

The right hand side is known from lemma 38. □

The behaviour of counterterms under a change of renormalization point is in principle straightforward from their definition, but great care is required regarding which quantity is a function of which variable. For clarity, we restrict ourselves to a theory with only a single Green function $G_{\mathcal{R}}$ and two Z-factors, Z_α for the coupling and Z_G for $G_{\mathcal{R}}$. The renormalized Green function $G_{\mathcal{R}}$ in MOM (def. 91) is related to the unrenormalized one via def. 104 and eq. (3.26),

$$G_{\mathcal{R}}(\alpha, \epsilon, L) = Z_G(\alpha, \epsilon) \cdot G(\alpha Z_\alpha(\alpha, \epsilon), \epsilon, L). \tag{4.30}$$

Firstly, we consider a linear Dyson-Schwinger equation, that is, the invariant charge (def. 92) is $Q = 1$ and consequently $Z_\alpha = 1$, and eq. (4.30) becomes

$$G_{\mathcal{R}}(\alpha, \epsilon, L) = Z_G(\alpha, \epsilon) G\left(\alpha, \epsilon, L\right). \tag{4.31}$$

By def. 112, $\tilde{\alpha}(\alpha, \epsilon) = \alpha'(\alpha, \epsilon)$ for a linear DSE. Let

$$\gamma'_0(\alpha, \epsilon) := G_{\mathcal{R}'}(\alpha, \epsilon, 0) = G_{\mathcal{R}}(\alpha, \epsilon, L = \delta(\alpha, \epsilon)). \tag{4.32}$$

Combining lemma 58 and eq. (4.31), the shifted Green function is

$$\begin{aligned} G_{\mathcal{R}'}(\alpha, \epsilon, L) &= \gamma'_0(\alpha, \epsilon) \cdot G_{\mathcal{R}}(\alpha'(\alpha, \epsilon), \epsilon, L) \\ &= \gamma'_0(\alpha, \epsilon) \cdot Z_G(\alpha'(\alpha, \epsilon), \epsilon) \cdot G(\alpha'(\alpha, \epsilon), \epsilon, L). \end{aligned} \tag{4.33}$$

Naively, from def. 104, we expect the form

$$G_{\mathcal{R}'}(\alpha, \epsilon, L) \stackrel{?}{=} Z'_G(\alpha, \epsilon) G\left(\alpha Z'_\alpha(\alpha, \epsilon), \epsilon, L\right). \tag{4.34}$$

This would mean that $\alpha Z'_\alpha \stackrel{?}{=} \alpha' = \alpha e^{-\epsilon\delta}$. In other words, with the definition eq. (4.34), the solution of a linear Dyson-Schwinger equation obtains a non-vanishing coupling counterterm $Z'_\alpha \stackrel{?}{=} e^{-\epsilon\delta}$. This is not only "unintuitive", but it also violates equations such as $Z_\alpha = Z_G^w$, which would otherwise guarantee that $Z_\alpha = 1$ if $w = 0$. We therefore *decide* that α' is the proper variable for $G_{\mathcal{R}'}$, so that in eq. (4.33), no Z_α is necessary. We stress that this is a choice, not a theorem. Essentially, it is the same choice that we commented on below def. 104 for factoring s_0^ϵ out of the definition of Z_α. We absorb $e^{-\epsilon\delta}$ into the definition of the coupling α' in the same way that we absorbed s_0^ϵ into α in eq. (3.24). With this understanding, we define

$$\begin{aligned} G'_{\mathcal{R}}(\alpha', \epsilon, L) &:= G_{\mathcal{R}'}\left(\alpha(\alpha', \epsilon), \epsilon, L\right) \\ \gamma'_0(\alpha', \epsilon) &:= G'_{\mathcal{R}}(\alpha', \epsilon, 0) = \gamma_0(\alpha(\alpha', \epsilon), \epsilon). \end{aligned} \tag{4.35}$$

Definition 113. Let $\mathcal{R}'$ be a shifted kinematic renormalization scheme (def. 111). We take the shifted coupling α' from def. 112 as a natural variable and define the *shifted counterterms* $Z'_G(\alpha',\epsilon), Z'_\alpha(\alpha',\epsilon)$ by the relation

$$G'_{\mathcal{R}}(\alpha',\epsilon,L) =: Z'_G(\alpha',\epsilon)\cdot G\left(\alpha' Z'_\alpha(\alpha',\epsilon),\epsilon,L\right).$$

The counterterms for the linear DSE can now be read off from comparing eq. (4.33) and def. 113 :

$$\begin{aligned} Z'_\alpha(\alpha',\epsilon) &= 1, \\ Z'_G(\alpha',\epsilon) &= \gamma'_0(\alpha',\epsilon) Z_G(\alpha',\epsilon). \end{aligned} \tag{4.36}$$

In the second equation, we insert α' as a variable into Z_G, without any implicit transformation $\alpha(\alpha')$.

Example 121: Multiedge linear DSE, shifted counterterm.

Consider the linear multiedge DSE from example 119. We introduce a shift $\delta = -3$. Equation (4.35) then takes the form

$$\begin{aligned} \gamma'_0(\alpha',\epsilon) = 1 - 3\alpha' + \frac{15}{2}\alpha'^2 - \frac{39}{2}\alpha'^3 + \frac{435}{8}\alpha'^4 + -\frac{6441}{40}\alpha'^5 + \dots \\ + \left(-\frac{3}{2}\alpha' + \frac{33}{2}\alpha'^2 + \left(-\frac{393}{4} + 6\zeta(3)\right)\alpha'^3 + \dots\right)\epsilon + \mathcal{O}\left(\epsilon^2\right). \end{aligned}$$

According to eq. (4.36), the shifted counterterm is

$$\begin{aligned} \ln Z'_G(\alpha',\epsilon) = \left(\alpha' - \frac{\alpha'^2}{2} + 2\frac{\alpha'^3}{3} - 5\frac{\alpha'^4}{4} + 14\frac{\alpha'^5}{5} \mp \dots\right)\frac{1}{\epsilon} \\ - \alpha' - \frac{1}{2}\alpha'^2 + \left(\frac{8}{3} - \frac{2}{3}\zeta(3)\right)\alpha'^3 + \left(-\frac{39}{4} + 2\zeta(3)\right)\alpha'^4 + \dots + \mathcal{O}(\epsilon). \end{aligned}$$

The singular term of this series coincides with the un-shifted one from example 119.

Theorem 59. Let $\mathcal{R}'$ be a shifted kinematic renormalization scheme (def. 111), and let α' be the shifted coupling (def. 112). Let Z_G, Z_α be the counterterms in kinematic renormalization without shift, and let

$$\gamma'_0(\alpha',\epsilon) := G'_{\mathcal{R}}(\alpha',\epsilon,0), \qquad \mathcal{Q}'_0(\alpha',\epsilon) := \mathcal{Q}'_{\mathcal{R}}\left(\alpha',\epsilon,0\right) = \mathcal{Q}_{\mathcal{R}'}\left(\alpha(\alpha'),\epsilon,0\right).$$

Then, the shifted counterterms of def. 113 are given by

$$Z'_\alpha\left(\alpha',\epsilon\right) = \mathcal{Q}'_0(\alpha',\epsilon)\cdot Z_\alpha(\alpha'\mathcal{Q}'_0(\alpha',\epsilon),\epsilon), \qquad Z'_G\left(\alpha',\epsilon\right) = \gamma'_0(\alpha',\epsilon)\cdot Z_G\left(\alpha'\mathcal{Q}'_0(\alpha',\epsilon),\epsilon\right).$$

Proof. For a non-linear DSE, from lemma 58, we obtain

$$G_{\mathcal{R}'}(\alpha,\epsilon,L) = \gamma_0'(\alpha,\epsilon)\cdot G_{\mathcal{R}}(\tilde{\alpha}(\alpha,\epsilon),\epsilon,L).$$

Note the presence of $\tilde{\alpha} = \alpha'\mathcal{Q}_0(\alpha,\epsilon)$ from def. 112. We take α' as a natural variable and define the shifted Z-factors according to def. 113. The un-shifted Green function is given by eq. (4.30), therefore

$$\gamma_0'(\alpha,\epsilon)\cdot Z_G(\tilde{\alpha},\epsilon)G(\tilde{\alpha}Z_\alpha(\tilde{\alpha},\epsilon),\epsilon,L) = Z_G'(\alpha',\epsilon)G\left(\alpha' Z_\alpha'(\alpha',\epsilon),\epsilon\right).$$

Comparing factors, and writing everything as a function of α', we obtain the claimed expressions. □

4.3.3. Shifted renormalization group functions

Knowing the shifted counterterms from theorem 59, we can compute the corresponding renormalization group functions from def. 110. We deliberatly expressed our shifted functions in terms of α', not α, because in this way, we can use the same derivations as in section 3.2.2, only replacing α by α'. This fits with our remark eq. (3.24): Renormalization and change of energy scale are one and the same operation, that is, with a shifted renormalization point, we obtain identical results, up to a different value of the coupling.

Theorem 60. Consider an arbitrarily shifted kinematic renormalization scheme, where the counterterms are given by theorem 59 as functions of α' (def. 112). The shifted renormalization group functions $\beta'(\alpha',\epsilon),\gamma'(\alpha',\epsilon)$ are computed as in def. 110, where every α is replaced by α'. Then, the Callan-Symanzik equation (theorem 43) holds for the shifted Green function eq. (4.35) as a function of α':

$$\left(\gamma'(\alpha',\epsilon) + \left(\beta'(\alpha',\epsilon) - \alpha'\epsilon\right)\frac{\partial}{\partial\alpha'}\right) G_{\mathcal{R}}'(\alpha',\epsilon,L) = \frac{\partial}{\partial L}G_{\mathcal{R}}'(\alpha',\epsilon,L).$$

Proof. Owing to our definitions in section 4.3.2, def. 113 is exactly the same as the un-shifted relation eq. (4.30), only with every α replaced by α' and Z replaced by Z'. Moreover, thanks to def. 110, the Z-factors are related to the renormalization group functions exactly as in the un-shifted case, up to replacing $\gamma\to\gamma'$ and $\beta\to\beta'$. Effectively, $G_{\mathcal{R}}'(\alpha,\epsilon,L)$ can be expressed in terms of γ',β' exactly the same way that $G_{\mathcal{R}}(\alpha,\epsilon,L)$ is expressed by γ,β, and both are based on the same un-renormalized Green function G. Consequently, both satisfy the same Callan-Symanzik equation theorem 43.

A different perspective is to use theorem 57: The shifted kinematic Green function is equal to some non-kinematic Green function, and by lemma 53, the latter satisfies the familiar Callan-Symanzik equation and the counterterm relations of def. 110. □

Similarly to eq. (3.2), the shifted Green function (eq. (4.35)) can be expanded in the logarithmic scale (def. 99):

$$G_{\mathcal{R}}'(\alpha',\epsilon,L) := \sum_{j=0}^{\infty}\gamma_j'(\alpha',\epsilon)L^j. \tag{4.37}$$

In this equation, all quantities are functions of α' from def. 112. But, unlike earlier notation, $\gamma_j'(\alpha') \neq \gamma_j(\alpha(\alpha'))$.

Lemma 61. Let $G'_{\mathcal{R}}(\alpha, \epsilon, L)$ be a renormalized Green function in a shifted kinematic scheme (def. 111) which is a solution of a DSE. Let $\gamma'_j(\alpha', \epsilon)$ be the coefficients of the log expansion eq. (4.37). Then,

$$\gamma'_{j>1}(\alpha', \epsilon) = \frac{1}{j}\left(\gamma'(\alpha', \epsilon) + \left(\beta'(\alpha', \epsilon) - \alpha'\epsilon\right) \cdot \frac{\partial}{\partial \alpha'}\right) \gamma'_{j-1}(\alpha', \epsilon).$$

Proof. Insert the expansion eq. (4.37) into the Callan-Symanzik equation (theorem 60). □

By theorem 60 and lemma 61, the shifted renormalization group is entirely expressed in terms of shifted couplings α', shifted Green functions $G_{\mathcal{R}'}$ and shifted renormalization group functions β', γ'. On the other hand, for a given shift δ, the expansion functions can also be computed directly from the un-shifted ones.

Theorem 62. Let $\gamma'_j(\alpha', \epsilon)$ be the expansion functions from eq. (4.37), where $G'_{\mathcal{R}}$ is a shifted Green function according to eq. (4.35) and def. 111, and let $\gamma_j(\alpha, \epsilon)$ be the corresponding expansion functions in MOM from eq. (3.2). Let $\alpha(\alpha') = \alpha' e^{+\epsilon\delta'(\alpha', \epsilon)}$, where $\delta'(\alpha', \epsilon) = \delta(\alpha(\alpha', \epsilon), \epsilon)$ from def. 112. Then,

$$\gamma'_k(\alpha', \epsilon) = \gamma'_0(\alpha', \epsilon) \cdot \gamma_k(\tilde{\alpha}(\alpha', \epsilon), \epsilon)$$
$$\gamma'_k(\alpha', \epsilon) = \sum_{j=k}^{\infty} \binom{j}{k} \gamma_j(\alpha(\alpha', \epsilon), \epsilon) \delta^{j-k}(\alpha(\alpha', \epsilon), \epsilon).$$

Proof. The first equation follows if we insert the expansion eq. (4.37) into lemma 58.
From def. 111, we obtain

$$G_{\mathcal{R}'}(\alpha, \epsilon, L) = G_{\mathcal{R}}(\alpha, \epsilon, L + \delta).$$

Insert the expansions eqs. (3.2) and (4.37),

$$\sum_{j=0}^{\infty} \gamma'_j(\alpha, \epsilon) L^j = \sum_{j=1}^{\infty} \gamma_j(\alpha, \epsilon)(L + \delta)^j.$$

Expand the right hand side with the binomial theorem and consider order L^k.

$$\sum_{j=0}^{\infty} \gamma_j(\alpha, \epsilon) \sum_{k=0}^{j} \binom{j}{k} L^k \delta^{j-k} = \sum_{k=0}^{\infty} L^k \sum_{j=k}^{\infty} \binom{j}{k} \gamma_j(\alpha, \epsilon) \delta^{j-k}.$$

$$\gamma'_k(\alpha, \epsilon) = \sum_{j=k}^{\infty} \binom{j}{k} \gamma_j(\alpha, \epsilon) \delta^{j-k}.$$

This is a function of α, so we need to insert $\alpha(\alpha')$ everywhere. □

So far, we have worked with the full ϵ-dependent functions, which is necessary for a consistent treatment of counterterms. If we are only interested in the $\epsilon = 0$ case, then the situation simplifies considerably.

Theorem 63. Assume that the MOM expansion functions $\gamma_k(\alpha)$ from eq. (3.2) are formal power series and satisfy the Callan-Symanzik equation theorem 39, and the kinematic renormalization point is shifted by a factor $\delta(\alpha)$ according to def. 111, which is a power series in α. Assume further that $G_{\mathcal{R}}$ is a solution to a DSE of type eq. (3.35), where the invariant charge (def. 92) is $Q = G^w$. Then, in the limit $\epsilon = 0$,

1. The shifted anomalous dimension and beta functions of theorem 60, for $\epsilon = 0$, are

$$\gamma'(\alpha) := \frac{\gamma(\alpha)}{1 + w\gamma(\alpha) \cdot \alpha\partial_\alpha \delta(\alpha)}, \qquad \beta'(\alpha) := w\alpha\gamma'(\alpha),$$

2. The shifted anomalous dimension satisfies $\gamma'(\alpha) = \gamma(\alpha) + \mathcal{O}\left(\alpha^3\right)$, and the shifted beta function satisfies $\beta'(\alpha) = \beta(\alpha) + \mathcal{O}(\alpha^4)$.

Proof. 1. Consider the limit $\epsilon \to 0$ in theorem 62. In that limit, $\alpha' \to \alpha$ and the ϵ-dependence of all quantities can be left out because they are regular (lemma 52). Compute the derivative of this series, using the fact that $\gamma_j(\alpha)$ satisfy the Callan-Symanzik equation (theorem 40), and identify the resulting series to obtain

$$\alpha\partial_\alpha\gamma'_k(\alpha) = -\frac{\gamma}{w\gamma}\gamma'_k + \frac{1}{w\gamma}\sum_{j=k+1}^{\infty} \frac{j!(k+1)\gamma_j\delta^{j-1-k}}{(j-1-k)!(k+1)!} + \alpha\partial_\alpha\delta \cdot \sum_{j=k}^{\infty} \frac{j!(k+1)\gamma_j\delta^{j-k-1}}{(j-k-1)!(k+1)!}$$
$$(k+1)\gamma'_{k+1} = \frac{\gamma}{1 + w\gamma\alpha\partial_\alpha\delta} \cdot \gamma'_k + \frac{s\gamma}{1 + w\gamma\alpha\partial_\alpha\delta} \cdot \alpha\partial_\alpha\gamma'_k.$$

This is again the Callan-Symanzik equation, but with a different anomalous dimension and beta function as claimed.

2. Follows from 1. and lemma 41 upon noticing that $\gamma(\alpha) \cdot \alpha\partial_\alpha \ln\delta(\alpha) \in \mathcal{O}(\alpha^2)$. □

For the linear DSE, $w = 0$, we recover $\gamma'(\alpha) = \gamma(\alpha)$, known from theorem 56. Point 2. is an extension of point 1 in theorem 56.

Lemma 64. For a linear DSE, the shifted anomalous dimension $\gamma'(\alpha', \epsilon)$ is

$$\gamma'(\alpha', \epsilon) = \gamma(\alpha', \epsilon) + \epsilon\partial_{\alpha'} \ln\gamma'_0(\alpha', \epsilon).$$

Here, $\gamma(\alpha', \epsilon)$ is the un-shifted anomalous dimension where the argument is α', that is, we do not insert the transformation $\alpha(\alpha')$. Especially, $[\epsilon^0]\gamma'(\alpha, \epsilon) = [\epsilon^0]\gamma(\alpha, \epsilon)$, so γ and γ' coincide for $\epsilon = 0$.

Proof. First note that in the linear case, $\beta'(\alpha', \epsilon) = 0$. Using def. 110 on eq. (4.36) results in

$$\gamma'(\alpha', \epsilon) = \epsilon\alpha'\epsilon\partial_{\alpha'} \ln Z_G(\alpha', \epsilon) = \partial_{\alpha'} \ln\gamma'_0(\alpha', \epsilon) + \alpha'\epsilon\partial_{\alpha'} \ln Z_G(\alpha', \epsilon).$$

The last summand is the un-shifted anomalous dimension with argument α'. γ' is regular in ϵ, since it appears in the Callan-Symanzik equation (theorem 60) where $G_{\mathcal{R}'}$ is regular and non-vanishing for $\epsilon \to 0$. The difference of γ and γ' is proportional to ϵ because neither of them contains poles in ϵ. □

Summary of section 4.3.

1. All solutions of the same DSE, but in different renormalization schemes, are identical up to different renormalization points. In non-kinematic renormalization schemes, the renormalization point $\delta(\alpha, \epsilon)$ is a function of α (section 4.3.1).
2. In order to obtain the correct counterterms and renormalization group functions for $\epsilon \neq 0$, one needs to introduce a shifted coupling $\alpha' = \alpha e^{-\epsilon\delta}$ (section 4.3.2).
3. For a given shift $\delta(\alpha)$, the shifted counterterms and renormalization group functions can be computed from the un-shifted ones, and they satisfy all the usual renormalization group equations (section 4.3.3).

4.4. MS as a shifted MOM scheme

All renormalization schemes can be interpreted as shifted kinematic renormalization schemes (def. 111), where the renormalization point $\delta(\alpha, \epsilon)$ in general depends both on α and on ϵ. This follows from theorem 57, and is valid up to the exceptions discussed there. In the present section, we narrow down the setting to a comparison between kinematic renormalization and concretely Minimal Subtraction, instead of arbitrary non-kinematic schemes.

4.4.1. Relation between MS and MOM

As described in section 4.1.1, kinematic renormalization (def. 91) has pleasant analytic features and straightforward interpretation, while Minimal Subtraction (def. 91) is technically easiest for solving Feynman integrals. Moreover, in MS, but presumably not in MOM, the beta function is expected to be dominated by primitive diagrams (def. 86) [479]. In section 4.2.4, we saw explicit examples for the fact that the perturbative beta function can differ substantially between MS and MOM. Finally, we can expect that low-order perturbation theory is reliably where quantum corrections are small, that is, in the vicinity of the renormalization point δ, not necessarily near $L = 0$ [477, 478]. For all these reasons, we want to improve our understanding of the relationship between MS and MOM by concretely determining the shift $\delta(\alpha, \epsilon)$.

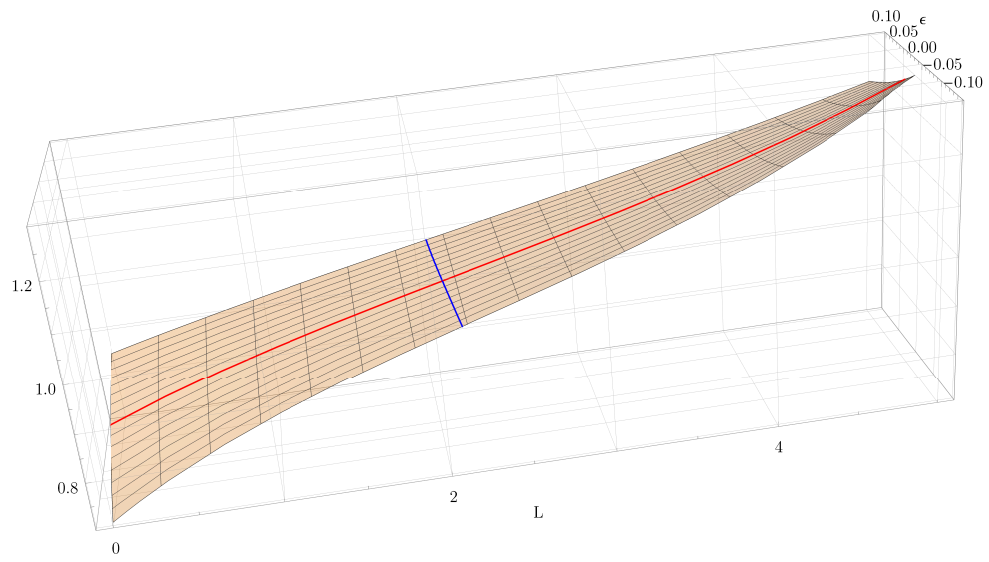

Figure 4.3.: Sketch of the situation discussed in the present section. The orange surface is a Green function $\bar{G}_{\mathcal{R}}(\alpha, \epsilon, L)$ in MS-bar for some fixed value of α. The red line indicates its value for $\epsilon = 0$. Our goal is to find the blue line. The blue line is the function $-\delta(\alpha, \epsilon)$, for the same fixed value of α, where $\bar{G}_{\mathcal{R}}(\alpha, \epsilon, -\delta) = 1$.

The qualitative situation is sketched in fig. 4.3: The Green function $\hat{G}_{\mathcal{R}}$ in MS is some function of α, ϵ and L and we want to determine the values $L = -\delta(\alpha, \epsilon)$ where it has unit value. There are three approaches to finding δ:

1. Compute the MS solution $\hat{G}_{\mathcal{R}}$ and determine δ from the condition def. 111, by reversing the series.

2. Compute the MOM solution and the MS solution and determine δ without extensive series reversions.

3. Derive δ from a known MOM solution without explicitly computing the MS solution.

We shall discuss the first approach in section 4.4.2, the second one in section 4.4.3 and the third one in section 4.4.4.

In all cases, we will actually be working with MS-bar and not MS (def. 108) in order to eliminate trivial constants. The transition between MOM and MS is described in section 4.2.2, and for our concrete examples it is given in [480]. Moreover, we again restrict ourselves to propagator-DSEs of type eq. (3.35) where $Q = G^w$ with $w \in \mathbb{Q}$.

4.4.2. Brute-force computation

With the algorithm described in section 4.2, we can in principle find the MS-bar solution $\bar{G}_{\mathcal{R}}(\bar{\alpha}, \epsilon, L)$ to any finite order, and then determine $\delta(\alpha, \epsilon)$ by "reversing" the resulting series in L. A first order computation was shown in example 120.

In the framework of shifted kinematic renormalization (section 4.3), the MS-bar Green function is to be interpreted as the shifted Green function, that is, it is expressed in the variable $\bar{\alpha}$, corresponding to α' in def. 112. The shifted renormalization condition (def. 111),

$$\bar{G}_{\mathcal{R}}(\bar{\alpha}, \epsilon, -\bar{\delta}) \stackrel{!}{=} 1, \tag{4.38}$$

represents a linear system for the expansion coefficients of the power series $\delta(\bar{\alpha}, \epsilon)$. In practice, finding the inverse series $\bar{\delta}(\bar{\alpha}, \epsilon)$ of eq. (4.38) is a computationally demanding task since we are dealing with a double series where the coefficients are large polynomials in π^2 and zeta values.

In solving eq. (4.38), observe that we are performing the transformations of section 4.3 in "reverse direction". Concretely, in section 4.3, we started with a MOM-renormalized amplitude, expressed as a function of α, and computed the shifted amplitude, expressed via $\bar{\alpha} = \alpha e^{-\epsilon\delta(\alpha,\epsilon)}$. In the present case, the coupling that we are using in MS represents $\bar{\alpha}$, and we have $\alpha = \bar{\alpha} e^{+\epsilon\bar{\delta}(\bar{\alpha},\epsilon)}$, where

$$\bar{\delta}(\bar{\alpha}, \epsilon) = \delta(\alpha(\bar{\alpha}, \epsilon), \epsilon). \tag{4.39}$$

If $G_{\mathcal{R}}(\alpha, \epsilon, L)$ is the solution of the same DSE in MOM, then

$$\bar{G}_{\mathcal{R}}(\bar{\alpha}, \epsilon, L) = G_{\mathcal{R}}(\alpha(\bar{\alpha}), \epsilon, L + \bar{\delta}(\bar{\alpha}, \epsilon)).$$

To be explicit: The shift $\delta(\alpha, \epsilon)$ that translates from MOM to MS, for $\epsilon \neq 0$, is not the same as the function $\bar{\delta}(\bar{\alpha}, \epsilon)$ in the opposite direction, because they depend on different variables. This conundrum disappears as soon as one consistently uses $\bar{\alpha}$ as the name of the coupling in MS, but it is not obvious from def. 108 why in MS, one would suddenly give a different name to the coupling compared to MOM. Owing to $\bar{\alpha} = \alpha + \mathcal{O}(\epsilon)$, the functions $\bar{\delta}(\bar{\alpha})$ and $\delta(\alpha)$ coincide for $\epsilon = 0$, so the distinction is unnecessary as long as we are only interested in $\epsilon = 0$.

Example 122: Multiedge linear DSE, brute force shift.

In example 116, we quoted the constant term $\bar{\gamma}_0(\bar{\alpha}, \epsilon)$, similarly, all higher $\bar{\gamma}_j(\bar{\alpha}, \epsilon)$ can be determined from the coefficients (example 111). Here, $\bar{\alpha}$ is merely the name of the variable, it is not computed from some underlying α. Knowing the power series $\bar{G}_{\mathcal{R}}(\bar{\alpha}, \epsilon, L)$, we obtain from eq. (4.38):

$$\begin{aligned}\bar{\delta}(\bar{\alpha}, \epsilon) = -2 + \frac{3}{2}\bar{\alpha} + \left(-\frac{19}{6} + \frac{2}{3}\zeta(3)\right)\bar{\alpha}^2 + \left(\frac{103}{12} - \frac{4}{3}\zeta(3)\right)\bar{\alpha}^3 + \dots \\ + \left(-2 + \frac{\pi^2}{12} + \left(\frac{9}{2} - 3\zeta(3)\right)\bar{\alpha} + \left(-\frac{403}{24} + \frac{\pi^2}{90} + 5\zeta(3)\right)\bar{\alpha}^2 + \dots\right)\epsilon + \mathcal{O}\left(\epsilon^2\right).\end{aligned}$$

With this, we compute $\alpha(\bar{\alpha}) = \alpha e^{+\epsilon\bar{\delta}(\bar{\alpha},\epsilon)}$. We invert the latter series to find $\bar{\alpha}(\alpha)$, which results in

$$\begin{aligned}\delta(\alpha, \epsilon) &= -\frac{1}{\epsilon}\ln\frac{\bar{\alpha}(\alpha)}{\alpha} = \bar{\delta}(\bar{\alpha}(\alpha), \epsilon) \\ &= -2 + \frac{3}{2}\alpha + \left(-\frac{19}{6} + \frac{2}{3}\zeta(3)\right)\alpha^2 + \left(\frac{103}{12} - \frac{4}{3}\zeta(3)\right)\alpha^2 + \dots \\ &\quad + \left(-2 + \frac{\pi^2}{12} + \left(\frac{15}{2} - 3\zeta(3)\right)\alpha + \left(-\frac{761}{24} + \frac{\pi^4}{90} + \frac{23}{3}\zeta(3)\right)\alpha^2 + \dots\right)\epsilon + \mathcal{O}\left(\epsilon^2\right).\end{aligned}$$

As expected, the functions δ and $\bar{\delta}$ coincide for $\epsilon = 0$, but they differ for $\epsilon \neq 0$.

4.4.3. Relation of the shift to renormalization group functions

The brute force method (eq. (4.38)) is computationally demanding for $\epsilon \neq 0$. It becomes significantly faster if we restrict ourselves to $\epsilon = 0$. In that case, the distinction eq. (4.39) does not exist, $\bar{\alpha} = \alpha$ and $\bar{\delta} = \delta$. Furthermore, we can accelerate the computation by exploiting the particular analytic structure of $\bar{G}_{\mathcal{R}}$.

First consider a linear DSE, $w = 0$. In MS-bar, it has a scaling solution eq. (4.6),

$$\bar{G}_{\mathcal{R}}(\alpha, L) = \bar{\gamma}_0(\alpha) \cdot L^{\gamma(\alpha)}. \tag{4.40}$$

By theorem 56, the anomalous dimension $\gamma(\alpha)$ of a linear DSE is independent of the renormalization scheme.

Theorem 65. Consider two perturbative solutions of the same linear Dyson-Schwinger equation (eq. (3.35) with $Q = 1$). Let $\gamma(\alpha)$ be the anomalous dimension and assume that both $\gamma_0(\alpha)$ and $\gamma_0'(\alpha) = 1 + \mathcal{O}(\alpha)$ are formal power series (def. 51) starting with unity. Then, the Green functions are equal up to an α-dependent shift δ (def. 111) given by the power series

$$\delta(\alpha) = \frac{1}{\gamma(\alpha)}\ln\left(\frac{\gamma_0'(\alpha)}{\gamma_0(\alpha)}\right).$$

Proof. In the linear case, $w = 0$, the renormalized Green function has the form eq. (4.40). Using def. 111, we demand $\gamma_0' = \gamma_0 \delta^\gamma$, which leads to the claimed formula. The functions $\gamma(\alpha), \gamma_0(\alpha)$ and $\gamma_0'(\alpha)$ are power series and $\gamma_0'(\alpha)/\gamma(\alpha) = 1 + \mathcal{O}(\alpha)$ by assumption. Therefore $\ln(\gamma_0'/\gamma_0) \in \mathcal{O}(\alpha)$ and the pole $1/\alpha$ of $1/\gamma(\alpha)$ from lemma 41 is cancelled. The claimed formula $\delta(\alpha) = \frac{1}{\gamma} \ln \frac{\gamma_0'}{\gamma_0}$ is a formal power series indeed. □

In MOM, we have $\gamma_0(\alpha) = 1$ by the renormalization condition def. 91. In MS-bar, the solution will have some $\bar{\gamma}_0(\alpha) \neq 1$. Theorem 65 thus specializes to

$$\delta(\alpha) = \frac{\ln \bar{\gamma}_0(\alpha)}{\gamma(\alpha)}. \tag{4.41}$$

Lemma 66. Consider a DSE of the form eq. (4.7) and let $f_n^{(k)}$ be the expansion coefficients of the kernel (eq. (4.9)). Then, the shift δ between MS-bar and MOM (def. 111), regardless of w, starts with

$$\delta(\alpha) = -\frac{f_0^{(0)}}{f_{-1}^{(0)}} + \mathcal{O}(\alpha).$$

Proof. By explicit calculation, the first coefficients of an explicit perturbative solution of eq. (4.7) in MOM respectively MS-bar are

$$\begin{aligned}
\gamma(\alpha) &= -f_{-1}^{(0)}\alpha + (w+1)\left(-2f_{-1}^{(0)}f_0^{(1)} - 2f_0^{(0)}f_{-1}^{(1)} + 2f_{-1}^{(0)}f_0^{(0)}\right)\alpha^2 + \mathcal{O}\left(\alpha^3\right), \\
\bar{\gamma}_1(\alpha) &= -f_{-1}^{(0)}\alpha + (w+1)\left(-2f_{-1}^{(0)}f_0^{(1)} - 2f_0^{(0)}f_{-1}^{(1)} + f_{-1}^{(0)}f_0^{(0)}\right)\alpha^2 + \mathcal{O}\left(\alpha^3\right), \\
\bar{\gamma}_0(\alpha) &= 1 + \alpha f_0^{(0)} + \mathcal{O}(\alpha^2), \qquad \alpha\partial_\alpha \hat{G}\big|_{x=1} = \alpha f_0^{(0)} + \mathcal{O}(\alpha^2).
\end{aligned}$$

Using theorems 39 and 63, the anomalous dimension in MS is

$$\bar{\gamma}(\alpha) = \frac{\bar{\gamma}_1(\alpha)}{\bar{\gamma}_0(\alpha) + w\alpha\partial_\alpha \bar{G}|_{x=1}} = \frac{\bar{\gamma}_1(\alpha)}{1 + (w+1)\alpha f_0^{(0)} + \mathcal{O}(\alpha^2)} = \gamma(\alpha) + \mathcal{O}\left(\alpha^3\right).$$

□

Note that $f_{-1}^{(0)} \neq 0$ in physically sensible kernels, because the pole $\frac{1}{\rho}$ in the "regulator" ρ expresses that the kernel graph is primitively divergent. Remarkably, $\delta(0) \neq 0$ unless $f_0^{(0)} = 0$, so the shift does not necessarily vanish for vanishing coupling. This result does not depend on the invariant charge in the DSE, but just on the kernel.

Example 123: Multiedge DSE, first order of shift.

For the multiedge DSE, the first coefficients $f_n^{(k)}$ are listed in example 109, $f_{-1}^{(0)} = 1$ and $f_0^{(0)} = 2$. By lemma 66,

$$\delta(\alpha) = -2 + \mathcal{O}(\alpha).$$

This coincides with our earlier finding in example 122.

Theorem 67. Let $G_{\mathcal{R}}(\alpha, x)$ and $\bar{G}_{\mathcal{R}}(\alpha, x)$ be the perturbative solutions of the same propagator-type Dyson-Schwinger equation eq. (4.7) with $w \neq 0$, where $G_{\mathcal{R}}$ uses kinematic renormalization and $\bar{G}_{\mathcal{R}}$ uses Minimal Subtraction. Assume that the anomalous dimensions (def. 110) $\gamma(\alpha), \bar{\gamma}(\alpha)$ are power series with a non-vanishing term $\propto \alpha$. Then there is a unique power series $\delta(\alpha)$ such that $G_{\mathcal{R}}(\alpha, L + \delta(\alpha)) = \bar{G}(\alpha, L)$ (def. 111) for all L, given by lemma 66 and

$$\frac{\partial}{\partial\alpha}\delta(\alpha) = \frac{1}{w\alpha}\left(\frac{1}{\bar{\gamma}(\alpha)} - \frac{1}{\gamma(\alpha)}\right) = \frac{\gamma(\alpha) - \bar{\gamma}(\alpha)}{w\alpha\bar{\gamma}(\alpha)\gamma(\alpha)}.$$

Proof. The fact *that* MS and MOM are related via a change in renormalization point is known from theorem 57. It remains to show that, in our setup, the shift $\delta(\alpha)$ is a well-defined power series.

From theorem 63 we know how shifting the kinematic renormalization point induces a change in the anomalous dimension. Solving the latter relation for $\delta(\alpha)$ produces the claimed expression.

By lemma 41 and point 2 of theorem 63, using the assumption, the denominator of the last fraction in the present theorem is proportional to α^3. But, since $\bar{\gamma}(\alpha)$ is the anomalous dimension in MS, the numerator is $\gamma(\alpha) - \hat{\gamma}(\alpha) \in \mathcal{O}(\alpha^3)$ by theorem 63. Therefore the right hand side is a well defined power series in α. It uniquely defines the power series $\delta(\alpha)$ up to a constant summand, which is fixed by lemma 66. □

Given the solutions of a DSE in MOM and MS-bar, there are at least three approaches to calculate $\delta(\alpha)$ from this data. The first approach uses theorem 67, where the anomalous dimensions $\gamma(\alpha), \hat{\gamma}(\alpha)$ can be extracted from the corresponding Z-factors according to def. 110.

The second approach utilizes the renormalization group equation in MS-bar derived in theorem 63,

$$(k+1)\bar{\gamma}_{k+1}(\alpha) = \frac{\gamma(\alpha)}{1 + w\gamma(\alpha)\alpha\partial_\alpha\delta(\alpha)} \cdot (1 + w\alpha\partial_\alpha)\,\bar{\gamma}_k(\alpha). \tag{4.42}$$

If any two of the MS functions $\hat{\gamma}_k(\alpha)$, together with the MOM anomalous dimension $\gamma(\alpha)$, are known, then $\delta(\alpha)$ can be computed. For example, using $\bar{\gamma}_0$ and $\bar{\gamma}_1$, one has

$$\frac{\partial}{\partial\alpha}\delta(\alpha) = \frac{\gamma \cdot \hat{\gamma}_0 - \bar{\gamma}_1}{w\alpha \cdot \bar{\gamma}_1} + \frac{1}{\bar{\gamma}_1}\frac{\partial}{\partial\alpha}\bar{\gamma}_0 \qquad (\text{for } w \neq 0). \tag{4.43}$$

The third approach is to compute all MS-bar functions $\bar{\gamma}_j(\alpha)$ up to some desired maximum j and additionally all MOM functions $\gamma_j(\alpha)$. Next, one writes a power series ansatz for $\delta(\alpha)$ and uses this to formally compute the powers $\delta(\alpha)^k$. Then the right side of eq. (4.37),

$$G'_{\mathcal{R}}(\alpha', \epsilon, L) := \sum_{j=0}^{\infty} \gamma'_j(\alpha', \epsilon) L^j \tag{4.44}$$

is a linear system for the unknown coefficients of $\delta(\alpha)$ which can be solved.

The resulting $\delta(\alpha)$ agrees in all three approaches. The difference between them is about which input data they need, and how computationally efficient they are. The third approach does not involve a derivative and therefore it produces one order higher in α compared to the first two, for the same order of input data.

In all approaches, we need both the MOM- and the MS-bar solution in order to compute $\delta(\alpha)$. As long as we restrict ourselves to $\epsilon = 0$, it is not possible to obtain $\delta(\alpha)$ without knowing data from both of the renormalized Green functions.

4.4.4. Deriving the shift from the MOM solution

As outlined above, we can find the shift function $\delta(\alpha, \epsilon)$ if we are given two different renormalized Green functions. On the other hand, for $\epsilon = 0$, the renormalization point is really only a single number, and the rest of the Green function is determined from the DSE. It is therefore conceivable that one can alternate between MOM and MS from first principles, without needing to explicitly know both Green functions.

Def. 108 makes explicit reference to the ϵ-dependence of counterterms. This already indicates that in order to go from MOM to MS or vice versa, we need to know the solution in one of the schemes for $\epsilon \neq 0$. For systematic derivations, we need an analytic statement comparable to the condition $G_{\mathcal{R}}(\alpha, \epsilon, 0) = 1$ for MOM. This is theorem 54, the condition that the shifted anomalous dimension $\gamma'(\alpha, \epsilon)$ is independent of ϵ.

Theorem 68. Consider a linear DSE of type eq. (3.38). Let $\gamma(\alpha, \epsilon) = \partial_L G_{\mathcal{R}}(\alpha, \epsilon, L)|_{L=0}$ be the anomalous dimension in MOM. Then, the solution in MS-bar at $L = 0$ has the amplitude

$$G_{\bar{\mathcal{R}}}(\alpha, \epsilon, L = 0) = \bar{\gamma}_0(\alpha, \epsilon) = \exp\left(- \int_0^\alpha \mathrm{d}u \, \frac{\gamma(u, \epsilon) - \gamma(u, 0)}{u\epsilon} \right).$$

Here, $G_{\bar{\mathcal{R}}}(\alpha, \epsilon, L)$ is a function of α, not of $\bar{\alpha}$, compare eq. (4.32) to eq. (4.35).

Proof. Use lemma 64, where γ' represents the anomalous dimension in MS. By theorem 54, the latter is independent from ϵ. By theorem 63, it coincides with the MOM anomalous dimension $\gamma(\alpha)$ for $\epsilon = 0$. Therefore

$$\bar{\gamma}(\alpha, \epsilon) = \gamma(\alpha) + \epsilon \partial_\alpha \ln \bar{\gamma}_0(\alpha, \epsilon).$$

In lemma 64, α' is merely a renamed variable, since all quantities are functions of α'. □

Lemma 69. Consider a linear DSE of type eq. (3.38) for $\epsilon = 0$, where $\gamma(\alpha)$ is the anomalous dimension and $g(\alpha)$ is the coefficient given by theorem 47. Then, the shift between MS and MOM (def. 111) is

$$\delta(\alpha) = -\frac{1}{\gamma(\alpha)} \int_0^\alpha \frac{\mathrm{d}u}{u} \, g(u).$$

Proof. For a linear DSE, γ_0' directly corresponds to δ via theorem 65. Insert theorem 68 into eq. (4.41):

$$\delta(\alpha) = \frac{1}{\gamma(\alpha)} [\epsilon^0] \ln \bar{\gamma}_0(\alpha) = -\frac{1}{\gamma(\alpha)} [\epsilon^0] \int_0^\alpha \mathrm{d}u \, \frac{\gamma(u, \epsilon) - \gamma(u, 0)}{u\epsilon}$$

□

The further transition from MS-bar to MS is a trivial rescaling, discussed in section 4.2 and in [480]. Using lemma 69 and theorem 47, we can indeed deduce the MS amplitude of a linear DSE directly from the Mellin transform in a comparable way as we can for MOM (theorem 44). Especially, we can obtain the solution in MS with purely analytic operations, without solving the DSE order by order. This result represents one of the key findings of the present thesis.

Example 124: Multiedge linear DSE, exact shift.

From example 106, we know

$$g(\alpha) = 1 + \frac{\alpha}{1+4\alpha} + \frac{\gamma(\alpha)+1}{2\gamma(\alpha)+1}\left(2\gamma(\alpha)\cdot\gamma_E + \rho\partial_\rho \ln\frac{\Gamma(1+\rho)}{\Gamma(1-\rho)}\Big|_{\rho\to\gamma(\alpha)} - 1\right),$$

where $\gamma = \frac{1}{2}\left(\sqrt{1+4\alpha}-1\right)$ from example 104. This function satisfies $\frac{\mathrm{d}\gamma(\alpha)}{\mathrm{d}\alpha} = \frac{1}{\sqrt{1+4\alpha}} = \frac{1}{2\gamma(\alpha)+1}$. Consequently, $\frac{\mathrm{d}u}{2\gamma(u)+1} = \mathrm{d}\gamma(u)$. Upon integration, we obtain

$$\ln\bar{\gamma}_0(\alpha) = -\int_0^\alpha \frac{\mathrm{d}u}{u} g(u) = \ln\frac{\gamma(\alpha)}{\alpha} - \frac{1}{4}\ln(1+4\alpha) - 2\gamma(\alpha)\gamma_E + \ln\frac{\Gamma(1-\gamma(\alpha))}{\Gamma(1+\gamma(\alpha))}.$$

This confirms the formula we had found empirically in example 116. By lemma 69, the shift between MS-bar and MOM is

$$\begin{aligned}\bar{\delta}(\alpha) = \frac{\ln\bar{\gamma}_0(\alpha)}{\gamma(\alpha)} &= \frac{1}{\gamma(\alpha)}\ln\frac{\gamma(\alpha)}{\alpha} - \frac{\ln(1+4\alpha)}{4\gamma(\alpha)} - 2\gamma_E + \frac{1}{\gamma(\alpha)}\ln\frac{\Gamma(1-\gamma(\alpha))}{\Gamma(1+\gamma(\alpha))} \\ &= -2 + \frac{3}{2}\alpha + \left(-\frac{19}{6} + \frac{2}{3}\zeta(3)\right)\alpha^2 + \left(\frac{103}{12} - \frac{4}{3}\zeta(3)\right)\alpha^3 + \dots\end{aligned}$$

The first coefficient coincides with example 123. We stress again that this shift $\bar{\delta}(\alpha)$ was derived exactly and from first principles, without heuristically matching a series expansion and without doing any explicit calculation in MS-bar.

Example 125: Toy model linear DSE, exact shift.

For the linear toy model DSE (example 102), the function $\bar{\gamma}_0(\alpha)$ is particularly simple, see example 118. Using lemma 69, we conclude

$$\delta(\alpha) = \frac{\pi\ln\left(1-\alpha^2\pi^2\right)}{4\arcsin(\alpha\pi)} = -\frac{\pi^2}{4}\alpha - \frac{\pi^4}{12}\alpha^3 - \frac{73\pi^6}{1440}\alpha^5 - \mathcal{O}(\alpha^7),$$

Observe that this time, the constant coefficient $[\alpha^0]\delta(\alpha)$ vanishes, in accordance with lemma 66, since for the toy model $f_0 = f_0^{(0)} = 0$.

Summary of section 4.4.

1. Each of the two renormalization schemes MS and MOM has conceptually unique features which make them indispensable in certain applications. Therefore, it is highly desirable to find the precise relation between the two Green functions, in the form of a shift $\delta(\alpha, \epsilon)$ of the renormalization point (section 4.4.1).

2. Knowing the MS-solution explicitly to some finite order in perturbation theory, one can compute $\delta(\alpha, \epsilon)$ by finding the point where the amplitude is unity (section 4.4.2).

3. Skipping the full ϵ-dependence, one can infer $\delta(\alpha)$ in various ways from the log-expansion of the MS-solution (section 4.4.3). For a linear DSE, $\delta(\alpha)$ is determined explicitly from $\gamma(\alpha)$ and $\bar{\gamma}_0(\alpha)$ alone (theorem 65).

4. Conceptually, it is possible to derive $\delta(\alpha, \epsilon)$ and the full MS-solution from the MOM-solution at $\epsilon \neq 0$ (section 4.4.4), which in turn only depends on the Mellin transform of the kernel. For linear DSEs, we derived an explicit formula which allows to compute $\delta(\alpha)$ from a given, ϵ-dependent Mellin transform (lemma 69 and theorem 47).

4.5. Shift between MS and MOM in non-linear examples

In the present section, we present empirical results for the shift $\delta(\alpha)$ for non-linear Dyson-Schwinger equations, computed with the methods discussed in section 4.4.3.

4.5.1. Multiedge DSE in D=4 dimensions

The multiedge DSE was introduced in example 103. The shift between MS and MOM can be derived exactly in the linear case (example 124). For the non-linear versions of the DSE, the solutions in kinematic renormalization have been discussed in section 3.4.1. Again, we restrict ourselves to MS-bar and skip the transformation to MS.

We computed the coefficients $g_{t,r}^{(n)}$ of section 4.2 in MS for $w \in \{-5, \dots, +5\}$ symbolically at least up to order α^{11}. By using numerical approximations of the various constants $\zeta(n)$ and π^m, we reached order α^{20}. It was verified in all cases that the first three orders of the leading-log expansion fulfil eq. (3.42). The shift from MOM- to MS-bar-renormalization has been computed as discussed in section 4.4.3. The first coefficients are reported in table 4.1.

w	$\bar{\delta}(\alpha)$	f_{n+1}/f_n
5	$-2 + 9\alpha + (-139 + 14\zeta(3))\,\alpha^2 + \left(3464 + \frac{7\pi^4}{12} - 233\zeta(3)\right)\alpha^3$	30.22 ± 0.09
4	$-2 + \frac{15}{2}\alpha + \left(-\frac{575}{6} + 10\zeta(3)\right)\alpha^2 + \left(\frac{23525}{12} + \frac{\pi^4}{3} - \frac{410}{3}\zeta(3)\right)\alpha^3$	25.09 ± 0.06
3	$-2 + 6\alpha + \left(-\frac{182}{3} + \frac{20}{3}\zeta(3)\right)\alpha^2 + \left(\frac{2911}{3} + \frac{\pi^4}{6} - \frac{214}{3}\zeta(3)\right)\alpha^3$	19.96 ± 0.04
2	$-2 + \frac{9}{2}\alpha + \left(\frac{-67}{2} + 4\zeta(3)\right)\alpha^2 + \left(\frac{773}{2} + \frac{\pi^4}{15} - 31\zeta(3)\right)\alpha^3$	14.80 ± 0.02
1	$-2 + 3\alpha + \left(-\frac{43}{3} + 2\zeta(3)\right)\alpha^2 + \left(\frac{305}{3} + \frac{\pi^4}{60} - \frac{29}{3}\zeta(3)\right)\alpha^3$	9.60 ± 0.01
0	$-2 + \frac{3}{2}\alpha + \left(-\frac{19}{6} + \frac{2}{3}\zeta(3)\right)\alpha^2 + \left(\frac{103}{12} - \frac{4}{3}\zeta(3)\right)\alpha^3$	
-1	-2	
-2	$-2 - \frac{3}{2}\alpha - \frac{29}{6}\alpha^2 - \left(\frac{94}{3} - \frac{1}{3}\zeta(3)\right)\alpha^3$	5.8 ± 1.8
-3	$-2 - 3\alpha + \left(-\frac{53}{3} + \frac{2}{3}\zeta(3)\right)\alpha^2 - \left(\frac{578}{3} + \frac{\pi^4}{60} - \frac{17}{3}\zeta(3)\right)\alpha^3$	10.50 ± 0.11
-4	$-2 - \frac{9}{2}\alpha + \left(-\frac{77}{2} + 2\zeta(3)\right)\alpha^2 - \left(\frac{2365}{4} + \frac{\pi^4}{15} - 22\zeta(3)\right)\alpha^3$	15.69 ± 0.05
-5	$-2 - 6\alpha + \left(-\frac{202}{3} + 4\zeta(3)\right)\alpha^2 - \left(\frac{4003}{3} + \frac{\pi^4}{6} - \frac{166}{3}\zeta(3)\right)\alpha^3$	20.85 ± 0.07

Table 4.1.: Non-linear multiedge DSE in $D = 4$ dimensions. $\bar{\delta}(\alpha)$ is the shift of the renormalization point between MOM- and MS-scheme def. 111. Shown are the first four terms of its perturbative power series. f_{n+1}/f_n is the growth rate of the function $f(\alpha)$ to be introduced in eq. (4.53).

We are interested in the asymptotic behaviour of the power series $\bar{\delta}(\alpha)$ at high order. To this end, we use the expansion eq. (3.44),

$$\gamma(\alpha) =: \sum_{j=1}^{\infty} c_j \alpha^j, \qquad \bar{\delta}(\alpha) := \sum_{j=0}^{\infty} d_j \alpha^j. \tag{4.45}$$

The asymptotics of c_j in MOM is known from eq. (3.50). To visualize it, we consider

$$\frac{c_{n+1}/\Gamma(n+1-\beta(w))}{-c_n/\Gamma(n-\beta(w))} \equiv \frac{-c_{n+1}}{(n+\frac{3+2w}{w})c_n} = w - b^{(1)}(w)\frac{1}{n^2} + \mathcal{O}\left(\frac{1}{n^3}\right). \tag{4.46}$$

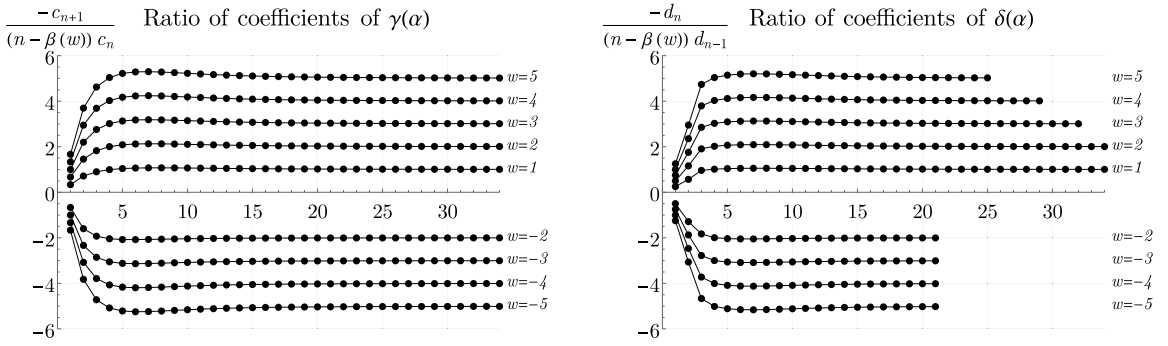

(a) (b)

Figure 4.4.: (a) Ratio of successive coefficients c_n of $\gamma(\alpha) = \sum c_n \alpha^n$ for the multiedge DSE in $D = 4$ dimensions. The denominator $(n - \beta(w))$ is chosen to match the known asymptotics eq. (3.50). The ratio quickly converges towards the limit w, see eq. (4.46). (b) Ratio of successive coefficients d_n from eq. (4.45). This ratio behaves very similarly to the ratio in (a).

There is no $1/n$ correction to this quantity, hence it converges quickly, see Figure 4.4 (a).

Similarly to eq. (4.46), we examine the ratio of successive d_n,

$$\frac{-d_n}{(n-\beta(w))d_{n-1}} = \frac{-d_n}{(n+\frac{3+2w}{w})d_{n-1}}, \tag{4.47}$$

where we used the same parameter $\beta(w) = \frac{-3-2w}{w}$ (from eq. (3.49)) as in eq. (4.46). A priori, this choice is a guess, but the results shown in fig. 4.4 (b), suggest that it is correct. Consequently, we write for d_n an ansatz similar to eq. (3.50),

$$d_n \sim \tilde{S}(w) \cdot (-\tilde{F}(w))^n \cdot \Gamma\left(n - \tilde{\beta}(w)\right) \left(1 + \frac{\tilde{b}^{(1)}(w)}{(n - \tilde{\beta}(w) - 1)} + \dots\right). \tag{4.48}$$

We extract the free parameters using Richardson extrapolation (def. 59) of orders 2,3,4 and 5 and take their mean as the estimation and the largest absolute difference between any of these as uncertainty. Experiments with the coefficients c_n of $\gamma(\alpha)$ show that this procedure likely overestimates the uncertainties. The results are reported in table 4.2. They are consistent with $\tilde{S}(w) = w \cdot S(w), \tilde{F}(w) = w$ and $\tilde{\beta}(w) = \beta(w) - 1$ within around 1% relative uncertainty. Unlike the analysis of $\gamma(\alpha)$ in section 3.4.1, at this level of uncertainty, our findings of "rational numbers" are to be understood as educated guesswork rather than numerical proofs. The estimates obtained for $\tilde{b}^{(1)}(w)$ are too imprecise to deduce a formula at this point.

Motivated by the formula eq. (4.48), we directly compare the coefficients d_n to c_{n+1}. Using eq. (4.48) with table 4.2, we expect that $d_n/c_{n+1} \to 1$. By eq. (3.49), $w \cdot \lambda(w) = 1$ in our case, but we include this factor for consistency, and examine the ratio

$$\frac{-d_n}{w\lambda c_{n+1}} \sim r(w) + r_1(w)\frac{1}{n} + r_2(w)\frac{1}{n^2} + \dots, \qquad n \to \infty. \tag{4.49}$$

This ratio is plotted in fig. 4.5.

As before, the free parameters of eq. (4.49) are extracted using Richardson extrapolation (def. 59). We confirm numerically that $r(w) = 1 \pm 10^{-5}$. The results for the corrections r_j

w	$n_{\max}$	$\tilde{S}(w)/w$	$\tilde{F}(w)$	$\tilde{\beta}(w)$	$\tilde{b}^{(1)}(w)$
5	24	-0.02532 ± 0.00037	4.987 ± 0.062	-3.59 ± 0.12	-2.61 ± 0.18
4	27	-0.02709 ± 0.00019	3.993 ± 0.036	-3.74 ± 0.08	-2.79 ± 0.11
3	32	-0.02749 ± 0.00011	2.997 ± 0.017	-3.99 ± 0.04	-3.10 ± 0.06
2	38	-0.02272 ± 0.00010	1.999 ± 0.009	-4.50 ± 0.03	-3.74 ± 0.05
1	38	-0.00541 ± 0.00009	0.999 ± 0.007	-6.00 ± 0.04	-5.97 ± 0.12
-2	21	0.2080 ± 0.0018	-1.998 ± 0.012	-1.49 ± 0.05	-0.74 ± 0.08
-3	21	0.1295 ± 0.0014	-2.995 ± 0.026	-1.99 ± 0.07	-1.10 ± 0.11
-4	21	0.0882 ± 0.0011	-3.993 ± 0.040	-2.24 ± 0.09	-1.30 ± 0.14
-5	21	0.0655 ± 0.0009	-4.991 ± 0.054	-2.40 ± 0.10	-1.43 ± 0.15

Table 4.2.: Numerical findings of the growth parameters of $\bar{\delta}(\alpha)$ according to eq. (4.48). They are consistent with table 3.2 and eq. (3.49). $\bar{\delta}(\alpha)$ was computed including order $\alpha^{n_{\max}}$.

are reported in table 4.3. We emphasize the relatively low uncertainties, which indicate that the ratio eq. (4.49) converges quickly. From the numerical results, we guess the expressions

$$r(w) = 1, \qquad r_1(w) = \frac{w+1}{w}, \qquad r_{j\geq 2}(w) = 0. \tag{4.50}$$

Together with the known behaviour of c_{n+1} (eq. (3.50)), and $\beta(w) = -(3+2w)/w$, we can give an explicit formula for the corrections to the leading asymptotics of d_n:

$$\begin{aligned} d_n \sim\ & S(w)(-w)^{n+1}\Gamma\left(n-\beta(w)+1\right) \\ & \cdot\left(1 + \frac{-\frac{1+3w+2w^2}{w^2}}{n-\beta(w)} + \frac{\frac{1+4w+4w^2-6w^3-7w^4}{2w^4}}{(n-\beta(w))(n-\beta(w)-1)} + \mathcal{O}\left(\frac{1}{n^3}\right)\right). \end{aligned} \tag{4.51}$$

The subleading coefficient is consistent with the value $\tilde{b}^{(1)}(w)$ which we found in table 4.2.

w	$r_1(w)$	$r_2(w)$	$r_3(w)$	$r_4(w)$	$r_5(w)$
5	1.20002 ± 0.00012	0.0003 ± 0.0019	0.005 ± 0.031	0.09 ± 0.50	1.3 ± 7.9
4	1.25000 ± 0.00001	0.0000 ± 0.0002	0.000 ± 0.003	0.01 ± 0.05	0.18 ± 0.95
3	1.33333 ± 0.00001	0.0000 ± 0.0001	0.000 ± 0.001	0.01 ± 0.01	0.00 ± 0.02
2	1.50000 ± 0.00001	0.0000 ± 0.0001	0.000 ± 0.001	0.00 ± 0.01	0.00 ± 0.01
1	2.00000 ± 0.00001	0.0000 ± 0.0001	0.000 ± 0.001	0.00 ± 0.01	0.00 ± 0.01
-2	0.50000 ± 0.00001	0.0000 ± 0.0001	0.000 ± 0.001	0.00 ± 0.01	0.00 ± 0.02
-3	0.66667 ± 0.00001	0.0000 ± 0.0002	0.000 ± 0.002	0.01 ± 0.03	0.07 ± 0.39
-4	0.75001 ± 0.00004	0.0001 ± 0.0005	0.001 ± 0.007	0.02 ± 0.09	0.20 ± 1.24
-5	0.80001 ± 0.00006	0.0002 ± 0.0009	0.002 ± 0.012	0.03 ± 0.17	0.4 ± 2.3

Table 4.3.: Parameters of the ratio d_n/c_{n+1} for $D = 4$ from eq. (4.49). $r_0 = 1$ is not included, $r_{\geq 2}$ is consistent with zero as claimed in eq. (4.50).

For the higher order corrections in table 4.3, the uncertainties are increasing. If we nonetheless speculate that eq. (4.50) is correct for all r_j, we obtain

$$d_n = -\left(1 + \frac{w+1}{wn}\right) \cdot c_{n+1} + e_n. \tag{4.52}$$

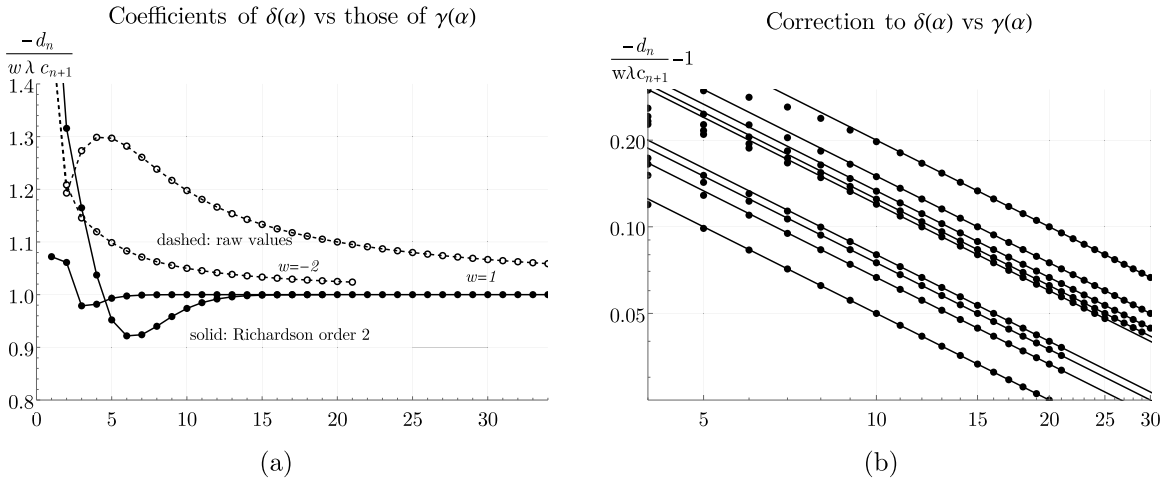

(a) (b)

Figure 4.5.: (a) Ratio of the coefficients of $\delta(\alpha) = \sum d_n \alpha^n$ and $\gamma(\alpha) = \sum c_n \alpha^n$. Shown are two representative sequences, namely $w = -2$ and $w = 1$. For each of them, the dashed line indicates the raw values while the solid line is the order-2 Richardson extrapolation. The ratio $-d_n/c_{n+1}$ approaches unity in the limit $n \to \infty$. (b) Correction to this ratio. Each sequence corresponds to one value of w. Solid lines are the functions $\frac{w+1}{wn}$, they match the points surprisingly well even for low orders. The remaining difference falls of faster than $1/n^2$.

The numerical values suggest that the remainder e_n falls off factorially, see fig. 4.6 (a). This asymptotic statement for factorially divergent power series (section 2.1.1) can be translated to a relation between the corresponding generating functions[1]:

$$\bar{\delta}(\alpha) = -\frac{\gamma(\alpha)}{\alpha} - \frac{w+1}{w} \int^{\alpha} \frac{\mathrm{d}a}{a} \frac{\gamma(a)}{a} + f(\alpha), \qquad w \neq 0. \tag{4.53}$$

From our data, we can extract the first coefficients of the power series $f(\alpha) := \sum_{n=1}^{\infty} f_n \alpha^n$. These coefficients contain, besides rational factors, zeta values, which appear in $\delta(\alpha)$ but not in $\gamma(\alpha)$, so they can not arise from the first two summands of eq. (4.53). Figure 4.6 (b) suggests that the coefficients f_n grow geometrically, not factorially. The growth rate is reported in the last column of table 4.1. This geometric growth indicates that $f(\alpha)$ is a convergent power series around $\alpha = 0$.

[1]The author thanks Michael Borinsky for pointing out this implication of eq. (4.52).

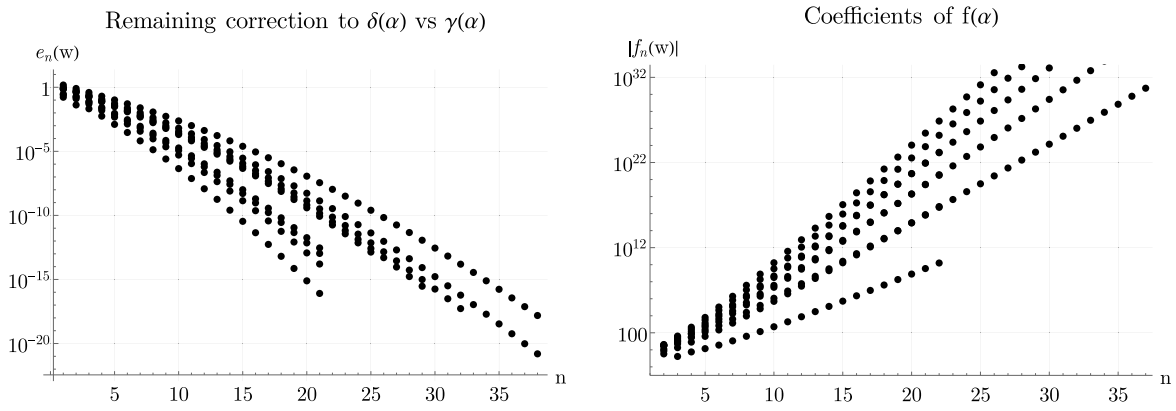

Figure 4.6.: (a) Remainder coefficients e_n from eq. (4.52), for different values of w. This is a logarithmic plot, they decay faster than exponentially. (b) Coefficients of the function $f(\alpha)$ in eq. (4.53). The data points overlap for different w. The coefficients grow geometrically, which suggests that $f(\alpha)$ is an analytic function.

4.5.2. Multiedge DSE in D=6 dimensions

w	$\delta(\alpha)$
5	$-\frac{8}{3}-\frac{61}{24}\alpha+\left(-\frac{80213}{7776}+\frac{7}{18}\zeta(3)\right)\alpha^2-\left(\frac{8813575}{139968}+\frac{7\pi^4}{2592}-\frac{2563}{1296}\zeta(3)\right)\alpha^3$
4	$-\frac{8}{3}-\frac{305}{144}\alpha+\left(-\frac{331345}{46656}+\frac{5}{18}\zeta(3)\right)\alpha^2-\left(\frac{119812205}{3359232}+\frac{\pi^4}{648}-\frac{2255}{1944}\zeta(3)\right)\alpha^3$
3	$-\frac{8}{3}-\frac{61}{36}\alpha+\left(-\frac{52325}{11664}+\frac{5}{27}\zeta(3)\right)\alpha^2-\left(\frac{14842891}{839808}+\frac{\pi^4}{1296}-\frac{1177}{1944}\zeta(3)\right)\alpha^3$
2	$-\frac{8}{3}-\frac{61}{48}\alpha+\left(-\frac{38381}{15552}+\frac{1}{9}\zeta(3)\right)\alpha^2-\left(\frac{3947825}{559872}+\frac{\pi^4}{3240}-\frac{341}{1296}\zeta(3)\right)\alpha^3$
1	$-\frac{8}{3}-\frac{61}{72}\alpha+\left(-\frac{24437}{23328}+\frac{1}{18}\zeta(3)\right)\alpha^2+\left(\frac{1560359}{839808}+\frac{\pi^4}{12960}-\frac{319}{3888}\zeta(3)\right)\alpha^3$
0	$-\frac{8}{3}-\frac{61}{144}\alpha+\left(-\frac{10493}{46656}+\frac{1}{54}\zeta(3)\right)\alpha^2+\left(\frac{518095}{3359232}-\frac{11}{972}\zeta(3)\right)\alpha^3$
-1	$-\frac{8}{3}$
-2	$-\frac{8}{3}+\frac{61}{144}\alpha-\frac{17395}{46656}\alpha^2-\left(-\frac{114361}{209952}+\frac{11}{3888}\zeta(3)\right)\alpha^3$
-3	$-\frac{8}{3}+\frac{61}{72}\alpha+\left(\frac{31339}{23328}+\frac{1}{54}\zeta(3)\right)\alpha^2-\left(-\frac{359005}{104976}-\frac{\pi^4}{12960}+\frac{187}{3888}\zeta(3)\right)\alpha^3$
-4	$-\frac{8}{3}+\frac{61}{48}\alpha+\left(-\frac{45283}{15552}+\frac{1}{18}\zeta(3)\right)\alpha^2-\left(-\frac{11830593}{1119744}-\frac{\pi^4}{3240}+\frac{121}{648}\zeta(3)\right)\alpha^3$
-5	$-\frac{8}{3}+\frac{61}{36}\alpha+\left(-\frac{59227}{11664}+\frac{1}{9}\zeta(3)\right)\alpha^2-\left(-\frac{20089615}{839808}-\frac{\pi^4}{1296}+\frac{913}{1944}\zeta(3)\right)\alpha^3$

Table 4.4.: First perturbative coefficients of $\delta(\alpha)$ for $D = 6$ dimensions.

For the 6-dimensional case (example 103), the procedure is completely analogous to the one described in the previous section 4.5.1. We use the same symbols as in the $D = 4$ case in order to not clutter notation. Again, results for the linear DSE have been reported earlier (examples 104 and 117) and will not be discussed here.

The power series coefficients of the shift $\bar{\delta}(\alpha)$ have been computed symbolically up to order α^{10}, and numerically at least to order α^{20}, the first coefficients are reported in table 4.4. The ratio of successive coefficients (eq. (4.47)), this time with $\beta(w)$ from table 4.5, is shown in fig. 4.7(a). The plot suggests that d_n grow at a similar rate as c_n.

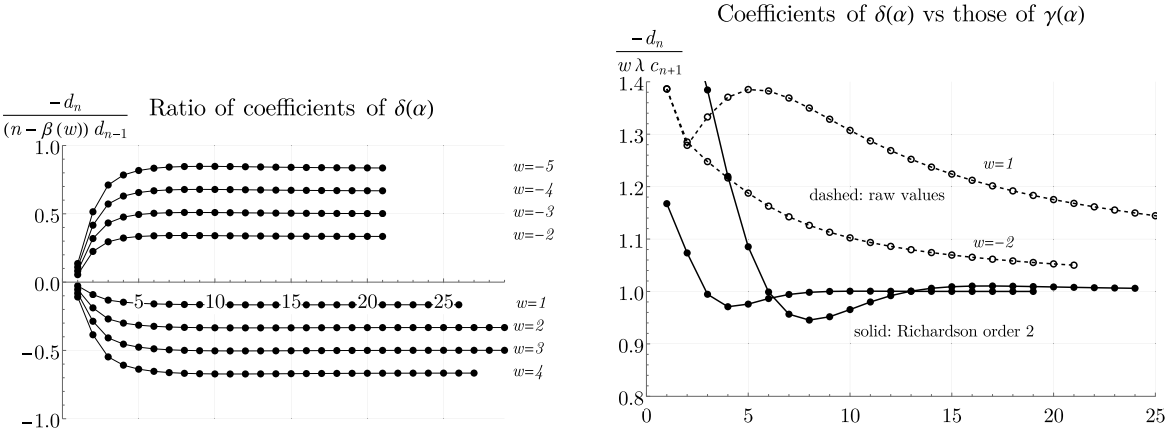

(a) (b)

Figure 4.7.: (a) Ratio of successive coefficients d_n of $\delta(\alpha)$ (eq. (4.45)), divided by the assumed leading asymptotic behaviour from eq. (3.55), for the multiedge DSE in $D = 6$. This quantity quickly approaches the limit $-w/6$. (b) Ratio between the coefficients d_n of $\delta(\alpha)$ and the coefficients c_{n+1} of $\gamma(\alpha)$. Compared to fig. 4.5 (a), the Richardson extrapolation converges slower, indicating a significant $1/n^2$-correction, see table 4.6.

We extracted numerical estimates of the parameters in eq. (4.48) with the procedure explained in section 4.5.1. The results are reported in table 4.5 and are consistent with $\tilde{S}(w) = w \cdot S(w), \tilde{F}(w) = -w/6$ and $\tilde{\beta}(w) = \beta_1(w) - 1$.

w	$n_{\max}$	$10^6 \cdot \tilde{S}(w)/w$	$\tilde{F}(w)$	$\tilde{\beta}(w)$
5	24	-50.1 ± 4.5	-0.833 ± 0.018	-7.00 ± 0.37
4	27	-34.5 ± 2.4	-0.666 ± 0.012	-7.25 ± 0.23
3	29	-16.6 ± 1.2	-0.500 ± 0.007	-7.72 ± 0.19
2	29	-2.97 ± 0.28	-0.333 ± 0.006	-8.68 ± 0.26
1	26	-0.0054 ± 0.0015	-0.167 ± 0.006	-11.64 ± 0.75
-2	21	87900 ± 1600	0.333 ± 0.005	-2.92 ± 0.12
-3	21	18000 ± 560	0.500 ± 0.009	-3.90 ± 0.21
-4	21	6690 ± 290	0.666 ± 0.013	-4.39 ± 0.26
-5	21	3410 ± 180	0.833 ± 0.018	-4.69 ± 0.29

Table 4.5.: Numerical findings of the growth parameters of $\bar{\delta}(\alpha)$ for the $D = 6$ multiedge DSE, according to eq. (4.48). They are consistent with eq. (3.55) and table 3.3.

The ratio from eq. (4.49),

$$\frac{-d_n}{w\lambda(w)c_{n+1}} = \frac{d_n}{6c_{n+1}},$$

w	$r(w)$	$r_1(w)$	$r_2(w)$
5	1.0010 ± 0.0017	2.573 ± 0.072	-6.91 ± 0.84
4	1.0007 ± 0.0019	2.685 ± 0.072	-7.3 ± 1.4
3	1.0007 ± 0.0024	2.863 ± 0.078	-8.4 ± 1.8
2	1.0010 ± 0.0026	3.21 ± 0.11	-11.2 ± 1.8
1	1.0032 ± 0.0048	4.22 ± 0.23	-22.3 ± 1.3
-2	1.0000 ± 0.0002	1.083 ± 0.003	-1.10 ± 0.34
-3	1.0002 ± 0.0004	1.441 ± 0.012	-1.80 ± 0.07
-4	1.0003 ± 0.0007	1.619 ± 0.018	-2.33 ± 0.16
-5	1.0004 ± 0.0008	1.726 ± 0.022	-2.71 ± 0.22

Table 4.6.: Numerical parameters of the ratio $d_n/(6c_{n+1})$ for $D = 6$ from eq. (4.49).

is depicted in fig. 4.7 (b) for two particular values of w. The asymptotic parameters, according to eq. (4.49), are reported in table 4.6. Unlike for $D = 4$, this ratio does not converge particularly quickly. A fit suggests that $r_1(w) = (2.12 + 2.15w)/w$, but the uncertainties are too large to identify the numbers as rational. This is reflected by the large absolute values we obtain for the $1/n^2$-correction $r_2(w)$, see table 4.6.

For $D = 4$ (section 4.5.1), the suspected vanishing of $r_{j\geq 2}$ allowed us to explicitly deduce the asymptotics of d_n, eq. (4.51). This is not possible in $D = 6$ since the $r_{j\geq 2}$ do not vanish. Our findings suggest that the leading growth coincides with the one of c_{n+1}, that is

$$d_n \sim S(w) w \left(\frac{w}{6}\right)^n \Gamma\left(n + 1 + \frac{35 + 29w}{6w}\right). \tag{4.54}$$

4.5.3. Toy model

The DSE of the toy model was introduced in example 102, the shift for the linear case is given in example 125.

We solved the non-linear toy model DSE for $w \in \{-5, \dots, +4\}$ symbolically to order α^{16}. Numerically, we reached order α^{23}, but since $c_n = 0$ for every even n, we effectively have only 12 coefficients at our disposal for asymptotic analysis.

The leading-log functions H_1, H_2 and H_3 agree with the general formula eq. (3.42) of [380] for the appropriate choice $c_1 = 1, c_2 = 0, c_3 = \pi^2/2$ and for all values of w. Especially, we confirm $H_2 = H_4 = H_6 = 0$, and, for $w = -2$, the formula for H_1 from [308, Cor. 3.6.4].

By lemma 66, the shift $\delta(\alpha)$ does not have a constant term in the toy model, compare example 125. We compute and analyze the series expansion eq. (4.45) of the shift in the same way we did in sections 4.5.1 and 4.5.2 for the multiedge DSE. The first coefficients for the shift are reported in table 4.8, while table 4.7 contains the numerical estimates for their growth parameters.

The toy model has the property that both c_n and d_n from eq. (4.45) vanish for even n. Consequently, the ratio eq. (4.49) is not well defined. Instead, we mimic the latter ratio by considering the following two ratios for odd n:

$$R^{(\delta)} := \sqrt{\frac{d_{n+2}}{(n - \beta(w) + 1)(n - \beta(w) + 2)d_n}}, \qquad R^{(\delta/\gamma)} := \frac{d_n}{w \cdot (n - \beta(w) + 1)c_n}. \tag{4.55}$$

w	$n_{\max}$	$\tilde{S}(w)/w$	$\tilde{F}(w)$	$\tilde{\beta}(w)$
4	23	-0.389 ± 0.010	3.985 ± 0.081	-2.50 ± 0.21
3	23	-0.485 ± 0.015	2.988 ± 0.068	-2.68 ± 0.24
2	23	-0.612 ± 0.023	1.991 ± 0.059	-3.02 ± 0.31
1	23	-0.572 ± 0.037	0.996 ± 0.056	-4.09 ± 0.56
-2	23	0.6382 ± 0.0067	1.997 ± 0.012	-0.991 ± 0.050
-3	23	0.5275 ± 0.0076	2.994 ± 0.024	-1.322 ± 0.071
-4	23	0.4202 ± 0.0069	3.991 ± 0.037	-1.488 ± 0.082
-5	23	0.3443 ± 0.0060	4.988 ± 0.051	-1.588 ± 0.088

Table 4.7.: Numerical findings of the growth parameters of $\bar{\delta}(\alpha)$ in the toy model, according to eq. (4.48). $\tilde{S}(w)$ is consistent with table 3.4.

Figure 4.8 (a) indicates that $R^{(\delta)}$ approaches the limit $|w|$, which suggests that d_n scale asymptotically $\sim w^n \Gamma(n - \beta(w) + 1)$, with (approximately) the same $\beta(w)$ (eq. (3.57)) as the coefficients c_n of $\gamma(\alpha)$.

The quantity $R^{(\delta/\gamma)}$, shown in fig. 4.8 (b), allows us to fix the Stokes constant. The limit of $R^{(\delta/\gamma)}$ is 1.00 ± 0.02, suggesting that the Stokes constant agrees with the one of $\gamma(\alpha)$. Table 4.7 contains estimates of the asymptotic growth. Even for the anomalous dimension $\gamma(\alpha)$, the subleading asymptotic corrections are only known numerically (table 3.4), we make no attempt to identify rational values for the corrections of $\delta(\alpha)$. All in all, we estimate the following asymptotic growth for the coefficients of $\delta(\alpha)$ in the toy model:

$$d_n \sim S(w) w^{n+1} \Gamma\left(n + \frac{2+2w}{w}\right). \tag{4.56}$$

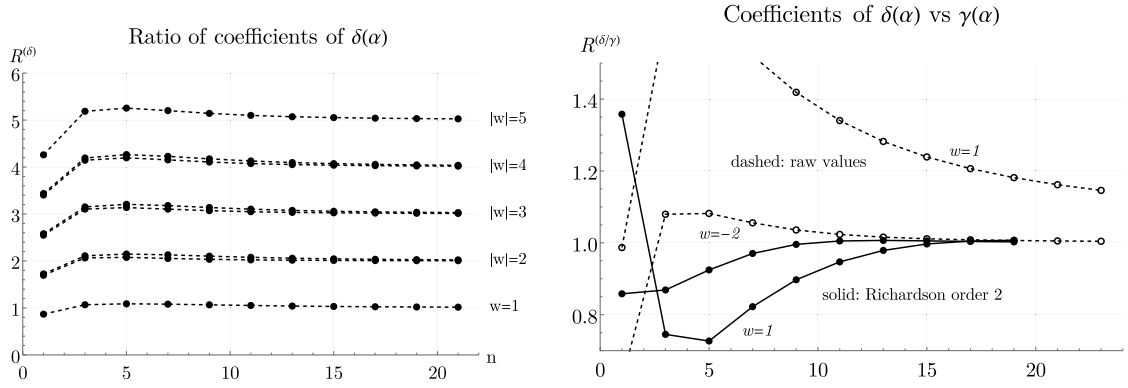

Figure 4.8.: (a) Ratio $R^{(\delta)}$ (eq. (4.55)) of successive coefficients of $\delta(\alpha)$. The ratio visibly approaches $|w|$. (b) Ratio $R^{(\delta/\gamma)}$ (eq. (4.55)) between coefficients of $\delta(\alpha)$ and $\gamma(\alpha)$ and its order-2-Richardson extrapolation. limit seems to be consistent with unity, compare fig. 4.5 (a).

Some coefficients of the counterterm Z of the toy model in kinematic renormalization are listed in the appendix of [480]. They satisfy the relations of theorem 49.

w	$\alpha\bar{\delta}(\alpha(A))$
5	$-6A - \frac{2009}{3}A^2 - \frac{11563106}{45}A^3 - \frac{173306477104}{945}A^4 - \frac{1228737945883358}{6075}A^5 - \frac{46235332362117842849}{147015}A^6$
4	$-5A - \frac{1130}{3}A^2 - \frac{4316822}{45}A^3 - \frac{59632972484}{1323}A^4 - \frac{461687074578658}{14175}A^5 - \frac{34025588969113725668}{1029105}A^6$
3	$-4A - \frac{554}{3}A^2 - \frac{1263424}{45}A^3 - \frac{10282878575}{1323}A^4 - \frac{46540947260036}{14175}A^5 - \frac{3987378396925321 22}{205821}A^6$
2	$-3A - \frac{217}{3}A^2 - \frac{1233338}{225}A^3 - \frac{4881119933}{6615}A^4 - \frac{3528108924854}{23625}A^5 - \frac{1074400592111547046}{25727625}A^6$
1	$-2A - \frac{55}{3}A^2 - \frac{106898}{225}A^3 - \frac{135875429}{6615}A^4 - \frac{272890120256}{212625}A^5 - \frac{2770658834393158}{25727625}A^6$
0	$-A - \frac{4}{3}A^2 - \frac{146}{45}A^3 - \frac{8864}{945}A^4 - \frac{417682}{14175}A^5 - \frac{9095176}{93555}A^6$
-1	0
-2	$A + 7A^2 + 242A^3 + 17771A^4 + 2189294A^5 + 404590470A^6$
-3	$2A + 41A^2 + \frac{92518}{25}A^3 + \frac{503885698}{735}A^4 + \frac{1639676026462}{7875}A^5 + \frac{266517331818761291}{2858625}A^6$
-4	$3A + \frac{370}{3}A^2 + \frac{4782122}{225}A^3 + \frac{48904622516}{6615}A^4 + \frac{887103429351554}{212625}A^5 + \frac{88600913717695595572}{25727625}A^6$
-5	$4A + \frac{826}{3}A^2 + \frac{3478864}{45}A^3 + \frac{287007344207}{6615}A^4 + \frac{185545372999796}{4725}A^5 + \frac{53252838327756373006}{1029105}A^6$

Table 4.8.: First coefficients of $\delta(\alpha)$ in the toy model, up to order α^{11}. Here, $A := (\alpha\pi)^2/4$.

4.5.4. The chain approximation in D=4

As an example of a model where MS and MOM can not be related by a shift $\delta(\alpha)$, we consider the chain approximation. We restrict ourselves to $D = 4 - 2\epsilon$ and consider renormalized quantities only at $\epsilon = 0$.

The chain approximation of the multiedge propagator DSE contains the sum of all chain graphs, that is, multiedges where a chain of subgraphs is inserted into one of the edges, without recursive insertions. From a Hopf-algebra perspective, the chain graphs correspond to corollas C_j,

$C_1 = \bullet$, $C_2 =$, $C_3 =$, $C_4 =$.

The second chain graph from example 26 is $S \simeq C_3$ in this sequence. The chain approximation is non-recursive by nature, and it is not generated by a DSE. Nevertheless, it is sometimes viewed as an intermediate step between the linear ($w = 0$) and the full recursive ($w = -2$) DSE, see for example [253]. The first function of the log-expansion (eq. (3.2)) in MOM is

$$\gamma_1(\alpha) = -\sum_{n=1}^{\infty}(n-1)!(-\alpha)^n = e^{\frac{1}{\alpha}}\int_{\frac{1}{\alpha}}^{\infty}\frac{\mathrm{d}t}{t}e^{-t}, \tag{4.57}$$

where the resummed series is the exponential integral (example 43). Explicit computation of the higher $\gamma_t(\alpha)$ in MOM produces coefficients which can again be identified,

$$\gamma_{t\geq 1} = (-1)^t\frac{1}{t!}\sum_{n=t}^{\infty}(n-1)!(-\alpha)^n, \qquad k\gamma_k(\alpha) = \alpha\cdot\alpha\partial_\alpha\gamma_{k-1}(\alpha)$$
$$\Rightarrow \qquad \partial_L G_{\mathcal{R}}(\alpha, L) = \gamma_1(\alpha) + \alpha\cdot\alpha\partial_\alpha G_{\mathcal{R}}(\alpha, L). \tag{4.58}$$

Although the last equation is reminiscent of the Callan-Symanzik equation theorem 39 for a beta function $\beta(\alpha) = \alpha$, it is structurally different. The function $\gamma_1(\alpha)$ is not the anomalous

dimension of this model in the conventional physical sense, because it is not a prefactor of $G_{\mathcal{R}}(\alpha, L)$.

In Minimal Subtraction, we find

$$\begin{aligned}\bar{\gamma}_0(\alpha) &= 1 - 2a + \frac{11}{2}\alpha^2 - \left(\frac{37}{3} + \frac{2}{3}\zeta(3)\right)a^3 + \left(\frac{169}{4} - \frac{1}{120}\pi^4 + \frac{1}{2}\zeta(3)\right)a^4 + \dots \\ &=: \sum_{r=0}^{\infty} r_k(-\alpha)^k.\end{aligned}$$

The coefficients grow approximately as $r_k \sim (k-1)!$. The other expansion functions $\bar{\gamma}_{t>0}(\alpha)$ do not contain zeta values and are purely rational. The first of them is

$$\bar{\gamma}_1(\alpha) = \alpha - 3\alpha^2 + 10\alpha^3 - 38\alpha^4 + 168\alpha^5 - 872\alpha^6 + 5296\alpha^7 \pm \dots = \sum_{n=1}^{\infty} c_n(-\alpha)^n. \quad (4.59)$$

Empirically, the coefficients agree with [A010842] [473], $c_n = (n-1)![x^{n-1}]\frac{e^{2x}}{x-1}$.

The higher $\bar{\gamma}_j$, but not $\bar{\gamma}_0$, satisfy the recursion

$$k\bar{\gamma}_k(\alpha) = \alpha \cdot \alpha\partial_\alpha \bar{\gamma}_{k-1}(\alpha),$$

which is reminiscent of theorem 40. $\bar{\gamma}_0$ can not possibly satisfy the same equation because it is the only function to contain zeta values. Again, the function $\bar{\gamma}(\alpha) = \alpha$ can not be interpreted as the anomalous dimension in the conventional physical sense.

For the chain approximation, it is not possible to consistently define a shift $\delta(\alpha)$ between MS and MOM. The algorithms of section 4.4.3 are not even applicable since they require a value w from the DSE. The brute-force algorithm (section 4.4.2) does produce some solution $\delta(\alpha)$ if the series are truncated. However, the solutions differ depending on whether $\bar{\gamma}_0$ was included in the linear system or not. This was to be expected because the underlying formula $\tau = e^{\star\delta\sigma}$ (theorem 57) is only valid for solutions of Dyson-Schwinger equations.

Regarding the physical validity of the chain approximation, we conclude the following: It is surely valid as an "approximation" in the sense that it includes a proper subset of the graphs of the full solution $w = -2$. Consequently, the would-be "anomalous dimension" eq. (4.57) qualitatively resembles the true solution, see fig. 4.9.

However, the chain approximation is not self-consistent in perturbation theory, it does not satisfy a Callan-Symanzik equation and therefore transforms inconsistently in the renormalization group. Concretely, in different renormalization schemes, the chain approximation will give rise to physically inequivalent solutions, which can not be mapped one another by rescaling of arguments. The combinatorial reason for this is obvious: The chain approximation does not arise from a DSE and therefore does not have the "recursive" features to be expected from a QFT amplitude. Our verdict is that the chain approximation, without further justifications, is not a valid model to establish combinatorial properties of QFT, such as the presence of *renormalons* [481–483], because it systematically misses one of the key features of QFT combinatorics.

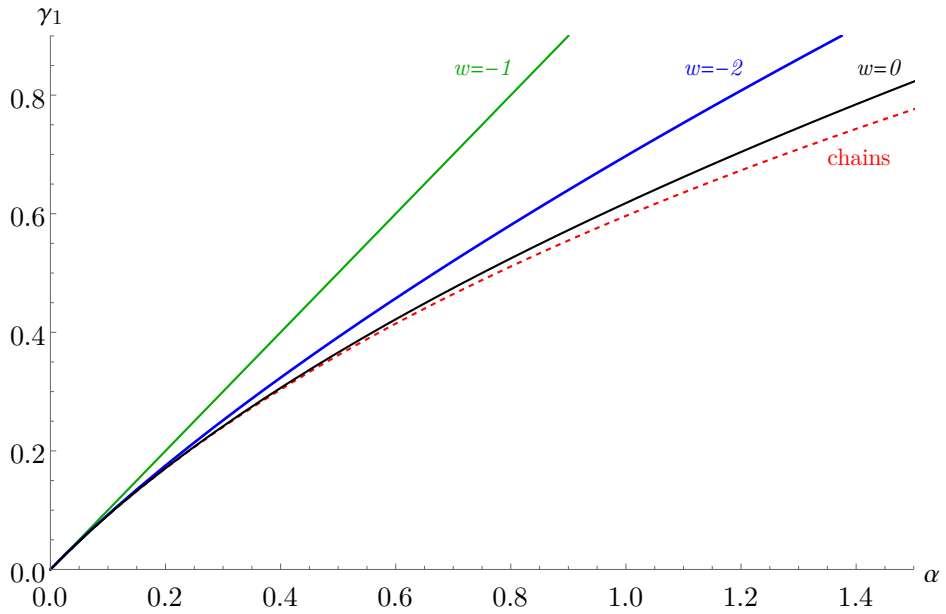

Figure 4.9.: The function $\gamma_1(\alpha)$ in MOM for various forms of the multiedge DSE in $D = 4$ (example 103). Green: trivial solution $\gamma = \alpha$ for $w = -1$. Black: linear DSE (example 114). Blue: exact solution for $w = -2$ from [390]. Red: chain approximation eq. (4.57). Even if these four functions have significantly different properties in perturbation theory, $w = 0$ and $w = -1$ being convergent series while the other ones are asymptotic, their graphs look surprisingly similar.

Summary of section 4.5.

1. For the non-linear multiedge DSE in $D = 4$, the shift $\delta(\alpha)$ is given by a factorially divergent power series very similar to the anomalous dimension $\gamma(\alpha)$. From our numerical data, we guessed closed formulas for all the asymptotic coefficients and gave a tentative equation which relates $\delta(\alpha)$ and $\gamma(\alpha)$ up to an unknown convergent power series (section 4.5.1).

2. For the non-linear multiedge DSE in $D = 6$, the asymptotic growth of the coefficients of $\delta(\alpha)$ is very similar to the one of $\gamma(\alpha)$. This time, we did not find an explicit formula for all subleading corrections (section 4.5.2).

3. The non-liner toy model DSE, again, behaves qualitatively similar to the multiedge case, but the concrete relation between γ and δ is even less accurate than in 2 (section 4.5.3).

4. The chain approximation does not satisfy a Dyson-Schwinger equation and its amplitudes are truly different in different renormalization schemes. We argued that the chain approximation is systematically inconsistent and should not be used for combinatorial arguments, even if it gives rise to approximately similar Green functions as the other models (section 4.5.4).

5. Field Diffeomorphisms and Symmetries

5.1. Symmetries and Hopf ideals

We have so far only considered a one-component scalar quantum field, which is sufficient to establish most of the principles of renormalization. In the present section, we examine how symmetries are encoded in the Hopf algebra.

5.1.1. Symmetries

Theorem 70 (Coleman-Mandula-Haag [484, 485])**.** Under technical conditions listed in the cited works, every symmetry group G of the S-matrix (def. 18) is isomorphic to the direct product of

1. The Poincaré group (def. 3),
2. The group of supersymmetric transformations between bosons and fermions,
3. internal symmetry groups of the fields (def. 114).

All our quantum field theories are Poincaré-symmetric by construction (def. 6), supersymmetry has never been observed in particle physics, consequently, the most relevant part of G for us is the *internal* symmetry.

Definition 114. An *internal symmetry* of a quantum field theory, defined by a Lagrangian $\mathcal{L}$ (def. 6), is a group G such that the quantum field operators are representations of G, acted upon by an unitary operator $U(g)$ which leaves the action (def. 7) invariant:

$$\int \mathrm{d}^D\underline{x}\, U^\dagger(g)\mathcal{L}U(g) = \int \mathrm{d}^D\underline{x}\, \mathcal{L} = S[\phi], \qquad \forall g \in G.$$

Example 126: Gauge transformation of complex scalar field.

If the field variable ϕ of a scalar field (example 6) is not real, but complex, then the theory can have a global $U(1)$ symmetry given by the transformations, which are independent of spacetime:

$$\phi \mapsto e^{i\alpha}\phi, \qquad \phi^* \mapsto e^{-i\alpha}\phi^*, \qquad \alpha \in \mathbb{R}.$$

These transformations are given by one real parameter, the gauge group is the Lie group $U(1)$. A square of fields transforms as $\phi^*\phi \mapsto \phi^* e^{-i\alpha}e^{i\alpha}\phi = \phi^*\phi$.

Consequently, to be symmetric under these transformations, the Lagrangian must be a function of products $\phi^*\phi$. The complex analogue of the ϕ^4-Lagrangian is

$$\mathcal{L} = -\frac{1}{2}\partial_\mu\phi^*\partial^\mu\phi - \frac{\lambda_4}{4!}(\phi^*\phi)^2.$$

An internal symmetry (def. 114) is *local* if the transformation parameters depend on spacetime. In that case, the kinetic term of the Lagrangian gives rise to derivatives of the transformation parameter, which destroy the symmetry of the action. In order to restore symmetry, one needs to introduce a second field, which couples to the original one in a particular way called *gauge covariant derivative* and which transforms in a way to absorb the superfluous terms. This field is called *gauge boson*, the corresponding QFT is a *gauge theory*.

Example 127: Gauge transformation in QED.

Quantum electrodynamics (example 22) contains two fields, the potential $A^\mu(\underline{x}) := (\Phi(\underline{x}), \mathbf{A}(\underline{x}))$, and the fermion field $\psi(\underline{x})$. The Lagrangian is

$$\mathcal{L} = \bar{\psi}\left(i\gamma^\mu D_\mu - m\right)\psi - \frac{1}{4}F_{\mu\nu}F^{\mu\nu}, \qquad D_\mu := \partial_\mu - ieA_\mu.$$

The Lagrangian of the fermion field ψ alone, without coupling to A^μ, has the freedom to globally transform under the group $U(1)$, $\psi(\underline{x}) \mapsto e^{-ie\alpha}\psi(\underline{x})$. Here, e is the electromagnetic charge of the fermion and α is a constant.

The potential A^μ has a gauge freedom $A^\mu(\underline{x}) \mapsto A^\mu(\underline{x}) - \partial^\mu\alpha(\underline{x})$ for any differentiable function $\alpha(\underline{x})$, because all observables are functions of the field strength tensor $F_{\mu\nu} := \partial_\mu A_\nu - \partial_\nu A_\mu$. Consequently, also the pure electromagnetic Lagrangian $F_{\mu\nu}F^{\mu\nu}$ is gauge invariant.

If ψ is coupled to A^μ with the interaction term $e\bar{\psi}\gamma^\mu A_\mu$, arising from the gauge covariant derivative D_μ, then the gauge transformation of ψ can be promoted to a local transformation as well, because the transformation of A^μ cancels the non-invariant term arising from ψ. The photon field A^μ is the gauge boson of QED since it allows the fermion field to be locally gauge invariant.

Internal symmetries are often related to the spin of particles by the following heuristics: The free part of quantum field theory of higher spin particles is typically based on the *Fierz-Pauli-Dirac* Lagrangian [486–488]. There, a particle with integer spin n is represented by a symmetric tensor with n indices (As Fierz pointed out later [489], this setup equivalently describes a non-local scalar field [490]). Nevertheless, by representation theory of the Lorentz group [11], a massless particle has only two degrees of freedom. This entails that many of the tensor entries are not independent, and the form of possible interaction terms is restricted. A symmetry then amounts to the equivalence of different choices of the two independent degrees of freedom. For spin 1 and spin 2 massless unconfined particles, one finds that the Maxwell equations ([25], example 7) and the Einstein equations ([95], section 5.2.1) – together with their corresponding local gauge symmetries – follow automatically from Lorentz covariance [107, 108, 491]. Similarly, for spin 3 or higher, there are only very few consistent types of interactions [137, 492–496].

Within a gauge theory, the n-point Green functions (def. 14) are a priori not well defined, because with a suitable local gauge transform, the field can be altered almost arbitrarily at any given point. In order to calculate Green functions, one needs to fix the gauge and introduce fictitious particles with opposite statistics, called *gauge ghost particles*, which cancel superfluous degrees of freedom. This procedure gives rise to additional terms in the Lagrangian, and to corresponding vertices and propagators in Feynman graphs. The choice of gauge is arbitrary [497] within the limit that it must not destroy renormalizability of the theory [498, 499]. Physical observables are independent of the chosen gauge, compare [500]. We skip details because in the present thesis, we never need gauge fixing explicitly.

5.1.2. Ward identities

As seen in example 127, gauge invariance of the theory crucially depends on the presence, and precise numerical relation, of certain monomials in the Lagrangian. During renormalization, each monomial is rescaled by its corresponding Z-factor (section 3.2.2), which depend on the energy scale in question. The renormalized QFT is gauge invariant if and only if the classical theory is, and all monomials in question are rescaled with the same Z-factor.

Definition 115. Consider a QFT where the underlying Lagrangian has an internal symmetry (def. 114). A *Ward identity* or *Slavnov-Taylor identity* is an algebraic relation between the Z-factors (def. 104) of those terms of the Lagrangian which are involved in the symmetry.

Example 128: Ward identity in QED.

The Z-factors for the QED Lagrangian (example 22) can be chosen (e.g. [501])

$$\mathcal{L} = Z_2\bar{\psi}\left(i\gamma^\mu\partial_\mu + \frac{Z_1}{Z_2}e\gamma^\mu A_\mu - Z_m m\right)\psi - \frac{1}{4}Z_3 F_{\mu\nu}F^{\mu\nu}.$$

If the renormalized theory is to be gauge invariant, then the gauge-covariant derivative must retain its form $D_\mu = \partial_\mu - ieA_\mu$ after renormalization. This is possible only if the Ward identity (def. 115)

$$\frac{Z_1}{Z_2} = 1 \qquad \Leftrightarrow \qquad Z_1 = Z_2$$

holds. This identity was suspected by Dyson in [215], and little after proven in a remarkably short article [502] by Ward.

From the perspective of Feynman graphs, the Ward identity in QED holds because one obtains all vertex graphs by adding exactly one more vertex into any of the internal fermion edges of the propagator graphs, see [299, 503, 504].

The precise value of Z-factors depends on renormalization conditions [477]. If one uses kinematic renormalization (def. 91), then the momentum of the individual edges of the vertex at the renormalization point must match the corresponding 2-point functions, [505, 506]. In Minimal Subtraction (def. 108), Ward identities typically hold without additional

constraints [503, 507]. Further, the concrete form of Ward identities heavily depends on the chosen gauge [174, 175, 508]. Finally, a Ward identity is valid in a regularized theory (where the regulator is not yet removed) only under the condition that the regularization procedure respects the symmetry, compare for example [440, 509]. A main reason for the popularity of dimensional regularization (section 2.3.3) is that this regularization scheme does not spoil Ward identities in QED and QCD, while, for example, cutoff regularization does.

By def. 115, Ward identities are equations for the Z-factors. Alternatively, they be expressed as identities for renormalized Green functions, compare for example [510].

Example 129: Alternative forms of the Ward identity in QED.

The Ward identity in QED can be stated in the following forms. We do not claim that all forms are equivalent in full generality.

1. $Z_1 = Z_2$
2. The transversally projected 1PI vertex is the difference of electron propagators,

$$\left(\underline{p}_2 - \underline{p}_1\right)^\mu G^{\wwvert}_{\mathcal{R},\mu}(\underline{p}_1, -\underline{p}_2) = G^{\succ}_{\mathcal{R}}(\underline{p}_1) - G^{\succ}_{\mathcal{R}}(\underline{p}_2),$$

   where $\underline{p}_1, -\underline{p}_2$ are the momenta of the two electron edges entering the vertex.
3. The vertex at zero momentum transfer is the derivative of the electron propagator,

$$G^{\wwvert}_{\mathcal{R},\mu}(\underline{p}, -\underline{p}) = -\frac{\partial}{\partial p^\mu} G^{\succ}_{\mathcal{R}}(\underline{p}).$$

4. All renormalized photon n-point S-matrix elements are transversal,

$$p_1^{\mu_1} G^{(n)}_{\mathcal{R},\mu_1,\ldots}(\underline{p}_1, \ldots) = 0 \quad \text{for} \quad \underline{p}_1^2 = 0.$$

5. The renormalized photon propagator is massless.

Example 130: QCD.

Quantum Chromodynamics (QCD) is a gauge theory similar to QED (example 22), but for an underlying non-Abelian symmetry group $SU(3)$. It can be formulated in terms of gauge-covariant derivatives $D_\mu = \partial_\mu + ieA_\mu$ just like QED. The gauge field $A^a_\mu = t^a A_\mu$ represents gluons, it carries an index $a \in \{1, \ldots, 8\}$ of the $SU(3)$ adjoint representation matrix t^a. Since $SU(3)$ is not Abelian, the structure constants f^{abc}, defined as $[t^a, t^b] = if^{abc}t^c$, do not vanish, and the field strength tensor involves a quadratic term in A^a_μ,

$$F^a_{\mu\nu} = \frac{1}{-ig}\left[D_\mu, D_\nu\right] = \partial_\mu A^a_\nu t^a - \partial_\nu A^a_\mu t^a + g f^{abc} A^b_\mu A^c_\nu t^a,$$

where g is the QCD coupling constant.

Unlike QED (example 22), the Lagrangian of the gluon field in QCD, called Yang-Mills Lagrangian [511], contains cubic and quartic summands, expressing a self-interaction among gluons:

$$\mathcal{L} = -\frac{1}{4}\left(\partial_\mu A^a_\nu - \partial_\nu A^a_\mu + g\, f^{abc} A^b_\mu A^c_\nu\right)\left(\partial^\mu A^{a\nu} - \partial^\nu A^{a\mu} + g\, f^{abc} A^{b\mu} A^{c\nu}\right).$$

The case of the Abelian gauge group $U(1)$ in QED is reproduced in the limit of vanishing strucutre constants f^{abc}.

For theories with more than one vertex, such as QCD, each vertex comes with an invariant charge (see example 81) and a beta function (def. 103), which determines how the amplitude of that vertex changes with the energy scale (def. 102). The presence of a symmetry should not depend on the energy scale, therefore a Ward identity should hold all energy scales. Consequently, all vertices involved in the Ward identity must scale with the same beta function. This entails that their invariant charges must agree.

Example 131: Slavnov-Taylor identities in QCD.

The gluon in Quantum chromodynamics (example 130) is a massless spin-1 particle, it has only two degrees of freedom, which are transversal [11, 105, 107, 108].

The Yang-Mills Lagrangian (example 130) has a 3-valent and a 4-valent gluon vertex. The 3-gluon vertex scales $\sim \underline{p}$ for the incoming momenta. If two 3-gluon vertices are joined with an intermediate gluon propagator $\sim \frac{1}{q^2}$, then the overall amplitude of this 4-valent tree scales as $\underline{q}^0$, and it has summands which do not vanish when projected onto the external momenta. The 4-gluon vertex cancels this non-transversal term.

In order for the cancellation to work at all energy scales, both types of graphs, the 4-point function and the product of two 3-point functions, must scale identically. Consequently, the invariant charges (example 81) which determine their scaling (def. 102), must agree:

$$\sqrt{Q_{\text{gluon}}} \cdot \sqrt{Q_{\text{gluon}}} \overset{!}{=} Q_{\text{gluon}}.$$

Q_{gluon} already contains the appropriate factor for the intermediate gluon propagator.

Inspecting the cancellation mechanism for non-transversal terms in other vertices, one finally arrives at $Q_{\text{gluon}} = Q_{\text{gluon}} = Q_{\text{ghost}} = Q_{\text{ghost}}$. These are the Slavnov-Taylor identities [503, 512, 513]. They express that QCD has only one beta function, which scales *all* vertices simultaneously.

A more conventional notation is to write the Slavnov-Taylor identities directly for the Z-factors, or, equivalently, as identities for combinatorial 1PI Green functions:

$$\frac{Z^{\text{gluon}}}{Z^{\text{gluon}}} = \frac{Z^{\text{gluon}}}{Z^{\text{quark}}} = \frac{Z^{\text{ghost}}}{Z^{\text{ghost}}} = \frac{Z^{\text{ghost}}}{Z^{\text{quark}}}, \quad \text{or, at fixed angles,} \quad \frac{\Gamma^{\text{gluon}}}{\Gamma^{\text{gluon}}} = \frac{\Gamma^{\text{gluon}}}{\Gamma^{\text{quark}}} = \frac{\Gamma^{\text{ghost}}}{\Gamma^{\text{ghost}}} = \frac{\Gamma^{\text{ghost}}}{\Gamma^{\text{quark}}}.$$

Much like in QED (example 128), the validity of the Slavnov-Taylor identities can be established order by order in graph theory. But the QCD graphs often involve non-trivial symmetry factors (section 1.3.8). Here, the mechanism of example 29 comes into play, ensuring that symmetry factors match when vertices are being merged and split.

Another interesting perspective on the Slavnov-Taylor identities is the *corolla polynomial* [169–171, 201]. It encodes a combinatorial algorithm to obtain the full QCD integrand from the graphs of scalar ϕ^3 theory. The validity of the Slavnov-Taylor identities, and therefore gauge symmetry and transversality of the resulting theory, is then a consequence of the fact that all gluon graphs arise from the same algebraic operations, applied to the same underlying scalar graphs.

By def. 115, a Ward identity reduces the number of independent Z-factors and hence the number of necessary renormalization conditions. If the Ward identities in QED and QCD would not hold, then all vertices need their individual, independent renormalization conditions. The quantized theory is no longer gauge invariant, and the bosons (photon or gluon) are massive, completely altering the nature of their interactions. Nonetheless, QED and QCD would be renormalizable (def. 98) by power counting (theorem 28) even without these identities. As phrased by 't Hofft and Veltman [86, Chap. 13.1]:

> Indeed, Ward identities have nothing to do with renormalizability but everything to do with unitarity.

5.1.3. Hopf ideals

On the level of Feynman graphs, a Ward identity (def. 115) amounts to setting certain classes of graphs equal, or, alternatively, assigning the value of zero to their difference. In order to be a physical symmetry, such identification must hold for all momentum scales L (def. 81).

Example 132: Ward identity in QED, identification of graphs.

The Ward identity $Z_1 - Z_2 = 0$ in QED (example 128) is, with our sign convention (def. 47), $S^{\mathcal{F}}_{\mathcal{R}}[\Gamma^{\wwvec}] + S^{\mathcal{F}}_{\mathcal{R}}[\Gamma^{\vec{}}] = 0$. Here, Γ^r is the combinatorial 1PI Green function (def. 45). At 1-loop level, we denote the Ward identity by

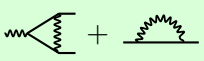

This is meant to hold for the corresponding renormalized amplitudes for all momenta $\underline{p}$, but only if the vertex has zero momentum transfer, as in point 3 in example 129.

By def. 100, theorem 48, and lemma 37, the behaviour of $\mathcal{F}_{\mathcal{R}}[\Gamma]$ under change of momentum scale is encoded in the coproduct $\Delta(\Gamma)$:

$$\frac{\partial}{\partial L}\mathcal{F}_{\mathcal{R}}[\Gamma^a](L) = \left(\sigma \star \tau \star e^{L\sigma}\right)\Gamma^a = \left(\sigma \star \mathcal{F}_{\mathcal{R}}(L)\right)\Gamma^a = m\left(\sigma \otimes \mathcal{F}_{\mathcal{R}}\right)\Delta(\Gamma^a).$$

If we want a Ward identity to hold at all scales, then the coproduct of the graphs involved in that identity must behave in an appropriate way. To understand the mechanism, we firstly

consider the solution Γ^a of a Dyson-Schwinger equation (theorem 26) $\Gamma^a = 1 + \alpha B_+(\Gamma^a Q_a)$, and we let $\gamma_j^a = [\alpha^j]\Gamma^a$. By theorem 24,

$$\Delta(\Gamma^a) = \sum_j \Gamma^a Q_a^j \alpha^j \otimes \gamma_j^a.$$

If $\gamma_j^a = 0$ for all j, then $\partial_L \mathcal{F}_{\mathcal{R}}[\Gamma^a](L) = 0$ and $\mathcal{F}_{\mathcal{R}}[\Gamma^a] = 0$ holds at all scales.

Now consider the sum of two solutions to different DSEs, $\Gamma^a + \Gamma^b =: W$. We have

$$\Delta(W) = \Delta(\Gamma^a + \Gamma^b) = \sum_j \alpha^j \left(\Gamma^a Q_a^j \otimes \gamma_j^a + \Gamma^b Q_b^j \otimes \gamma_j^b \right).$$

In general, $Q_a \neq Q_b$ and the summands do not factorize into the form $(\Gamma^a + \Gamma^b) \otimes (\gamma_j^a + \gamma_j^b)$. Consequently, even if we demand $\gamma_j^a + \gamma_j^b = 0$ for all $j < n$ then, at order n, not all factors in the coproduct of $\gamma_n^a + \gamma_n^b$ will vanish. Expressed in terms of Feynman amplitudes, this means that even if the Ward identity is enforced for all graphs of loop order $j < n$, the corresponding identity at order n will still depend on the scale non-trivially. If we demand $\mathcal{F}_{\mathcal{R}}[\Gamma^a + \Gamma^b](L) = 0$ at some scale L, then this identity will generally not hold for other values of L.

If some identity of the form $W = 0$ is supposed to be valid for all scales L, then we must require $\Delta(W) \subseteq W \otimes H + H \otimes W$. That is, W generates a Hopf ideal (def. 69). In that case, we can impose $W = 0$ and by lemma 19, the quotient $U := \frac{H}{W}$ is closed under the coproduct and antipode. The Hopf algebra U represents the theory where the Ward identity is imposed, it replaces the ordinary renormalization Hopf algebra H. This algebraic perspective on symmetries is described in [200, 355].

Example 133: Ward identity in QED as a Hopf ideal.

To see a nontrivial effect for the coproduct, we need to examine non-primitive (def. 86) graphs. We look at the non-primitive 2-loop graphs of QED (example 22). A fully worked out example for QCD (example 130), including primitive graphs, spans 9 pages in [200].

By $\langle 2 \rangle$ we denote two different orientations of the same graph (def. 17). Let

$\Gamma^{\nearrow} :=$ 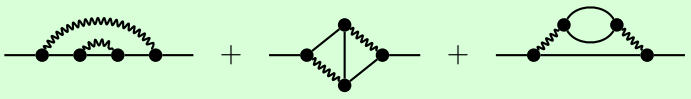

$\Gamma^{\nwarrow\!\!\nearrow} :=$ $\langle 2 \rangle$ 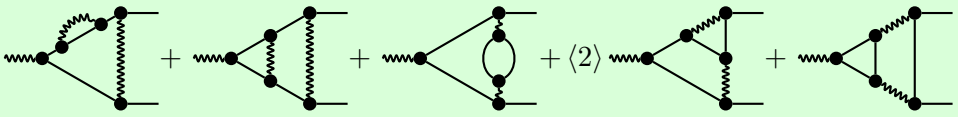

The last graph of $\Gamma_{\nwarrow\!\!\nearrow}$ does not contribute because its 3-photon subgraph vanishes due to Furry's theorem [514]. The reduced coproducts (def. 64) are

$\Delta_1\left(\Gamma^{\nearrow}\right) =$ 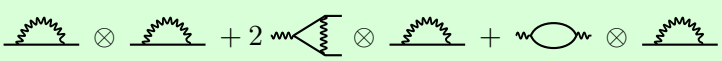

$\Delta_1\left(\Gamma^{\nwarrow\!\!\nearrow}\right) = 2$ 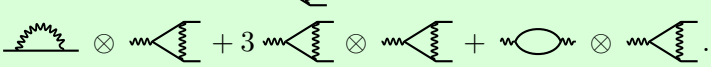

Define $W_2 := \Gamma^{\text{  }} + \Gamma^{\text{}}$ and observe

$\Delta_1(W_2) =$

The Ward identity (example 128) at one-loop level is

$0 = \left(S^{\mathcal{F}}_{\mathcal{R}}[\Gamma^{\text{  }}] + S^{\mathcal{F}}_{\mathcal{R}}[\Gamma^{\text{}}]\right)\Big|_{1\text{ loop}} =$ 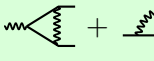 $=: W_1.$

We see that $\Delta_1(W_2) \subseteq W_1 \otimes H + H \otimes W_1$, so W_2 indeed lies in a Hopf ideal (def. 69). Further,

$$S^{\mathcal{F}}_{\mathcal{R}}[W_2] = -\mathcal{R}[W_2] - \mathcal{R}\left[S^{\mathcal{F}}_{\mathcal{R}}[W_1] \cdot H + S^{\mathcal{F}}_{\mathcal{R}}[H] \cdot W_1\right] = -\mathcal{R}[W_2].$$

But if we impose the Ward identity in general, not only at one-loop level, then $-\mathcal{R}[W_2] = 0$. Note that this construction is not tautological: If W_2 would not lie in a Hopf ideal, then $S^{\mathcal{F}}_{\mathcal{R}}[W_2]$ would contain additional summands which we have no information about. Demanding that $S^{\mathcal{F}}_{\mathcal{R}}[W_2] = 0$, in that case, would lead to identities between one-loop graph other than $W_1 = 0$. The Ward identity would then not be compatible with renormalization.

We want to stress that being a Hopf ideal is a necessary, but not a sufficient condition for a physical symmetry. Whether or not $W_i = 0$ is a Hopf ideal, is determined by the combinatorics of Feynman graphs, this does not automatically mean that $\mathcal{F}[W_i] = 0$ under physically sensible kinematic conditions.

5.1.4. Tadpoles

In section 1.3.1, we announced to leave out all tadpole graphs (def. 29). In the present section, we motivate this decision. Tadpoles have only one external momentum, which vanishes by momentum conservation, hence they are independent of momenta altogether. The second Symanzik polynomial (def. 37) of a tadpole T is

$$\phi_T = \psi_T \cdot \sum_{e \in E_T} m_e^2 a_e.$$

This leads to a parametric Feynman integral (eq. (1.49)) of the form

$$\mathcal{F}[T] = \frac{i^{|E_T|}}{(4\pi)^{|L_T|\frac{D}{2}}} \prod_{v \in V_T} (-i\lambda_{|v|}) \prod_{e \in E_\Gamma} \int_0^\infty \frac{\mathrm{d}a_e \; a_e^{\nu_e - 1}}{\Gamma(\nu_e)} \frac{\exp\left(-\sum_{e \in E_T} m_e^2 a_e\right)}{\psi_\Gamma^{\frac{D}{2}}}. \tag{5.1}$$

For a massless theory, all $m_e = 0$ and the integrand is a rational function of the parameters a_e. By lemma 12 and def. 41, it is homogeneous of degree $\omega_T - |E_T|$. An integral from 0 to ∞ over a homogeneous function is divergent. This means that $\mathcal{F}[T]$ for a massless tadpole T will be infinite, regardless of the values of ν_e and D. Observe that eq. (5.1) for $m_e = 0$ is not the same as the period (def. 96): The latter is the same integrand, but integrated over a compact domain given by the constraint $\sum a_e = 1$.

It is not possible to regularize massless tadpole graphs using either analytic (section 2.3.2) or dimensional (section 2.3.3) regularization. One can, however, regularize the integral by introducing an UV- and an IR- cutoff like in eq. (2.42). Once the integrals are regularized, they factorize at single intermediate edges according to eq. (1.52).

We will now argue that one can choose to leave out tadpoles from calculations as claimed in section 1.3.1. Firstly, vacuum graphs (fig. 5.1(a)) can be considered a special class of tadpoles. They are not observable in QFT because their contribution is always cancelled when Green functions are normalized (theorem 6). Hence, they can be left out.

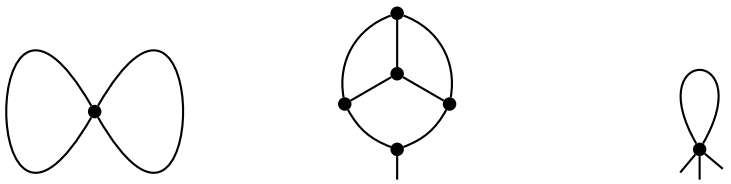

(a) (b) (c)

Figure 5.1.: Three contributions of tadpole graphs. (a) vacuum graph. (b) 1-point function. (c) 3-point function.

Secondly, the 1-point function $G^{(1)}(\underline{x})$ consists entirely of tadpoles (fig. 5.1(b)). Their amplitude is position-independent and $G^{(1)}(\underline{x}) = G^{(1)}$ is a mere number; it can depend on masses. Effectively, tadpoles lead to a global shift $\langle\phi(\underline{x})\rangle \to \langle\phi(\underline{x})\rangle + \delta(m)$. One can remove it by imposing the renormalization condition eq. (1.18),

$$\langle\phi(\underline{x})\rangle \stackrel{!}{=} 0.$$

Thereby, one leaves out all tadpoles, massless or not, which contribute to the 1-point function.

Thirdly, tadpoles can contribute to $(n \geq 2)$-valent Green functions $G^{(n)}(\underline{x})$, if they involve a vertex of sufficiently high valence (fig. 5.1(c)). There, the tadpoles constitute a mass-dependent shift of the corresponding vertex amplitude. In kinematic renormalization (def. 91), the renormalized value of every vertex is fixed by a renormalization condition, therefore, tadpole contributions are always absorbed into this value, and all graphs which include tadpoles evaluate to zero in kinematic renormalization,

$$\mathcal{F}_{\mathcal{R}}[\Gamma] = \mathcal{F}_{\mathcal{R}}\Big[\frac{\Gamma}{T}\Big] \cdot (\mathcal{F}[T] - C_T) = \mathcal{F}_{\mathcal{R}}\Big[\frac{\Gamma}{T}\Big] \cdot 0 = 0.$$

Theorem 71. In kinematic renormalization, all graphs that contain tadpoles vanish, and they can be left out from the start.

Theorem 71 does not imply that we are forced to use cutoff regularization for all graphs. Tadpoles are a Hopf ideal (def. 69) [169, 303], this means that it is possible to first use cutoff regularization so that tadpoles factorize, then divide by the tadpole Hopf ideal and then

remove cutoff regularization. In the remaining tadpole-free sub Hopf algebra, we are free to use any regularization scheme of our choice.

In the Minimal Subtraction scheme (def. 108), we are facing an obstacle: The latter is explicitly based on dimensional or analytic regularization, but tadpoles can not be regularized this way. Consequently, one must introduce a second, explicit, renormalization condition for tadpoles, independent of the ordinary MS renormalization condition. Tadpoles introduce a new, arbitrary, mass scale into the otherwise massless theory, therefore one typically demands them to vanish, but this is a choice, not a theorem, compare example 91. We stress that such a choice, without altering the theory, is only possible for tadpoles because they are momentum-independent. If tadpoles vanish, then all multiedge graphs $M^{(l)}$ (example 18) are primitive (def. 86) since their cographs are tadpoles.

The situation is different for massive tadpoles. They do not vanish automatically in MS renormalization conditions, and this time, the theory has a mass which they can depend on. Consequently, tadpoles will show up as non-vanishing cographs and massive multiedges are not primitive unless we use kinematic renormalization. We can still leave out tadpoles, but this requires to engineer a non-vanishing mass counterterm which absorbs them. If we choose to do so, then we are leaving the conventional MS scheme by imposing a non-MS renormalization condition specifically on tadpole graphs.

Example 134: Violation of the tadpole Hopf ideal.

A massive theory in the Minimal Subtraction scheme (def. 108) is an example that Hopf ideals are only necessary, but not sufficient, for Ward identities to hold. The combinatorics, and hence the Hopf algebra structure, of the massive theory is the same for all renormalization schemes. If we choose MOM, then the tadpole Hopf ideal is respected by default. The renormalized Feynman rules in MS violate the Hopf ideal, restoring it amounts to an additional condition.

Summary of section 5.1.

1. A quantum field theory can have different types of symmetries. We restrict our attention to internal gauge symmetries (section 5.1.1).
2. A symmetry of the classical action does not automatically hold in the renormalized quantum theory because in renormalization, the monomials of the Lagrangian are rescaled by scale-dependent Z-factors. A Ward identity expresses that certain Z-factors scale identically, preserving the original symmetry (section 5.1.2).
3. In the abstract Hopf algebra formulation of renormalization, Ward identities generate Hopf ideals by formally setting certain classes of graphs equal (section 5.1.3).
4. Tadpole graphs form a Hopf ideal as well, it is algebraically consistent to set all tadpoles to zero. The Feynman rules in kinematic renormalization respect this ideal and tadpoles vanish automatically. For Minimal Subtraction, leaving out tadpoles is a dedicated choice (section 5.1.4).

5.2. Diffeomorphisms of scalar fields

Intuitively, it should be possible to describe the same physical system by different choices of variables. In the present section, we examine the behaviour of a scalar quantum field theory under non-linear transformations of the field variable. We derive the Feynman rules for the transformed theory both in position space and in momentum space, and we establish that the transformation indeed does not alter physical observables.

5.2.1. Digression: The numerous problems of quantum gravity

General relativity [95] is based on the Einstein-Hilbert Lagrangian [515],

$$\mathcal{L} = \sqrt{\det g} R, \tag{5.2}$$

where the field degrees of freedom are the entries of the curved metric tensor $g_{\mu\nu}$, the non-static analogue of the Minkowski metric (def. 1). R denotes the scalar Riemann curvature, which is the trace of the curvature tensor $R^{\tau}_{\mu\tau\nu}$. With a tedious calculation, we can express R concretely in terms of g (for example [516, eq. (36)]):

$$\begin{aligned} R := g^{\mu\nu} R^{\tau}_{\mu\tau\nu} = g^{\mu\nu} g^{\rho\sigma} \Bigg(& (\partial_\rho \partial_\sigma g_{\mu\nu} - \partial_\rho \partial_\mu g_{\nu\sigma}) \\ & + g^{\tau\omega} \left(\frac{1}{2} \partial_\mu g_{\omega\sigma} \partial_\tau g_{\nu\rho} - \frac{3}{4} \partial_\mu g_{\tau\sigma} \partial_\nu g_{\omega\rho} + \partial_\mu g_{\nu\tau} \partial_\rho g_{\omega\sigma} - \partial_\mu g_{\nu\omega} \partial_\tau g_{\rho\sigma} + \frac{1}{4} \partial_\mu g_{\tau\omega} \partial_\nu g_{\rho\sigma} \right) \Bigg). \end{aligned} \tag{5.3}$$

Here, $g^{\mu\nu}$ is the inverse matrix of $g_{\mu\nu}$, which can be expressed as a Neumann series [210], and to obtain the Lagrangian (eq. (5.2)), we still need to multiply R by $\sqrt{\det g}$, which is another power series in $g_{\mu\nu}$. General relativity is a gauge theory (section 5.1.1), the gauge group is the group of general coordinate transformations in 4-dimensional spacetime.

Quantum Einstein gravity is the quantum field theory obtained from the Einstein-Hilbert Lagrangian eq. (5.2), where the metric tensor is interpreted as a graviton particle. Irrespective of technical details, a superficial inspection of eq. (5.3) already indicates two qualitative features of quantum gravity in perturbation theory: Firstly, due to the power series expansion of $\sqrt{g}$, there are n-graviton-vertices of any valence $n \in \mathbb{N}$. And secondly, since all summands in eq. (5.3) involve second derivatives, the vertices scale as

$$v_n \sim \underline{p}^2. \tag{5.4}$$

The graviton propagator constructed from eq. (5.2) scales as $\underline{p}^{-2}$. This scaling behaviour has two closely related consequences for the n-graviton Feynman amplitudes $G^{(n)}$:

1. There are infinitely many $G^{(n\geq 2)}$ which are superficially divergent (def. 94).
2. For a concrete function $G^{(n)}$, the degree of divergence (def. 41) of the contributing graphs grows indefinitely with loop number.

By lemma 33, a theory with these properties is not renormalizable. As introduced in section 2.2.1, renormalization amounts to redefinition of finitely many constants in terms of their observable values. The above behaviour of quantum gravity poses a double problem:

1. For each $G^{(n)}$, one would need an experimental input to fix their Z-factors, hence infinitely many measurements to render the complete theory predictive.

2. The interpretation of these experiments as measuring a coupling constant would be questionable, since the divergent part of $G^{(n)}$ is an unknown power series in momenta.

Probably, this naive picture is too pessimistic [517] and the two infinite sets mentioned above are not mutually independent. But even in that case, one infinite set of unknown parameters remains to be determined by renormalization.

The theorist's conclusion appears to be that a quantum theory with Lagrangian eq. (5.2) is impossible. But experiments confirm that both quantum theory, and general relativity, exist in nature, therefore the conclusion that they are mutually exclusive is unacceptable. Over the last century, countless approaches to the renormalization problem of quantum gravity have been proposed. We review four of the more popular ones.

The first possible solution is to introduce a graviton propagator which scales $\sim \underline{p}^{-4}$ [379, 518–523]. One prominent 4^{th}-order theory of gravity is *conformal gravity*, given by the Weyl equations [353, 524–528]. In section 2.4, we have presented various arguments against propgators of 4^{th} order, but they might not apply to the case of gravity: Since gravity is associated with a curved spacetime, it is not obvious whether eq. (2.53) gives the correct short-distance scaling and the argument about conserved fluxes does not necessarily exclude $n \neq 1$. Similarly, the presence of Ostrogradsky ghosts can possibly be avoided by viewing the massless 4^{th} order propagator as a particular limit of massive fields [519].

A second approach to the renormalization problem is the assumption that, instead of changing the propagator, the spacetime dimension changes for short distances, being effectively 2-dimensional, which would render gravity renormalizable [529–531]. We know from everyday experience and from various theoretical considerations [532, 533] that spacetime is 4-dimensional on observable scales. But these arguments do not apply to scales well below the size of nuclei. Several hypothetical mechanisms describe how and why spacetime can effectively become 2-dimensional at short distances [534–537].

Thirdly, quantum gravity in 4 dimensions can potentially still be finite, despite being perturbatively non-renormalizable, by having a non-trivial UV fixed point (see section 3.2.4). This possibility has a certain overlap with the first two. For example, by quantum corrections, the propagator for high energies could deviate from the $\underline{p}^{-2}$ scaling (def. 103), or the scaling behaviour of propagators can even be taken as a *definition* of the dimension of spacetime at this scale [537–540]. From that perspective, whether spacetime changes its dimension or the propagator obtains a non-standard power is almost the same question.

Fourthly, it is conceivable that, due to the tensorial character of gravity, the mere scaling of the vertex (eq. (5.4)) is too imprecise to capture the true behaviour and that the infinitely many involved counterterms are not independent. An example of this phenomenon are the Slavnov-Taylor identities in QCD (example 131): There are seven different divergent Green functions in QCD, but all of their counterterms are related and a single measurement – determining the physical value of the QCD coupling constant g – is sufficient to uniquely determine all seven divergent amplitudes. The hope is that for gravity, being based on the gauge group of arbitrary coordinate transformations, a similar mechanism might be at play, involving infinitely many Ward identities to fix all but finitely many counterterms [517, 541]. This approach to the renormalization problem fits into a broader set of considerations, that a theory with non-polynomial interaction can potentially be renormalizable if its amplitudes have particular extra properties [542–545]. A necessary condition for the validity of such

Ward identities is that they form a Hopf ideal (def. 69) in the core Hopf algebra (def. 85) which underlies the perturbation theory of gravity, compare section 5.1.3. It has been verified that they do [516, 546–548].

Even if Hopf ideals are present, the Feynman rules can potentially violate them, compare example 134. To check the validity of Ward identities, we would need to examine concrete Feynman rules of quantum gravity. Unfortunately, the construction of a QFT from the Einstein-Hilbert Lagrangian (eq. (5.2)) faces significant technical and philosophical challenges. De Witt [549] observes that

> Some of the field variables possess no conjugate momenta; the momenta conjugate to the remaining field variables are not all dynamically independent; the field equations themselves are not linearly independent, and some of them involve no second time derivatives [...].

In general relativity, the Hamiltonian (def. 10), a cornerstone of canonical quantization (section 1.2.2), vanishes identically, and it is not obvious which quantity should be interpreted as the total energy [550]. Moreover, scattering theory relies on the existence of asymptotic states (def. 18) in infinite distances, which, in a globally curved spacetime, might propagate in a different effective metric.

Often, one defines the graviton $h_{\mu\nu}$ to be a small perturbation around a background spacetime $b_{\mu\nu}$, $h_{\mu\nu} := g_{\mu\nu} - \eta_{\mu\nu}$. This approach suffers from ambiguities by possibly inequivalent choices of background metrics $b_{\mu\nu}$ and field variables $h_{\mu\nu}$. The obvious choice $b_{\mu\nu} = \eta_{\mu\nu}$, excludes the physical possibility of non-trivial topologies of the universe, but conversely, if $b_{\mu\nu}$ is not a flat metric, then one faces all the problems of formulating QFT on a curved background [551–553]. Various different definitions of background and graviton field have been considered [73, 175, 549, 554–557], including non-linear redefinitions (def. 116) of $h_{\mu\nu}$ [558]. At least, it has been established that gravity can not be formulated as a non-linear transformation of a free spin-2 field [559]. The perturbative formulations of quantum gravity considered so far typically reproduce (non quantum) general relativity in treelevel graphs [560–563], but this does not imply that they are the correct framework to compute quantum corrections.

Alternatively, one identifies the full metric tensor $g_{\mu\nu}$ as the graviton field variable, but this results in a strongly coupled theory, making perturbation theory inapplicable. Effectively, most issues with the construction of quantum gravity are related to the identification of suitable physical observables, field variables, or gauge conditions [558], and the question unanswered so far is whether there exists any choice such that the above Ward identities render gravity renormalizable. As a side remark, small perturbative deviations from a background field [564] and Feynman graphs [565] are also useful in general relativity itself, irrespective of its possible quantization.

The present thesis does not propose a solution to the renormalization of quantum gravity. But the quantum field diffeomorphisms to be examined in the subsequent sections can be viewed as as a toy model for a quantum field theory where vertices are proportional to inverse propagators. We will see in theorem 90 that the diffeomorphism field indeed satisfies infinitely many Ward identities, but nevertheless, infinitely many counterterms remain undetermined. Examining the diffeomorphism toy model does not solve the gravity problem, but it helps to clarify what type of mechanism is needed concretely to make Ward identities work in the proposed sense.

5.2.2. Field diffeomorphisms

In the present chapter, we consider diffeomorphisms of the field variable in quantum field theory. This setting is different from non-linear coordinate transformations in general relativity (section 5.2.1), which are often called diffeomorphism as well.

Definition 116. Let $\phi(\underline{x})$ be the variable of a scalar quantum field, and let $a_n \in \mathbb{C}$, where $a_0 = 1$. A (global) *field diffeomorphism* is a transformation of ϕ to a new field variable ρ, related by a formal power series (def. 51),

$$\phi(\underline{x}) = \sum_{n=0}^{\infty} a_n \rho^{n+1}(\underline{x}).$$

Likewise, with a set of coefficients b_n, we denote the inverse diffeomorphism by

$$\rho(\underline{x}) =: \sum_{n=1}^{\infty} \frac{b_{n+1}}{n!} \phi^n(\underline{x}). \tag{5.5}$$

The coefficients a_n and b_n in def. 116 are related by theorem 17,

$$\begin{aligned} a_n &= \frac{1}{(n+1)!} \sum_{k=1}^{n} B_{n+k,k}\left(0, -b_3, -b_4, -b_5, \ldots\right) \\ b_{n+2} &= \sum_{k=1}^{n} \frac{(n+k)!}{n!} B_{n,k}\left(-1!a_1, -2!a_2, \ldots, -n!a_n\right). \end{aligned} \tag{5.6}$$

Here, $B_{n,k}$ are the Bell polynomials (def. 52). The diffeomorphism (def. 116) is called *global* in the sense of a global symmetry, which does not depend on the position (section 5.1.1). Conversely, it could be called local in the sense that it is a transformation between fields at the same spacetime point.

Field diffeomorphisms of this type have been examined in the literature repeatedly and for different reasons. Some motivations are the following:

1. Non-linear field redefinitions do not alter the S-matrix (def. 18), which has been established in various different frameworks (theorem 78, [24, 86, 199, 202, 566–569]). This invariance is frequently used to simplify the Lagrangian, for example in gauge theories [328, ch. 6.3], in non-local interactions [570], or in effective field theories [571].

2. Linear shifts in the field variable of an interacting field alter the type of interaction, but they do not impede renormalizability, which is important for theories with spontaneous symmetry breaking [5, 402].

3. By power counting, the Feynman graphs of a field diffeomorphism reside in the core Hopf algebra (def. 85). The same is true for quantum Einstein gravity (section 5.2.1). This makes field diffoemophisms a toy model for the algebraic behaviour of gravity.

4. For quantum gravity, it is notoriously different to identify the correct field variables, see section 5.2.1. A better understanding of field diffeomorphisms can help to classify and restrict the possible choices.

5. By a field diffeomorphism, the Lagrangian of a theory with non-polynomial interaction can be transformed to a theory with polynomial interaction but non-standard kinetic term [572]. This has been used to examine the possibility of non-polynomial interactions in QFT, see example 143.

In the present chapter, we touch upon most of these points, but the focus will be on the offshell Green functions, divergences and renormalizability of field diffeomorphisms. The perturbation theory of scalar field diffeomorphisms has been studied recently [199, 566, 567]. The remainder of the present chapter will follow the author's own works [202, 573].

For a diffeomorphism (def. 116), the underlying field ϕ can be either a free (example 1) or an interacting (example 6) field. We concentrate mostly on the first case, because it already gives rise to all the non-trivial phenomena of field diffeomorphisms, whereas an underlying interaction only makes calculations more cumbersome without adding qualitatively new effects. We write the free Lagrangian of the underlying field ϕ in the form eq. (1.4),

$$\mathcal{L} = \frac{1}{2}\phi(\underline{x})\hat{s}\phi(\underline{x}). \tag{5.7}$$

By Wick's theorem (theorem 2), the correlation functions of ϕ are products of Feynman propagators (eq. (1.23))

$$G_F(\underline{x}_1, \underline{x}_2) := G_F(\underline{x}_2 - \underline{x}_1) = \int \frac{\mathrm{d}^D \underline{k}}{(2\pi)^D} \frac{i}{s_k} e^{-i\underline{k}(\underline{x}_2 - \underline{x}_1)}, \tag{5.8}$$

where s_k is the offshell variable (def. 8).

Example 135: Analogy between QCD and a scalar field diffeomorphism.

Consider the diffeomorphism (def. 116) $a_1 = \frac{-g}{2}$ and $a_{n>1} = 0$, that is, $\phi(\underline{x}) = \rho(\underline{x}) - \frac{g}{2}\rho^2(\underline{x})$. If the underlying field ϕ is a free field (eq. (5.7)) with offshell variable (def. 8) $s_p = \underline{p}^2$, then, using $\partial_\mu \rho^2 = 2\rho\partial_\mu\rho$, the Lagrangian of ρ is

$$\mathcal{L} = \frac{1}{2}\left(-\partial_\mu\rho + g\ \rho\partial_\mu\rho\right)\left(-\partial^\mu\rho + g\ \rho\partial^\mu\rho\right).$$

This Lagrangian is reminiscent of the Yang-Mills-Lagrangian of QCD (example 130), up to the tensor structure which is necessarily different between a scalar field and a vector-valued gauge field.

5.2.3. Diffeomorphism Feynman rules in position space

We examine the Feynman rules of the field diffeomorphism $\rho(\underline{x})$ (def. 116) in position space. The time ordered correlation functions $\tilde{G}^{(n)}(\underline{x}_1, \ldots, \underline{x}_n) = \langle T\rho(\underline{x}_1)\cdots\rho(\underline{x}_n)\rangle$ (def. 14) of ρ can be computed by expanding the series $\rho(\phi(\underline{x}))$ in def. 116 in powers of $\phi(\underline{x})$.

The 1-point function $\langle T\rho(\underline{x})\rangle$ is

$$\tilde{G}^{(1)}(\underline{x}) = \langle\rho(\underline{x})\rangle = \sum_{n=1}^{\infty} \frac{b_{n+1}}{n!} \langle T\phi(\underline{x})\cdots\phi(\underline{x})\rangle.$$

By Wick's theorem (theorem 2), the correlation functions $\langle T\phi^n(\underline{x})\rangle$ are propagators (eq. (5.8)) evaluated at the same spacetime point,

$$\langle T\phi(\underline{x})\rangle = 0, \qquad \left\langle T\phi^2(\underline{x})\right\rangle = G_F(\underline{0}), \qquad \left\langle T\phi^4(\underline{x})\right\rangle = 3\cdot G_F(\underline{0})\cdot G_F(\underline{0}), \quad \ldots.$$

These products correspond to tadpole graphs (section 5.1.4). We demand that they vanish,

$$G_F(\underline{0}) \stackrel{!}{=} 0. \tag{5.9}$$

Equivalently, we demand that eq. (1.18) holds for the transformed field, $\langle\rho(\underline{x})\rangle \stackrel{!}{=} 0$.

For the 2-point function, the expansion of the diffeomorphism (def. 116) reads

$$\tilde{G}^{(2)}(\underline{x}_1,\underline{x}_2) = \langle T\rho(\underline{x}_1)\rho(\underline{x}_2)\rangle = \sum_{t_1=1}^{\infty}\sum_{t_2=1}^{\infty}\frac{b_{t_1+1}b_{t_2+1}}{t_1!t_2!}\left\langle T\phi^{t_1}(\underline{x}_1)\phi^{t_2}(\underline{x}_2)\right\rangle.$$

The right hand side are correlation functions of a free field ϕ. By Wick's theorem and vanishing of tadpoles eq. (5.9), the terms contributing to the 2-point function consist of an arbitrary number of edges between the two spacetime points $\underline{x}_1$ and $\underline{x}_2$. They can be interpreted as Feynman diagrams on two external vertices, see graph A in fig. 5.2. There are $t_1!$ different Wick contractions for each summand, consequently

$$\tilde{G}^{(2)}(\underline{x}_1,\underline{x}_2) = \sum_{t_1=1}^{\infty}\frac{b_{t_1+1}^2}{t_1!t_1!}t_1!G_F^{t_1}(\underline{x}_2-\underline{x}_1) = \sum_{t=1}^{\infty}\frac{b_{t+1}^2}{t!}G_F^{t}(\underline{x}_2-\underline{x}_1). \tag{5.10}$$

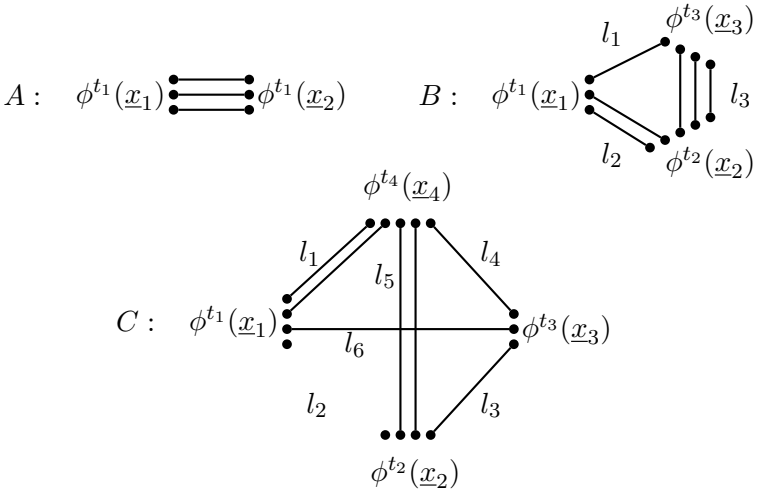

Figure 5.2.: Contributions to connected correlation functions in position space. Each dot represents a factor of ϕ. Graphs where dots of the same monomial ϕ^j (i.e. same spacetime-point) are connected, are excluded due to eq. (5.9). A : 2-point function, B : 3-point function, C : 4-point function.

The time-ordered 3-point function is sketched in graph B in fig. 5.2 and can be written as

$$\tilde{G}^{(3)}(\underline{x}_1,\underline{x}_2,\underline{x}_3) = \sum_{t_1=1}^{\infty}\sum_{t_2=1}^{\infty}\sum_{t_3=1}^{\infty}\frac{b_{t_1+1}b_{t_2+1}b_{t_3+1}}{t_1!t_2!t_3!}\left\langle\phi^{t_1}(\underline{x}_1)\phi^{t_2}(\underline{x}_2)\phi^{t_3}(\underline{x}_3)\right\rangle.$$

Let l_1, l_2, l_3 be the number of propagators between the points as indicated in fig. 5.2, then

$$\begin{aligned} & t_1 = l_1 + l_2, \qquad t_2 = l_2 + l_3, \qquad t_3 = l_1 + l_3 \\ \Leftrightarrow \quad & l_1 = \frac{1}{2}(t_1 + t_3 - t_2), \quad l_2 = \frac{1}{2}(t_1 + t_2 - t_3), \quad l_3 = \frac{1}{2}(t_2 + t_3 - t_1). \end{aligned}$$

Rewriting the sums over t_i in terms of l_i, the non-tadpole part of the 3-point function reads

$$\tilde{G}^{(3)}(\underline{x}_1, \underline{x}_2, \underline{x}_3) = \sum_{\substack{l_j \in \mathbb{N}_0 \\ l_1+l_2+l_3 \geq 2}} \frac{b_{t_1+1} b_{t_2+1} b_{t_3+1}}{l_1! l_2! l_3!} G_F^{l_1}(\underline{x}_2 - \underline{x}_1)^{l_2} G_F(\underline{x}_3 - \underline{x}_2) G_F^{l_3}(\underline{x}_3 - \underline{x}_1). \quad (5.11)$$

The construction of higher $\tilde{G}^{(n)}$ follows the same scheme, the resulting sum can always be interpreted as a sum over all possible graphs involving exactly n vertices. A graph contributing to $\tilde{G}^{(4)}$ is shown in fig. 5.2 C. Equivalently, this construction can be viewed as a sum over complete graphs K_n on n vertices, where each edge of K_n is replaced by any number, including zero, of propagators. A detailed examination shows that the combinatorial prefactors have the form analogous to eq. (5.11) in the general case.

Theorem 72 ([202])**.** Let ρ be a diffeomorphism (def. 116) of a free scalar field ϕ with propagator $G_F(\underline{z})$ in position space (eq. (5.8)). Assume that tadpoles vanish, and let $k = \frac{n(n-1)}{2}$. Then, the time-ordered n-point amplitude (def. 14) of ρ in position space is

$$\tilde{G}^{(n)}(\underline{x}_1, \ldots, \underline{x}_n) = \sum_{\substack{l_1, \ldots, l_k \in \mathbb{N}_0 \\ t_j \geq 1 \; \forall j}} \frac{b_{t_1+1} \cdots b_{t_n+1}}{l_1! \cdots l_k!} G_F^{l_1}(\underline{x}_1 - \underline{x}_2) G_F^{l_2}(\underline{x}_1 - \underline{x}_3) \cdots G_F^{l_k}(\underline{x}_{n-1} - \underline{x}_n)$$

The indices l_i are labels of the edges of a completely connected graph on n vertices, and t_j are the sum of all l_i incident to the vertex j, compare fig. 5.2. Each l_i contributes to precisely two distinct t_j and each pair $\{t_i, t_j\}$ shares precisely one l_i and the summation is such that no t_j is zero.

The index t_j of b_{t_j} depends on $(n-1)$ of the summation indices l_j, consequently, the k sums in theorem 72 are not independent from each other. The prefactor obtained in theorem 72,

$$\frac{b_{t_1+1} \cdots b_{t_n+1}}{l_1! \cdots l_k!}, \quad (5.12)$$

equals the prefactor of an ordinary Feynman graph in position space (def. 39): The numerator represents vertex Feynman rules, where a j-valent vertex has the amplitude $\frac{b_j}{j!}$. In the graphs constructed in theorem 72, all n vertices are external, therefore, the symmetry factor (theorem 13) arises entirely from permutations of the multiedges, $l!$ for each G_F^l. This factor is the denominator in eq. (5.12). Consequently, theorem 72 reproduces the know Feynman rules in position space (def. 39). The case of field diffeomorphisms is special only insofar as the resulting graphs do not contain internal vertices, and therefore no integrations.

5.2.4. Diffeomorphism Feynman rules in momentum space

Applied to a free Lagrangian (eq. (5.7)), a diffeomorphism (def. 116) gives rise to a theory with an infinite set of interaction vertices.

Lemma 73 ([202])**.** Let ρ be the diffeomorphism (def. 116) of a free field (eq. (5.7)) with offshell variable s (def. 8). Then, ρ has vertices of every valence $n \geq 2$ with Feynman rule

$$iv_n := i\frac{1}{2}\sum_{k=1}^{n-1} a_{n-k-1}a_{k-1}(n-k)!k! \sum_{P\in Q^{(n,k)}} s_P.$$

Here, $Q^{(n,k)}$ is the set of all possibilities to choose k out of n external edges without distinguishing the order, P is one of these sets and s_P is the offshell variable corresponding to the momenta in P.

Example 136: Diffeomorphism vertices.

Let s be the offshell variable (def. 8), with the usual shorthand notation $s_{i+j} := s_{p_i+p_j}$. The first vertices from lemma 73 read

$$\begin{aligned} iv_2 &= is_1, \\ iv_3 &= 2ia_1\left(s_1+s_2+s_3\right), \\ iv_4 &= 6ia_2\left(s_1+s_2+s_3+s_4\right) + 4ia_1^2\left(s_{1+2}+s_{1+3}+s_{2+3}\right). \end{aligned}$$

In general, it is not possible to reduce the offshell variables $s_{i+j+\ldots}$, appearing in lemma 73, to polynomials in the n external offshell variables $\{s_i\}$, except for the special cases $s = \underline{p}^2$ or $s = \underline{p}^2 - m^2$ [199].

Theorem 74 ([202])**.** Let ϕ be a scalar field with interacting Lagrangian (eq. (1.5)),

$$\mathcal{L} = \frac{1}{2}\phi\hat{s}\phi - \sum_{t=3}^{\infty}\frac{\lambda_t}{t!}\phi^t,$$

and let ρ be a diffeomorphism (def. 116) of ϕ. Then, ρ has vertices iv_n according to lemma 73, and additionally, for each $n \geq 3$, $t \leq n$, a vertex

$$-iw_n^{(t)} = -i\lambda_t B_{n,t}\left(1!a_0, 2!a_1, 3!a_2, 4!a_3, \ldots\right),$$

where $B_{n,t}$ are the Bell polynomials (def. 52).

For scalar fields where the propagator is of quadratic order in momentum, so $s_p = p^2$ or $s_p = p^2 + m^2$, all propagator-cancelling theories are diffeomorphisms of a free field.

Theorem 75. Consider a scalar field theory ρ with propagator (def. 8) $s = \underline{p}^2 - m^2$, where $m^2 \geq 0$.

1. If ρ has interaction vertices $iv_n = k_n \cdot (p_1^2 + \ldots + p_n^2) + r_n \; \forall n > 2$ where $k_n, r_n \in \mathbb{R}$, then ρ is a unique diffeomorphism of a field ϕ such that the vertices of ϕ are independent of momenta, $iv'_n = ir'_n$ where $r'_n \in \mathbb{R}$.
2. If ρ is a massless field and has interaction vertices $iv_n = k_n \cdot (p_1^2 + \ldots + p_n^2)$, with arbitrary $k_n \in \mathbb{R}$, then ρ is a diffeomorphism of a free massless scalar field.
3. There is no diffeomorphism between two power-counting renormalizable theories.

Proof. The statements are a corollary of theorem 74. Consider the general form of a vertex of the diffeomorphism theory, $iv_n - iw_n^{(t)}$. For $s = \underline{p}^2 - m^2$, this vertex is of the form stated in point 1. In this setting, both the diffeomorphism parameters $\{a_n\}$ and the coupling constants $\{\lambda_t\}$ are free parameters. Using the formulas in lemma 73 and theorem 74, one can determine these parameters to reproduce any given sets $\{k_n, r_n\}$.

A theory with propagator $\sim \underline{p}^{-2}$ can only be power-counting renormalizable (lemma 33) if no vertex is proportional to squared momenta. The most general form of such a scalar theory is the interacting Lagrangian of theorem 74. By lemma 73, every diffeomorphism of such a theory contains vertices scaling as $\underline{p}^2$ and is therefore not renormalizable. □

5.2.5. Propagator cancellations and the connected perspective

From now on, we restrict ourselves to an underlying free field. The vertices of the diffeomorphism (lemma 73) are proportional to inverse offshell variables (def. 8). Hence, they are capable of cancelling a propagator $\frac{i}{s_e}$ (eq. (5.8)), by the identity

$$s_e \cdot \frac{i}{s_e} = i.$$

If a Feynman graph contains vertices iv_n (lemma 73) then the corresponding Feynman amplitude can have a different topology than the graph, in the sense that not every propagator of the graph appears as a factor $\frac{i}{s_e}$ in the amplitude.

The sum over offshell variables s_P in the vertex iv_n (lemma 73) corresponds to all possibilities to choose k out of the n external edges. Pictorially, such a choice means splitting the external edges of the vertex into two disjoint sets. The same splitting happens if we replace the vertex iv_n by two smaller vertices $iv_j \frac{i}{s_P} iv_k$, where $j + k - 2 = n$ and s_P is the intermediate propagator joining iv_j and iv_k. The mechanism is depicted in fig. 5.3.

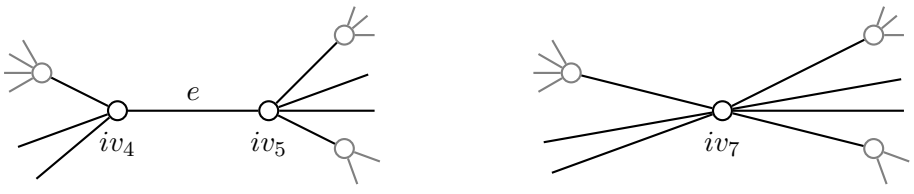

Figure 5.3.: Illustration of splitting the vertex iv_7 into $iv_4 \frac{i}{e} iv_5$.

The product $iv_j \frac{i}{s_P} iv_k = -iv_j \frac{1}{s_P} v_k$ has the opposite sign as the corresponding term in v_n, and a closer examination [202] shows that the combinatorial factors match so that both terms exactly cancel each other. The only remaining summands in iv_n (lemma 73) are those which do not correspond to splitting the vertex, that is, those where the partition P is a single external edge e. Such terms are proportional to an external offshell variable $s_P = s_e$.

$$\left(iv_n + \sum_{v_j \star v_k = v_n} iv_j \frac{i}{s_P} iv_k \right) \Bigg|_{\text{Terms not proportional to an external } s_e} = 0. \tag{5.13}$$

Here, the product $v_j \star v_k$ denotes summation over all ways to choose the valences j, k and also all possible permutations of external edges. By eq. (5.13), the connected tree-level n-point amplitude is proportional to the external offshell variables s_e, it has the form

$$-ib_n(s_1 + \ldots + s_n) =: iV_n \tag{5.14}$$

where $b_n \in \mathbb{R}$ is independent of kinematics.

Definition 117. For $n \geq 3$, the *tree sums* b_n are defined as the sum of all connected tree-level Feynman graphs of the field ρ with a total of n external edges, where $n-1$ external edges are onshell (i.e. $s_e = 0$ for these edges e) and the last external edge is offshell. The propagator $\frac{i}{s_e}$ of this offshell edge e is included in b_n. Finally, $b_2 := 1$.

Example 137: Diffeomorphism tree sums.

An explicit calculation of the first tree sums b_n (def. 117), using lemma 73, yields

$$\begin{aligned} b_3 &= \frac{i}{x_{1+2}} \cdot 2ia_1 \left(x_1 + x_2 + x_{1+2}\right) \Big|_{x_1=0=x_2} = -2a_1, \\ b_4 &= -6a_2 + 12a_1^2. \end{aligned}$$

Graphically, we denote the tree sums b_n by a square vertex, and indicate the cancelled offshell external edge by an arrow. For the ordinary vertices iv_n, we indicate an onshell edge by a perpendicular line.

$b_2 =$  $= 1$

$b_3 =$ 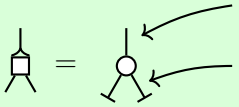

$b_4 =$ 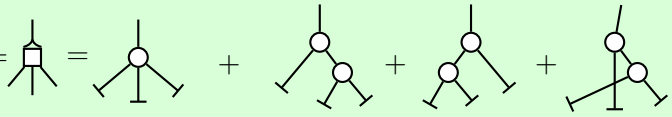

Theorem 76 ([199, 202, 567])**.** The tree sums b_n (def. 117) are the coefficients b_n of the inverse diffeomorphism (def. 116), for arbitrary offshell variable s_p (def. 8).

Example 138: Berends-Giele relations and Parke-Taylor formula.

In QCD (example 130), the n-gluon currents $\hat{J}^x_\xi(1,2,\dots,n)$ are defined as the connected $(n+1)$-point gluon functions where precisely one leg is offshell. They can be constructed recursively with the Berends-Giele (BG) relations [127]. The definition of $\hat{J}^x_\xi$ is almost verbatim def. 117 of the tree sums b_{n+1}. Consequently, the proof of theorem 76 in [199] is strikingly similar to the derivation of BG relations in [127].

The maximum helicity violating (MHV) amplitudes in QCD are those onshell (def. 8) n-gluon amplitudes where precisely two out of n external onshell gluons have a different helicity than the remaining ones. To leading order in N of the gauge group $SU(N)$, their matrix element is given by the Parke-Taylor formula [129],

$$\left|M_{\text{MHV}}(1^-,2^-,3^+,\dots)\right|^2 = \frac{g^{2n-4}}{2^{2n-4}}\frac{N^{n-2}(N^2-1)}{n}(p_1\cdot p_2)^4\sum_P \frac{1}{(p_1\cdot p_2)(p_2\cdot p_3)\cdots(p_n\cdot p_1)}$$

where P ranges over all permutations of $1,\dots,n$. The Parke-Taylor formula is a consequence of Berends-Giele relations.

In this sense, the connected amplitudes $iV_n \sim ib_n$ in eq. (5.14) are a scalar analogue of the MHV-amplitudes in QCD. Especially, if we restrict the diffeomorphism to example 135, which closely resembles QCD, then the tree-level matrix element with one external edge offshell is the square of eq. (5.14),

$$|V_n|^2 = |b_n|^2\sum_{i=1}^n s_i^2 = g^{2n-4}\left((2n-1)!!\right)^2\sum_{i=1}^n (p_i\cdot p_i)^2\,.$$

This amplitude vanishes in the onshell limit $p^2=0$, see theorem 78.

A scalar field diffeomorphism (example 135) is not QCD, therefore we can not expect to precisely recover the Parke-Taylor formula, but it is interesting to observe that, despite the striking difference in tensor structure, qualitatively similar amplitudes arise.

The fact that the tree sums b_n (def. 117) are mere numbers, without any remaining internal propagators, motivates to use these tree sums as *metavertices* in computing connected correlation functions. This approach is dubbed *connected perspective*, as opposed to the *ordinary perspective*, where the vertex Feynman rules are lemma 73. The Feynman rules of the connected perspective differ from the ordinary momentum space Feynman rules (def. 40).

Theorem 77 ([202, 573])**.** Assume that tadpoles vanish. The connected n-point amplitude (def. 14) of a diffeomorphism ρ (def. 116) of a free field (eq. (5.7)) is obtained by summing over all graphs Γ (def. 24) such that

1. Each internal edge $e \in \Gamma$ contributes a propagator factor $\frac{i}{s_e}$.
2. Γ is built from $(k > 2)$-valent metavertices with amplitude $iV_k = -ib_k(s_1 + s_2 + \ldots + s_k)$. Keeping a summand s_e in this amplitude amounts to cancelling the adjacent edge e.
3. The metavertices do not cancel internal edges of Γ.
4. The Graph Γ does not contain internal metavertices, that is, every metavertex is adjacent to at least one external edge.

When using theorem 77, all cancellations have been taken into account, and the topology of the graph equals the topology of the corresponding amplitude. The metavertex Feynman rule (eq. (5.14)) implies that all graphs are proportional to at least one external offshell variable. Consequently, every non-trivial graph of the connected perspective vanishes as soon as all external momenta are taken onshell (def. 8). An analogous statement holds if the underlying theory is interacting, where only the original interaction vertices remain in the onshell limit.

Theorem 78 ([202])**.** Let ρ be a diffeomorphism (def. 116) of a free or interacting scalar field ϕ. Assume that tadpoles vanish. Then, as soon as all external momenta are onshell, the time ordered Green functions (def. 14) of ρ coincide with the ones of ϕ. The diffeomorphism does not alter the S-matrix (def. 18).

We can understand the Feynman rules of the connected perspective (theorem 77) from the diffeomorphism Feynman rules in position space (theorem 72), compare fig. 5.4. The metavertices in the connected perspective, cancelling the adjacent external propagator, can be identified as the external powers $\phi^j(\underline{x})$ in position space. This correspondence indicates that the perturbative treatment in momentum space – which involves significant combinatorial effort in [199, 202, 573] – has indeed yielded the correct results.

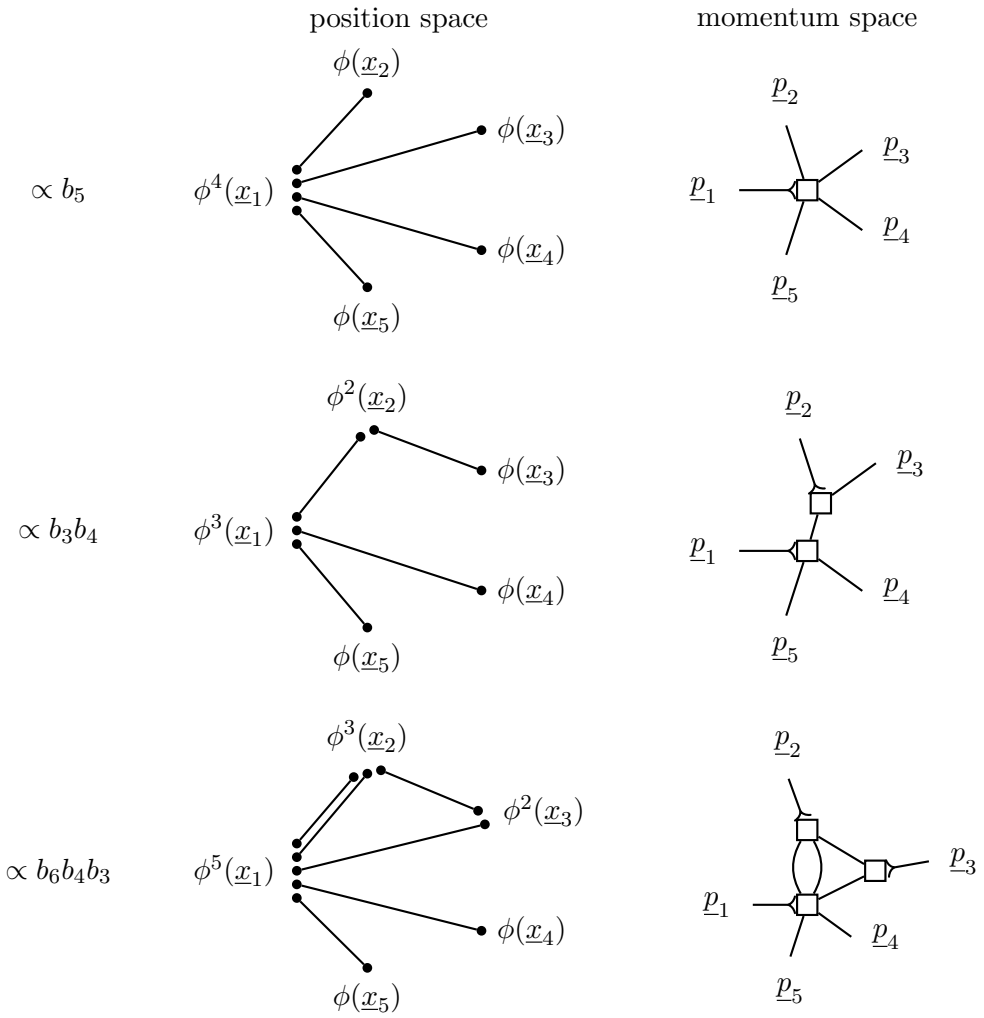

Figure 5.4.: Correspondence between momentum space (theorem 77) and position space (theorem 72) Feynman rules for a diffeomorphism ρ (def. 116). A momentum $\underline{p}_i$ is the Fourier transform of a position $\underline{x}_i$. Metavertices are indicated by squares, the edge which is cancelled is marked with an arrow.

5.2.6. Two-point function in momentum space

Lemma 79. Assume that tadpoles vanish (section 5.1.4). Let ρ be a field diffeomorphism (def. 116) of a free field. Then, the connected 2-point function $\bar{G}_2$ (def. 20) of ρ, excluding the two external propagators, is a sum of multiedges $M^{(l)}$ (example 18),

$$\bar{G}_2(s) = -is + \sum_{l=1}^{\infty} (-ib_{l+2}s)^2 \frac{\mathcal{F}\big[M^{(l)}\big](s)}{(l+1)!}.$$

Proof. Using the Feynman rules of the connected perspective (theorem 77), the connected amplitude with two external momenta $\bar{G}_2$ is supported on Feynman graphs with up to two metavertices. Excluding tadpoles, the only remaining graph topology is that of l-loop multiedges $M^{(l)}$. The metavertices have valence $(l+2)$ and Feynman rule $iV_{l+2} = -ib_{l+2} \cdot s$ (eq. (5.14)), see fig. 5.5. □

$$\bar{G}_2(s) = \quad + \quad + \quad + \ldots$$

$$= -is + (-ib_3 s)^2 \tfrac{1}{2!} \mathcal{F}\big[M^{(1)}\big](s) + (-ib_4 s)^2 \tfrac{1}{3!} \mathcal{F}\big[M^{(2)}\big](s) + \ldots$$

Figure 5.5.: The amputated connected two-point-amplitude $\bar{G}_2$ in momentum-space in the connected perspective. Both external propagators are being cancelled.

Even if all multiedges are 1PI graphs (def. 44), $\bar{G}_2$ is the connected, not the 1PI 2-point function. If tadpoles vanish then multiedge graphs are primitive, so their divergence is local (theorem 30). In dimensional regularization (section 2.3.3), we split $\bar{G}_2$ (lemma 79) into a finite and a divergent part,

$$\bar{G}_2(s) =: -is \left(1 + \bar{G}_2^{\text{fin}}(s) + \bar{G}_2^{\text{div}}(s)\right) + \mathcal{O}(\epsilon) .$$

The divergent part is $\bar{G}_2^{\text{div}}(s) := \hat{\mathcal{R}}[\bar{G}_s(s)]$, where $\hat{\mathcal{R}}$ is the MS subtraction operator (def. 108). It is specific to the 2-point function that $\bar{G}_2$ contains only local divergences $\bar{G}^{\text{div}}$. In general, the diffeomorphism requires a systematic recursive renormalization procedure. We come back to this question in section 5.4.

Example 139: Massless two-point function of diffeomorphism.

If we restrict ourselves to an underlying theory with offshell variable $s = \underline{p}^2$, then the finite and divergent part of $\bar{G}_2$ are given by lemma 29,

$$\bar{G}_2^{\text{div}}(s) = -\frac{b_{l+2}^2 (-is)^l}{(4\pi)^{2l} (l!)^2 (l+1)!}$$

$$\bar{G}_2^{\text{fin}}(s) = -\sum_{l=1}^{\infty} \frac{b_{l+2}^2}{(l+1)!} \frac{(-is)^l}{(4\pi)^{2l} (l!)^2} \left((2l+1)H_l - 1 - l\gamma_E + l\ln(4\pi) - l\ln\frac{s}{s_0}\right).$$

As expected from theorem 78, we reproduce the free connected 2-point function $-is$, i.e. the inverse propagator (eq. (5.8)) in the onshell limit $s \to 0$:

$$\lim_{s\to 0} \frac{i}{s} \bar{G}_2(s) = 1.$$

Moreover, if we demand that $\bar{G}_2(s) = -is$ for all $s \neq 0$ then necessarily all $b_{n>2} = 0$ and ρ is equal to the underlying free theory. Demanding the 2-point function to be that of a free field is sufficient that the theory is free altogether, compare theorem 1.

Summary of section 5.2.

- The quantization of general relativity faces numerous technical and philosophical obstacles. Quantum gravity is unrenormalizable by power counting. There are various possible remedies. Gravity might still be predictive if the counterterms are related by infinitely many Ward identities (section 5.2.1).
- A field diffeomorphism is a non-linear global redefinition of the field variable. Diffeomorphisms have applications in various settings in QFT (section 5.2.2).
- In position space, the Feynman rules of a diffeomorphism are straightforward from the definitions. They give rise to graphs without internal vertices, that is, without integrations (section 5.2.3).
- In momentum space, the Feynman rules of a diffeomorphism contain vertices of any valence, which scale like inverse propagators. Every diffeomorphism is unrenormalizable by powercounting (section 5.2.4).
- Momentum space Feynman rules can be simplified dramatically for connected amplitudes by introducing metavertices, which do not cancel internal edges of graphs (section 5.2.5).
- The connected 2-point function is given by a sum of all multiedge graphs. For an underlying massless theory, the resulting amplitude can be computed explicitly (section 5.2.6).

5.3. Exponential diffeomorphism

In the field diffeomorphisms introduced in section 5.2, the parameters $\{a_n\}$ have been left undetermined. In the present section, we examine a certain family of diffeomorphisms where these parameters are powers of a single constant.

5.3.1. Field transformations

Definition 118. Let $u \in \mathbb{N}$ and $\lambda \in \mathbb{C}$. The *exponential diffeomorphism* is defined as the diffeomorphism (def. 116) with parameters

$$b_n = \begin{cases} 1 & n = 2 \\ \lambda^{n-2} & \exists k \in \mathbb{N}_0 : uk = n-2 \\ 0 & \text{else.} \end{cases}$$

Def. 118 implies that the connected n-point function (def. 20) is proportional to λ^{n-2}. In the following, we examine which transformation function $\rho(\phi)$ or $\phi(\rho)$ corresponds to the choice of coefficients given in def. 118.

Definition 119 ([574])**.** The *generalized hypergeometric function* is

$${}_pF_q\left(\{a_1,\dots,q_p\},\{b_1,\dots,b_q\}\,\middle|\,z\right) := \sum_{k=0}^{\infty}\prod_{i=1}^{p}\frac{\Gamma(k+a_i)}{\Gamma(a_i)}\prod_{j=1}^{q}\frac{\Gamma(b_j)}{\Gamma(k+b_j)}\frac{z^k}{k!}.$$

Definition 120 ([575])**.** The *hyperbolic function* of order u of the r^{th} kind is

$$H_{u,r}(x) := \sum_{k=0}^{\infty}\frac{x^{uk+r}}{\Gamma\left(uk+1+r\right)}.$$

Lemma 80 ([573])**.** Hyperbolic (def. 120) and hypergeometric (def. 119) functions satisfy

$$H_{u,1}(z) = z\cdot\begin{cases} {}_1F_1(1;2|z), & u=1 \\ {}_0F_{u-1}\left(\{\};\left\{\frac{2}{u},\frac{3}{u},\dots,\frac{u-1}{u},\frac{u+1}{u}\right\}\,\middle|\,\left(\frac{z}{u}\right)^u\right) & u\geq 2. \end{cases}$$

Lemma 81. The exponential diffeomorphism def. 118 corresponds to $\rho(\phi)$ by

$$\rho(\underline{x}) = \frac{1}{\lambda}H_{u,1}(\lambda\phi(\underline{x})),$$

where $H_{u,1}$ is the hyperbolic function (def. 120) .

Proof. Using the diffeomorphism coefficients of def. 118, the mapping $\rho(\phi)$ is the series def. 116,

$$\rho(x) = \sum_{n=1}^{\infty} \frac{b_{n+1}}{n!}\phi^n(x) = \phi \sum_{k=0}^{\infty} \frac{(\lambda\phi)^{ku}}{(uk+1)!} = \phi \sum_{k=0}^{\infty} \frac{(\lambda\phi)^{ku}}{\Gamma(uk+2)}.$$

This series is the hyperbolic function of order $r = 2 - 1 = 1$ (def. 120). □

The diffeomorphism given by lemma 81 satisfy the differential equation [575]

$$\frac{\mathrm{d}^u}{\mathrm{d}\phi^u}\rho = \lambda^u \cdot \rho.$$

The solutions $\rho(\phi)$ are are sums of terms $\rho \propto e^{q_i\lambda\phi}$ where q_i are u^{th} roots of unity, see example 140. This fact motivates the name *exponential diffeomorphisms*.

Example 140: Inverse exponential diffeomorphism.

For small u, the hyperbolic functions in lemma 81 evaluate to

$$\begin{aligned}
u = 1: &\quad \rho = \lambda^{-1}\left(e^{\lambda\phi} - 1\right), \\
u = 2: &\quad \rho = (2\lambda)^{-1}\left(e^{\lambda\phi} - e^{-\lambda\phi}\right) = \lambda^{-1}\sinh(\lambda\phi), \\
u = 3: &\quad \rho = (3\lambda)^{-1}\left(e^{\lambda\phi} + (-1)^{\frac{1}{3}}e^{-(-1)^{\frac{1}{3}}\lambda\phi} + (-1)^{\frac{2}{3}}e^{(-1)^{\frac{2}{3}}\lambda\phi}\right).
\end{aligned}$$

Next, consider the diffeomorphism in the opposite direction, the function $\phi(\rho)$. Using eq. (5.6), the diffeomorphism coefficients a_n can be computed in principle from the b_n in def. 118, but there seems to be no easy explicit formula. One obtains

$$\begin{aligned}
u = 1: &\quad a_n = \frac{(-1)^n\lambda^n}{n+1}, \\
u > 1: &\quad a_n = \begin{cases} \frac{(-1)^k\lambda^n}{(n+1)!} \cdot \alpha_k, & n = k \cdot u \\ 0 & \text{else,} \end{cases}
\end{aligned} \tag{5.15}$$

where the sequences $\{\alpha_k\}_{k\in\mathbb{N}}$ have been interpreted in terms of Whitney numbers [576].

Example 141: Coefficients of the exponential diffeomorphism.

The case $u = 1$ in eq. (5.15) amounts to $\alpha_n = n!$. Other examples of $\{\alpha_k\}$ are

$$\begin{aligned}
u = 2: &\quad \{1, 9, 225, 11025, 893025, \ldots\} \quad [473,\ \text{A001818}], \\
u = 3: &\quad \{1, 34, 5446, 2405116, 2261938588, \ldots\} \quad [473,\ \text{A292750}], \\
u = 4: &\quad \{1, 125, 124125, 477257625, \ldots\}.
\end{aligned}$$

Example 142: Forward exponential diffeomorphism.

In the special cases $u = 1, 2$, the function $\phi(\rho)$ can be obtained by inverting the function $\rho(\phi)$ from example 140:

$$\begin{aligned} u = 1: &\quad \phi = \lambda^{-1} \ln(1 + \lambda\rho) \\ u = 2: &\quad \phi = \lambda^{-1} \operatorname{asinh}(\lambda\rho) = \lambda^{-1} \ln(\sqrt{1 + (\lambda\rho)^2} + \lambda\rho). \end{aligned}$$

It is instructive to write down the Lagrangian for $u = 1$ in the case $s = p^2 - m^2$,

$$\mathcal{L} = -\frac{1}{2}\partial_\mu\phi\partial^\mu\phi - \frac{1}{2}m^2\phi^2 = -\frac{1}{2}\frac{1}{(1+\lambda\rho)^2}\partial_\mu\rho\partial^\mu\rho - \frac{1}{2}\frac{m^2}{\lambda^2}\ln^2(1+\lambda\rho). \tag{5.16}$$

Setting $m = 0$ and defining a field $\varrho := 1 + \lambda\rho$, eq. (5.16) reads

$$\mathcal{L} = -\frac{1}{2\lambda^2} \cdot \varrho^{-2} \cdot \partial_\mu\varrho\partial^\mu\varrho. \tag{5.17}$$

This form vaguely reminds of the Einstein-Hilbert-Lagrangian (eq. (5.2)) $\mathcal{L} \sim \sqrt{g} \cdot g^{-2}\partial_\mu g\partial_\nu g$. Alternatively, from eq. (5.15) we find $a_n = \frac{(-1)^n g^n}{n+1}$ and the Lagrangian can be written as

$$\mathcal{L} = \frac{1}{2}\left(-\partial_\mu\rho + g\ \rho\partial_\mu\rho - g^2\ \rho^2\partial_\mu\rho + g^3\ \rho^3\partial_\mu\rho \mp \ldots\right)^2.$$

To first order, this Lagrangian equals the choice of example 135, which we argued to be analogous to QCD. Conversely, for the present case, the analogue to the Parke-Taylor formula (example 138) has the particularly simple form

$$|V_n|^2 = g^{2n-4}\sum_{i=1}^{n}\left(\underline{p}_i \cdot \underline{p}_i\right)^2.$$

The rough qualitative analogy between field diffeomorphisms and gauge theory is probably of little help in practice, but it is pleasing to see that both the QCD-analogue and the gravity-analogue correspond to particularly simple, natural choices of diffeomorphisms – the first to a quadratic function, the second to an exponential one.

5.3.2. Correlation functions of the exponential diffeomorphism

Lemma 82 ([573])**.** Let $\rho(x)$ be an exponential diffeomorphism (def. 118), for a fixed $u \in \mathbb{N}$, of a free field ϕ with propagator $G_F(\underline{z})$ in position space. Assume that tadpoles vanish. Then, the connected full two-point function (def. 20) of ρ in position space is

$$\bar{G}_2(\underline{z}) = \frac{1}{\lambda}H_{u,1}(\lambda^2 G_F(\underline{z})),$$

where $H_{u,1}$ is the hyperbolic function (def. 120).

Example 143: Exponential superpropagator.

Consider the massless theory with offshell variable $s = \underline{p}^2$, its propagator is eqs. (1.26) and (2.49). One obtains the same functions as in example 140. Especially, for $u = 1$, the resulting function is known as the *exponential superpropagator*,

$$\begin{aligned}\bar{G}_2(\underline{z}) &= \lambda^{-3}\left(e^{\lambda^2 G_F(\underline{z})} - 1\right) \\ &= \lambda^{-2}\left(\exp\left(\frac{i\Gamma(1-\epsilon)\lambda^2}{(\underline{z}^2)^{1-\epsilon}4\pi^{2-\epsilon}}\right) - 1\right) = \lambda^{-2}\left(e^{i\frac{\lambda^2}{\underline{z}^2(2\pi)^2}} - 1\right) + \mathcal{O}(\epsilon).\end{aligned}$$

The superpropagator in position space is finite in the limit $\epsilon \to 0$. But, in stark contrast to the free propagator G_F (eq. (1.26)), or the perturbative 2-point function of any renormalizable theory, this function has an essential singularity at $\underline{z}^2 = 0$ and it is not a tempered distribution [577]. Qualitatively, the essential singularity allows to add terms of the form $(\partial_\mu\partial^\mu)\delta(\underline{z})$. In a Fourier transform to position space (eq. (1.2)), these terms become summands $\propto (\underline{p}^2)^n$. Consequently, the superpropagator in momentum space allows the addition of an arbitrary power series $f(\underline{p}^2)$, it is unpredictive. The diffeomorphism is a non-renormalizable theory (theorem 75), the non-predictive Fourier transform is exactly what is expected in such a case ([477], section 2.3.4). We know the amplitude of multiedges from lemma 29. The infinitely many free constants correspond to the freedom to add finite terms into the counterterm of each $M^{(l)}$. Equivalently, the overall counterterm is not a constant, but a power series in $\underline{p}^2$, see example 139.

By a a field diffeomorphism, Liouville theory (example 93) can be turned into a theory with polynomial interaction, but with the exponential superpropagator as 2-point function. Intuitively, 4-dimensional Liouville theory can be rendered predictive if one succeeds to remove the ambiguity from the superpropagator. Various prescriptions with conflicting results have appeared in the literature [545, 578–580].

The higher n-point functions of the exponential diffeomorphism (def. 118) in position space are computable from theorem 72. In the case $u = 1$, none of the b_n vanishes and the sum in theorem 72 simplifies to

$$\tilde{G}^{(n)}(\underline{x}_1, \dots, \underline{x}_n) = \frac{1}{\lambda^n} \sum_{\substack{l_1,\dots,l_k \in \mathbb{N}_0 \\ t_j \geq 1 \ \forall j}} \frac{\lambda^{2l_1} \cdots \lambda^{2l_k}}{l_1! \cdots l_k!} G_F^{l_1}(\underline{x}_1 - \underline{x}_2) G_F^{l_2}(\underline{x}_1 - \underline{x}_3) \cdots G_F^{l_k}(\underline{x}_{n-1} - \underline{x}_n). \tag{5.18}$$

On the other hand, for $u = 1$, the connected 2-point function (lemma 82) is the exponential superpropagator (example 143),

$$\bar{G}_2(\underline{z}) := \sum_{l=0}^{\infty} \frac{\lambda^{2l}}{l!} G_F^l(\underline{z}).$$

The sum eq. (5.18) amounts to all ways to connect the n spacetime points by superpropagators. This implies yet another interpretation of the exponential diffeomorphism (def. 118): The latter is the unique choice of parameters b_n for which the position-space correlation functions factorize into products of superpropagators.

Theorem 83 ([573]). Let ρ be an exponential diffeomorphism (def. 118) of a free field. Assume further that tadpoles vanish. Then the connected Green functions $\bar{G}^{(n>2)}$ (def. 20) of ρ in momentum space are given by a sum over all the following connected graphs Γ:

1. Γ contains at most n vertices.
2. The j-valent vertices of Γ are metavertices $V_j = -i\lambda^{n-2}(s_1 + \ldots + s_j)$.
3. There is at most one edge directly between any two metavertices.
4. Edges correspond to superpropagators in momentum space $\bar{G}_2(s)$ (example 143).
5. Every metavertex cancels precisely one of the n external edges, the uncancelled external edges are superpropagators $\bar{G}_2(s)$.
6. Γ carries a symmetry factor (theorem 13) unity.

On first sight, theorem 83 appears to be very similar to Dyson-Schwinger equations (theorem 14). But that view is deceiving: theorem 83 does not describe fixed-point equations. To compute $\bar{G}_n$, assuming $\bar{G}_2$ is known, only finitely many integrals remain to be solved and none of them involves $\bar{G}_n$ itself.

Example 144: Green functions of the exponential diffeomorphism.

For the 2-, 3- and 4-point function, the graphs obtained from theorem 83 are shown below. The brackets $\langle k \rangle$ indicate a sum over n permutations (def. 17).

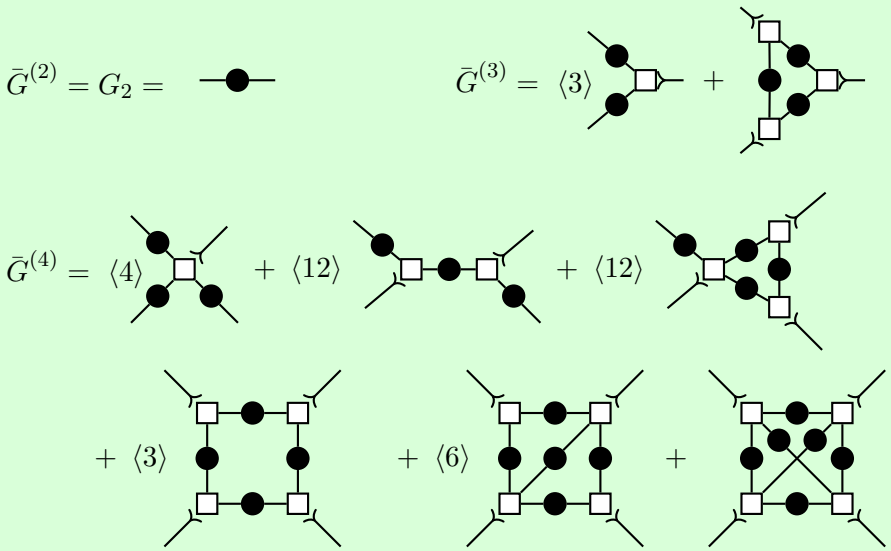

In a Dyson-Schwinger equation (example 36), the full 3-point function itself appears inside the integrals of $\bar{G}^{(3)}$, in the present case, it does not.

Summary of section 5.3.

- If the parameter of a diffeomorphism are chosen to be powers of one constant, then the diffeomorphism simplifies considerably and becomes a hypergeometric function. In the simplest such case, where the transformation is an exponential function, the resulting Lagrangian is qualitatively reminiscent of quantum gravity (section 5.3.1).
- In position space, the correlation functions of the exponential diffeomorphism factorize into superpropagators. The superpropagator is not a tempered distribution and, in momentum space, it requires infinitely many renormalization conditions. Once the superpropagator is fixed, the higher correlation functions in momentum space are given by finitely many integrals (section 5.3.2).

5.4. Divergences of field diffeomorphisms

In this section, we extend the formalism of the connected perspective (section 5.2.4) to incorporate counterterms. We concentrate on the combinatorial properties and skip questions of physical interpretation. Moreover, the general proofs of the statements in the present section are rather tedious, but unilluminating combinatorial exercises. Instead of reproducing them here, we generally refer to the original article [573].

5.4.1. Metacounterterms

The connected perspective (theorem 77) is based on metavertices which do not cancel adjacent internal edges. For a consistent treatment of divergences in the connected perspective, we need to define *metacounterterms* C_k which share the combinatorial properties of metavertices: they absorb all possible internal cancellations and appear in graphs without changing the graph topology. For brevity and concreteness, we only consider metacounterterms for the case that the underlying field (def. 116) is a free field, we work in dimensional regularization (section 2.3.3) and Minimal Subtraction (def. 108), we assume that the divergent part of a 1-loop multiedge (example 86) is independent of momenta, and we assume the vanishing of tadpoles (section 5.1.4).

Metacounterterms can be classified by three integers j, k, l corresponding to the graphs they arise from. A metacounterterm $C^{(l)}_{n,k}$ cancels the superficial divergence of graphs with

- n external edges,
- $k \leq n$ external edges offshell (which implies precisely k metavertices), and
- l loops.

A graph with n external edges can not have more than n external edges offshell, consequently we define

$$C^{(l)}_{n,k>n} := 0 \qquad \forall n, k, l.$$

Theorem 84 ([573])**.** Consider a diffeomorphism (def. 116) of a free field. Assume that tadpoles vanish. Then, all connected Green functions $\bar{G}^{(n)}$ (def. 20) can be rendered finite if metacounterterms are included according to the following rules:

1. Construct the graphs of the connected perspective according to theorem 77.
2. Proceed according to the BPHZ renormalization algorithm (theorem 32), recursively replacing divergent subgraphs $\gamma \subset \Gamma$ by their corresponding metacounterterm which subtracts the divergence. Finally, remove the superficial divergence.
3. The metacounterterm $C_{n,k}$ is inserted in place of a graph on k metavertices, it cancels exactly k out of its n adjacent edges simultaneously.
4. Neither metavertices nor metacounterterms cancel internal edges of the graph.
5. There are neither internal metavertices nor internal metacounterterms.

In terms of cancellations, the only difference between metavertices and metacounterterms is that the former, by eq. (5.14), cancel exactly one of their adjacent external edges, while metacounterterms $C_{n,k}$ cancel $k \leq n$ adjacent external edges.

Example 145: Metacounterterm in the 3-point-function.

The requirement of not cancelling internal edges automatically selects the correct parts of the metacounterterms. Consider the three-loop graph Γ_1:

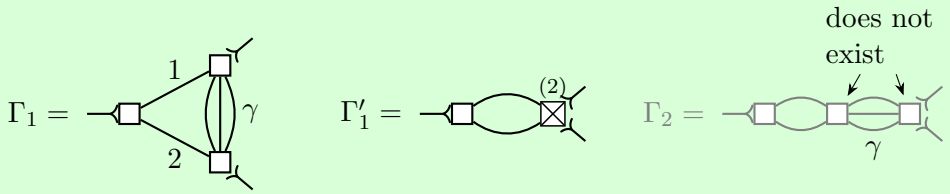

Γ_1 has a divergent subgraph $\gamma \subset \Gamma_1$. This subdivergence is removed by the counterterm graph Γ_1' where a metacounterterm $C^{(2)}_{4,2}$ (indicated by a crossed-out vertex) is inserted into the cograph $\frac{\Gamma_1}{\gamma}$. On the other hand, the graph Γ_2 amounts to a different orientation of γ in the same cograph. However, Γ_2 is not present in the connected perspective since it has an internal metavertex. This restriction is automatically respected by the metacounterterm $C^{(2)}_{4,2}$: When cancelling two edges, only those graphs contribute to $C^{(2)}_{4,2}$ where the two cancelled edges are incident to two distinct metavertices, see the following figure:

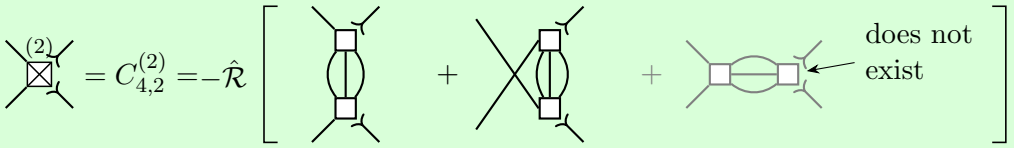

If we label the edges of $C^{(2)}_{4,2}$ as $1, 2, 3, 4$, then the graphs shown in the above figure are proportional to sums of two external momenta, that is, terms such as s_{1+2}, but not to s_j where $j \in \{1, 2, 3, 4\}$. Phrased differently: The cancellations of adjacent edges, which are caused by $C^{(2)}_{4,2}$, stem from metavertices of the underlying graphs, but not from the amplitudes $\mathcal{F}[\Gamma]$ of the graphs themselves, because the latter always depend on sums s_{i+j} and not on individual s_i.

5.4.2. Metacounterterms for less than 3 edges offshell

If all external edges are onshell, i.e. $k = 0$ in $C^{(l)}_{n,k}$, then the amplitudes of the connected perspective vanish, consequently there is no divergence.

$$C^{(l)}_{n,0} = 0 \qquad \forall n, l \qquad \Rightarrow \quad C_{n,0} = 0. \tag{5.19}$$

If only one external edge is offshell, the amplitude is supported on graphs with a single metavertex. Such graphs are tadpoles and we assume them to vanish. We therefore have

$$C^{(l)}_{n,1} = 0 \qquad \forall n, l \qquad \Rightarrow \quad C_{n,1} = 0. \tag{5.20}$$

Graphically, these two identities are shown in fig. 5.6.

Figure 5.6.: The metacounterterms $C_{n,k}$ for connected amplitudes vanish identically if $k = 0$ or $k = 1$, i.e. zero or one external edge is offshell.

As discussed in section 5.2.6, the 2-point-function $n = 2$ is supported on l-loop multiedge graphs $M^{(l)}(s)$ which have no subdivergence and therefore do not require metacounterterms for subdivergences. Consequently, to render the 2-point function finite, all that is needed is the counterterm $C_{2,2}$. The l-loop metacounterterm for the 2-point-function is the divergent part $-M^{(l)}_{\text{div}}$of $M^{(l)}$,

$$C^{(l)}_{2,2}(s) = -(-ib_{l+2}s)^2 \frac{M^{(l)}_{\text{div}}(p^2)}{(l+1)!} = b^2_{l+2}s^2 \frac{M^{(l)}_{\text{div}}(p^2)}{(l+1)!}. \tag{5.21}$$

For $n > 2$ external edges, the metacounterterm with $k = 2$ offshell edges still represents the superficial divergence of a graph on 2 metavertices i.e. a multiedge. The only difference to the case $n = 2$ in eq. (5.21) is that for $n > 2$, there are multiple possible orientations of the 2-vertex multiedge.

With $n = 3$ external edges and $k = 2$, one of the metavertices is adjacent to one external edge and the other one to the remaining two, see fig. 5.7, and there are three ways to choose which two edges are offshell. The l-loop metacounterterm reads

$$C^{(l)}_{3,2} = \frac{b_{l+2}b_{l+3}}{(l+1)!} \Big(s_1(s_2+s_3)M^{(l)}_{\text{div}}(s_1) + s_2(s_1+s_3)M^{(l)}_{\text{div}}(s_2) + s_3(s_1+s_2)M^{(l)}_{\text{div}}(s_3) \Big). \tag{5.22}$$

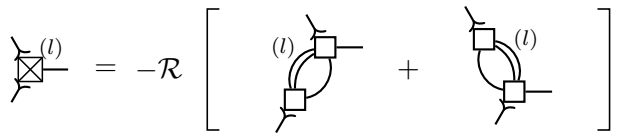

Figure 5.7.: Metacounterterm $C^{(l)}_{3,2}$ according to eq. (5.22). For the indicated orientation of cancelled edges, only two graphs contribute.

With $n = 4$ external edges and $k = 2$ metavertices, two different configurations of multiedges are possible: Either each metavertex is adjacent to two external edges, or one of them to three and one to only one external edge. In the former case, the multiedge depends on a sum offshell variable s_{i+j}. There are six possibilities to choose two out of four edges offshell, each of them contributes four graphs as shown in fig. 5.8; the sum can be written as

$$C^{(l)}_{4,2} = \langle 4 \rangle \cdot b_{l+2}b_{l+4}s_1(s_2+s_3+s_4)\frac{M^{(l)}_{\text{div}}(s_1)}{(l+1)!} + \langle 3 \rangle \cdot b^2_{l+3}(s_1+s_2)(s_3+s_4)\frac{M^{(l)}_{\text{div}}(s_{1+2})}{(l+1)!}. \tag{5.23}$$

As expected, $C^{(l)}_{4,2}$ again cancels exactly two out of its four external edges. Observe that $M^{(l)}_{\text{div}}(s_1)$ in general is a monomial in s_1, and consequently the edge e_1 gets cancelled multiple times.

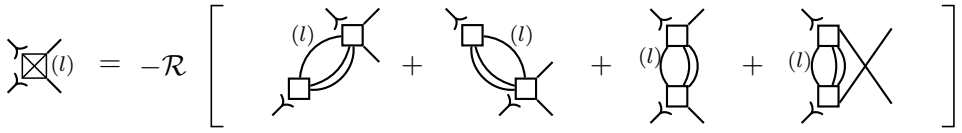

Figure 5.8.: Metacounterterm $C^{(l)}_{4,2}$ according to eq. (5.23) for one of six orientations.

Computing the higher valent metacounterterms, this pattern continues:

$$C^{(l)}_{5,2} = \langle 5 \rangle \cdot b_{l+2} b_{l+5} s_1 (s_2 + s_3 + s_4 + s_5) \frac{M^{(l)}_{\text{div}}(s_1)}{(l+1)!} \tag{5.24}$$
$$+ \langle 10 \rangle \cdot b_{l+3} b_{l+4} (s_1 + s_2)(s_3 + s_4 + s_5) \frac{M^{(l)}_{\text{div}}(s_{1+2})}{(l+1)!}.$$

Lemma 85 ([573])**.** The l-loop metacounterterm $C^{(l)}_{n,k}$ with n edges, two of which are cancelled, is

$$C^{(l)}_{n,2} = \frac{1}{2} \sum_{j=1}^{n-1} \langle K_j \rangle \, b_{l+1+j} b_{l+n+1-j} (s_1 + \ldots + s_j)(s_{j+1} + \ldots + s_n) \frac{M^{(l)}_{\text{div}}(s_{1+\ldots+j})}{(l+1)!},$$

where $K_j = \binom{n}{j}$, and $\langle K_j \rangle$ indicates a symmetric sum over permutations (def. 17).

Example 146: 1-loop metacounterterms for the massless theory.

Assume that $M^{(1)}_{\text{div}}$ is independent of momenta, this is true for example in $D = 4 - 2\epsilon$ dimensions for quadratic propagators (example 86). Then, the explicit prefactors in lemma 85 constitute the only momentum-dependence. The product $(s_1 + \ldots + s_j)(s_{j+1} + \ldots + s_n)$ contains $j \cdot (n-j)$ summands. There are $K_j = \binom{n}{j}$ such terms and the sum is symmetric. The elementary symmetric polynomial of order two in n variables is

$$E_2(s_1, s_2, \ldots, s_n) = \left\langle \frac{n(n-1)}{2} \right\rangle s_1 s_2,$$

where $\langle j \rangle$ denotes permutations (def. 17). $E_2(s_1, \ldots, s_n)$ has $\frac{n(n-1)}{2}$ factors, therefore

$$\langle K_j \rangle \, (s_1 + \ldots + s_j)(s_{j+1} + \ldots + s_n) = 2 \binom{n-2}{j-1} E_2(s_1, \ldots, s_n)$$

and

$$C^{(1)}_{n,2} = E_2(s_1, \ldots, s_n) M^{(1)}_{\text{div}} \sum_{j=1}^{n-1} \binom{n-2}{j-1} b_{j+2} b_{n-j+2}.$$

If we further restrict ourselves to the exponential diffeomorphism (def. 118) for $u = 1$, then $b_{n+2} = \lambda_n$. In $D = 4 - 2\epsilon$ and for $s = \underline{p}^2$, the multiedge is the only divergent 1-loop graph, there are no divergent 1-loop graphs which involve $k \geq 3$ metavertices.

Therefore, $\sum_k C^{(1)}_{n,k} = C^{(1)}_{n,2}$ actually represents the complete 1-loop counterterm. We can give its amplitude explicitly since we know the divergent part of the multiedge from example 89:

$$C^{(1)}_n \equiv C^{(1)}_{n,2} = -\lambda^n \frac{2^{n-3}}{(4\pi)^2} \frac{1}{\epsilon} E_2\left(s_1, \ldots, s_n\right).$$

For $k > 2$ external edges offshell, the amplitudes in the connected perspective are no longer based on multiedge graphs exclusively. For $k = 3$, the new topology is triangle graphs, where each of the three internal edges is replaced by a multiedge. Additionally, there are contributions of two adjacent multiedges, see fig. 5.9 for the topology at 2-loop order. The general principle of metacounterterms works as above, but from $k = 3$ on, it is necessary to subtract subdivergences. A more detailed exposition can be found in [573]

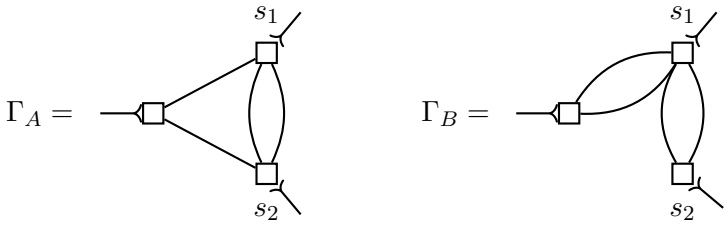

Figure 5.9.: The two topologies of two-loop graphs contributing to the connected three-vertex correlation function where all three edges are cancelled. Each graph has three different permutations $s_1 \to s_2 \to s_3$, they are not indicated.

Example 147: 3-point 2-loop metacounterterm for the massless theory.

Consider the massless theory with $s = \underline{p}^2$ in $D = 4 - 2\epsilon$. At two loops, the metacounterterm $C^{(2)}_{3,3}$ involves the graph topologies shown in fig. 5.9. Divergent parts of the multiedges are derived in lemma 29, the divergent part of the dunce's cap is quoted in example 87. Together, and including permutations and symmetry factors, they give rise to the metacounterterm

$$C^{(2)}_{3,3} = i s_1 s_2 s_3 \frac{3}{4(4\pi)^4} \left(\left(b_3 b_4^2 + b_3^2 b_5\right) \frac{1}{\epsilon^2} - b_3 b_4^2 \frac{1}{\epsilon} \right).$$

5.4.3. 1PI counterterms

The metacounterterms $C^{(l)}_{n,k}$ (section 5.4.1) cancel the divergences of connected amplitudes, considered in the connected perspective. If we want to use the ordinary perspective, that is, the Feynman rules lemma 73, then we need 1PI counterterms $c^{(l)}_{n,k}$. Their indices n, l, k have the same meaning as for the metacounterterms in section 5.4.1. The sum $c^{(l)}_n := \sum_{k=0}^n c^{(l)}_{n,k}$ represents the l-loop counterterm of the 1PI n-point function, that is, the l-loop order of the conventional counterterm $Z^{(n)}$ in the sense of defs. 89 and 104.

We know the metacounterterms from section 5.4.2. At the same time, being counterterms for connected amplitudes, they correspond to all possible trees of 1PI counterterms $c^{(l)}_{n,k}$ and 1PI vertices iv_n (lemma 73). Extracting the 1PI counterterms is a question of combinatorics, namely a Legendre transform (def. 53), they do not require any new evaluation of integrals.

In the present section, we demonstrate with a few explicit examples how the 1-loop 1PI counterterms can be obtained. Firstly, for the 2-point function, the 1PI one-loop amplitude and the amputated connected amplitude (eq. (5.21)) are identical, therefore

$$C^{(1)}_2 = C^{(1)}_{2,2} = b_3^2 s^2 \frac{M^{(1)}_{\text{div}}}{2} = c^{(1)}_2. \tag{5.25}$$

For the 3-point function, the connected 3-point divergence is the product of the 1PI 3-point divergence $c^{(1)}_3$ and three adjacent connected 2-point divergences, see fig. 5.10. To one-loop order, this product can contain only one divergent term in total, either $c^{(1)}_3$ or one of the propagator counterterms $c_{2,2}$, consequently

$$C^{(1)}_3 = c^{(1)}_3 + \langle 3 \rangle \; iv_3 \frac{i}{s_1} c^{(1)}_{2,2}(s_1). \tag{5.26}$$

Here, $\langle 3 \rangle$ denotes 3 permutations (def. 17).

First consider the case of $n = 3$ where all external edges are onshell, i.e. $C^{(1)}_{3,0}$. Then the metacounterterms $C^{(1)}_3$ and $C^{(1)}_2$ vanish due to eq. (5.19), and eq. (5.26) simplifies to

$$0 = c^{(1)}_{3,0} + 0. \tag{5.27}$$

Now let one of the edges be offshell. The metacounterterm $C^{(1)}_{3,1}$ vanishes due to eq. (5.20), but one of the terms $c^{(1)}_{2,2}$ in eq. (5.26) remains, so

$$C^{(1)}_{3,1} = 0 = c^{(1)}_{3,1} + \langle 3 \rangle b_3 (-i s_1) \frac{i}{s_1} c^{(1)}_{2,2}(s_1). \tag{5.28}$$

This implies that

$$c^{(1)}_{3,1} = - \langle 3 \rangle \, b_3 c^{(1)}_{2,2}(s_1) = -b_3^3 \left(s_1^2 + s_2^2 + s_3^2 \right) \frac{M^{(1)}_{\text{div}}}{2}. \tag{5.29}$$

For $c^{(1)}_{3,2}$, the metacounterterm $C^{(1)}_{3,2}$ does not vanish, see eq. (5.22). The construction of $c^{(1)}_{3,2}$ is shown in fig. 5.11, it yields

$$\begin{aligned} c^{(1)}_{3,2} &= C^{(1)}_{3,2} - \langle 3 \rangle \, (-i b_3 s_1) \frac{i}{s_2} c^{(1)}_{2,2}(s_2) - \langle 3 \rangle \, (-i b_3 s_2) \frac{i}{s_1} c^{(1)}_{2,2}(s_1) \\ &= \langle 6 \rangle \, b_3 \left(b_4 - b_3^2 \right) s_1 s_2 \frac{M^{(1)}_{\text{div}}}{2} = b_3 \left(b_4 - b_3^2 \right) \frac{M^{(1)}_{\text{div}}}{2} \cdot 2E_2 \left(s_1, s_2, s_3 \right). \end{aligned} \tag{5.30}$$

To streamline notation, we assumed that $M^{(1)}_{\text{div}}$ is independent of momenta.

Finally, $C^{(1)}_{3,3} = 0$ as there is no divergent connected graph that cancels three external edges at one loop (example 146), therefore

$$c^{(1)}_{3,3} = 0. \tag{5.31}$$

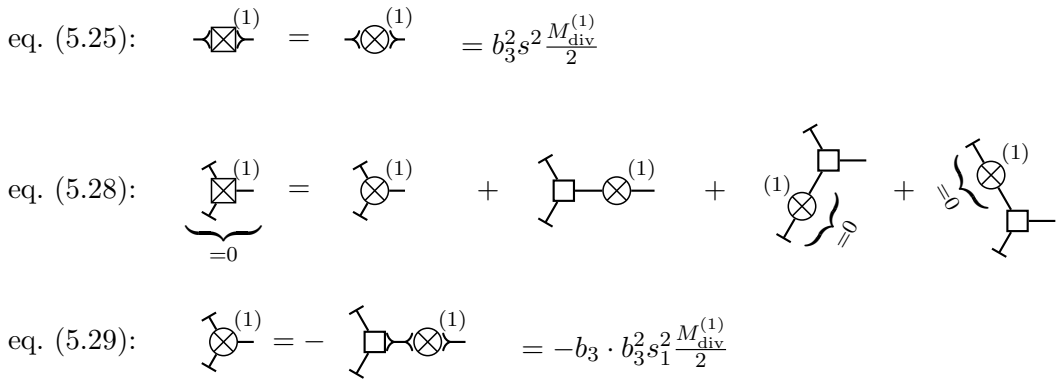

Figure 5.10.: Graphical representation for the computation of $c_{3,1}^{(1)}$. The perpendicular line indicates an external edge which must not be cancelled by the adjacent vertex.

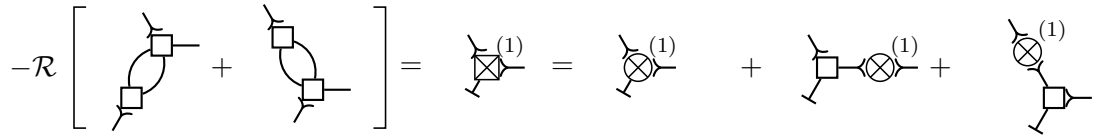

Figure 5.11.: Graphical notation for the computation of $c_{3,2}^{(1)}$. The metacounterterm has been taken from fig. 5.7.

This finishes our survey of 3-point 1PI counterterms at 1 loop order.

The higher n-point 1PI counterterms can be constructed similarly. For $n = 4$ and $k = 0$, the mechanism is depicted in fig. 5.12. The resulting 1PI counterterm is

$$c_{4,0}^{(1)} = -\langle 3\rangle c_{3,1}^{(1)} \frac{i}{s_{1+2}}(-ib_3 s_{1+2}) = -b_3^4 \left(s_{1+2}^2 + s_{1+3}^2 + s_{1+4}^2\right) \frac{M_{\rm div}^{(1)}}{2} \frac{1}{\epsilon}. \tag{5.32}$$

Observe that this 1PI counterterm does not vanish, even if the corresponding metacounterterm $C_{4,0}^{(1)}$ does (eq. (5.19)). With one external edge offshell, the metacounterterm $C_{4,1}^{(1)}$ still vanishes (eq. (5.20)) and we obtain the 1PI counterterm as shown in fig. 5.13. Equation (5.29) implies that the second and third graph cancel and therefore

$$c_{4,1}^{(1)} = \langle 4\rangle \left(b_4 - 3b_3^2\right) b_3^2 \frac{1}{2} M_{\rm div}^{(1)} s_1^2 - \langle 4\rangle\, 2b_3^2 \left(b_4 - b_3^2\right) \frac{1}{2} M_{\rm div}^{(1)} \left(s_{1+2} + s_{1+3} + s_{1+4}\right) s_1.$$

This is the first instance of a 1PI counterterm which cancels a single of its external edges twice, as indicated by a double arrow in fig. 5.13.

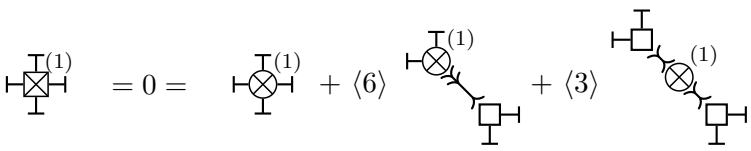

Figure 5.12.: Construction of the onshell 4-point metacounterterm from metavertices 1PI counterterms. The metacounterterm $C_{4,0}^{(1)}$ vanishes, see fig. 5.6.

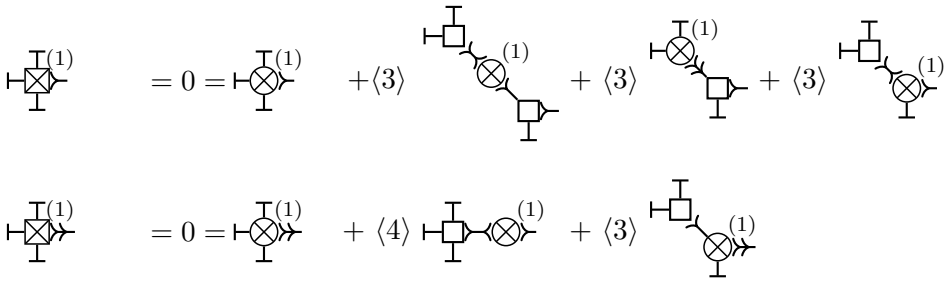

Figure 5.13.: 4-valent metacounterterm with one external leg offshell, which can be cancelled once or twice, indicated by arrows. Edges with perpendicular lines must not be cancelled.

The structure of higher $c^{(1)}_{n,k}$ is restricted by two mechanisms. Firstly, by power-counting, the one-loop 1PI counterterm $c^{(1)}_n$ is proportional to two powers of offshell variables, hence, five different dependencies are possible: Square of an external offshell variable s_j^2, square of an internal one $s^2_{i+j+\ldots}$, two different external ones $s_i s_j$, two different internal ones $s_{i+j+\ldots}s_{k+l+\ldots}$ or a mixture of both types $s_j s_{k+l+\ldots}$.

Secondly, since $M^{(1)}_{\text{div}}$ is independent of momenta by assumption, the metacounterterms $C^{(1)}_{n,k}$ are polynomials in only the external offshell variables s_j, but not in internal ones $s_{i+j+\ldots}$. Both observations together severely restrict the structure of $c^{(1)}_{n,k}$. A rigorous proof requires a tedious recursive construction of trees, we skip the technical details and merely quote the results from [573].

Lemma 86 ([573])**.** Assume that $M^{(1)}$ is the only divergent 1-loop graph and that its divergent part $M^{(1)}_{\text{div}}$ is independent of momenta. The summand in $c^{(1)}_n$, which is proportional to a square of an external offshell variable, is

$$+(n-1)!a_{n-2}b_3^2\frac{M^{(1)}_{\text{div}}}{2}\left(s_1^2+\ldots+s_n^2\right),$$

where a_n is given by eq. (5.6).

Lemma 87 ([573])**.** Assume that $M^{(1)}$ is the only divergent 1-loop graph and $M^{(1)}_{\text{div}}$ is independent of momenta. In the 1PI counterterm $c^{(1)}_n$, the contributions proportional to s_p^2, the square of the offshell variable of some partition p of the external momenta, is

$$b_3^2\frac{M^{(1)}_{\text{div}}}{2}\frac{1}{2}\sum_{k=2}^{n-2}\sum_{p\in Q^{(n,k)}}k!a_{k-1}a_{n-k-1}(n-k)!s_p^2$$

where $Q^{(n,k)}$ denotes the set of all possibilities to choose k out of n external legs.

Lemma 88. Assume that $M^{(1)}$ is the only divergent 1-loop graph and that its divergent part $M^{(1)}_{\text{div}}$ is independent of momenta. If $b_n = \lambda^{n-2}$ then $c^{(1)}$ does not contain any summands which are proportional to $s_e \cdot s_f$, where $e \neq f$ can be external or internal offshell variables.

Theorem 89. For the exponential diffeomorphism (def. 118), $b_n = \lambda^{n-2}$, the 1-loop counterterm $c^{(1)}_n$ has the same structure as the 1PI vertex v_n (lemma 73), up to a non-linear replacement of the offshell variable (def. 8),

$$c^{(1)}_n = v_n \Big|_{s_e \to s_e \cdot \frac{M^{(1)}_{\text{div}}}{2} \lambda^2 s_e}.$$

Proof. Add the contributions of lemmas 86 and 87 to obtain

$$\begin{aligned} c^{(1)}_n &= (n-1)! a_{n-2} b_3^2 \frac{M^{(1)}_{\text{div}}}{2} \left(s_1^2 + \ldots + s_n^2\right) + b_3^2 \frac{M^{(1)}_{\text{div}}}{2} \frac{1}{2} \sum_{k=2}^{n-2} \sum_{p \in Q^{(n,k)}} a_{n-k-1} a_{k-1} (n-k)! k! s_p^2 \\ &= \frac{1}{2} \sum_{k=1}^{n-2} \sum_{p \in Q^{(n,k)}} a_{n-k-1} a_{k-1} (n-k)! k! s_p^2 b_3^2 \frac{M^{(1)}_{\text{div}}}{2}. \end{aligned}$$

This equals the vertex lemma 73 up to the claimed replacement of s_e. Given $b_n = \lambda^{n-2}$, lemma 88 guarantees the absence of other terms. □

Theorem 89 asserts that if we set

$$is_{\mathcal{R}} := is - (is)^2 b_3^2 \frac{M^{(1)}_{\text{div}}}{2}, \tag{5.33}$$

then

$$iv_{\mathcal{R},n} := \frac{1}{2} \sum_{k=1}^{n-1} a_{n-k-1} a_{k-1} (n-k)! k! \sum_{p \in Q^{(n,k)}} is_{\mathcal{R},p} = iv_n + c^{(1)}_n$$

is a "renormalized" vertex in the sense that using $iv_{\mathcal{R},n}$ in place of iv_n, all one-loop divergences are removed from the theory. The "renormalization" eq. (5.33) is a divergent non-linear rescaling of a quantity, much like the rescaling $\alpha = \alpha_0 + \mathcal{O}(\alpha_0^2)$ in conventional renormalization (eq. (2.33)), only that it is not a rescaling of a coupling parameter, but, in a certain sense, a non-linear rescaling of spacetime. This finding is exciting, but it can not be generalized to higher loop orders, see example 148. The failure at higher loop order is plausible from the involved Feynman graphs: From two loops on, there are divergent graphs which are not of propagator type, such as the dunce's cap (fig. 5.9). The divergence of non-propagator graphs can not possibly be cancelled by modifications of the propagator alone, because, even in ordinary renormalization, they require the presence of vertex counterterms.

Interestingly, this finding is reminiscent of quantum gravity (section 5.2.1), uncoupled to matter: All 1-loop divergences can be removed by suitable redefinitions [581], but 2-loop divergences, at least in some formulation of gravity, require counterterms which are not present in the original Lagrangian [582, 583].

Example 148: 2-loop 1PI counterterms of the exponential diffeomorphism.

Consider the exponential diffeomorphism (def. 118) with $u = 1$, $b_n = \lambda^{n-2}$, of a massless field with $s = \underline{p}^2$ in $D = 4 - 2\epsilon$ dimensions. Then, the 1PI 2-loop counterterms are [573]

$$\begin{aligned}
c^{(2)}_{2,2} &= \frac{is^3}{24(4\pi)^4}\lambda^4\left(\frac{1}{\epsilon} - 6\frac{1}{\epsilon^2}\right),\\
c^{(2)}_{3,1} &= \frac{i\left(s_1^3 + s_2^2 + s_3^2\right)}{24(4\pi)^4}\lambda^5\left(6\frac{1}{\epsilon^2} - \frac{1}{\epsilon}\right),\\
c^{(2)}_{3,2} &= -\frac{2i\left(s_1^2 s_2 + s_1^2 s_3 + s_2^2 s_1 + s_2^2 s_3 + s_3^2 s_1 + s_3^2 s_2\right)}{4(4\pi)^4}\lambda^5\frac{1}{\epsilon^2}\\
c^{(2)}_{3,3}, &= \frac{3is_1 s_2 s_3}{4(4\pi)^4}\lambda^5\left(\frac{1}{\epsilon^2} - \frac{1}{\epsilon}\right).
\end{aligned}$$

Their tensor structure is not proportional to the vertext $iv_3 = 2ia_2(s_1 + s_2 + s_3)$ (example 136). This shows that, contrary to the 1-loop counterterms in theorem 89, the 2-loop counterterms can not be generated by a rescaling of the momenta in the bare vertices like eq. (5.33). Compare example 144: The 3-point function $\bar{G}^{(3)}$ involves a triangle graph with superpropagators as edges. From 2 loops on, this graph is divergent, and requires a renormalization condition, even if the superpropagators themselves are finite (by a non-linear rescaling of s).

We conclude that it is not possible to renormalize a field diffeomorphism by rescaling the offshell variable, not even in the special case of an exponential diffeomorphism (def. 118). Instead, we need 1PI counterterms of all valences $n \geq 2$.

5.4.4. Ward identities of the field diffeomorphism

The non-vanishing metacounterterms $C^{(l)}_n$ (section 5.4.1) are proportional to at least two different external offshell variables s_j. Conversely, the 1PI counterterms of the same order can be proportional to inner offshell variables s_{i+j}, too, see for example eq. (5.32). This means that the 1PI counterterms do not necessarily vanish in the onshell limit $s_j \to 0$ of the external edges. Consequently, there must be identities amongst the 1PI counterterms which ensure that they do not contribute to the S-matrix (def. 18) once all graphs are added up.

This behaviour is completely analogous to the 1PI vertices iv_n lemma 73 which, unlike the metavertices iV_n (eq. (5.14)), contain such internal offshell variables in order to fulfil eq. (5.13). Consequently, there is an analogue of eq. (5.13) for counterterms, the following Ward identity (def. 115):

Theorem 90. Consider a diffeomorphism (def. 116) of a free field. Let $c_n^{(l)} := \sum_{k=0}^{n} c_{n,k}^{(l)}$ be the l-loop n-valent 1PI counterterms and let

$$\Gamma_2 := -is - \sum_{l=1}^{\infty} c_2^{(l)}(s), \qquad \Gamma_{n\geq 3} := iv_n + \sum_{l=1}^{\infty} c_n^{(l)},$$

and assume that tadpoles vanish (section 5.1.4). Then, for $n \geq 2$,

1. $$\left[\Gamma_n \frac{1}{\Gamma_2}(-is)\right]_{\text{only } s \text{ offshell}} = iv_n\Big|_{\text{only } s \text{ offshell}},$$
2. $$\sum_{\Gamma_j \star \Gamma_k = \Gamma_n} \left[\Gamma_j \frac{1}{\Gamma_2}\Gamma_k\right]_{\text{onshell}} = -\Gamma_n\Big|_{\text{onshell}},$$

where the product $\star$ implies that $j+k = n+2$ and the sum extends over all orientations of the involved graphs.

Proof. First note that

$$\frac{1}{\Gamma_2} = \frac{i}{s - ic_2} = \frac{i}{s}\sum_{j=0}^{\infty}\left(\frac{i}{s}c_2\right)^j$$

is the non-amputated chain of all 1PI 2-point counterterms, which equals the 2-point metacounterterm. $\frac{1}{\Gamma_2}\cdot(-is)$ is the same chain where the outermost propagator is removed.

For any $n \geq 3$, the connected n-point correlation function vanishes if not more than one external edge is offshell due to theorem 77. Consequently, its divergent part vanishes and $C_{n,0} = C_{n,1} = 0$, see eqs. (5.19) and (5.20). It suffices to consider connected graphs where all internal edges are cancelled since the remaining graphs are products of the former type.

First prove point 1. Use induction on n. For $n = 2$, the statement becomes $(-is) = iv_2$ which is true. For $n = 3$, since c_2 vanishes onshell, the connected graph where only s is offshell is $\Gamma_3\frac{1}{\Gamma_2}(-is)$ where Γ_2 is the counterterm of edge s. But $C_{3,1} = 0$ and hence only the regular term survives of this sum, which is iv_3 as claimed in point 1. Now assume the claim holds for $j < n$. Then, in the sum of all connected graphs, all divergent contributions cancel where s is adjacent to a j-valent counterterm, either directly or via a string of propagator counterterms. The only non-vanishing terms are those where a n-valent counterterm is involved. But again, the sum over all divergent terms has to vanish and the only remaining term is iv_n. This proves point 1.

For point 2, the case $n = 2$ reads $\Gamma_2|_{\text{onshell}} = -\Gamma_2|_{\text{onshell}}$ which is true since $\Gamma_2|_{\text{onshell}} = 0$. The same holds for $n = 3$ since, by eq. (5.19), $\Gamma_3|_{\text{onshell}} = 0$.

Assume point 2 holds for $j, k < n$. The onshell connected amplitude can only be proportional to powers of internal momenta s_e. If there is only one such internal momentum, corresponding to one internal edge e, then all terms proportional to s_e arise from $\Gamma_j\frac{1}{\Gamma_2(e)}\Gamma_k$. Since these terms are not present in the end result, we know Γ_n must absorb them. If there is more than one edge, pick one and call it e. Then, there are two subtrees T_j, T_k, each of which has valence $< n$ and only one external edge offshell, namely e. But by eq. (5.20), such trees do not contain divergent terms. In fact, as a consequence of point 1, such trees do not even contain powers of internal momenta since they are made from tree-level vertices iv_k and such trees evaluate to b_j by theorem 76. Therefore, the only relevant contribution stems from trees with exactly one internal multi-cancelled edge, which proves point 2. □

The compatibility of theorem 90 with locality is expressed by the fact that such identifications between different n-point-functions represent Hopf ideals in the core Hopf algebra [547, 548].

Note also that eq. (5.13) is the tree-level version of statement 2. Technically, only statement 1 of theorem 90 requires the vanishing of tadpoles, i.e. $C_{n,1} = 0$, whereas statement 2 holds regardless. Furthermore, theorem 90 is compatible with BCFW relations [116, 117], in the sense that the overall divergence of a connected graph is given by products of *onshell* subtrees, each of which vanishes.

The Ward identities of theorem 90 play exactly the same role as they do in renormalizable theories: They implement a symmetry. In the case of field diffeomorphisms, the symmetry in question is invariance of the S-matrix (theorem 78) under field diffeomorphisms. Point 2 of theorem 90 ensures that, even at loop level, no counterterms arise which could alter the S-matrix.

Theorem 90 allows for a generalization of the lemmas at the end of section 5.4.3. Point 1 of theorem 90 can equivalently be written in the form

$$\Gamma_n\Big|_{\text{only } s \text{ offshell}} = \left[iv_n \frac{i}{s}\Gamma_2(s)\right]_{\text{only } s \text{ offshell}} .$$

Upon expanding the series $c_n^{(l)}$, this implies

$$c_n^{(l)}\Big|_{\text{only } s \text{ offshell}} = \left[v_n s^{-1} c_2^{(l)}(s)\right]_{\text{only } s \text{ offshell}} .$$

Consequently, the part of $c_n^{(l)}$ proportional to powers of a single offshell variable is always given by the 2-point counterterm, lemma 86 holds to all orders in perturbation theory. Similarly, inserting point 1 of theorem 90 into point 2 produces

$$-\Gamma_n\Big|_{\text{onshell}} = \sum_{\Gamma_j \star \Gamma_k = \Gamma_n} \left[iv_n \frac{i}{s}\Gamma_k\right]_{\text{onshell}} = \sum_{\Gamma_j \star \Gamma_k = \Gamma_n} \left[iv_n \frac{i}{s}\Gamma_2(s)\frac{i}{s}iv_k\right]_{\text{onshell}}$$

and thereby also lemma 87 holds to all orders.

It is lemma 88 which fails at higher than one-loop order: To all orders, those parts of the counterterms which have the same momentum dependence as the vertices iv_n can be obtained by replacing $-is \to \Gamma_2(s)$. But starting from two-loop order, there are additional kinematic form factors in the counterterms which are not obtained in this way.

In renormalizable theories, by lemma 33, each divergent amplitude has one single tensor structure and renormalization amounts to determining the scalar prefactor Z of this tensor. In the present case, on the other hand, a single amplitude obtains at higher loop order infinitely many additional tensor structures, each of which requires their own Z factor. Not all of these terms can be constructed recursively from theorem 90, even if an infinite family can. It is this effect which ultimately renders the theory non-predictive despite the validity of theorem 90.

This negative result for field diffeomorphisms does not directly translate to gravity (section 5.2.1). The latter has a highly non-trivial tensor structure and we would need a dedicated examination to find out if, for a fixed n-graviton amplitude, the number of independent tensors can grow in a similarly uncontrolled way as it can for scalar fields. Such examination is beyond the scope of the present thesis.

Summary of section 5.4.

1. Divergences of connected amplitudes of a field diffeomorphism can be cancelled by metacounterterms, which work analogously to metavertices (section 5.4.1). They are computed from Feynman graphs in the connected perspective (section 5.4.2).

2. Ordinary counterterms, which cancel divergences of 1PI graphs, can be reconstructed from the metacounterterms by a Mellin transform (section 5.4.3). For an exponential diffeomorphism, and only at 1-loop order, all counterterms amount to a non-linear rescaling of the offshell variable (theorem 89).

3. A field diffeomorphism satisfies infinitely many Ward identities, which ensure that counterterms do not alter the S-matrix. These identities are not sufficient to render the theory predictive, as another infinite class of counterterms remains undetermined (section 5.4.4).

6. Conclusion

6.1. Summary

We have examined the high-order perturbative renormalization of quantum field theory. Besides an extensive review of known concepts, we have reached the following results:

1. We extended the differential-equation version of Dyson-Schwinger equations to incorporate ϵ-dependence (section 3.3.4). For non-linear DSEs, the resulting equation is complicated, but we found an explicit formula for the order-ϵ-coefficient of the anomalous dimension of a linear DSE (theorem 47). These results are new and so far unpublished.

2. We examined three popular example DSEs for an undetermined exponent $w \in \mathbb{Z}$ of the invariant charge Q, and derived the leading asymptotic behaviour of the coefficients of their anomalous dimensions (sections 3.4.1, 3.4.3 and 3.4.4). These results have been published in the author's article [480].

3. We found two seemingly exact solutions of non-linear toy model DSEs (section 4.2.4) and two tentative exact values for the Stokes constant of the $D = 4$ multiedge DSE (section 3.4.1), all of which are contained in [480].

4. We computed the Stokes constant of the aysmptotic growth of series coefficients as a function of $w \in \mathbb{Q}$. The result is a smooth, oscillating function, singular as $w \to 0_-$. We gave a tentative explanation (section 3.4.2). This phenomenon is published so far only as a footnote in [480].

5. We examined counterterms and renormalization group equations in detail, for different renormalization conditions, including the full ϵ-dependence, and relating all quantities to the Hopf algebra formulation of renormalization (sections 3.2, 4.1 and 4.3). Although these statements are in principle known, the author is not aware of an exposition at a similar level of detail in the literature.

   This study led us to the conclusion that Green functions in kinematic renormalization and in Minimal Subtraction are equivalent, up to a different choice of renormalization point $\delta(\alpha, \epsilon)$, which, in perturbation theory, is a power series in α and ϵ.

6. We derived multiple formulas to compute $\delta(\alpha, \epsilon)$ under the condition that the Green function is known both in MOM and in MS. To compute the ϵ-independent part $\delta(\alpha)$, it is sufficient to know the renormalized Green functions for $\epsilon = 0$ (sections 4.4.2 and 4.4.3). The case $\epsilon = 0$ had been published in [480], the case $\epsilon \neq 0$ is new.

7. We computed the shifts $\delta(\alpha)$ for the three non-linear example DSEs and examined their power series coefficients. We found that the coefficients grow similarly to the ones of the anomalous dimension. These results are contained in [480].

8. For a linear DSE, we gave an explicit relation between the solution in MS at $\epsilon = 0$ and the solution in MOM at $\epsilon \neq 0$. Using the above result, this allows us to compute the solution of a linear DSE in MS from the ϵ-dependent Mellin transform alone, in a similar way as the MOM-solution can be found directly from the Mellin transform (section 4.4.4). This result constitutes a central new contribution of the present thesis.

9. We examined the chain approximation and found that it does not arise from a Dyson-Schwinger equation. Physically, this means that it violates the fundamental principle of quantum mechanics, that all possible quantum processes must be summed. Consequences of this shortcoming are that the chain approximation does not fulfil the renormalization group equations and it has inequivalent solutions in different renormalization schemes (section 4.5.4). We conclude that the chain approximation is not a valid model for combinatorial properties of QFT. Parts of this argument are contained in [480].

10. We stated, skipping most of the proofs, the Feynman rules of a field diffeomorphism in momentum space and in position space. A diffeomorphism constitutes a perturbatively non-renormalizable theory, but its S-matrix coincides with the underlying field (section 5.2). These results have been published in [202].

11. There is exactly one choice of diffeomorphism parameters with remarkably pleasant combinatorial properties, the exponential diffeomorphism (section 5.3). In this case, some correlation functions of the diffeomorphism theory can be computed to all order. This has been discussed in the author's preprint [573].

12. We examined the structure of divergences of a field diffeomorphism, following the preprint [573]. The outcome is that the divergences satisfy infinitely many Ward identities, which ensure that there are no divergent terms in the S-matrix. However, these identities still leave infinitely many divergences unconstrained. We conclude that the diffeomorphism theory is truly unrenormalizable (section 5.4).

13. We included five remarks beyond the scope of the present thesis (sections 1.2.8, 1.3.9, 2.4, 3.2.4 and 5.2.1). They do not contain any new insights, but are perhaps useful for future doctoral candidates, a they concern topics which are rarely discussed explicitly in typical introduction courses.

6.2. Outlook: Numerical integration of Feynman periods

Apart from renormalization conditions and field diffeomorphisms, which have been presented in the main part of the thesis, the author devoted significant time of his doctorate to a third project, the numerical integration of Feynman periods. To keep the thesis at a reasonable length, the present section contains only a short outlook. The detailed results, together with a discussion of algorithms and implementation, are subject of an upcoming publication.

6.2.1. Symmetries of the period

The Feynman period $\mathcal{P}[\Gamma]$ (def. 96) is the coefficient of the logarithm of the scale and of the first-order pole in ϵ (theorem 30), of a primitive (def. 86) Feynman amplitude. Equally, $\mathcal{P}[\Gamma] = c_0$ is the first term of the Mellin transform (def. 101) of the graph,

$$F_\Gamma(\rho) = \sum_{j=0}^{\infty} c_j \rho^{j-1}.$$

As discussed in section 3.3, the Mellin transform is the input needed for Dyson-Schwinger equations in order to compute the all-order perturbative Green function $G_{\mathcal{R}}$ and inform a resurgence analysis (section 2.1.2) of the non-perturbative properties (section 3.4).

To derive the full Green function, we need to know the entire series expansion of the Mellin transform, for all (infinitely many) kernel graphs (def. 50) of the DSE in question. Computing all of these series is beyond our current capabilities. The three examples discussed in the main text – the multiedge (example 103) in $D = 4$ and $D = 6$, and the toy model (example 102) – were based on the intuition that a good approximation to the DSE can be obtained by considering the full Mellin transform of only a single kernel graph. The present section follows the opposite approach: Include as many kernel graphs as possible, but only the first coefficient of their Mellin transform. If the Mellin transform is truncated after c_0, then the DSE effectively becomes trivial, that is, its solution $G_{\mathcal{R}}$ is merely a sum of the primitive kernel graphs, without any insertions of divergent subgraphs.

We restrict ourselves to massless ϕ^4 theory in $D = 4$ spacetime dimensions, and to the 4-point function. The resulting amplitudes are then contributions to the β-function (def. 110) of ϕ^4 theory.

Computing the β-function to high loop order is relevant for conceptual questions of QFT, such as the existence of renormalons, see [483]. Moreover, as mentioned in section 4.4.1, it is believed that in Minimal Subtraction, the beta function is dominated by primitive graphs, although a theoretical derivation of this result is still lacking [479]:

> Since there are no citations given to substantiate these claims, their status is uncertain. The second of the [historic papers claiming that the beta function is dominated by primitive graphs] was written by the present author, but he recalls only that there was a general belief in the correctness of the assertion at the time.

For further applications, and concrete values, of the β-function in ϕ^4 theory, see [584–587].

Definition 121. A *n-edge-cut* of a graph Γ (def. 24) is a set $E_C := \{e_1, \dots, e_n\} \in E_\Gamma$ such that removing the edges E_C, Γ is split into at least two connected components (def. 22), where none of the components is a single vertex.

Lemma 91. In massless ϕ^4 theory in $D = 4$ dimensions, a graph Γ is primitive if and only if it is internally 6-edge connected (def. 22). That is, it has no k-edge-cut (def. 121) with $k < 6$.

Proof. Let $\Gamma = \Gamma_1 \cup \Gamma_2$ be a split into two connected components. By eq. (1.43), ϕ^4 theory does not contain graphs with an odd number of external edges. Therefore, all three graphs $\Gamma, \Gamma_1, \Gamma_2$ have an even number of external edges, and there are no cuts with an odd number of edges.

By lemma 33, a superficially divergent graph of ϕ^4 theory has 2 or 4 external edges. Assume that Γ has a divergent subgraph γ. Then γ has 2 or 4 external edges, that is, γ is connected to $\frac{\Gamma}{\gamma}$ with 2 or 4 edges. Consequently, Γ has a 2-cut or a 4-cut. Conversely, if Γ is 6-connected, then there is no subgraph with less than 6 external edges, and therefore all subgraphs are convergent. □

Definition 122. A *completion* of a graph Γ is the graph $\Gamma' = \Gamma \cup v$, where v is an additional vertex and all external edges of Γ are incident to v, such that Γ' does not have any external edges. A *decompletion* of a completion Γ is obtained by removing any vertex of Γ.

Every 4-point graph has a unique completion (def. 122). On the other hand, a single completed graph typically gives rise to multiple non-isomorphic decompletions.

Example 149: Wheel with spokes, completion.

$\Gamma =$ 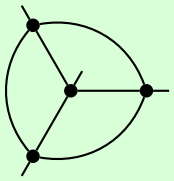 $K_5 =$ 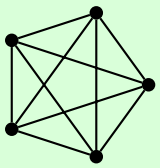

The graph Γ is called *wheel on three spokes*, its period is $\mathcal{P}[\Gamma] = 6\zeta(3)$ [588] and its completion is K_5. In this particular case, all decompletions of K_5 are isomorphic to Γ.

Definition 123. A *n-vertex-cut* of a graph Γ (def. 24) is a set $V_C := \{v_1, \dots, v_n\} \in V_\Gamma$ such that removing the vertices V_C, Γ is split into at least two connected components (def. 22), where none of the components is a single vertex.

The period $\mathcal{P}[\Gamma]$ (def. 96) is symmetric under certain operations on the graph Γ. Below, we list the known symmetries, a precise description can be found in [193, 339, 341].

Completion: If Γ_1 and Γ_2 have the same completion Γ', then $\mathcal{P}[\Gamma_1] = \mathcal{P}[\Gamma_2]$.

Product: If $\Gamma = \Gamma_1 \cup \Gamma_2$ is a 3-vertex cut (def. 123), then $\mathcal{P}[\Gamma] = \mathcal{P}[\Gamma_1] \cdot \mathcal{P}[\Gamma_2]$.

Fourier: If Γ is a planar graph with planar dual $\tilde{\Gamma}$, then $\mathcal{P}[\Gamma] = \mathcal{P}[\tilde{\Gamma}]$.

Extended Fourier: If the planar dual $\tilde{\Gamma}$ of a graph contains one vertex v of valence higher than 4, construct the completion, remove v, and take the planar dual again. If the result is a valid graph in ϕ^4 theory, then its period coincides with $\mathcal{P}[\Gamma]$. Repeat until the resulting graph has either none or more than one vertex of higher valence.

Twist: If Γ has a 4-vertex cut (def. 123), then a pairwise exchange of the edges adjacent to the cut vertices does not alter the period.

Fourier split: Assume that Γ has a 4-vertex cut $\Gamma = \Gamma_1 \cup \Gamma_2$ (def. 123). Taking the planar dual of one of the components, and reconnecting in a particular way, does not alter the period, $\mathcal{P}[\Gamma] = \mathcal{P}[\tilde{\Gamma}_1 \cup \Gamma_2]$.

6.2.2. Numerical quadrature

The number of primitive graphs grows factorially (def. 58) with the loop number [194, 252]. There is a single period at 1 loop (the multiedge example 18), a single one at 3 loops (the wheel with 3 spokes example 149), but there are already more than 13000 periods at 10 loops. Even if by now, the periods of hundreds of graphs are known analytically [191, 339, 340, 342, 589, 590], a sensible study of the high-order asymptotics of periods requires significantly more data. One therefore resorts to numerical calculation of Feynman periods.

The integral in def. 96,

$$\mathcal{P}[\Gamma] = \prod_{e \in E_\Gamma} \int_0^\infty \frac{\mathrm{d}a_e \; a_e^{\nu_e - 1}}{\Gamma(\nu_e)} \; \delta\left(1 - \sum_{e=1}^{|E_\Gamma|} a_e\right) \frac{1}{\psi^2}, \tag{6.1}$$

is of high dimensionality, the method of choice for numerical quadrature is a Monte Carlo integration [591]. However, a direct Monte Carlo integration of eq. (6.1) is impossible because the integral is generally infrared divergent (section 2.3.1). The divergences can be isolated by splitting the integration domain into finitely many *Hepp sectors* [356], such that the integral is free of divergences within each sector, and each of the sectors can be integrated with the Monte Carlo algorithm. This *sector decomposition* [592–595] can be automated, but for a given primitive ϕ^4-graph Γ, it results in $2^{|E_\Gamma|} = 4^{|L_\Gamma|}$ sectors. Consequently, the numerical computation of the period, for a single graph of 10 or more loops, requires the evaluation of millions of sector integrals.

The magnitudes of the individual sector integrals vary significantly. Borinsky [596] has achieved a breakthrough in computation efficiency by weighting each sector according to the Hepp bound (def. 124), recently investigated by Panzer [193]. Using this weighting, a Monte-Carlo integration concentrates the sampling to sectors which give the largest contributions to the end result. The algorithm requires a table of Hepp bounds for all $4^{|L_\Gamma|}$ Hepp sectors. This table, and not so much the actual computing time, is the limiting factor with regards to loop number. Computing 18-loop ϕ^4-periods requires slightly more than 1TB of RAM.

Definition 124 ([193, 356])**.** Let Γ be a Feynman graph and σ a permutation of the edges E_Γ, and let the graph $G_k^\sigma := \{\sigma(1), \dots, \sigma(k)\}$ be the first k edges in σ. Let $\mathcal{S}_n$ be the symmetric group of all $|E_\Gamma|!$ permutations of E_Γ. The *Hepp bound* of a Feynman graph Γ is the rational function

$$\mathcal{H}[\Gamma] := \sum_{\sigma \in \mathcal{S}_n} \frac{1}{\omega(G_1^\sigma) \cdots \omega(G_{|E_\Gamma|-1}^\sigma)},$$

where $\omega(G_k^\sigma)$ is the superficial degree of convergence (def. 41) of the graph G_k^σ.

The Hepp bound is indeed a bound of the period, which was its original motivation in the study of convergence of Feynman integrals [356]:

$$\mathcal{H}[\Gamma] \cdot \left| T_\Gamma^{(1)} \right|^{-2} \leq \mathcal{P}[\Gamma] \leq \mathcal{H}[\Gamma], \tag{6.2}$$

where $T_\Gamma^{(1)}$ is the set of all spanning trees (def. 34).

The Hepp bound (def. 124) satisfies all known symmetries of the period. Moreover, there are pairs of graphs where the Hepp bounds coincide, but the two graphs are not related by any of the known symmetries. It is conjectured that the periods of two graphs coincide whenever the Hepp bounds do [193].

Example 150: Wheel with spokes, Hepp bound.

The wheel with three spokes from example 149 has 6 edges and therefore, the sum in def. 124 is over $6! = 720$ permutations. Its Hepp bound (def. 124) is $\mathcal{H}[\Gamma] = 84$. There are 12 spanning trees (def. 34) and eq. (6.2) is satisfied:

$$\frac{8}{12} = \mathcal{H}[\Gamma] \cdot 12^{-2} \leq 6\zeta(3) \leq \mathcal{H}[\Gamma] = 84.$$

This example indicates that the Hepp bound is a rather crude approximation of the period.

6.2.3. Results

Our own contribution consists of two parts. Firstly, we implemented all known symmetries of the period (section 5.1.1) in native C++ code. The extended dual symmetry has been mentioned in [339], but apparently it has not actually been used in current implementations. It is also possible to combine the Fourier split with the extended Fourier symmetry on the components. The extended Fourier symmetry sometimes leads to sequences of many intermediate graphs until it finally produces a symmetric ϕ^4-graph. This entails that, to find all symmetries of a given graph, the program typically has to construct thousands of candidate graphs, which is computationally demanding. Details of the implementation, as well as more statistical information regarding the symmetries, will be reported elsewhere.

We generated all completed (def. 122) 4-point graphs of ϕ^4 theory up to 14 loops using nauty [597], and filtering for primitive graphs according to lemma 91. For the graphs up to 13 loops, we determined the precise count of all known symmetries, including the extended Fourier split, see table 6.1. The number of symmetries we find is slightly higher than what has been reported so far in the literature [193, 339]. The number of cases where Hepp bounds coincide, but the coincidence is not explained by a known symmetry, is therefore actually lower than the numbers in [193]. Nevertheless, from 8 loops on, there are unexplained identities. We have verified in every single case that if two graphs are related by a known symmetry, their Hepp bounds coincide.

Our second contribution is the actual numerical computation of Feynman periods. The article [596] already contains a C++ reference implementation. We did some trivial modifications on this program in order to fine-tune it especially for ϕ^4-periods. Moreover, the whole process – generation of graphs, numerical integration, and computation of symmetry factors, n-edge cuts (def. 121) and other statistical quantities – has been fully automated, reading and saving all intermediate steps directly to compressed files, and ran on various computers at Humboldt-Universität zu Berlin since late 2020.

L	Decomp.	Planar dec.	Irred. compl.	Twists	F	T+F	F split	Indep. periods	Hepp	Unexpl. Hepp
5	3	2	1	0	0	0	0	1	1	0
6	10	5	4	0	0	0	0	4	4	0
7	44	19	11	1	2	2	2	9	9	0
8	248	58	41	9	3	10	9	31	29	2
9	1688	235	190	48	14	55	53	134	129	5
10	13094	880	1182	336	21	350	334	819	776	42
11	114016	3623	8687	2387	43	2420	2276	6197	6030	158
12	1081529	14596	74204	18680	60	18728	17040	55196	54552	618
13	11048898	60172	700242	155547	90	155630	138164	543535	541196	2246
14	120451435		7160643	1386809	117			5773724		

Table 6.1.: Statistical information on ϕ_4^4-periods. **L** Loop order of the decompletion; Total number of... **Decomp.** non-isomorphic decompletions (= primitive 4-valent graphs); **Planar dec.** planar decompletions; **Irred. compl.** 3-vertex-irreducible completions; **Twist** twist identities; F extended Fourier identities; **T+F** Twist and extended Fourier combined; **F split** extended Fourier splits; **Indep. periods** independent irreducible periods exploiting all known symmetries; **Hepp** numerically distinct Hepp bounds at machine precision; **Unexpl. Hepp**: Unique Hepp bounds coinciding for (sets of) graphs not related by known symmetries. This number is not equal 'independent periods'-'distinct Hepp bounds' since sometimes, more than two sets have the same identical Hepp bounds.
"One identity" means a reduction of the number of independent graphs by one. The symmetry counts refer to irreducible graphs only, the reducible ones have additional symmetries. Note that many identities can be interpreted both as twist or as planar dual identity at the same time, and that planar duals are overall very rare.

We deliberately chose to compute *all* completed graphs, and not just the remaining ones after application of symmetries, because this allows us to verify that expected symmetries are satisfied in every single case. No computation time is wasted because, after verification of symmetries, we combine the individual results of all symmetric graphs to obtain higher accuracy in the end result.

L	computed	proportion	rel. error	irreducible	Hepp	5σ-d	constr.
5	2	1	85 / 85	1	1	1	-
6	5	1	86 / 90	4	4	4	-
7	14	1	80 / 89	11	9	9	-
8	49	1	74 / 90	41	29	28	-
9	227	1	70 / 90	190	129	127	-
10	1354	1	68 / 90	1182	776	578	-
11	9722	1	69 / 90	8687	6030	1563	-
12	81305	1	57 / 90	55196	54706	3002	-
13	755643	1	218 / 288	700242	541196	1346	-
14	215738	$2.8 \cdot 10^{-2}$	246 / 289	208121	205335	1030	273462
15	99212	$1.1 \cdot 10^{-3}$	222 / 308	97178	96177	1198	142040
16	9996	$1.0 \cdot 10^{-5}$	219 / 273	9733	9733	997	21437
17	5144		172 / 261	5043	5043	999	11578
18	789		113 / 220	764	764	579	1448

Table 6.2.: Statistical information on the graphs considered in this work. **L** Loop order; **computed** Number of numerically computed completed primitives, without using symmetries; **proportion** ratio of the computed completed primitives to the total number at that loop order; **rel. error** average / maximum relative uncertainty, in ppm, after imposing symmetries, where the average is taken over all computed graphs. The uncertainty refers to the computed graphs only, not also the ones constructed. **irreducible** number of irreducible graphs computed, **Hepp** number of distinct Hepp bounds within the irreducible graphs, **5 σ-d** number of irreducible graphs which are at least 5σ-distinct from any other computed graph. **constr.** number of completed primitives, including the computed ones, constructed from the computed graphs by symmetries .

We have computed all periods up to 12 loops to at least $90 \cdot 10^{-6}$ relative accuracy, and all 13-loop periods to at least $290 \cdot 10^{-6}$ relative accuracy. Moreover, we have computed a total of over $3 \cdot 10^5$ randomly selected graphs with 14 to 18 loops. The precise numbers are reported in table 6.2. In total, we computed more than 1.1 million completed graphs, which amounts to the period values of round about 12 million non-isomorphic graphs of the 4-point function in ϕ^4 theory.

In all cases, the numerical results satisfy the expected symmetries. Moreover, the periods agree, within the numerical accuracy, in all cases where Hepp bounds agree. The correspondence between symmetries, Hepp bounds, and numerical results indicates that our implementation of symmetries is likely correct.

Although we know some symmetries of the period, it is still possible that even more periods coincide by unknown symmetries, perhaps even if their Hepp bounds are unequal. We tried to estimate a lower bound on the number of distinct periods. To this end, we counted how

many numerical periods are distinct from all others of the same loop order by at least five standard deviations. However, due to the high number of periods, our numerical accuracy is not sufficient to tell most of them apart, and the so-obtained lower bound is weak, see table 6.2.

In the cases where we computed only a random sample of periods, we used the symmetries to construct all symmetric graphs, whose value thereby is known as well. The latter periods are, however, not usable for the estimation of the asymptotics, because using them would distort the random sample of graphs, giving more weight to graphs which have more symmetries.

At this point, we do not report the concrete numerical values we obtained, because statistical evaluation is still ongoing and the results would need significant explanation, which is beyond the scope of this thesis. As an illustration, fig. 6.1 shows all our periods.

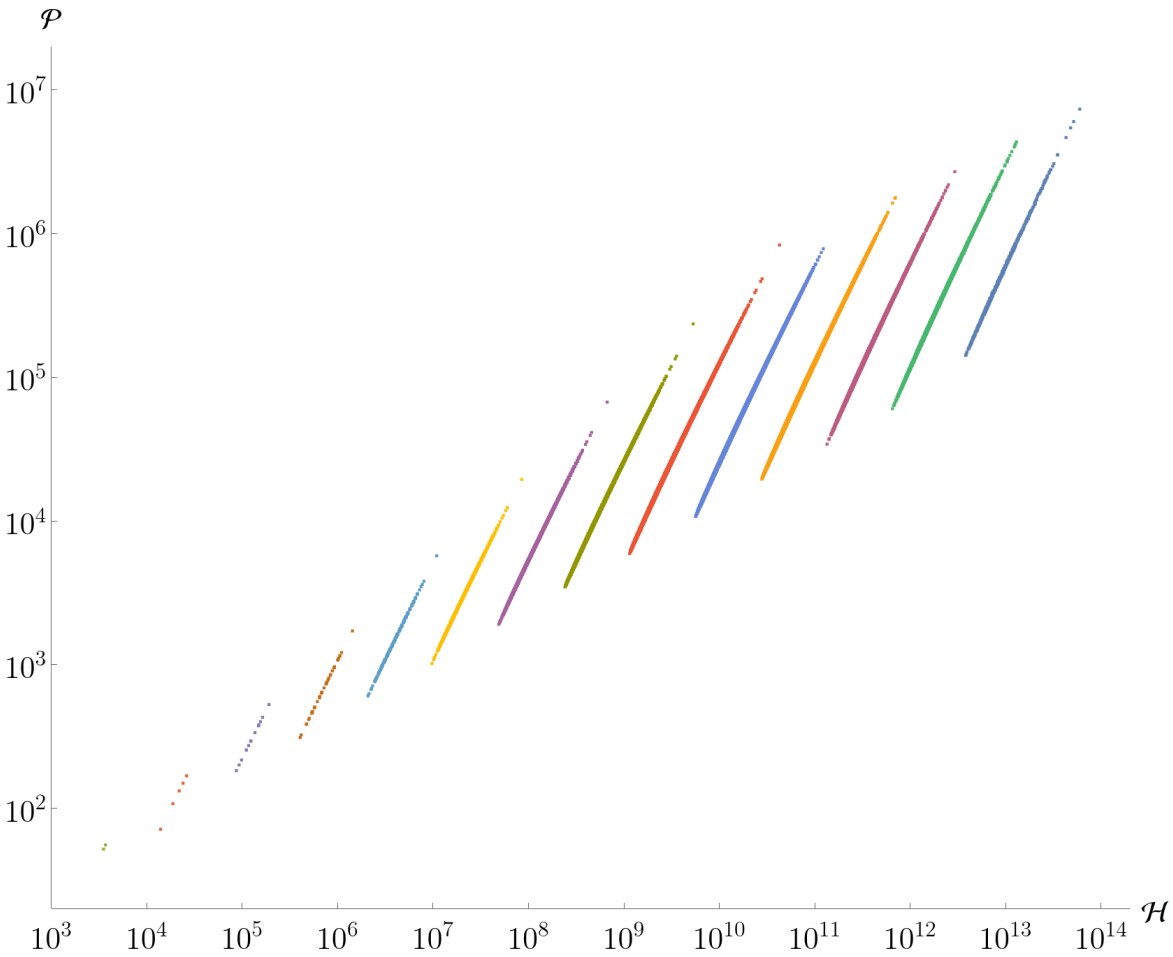

Figure 6.1.: All computed periods, as a function of their Hepp bound (def. 124). Colours indicate loop order, starting from 5 loops on the left. We see that, within the same loop order, the period is strongly correlated with the Hepp bound. This plot contains 1.1 million data points.

Selbstständigkeitserklärung

Ich erkläre, dass ich die Dissertation selbständig und nur unter Verwendung der von mir gemäß § 7 Abs. 3 der Promotionsordnung der Mathematisch-Naturwissenschaftlichen Fakultät, veröffentlicht im Amtlichen Mitteilungsblatt der Humboldt-Universität zu Berlin Nr. 42/2018 am 11.07.2018 angegebenen Hilfsmittel angefertigt habe.
Ich habe mich nicht anderwärts um einen Doktorgrad in dem Promotionsfach beworben und besitze keinen entsprechenden Doktorgrad.
Die Promotionsordnung der Mathematisch-Naturwissenschaftlichen Fakultät, veröffentlicht im Amtlichen Mitteilungsblatt der Humboldt-Universität zu Berlin Nr. 42 am 11. Juli 2018, habe ich zur Kenntnis genommen.

Berlin, den 13.10.2022

A. Publications

Appeared

Paul-Hermann Balduf: "Perturbation Theory of Transformed Quantum Fields", *Math Phys Anal Geom* ***23****, 33 (2020).* doi 10.1007/s11040-020-09357-z, 37 pages. [202]

A. Sternbeck, Paul-Hermann Balduf, A. Kızılersü, O. Oliveira, P.J. Silva, J. Skullerud, A. G. Williams: "Triple-Gluon and Quark-Gluon Vertex from Lattice QCD in Landau Gauge", *PoS, Talk given at 34th annual International Symposium on Lattice Field Theory*, Feb. 2, 2017. arXiv:1702.00612[hep-lat], 7 pages. [471]

Paul-Hermann Balduf, A. Glück: "Fallbeispiele der Promotionsbedingungen für interne und externe Promovierende an der Humboldt-Universität zu Berlin". *Qualität in der Wissenschaft* ***3+4****, 2022.* 7 pages. [598] Raw data available from docs.hu-berlin.de

Accepted for publication

Paul-Hermann Balduf: "Dyson-Schwinger Equations in Minimal Subtraction", Sept. 28, 2021. *Annales de l'Institut Henri Poincaré D.* arXiv:2109.13684, 30 pages. [480]

Preprint

Paul-Hermann Balduf: "Propagator-cancelling scalar fields", Feb 8, 2021. arXiv:2102.04315, 46 pages. [573]

In preparation

Paul-Hermann Balduf, A. Cantwell, K. Ebrahimi-Fard, L. Nabergall, N. Olson-Harris, K. Yeats: "Tubings, Chord diagrams, and Dyson-Schwinger equations".

Paul-Hermann Balduf: "Numerical tables of ϕ^4 periods".

B. Curious quotes from the literature

The ideas and results presented in this paper lead to many questions.
Erik Verlinde [536]

Eine physikalische Theorie glauben wir dann anschaulich zu verstehen, wenn wir uns in allen einfachen Fällen die experimentellen Konsequenzen dieser Theorie qualitativ denken können, und wenn wir gleichzeitig erkannt haben, daß die Anwendung der Theorie niemals innere Widersprüche enthält.
Werner Heisenberg [29]

An elucidation of the mathematical nature of quantum field theory is greatly desirable, particularly in view of current metaphysical pronouncements on this subject. More pertinently, one neither knows entirely satisfactory calculational techniques in elementary particle physics nor, what is more fundamental, whether any proposed schemes have any solutions in principle.
William M. Frank [599]

Quantum mechanics itself is not at all a mystery to me.
Gerard 't Hooft [534]

I've analyzed this method both by doing a number of problems, and by a mathematical high-class elegant technique – I can do high class mathematics too, but I don't believe in it, that's the difference. [...] I'm lousy at proving things – I always make a mistake. [...] So I always have to check with calculations; and I'm very poor at calculations – I always get the wrong answer.
Richard P. Feynman [73]

Well, brothers and sisters, I am here today to tell you: If you love these formulas, you need no longer hide in the shadows! The answer to all of these woes is here.
Gerald A. Edgar [258]

Section II contains the proof. Although at times this attains mathematical levels of obscurity, we make no claim for corresponding standards of rigor.
Sidney Coleman & Jeffrey Mandula [484]

Generalized hyperbolic functions [...] have a compelling intrinsic beauty.
Abraham Ungar [575]

Here I argue that mathematical soundness only is not enough when we are interested in processes of physical content.
Alfredo T. Suzuki [209]

The Yang-Mills theory with zero mass obviously does not exist, because a zero mass field would be obvious; it would come out of nuclei right away.

Richard P. Feynman [73]

The success of the quark-constituent picture both for resonances and for deep-inelastic electron and neutrino processes makes it difficult to believe quarks do not exist. The problem is that quarks have not been seen.

Kenneth G. Wilson [89]

Indeed, we do not believe that physical quarks exist.

David J. Gross, [397, p.209]

Knowledge of the effective potential is knowledge of the structure of spontaneous symmetry breakdown. Unfortunately, we do not know the effective potential.

Sidney Coleman & Erick Weinberg [354]

This result stands out from other multi-loop calculations because it is very likely correct.

Oliver Schnetz [339]

The aim of the present paper is to discuss in some detail established results on the field [of quantum gravity]. In some strong sense, the review could be finished at once, because there are none.

Enrique Alvarez [600]

The appearance of this tiny fundamental length is a gentle reminder that, with conceptual problems no longer barring the way to performing the calculations, the practical interest attached to such refinements of gravitational dynamics is, and for the foreseeable future will remain, nil.

Julian Schwinger [491]

It would be difficult to pretend that the gravitational infrared divergence problem is very urgent. My reasons for now attacking this question are (1) Because I can [...] (2) Because something might go wrong, and that would be interesting. Unfortunately, nothing does go wrong.

Steven Weinberg [601]

Durch mehrere Wahrnehmungen veranlasst, habe ich sorgfältige und vielfach wiederholte Versuche über die Fortleitung der Contaktelektricität in Metallen angestellt und Resultate erhalten, zu deren schleunigser Mittheilung ich mich um so mehr bewogen fühle, als meine geringe, ziemlich verkümmerte Musse mir es nicht verstattet, das Ende dieser Untersuchung so bald herbeizuführen.

Georg S. Ohm [203]

C. Statistics

Excluding the appendices, the thesis is 69100 words long. There are 4633 inline mathematical formulae, and 802 display formulae. This illustrates the scale of section 6.2.3: We have computed 16 period graphs for every word in this thesis.

The thesis contains references to 612 works, 526 of which are journal articles (including preprints), 42 books, 15 book sections, 10 conference papers, 6 theses, and the rest other types of documents. The average document is from the year 1984, that is, 38 years old. The distribution below corresponds to main topics – 1930s QFT basics, 1970s renormalization group theory and 2010s Hopf algebra theory.

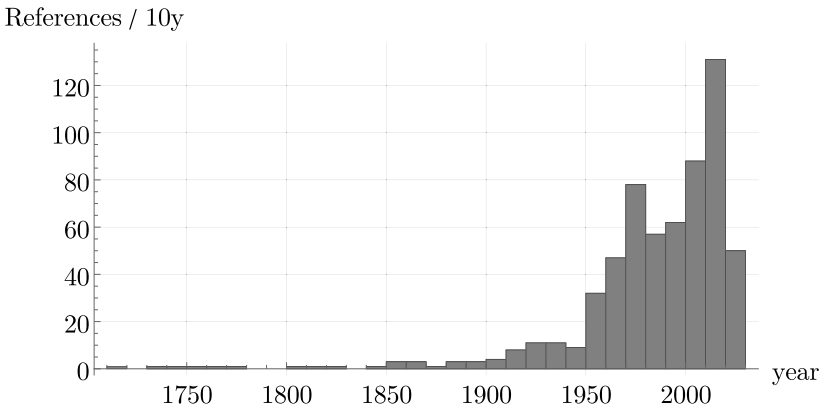

Relying on references which are typically 40 years old appears somewhat bizarre. But a trend towards older references has been observed empirically in many fields [602], and it is sometimes interpreted as a sign that scientific progress is slowing down [603]. The supposed mechanism is that, if the references of a work are decades old, this indicates that recent publications contribute little to the progress of the field.

The author is sceptical about this mechanism. The present thesis uses and refers to dozens of recent articles, the high average age arises mainly because we opted to refer to original sources even for widely known basics. But beyond the age of cited work, other indicators for a slowdown of scientific progress have been observed, despite an exponential growth in number of published papers [604–607]. The interpretation of these findings is disputed [608], and details of the claim – such as a slowdown in total numbers, or rather in productivity per researcher, or per money spent – vary, as well as the supposed reasons – incentive to work on well-funded mainstream questions instead of risky projects, overloading by the flood of published papers, by bureaucracy, teaching and communication tasks or simply the unbearable employment conditions of early career researchers. Our own findings [598] and the ongoing postdoc crisis [609–612] – postdoc positions sitting vacant because they are too unattractive to even apply – do support the last explanation, even if all the points are to some degree entangled. In any case, the author is much less concerned about the age of his references than about the employment situation of early career researchers.

D. List of Examples

E. Bibliography

[1] A. Das, *Lectures on Quantum Field Theory* (World Scientific, Singapore, 2010).

[2] C. Itzykson and J.-B. Zuber, *Quantum Field Theory* (Dover publications, Mineola, New York, 2005).

[3] N. Nakanishi and I. Ojima, *Covariant Operator Formalism of Gauge Theories and Quantum Gravity* (WORLD SCIENTIFIC, 1990), 452 pp., URL: https://www.worldscientific.com/doi/abs/10.1142/0362.

[4] S. Weinberg, *The Quantum Theory of Fields. Volume 1: Foundations*, Vol. 1 (Cambridge University Press, Cambridge, 1996), URL: https://doi.org/10.1017/CBO9781139644167.

[5] M. E. Peskin and D. V. Schroeder, *An Introduction to Quantum Field Theory* (1995), 842 pp., URL: https://cds.cern.ch/record/257493.

[6] R. Ticciati, *Quantum Field Theory for Mathematicians*, Encyclopedia of Mathematics and Its Applications (Cambridge University Press, Cambridge, 1999), URL: https://www.cambridge.org/core/books/quantum-field-theory-for-mathematicians/4783BB717856D3572422F05714CA3D5A.

[7] B. E. Baaquie, *Quantum Field Theory for Economics and Finance — Econophysics, Financial Physics and Social Physics* (Cambridge, 2018), 714 pp., URL: https://www.cambridge.org/de/academic/subjects/physics/econophysics-and-financial-physics/quantum-field-theory-economics-and-finance,%20https://www.cambridge.org/de/academic/subjects/physics/econophysics-and-financial-physics.

[8] T. Lancaster and S. Blundell, *Quantum Field Theory for the Gifted Amateur*, First Edition (Oxford University Press, Oxford, 2014), 485 pp.

[9] E. Weinkötz, "Gedichte", in *27. open mike Wettbewerb für junge Literatur* (Allitera Verlag, München, 2019), p. 182.

[10] H. A. Lorentz, "Versuch Einer Theorie der Electrischen und Optischen Erscheinungen in Bewegten Körpern", in *Collected Papers: Volume V*, edited by H. A. Lorentz (Springer Netherlands, Dordrecht, 1895), pp. 1–138,

[11] E. Wigner, "On Unitary Representations of the Inhomogeneous Lorentz Group", Annals of Mathematics **40**, 149 (1939).

[12] E. C. Zeeman, "Causality Implies the Lorentz Group", Journal of Mathematical Physics **5**, 490–493 (1964),

[13] M. H. Poincaré, "Sur la dynamique de l'électron", Rendiconti del Circolo Matematico di Palermo (1884-1940) **21**, 129–175 (1906),

[14] M. Planck, "Ueber Irreversible Strahlungsvorgänge", Annalen der Physik **306**, 69–122 (1900),

[15] L. Euler, "De Progressionibus Transcendentibus Seu Quarum Termini Generales Algebraice Dari Nequeunt", Commentarii academiae scientiarum Petropolitanae, 36–57 (1738),

[16] R. P. Kanwal, *Generalized Functions, Theory and Applications*, 3rd ed. (Springer, 2004).

[17] C. F. Gauss, *Theoria motus corporum coelestium in sectionibus conicis solem ambientium* (1809), URL: http://www.deutsche-digitale-bibliothek.de/item/3VB4VDOTEM5XBYLK3VV7VQY5JK6SZJWO.

[18] J. Liouville, "Sur l'equation Aux Differences Partielles D2logdu Dv2a2=0", Journal de mathematiques pures et appliquees 1re serie **18**, 71–72 (1853).

[19] O. Klein, "Elektrodynamik und Wellenmechanik vom Standpunkt des Korrespondenzprinzips", Zeitschrift für Physik A Hadrons and nuclei **41**, 407–442 (1927),

[20] W. Gordon, "Der Comptoneffekt nach der Schrödingerschen Theorie", Zeitschrift für Physik **40**, 117–133 (1926),

[21] E. Schrödinger, "Quantisierung Als Eigenwertproblem", Annalen der Physik **386**, 109–139 (1926),

[22] P. T. Kristensen, K. Herrmann, F. Intravaia, K. Busch, and K. Busch, "Modeling Electromagnetic Resonators Using Quasinormal Modes", Advances in Optics and Photonics **12**, 612–708 (2020),

[23] M. Veltman, "Unitarity and Causality in a Renormalizable Field Theory with Unstable Particles", Physica **29**, 186–207 (1963).

[24] A. A. Mahmoud, "On the Enumerative Structures in Quantum Field Theory", 2020, ARXIV: 2008.11661.

[25] J. C. Maxwell, "A Dynamical Theory of the Electromagnetic Field", Philosophical Transactions of the Royal Society of London **155**, 459–512 (1865),

[26] P. A. M. Dirac and R. H. Fowler, "The Quantum Theory of the Electron", Proceedings of the Royal Society of London. Series A, Containing Papers of a Mathematical and Physical Character **117**, 610–624 (1928),

[27] W. Heisenberg, "Über quantentheoretische Umdeutung kinematischer und mechanischer Beziehungen.", Zeitschrift für Physik **33**, 879–893 (1925),

[28] M. Born, W. Heisenberg, and P. Jordan, "Zur Quantenmechanik. II.", Zeitschrift für Physik **35**, 557–615 (1926),

[29] W. Heisenberg, "Über den anschaulichen Inhalt der quantentheoretischen Kinematik und Mechanik", Zeitschrift für Physik **43**, 172–198 (1927),

[30] I. J. R. Aitchison, D. A. MacManus, and T. M. Snyder, "Understanding Heisenberg's 'Magical' Paper of July 1925: A New Look at the Calculational Details", version 1, American Journal of Physics **72**, 1370–1379 (2004),

[31]F. Bayen, M. Flato, C. Fronsdal, A. Lichnerowicz, and D. Sternheimer, "Deformation Theory and Quantization. I. Deformations of Symplectic Structures", Annals of Physics **111**, 61–110 (1978),

[32]F. Bayen, M. Flato, C. Fronsdal, A. Lichnerowicz, and D. Sternheimer, "Deformation Theory and Quantization. II. Physical Applications", Annals of Physics **111**, 111–151 (1978),

[33]M. Kontsevich, "Deformation,Quantization and Beyond", Rutgers Algebra Seminar, 1997.

[34]M. Kontsevich, "Deformation Quantization of Poisson Manifolds", Letters in Mathematical Physics **66**, 157–216 (2003),

[35]S. T. Ali and M. Engliš, "Quantization Methods: A Guide for Physicists and Analysts", Reviews in Mathematical Physics **17**, 391–490 (2005),

[36]S. Bates and A. Weinstein, "Lectures on the Geometry of Quantization", 134 (1994).

[37]N. M. J. Woodhouse, *Geometric Quantization*, Second Edition, Oxford Mathematical Monographs (Oxford University Press, Oxford, New York, 1997), 320 pp.

[38]P. C. Grange and E. Werner, "Quantum Fields as Operator Valued Distributions and Causality", 2007, ARXIV: math-ph/0612011.

[39]F. Gieres, "Mathematical Surprises and Dirac's Formalism in Quantum Mechanics", Reports on Progress in Physics **63**, 1893–1931 (2000),

[40]M. J. Gotay, H. B. Grundling, and G. M. Tuynman, "Obstruction Results in Quantization Theory", Journal of Nonlinear Science **6**, 469–498 (1996),

[41]D. Buchholz and R. Haag, "The Quest for Understanding in Relativistic Quantum Physics", version 2, Journal of Mathematical Physics **41**, 3674–3697 (2000),

[42]L. Klaczynski, "Haag's Theorem in Renormalised Quantum Field Theories", 2016, ARXIV: 1602.00662.

[43]O. Müller, "On the von Neumann Rule in Quantization", 2019, ARXIV: 1903.10494.

[44]A. S. Wightman, "Quantum Field Theory in Terms of Vacuum Expectation Values", Physical Review **101**, 860–866 (1956),

[45]A. S. Wightman and L. Gårding, "Fields as Operator-Valued Distributions in Relativistic Quantum Theory.", Ark. Fys. **28**, 129–184 (1965).

[46]K. Osterwalder and R. Schrader, "Axioms for Euclidean Green's Functions", Commun. Math. Phys. **31**, 83–112 (1973).

[47]G. Mack, "Osterwalder-Schrader Positivity in Conformal Invariant Quantum Field Theory", in Trends in Elementary Particle Theory, edited by H. Rollnik and K. Dietz, Lecture Notes in Physics (1975), pp. 66–91.

[48]H. P. Stapp, "The Copenhagen Interpretation", American Journal of Physics **40**, 1098–1116 (1972),

[49]R. P. Feynman, "Mathematical Formulation of the Quantum Theory of Electromagnetic Interaction", Physical Review **80**, 440–457 (1950),

[50]R. P. Feynman, "Space-Time Approach to Quantum Electrodynamics", Physical Review **76**, 769–789 (1949),

[51]R. P. Feynman, "Space-Time Approach to Non-Relativistic Quantum Mechanics", Rev. Mod. Phys. **20**, 367–387 (1948),

[52]H. Lehmann, K. Symanzik, and W. Zimmermann, "Zur Formulierung Quantisierter Feldtheorien", Il Nuovo Cimento (1955-1965) **1**, 205–225 (1955),

[53]S. Fubini, A. J. Hanson, and R. Jackiw, "New Approach to Field Theory", Physical Review D **7**, 1732–1760 (1973),

[54]K. Huang, *Quantum Field Theory: From Operators to Path Integrals* (Wiley, New York, 1998), 426 pp.

[55]R. Jost, "Properties of Wightman Functions", in *Lectures on Field Theory and the Many-Body Problem Edited by E. R. Caianiello* (Academic Press, New York, 1961).

[56]P. G. Federbush and K. A. Johnson, "Uniqueness Property of the Twofold Vacuum Expectation Value", Physical Review **120**, 1926–1926 (1960),

[57]K. Pohlmeyer, "The Jost-Schroer Theorem for Zero-Mass Fields", Communications in Mathematical Physics **12**, 204–211 (1969),

[58]G. C. Wick, "The Evaluation of the Collision Matrix", Phys. Rev. **80**, 268–272 (1950),

[59]L. Isserlis, "On a Formula for the Product-Moment Coefficient of Any Order of a Normal Frequency Distribution in Any Number of Veriables", Biometrika **12**, 134–139 (1918),

[60]O. Steinmann, "Perturbation Theory of Wightman Functions", Communications in Mathematical Physics **152**, 627–645 (1993),

[61]J. Schwinger, "Quantum Electrodynamics. I. A Covariant Formulation", Physical Review **74**, 1439–1461 (1948),

[62]J. Schwinger, "Quantum Electrodynamics. II. Vacuum Polarization and Self-Energy", Physical Review **75**, 651–679 (1949),

[63]J. Schwinger, "Quantum Electrodynamics. III. The Electromagnetic Properties of the Electron—Radiative Corrections to Scattering", Physical Review **76**, 790–817 (1949),

[64]F. J. Dyson, "The Radiation Theories of Tomonaga, Schwinger, and Feynman", Physical Review **75**, 486–502 (1949),

[65]P. Duch, "Massless Fields and Adiabatic Limit in Quantum Field Theory" (2017), ARXIV: 1709.09907.

[66]R. Haag, "On Quantum Field Theories", Det Kongelige Danske Videnskabernes Selskab Matematisk-fysiske Meddelelser **29**, 19 (1955).

[67]H. Araki, K. Hepp, and D. Ruelle, "On the Asymptotic Behaviour of Wightman Functions in Space-like Directions", Helv. Phys. Acta **35**, 164–174 (1962).

[68]D. A. Slavnov, "Asymptotic States in the Quantum Field Theory", Theoretical and Mathematical Physics **1**, 251–256 (1969),

[69]N. N. Bogolubov, A. A. Logunov, A. I. Oksak, I. T. Todorov, and G. G. Gould, "Haag-Ruelle Scattering Theory", in *General Principles of Quantum Field Theory*, edited by N. N. Bogolubov, A. A. Logunov, A. I. Oksak, and I. T. Todorov, Mathematical Physics and Applied Mathematics (Springer Netherlands, Dordrecht, 1990), pp. 486–502,

[70]D. L. Fraser, "Haags Theorem and the Interpretation of Quantum Field Theories with Interactions. Doctoral Dissertation" (2006), URL: http://d-scholarship.pitt.edu/8260/.

[71]W. Heisenberg, "Die beobachtbaren Größen in der Theorie der Elementarteilchen", Zeitschrift für Physik **120**, 513–538 (1943),

[72]V. Fock, "Konfigurationsraum und zweite Quantelung", Zeitschrift für Physik **75**, 622–647 (1932),

[73]R. P. Feynman, "Quantum Theory of Gravitation", Acta Phys.Polon. **24**, 697–722 (1963).

[74]R. Runkel, Z. Szőr, J. P. Vesga, and S. Weinzierl, "Causality and Loop-Tree Duality at Higher Loops", Physical Review Letters **123**, 059902 (2019),

[75]J. J. Aguilera-Verdugo, F. Driencourt-Mangin, J. Plenter, S. Ramírez-Uribe, G. Rodrigo, G. F. R. Sborlini, W. J. T. Bobadilla, and S. Tracz, "Causality, Unitarity Thresholds, Anomalous Thresholds and Infrared Singularities from the Loop-Tree Duality at Higher Orders", 2019, ARXIV: 1904.08389.

[76]Z. Capatti, V. Hirschi, D. Kermanschah, A. Pelloni, and B. Ruijl, "Manifestly Causal Loop-Tree Duality", 2020, ARXIV: 2009.05509.

[77]J. J. Aguilera-Verdugo, R. J. Hernandez-Pinto, G. Rodrigo, G. F. R. Sborlini, and W. J. T. Bobadilla, "Mathematical Properties of Nested Residues and Their Application to Multi-Loop Scattering Amplitudes", Journal of High Energy Physics **2021**, 112 (2021),

[78]M. Berghoff and D. Kreimer, "Graph Complexes and Feynman Rules", 2020, ARXIV: 2008.09540.

[79]N. Wiener, "Differential-Space", Journal of Mathematics and Physics **2**, 131–174 (1923),

[80]P. a. M. Dirac, "The Lagrangian in Quantum Mechanics", Physikalische Zeitschrift der Sovjetunion **3**, 10.1142/9789812567635_0003 (1933),

[81]A. Connes and M. Marcolli, *Noncommutative Geometry, Quantum Fields and Motives*, Vol. 55, Colloquium Publications (American Mathematical Society, Providence, Rhode Island, 2007), URL: http://www.ams.org/coll/055.

[82]G. Jona-Lasinio, "Relativistic Field Theories with Symmetry-Breaking Solutions", Il Nuovo Cimento (1955-1965) **34**, 1790–1795 (1964),

[83]A. Wipf, *Statistical Approach to Quantum Field Theory: An Introduction*, Lecture Notes in Physics volume 864 (Springer, Heidelberg ; New York, 2013), 390 pp.

[84]F. A. Berezin, "Feynman Path Integrals in a Phase Space", Soviet Physics Uspekhi **23**, 763 (1980),

[85]L. F. Abbott and M. B. Wise, "Dimension of a Quantum-mechanical Path", American Journal of Physics **49**, 37–39 (1981),

[86]G. 't Hooft and M. Veltman, "Diagrammar", Geneva, 1973, URL: http://cds.cern.ch/record/186259/files/CERN-73-09.pdf?version=1.

[87]S. Laporta, "High-Precision Calculation of the 4-Loop Contribution to the Electron g-2 in QED", Phys. Lett. **B772**, 232–238 (2017).

[88]P. Cvitanović, "Asymptotic Estimates and Gauge Invariance", Nuclear Physics B **127**, 176–188 (1977),

[89]K. G. Wilson, "Confinement of Quarks", Physical Review D **10**, 2445–2459 (1974),

[90]H. J. Rothe, *Lattice Gauge Theories: An Introduction (Fourth Edition)* (World Scientific Publishing Company, 2012), URL: https://library.oapen.org/handle/20.500.12657/50492.

[91]J. Ginibre, "Some Applications of Functional Integration in Statistical Mechanics", in Les Houches Summer School of Theoretical Physics: Statistical Mechanics and Quantum Field Theory (1971), pp. 327–429.

[92]E. H. Wichmann and J. H. Crichton, "Cluster Decomposition Properties of the S-Matrix", Physical Review **132**, 2788–2799 (1963),

[93]F. Alpeggiani, N. Parappurath, E. Verhagen, and L. Kuipers, "Quasinormal-Mode Expansion of the Scattering Matrix", Physical Review X **7**, 021035 (2017),

[94]S. V. Lobanov, W. Langbein, and E. A. Muljarov, "Resonant-State Expansion of Three-Dimensional Open Optical Systems: Light Scattering", Physical Review A **98**, 033820 (2018),

[95]A. Einstein, "Die Grundlage Der Allgemeinen Relativitätstheorie", Annalen der Physik **49**, 769 (1916).

[96]S. Weinberg, "What Is Quantum Field Theory, and What Did We Think It Is?", 1997, ARXIV: hep-th/9702027.

[97]G. Källén, "On the Definition of the Renormalization Constants in Quantum Electrodynamics", 10.5169/seals-112316 (1952), URL: https://www.e-periodica.ch/digbib/view?pid=hpa-001:1952:25::814.

[98]H. Lehmann, "Über Eigenschaften von Ausbreitungsfunktionen und Renormierungskonstanten quantisierter Felder", Il Nuovo Cimento (1943-1954) **11**, 342–357 (1954),

[99]L. D. Landau, "On Analytic Properties of Vertex Parts in Quantum Field Theory", Nuclear Physics **13**, 181–192 (1959),

[100]S. Mandelstam, "Determination of the Pion-Nucleon Scattering Amplitude from Dispersion Relations and Unitarity. General Theory", Physical Review **112**, 1344–1360 (1958),

[101]S. Mandelstam, "Analytic Properties of Transition Amplitudes in Perturbation Theory", Physical Review **115**, 1741–1751 (1959),

[102]R. E. Cutkosky, "Singularities and Discontinuities of Feynman Amplitudes", Journal of Mathematical Physics **1**, 429–433 (1960),

[103]D. Amati and S. Fubini, "Dispersion Relation Methods in Strong Interactions", Annual Review of Nuclear Science (1962),

[104]S. Weinberg, "Feynman Rules for Any Spin", Physical Review **133**, B1318–B1332 (1964),

[105]S. Weinberg, "Feynman Rules for Any Spin. II. Massless Particles", Physical Review **134**, B882–B896 (1964),

[106]S. Weinberg, "Feynman Rules for Any Spin. III", Physical Review **181**, 1893–1899 (1969),

[107]S. Weinberg, "Photons and Gravitons in S-Matrix Theory: Derivation of Charge Conservation and Equality of Gravitational and Inertial Mass", Physical Review B **135**, B1049–B1056 (1964),

[108]S. Weinberg, "Photons and Gravitons in Perturbation Theory: Derivation of Maxwell's and Einstein's Equations", Physical Review B **138**, B988–B1002 (1965),

[109]O. Steinmann, "Ueber den Zusammenhang zwischen den Wightmanfunktionen und den retardierten Kommutatoren", Doctoral Thesis (ETH Zurich, 1960), URL: https://www.research-collection.ethz.ch/handle/20.500.11850/135473.

[110]O. Steinmann, "Wightman-Funktionen und retardierte Kommutatoren. II", Helv. Phys. Acta **33**, 10.5169/SEALS-113079 (1960),

[111]E. Remiddi, "Dispersion Relations for Feynman Graphs", Helvetica Physica Acta **54**, 364–382 (1982),

[112]W. L. Van Neerven, "Dimensional Regularization of Mass and Infrared Singularities in Two-Loop on-Shell Vertex Functions", Nuclear Physics B **268**, 453–488 (1986),

[113]J. Bosma, M. Sogaard, and Y. Zhang, "Maximal Cuts in Arbitrary Dimension", Journal of High Energy Physics **2017**, 51 (2017),

[114]E. Remiddi, "Generalised Cuts and Wick Rotations", in Proceedings of Loops and Legs in Quantum Field Theory — PoS(LL2018) (2018), p. 086,

[115]E. Remiddi, "SCHOONSCHIP, the Largest Time Equation and the Continuous Dimensional Regularisation", Acta Phys. Polon. B **52**, 513 (2021).

[116]R. Britto, F. Cachazo, and B. Feng, "New Recursion Relations for Tree Amplitudes of Gluons", Nuclear Physics B **715**, 499–522 (2005),

[117]R. Britto, F. Cachazo, B. Feng, and E. Witten, "Direct Proof Of Tree-Level Recursion Relation In Yang-Mills Theory", Physical Review Letters **94**, 181602 (2005),

[118]R. Zwicky, "A Brief Introduction to Dispersion Relations and Analyticity", in Proceedings, Quantum Field Theory at the Limits: From Strong Fields to Heavy Quarks (HQ 2016): Dubna, Russia, July 18-30, 2016 (2017), pp. 93–120,

[119]S. Bloch and D. Kreimer, "Feynman Amplitudes and Landau Singularities for One-Loop Graphs", Communications in Number Theory and Physics **4**, 709–753 (2010),

[120]S. Bloch and D. Kreimer, "Cutkosky Rules and Outer Space", 2015, ARXIV: 1512.01705.

[121]S. Abreu, R. Britto, C. Duhr, and E. Gardi, "The Diagrammatic Coaction and the Algebraic Structure of Cut Feynman Integrals", 2018, ARXIV: 1803.05894.

[122]F. V. Tkachov, "A Theorem on Analytical Calculability of 4-Loop Renormalization Group Functions", Physics Letters B **100**, 65–68 (1981),

[123]S. Laporta, "High-Precision Calculation of Multi-Loop Feynman Integrals by Difference Equations", International Journal of Modern Physics A **15**, 5087 (2000),

[124]K. G. Chetyrkin and F. V. Tkachov, "Integration by Parts: The Algorithm to Calculate Beta-functions in 4 Loops", Nuclear Physics B **192**, 159–204 (1981),

[125]D. Broadhurst, "Quadratic Relations between Feynman Integrals", in Proceedings of Loops and Legs in Quantum Field Theory — PoS(LL2018) (2018), p. 053,

[126]H. J. Munch, *Feynman Integral Relations from GKZ Hypergeometric Systems*, 2022, ARXIV: 2207.09780.

[127]F. A. Berends and W. T. Giele, "Recursive Calculations for Processes with n Gluons", Nuclear Physics B **306**, 759–808 (1988),

[128]L. Dixon, "Calculating Scattering Amplitudes Efficiently", 1996, ARXIV: hep-ph/9601359.

[129]S. J. Parke and T. R. Taylor, "Amplitude for N-Gluon Scattering", Physical Review Letters **56**, 2459–2460 (1986),

[130]N. Arkani-Hamed, J. L. Bourjaily, F. Cachazo, A. Postnikov, and J. Trnka, "On-Shell Structures of MHV Amplitudes Beyond the Planar Limit", 2014, ARXIV: 1412.8475.

[131]S. Badger, "Automating QCD Amplitudes with On-Shell Methods", Journal of Physics: Conference Series **762**, 012057 (2016),

[132]D. Forde, "On-Shell Recursion Relations for n-Point QCD", Continuous Advances in QCD 2006, 472–478 (2007),

[133]C. Schwinn and S. Weinzierl, "On-Shell Recursion Relations for All Born QCD Amplitudes", Journal of High Energy Physics **2007**, 072–072 (2007),

[134]N. Arkani-Hamed, J. L. Bourjaily, F. Cachazo, A. B. Goncharov, A. Postnikov, and J. Trnka, "Scattering Amplitudes and the Positive Grassmannian", 2014, ARXIV: 1212.5605.

[135]L. Mason and D. Skinner, "Scattering Amplitudes and BCFW Recursion in Twistor Space", Journal of High Energy Physics **2010**, 64 (2010),

[136]T. Cohen, H. Elvang, and M. Kiermaier, "On-Shell Constructibility of Tree Amplitudes in General Field Theories", Journal of High Energy Physics **2011**, 10.1007/JHEP04(2011)053 (2011),

[137]D. A. McGady and L. Rodina, "Higher-Spin Massless S Matrices in Four Dimensions", Physical Review D **90**, 084048 (2014),

[138]N. Arkani-Hamed, T.-C. Huang, and Y.-t. Huang, "Scattering Amplitudes For All Masses and Spins", 2017, ARXIV: 1709.04891.

[139]F. Cachazo and A. Strominger, "Evidence for a New Soft Graviton Theorem", 2014, ARXIV: 1404.4091.

[140]W.-M. Chen, Y.-t. Huang, and D. A. McGady, "Anomalies without an Action", 2014, ARXIV: 1402.7062.

[141]D. Neill and I. Z. Rothstein, "Classical Space–Times from the S-matrix", Nuclear Physics B **877**, 177–189 (2013),

[142]P. Benincasa, C. Boucher-Veronneau, and F. Cachazo, "Taming Tree Amplitudes In General Relativity", Journal of High Energy Physics **2007**, 057–057 (2007),

[143]N. E. J. Bjerrum-Bohr, J. F. Donoghue, and P. Vanhove, "On-Shell Techniques and Universal Results in Quantum Gravity", Journal of High Energy Physics **2014**, 111 (2014),

[144]N. E. J. Bjerrum-Bohr, P. H. Damgaard, G. Festuccia, L. Planté, and P. Vanhove, "General Relativity from Scattering Amplitudes", Physical Review Letters **121**, 171601 (2018),

[145]M. Campiglia and A. Laddha, "Sub-Subleading Soft Gravitons: New Symmetries of Quantum Gravity?", Physics Letters B **764**, 218–221 (2017),

[146]D. Meltzer, "Dispersion Formulas in QFTs, CFTs and Holography", Journal of High Energy Physics **2021**, 98 (2021),

[147]N. Dragon, "The Relativistic String", in Trends in Elementary Particle Theory, edited by H. Rollnik and K. Dietz, Lecture Notes in Physics (1975), pp. 331–351.

[148]A. M. Polyakov, "Quantum Geometry of Bosonic Strings", Physics Letters B **103**, 207–210 (1981),

[149]W. Siegel, "Introduction to String Field Theory", 1988, ARXIV: hep-th/0107094.

[150]R. Loll, "Discrete Approaches to Quantum Gravity in Four Dimensions", Living Reviews in Relativity **1**, 13 (1998),

[151]J. Ambjørn, A. Görlich, J. Jurkiewicz, R. Loll, J. Gizbert-Studnicki, and T. Trześniewski, "The Semiclassical Limit of Causal Dynamical Triangulations", Nuclear Physics B **849**, 144–165 (2011),

[152]F. Finster, "The Principle of the Fermionic Projector: An Approach for Quantum Gravity?", Quantum Gravity, 263–281 (2006),

[153]D. M. Jackson, A. Kempf, and A. H. Morales, "A Robust Generalization of the Legendre Transform for QFT", Journal of Physics A: Mathematical and Theoretical **50**, 225201 (2017),

[154]L. Euler, "Elementa Doctrinae Solidorum", Novi Commentarii academiae scientiarum Petropolitanae, 109–140 (1758),

[155]B. Bollobás, *Modern Graph Theory* (Springer, New York, NY, 1998), 394 pp., URL: https://doi.org/10.1007/978-1-4612-0619-4.

[156]C. W. Borchhardt, "Über eine Interpolationsformel für eine Art symmetrischer Functionen un über deren Anwendung", Abhandlungen der Königlichen Akademie der Wissenschaften in Berlin, 1–20 (1860),

[157]A. Cayley, "A Theorem on Trees", Quaterly Journal of Pure and Applied Mathematics **23**, 376–378 (1889).

[158]J. W. Moon, *Counting Labelled Trees*, Canadian Mathematical Monographs 1 (William Clowes and Sons, London, 1970).

[159]S. Nakamoto, "Bitcoin: A Peer-to-Peer Electronic Cash System", 2008, URL: https://bitcoin.org/bitcoin.pdf.

[160]G. Kirchhoff, "Ueber die Auflösung der Gleichungen, auf welche man bei der Untersuchung der linearen Vertheilung galvanischer Ströme geführt wird", Annalen der Physik **148**, 497–508 (1847),

[161]S. Chaiken and D. J. Kleitman, "Matrix Tree Theorems", Journal of Combinatorial Theory, Series A **24**, 377–381 (1978),

[162]K. Yeats, *A Combinatorial Perspective on Quantum Field Theory*, Vol. 15, SpringerBriefs in Mathematical Physics (Springer International Publishing, Cham, 2017), URL: http://link.springer.com/10.1007/978-3-319-47551-6.

[163]F. Brown and K. Yeats, "Spanning Forest Polynomials and the Transcendental Weight of Feynman Graphs", Communications in Mathematical Physics **301**, 357–382 (2011),

[164]C. Bogner and S. Weinzierl, "Feynman Graph Polynomials", International Journal of Modern Physics A **25**, 2585–2618 (2010),

[165]C. G. Bollini and J. J. Giambiagi, "Dimensional Regularization in Configuration Space", Physical Review D **53**, 5761–5764 (1996),

[166]N. Nakanish, *Graph Theory and Feynman Integrals*, Vol. 11, Mathematics and Its Applications (Gordon and Breach, Science Publishers, Inc, New York London Paris, 1971).

[167]E. Panzer, "Feynman Integrals and Hyperlogarithms", 2015, ARXIV: 1506.07243.

[168]N. N. Bogoliubow and O. S. Parasiuk, "Ueber die Multiplikation der Kausalfunktionen in der Quantentheorie der Felder", Acta Mathematica **97**, 227–266 (1957),

[169]D. Kreimer, M. Sars, and W. D. van Suijlekom, "Quantization of Gauge Fields, Graph Polynomials and Graph Homology", Annals of Physics **336**, 180–222 (2013),

[170]D. Kreimer and K. Yeats, "Properties of the Corolla Polynomial of a 3-Regular Graph", The Electronic Journal of Combinatorics, P41–P41 (2013),

[171]D. Prinz, "The Corolla Polynomial for Spontaneously Broken Gauge Theories", Mathematical Physics, Analysis and Geometry **19**, 18 (2016),

[172]H. Amann and J. Escher, *Analysis*. 2., korr. Aufl., 1. Nachdr, Grundstudium Mathematik (Birkhäuser, Basel, 2008), 415 pp.

[173]N. I. Usyukina, "On a Representation for the Three-Point Function", Theoretical and Mathematical Physics **22**, 210–214 (1975),

[174]D. M. Capper and G. Leibbrandt, "Ward Identities in a General Axial Gauge. I. Yang-Mills Theory", Physical Review D **25**, 1002–1008 (1982),

[175]D. M. Capper and G. Leibbrandt, "Ward Identities in a General Axial Gauge. II. Quantum Gravity", Physical Review D **25**, 1009–1018 (1982),

[176]M. S. Milgram and H. C. Lee, "Tables of Divergent Feynman Integrals in the Axial and Light-Cone Gauges", Journal of Computational Physics **59**, 331–346 (1985),

[177]G. Kramer and B. Lampe, "Integrals for Two-loop Calculations in Massless QCD", Journal of Mathematical Physics **28**, 945–956 (1987),

[178]K. Bönisch, F. Fischbach, A. Klemm, C. Nega, and R. Safari, "Analytic Structure of All Loop Banana Amplitudes", Journal of High Energy Physics **2021**, 66 (2021),

[179]D. Kreimer, "Bananas: Multi-Edge Graphs and Their Feynman Integrals", 2022, ARXIV: 2202.05490.

[180]R. N. Lee and A. A. Pomeransky, "Critical Points and Number of Master Integrals", Journal of High Energy Physics **2013**, 165 (2013),

[181]I. M. Gelfand, M. M. Kapranov, and A. V. Zelevinsky, *Discriminants, Resultants, and Multidimensional Determinants* (Springer, 1994), URL: https://link.springer.com/book/10.1007/978-0-8176-4771-1.

[182]P. Vanhove, *Feynman Integrals, Toric Geometry and Mirror Symmetry*, 2018, ARXIV: 1807.11466.

[183] R. P. Klausen, "Hypergeometric Series Representations of Feynman Integrals by GKZ Hypergeometric Systems", 2019, ARXIV: 1910.08651.

[184] P. A. Baikov, "Explicit Solutions of the 3–Loop Vacuum Integral Recurrence Relations", Physics Letters B **385**, 404–410 (1996),

[185] P. A. Baikov, "Explicit Solutions of the N–Loop Vacuum Integral Recurrence Relations", 1996, ARXIV: hep-ph/9604254.

[186] P. A. Baikov, "A Practical Criterion of Irreducibility of Multi–Loop Feynman Integrals", Physics Letters B **634**, 325–329 (2006),

[187] A. V. Kotikov, "Differential Equations Method. New Technique for Massive Feynman Diagram Calculation", Physics Letters B **254**, 158–164 (1991),

[188] A. V. Kotikov, "Differential Equation Method. The Calculation of N-point Feynman Diagrams", Physics Letters B **267**, 123–127 (1991),

[189] E. Remiddi, "Differential Equations for Feynman Graph Amplitudes", Il Nuovo Cimento A **110**, 1435–1452 (1997),

[190] T. Gehrmann and E. Remiddi, "Differential Equations for Two-Loop Four-Point Functions", Nuclear Physics B **580**, 485–518 (2000),

[191] E. Nasrollahpoursamami, *Periods of Feynman Diagrams and GKZ D-Modules*, 2016, ARXIV: 1605.04970.

[192] C. Berkesch, J. Forsgård, and M. Passare, *Euler–Mellin Integrals and A-hypergeometric Functions*, 2013, ARXIV: 1103.6273.

[193] E. Panzer, "Hepp's Bound for Feynman Graphs and Matroids", 2019, ARXIV: 1908.09820.

[194] M. Borinsky, *Graphs in Perturbation Theory: Algebraic Structure and Asymptotics*, Springer Theses (Springer International Publishing, Cham, 2018), URL: http://link.springer.com/10.1007/978-3-030-03541-9.

[195] G. Frobenius, "Ueber die Congruenz nach einem aus zwei endlichen Gruppen gebildeten Doppelmodul", Journal für die reine und angewandte Mathematik **101**, 273–299 (1887),

[196] W. Burnside, *Theory of Groups of Finite Order* (Cambridge University Press, Cambridge, 1897), URL: https://www.gutenberg.org/ebooks/40395.

[197] J. H. Redfield, "The Theory of Group-Reduced Distributions", American Journal of Mathematics **49**, 433–455 (1927).

[198] G. Pólya, "Kombinatorische Anzahlbestimmungen für Gruppen, Graphen und chemische Verbindungen", Acta Mathematica **68**, 145–254 (1937),

[199] D. Kreimer and K. Yeats, "Diffeomorphisms of Quantum Fields", Mathematical Physics, Analysis and Geometry **20**, 16, 16 (2017).

[200] D. Kreimer, "Anatomy of a Gauge Theory", Annals of Physics **321**, 2757–2781 (2006),

[201] M. Berghoff and A. Knispel, "Complexes of Marked Graphs in Gauge Theory", Letters in Mathematical Physics **110**, 2417–2433 (2020),

[202] P.-H. Balduf, "Perturbation Theory of Transformed Quantum Fields", Mathematical Physics, Analysis and Geometry **23**, 33 (2020),

[203] G. S. Ohm, "Vorläufige Anzeige Des Gesetzes, Nach Welchem Metalle Die Contaktelektricität Leiten", Annalen der Physik **80**, 79–88 (1825),

[204] J. Mathews, "Application of Linear Network Analysis to Feynman Diagrams", Physical Review **113**, 381–381 (1959),

[205] M. D'eramo, L. Peliti, and G. Parisi, "Theoretical Predictions for Critical Exponents at the λ-Point of Bose Liquids", Lettere al Nuovo Cimento (1971-1985) **2**, 878–880 (1971),

[206] A. N. Vasil'ev, Y. M. Pis'mak, and Y. R. Khonkonen, "1/n Expansion: Calculation of the Exponents Eta and Nu in the Order 1/N2 for Arbitrary Number of Dimensions", Theoretical and Mathematical Physics **47**, 465–475 (1981),

[207] N. I. Usyukina, "Calculation of Many-Loop Diagrams of Perturbation Theory", Theoretical and Mathematical Physics **54**, 78–81 (1983),

[208] D. I. Kazakov, "Calculation of Feynman Diagrams by the 'Uniqueness' Method", Theoretical and Mathematical Physics **58**, 223–230 (1984),

[209] A. Suzuki, "Analytic Result for the One-Loop Massless Triangle Feynman Diagram", (2007).

[210] C. G. Neumann, *Untersuchungen Über Das Logarithmische Und Newton'sche Potential* (B.G. Teubner, Leipzig, 1877).

[211] B. S. DeWitt and R. Stora, *Relativity, Groups and Topology: No. 2: Summer School Proceedings* (Elsevier Science Ltd, Amsterdam ; New York : New York, N.Y, 1984), 1360 pp.

[212] D. M. Jackson, A. Kempf, and A. H. Morales, "Algebraic Combinatorial Fourier and Legendre Transforms with Applications in Perturbative Quantum Field Theory", 2019, ARXIV: 1805.09812.

[213] K. Yeats, "Growth Estimates for Dyson-Schwinger Equations", 2008, ARXIV: 0810.2249.

[214] M. P. Bellon and E. I. Russo, "Ward–Schwinger–Dyson Equations in Phi3_6 Quantum Field Theory", Letters in Mathematical Physics **111**, 42 (2021),

[215] F. J. Dyson, "The S Matrix in Quantum Electrodynamics", Physical Review **75**, 1736–1755 (1949),

[216] J. Schwinger, "On the Green's Functions of Quantized Fields. I", Proceedings of the National Academy of Sciences **37**, 452–455 (1951),

[217] J. Schwinger, "On the Green's Functions of Quantized Fields. II", Proceedings of the National Academy of Sciences **37**, 455–459 (1951),

[218] M. Gell-Mann and F. Low, "Bound States in Quantum Field Theory", Physical Review **84**, 350–354 (1951),

[219] P. Cvitanovic, *Field Theory* (Nordita Lecture Notes, 1983), 115 pp., URL: https://chaosbook.org/FieldTheory/pdf.html.

[220] H. S. Wilf, *Generatingfunctionology* (Academic Press, 1994), URL: https://www.math.upenn.edu/%7Ewilf/gfologyLinked2.pdf.

[221] D. Pavlovic and M. Escardo, "Calculus in Coinductive Form", in Proceedings. Thirteenth Annual IEEE Symposium on Logic in Computer Science (Cat. No.98CB36226) (1998), pp. 408–417,

[222] E. T. Bell, "Exponential Polynomials", Annals of Mathematics **35**, 258–277 (1934).

[223]L. Comtet, *Advanced Combinatorics* (D. Reidel Publishing Company, Dordrecht, Holland, 1974).

[224]D. Cvijovic, "New Identities for the Partial Bell Polynomials", Applied Mathematics Letters **24**, 1544–1547 (2011),

[225]A. Schreiber, "Inverse Relations and Reciprocity Laws Involving Partial Bell Polynomials and Related Extensions", 2020, ARXIV: 2009.09201.

[226]F. Qi, D.-W. Niu, D. Lim, and Y.-H. Yao, "Special Values of the Bell Polynomials of the Second Kind for Some Sequences and Functions", Journal of Mathematical Analysis and Applications **491**, 124382 (2020),

[227]J.-L. de Lagrange, "Nouvelle Methode Pour Resoudre Les Equations Litterales Par La Moyen Des Series", Mem. Acad. Royale des Sciences et Belles-Lettres de Berlin, 251–326 (1770).

[228]Henrici, "An Algebraic Proof of the Lagrange-Buermann Formula", Journal of mathematical analysis and applications **8**, 218–224 (1964).

[229]D. Merlini, R. Sprugnoli, and M. C. Verri, "Lagrange Inversion: When and How", Acta Applicandae Mathematica **94**, 233–249 (2006),

[230]W. P. Johnson, "The Curious History of Faa Du Bruno's Formula", The American Mathematical Monthly **109**, 217–234 (2002),

[231]É. Borel, *Leçons Sur Les Séries Divergentes*, Nouvelles Lecons Sur La Theorie Des Fonctions (Gauthier-Villars, Paris, 1901).

[232]G. G. Stokes, "On the Discontinuity of Arbitrary Constants Which Appear in Divergent Developments", Transactions of the Cambridge Philosophical Society **10**, 105 (1864),

[233]M. V. Berry and C. J. Howls, "Hyperasymptotics for Integrals with Saddles", Proceedings of the Royal Society of London. Series A: Mathematical and Physical Sciences **434**, 657–675 (1991),

[234]O. Costin, "On Borel Summation and Stokes Phenomena for Rank-1 Nonlinear Systems of Ordinary Differential Equations", Duke Mathematical Journal **93**, 289–344 (1998),

[235]I. M. Suslov, "Divergent Perturbation Series", Journal of Experimental and Theoretical Physics **100**, 1188–1233 (2005),

[236]D. Sauzin, "Introduction to 1-Summability and Resurgence", 2014, ARXIV: 1405.0356.

[237]I. Aniceto, G. Başar, and R. Schiappa, "A Primer on Resurgent Transseries and Their Asymptotics", Physics Reports, A Primer on Resurgent Transseries and Their Asymptotics **809**, 1–135 (2019),

[238]D. Dorigoni, "An Introduction to Resurgence, Trans-Series and Alien Calculus", Annals of Physics **409**, 167914 (2019),

[239]J. Zinn-Justin, "Perturbation Series at Large Orders in Quantum Mechanics and Field Theories: Application to the Problem of Resummation", Physics Reports **70**, 109–167 (1981),

[240]G. V. Dunne and M. Unsal, "WKB and Resurgence in the Mathieu Equation", 2016, ARXIV: 1603.04924.

[241]P. J. Clavier, "Borel-Écalle Resummation of a Two-Point Function", Annales Henri Poincaré **22**, 2103–2136 (2021),

[242]M. Kontsevich and Y. Soibelman, "Analyticity and Resurgence in Wall-Crossing Formulas", 2021, ARXIV: 2005.10651.

[243]A. Maiezza and J. C. Vasquez, "Non-Wilsonian Ultraviolet Completion via Transseries", International Journal of Modern Physics A **36**, 2150016 (2021),

[244]M. Borinsky and D. Broadhurst, "Resonant Resurgent Asymptotics from Quantum Field Theory", 2022, ARXIV: 2202.01513.

[245]M. P. Bellon and E. I. Russo, "Resurgent Analysis of Ward-Schwinger-Dyson Equations", SIGMA. Symmetry, Integrability and Geometry: Methods and Applications **17**, paper 075, 18 (2021),

[246]P. C. Argyres and M. Ünsal, "The Semi-Classical Expansion and Resurgence in Gauge Theories: New Perturbative, Instanton, Bion, and Renormalon Effects", Journal of High Energy Physics **2012**, 63 (2012),

[247]G. Basar, G. V. Dunne, and M. Unsal, "Resurgence Theory, Ghost-Instantons, and Analytic Continuation of Path Integrals", Journal of High Energy Physics **2013**, 41 (2013),

[248]L. Klaczynski, "Resurgent Transseries & Dyson-Schwinger Equations", Annals of Physics **372**, 397–448 (2016),

[249]M. Borinsky, "Generating Asymptotics for Factorially Divergent Sequences", 2018, ARXIV: 1603.01236.

[250]G. V. Dunne and M. Unsal, "Resurgence and Transseries in Quantum Field Theory: The CP(N-1) Model", Journal of High Energy Physics **2012**, 170 (2012),

[251]G. V. Dunne and M. Ünsal, "Generating Nonperturbative Physics from Perturbation Theory", Physical Review D **89**, 041701 (2014),

[252]M. Borinsky, "Renormalized Asymptotic Enumeration of Feynman Diagrams", Annals of Physics **385**, 95–135 (2017),

[253]M. Borinsky and G. V. Dunne, "Non-Perturbative Completion of Hopf-algebraic Dyson-Schwinger Equations", Nuclear Physics B **957**, 115096 (2020),

[254]F. J. Dyson, "Divergence of Perturbation Theory in Quantum Electrodynamics", Physical Review **85**, 631–632 (1952),

[255]A. Sommerfeld, "Zur Quantentheorie Der Spektrallinien", Annalen der Physik **356**, 1–94 (1916),

[256]M. Gevrey, "Sur La Nature Analytique Des Solutions Des Équations Aux Dérivées Partielles. Premier Mémoire", Annales scientifiques de l'École Normale Supérieure **35**, 129–190 (1918),

[257]L. Euler, "De Seriebus Divergentibus", Novi Commentarii academiae scientiarum Petropolitanae **5**, 205–237 (1760).

[258]G. A. Edgar, "Transseries for Beginners", 2009, ARXIV: 0801.4877.

[259]B. Dahn and P. Göring, "Notes on Exponential-Logarithmic Terms", Fundamenta Mathematicae **127**, 45–50 (1987),

[260]Y. S. Il'yashenko, "Finiteness Theorems for Limit Cycles", Russian Mathematical Surveys **45**, 129–203 (1990),

[261] J. Ecalle, *Introduction Aux Fonctions Analysables et Preuve Constructive de La Conjecture de Dulac*, Actualités Mathématiques (Hermann, Paris, 1992).

[262] L. van den Dries, A. Macintyre, and D. Marker, "Logarithmic-Exponential Power Series", Journal of the London Mathematical Society **56**, 417–434 (1997),

[263] J. Hoeven, *Transseries and Real Differential Algebra*, 1st ed., Lecture Notes in Mathematics 1888 (Springer Berlin Heidelberg, 2006), 260 pp., URL: https://doi.org/10.1007/3-540-35590-1.

[264] O. Costin, "Exponential Asymptotics, Transseries, and Generalized Borel Summation for Analytic Rank One Systems of ODE's", 2006, ARXIV: math/0608414.

[265] R. B. Dingle, *Asymptotic Expansions: Their Derivation and Interpretation* (Academic Press, London, New York, 1973).

[266] J. Ecalle, *Les fonctions résurgentes*, Vol. 1, 3 vols., Publ. Math. Orsay (Orsay, 1981), 248 pp.

[267] L. F. Richardson and R. T. Glazebrook, "The Approximate Arithmetical Solution by Finite Differences of Physical Problems Involving Differential Equations, with an Application to the Stresses in a Masonry Dam", Philosophical Transactions of the Royal Society of London. Series A **210**, 307–357 (1911),

[268] C. Kassel, *Quantum Groups*, Vol. 155, Graduate Texts in Mathematics (Springer New York, New York, NY, 1995), URL: http://link.springer.com/10.1007/978-1-4612-0783-2.

[269] A. Connes and D. Kreimer, "Hopf Algebras, Renormalization and Noncommutative Geometry", in *Quantum Field Theory: Perspective and Prospective*, edited by C. DeWitt-Morette and J.-B. Zuber, NATO Science Series (Springer Netherlands, Dordrecht, 1999), pp. 59–109,

[270] C. Bergbauer and D. Kreimer, "Hopf Algebras in Renormalization Theory: Locality and Dyson-Schwinger Equations from Hochschild Cohomology", 2005, ARXIV: hep-th/0506190.

[271] D. Kreimer and E. Panzer, "Renormalization and Mellin Transforms", Computer Algebra in Quantum Field Theory, Texts & Monographs in Symbolic Computation, 195–223 (2013),

[272] S. Raianu, "Coalgebras from Formulas", in , Vol. 237, Lecture Notes In Pure and Applied Mathematics (2004), pp. 215–224, URL: http://math.csudh.edu/~sraianu/coalgfor.pdf.

[273] J. W. Milnor and J. C. Moore, "On the Structure of Hopf Algebras", Annals of Mathematics **81**, 211–264 (1965).

[274] E. Abe, *Hopf Algebras*, Cambridge Tracts in Mathematics 74 (Cambridge University Press, Cambridge, 1980), 300 pp.

[275] G. Bogfjellmo and A. Schmeding, "The Geometry of Characters of Hopf Algebras", in Computation and Combinatorics in Dynamics, Stochastics and Control. Abel Symposia, Vol 13, Vol. 13 (2016), pp. 159–185,

[276] G. Bogfjellmo, R. Dahmen, and A. Schmeding, "Character Groups of Hopf Algebras as Infinite-Dimensional Lie Groups", Annales de l'Institut Fourier **66**, 2101–2155 (2016),

[277] S. A. Joni and G.-C. Rota, "Coalgebras and Bialgebras in Combinatorics", Studies in Applied Mathematics **61**, 93–139 (1979),

[278] A. Abdesselam, *Feynman Diagrams in Algebraic Combinatorics*, 2002, ARXIV: math/0212121.

[279] H. Figueroa, J. M. Gracia-Bondia, and J. C. Varilly, "Faa Di Bruno Hopf Algebras", 2005, ARXIV: math/0508337.

[280] H. Figueroa and J. M. Gracia-Bondía, "Combinatorial Hopf Algebras in Quantum Field Theory i", Reviews in Mathematical Physics **17**, 881–976 (2005),

[281] A. Connes and D. Kreimer, *Lessons from Quantum Field Theory - Hopf Algebras and Spacetime Geometries*, 1999, ARXIV: hep-th/9904044.

[282] R. P. Stanley, *Enumerative Combinatorics II*, Vol. 2, 2 vols., Cambridge Studies in Advanced Mathematics (Cambridge University Press, Cambridge, 1999), URL: https://www.cambridge.org/core/books/enumerative-combinatorics/D8DDDFF7E8EBF0BCFE99F5E6918CE2A8.

[283] A. Connes and H. Moscovici, "Hopf Algebras, Cyclic Cohomology and the Transverse Index Theorem", Communications in Mathematical Physics **198**, 199–246 (1998),

[284] D. Kreimer, "Chen's Iterated Integral Represents the Operator Product Expansion", 1999, ARXIV: hep-th/9901099.

[285] J. C. Butcher, "Coefficients for the Study of Runge-Kutta Integration Processes", Journal of the Australian Mathematical Society **3**, 185–201 (1963),

[286] T. Krajewski and P. Martinetti, "Wilsonian Renormalization, Differential Equations and Hopf Algebras", 2008, ARXIV: 0806.4309.

[287] C. Brouder, "Runge–Kutta Methods and Renormalization", The European Physical Journal C - Particles and Fields **12**, 521–534 (2000),

[288] B. R. Jones and K. Yeats, "Tree Hook Length Formulae, Feynman Rules and B-series", 2014, ARXIV: 1412.6053.

[289] C. Runge, "Ueber die numerische Auflösung von Differentialgleichungen", Mathematische Annalen **46**, 167–178 (1895),

[290] W. Kutta, "Beitrag Zur Näherungsweisen Integration Totaler Differentialgleichungen", Zeitschrift für Mathematik und Physik **46**, 435–453 (1901).

[291] J. P. Bell, S. N. Burris, and K. A. Yeats, "Counting Rooted Trees: The Universal Law $t(n) \sim C\rho^{-n}n^{-3/2^n}$", The Electronic Journal of Combinatorics, R63–R63 (2006),

[292] D. Kreimer, "On Overlapping Divergences", Communications in Mathematical Physics **204**, 669–689 (1999),

[293] D. Kreimer, "Combinatorics of (Perturbative) Quantum Field Theory", Physics Reports, Renormalization Group Theory in the New Millennium. IV **363**, 387–424 (2002),

[294] R. L. Grossman and R. G. Larson, *Hopf-Algebraic Structures of Families of Trees*, 1987, ARXIV: 0711.3877.

[295]L. Foissy, "Les algèbres de Hopf des arbres enracinés décorés, I", Bulletin des Sciences Mathématiques **126**, 193–239 (2002),

[296]L. Foissy, "Les algèbres de Hopf des arbres enracinés décorés, II", Bulletin des Sciences Mathématiques **126**, 249–288 (2002),

[297]F. Chapoton and M. Livernet, "Pre-Lie Algebras and the Rooted Trees Operad", IMRN 2001 **8**, 395–408 (2000),

[298]D. J. Broadhurst and D. Kreimer, "Renormalization Automated by Hopf Algebra", 1998, ARXIV: hep-th/9810087.

[299]W. D. van Suijlekom, "Renormalization of Gauge Fields: A Hopf Algebra Approach", Communications in Mathematical Physics **276**, 773–798 (2007),

[300]L. Foissy, "General Dyson–Schwinger Equations and Systems", Communications in Mathematical Physics **327**, 151–179 (2014),

[301]B. Delamotte, "A Hint of Renormalization", Am. J. Phys. **72**, 170–184 (2004).

[302]F. Brown and D. Kreimer, "Decomposing Feynman Rules", in (2012), ARXIV: 1212.3923.

[303]F. Brown and D. Kreimer, "Angles, Scales and Parametric Renormalization", 2011, ARXIV: 1112.1180.

[304]A. M. Polyakov, "Conformal Symmetry of Critical Fluctuations", JETP Letters **12**, 381 (1970),

[305]G. Mack and I. T. Todorov, "Conformal-Invariant Green Functions Without Ultraviolet Divergences", Physical Review D **8**, 1764–1787 (1973),

[306]R. Penrose, "Twistor Algebra", Journal of Mathematical Physics **8**, 345–366 (1967),

[307]D. Kreimer, "On the Hopf Algebra Structure of Perturbative Quantum Field Theories", Adv. Theor. Math. Phys. **2**, 303–334 (1998).

[308]E. Panzer, "Hopf Algebraic Renormalization of Kreimer's Toy Model", 2012, ARXIV: 1202.3552.

[309]E. Panzer, "Renormalization, Hopf Algebras and Mellin Transforms", 2015, ARXIV: 1407.4943.

[310]A. Connes and D. Kreimer, "Renormalization in Quantum Field Theory and the Riemann-Hilbert Problem I: The Hopf Algebra Structure of Graphs and the Main Theorem", Communications in Mathematical Physics **210**, 249–273 (2000),

[311]A. Connes and D. Kreimer, "Renormalization in Quantum Field Theory and the Riemann-Hilbert Problem II: The Beta-Function, Diffeomorphisms and the Renormalization Group", Communications in Mathematical Physics **216**, 215–241 (2001),

[312]C. Brouder, A. Frabetti, and C. Krattenthaler, "Non-Commutative Hopf Algebra of Formal Diffeomorphisms", 2004, ARXIV: math/0406117.

[313]K. Ebrahimi-Fard, L. Guo, and D. Kreimer, "Integrable Renormalization II: The General Case", Annales Henri Poincaré **6**, 369–395 (2005),

[314]D. Manchon, "Hopf Algebras in Renormalisation", in *Handbook of Algebra*, Vol. 5, edited by M. Hazewinkel (North-Holland, 2008), pp. 365–427,

[315]G. Baxter, "An Analytic Problem Whose Solution Follows from a Simple Algebraic Identity", Pacific Journal of Mathematics **10**, 731–742 (1960),

[316]G.-C. Rota, "Baxter Algebras and Combinatorial Identities. I", Bulletin of the American Mathematical Society **75**, 325–329 (1969),

[317]S. Weinberg, "High-Energy Behavior in Quantum Field Theory", Physical Review **118**, 838–849 (1960),

[318]J. H. Lowenstein and W. Zimmermann, "The Power Counting Theorem for Feynman Integrals with Massless Propagators", Communications in Mathematical Physics **44**, 73–86 (1975),

[319]D. Yennie, S. Frautschi, and H. Suura, "The Infrared Divergence Phenomena and High-Energy Processes", Annals of Physics **13**, 379–452 (1961).

[320]T. Kinoshita, "Mass Singularities of Feynman Amplitudes", Journal of Mathematical Physics **3** (1962),

[321]K. Harada and R. Kubo, "Infrared Singularity in the Electron Propagator in Quantum Electrodynamics", Nuclear Physics B **191**, 181–188 (1981),

[322]R. Akhoury, M. G. Sotiropoulos, and V. I. Zakharov, "The KLN Theorem and Soft Radiation in Gauge Theories: Abelian Case", Physical Review D **56**, 377–387 (1997),

[323]A. A. Vladimirov, "Method of Calculating Renormalization-Group Functions in the Scheme of Dimensional Regularization", Theoretical and Mathematical Physics **43**, 417–422 (1980),

[324]L. Euler, "De Progressionibus Harmonicis Observationes", Commentarii academiae scientiarum Petropolitanae **7**, 150–161 (1740),

[325]B. Riemann, "Ueber die Anzahl der Primzahlen unter einer gegebenen Grösse", in *Bernard Riemann's gesammelte mathematische Werke und wissenschaftlicher Nachlass*, edited by R. Dedekind and H. M. Weber, 1st ed. (Cambridge University Press, 1859), pp. 136–144,

[326]C. G. Bollini and J. J. Giambiagi, "Dimensional Renormalization : The Number of Dimensions as a Regularizing Parameter", Il Nuovo Cimento B (1971-1996) **12**, 20–26 (1972),

[327]G. 't Hooft and M. Veltman, "Regularization and Renormalization of Gauge Fields", Nuclear Physics B **44**, 189–213 (1972),

[328]B. W. Lee, "Gauge Theories", in *Methods in Field Theory, Les Houches Session 1975*, edited by R. Balian and J. Zinn-Justin, Les Houches Session 28 (North Holland / World Scientific, 1981), pp. 79–140,

[329]K. G. Chetyrkin and V. A. Smirnov, "R_*-Operation Corrected", Physics Letters B **144**, 419–424 (1984),

[330]V. Sudakov, "Vertex Parts at Very High-Energies in Quantum Electrodynamics", Sov. Phy. JETP **3**, 65–71 (1956).

[331]*DLMF: NIST Digital Library of Mathematical Functions*, URL: `https://dlmf.nist.gov/`.

[332]E. E. Boos and A. I. Davydychev, "Method for calculating vertex-type Feynman integrals", Vestnik Moskovskogo Universiteta, Seriya 3. Fizika, Astronomiya **28**, 8–12 (1987),

[333]A. T. Suzuki, E. S. Santos, and A. G. M. Schmidt, "Massless and Massive One-Loop Three-Point Functions in Negative Dimensional Approach", The European Physical Journal C **26**, 125–137 (2002),

[334] A. I. Davydychev, "Recursive Algorithm for Evaluating Vertex-Type Feynman Integrals", Journal of Physics A: Mathematical and General **25**, 5587–5596 (1992),

[335] N. I. Ussyukina and A. I. Davydychev, "New Results for Two-Loop off-Shell Three-Point Diagrams", Physics Letters B **332**, 159–167 (1994),

[336] T. Gehrmann, G. Heinrich, T. Huber, and C. Studerus, "Master Integrals for Massless Three-Loop Form Factors: One-Loop and Two-Loop Insertions", Physics Letters B **640**, 252–259 (2006),

[337] J. A. Gracey, "Off-Shell Two Loop QCD Vertices", Physical Review D **90**, 025014 (2014),

[338] P. Belkale and P. Brosnan, "Periods and Igusa Zeta Functions", 2003, ARXIV: math/0302090.

[339] O. Schnetz, "Quantum Periods: A Census of Phi4-transcendentals", 2009, ARXIV: 0801.2856.

[340] F. C. S. Brown, "On the Periods of Some Feynman Integrals", 2010, ARXIV: 0910.0114.

[341] S. Hu, O. Schnetz, J. Shaw, and K. Yeats, "Further Investigations into the Graph Theory of Phi4-periods and the C2 Invariant", 2018, ARXIV: 1812.08751.

[342] E. Panzer and O. Schnetz, "The Galois Coaction on ϕ^4 Periods", Communications in Number Theory and Physics **11**, 657–705 (2017),

[343] M. Kontsevich and D. Zagier, "Periods", in *Mathematics Unlimited - 2001 and Beyond* (Springer, 2001), pp. 771–808,

[344] S. Bloch, H. Esnault, and D. Kreimer, "On Motives Associated to Graph Polynomials", Communications in Mathematical Physics **267**, 181–225 (2006),

[345] L. Zambelli and O. Zanusso, "Lee-Yang Model from the Functional Renormalization Group", Physical Review D **95**, 085001 (2017),

[346] J. A. Gracey, "Renormalization of Scalar Field Theories in Rational Spacetime Dimensions", 2017, ARXIV: 1703.09685.

[347] J. A. Gracey, "Four Loop Renormalization of Phi$\hat{3}$ Theory in Six Dimensions", Physical Review D **92**, 025012 (2015),

[348] I. G. Halliday and R. M. Ricotta, "Negative Dimensional Integrals. I. Feynman Graphs", Physics Letters B **193**, 241–246 (1987),

[349] G. V. Dunne and I. G. Halliday, "Negative Dimensional Integration. II. Path Integrals and Fermionic Equivalence", Physics Letters B **193**, 247–252 (1987),

[350] D. J. Broadhurst, "Two-Loop Negative-Dimensional Integration", Physics Letters B **197**, 179–182 (1987),

[351] A. Kempf, D. M. Jackson, and A. H. Morales, "How to (Path-) Integrate by Differentiating", Journal of Physics: Conference Series **626**, 012015 (2015),

[352] D. Jia, E. Tang, and A. Kempf, "Integration by Differentiation: New Proofs, Methods and Examples", Journal of Physics A: Mathematical and Theoretical **50**, 235201 (2017),

[353] S. L. Adler, "Einstein Gravity as a Symmetry-Breaking Effect in Quantum Field Theory", Reviews of Modern Physics **54**, 729–766 (1982),

[354] S. Coleman and E. Weinberg, "Radiative Corrections as the Origin of Spontaneous Symmetry Breaking", Physical Review D **7**, 1888–1910 (1973),

[355] D. Kreimer, *Structures in Feynman Graphs – Hopf Algebras and Symmetries*, 2002, ARXIV: hep-th/0202110.

[356] K. Hepp, "Proof of the Bogoliubov-Parasiuk Theorem on Renormalization", Communications in Mathematical Physics **2**, 301–326 (1966),

[357] W. Zimmermann, "Convergence of Bogoliubovs Method of Renormalization in Momentum Space", Communications in Mathematical Physics **15**, 208–234 (1969),

[358] E. R. Speer, "Ultraviolet and Infrared Singularity Structure of Generic Feynman Amplitudes", Annales de l'I.H.P. Physique théorique **23**, 1–21 (1975),

[359] W. E. Caswell and A. D. Kennedy, "Simple Approach to Renormalization Theory", Physical Review D **25**, 392–408 (1982),

[360] S. Sakata, H. Umezawa, and S. Kamefuchi, "On the Structure of the Interaction of the Elementary Particles, I. The Renormalizability of the Interactions", Progress of Theoretical Physics **7**, 377–390 (1952),

[361] A. V. Bäcklund, "Zur Theorie Der Partiellen Differentialgleichung Erster Ordnung", Mathematische Annalen **17**, 285 (1880),

[362] E. Braaten, T. Curtright, and C. Thorn, "An Exact Operator Solution of the Quantum Liouville Field Theory", Annals of Physics **147**, 365–416 (1983),

[363] E. D'Hoker and R. Jackiw, "Classical and Quantal Liouville Field Theory", Physical Review D **26**, 3517–3542 (1982),

[364] E. P. Osipov, "Feynman Integral for Exponential Interaction in Four-Dimensional Space-Time. I", Theoretical and Mathematical Physics **47**, 475–480 (1981),

[365] G. V. Efimov, "Formulation of a Scalar Quantum Field Theory with an Essentially Non-Linear", Nuclear Physics **74**, 657–668 (1965),

[366] G. V. Efimov, "Nonlinear Interaction Lagrangians", Soviet Physics JETP **21**, 7 (1965).

[367] K. G. Chetyrkin and F. V. Tkachov, "Infrared R-operation and Ultraviolet Counterterms in the MS-scheme", Physics Letters B **114**, 340–344 (1982),

[368] V. A. Smirnov and K. G. Chetyrkin, "R_* Operation in the Minimal Subtraction Scheme", Theoretical and Mathematical Physics **63**, 462–469 (1985),

[369] F. Herzog and B. Ruijl, "The R_*-Operation for Feynman Graphs with Generic Numerators", Journal of High Energy Physics **2017**, 37 (2017),

[370] R. Beekveldt, M. Borinsky, and F. Herzog, "The Hopf Algebra Structure of the R_*-Operation", Journal of High Energy Physics **2020**, 61 (2020),

[371] H. A. Bethe, "The Electromagnetic Shift of Energy Levels", Physical Review **72**, 339–341 (1947),

[372] R. P. Woodard, "The Theorem of Ostrogradsky", 2015, ARXIV: 1506.02210.

[373] M. Ostrogradsky, "Mémoires Sur Les Équations Différentielles, Relatives Au Problème Des Isopérimètres", Mem. Acad. St. Petersbourg **6**, 385–517 (1850),

[374] H. Motohashi and T. Suyama, "Quantum Ostrogradsky Theorem", 2020, ARXIV: 2001.02483.

[375]D. Braak, "Integrability of the Rabi Model", Physical Review Letters **107**, 100401 (2011),

[376]G. W. Ford and R. F. O'Connell, "The Rotating Wave Approximation (RWA) of Quantum Optics: Serious Defect", Physica A: Statistical Mechanics and its Applications **243**, 377–381 (1997),

[377]Y.-M. P. Lam, "Perturbation Lagrangian Theory for Scalar Fields-Ward-Takahashi Identity and Current Algebra", Physical Review D **6**, 2145–2161 (1972),

[378]I. L. Buchbinder and S. L. Lyahovich, "Canonical Quantisation and Local Measure of R 2 Gravity", Classical and Quantum Gravity **4**, 1487–1501 (1987),

[379]A. Ganz and K. Noui, "Reconsidering the Ostrogradsky Theorem: Higher-derivatives Lagrangians, Ghosts and Degeneracy", 2020, ARXIV: 2007.01063.

[380]O. Krüger, "Log Expansions from Combinatorial Dyson–Schwinger Equations", Letters in Mathematical Physics **110**, 2175–2202 (2020),

[381]K. Johnson, "Solution of the Equations for the Green's Functions of a Two Dimensional Relativistic Field Theory", Il Nuovo Cimento (1955-1965) **20**, 773–790 (1961),

[382]C. G. Callan, "Broken Scale Invariance in Scalar Field Theory", Physical Review D **2**, 1541–1547 (1970),

[383]K. Symanzik, "Small Distance Behaviour in Field Theory and Power Counting", Communications in Mathematical Physics **18**, 227–246 (1970),

[384]K. Symanzik, "Massless Phi4 Theory in 4-Epsilon Dimensions. DESY Report 73/58", DESY Report 73/58, 1973.

[385]M. Gomes and B. Schroer, "Comment on "New Approach to the Renormalization Group"", Physical Review D **10**, 3525–3531 (1974),

[386]E. Brezin, J. C. Le Guillou, and J. Zinn-Justin, "Wilson's Theory of Critical Phenomena and Callan-Symanzik Equations in 4-Epsilon Dimensions", Physical Review D **8**, 434–440 (1973),

[387]S. Weinberg, "New Approach to the Renormalization Group", Physical Review D **8**, 3497–3509 (1973),

[388]S. W. MacDowell, "Generalized Callan-Symanzik Equations and the Renormalization Group", Physical Review D **12**, 1089–1092 (1975),

[389]D. Kreimer and K. Yeats, "An Etude in Non-Linear Dyson–Schwinger Equations", Nuclear Physics B - Proceedings Supplements, Proceedings of the 8th DESY Workshop on Elementary Particle Theory **160**, 116–121 (2006),

[390]D. J. Broadhurst and D. Kreimer, "Exact Solutions of Dyson-Schwinger Equations for Iterated One-Loop Integrals and Propagator-Coupling Duality", Nuclear Physics B **600**, 403–422 (2001),

[391]J. C. Collins, "Structure of Counterterms in Dimensional Regularization", Nuclear Physics B **80**, 341–348 (1974),

[392]G. 't Hooft, "Dimensional Regularization and the Renormalization Group", Nuclear Physics B **61**, 455–468 (1973),

[393]K. G. Wilson and J. Kogut, "The Renormalization Group and the ϵ Expansion", Physics Reports **12**, 75–199 (1974),

[394]L. S. Brown, "Dimensional Regularization of Composite Operators in Scalar Field Theory", Annals of Physics **126**, 135–153 (1980),

[395]L. T. Adzhemyan and M. V. Kompaniets, "Renormalization Group and the ε-Expansion: Representation of the β-Function and Anomalous Dimensions by Nonsingular Integrals", Theoretical and Mathematical Physics **169**, 1450–1459 (2011),

[396]J. C. Collins and A. J. Macfarlane, "New Methods for the Renormalization Group", Physical Review D **10**, 1201–1212 (1974),

[397]D. J. Gross, "Applications of the Renormalization Group to High-Energy Physics", in *Methods in Field Theory, Les Houches Session 1975*, edited by R. Balian and J. Zinn-Justin, Les Houches Session 28 (North Holland / World Scientific, 1981), pp. 141–250,

[398]A. N. Vasil'ev, M. M. Perekalin, and Y. M. Pis'mak, "On the Possibility of Conformal Infrared Asymptotic Behavior in Non-Abelian Yang-Mills Theory", Theoretical and Mathematical Physics **55**, 529–536 (1983),

[399]Ö. Gürdoğan and V. Kazakov, "New Integrable 4D Quantum Field Theories from Strongly Deformed Planar $\mathcal{N} = 4$ Supersymmetric Yang-Mills Theory", Physical Review Letters **117**, 201602 (2016),

[400]J. Caetano, O. Gurdogan, and V. Kazakov, "Chiral Limit of N = 4 SYM and ABJM and Integrable Feynman Graphs", 2018, ARXIV: 1612.05895.

[401]D. Kreimer, "Étude for Linear Dyson–Schwinger Equations", in *Traces in Number Theory, Geometry and Quantum Fields*, Aspects of Mathematics E38 (Friedr. Vieweg, Wiesbaden, 2008), pp. 155–160,

[402]A. N. Vasilev, *The Field Theoretic Renormalization Group in Critical Behavior Theory and Stochastic Dynamics* (2004).

[403]A. A. Migdal, "Phase Transitions in Gauge and Spin-Lattice Systems'", Zh. Eksp. Teor. Fiz **69**, 1457 (1975).

[404]L. P. Kadanoff, "Notes on Migdal's Recursion Formulas", Annals of Physics **100**, 359–394 (1976),

[405]R. Lipowsky and H. Wagner, "The Migdal-Kadanoff Renormalization Group Scheme for the Ising Model with a Free Surface", Zeitschrift für Physik B Condensed Matter **42**, 355–365 (1981),

[406]N. Benayad and J. Zittartz, "Real-Space Renormalization Group Investigation of the Three-Dimensional Semi-Infinite Mixed Spin Ising Model", Zeitschrift für Physik B Condensed Matter **81**, 107–112 (1990),

[407]L. D. Landau, A. A. Abrikosov, and I. M. Khalatnikov, "An Asymptotic Expression for the Photon Green Function in Quantum Electrodynamics", Dokl. Akad. Nauk SSSR **95**, 1177–1180 (1954).

[408]M. Gell-Mann and F. E. Low, "Quantum Electrodynamics at Small Distances", Physical Review **95**, 1300–1312 (1954),

[409]G. van Baalen, D. Kreimer, D. Uminsky, and K. Yeats, "The QED β-Function from Global Solutions to Dyson–Schwinger Equations", Annals of Physics **324**, 205–219 (2009),

[410]G. van Baalen, D. Kreimer, D. Uminsky, and K. Yeats, "The QCD β-Function from Global Solutions to Dyson–Schwinger Equations", Annals of Physics **325**, 300–324 (2010),

[411] K. G. Wilson and M. E. Fisher, "Critical Exponents in 3.99 Dimensions", Physical Review Letters **28**, 240–243 (1972),

[412] J. D. Bjorken, "Asymptotic Sum Rules at Infinite Momentum", Physical Review **179**, 1547–1553 (1969),

[413] C. G. Callan and D. J. Gross, "Bjorken Scaling in Quantum Field Theory", Physical Review D **8**, 4383–4394 (1973),

[414] D. Gross and F. Wilczek, "Ultraviolet Behavior of Non-Abelian Gauge Theories", Physical Review Letters **30**, 1343–1346 (1973).

[415] H. Politzer, "Reliable Perturbative Results for Strong Interactions?", Physical Review Letters **30**, 1346–1349 (1973).

[416] S. Coleman and D. J. Gross, "Price of Asymptotic Freedom", Physical Review Letters **31**, 851–854 (1973),

[417] H. D. Politzer, "Asymptotic Freedom: An Approach to Strong Interactions", Physics Reports **14**, 129–180 (1974),

[418] K. G. Wilson, "Non-Lagrangian Models of Current Algebra", Physical Review **179**, 1499–1512 (1969),

[419] K. G. Wilson, "Renormalization Group and Strong Interactions", Physical Review D **3**, 1818–1846 (1971),

[420] W. Zimmermann, "Normal Products and the Short Distance Expansion in the Perturbation Theory of Renormalizable Interactions", Annals of Physics **77**, 570–601 (1973),

[421] J. Polchinski, "Renormalization and Effective Lagrangians", Nuclear Physics B **231**, 269–295 (1984),

[422] H. E. Stanley, "Scaling, Universality, and Renormalization: Three Pillars of Modern Critical Phenomena", Reviews of Modern Physics **71**, S358–S366 (1999),

[423] D. J. E. Callaway, "Triviality Pursuit: Can Elementary Scalar Particles Exist?", Physics Reports **167**, 241–320 (1988),

[424] T. R. Hurd, "Renormalization Group Proof of Perturbative Renormalizability", Communications in Mathematical Physics **124**, 153–168 (1989),

[425] C. Wetterich, "Average Action and the Renormalization Group Equations", Nuclear Physics B **352**, 529–584 (1991),

[426] M. Reuter, "Nonperturbative Evolution Equation for Quantum Gravity", Physical Review D **57**, 971–985 (1998),

[427] H. Gies and J. Jaeckel, "Renormalization Flow of QED", Physical Review Letters **93**, 110405 (2004),

[428] J. M. Pawlowski, "Aspects of the Functional Renormalisation Group", Annals of Physics **322**, 2831–2915 (2007),

[429] S. Nagy, "Lectures on Renormalization and Asymptotic Safety", Annals of Physics **350**, 310–346 (2014),

[430] M. Reuter, N. Tetradis, and C. Wetterich, "The Large N Limit and the High Temperature Phase Transition for the ϕ^4 Theory", Nuclear Physics B **401**, 567–590 (1993),

[431] O. Lauscher, "Untersuchungen zum nichtstörungstheoretischen Renormierungsverhalten der Quanten-Einstein-Gravitation" (Johannes Gutenberg-Universität, Mainz, 2002), 306 pp., URL: `https://publications.ub.uni-mainz.de/theses/frontdoor.php?source_opus=391&la=de`.

[432] M. Reuter and F. Saueressig, "Functional Renormalization Group Equations, Asymptotic Safety, and Quantum Einstein Gravity", 2007, ARXIV: 0708.1317.

[433] M. Niedermaier and M. Reuter, "The Asymptotic Safety Scenario in Quantum Gravity", Living Reviews in Relativity **9**, 5 (2006),

[434] S. Weinberg, "Effective Field Theory, Past and Future", 2009, ARXIV: 0908.1964.

[435] T. Appelquist and J. Carazzone, "Infrared Singularities and Massive Fields", Physical Review D **11**, 2856–2861 (1975),

[436] C. P. Korthals Altes and E. de Rafael, "Infrared Structure of Form Factors in Quantum Electrodynamics and Their Behaviour at Large Momentum Transfer", Nuclear Physics B **106**, 237–268 (1976),

[437] A. I. Alekseev, B. A. Arbuzov, and V. A. Baikov, "Infrared Asymptotic Behaviour of Gluon Green's Functions in Quantum Chromodynamics", Theoretical and Mathematical Physics **52**, 739–746 (1982),

[438] B. A. Arbuzov, "Infrared Asymptotics of Gluon and Quark Propagators in QCD", Physics Letters B **125**, 497–500 (1983),

[439] I. Antoniadis and E. Mottola, "Four-Dimensional Quantum Gravity in the Conformal Sector", Physical Review D **45**, 2013–2025 (1992),

[440] U. Ellwanger, M. Hirsch, and A. Weber, "Flow Equations for the Relevant Part of the Pure Yang—Mills Action", Zeitschrift für Physik C Particles and Fields **69**, 687–697 (1996),

[441] R. Alkofer, C. S. Fischer, and L. von Smekal, "The Infrared Behaviour of the Running Coupling in Landau Gauge QCD", 2002, ARXIV: hep-ph/0205125.

[442] S. Moch, J. A. M. Vermaseren, and A. Vogt, "Three-Loop Results for Quark and Gluon Form Factors", Physics Letters B **625**, 245–252 (2005),

[443] C. S. Fischer, A. Maas, and J. M. Pawlowski, "On the Infrared Behavior of Landau Gauge Yang–Mills Theory", Annals of Physics **324**, 2408–2437 (2009),

[444] Z. Komargodski and A. Schwimmer, "On Renormalization Group Flows in Four Dimensions", Journal of High Energy Physics **2011**, 99 (2011),

[445] D. J. Broadhurst and D. Kreimer, "Combinatoric Explosion of Renormalization Tamed by Hopf Algebra: 30-Loop Pade-Borel Resummation", Physics Letters B **475**, 63–70 (2000),

[446] K. Yeats, *Rearranging Dyson-Schwinger Equations*, Vol. 211, Memoirs of the American Mathematical Society 995 (American Mathematical Society, 2011), URL: `https://www.ams.org/memo/0995/`.

[447] H. W. Hamber and L. H. S. Yu, "Dyson's Equations for Quantum Gravity in the Hartree–Fock Approximation", Symmetry **13**, 120 (2021),

[448]D. R. Hartree, "The Wave Mechanics of an Atom with a Non-Coulomb Central Field. Part II. Some Results and Discussion", Mathematical Proceedings of the Cambridge Philosophical Society **24**, 111–132 (1928),

[449]V. Fock, "Näherungsmethode zur Lösung des quantenmechanischen Mehrkörperproblems", Zeitschrift für Physik **61**, 126–148 (1930),

[450]J. C. Slater, "Note on Hartree's Method", Physical Review **35**, 210–211 (1930),

[451]M. Bellon and F. A. Schaposnik, "Renormalization Group Functions for the Wess-Zumino Model: Up to 200 Loops through Hopf Algebras", Nuclear Physics B **800**, 517–526 (2008),

[452]N. Marie and K. Yeats, "A Chord Diagram Expansion Coming from Some Dyson-Schwinger Equations", Communications in Number Theory and Physics **7**, 251–291 (2013),

[453]J. Courtiel and K. Yeats, "Terminal Chords in Connected Chord Diagrams", 2016, ARXIV: 1603.08596.

[454]M. Hihn and K. Yeats, "Generalized Chord Diagram Expansions of Dyson-Schwinger Equations", 2016, ARXIV: 1602.02550.

[455]A. A. Mahmoud, "Chord Diagrams and the Asymptotic Analysis of QED-type Theories", 2020, ARXIV: 2011.04291.

[456]M. P. Bellon, "Approximate Differential Equations for Renormalization Group Functions in Models Free of Vertex Divergencies", Nuclear Physics B **826**, 522–531 (2010),

[457]M. Bellon, "An Efficient Method for the Solution of Schwinger–Dyson Equations for Propagators", Letters in Mathematical Physics **94**, 77–86 (2010),

[458]M. Borinsky, G. Dunne, and M. Meynig, "Semiclassical Trans-Series from the Perturbative Hopf-Algebraic Dyson-Schwinger Equations: ϕ^3 QFT in 6 Dimensions", Symmetry, Integrability and Geometry: Methods and Applications **17**, 87–113 (2021),

[459]R. Delbourgo, A. C. Kalloniatis, and G. Thompson, "Dimensional Renormalization: Ladders and Rainbows", Physical Review D **54**, 5373–5376 (1996),

[460]R. Delbourgo, D. Elliott, and D. S. McAnally, "Dimensional Renormalization in Phi3 Theory: Ladders and Rainbows", Physical Review D **55**, 5230–5233 (1997),

[461]P. J. Larcombe, "The 18th Century Chinese Discovery of the Catalan Numbers", Mathematical Spectrum **32**, 5–7 (1999),

[462]R. P. Stanley, *Catalan Numbers* (Cambridge University Press, Cambridge, 2015), URL: https://www.cambridge.org/core/books/catalan-numbers/5441FB5B09E9C01185834D9CBB9DFAD9.

[463]L. Delage, "Leading Log Expansion of Combinatorial Dyson Schwinger Equations", 2016, ARXIV: 1602.08705.

[464]J. Courtiel and K. Yeats, "Next-to-k Leading Log Expansions by Chord Diagrams", Communications in Mathematical Physics **377**, 469–501 (2020),

[465]O. Krüger and D. Kreimer, "Filtrations in Dyson–Schwinger Equations: Next-to-j-leading Log Expansions Systematically", Annals of Physics **360**, 293–340 (2015),

[466]A. Petermann and E. Stueckelberg, "La normalisation des constantes dans la théorie des quanta", 10.5169/SEALS-112426 (1953), URL: https://www.e-periodica.ch/digbib/view?pid=hpa-001:1953:26::894.

[467]E. A. Uehling, "Polarization Effects in the Positron Theory", Physical Review **48**, 55–63 (1935),

[468]R. Serber, "Linear Modifications in the Maxwell Field Equations", Physical Review **48**, 49–54 (1935),

[469]G. Feldman and R. E. Peierls, "Modified Propagators in Field Theory (with Application to the Anomalous Magnetic Moment of the Nucleon)", Proceedings of the Royal Society of London. Series A. Mathematical and Physical Sciences **223**, 112–129 (1954),

[470]W. E. Pauli, *Niels Bohr and the Development of Physics: Essays Dedicated to Niels Bohr on the Occasion of His Seventieth Birthday* (McGraw-Hill Book Company, 1955), 195 pp.

[471]A. Sternbeck, P.-H. Balduf, A. Kızılersu, O. Oliveira, P. J. Silva, J.-I. Skullerud, and A. G. Williams, "Triple-Gluon and Quark-Gluon Vertex from Lattice QCD in Landau Gauge", 2017, ARXIV: 1702.00612.

[472]J. B. Kogut, E. Dagotto, and A. Kocic, "New Phase of Quantum Electrodynamics: A Nonperturbative Fixed Point in Four Dimensions", Physical Review Letters **60**, 772–775 (1988),

[473]N. J. A. Sloane (editor), *The On-Line Encyclopedia of Integer Sequences*, (2018) URL: https://oeis.org.

[474]D. Broadhurst, *Airy Tadpoles and Dyson-Schwinger Equations*, 2022.

[475]J. Bernoulli, *Ars conjectandi, opus posthumum. Accedit Tractatus de seriebus infinitis, et epistola gallicé scripta de ludo pilae reticularis* (impensis Thurnisiorum, fratrum, Basileae, 1713).

[476]K. Ebrahimi-Fard, J. M. Gracia-Bondia, L. Guo, and J. C. Varilly, "Combinatorics of Renormalization as Matrix Calculus", Physics Letters B **632**, 552–558 (2006),

[477]W. Celmaster and R. J. Gonsalves, "Renormalization-Prescription Dependence of the Quantum-Chromodynamic Coupling Constant", Physical Review D **20**, 1420–1434 (1979),

[478]W. Celmaster and R. J. Gonsalves, "Quantum-Chromodynamics Perturbation Expansions in a Coupling Constant Renormalized by Momentum-Space Subtraction", Physical Review Letters **42**, 1435–1438 (1979),

[479]A. J. McKane, "Perturbation Expansions at Large Order: Results for Scalar Field Theories Revisited", Journal of Physics A: Mathematical and Theoretical **52**, 055401 (2019),

[480]P.-H. Balduf, *Dyson-Schwinger Equations in Minimal Subtraction*, 2022, ARXIV: 2109.13684.

[481]M. Beneke, "Renormalons", Physics Reports **317**, 1–142 (1999),

[482]D. Espriu and R. Tarrach, "Ambiguities in QED: Renormalons versus Triviality", Physics Letters B **383**, 482–486 (1996),

[483]G. V. Dunne and M. Meynig, "Instantons or Renormalons? A Comment on Phi4_4 Theory in the MS Scheme", 2021, ARXIV: 2111.15554.

[484]S. Coleman and J. Mandula, "All Possible Symmetries of the S Matrix", Physical Review **159**, 1251–1256 (1967),

[485]R. Haag, J. T. Łopuszański, and M. Sohnius, "All Possible Generators of Supersymmetries of the S-matrix", Nuclear Physics B **88**, 257–274 (1975),

[486]M. Fierz, "Über Die Relativistische Theorie Kräftefreier Teilchen Mit Beliebigem Spin", Helvetica Physica Acta **12** (1939),

[487]A. Sagnotti, "Higher Spins and Current Exchanges", 2010, ARXIV: 1002.3388.

[488]A. Sagnotti, "Notes on Strings and Higher Spins", Journal of Physics A: Mathematical and Theoretical **46**, 214006 (2013),

[489]M. Fierz, "Non-Local Fields", Physical Review **78**, 184–184 (1950),

[490]H. Yukawa, "Quantum Theory of Non-Local Fields. Part I. Free Fields", Physical Review **77**, 219–226 (1950),

[491]J. Schwinger, "Sources and Gravitons", Physical Review **173**, 1264–1272 (1968),

[492]Y. Iwasaki, "Consistency Condition for Propagators", Physical Review D **2**, 2255–2256 (1970),

[493]V. Alba and K. Diab, "Constraining Conformal Field Theories with a Higher Spin Symmetry in D=4", 2013, ARXIV: 1307.8092.

[494]E. S. Fradkin and A. N. Vasil'ev, "On the Gravitation Interaction of Massless Higher-Spin Fields", Physics Letters B **189**, 89–95 (1987).

[495]E. S. Fradkin and M. A. Vasiliev, "Cubic Interaction in Extended Theories of Massless Higher-Spin Fields", Nuclear Physics B **291**, 141–171 (1987),

[496]N. Boulanger, P. Sundell, and S. Leclercq, "On the Uniqueness of Minimal Coupling in Higher-Spin Gauge Theory", Journal of High Energy Physics **2008**, 056–056 (2008),

[497]P. M. Lavrov and I. V. Tyutin, "Canonical Formalism of Gauge Theories with Reducible Constraints", Soviet Physics Journal **28**, 576–579 (1985),

[498]B. W. Lee and J. Zinn-Justin, "Spontaneously Broken Gauge Symmetries. II. Perturbation Theory and Renormalization", Physical Review D **5**, 3137–3155 (1972),

[499]G. Curci and R. Ferrari, "Slavnov Transformations and Supersummetry", Physics Letters B **63**, 91–94 (1976),

[500]E. S. Fradkin and I. V. Tyutin, "S Matrix for Yang-Mills and Gravitational Fields", Physical Review D **2**, 2841–2857 (1970),

[501]C. Brouder and A. Frabetti, "Renormalization of QED with Planar Binary Trees", The European Physical Journal C - Particles and Fields **19**, 715–741 (2001),

[502]J. C. Ward, "An Identity in Quantum Electrodynamics", Physical Review **78**, 182–182 (1950),

[503]G. 'tHooft, "Renormalization of Massless Yang-Mills Fields", Nuclear Physics B **33**, 173–199 (1971),

[504]W. D. Van Suijlekom, "The Hopf Algebra of Feynman Graphs in Quantum Electrodynamics", Letters in Mathematical Physics **77**, 265–281 (2006),

[505]B. W. Lee and J. Zinn-Justin, "Spontaneously Broken Gauge Symmetries. I. Preliminaries", Physical Review D **5**, 3121–3137 (1972),

[506]J. A. Gracey, H. Kissler, and D. Kreimer, "On the Self-Consistency of off-Shell Slavnov-Taylor Identities in QCD", 2019, ARXIV: 1906.07996.

[507]G. 't Hooft and M. Veltman, "Combinatorics of Gauge Fields", Nuclear Physics B **50**, 318–353 (1972),

[508]D. F. Litim and J. M. Pawlowski, "Flow Equations for Yang-Mills Theories in General Axial Gauges", Physics Letters B **435**, 181–188 (1998),

[509]G. Keller, M. Salmhofer, and Kopper, C, "Perturbative Renormalization and Effective Lagrangians in Phi44", Helvetica Physica Acta **65**, 32–52 (1992),

[510]M. Sars, "Parametric Representation of Feynman Amplitudes in Gauge Theories" (2015).

[511]C. N. Yang and R. L. Mills, "Conservation of Isotopic Spin and Isotopic Gauge Invariance", Physical Review **96**, 191–195 (1954),

[512]A. A. Slavnov, "Ward Identities in Gauge Theories", Theoretical and Mathematical Physics **10**, 99–104 (1972),

[513]J. C. Taylor, "Ward Identities and Charge Renormalization of the Yang-Mills Field", Nuclear Physics B **33**, 436–444 (1971),

[514]W. H. Furry, "A Symmetry Theorem in the Positron Theory", Physical Review **51**, 125–129 (1937),

[515]D. Hilbert, "Die Grundlagen der Physik . (Erste Mitteilung.)", Nachrichten von der Gesellschaft der Wissenschaften zu Göttingen, Mathematisch-Physikalische Klasse **1915**, 395–408 (1915),

[516]D. Prinz, "Algebraic Structures in the Coupling of Gravity to Gauge Theories", 2018, ARXIV: 1812.09919.

[517]D. Kreimer, "A Remark on Quantum Gravity", Annals of Physics **323**, 49–60 (2008),

[518]A. Pais and G. E. Uhlenbeck, "On Field Theories with Non-Localized Action", Physical Review **79**, 145–165 (1950),

[519]P. D. Mannheim, "Solution to the Ghost Problem in Fourth Order Derivative Theories", Foundations of Physics **37**, 532–571 (2007),

[520]L. Modesto and L. Rachwał, "Universally Finite Gravitational and Gauge Theories", Nuclear Physics B **900**, 147–169 (2015),

[521]A. Salvio and A. Strumia, "Quantum Mechanics of 4-Derivative Theories", The European Physical Journal C **76**, 227 (2016),

[522]J. A. Gracey and R. M. Simms, "Higher Dimensional Higher Derivative Phi4 Theory", Physical Review D **96**, 10.1103/PhysRevD.96.025022 (2017),

[523]F. Briscese and L. Modesto, "Unattainability of the Trans-Planckian Regime in Nonlocal Quantum Gravity", 2019, ARXIV: 1912.01878.

[524]H. Weyl, "Eine Neue Erweiterung Der Relativitätstheorie", Annalen der Physik **364**, 101–133 (1919),

[525]K. S. Stelle, "Renormalization of Higher-Derivative Quantum Gravity", Physical Review D **16**, 953–969 (1977),

[526]A. Zee, "Einstein Gravity Emerging from Quantum Weyl Gravity", Annals of Physics **151**, 431–443 (1983),

[527]P. D. Mannheim, "Conformal Gravity Challenges String Theory", 2007, ARXIV: 0707.2283.

[528]P. D. Mannheim, "Alternatives to Dark Matter and Dark Energy", Progress in Particle and Nuclear Physics **56**, 340–445 (2006),

[529]S. M. Christensen and M. J. Duff, "Quantum Gravity in 2 + Epsilon Dimensions", Physics Letters B **79**, 213–216 (1978),

[530]R. Gastmans, R. Kallosh, and C. Truffin, "Quantum Gravity near Two Dimensions", Nuclear Physics B **133**, 417–434 (1978),

[531]I. Jack and D. R. T. Jones, "The Epsilon-Expansion of Two-Dimensional Quantum Gravity", Nuclear Physics B **358**, 695–712 (1991),

[532]P. Ehrenfest, "Welche Rolle spielt die Dreidimensionalität des Raumes in den Grundgesetzen der Physik?", Annalen der Physik **366**, 440–446 (1920),

[533]J. H. C. Scargill, "Can Life Exist in 2 + 1 Dimensions?", 2019, ARXIV: 1906.05336.

[534]G. 't Hooft, "Dimensional Reduction in Quantum Gravity", 1993, ARXIV: gr-qc/9310026.

[535]J. Ambjørn, J. Jurkiewicz, and R. Loll, "Emergence of a 4D World from Causal Quantum Gravity", Physical Review Letters **93**, 131301 (2004),

[536]E. P. Verlinde, "On the Origin of Gravity and the Laws of Newton", version 1, Journal of High Energy Physics **2011**, 29 (2011),

[537]S. Carlip, "Dimension and Dimensional Reduction in Quantum Gravity", Classical and Quantum Gravity **34**, 193001 (2017),

[538]M. Saravani, S. Aslanbeigi, and A. Kempf, "Spacetime Curvature in Terms of Scalar Field Propagators", Physical Review D **93**, 045026 (2016),

[539]A. Kempf, "Quantum Gravity on a Quantum Computer?", Foundations of Physics **44**, 472–482 (2014),

[540]F. Antonsen and K. Bormann, *Propagators in Curved Space*, version 1, 1996, ARXIV: hep-th/9608141.

[541]D. Kreimer, "Not so Non-Renormalizable Gravity", in *Quantum Field Theory: Competitive Models*, edited by B. Fauser, J. Tolksdorf, and E. Zeidler (Birkhäuser, Basel, 2009), pp. 155–162,

[542]S. Kamefuchi and H. Umezawa, "On the Structure of the Interaction of the Elementary Pasticles, IV. On the Interaction of the Second Kind", Progress of Theoretical Physics **9**, 529–549 (1953),

[543]B. S. DeWitt, "Gravity: A Universal Regulator?", Physical Review Letters **13**, 114–118 (1964),

[544]G. Lazarides, A. A. Patani, and Q. Shafi, "High-Energy Behavior in a Model Nonpolynomial Lagrangian Field Theory", Physical Review D **6**, 2780–2788 (1972),

[545]S. Okubo, "Note on the Second Kind Interaction", Progress of Theoretical Physics **11**, 80–94 (1954),

[546]A. Bley, "Cutkosky Cuts at Core Hopf Algebra", MA thesis (Humboldt-Universität zu Berlin, Berlin, 2016), 42 pp., URL: `http://www2.mathematik.hu-berlin.de/~kreimer/wp-content/uploads/Bley.pdf`.

[547]D. Kreimer and W. D. van Suijlekom, "Recursive Relations in the Core Hopf Algebra", Nuclear Physics B **820**, 682–693 (2009),

[548]D. Prinz, *Gauge Symmetries and Renormalization*, 2022, ARXIV: 2001.00104.

[549]B. S. DeWitt, "Quantum Theory of Gravity. I. The Canonical Theory", Physical Review **160**, 1113–1148 (1967),

[550]J. N. Goldberg, "Conservation Laws in General Relativity", Physical Review **111**, 315–320 (1958),

[551]S. J. Avis, C. J. Isham, and D. Storey, "Quantum Field Theory in Anti-de Sitter Space-Time", Physical Review D **18**, 3565–3576 (1978),

[552]L. Parker, "Aspects of Quantum Field Theory in Curved Space-Time: Effective Action and Energy-Momentum Tensor", in *Recent Developments in Gravitation: Cargèse 1978*, edited by M. Lévy and S. Deser, NATO Advanced Study Institutes Series (Springer US, Boston, MA, 1979), pp. 219–273,

[553]B. S. DeWitt, "Quantum Field Theory in Curved Spacetime", Physics Reports **19**, 295–357 (1975),

[554]W. E. Thirring, "An Alternative Approach to the Theory of Gravitation", Annals of Physics **16**, 96–117 (1961),

[555]B. S. DeWitt, "Quantum Theory of Gravity. II. The Manifestly Covariant Theory", Physical Review **162**, 1195–1239 (1967),

[556]B. S. DeWitt, "Quantum Theory of Gravity. III. Applications of the Covariant Theory", Physical Review **162**, 1239–1256 (1967),

[557]D. M. Capper, G. Leibbrandt, and M. R. Medrano, "Calculation of the Graviton Self-Energy Using Dimensional Regularization", Physical Review D **8**, 4320–4331 (1973),

[558]C. J. Isham, A. Salam, and J. Strathdee, "Is Quantum Gravity Ambiguity-Free?", Physics Letters B **46**, 407–411 (1973),

[559]F. A. Berends, G. J. H. Burgers, and H. van Dam, "On Spin Three Self Interactions", Zeitschrift für Physik C Particles and Fields **24**, 247–254 (1984),

[560]M. J. Duff, "Quantum Tree Graphs and the Schwarzschild Solution", Physical Review D **7**, 2317–2326 (1973),

[561]G. U. Jakobsen, "General Relativity from Quantum Field Theory", Master thesis, 2020, URL: `https://arxiv.org/abs/2010.08839v1`.

[562]Y. Iwasaki, "Quantum Theory of Gravitation vs. Classical Theory: Fourth-Order Potential", Progress of Theoretical Physics **46**, 1587–1609 (1971),

[563]J. F. Donoghue, "Introduction to the Effective Field Theory Description of Gravity", 1995, ARXIV: gr-qc/9512024.

[564]A. Einstein, "Näherungsweise Integration der Feldgleichungen der Gravitation", Sitzungsber. Preuss. Akad. Wiss. **1**, 688 (1916),

[565]J. Blümlein, A. Maier, P. Marquard, and G. Schäfer, *Gravity in Binary Systems at the Fifth and Sixth Post-Newtonian Order*, 2022, ARXIV: 2208.04552.

[566]D. Kreimer and A. Velenich, "Field Diffeomorphisms and the Algebraic Structure of Perturbative Expansions", Lett. Math. Phys. **103**, 171–181 (2013).

[567] A. A. Mahmoud and K. Yeats, "Diffeomorphisms of Scalar Quantum Fields via Generating Functions", 2020, ARXIV: 2007.12341.

[568] M. Omote, "Point Canonical Transformations and the Path Integral", Nuclear Physics B **120**, 325–332 (1977),

[569] K. M. Apfeldorf, H. E. Camblong, and C. R. Ordonez, "Field Redefinition Invariance in Quantum Field Theory", Modern Physics Letters A **16**, 103–112 (2001),

[570] I. V. Chebotarev, V. A. Guskov, S. L. Ogarkov, and M. Bernard, "S-Matrix of Nonlocal Scalar Quantum Field Theory in Basis Functions Representation", Particles **2**, 103–139 (2019),

[571] M. Ruhdorfer, J. Serra, and A. Weiler, "Effective Field Theory of Gravity to All Orders", Journal of High Energy Physics **2020**, 83 (2020),

[572] M. K. Volkov, "Quantum Field Model with Unrenormalizable Interaction", Communications in Mathematical Physics **7**, 289–304 (1968),

[573] P.-H. Balduf, "Propagator-Cancelling Scalar Fields", 2021, ARXIV: 2102.04315.

[574] C. F. Gauss, "Disquisitiones Generales circa Seriem Infinitam", Commentationes Societatis Regiae Scientiarum Gottingensis, Recentiores classis mathematicae, 227–270 (1813),

[575] A. Ungar, "Generalized Hyperbolic Functions", The American Mathematical Monthly **89**, 688–691 (1982).

[576] J. Engbers, D. Galvin, and C. Smyth, "Restricted Stirling and Lah Number Matrices and Their Inverses", 2017, ARXIV: 1610.05803.

[577] A. M. Jaffe, "Form Factors at Large Momentum Transfer", Physical Review Letters **17**, 661–663 (1966),

[578] H. Lehmann and K. Pohlmeyer, "On the Superpropagator of Fields with Exponential Coupling", Communications in Mathematical Physics **20**, 101–110 (1971),

[579] R. J. Blomer and F. Constantinescu, "On the Zero-Mass Superpropagator", Nuclear Physics B **27**, 173–192 (1971),

[580] C. G. Bollini and J. J. Giambiagi, "On the Exponential Superpropagator", Journal of Mathematical Physics **15**, 125–128 (1974),

[581] G. 't Hooft and M. J. G. Veltman, "One Loop Divergencies in the Theory of Gravitation", Ann.Inst.H.Poincare Phys.Theor.A **20**, 69–94 (1974),

[582] M. H. Goroff and A. Sagnotti, "The Ultraviolet Behavior of Einstein Gravity", Nuclear Physics B **266**, 709–736 (1986),

[583] S. Abreu, F. Febres Cordero, H. Ita, M. Jaquier, B. Page, M. S. Ruf, and V. Sotnikov, "Two-Loop Four-Graviton Scattering Amplitudes", Physical Review Letters **124**, 211601 (2020),

[584] D. J. Broadhurst and D. Kreimer, "Knots and Numbers in ϕ^4 Theory to 7 Loops and Beyond", International Journal of Modern Physics C **06**, 519–524 (1995),

[585] L. T. Adzhemyan and M. V. Kompaniets, "Five-Loop Numerical Evaluation of Critical Exponents of the φ^4 Theory", Journal of Physics: Conference Series **523**, 012049 (2014),

[586] M. V. Kompaniets and E. Panzer, "Minimally Subtracted Six Loop Renormalization of $O(n)$ -Symmetric ϕ^4 Theory and Critical Exponents", Physical Review D **96**, 036016 (2017),

[587] M. V. Kompaniets and E. Panzer, "Renormalization Group Functions of ϕ^4 Theory in the MS-scheme to Six Loops", 2016, ARXIV: 1606.09210.

[588] D. Z. Freedman, K. Johnson, and J. Latorre, "Differential Regularization and Renormalization: A New Method of Calculation in Quantum Field Theory", Nuclear Physics B **371**, 353–414 (1992),

[589] M. Borinsky and O. Schnetz, *Recursive Computation of Feynman Periods*, 2022, ARXIV: 2206.10460.

[590] F. Brown and O. Schnetz, "Single-Valued Multiple Polylogarithms and a Proof of the Zig-Zag Conjecture", Journal of Number Theory **148**, 478–506 (2015),

[591] N. Metropolis, A. W. Rosenbluth, M. N. Rosenbluth, A. H. Teller, and E. Teller, "Equation of State Calculations by Fast Computing Machines", The Journal of Chemical Physics **21**, 1087–1092 (1953),

[592] T. Binoth and G. Heinrich, "An Automatized Algorithm to Compute Infrared Divergent Multi-Loop Integrals", Nuclear Physics B **585**, 741–759 (2000),

[593] C. Bogner and S. Weinzierl, "Resolution of Singularities for Multi-Loop Integrals", Computer Physics Communications **178**, 596–610 (2008),

[594] A. V. Smirnov and V. A. Smirnov, "Hepp and Speer Sectors within Modern Strategies of Sector Decomposition", Journal of High Energy Physics **2009**, 004–004 (2009),

[595] T. Kaneko and T. Ueda, "A Geometric Method of Sector Decomposition", Computer Physics Communications **181**, 1352–1361 (2010),

[596] M. Borinsky, "Tropical Monte Carlo Quadrature for Feynman Integrals", Annales de l'Institut Henri Poincaré D (2021),

[597] B. D. McKay and A. Piperno, "Practical Graph Isomorphism, II", Journal of Symbolic Computation **60**, 94–112 (2014),

[598] P.-H. Balduf and A. Glück, "Fallbeispiele der Promotionsbedingungen für interne und externe Promovierende an der Humboldt- Universität zu Berlin", Qualität in der Wissenschaft **3+4**, 7 (2022).

[599] W. M. Frank, "Comparison Theorems for Convergence of Regularized Field Theories", Annals of Physics **29**, 175–216 (1964),

[600] E. Alvarez, "Quantum Gravity", in *Planck Scale Effects in Astrophysics and Cosmology*, edited by J. Kowalski-Glikman and G. Amelino-Camelia, Lecture Notes in Physics (Springer, Berlin, Heidelberg, 2005), pp. 31–58,

[601] S. Weinberg, "Infrared Photons and Gravitons", Physical Review **140**, B516–B524 (1965),

[602] A. Verstak, A. Acharya, H. Suzuki, S. Henderson, M. Iakhiaev, C. C. Y. Lin, and N. Shetty, *On the Shoulders of Giants: The Growing Impact of Older Articles*, version 1, 2014, ARXIV: 1411.0275.

[603] M. Clancy, "Do Academic Citations Measure the Impact of New Ideas?", New Things Under the Sun (2022),

[604] J. S. G. Chu and J. A. Evans, "Slowed Canonical Progress in Large Fields of Science", Proceedings of the National Academy of Sciences **118**, e2021636118 (2021),

[605] J. A. Evans, "Is Scientific Progress Slowing? With James Evans: Big Brains Podcast", Podcast, Chicago, 2022, URL: https://news.uchicago.edu/scientific-progress-slowing-james-evans.

[606] N. Bloom, "Are Ideas Getting Harder to Find?", The american economic review **110**, 41 (2020).

[607] S. Alexander, *Is Science Slowing Down? - LessWrong*, LessWrong, (2018) URL: https://www.lesswrong.com/posts/v7c47vjta3mavY3QC/is-science-slowing-down.

[608] A. Guzey, "How Life Sciences Actually Work: Findings of a Year-Long Investigation", guzey.com (2019),

[609] A. Bahr, K. Eichhorn, and S. Kubon, *#IchBinHanna. Prekäre Wissenschaft in Deutschland*, 2nd ed. (Suhrkamp, 2022), URL: https://www.suhrkamp.de/buch/ichbinhanna-t-9783518029756.

[610] K. Langin, *As Professors Struggle to Recruit Postdocs, Calls for Structural Change in Academia Intensify*, (2022) URL: https://www.science.org/content/article/professors-struggle-recruit-postdocs-calls-structural-change-academia-intensify.

[611] "Postdocs in Crisis: Science Cannot Risk Losing the next Generation", Nature **585**, 160 (2020),

[612] B. Nogrady, *Pandemic Amplifies Postdoc Struggles*, The Scientist Magazine®, (2021) URL: https://www.the-scientist.com/news-opinion/pandemic-amplifies-postdoc-struggles-69558.